

Topics in Organometallic Chemistry 51

Jairton Dupont
László Kollár *Editors*

Ionic Liquids (ILs) in Organometallic Catalysis

 Springer

Editorial Board

M. Beller, Rostock, Germany

J.M. Brown, Oxford, United Kingdom

P.H. Dixneuf, Rennes, France

J. Dupont, Porto Alegre, Brazil

A. Fürstner, Mülheim, Germany

Frank Glorius, Münster, Germany

L.J. Gooßen, Kaiserslautern, Germany

T. Ikariya, Tokyo, Japan

S. Nolan, St Andrews, United Kingdom

Jun Okuda, Aachen, Germany

L.A. Oro, Zaragoza, Spain

Q.-L. Zhou, Tianjin, China

Aims and Scope

The series *Topics in Organometallic Chemistry* presents critical overviews of research results in organometallic chemistry. As our understanding of organometallic structure, properties and mechanisms increases, new ways are opened for the design of organometallic compounds and reactions tailored to the needs of such diverse areas as organic synthesis, medical research, biology and materials science. Thus the scope of coverage includes a broad range of topics of pure and applied organometallic chemistry, where new breakthroughs are being achieved that are of significance to a larger scientific audience.

The individual volumes of *Topics in Organometallic Chemistry* are thematic. Review articles are generally invited by the volume editors. All chapters from *Topics in Organometallic Chemistry* are published OnlineFirst with an individual DOI. In references, *Topics in Organometallic Chemistry* is abbreviated as *Top Organomet Chem* and cited as a journal.

More information about this series at
<http://www.springer.com/series/3418>

Jairton Dupont • László Kollár
Editors

Ionic Liquids (ILs) in Organometallic Catalysis

With contributions by

C.A.M. Afonso • C. Bruneau • D.A. Castillo-Molina •
C. Chiappe • M. Cokoja • P. Cotugno • M.M. Dell'Anna •
Q.-H. Fan • C. Fischmeister • T. Ghilardi • L.R. Graser •
Y.-M. He • C. Janiak • F.E. Kühn • M. Latronico • Y. Li •
P. Lignier • I.I.E. Markovits • P. Mastrorilli • A. Monopoli •
C.J. Münchmeyer • A. Nacci • A. Plikhta • C.S. Pomelli •
B. Rieger • A.A. Rosatella • R. Skoda-Földes •
A.M. Trzeciak • N. Yan

 Springer

Editors

Jairton Dupont
Institute of Chemistry - UFRGS
Porto Alegre
Brazil

László Kollár
Department of Inorganic Chemistry
Institute of Chemistry, University of Pécs
Pécs
Hungary

ISSN 1436-6002

ISBN 978-3-662-47856-1

DOI 10.1007/978-3-662-47857-8

ISSN 1616-8534 (electronic)

ISBN 978-3-662-47857-8 (eBook)

Library of Congress Control Number: 2015945264

Springer Heidelberg New York Dordrecht London

© Springer-Verlag Berlin Heidelberg 2015

This work is subject to copyright. All rights are reserved by the Publisher, whether the whole or part of the material is concerned, specifically the rights of translation, reprinting, reuse of illustrations, recitation, broadcasting, reproduction on microfilms or in any other physical way, and transmission or information storage and retrieval, electronic adaptation, computer software, or by similar or dissimilar methodology now known or hereafter developed.

The use of general descriptive names, registered names, trademarks, service marks, etc. in this publication does not imply, even in the absence of a specific statement, that such names are exempt from the relevant protective laws and regulations and therefore free for general use.

The publisher, the authors and the editors are safe to assume that the advice and information in this book are believed to be true and accurate at the date of publication. Neither the publisher nor the authors or the editors give a warranty, express or implied, with respect to the material contained herein or for any errors or omissions that may have been made.

Printed on acid-free paper

Springer-Verlag GmbH Berlin Heidelberg is part of Springer Science+Business Media
(www.springer.com)

Preface

The application of the right solvent in chemical reactions is always a key-point for a chemist. In addition to conventional organic solvents several alternative ones were tested. Among them ionic liquids (ILs) and especially room temperature ionic liquids (RT-ILs) play an important role due to their environmentally benign properties such as extremely low vapor pressure, chemical and thermal stability, high ionic conductivity, and good solvent properties towards both ionic and covalent compounds.

A major drive of these efforts with ionic liquid both in industry and in fundamental research is to find more environmentally friendly technologies for traditional ones in which damaging and volatile organic solvents are generally used. Ionic liquids are considered not only as promising surrogates of organic solvents in conventional text-book reactions, but also their applications show an upward tendency also in catalytic reactions.

In this book we intend to summarize the recent achievements in catalytic reactions carried out in ILs. Leading scientists worldwide accepted our invitation to contribute to this volume and write about the recent developments. Although most chapters of the book are mainly focused on the catalytic reactions of synthetic importance, where appropriate, theoretical and mechanistic aspects are included in order to help the reader understand the underlying principles. We are confident that this book will provide a comprehensive overview of topics of current interest for the non-specialist reader.

One of the fundamental issues, the homogeneous or heterogeneous catalysis in ILs, is discussed by N. Yan (chapter “The Nature of Metal Catalysts in Ionic Liquids: Homogeneous vs Heterogeneous Reactions”). The formation of nanoparticles, as well as their application in catalytic reactions (hydrogenation, coupling reactions, methanol synthesis), is discussed by Ch. Janiak (chapter “Metal Nanoparticle Synthesis in Ionic Liquids”). P. Lignier’s contribution is dealing with the size control of metal nanocrystals in ILs (chapter “Size Control of Monodisperse Metal Nanocrystals in Ionic Liquids”). C. Chiappe et al. report on the structural features and properties of metal complexes in ILs with special focus on anionic speciation of metals (chapter “Structural Features and Properties of Metal

Complexes in Ionic Liquids: Application in Alkylation Reactions”). The state of the art in ionic liquid-based hydroformylation is reviewed by B. Rieger et al. (chapter “Ionic Liquids in Transition Metal-Catalyzed Hydroformylation Reactions”). The research carried out recently in the field of carbonylation of alkenes and alkynes, as well as aryl and alkenyl halides in the presence of O- and N-nucleophiles, is summarized by R. Skoda-Földes (chapter “ILs in Transition Metal-Catalysed Alkoxy- and Aminocarbonylation”). Metal-catalyzed oxidations of alcohols and sulfides are discussed by A.M. Afonso et al. (chapter “Metal-Catalyzed Oxidation of C–X (X=S, O) in Ionic Liquids”). Recent results on epoxidation of various olefins by different transition metal complexes, as well as by metal-free compounds in ILs, are summarized by F.E. Kühn et al. (chapter “Epoxidation of Olefins with Molecular Catalysts in Ionic Liquids”). The beneficial effect of ILs in terms of activity, selectivity, and recyclability in cross-coupling reactions such as Heck, Suzuki–Miyaura, Stille, Sonogashira, Ullmann, and Negishi couplings is described by P. Mastrolilli et al. (chapter “Ionic Liquids in Palladium-Catalyzed Cross-Coupling Reactions”). The chapter of Ch. Bruneau et al. covers the catalytic olefin metathesis reactions carried out in RT-ILs (chapter “RTILs in Catalytic Olefin Metathesis Reactions”). Selected examples of polymerization and oligomerization catalyzed by transition metal complexes in ILs are presented by A.M. Trzeciak (chapter “Ionic Liquids in Transition Metal-Catalyzed Oligomerization/Polymerization”). The efficiency of transition metal-catalyzed asymmetric reactions providing precursors of pharmaceutical importance is described by Q.-H. Fan et al. (chapter “Ionic Liquids in Transition Metal-Catalyzed Enantioselective Reactions”).

We are indebted to all chapter authors for their careful work. The editors thank Elizabeth Hawkins (Springer, Chemistry Editorial) and Sujitha Shiney (Project Coordinator) for their kind cooperation in producing the present volume.

As volume editors we kindly recommend the present book entitled *Ionic Liquids in Organometallic Catalysis* to the attention of research scientists at universities or in industry, as well as graduate students.

Pécs, Hungary
Porto Alegre, Brazil

László Kollár
Jairton Dupont

Contents

The Nature of Metal Catalysts in Ionic Liquids: Homogeneous vs Heterogeneous Reactions	1
Ning Yan	
Metal Nanoparticle Synthesis in Ionic Liquids	17
Christoph Janiak	
Size Control of Monodisperse Metal Nanocrystals in Ionic Liquids . . .	55
Pascal Lignier	
Structural Features and Properties of Metal Complexes in Ionic Liquids: Application in Alkylation Reactions	79
Cinzia Chiappe, Tiziana Ghilardi, and Christian Silvio Pomelli	
Ionic Liquids in Transition Metal-Catalyzed Hydroformylation Reactions	95
Bernhard Rieger, Andriy Plikhta, and Dante A. Castillo-Molina	
ILs in Transition Metal-Catalysed Alkoxy- and Aminocarbonylation	145
Rita Skoda-Földes	
Metal-Catalyzed Oxidation of C–X (X = S, O) in Ionic Liquids	163
Andreia A. Rosatella and Carlos A.M. Afonso	
Epoxidation of Olefins with Molecular Catalysts in Ionic Liquids	185
Christian J. Münchmeyer, Lilian R. Graser, Iulius I.E. Markovits, Mirza Cokoja, and Fritz E. Kühn	
Ionic Liquids in Palladium-Catalyzed Cross-Coupling Reactions	237
Piero Mastrorilli, Antonio Monopoli, Maria Michela Dell’Anna, Mario Latronico, Pietro Cotugno, and Angelo Nacci	

RTILs in Catalytic Olefin Metathesis Reactions	287
Cédric Fischmeister and Christian Bruneau	
Ionic Liquids in Transition Metal-Catalyzed Oligomerization/Polymerization	307
Anna M. Trzeciak	
Ionic Liquids in Transition Metal-Catalyzed Enantioselective Reactions	323
Yong Li, Yan-Mei He, and Qing-Hua Fan	
Index	349

The Nature of Metal Catalysts in Ionic Liquids: Homogeneous vs Heterogeneous Reactions

Ning Yan

Abstract Despite the extensive investigations on transition-metal-catalyzed reactions in ionic liquids (ILs), the most fundamental issue, i.e., *whether the catalysis is homogenous or heterogeneous*, is not always clear. This chapter provides a brief description of the methods to distinguish the metal-complex-catalyzed homogenous reactions from the metal-particle-catalyzed heterogeneous reactions in ILs. Following that, a current understanding of the nature of transition metal catalysts in ILs, categorized by the types of reactions, is provided.

Keywords Metal catalyst · Homogeneous catalysis · Heterogeneous catalysis · Ionic liquid

Contents

1	Introduction	2
2	Methods to Distinguish Between Homogenous and Heterogeneous Catalysts in ILs	2
3	The Nature of Catalysts for Various Reactions in ILs	4
3.1	Hydrogenation	4
3.2	Oxidation	6
3.3	Coupling	7
3.4	Miscellaneous	9
4	Conclusion	11
	References	12

N. Yan (✉)

Department of Chemical and Biomolecular Engineering, National University of Singapore,
4 Engineering Drive 4, 117576, Singapore
e-mail: cheyann@nus.edu.sg

1 Introduction

We have witnessed a proliferation of the numbers of papers on transition-metal-catalyzed reactions in ionic liquids (ILs) in the past decade [1–6]. The nature of the metal catalysts in ILs is one of the most fundamental issues in these studies, as it is the dominant factor controlling catalytic processes. In addition, identifying the true catalyst is critically important for future advances in the rational design of better catalysts in ILs.

Many of the earlier research papers did not discuss the active forms of metal catalysts, or simply assumed precatalyst to be the real catalytic species. It was not until fairly recently that researchers focused on the question – what is the form of the true catalytic species in these transition-metal-catalyzed reactions in ILs? Is it homogenous or heterogeneous? Addressing this problem can be nontrivial, as no versatile technique exists for making this distinction. Many methods have been developed to distinguish between homogenous and heterogeneous catalysis, but each has limitations. This necessitates the combination of various experiments to reach a compelling conclusion. In addition, the “non-innocent” role of ILs [7, 8] in metal-catalyzed reactions is often observed, due to their unique interactions with the catalysts [2], which adds complexity to the systems.


In this chapter, we describe the current understanding of the nature of transition-metal catalysts in ILs. First, methods that have been successfully applied in distinguishing metal-complex homogeneous catalysts from metal-particle heterogeneous catalysts in ILs are introduced. Next, we put emphasis on the nature of the catalysts in various reactions in ILs, including the reactions whose active species are well established by direct or accumulated circumstantial evidence, as well as those that are less well understood. Only the studies from which reasonably robust inferences can be drawn are introduced in this chapter.

2 Methods to Distinguish Between Homogenous and Heterogeneous Catalysts in ILs

In this section, we briefly reviewed the experimental approaches that could be employed to distinguish between homogenous and heterogeneous catalysts. Only methods proved to be successful for reactions carried out in ILs are introduced (Table 1). A more general, extensive review focused on various experiments to determine the true catalyst under reducing condition is highly recommended to readers with further interests [9].

Reaction kinetics is a powerful way to identify the nature of catalysts. Some even argued that the most compelling evidence for the identity of the true catalyst will always be kinetic in nature [9]. Robust kinetic analysis on metal-catalyzed reactions in ILs is rare but does exist. Ir nanoparticle (NP) catalyzed alkene hydrogenation in $[\text{C}_4\text{C}_1\text{im}][\text{PF}_6]$ ($[\text{C}_4\text{C}_1\text{im}] = 1\text{-butyl-3-methylimidazolium}$) has

Table 1 Applicability and reliability of various methods to distinguish homogeneous from heterogeneous catalysts in ILs

	Homogeneous catalysts	Heterogeneous catalysts	Method reliability ^a	
Reaction selectivity patterns	√	√	Increasing Reliability 	
Ex-situ spectroscopic techniques	TEM	√		
	UV-vis	√		
	XRD	√		
	XPS	√		
Filtration/leaching	√	√		
Poisoning test	NHCs	√		
	CS ₂			√
	Mercury			√
Reaction kinetics	√	√		

√ indicates the method is applicable to prove/refute the homogeneous or heterogeneous nature of the catalysts

^aThe arrow shows the direction with enhanced reliability

been examined by detailed kinetic modeling which indicated that the NP catalysts follow a simple Langmuir adsorption mechanism [10]. This is strong evidence that the Ir NPs in ILs behave as heterogeneous catalysts, as they obey a classical surface reaction mechanism. In some cases, an induction period was observed for the reaction to occur in ILs. This gives clue that the true catalytic species is different from the precatalyst – NPs formed from metal complexes, or homogenous species leached from the metal surface, may be responsible for the catalytic activity.

Various poisons that could selectively hinder the catalytic activity of homogeneous/heterogeneous catalysts can be used to determine the nature of catalysts. To date, mercury [11, 12] and CS₂ [12, 13] poisoning are most popularly employed in metal-catalyzed reactions in ILs. If the reaction is catalyzed by heterogeneous metal catalyst, the addition of mercury to the reaction will give a mercury-metal amalgam deactivating the catalyst. CS₂ poisoning is based on another principle. A heterogeneous catalyst can possibly be completely poisoned with far less than 1 equivalent of added CS₂ per metal atom. The reason is that only a small fraction of metal atoms are on the surface of a heterogeneous metal-particle catalyst; hence, much less than one molar equivalent of ligand per metal atom will be sufficient to deactivate the catalyst. Another reason is that not all the surface atoms are catalytic active. Both mercury and CS₂ tests are aimed to deactivate the heterogeneous catalysts and both have limitations. For mercury poisoning, one should keep in mind that some metals, such as Rh and Ru, do not form amalgams with mercury and that they are not easily poisoned (adding large excess of mercury could still poison Rh NPs in ILs [11]). The limitation for CS₂ poisoning is that ligand dissociation occurs at temperatures higher than 50°C. Therefore, this test should ideally be performed under mild temperatures. Other ligands that could be used to poison heterogeneous catalysts, such as PPh₃ and thiophene, and ligands to poison homogenous catalysts, such as dibenzo[a,e]cyclooctatetraene (DCT) [14], have not yet been used to probe the nature of the catalysts in ILs.

N-heterocyclic carbenes (NHCs) from imidazolium-based ILs sometimes act as poisons, which can be used as markers for homogeneous catalysis. For example, Ru-(BINAP)(DPEN)Cl₂ was tested for the asymmetric hydrogenation of ketones in a 2-propanol/IL mixture [15]. [C₄C₁im][BF₄] and [C₄C₁im][PF₆] performed poorly compared to analogue ILs whose C₂ position was substituted by a methyl group. A plausible explanation is that the KOH co-catalyst could deprotonate the C₂ position of the imidazolium ring, leading to the formation of NHCs, which could then poison the catalyst. Similarly, Dyson et al. found a Pd NHC complex to be inactive in Suzuki coupling reaction in ILs [16]. On the other hand, the presence of NHCs did not influence the olefin hydrogenation activity of heterogeneous Ir NPs in ILs [17].

Transmission electron microscopy (TEM), X-ray diffractometry (XRD), X-ray absorption spectroscopy (XAS), and UV-vis spectroscopy are all widely used to identify the presence of metal particles in ILs, while electrospray mass spectroscopy (ESI-MS) is used to determine metal molecular species in ILs. These methods can only be used to demonstrate whether or not heterogeneous metal particles/complexes exist in the system, instead of proving that the reaction is actually catalyzed by these particles/complexes, and must be used in conjunction with other techniques to finally address if these particles/complexes are the true catalytic active species.

Some reactions are known to be heterogeneously/homogeneously catalyzed, and these reactions can be used to provide clue on the nature of the catalysts. It is generally accepted that metal homogeneous catalysts do not hydrogenate aromatic compounds [18], so arene hydrogenation has been used as a chemical probe for studying the surface properties of NPs in ILs. Another example is that the absence of isomerized products in the hydrogenation of 1,3-butadiene [19] and (Z)-alkenes [20] catalyzed by Pd NPs in [C₄C₁im][BF₄] and [C₄C₁im][PF₆] is believed to be an indication of the surface-like behavior of the catalysts.

Occasionally, filtration could be used to test the catalyst's identity in ILs [21]. It becomes more informative when combined with ICP-AES or ICP-MS analysis, as the exact metal content in both filter residue and filtrate can be determined. However, this method should be treated with caution as it is incapable to distinguish soluble NPs from homogenous complex. According to Finke's review [9], there are a few other methods such as Collman's test and light scattering technique that could be used to provide information on the catalyst identity, but to our knowledge these methods have not been extended to metal-catalyzed reactions in ILs.

3 The Nature of Catalysts for Various Reactions in ILs

3.1 Hydrogenation

Hydrogenation is one of the earliest reactions studied in ILs, which dates back to 1995 [22, 23]. All major types of hydrogenation are successfully transferred into IL

phase. It is believed that arene hydrogenation mainly occurs over heterogeneous catalysts [4]. In fact, it is even used to probe the presence of metal NPs, as mentioned in the last section. On the other hand, a vast majority of asymmetric hydrogenations appear to be homogeneously catalyzed. Other types of reactions, including C=O, C=C, C=C, C=N, and NO₂ hydrogenation, could be catalyzed by both homogenous and heterogeneous catalysts.

In some investigations, the heterogeneous nature of the catalyst in hydrogenation was revealed in ILs. The most employed technique is to use poisons. Mercury is by far most extensively used [11, 12, 24]. CS₂ was also tested but to a much less extent [12]. Significant activity drop in hydrogenation upon adding these reagents suggests that NPs are responsible for catalysis in these cases [11, 12, 24]. Kinetic modeling was also attempted. In one study, the alkene hydrogenation with Ir NPs as the precatalyst obeys the monomolecular surface reaction mechanism $r = k_c K[S] / (1 + K[S])$ (k_c = kinetic constant, K = adsorption constant and $[S]$ = substrate concentration), which supports a heterogeneous mechanism and that Ir NPs are the real catalysts [10].

Less attention was paid to elucidate the nature and the mechanism of homogeneous catalysts in ILs. However, transfer of homogeneous hydrogenation catalysts from molecular solvents into ILs may be unsuccessful without understanding the nature of the catalytic species. Dyson et al. carried out detailed mechanistic investigation on the catalytic activity of metal complexes in ILs [25–28]. By using temperature variant ¹H NMR technique, they measured the interactions between chloride and the cation [27]. The solvation enthalpy of the chloride in [C₄C₁im][OTf] was found to be strikingly low – merely –46.2 kJ/mol – almost eight times smaller than that of chloride in water. The low solvation enthalpy of chloride in such an IL resulted in a strong coordination ability of the chloride anion in [C₄C₁im] type ILs, exhibiting a profound effect on homogeneous catalysts. Chloride dissociation from a transition-metal complex can be thermodynamically disfavored or even inhibited in these ILs. Therefore, homogenous catalysts that need chloride dissociation to generate active catalytic species become inactive [25]. This finding also provides a guideline to increase activity of heterogeneous catalysts in ILs, i.e., ILs should be purified with extreme caution, as contaminants such as chloride in these ILs bind strongly on metal surface acting as poisons.

Due to this inhibition effect, [Ru(*p*-cymene)-(dppm)Cl]Cl exhibited very little activity in a variety of ILs when used as catalyst precursor. Nevertheless, some catalytic activity was found in [C₄C₁im][CH₃SO₄] and higher activity in [C₄C₁im][NTf₂]. Mercury could not poison the catalyst and attempt to identify NPs by TEM failed, indicating the catalyst to be homogeneous. Interestingly, the addition of [C₄mpy]Cl (1-butyl-3-methylpyridinium) to the reaction mixture in [C₄mpy][NTf₂] also gave a catalytically active solution, ruling out the possibility of an active catalytic species requiring chloride dissociation. Detailed kinetic analysis revealed the first-order kinetics in the addition of chloride and the loss of *p*-cymene, and the second-order kinetics in Ru(II) for the formation of active catalytic species, which strongly suggest the formation of cationic, electronically unsaturated dimer species to be postulated as a rate-limiting process in the formation of the active catalyst

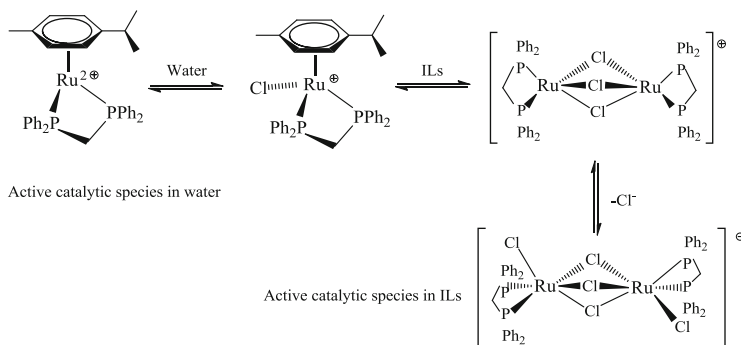


Fig. 1 Different activation pathways of $[\text{Ru}(\text{p-cymene})-(\text{dppm})\text{Cl}]\text{Cl}$ in water and in ILs

(see Fig. 1) [26]. This is one of the very few examples reported to date, which clearly demonstrated the mechanistic change in the homogeneous catalyst upon using ILs.

To overcome the inhibition of catalyst activity by chloride (and other) ions, functionalized ILs interacting much stronger with chloride could be used. For example, hydroxyl group functionalized ILs were found to be tolerant of chloride, even when chloride was in large excess to metal catalysts. Indeed, 1-(2'-hydroxyethyl)-3-methylimidazolium cation ($[\text{C}_2\text{OHC}_1\text{im}]$) based ILs were proved to be superior solvents compared to non-functionalized ILs for the immobilization of metal NP catalysts for a variety of reactions [29–31] including hydrogenation [31].

3.2 Oxidation

The potential of ILs for oxidation in the presence of metal catalysts has not escaped from the attention of chemists [32]. A majority of such studies are based on adapting the traditional organic solvent methods to ILs. Oxidations of alcohols, phenols, amines, imines, and alkenes have all been attempted, but efforts have rarely been paid to elucidate the nature of the catalysts. One exception comes from Hardacre and coworkers, and they employed MCM-41 and UVM-type mesoporous materials containing Ti or TiGe to catalyze the oxidation of thioether into sulfoxides and sulfones in both molecular solvents and ILs [21]. The leaching of Ti was carefully analyzed in both $[\text{C}_2\text{C}_1\text{im}][\text{BF}_4]$ and dioxane, and significantly more leaching (ca. 40%) was found in organic solvents than in ILs (18%) in the first run. Controlled experiments indicated that the Ti dissolution does not originate from the sulfoxidation reaction itself, but results from the interactions between the peroxy species and the catalyst. The leached Ti is active for the oxidation, but to a less extent compared with the heterogeneous catalysts. This, combined with the fact that leaching became insignificant from the second run, makes the authors conclude the reaction to be mainly heterogeneously catalyzed.

A majority of metal-catalyzed oxidation reactions in ILs use metal complexes or metal salts as precursors and their mechanism is often described by the classical homogenous catalytic cycle. However, the possibility of heterogeneous catalysis being responsible for some of the observed activity should be considered, especially when salts of precious metals, such as Au, Pt, Pd, and Ru, are used as the catalyst precursor. At least one report showed that metallic form of the metal was observed during the reaction. This reaction employed Pd(OAc)₂ in a range of 1,3-dialkylimidazolium-based ILs for the oxidation of benzyl alcohol to benzaldehyde using oxygen as oxidant [33]. The formation of the Pd metals may be due to the thermal decomposition of acetate anion, which serves as a reductant [20]. Zero valent forms of these metals are known to be catalytic active for alcohol and CO oxidation in molecular solvents [34]. The nature of the catalysts based on V and Mo should also be treated with caution. Despite the fact that their metal form is unstable and may not be able to promote the oxidation, their oxides are well practiced in industry for oxidations [35, 36].

3.3 Coupling

ILs have been used extensively for a variety of C–C coupling reactions with a wide range of substrates, as initially demonstrated in Heck reaction by the end of the last century [37]. Soon it was discovered that heterogeneous catalysts, such as Pd/C [38], exhibited considerable activity in ILs and this put the identity of genuine catalytic species under debate. Starting with Pd(OAc)₂, 1 nm Pd NPs were detected in [C₄C₄im]Br ([C₄C₄im] = 1-*n*-butyl-3-butylimidazolium) and [C₄C₄im][BF₄] after ultrasound promoted Heck reaction of aryl halides with alkylacrylate compounds at room temperature (see a TEM image in Fig. 2, left) [39]. Soon after this work, an in situ XAS study was performed, revealing that 0.8–1.6 nm Pd NPs were the main species present during the Heck reaction in a range of ILs employing Pd(OAc)₂ as precatalyst (Fig. 2, right, indicating the presence of Pd–Pd scattering peak after reaction) [40]. An induction period was observed, which was rationalized by the formation of Pd NPs as active catalysts. The presence of Pd NPs and their involvement in catalysis were also widely reported in Suzuki [41–43] Stille [44, 45], and Ullman [46, 47] coupling reactions.

Despite some of the earlier reports giving evidence suggesting, but not proving, a heterogeneous mechanism [48], it is now widely accepted that the leached soluble Pd is the genuine catalytically active species in most C–C coupling reactions. Dupont and coworkers pioneered the mechanistic investigation concerning the role of Pd NPs in Heck reactions using aryl halides and *n*-butyl acrylate as substrates [49]. There are some key findings in their study. First, 1.7-nm Pd NPs derived from N-containing palladacycle decomposition were active for Heck reaction when suspended in [C₄C₁im][PF₆]. Second, the Pd NPs dispersed in the IL after the reaction displayed an irregular shape with a monomodal size distribution of 6 nm. Third, ICP-MS showed leaching of considerable quantities of Pd from the IL into the organic

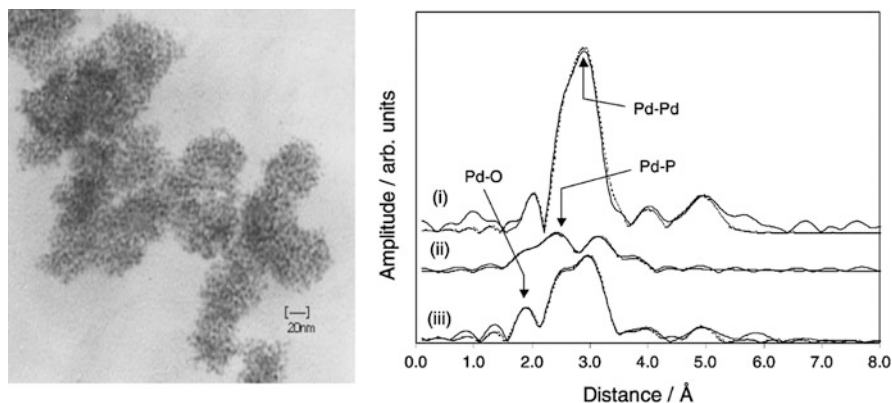


Fig. 2 *Left*: TEM image of Pd NPs formed from Pd(OAc)₂ in the Heck reaction in [Bbim]Br and [Bbim][BF₄]; *right*: radial distribution functions from palladium ethanoate in [C₄mim][PF₆] (i) without and (ii) with PPh₃ at 80°C and (iii) with PPh₃ and reagents at 50°C for 20 min. Reprinted with permission from references [39, 40] (Copyright Royal Chemical Society)

phase at the beginning of the reaction, and the level of leaching gradually decreased as the reaction progressed. Fourth, attempt to identify Pd NPs in the organic phase was unsuccessful, and the Pd species in the organic phase was inactive in the Heck reaction. Finally, competitive experiments of various bromoarenes and iodoarenes with *n*-butyl acrylate catalyzed by various palladacycles gave the same reaction constant (ρ). Since the ρ value depends only on the type of reaction but not on the substituent used, the data indicated that the same species in the oxidative addition step was generated [50]. These observations suggest that the Heck reaction pathway starts with oxidative addition of the aryl halide onto the metal surface, forming Pd(II) species, which detaches from the NP surface and enters the main catalytic cycle. The Pd(0) species generated after the reductive elimination step can either continue in the catalytic cycle or go back to the NP surface.

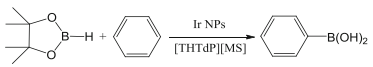
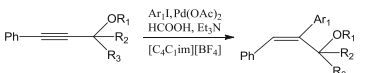
Subsequent studies indicated that Pd NPs acting as reservoirs for the catalytically active species in C–C coupling reactions in ILs appear to be general [1]. In this context, smaller Pd NPs are associated with an increased catalytic activity by providing more Pd surface atoms that can undergo oxidative addition with the aryl halide [5]. Preventing these NP reservoirs from aggregation and precipitation is the key to maintain a high catalytic performance of such reactions. To this end, several studies employing nitrile [51], ether [16], and hydroxyl functionalized [30] ILs as effective stabilizing species for Pd NPs were conducted, and indeed these functionalized ILs are superior in terms of activity and recyclability compared to non-functionalized counterparts. The roles for the functionalized ILs may be multiple: in addition to stabilizing the Pd NPs, they may also be responsible for stabilizing the active Pd(II) catalyst, facilitating Pd NP formation, and preventing Pd NPs from poisoning. The advantages of employing a hydroxyl functional IL for Suzuki coupling are illustrated in Fig. 3.

Table 2 Examples of various transitional metal catalytic reactions in ILs beyond hydrogenation, oxidation, and coupling reactions

Reaction type	A representative reaction scheme	Plausible catalyst nature	References
Olefin metathesis		Homogeneous	[58]
Dimerization		Homogeneous	[59]
Alkylcarbonylation		Homogeneous	[60]
Pauson–Khand		Homogeneous	[61]
Hydroformylation		Homogeneous	[62]
Hydroesterification		Homogeneous	[63]
Isomerization		Homogeneous	[64]
$^{10}\text{B}/^{11}\text{B}$ exchange		Heterogeneous	[55]
Fischer–Tropsch		Heterogeneous	[65, 66]
Dehalogenation		Heterogeneous	[67]
Hydrosilylation		Both possible	[56]

(continued)

Table 2 (continued)

Reaction type	A representative reaction scheme	Plausible catalyst nature	References
Phenylborylation		Unclear	[57]
Hydroarylation		Unclear	[68]

TPPTS tri(mulsulphonylphenyl) phosphine, trisodium salt, *TPP* 5,10,15,20-tetraphenylporphyrin

catalysts. In a very recent study, core-shell AuPd bimetallic NPs dispersed in $[\text{C}_2\text{OHC}_1\text{im}][\text{BF}_4]$ were found to be superior to monometallic Au or Pd NPs prepared under the same condition for the dehalogenation of bromo-aromatic compounds, due to the electron donating effect from Pd to Au. Indeed, this provides additional evidence that the dehalogenation reaction is heterogeneously catalyzed, as it is less likely that two homogeneous species can synergistically cooperate in a single reaction.

The reaction mechanism for a few reactions in ILs is not clear, but initial experiments were carried out to probe the active catalytic species. For example, Ru NPs catalyzed the isotope exchange between ^{10}B and ^{11}B nuclei in decaborane, which is believed to be heterogeneous in nature, since catalysis in the presence of mercury poison did not result in any $^{10}\text{B}/^{11}\text{B}$ exchange [55]. A biphasic hydrosilylation in $[\text{C}_4\text{py}][\text{BF}_4]$ ($[\text{C}_4\text{py}] = \text{N-butylpyridinium}$) employing K_2PtCl_4 or $\text{Pt}(\text{PPh}_3)_4$ as the precatalyst was conducted [56]. Pt NPs were observed after catalysis by TEM and adding mercury significantly reduced the catalytic activity. While there is no doubt that Pt NPs are formed in the course of hydrosilylation, the exact role of these NPs in catalysis, i.e., whether they served as catalyst reservoirs or as active catalysts, is not certain. For some reactions, little is known about the catalyst nature. For example, Ir NPs dispersed in $[\text{THTdP}][\text{MS}]$ ($[\text{THTdP}] = \text{trihexyltetradecylphosphonium}$; $[\text{MS}] = \text{methylsulfonate}$) can catalyze phenylborylation [57], but no mechanistic study was conducted to understand how this reaction occurred.

4 Conclusion

For transitional metal-catalyzed reactions in ILs, various techniques have been used to distinguish homogeneous from heterogeneous catalysis. Those include a number of instrumentation techniques, kinetic study, and various poison reagents. It is noteworthy that it is not possible to reach a definitive distinction from a single experiment. Each method has its own limitation and combined techniques have to

be used to understand the genuine nature of the catalysts. While there are reports with comprehensive investigations, which provided compelling evidence for the nature of the catalytic species in ILs, most studies simply assumed the catalysis to be homogeneous/heterogeneous without performing extensive experiments.

Unlike most molecular solvents, ILs are excellent stabilizers for metal NPs. Indeed, NPs appear to be more frequently encountered in transitional metal catalysis conducted in ILs than in molecular solvents. Special caution should be paid when precious metal salt/organometallic precursor is used as precatalyst and when the reaction is conducted under reductive condition, because the probability of forming NPs is high. The involvement of NPs complicates the specification on the nature of the catalysts. Whether the NPs act as the true catalytically active species, catalyst reservoirs, or simply spectators, has to be analyzed. Some cases are certainly worth further studying to rationalize the catalyst nature. Finally, ILs are found to be able to modify the reaction mechanism, not only in some organic reactions [69], but also in transitional metal-catalyzed reactions [26]. Whether it is possible that a homogeneously/heterogeneously catalyzed reaction in molecular solvents switches to a heterogeneously/homogeneously catalyzed one in ILs, or vice versa, remains a fundamental and intriguing question.

Acknowledgments We would like to thank the NUS start-up grant (R-279-000-368-133) for supporting our research, and Paul Dyson for the stimulating discussions.

References

1. Scholten JD, Leal BC, Dupont J (2012) Transition metal nanoparticle catalysis in ionic liquids. *ACS Catal* 2:184–200
2. Hallett JP, Welton T (2011) Room-temperature ionic liquids: solvents for synthesis and catalysis. 2. *Chem Rev* 111:3508–3576
3. Parvulescu VI, Hardacre C (2007) Catalysis in ionic liquids. *Chem Rev* 107:2615–2665
4. Dupont J, Scholten JD (2010) On the structural and surface properties of transition-metal nanoparticles in ionic liquids. *Chem Soc Rev* 39:1780–1804
5. Luska KL, Moores A (2012) Functionalized ionic liquids for the synthesis of metal nanoparticles and their application in catalysis. *ChemCatChem* 4:1534–1546
6. Yan N, Xiao C, Kou Y (2010) Transition metal nanoparticle catalysis in green solvents. *Coord Chem Rev* 254:1179–1218
7. Dupont J, Spencer J (2004) On the noninnocent nature of 1,3-dialkylimidazolium ionic liquids. *Angew Chem Int Ed* 43:5296–5297
8. Sowmiah S, Srinivasadesikan V, Tseng M-C, Chu Y-H (2009) On the chemical stabilities of ionic liquids. *Molecules* 14:3780–3813
9. Widegren JA, Finke RG (2003) A review of the problem of distinguishing true homogeneous catalysis from soluble or other metal-particle heterogeneous catalysis under reducing conditions. *J Mol Catal A Chem* 198:317–341
10. Fonseca GS, Domingos JB, Nome F, Dupont J (2006) On the kinetics of iridium nanoparticles formation in ionic liquids and olefin hydrogenation. *J Mol Catal A Chem* 248:10–16
11. Zhao C, Wang H-Z, Yan N, Xiao C-X, Mu X-D, Dyson PJ, Kou Y (2007) Ionic-liquid-like copolymer stabilized nanocatalysts in ionic liquids: II Rhodium-catalyzed hydrogenation of arenes. *J Catal* 250:33–40

12. Rossi L, Machado G, Fichtner PP, Teixeira S, Dupont J (2004) On the use of ruthenium dioxide in 1-n-butyl-3-methylimidazolium ionic liquids as catalyst precursor for hydrogenation reactions. *Catal Lett* 92:149–155
13. Vollmer C, Redel E, Abu-Shandi K, Thomann R, Manyar H, Hardacre C, Janiak C (2010) Microwave irradiation for the facile synthesis of transition-metal nanoparticles (NPs) in ionic liquids (ILs) from metal–carbonyl precursors and Ru-, Rh-, and Ir-NP/IL dispersions as biphasic liquid–liquid hydrogenation nanocatalysts for cyclohexene. *Chem—Eur J* 16:3849–3858
14. Anton DR, Crabtree RH (1983) Dibenzof[a, e]cyclooctatetraene in a proposed test for heterogeneity in catalysts formed from soluble platinum-group metal complexes. *Organometallics* 2:855–859
15. Ngo HL, Hu A, Lin W (2005) Catalytic asymmetric hydrogenation of aromatic ketones in room temperature ionic liquids. *Tetrahedron Lett* 46:595–597
16. Yang X, Fei Z, Geldbach TJ, Phillips AD, Hartinger CG, Li Y, Dyson PJ (2008) Suzuki coupling reactions in ether-functionalized ionic liquids: the importance of weakly interacting cations. *Organometallics* 27:3971–3977
17. Scholten JD, Ebeling G, Dupont J (2007) On the involvement of NHC carbenes in catalytic reactions by iridium complexes, nanoparticle and bulk metal dispersed in imidazolium ionic liquids. *Dalton Trans* 5554–5560
18. Dyson PJ (2003) Arene hydrogenation by homogeneous catalysts: fact or fiction? *Dalton Trans* 2964–974
19. Umpierre AP, Machado G, Fecher GH, Morais J, Dupont J (2005) Selective hydrogenation of 1,3-butadiene to 1-butene by Pd(0) nanoparticles embedded in imidazolium ionic liquids. *Adv Synth Catal* 347:1404–1412
20. Venkatesan R, Prechtl MHG, Scholten JD, Pezzi RP, Machado G, Dupont J (2011) Palladium nanoparticle catalysts in ionic liquids: synthesis, characterisation and selective partial hydrogenation of alkynes to Z-alkenes. *J Mater Sci* 21:3030–3036
21. Cimpeanu V, Parvulescu VI, Amorós P, Beltrán D, Thompson JM, Hardacre C (2004) Heterogeneous oxidation of pyrimidine and alkyl thioethers in ionic liquids over mesoporous Ti or Ti/Ge catalysts. *Chem—Eur J* 10:4640–4646
22. Chauvin Y, Mussmann L, Olivier H (1996) A novel class of versatile solvents for two-phase catalysis: hydrogenation, isomerization, and hydroformylation of alkenes catalyzed by rhodium complexes in liquid 1,3-dialkylimidazolium salts. *Angew Chem Int Ed* 34:2698–2700
23. Suarez PAZ, Dullius JEL, Einloft S, De Souza RF, Dupont J (1996) The use of new ionic liquids in two-phase catalytic hydrogenation reaction by rhodium complexes. *Polyhedron* 15:1217–1219
24. Julis J, Holscher M, Leitner W (2010) Selective hydrogenation of biomass derived substrates using ionic liquid-stabilized ruthenium nanoparticles. *Green Chem* 12:1634–1639
25. Daguinet C, Dyson PJ (2004) Inhibition of catalytic activity in ionic liquids: implications for catalyst design and the effect of cosolvents. *Organometallics* 23:6080–6083
26. Daguinet C, Dyson PJ (2006) Switching the mechanism of catalyst activation by ionic liquids. *Organometallics* 25:5811–5816
27. Daguinet C, Scopelliti R, Dyson PJ (2004) Mechanistic investigations on the hydrogenation of alkenes using ruthenium(II)-arene diphosphine complexes. *Organometallics* 23:4849–4857
28. Daguinet C, Dyson PJ (2007) A metallacage encapsulating chloride as a probe for a solvation scale in ionic liquids. *Inorg Chem* 46:403–408
29. Yuan X, Yan N, Katsyuba SA, Zvereva EE, Kou Y, Dyson PJ (2012) A remarkable anion effect on palladium nanoparticle formation and stabilization in hydroxyl-functionalized ionic liquids. *Phys Chem Chem Phys* 14:6026–6033
30. Yan N, Yang X, Fei Z, Li Y, Kou Y, Dyson PJ (2009) Solvent-enhanced coupling of sterically hindered reagents and aryl chlorides using functionalized ionic liquids. *Organometallics* 28:937–939
31. Yang X, Yan N, Fei Z, Crespo-Quesada RM, Laurenczy G, Kiwi-Minsker L, Kou Y, Li Y, Dyson PJ (2008) Biphasic hydrogenation over PVP stabilized Rh nanoparticles in hydroxyl functionalized ionic liquids. *Inorg Chem* 47:7444–7446

32. Muzart J (2006) Ionic liquids as solvents for catalyzed oxidations of organic compounds. *Adv Synth Catal* 348:275–295
33. Seddon KR, Stark A (2002) Selective catalytic oxidation of benzyl alcohol and alkylbenzenes in ionic liquids. *Green Chem* 4:119–123
34. Yuan Y, Yan N, Dyson PJ (2011) pH-sensitive gold nanoparticle catalysts for the aerobic oxidation of alcohols. *Inorg Chem* 50:11069–11074
35. Rodríguez JA, Stacchiola D (2010) Catalysis and the nature of mixed-metal oxides at the nanometer level: special properties of $\text{MO}_x/\text{TiO}_2(110)$ $M = \text{V, W, Ce}$ surfaces. *Phys Chem Chem Phys* 12:9557–9565
36. Ono T, Ogata N, Numata H, Miyaryo Y (2001) A study of active sites for alkene and alkane oxidation over Mo and V mixed oxide catalysts using ^{18}O tracer and Raman spectroscopy. *Top Catal* 15:229–234
37. Carmichael AJ, Earle MJ, Holbrey JD, McCormac PB, Seddon KR (1999) The Heck reaction in ionic liquids: a multiphase catalyst system. *Org Lett* 1:997–1000
38. Hagiwara H, Shimizu Y, Hoshi T, Suzuki T, Ando M, Ohkubo K, Yokoyama C (2001) Heterogeneous Heck reaction catalyzed by Pd/C in ionic liquid. *Tetrahedron Lett* 42:4349–4351
39. Deshmukh RR, Rajagopal R, Srinivasan KV (2001) Ultrasound promoted C–C bond formation: Heck reaction at ambient conditions in room temperature ionic liquids. *Chem Commun* 1544–1545
40. Hamill NA, Hardacre C, McMath SEJ (2002) In situ XAFS investigation of palladium species present during the Heck reaction in room temperature ionic liquids. *Green Chem* 4:139–142
41. Fernandez F, Cordero B, Durand J, Muller G, Malbosc F, Kihn Y, Teuma E, Gomez M (2007) Palladium catalyzed Suzuki C–C couplings in an ionic liquid: nanoparticles responsible for the catalytic activity. *Dalton Trans* 5572–5581
42. Durand J, Teuma E, Malbosc F, Kihn Y, Gómez M (2008) Palladium nanoparticles immobilized in ionic liquid: an outstanding catalyst for the Suzuki C–C coupling. *Catal Commun* 9:273–275
43. Song H, Yan N, Fei Z, Kilpin KJ, Scopelliti R, Li X, Dyson PJ (2012) Evaluation of ionic liquid soluble imidazolium tetrachloropalladate pre-catalysts in Suzuki coupling reactions. *Catal Today* 183:172–177
44. Prechtl MHG, Scholten JD, Dupont J (2010) Carbon–carbon cross coupling reactions in ionic liquids catalysed by palladium metal nanoparticles. *Molecules* 15:3441–3461
45. Zhao D, Fei Z, Geldbach TJ, Scopelliti R, Dyson PJ (2004) Nitrile-functionalized pyridinium ionic liquids: synthesis, characterization, and their application in carbon–carbon coupling reactions. *J Am Chem Soc* 126:15876–15882
46. Calò V, Nacci A, Monopoli A, Cotugno P (2009) Palladium-nanoparticle-catalysed Ullmann reactions in ionic liquids with aldehydes as the reductants: scope and mechanism. *Chem—Eur J* 15:1272–1279
47. Cheng J, Tang L, Xu J (2010) An economical, green pathway to biaryls: palladium nanoparticles catalyzed Ullmann reaction in ionic liquid/supercritical carbon dioxide system. *Adv Synth Catal* 352:3275–3286
48. Yin L, Liebscher J (2007) Carbon–carbon coupling reactions catalyzed by heterogeneous palladium catalysts. *Chem Rev* 107:133–173
49. Cassol CC, Umpierre AP, Machado G, Wolke SI, Dupont J (2005) The Role of Pd nanoparticles in ionic liquid in the Heck reaction. *J Am Chem Soc* 127:3298–3299
50. Consorti CS, Flores FR, Dupont J (2005) Kinetics and mechanistic aspects of the Heck reaction promoted by a CN–palladacycle. *J Am Chem Soc* 127:12054–12065
51. Fei Z, Zhao D, Pieraccini D, Ang WH, Geldbach TJ, Scopelliti R, Chiappe C, Dyson PJ (2007) Development of nitrile-functionalized ionic liquids for C–C coupling reactions: implication of carbene and nanoparticle catalysts. *Organometallics* 26:1588–1598
52. Dupont J, de Souza RF, Suarez PAZ (2002) Ionic liquid (molten salt) phase organometallic catalysis. *Chem Rev* 102:3667–3691

53. Haumann M, Jakuttis M, Franke R, Schönweiz A, Wasserscheid P (2011) Continuous gas-phase hydroformylation of a highly diluted technical C4 feed using supported ionic liquid phase catalysts. *ChemCatChem* 3:1822–1827
54. Shi F, Zhang Q, Gu Y, Deng Y (2005) Silica gel confined ionic liquid + metal complexes for oxygen-free carbonylation of amines and nitrobenzene to ureas. *Adv Synth Catal* 347:225–230
55. Yinghuai Z, Widjaja E, Pei Sia SL, Zhan W, Carpenter K, Maguire JA, Hosmane NS, Hawthorne MF (2007) Ruthenium(0) nanoparticle-catalyzed isotope exchange between 10B and 11B nuclei in decaborane(14). *J Am Chem Soc* 129:6507–6512
56. Geldbach TJ, Zhao D, Castillo NC, Laurenczy G, Weyershausen B, Dyson PJ (2006) Biphasic hydrosilylation in ionic liquids: a process set for industrial implementation. *J Am Chem Soc* 128:9773–9780
57. Yinghuai Z, Chenyan K, Peng AT, Emi A, Monalisa W, Kui-Jin Louis L, Hosmane NS, Maguire JA (2008) Catalytic phenylborylation reaction by iridium(0) nanoparticles produced from hydrido-iridium carborane. *Inorg Chem* 47:5756–5761
58. Thomas P, Marvey B (2009) C18:1 methyl ester metathesis in [bmim][X] type ionic liquids. *Int J Mol Sci* 10:5020–5030
59. Conte V, Elakkari E, Floris B, Mirruzzo V, Tagliatesta P (2005) The cyclooligomerization of arylethyne in ionic liquids catalysed by ruthenium porphyrins: a case of real catalyst recycling. *Chem Commun* 1587–1588
60. Lin Q, Yang C, Jiang W, Chen H, Li X (2007) Carbonylation of iodobenzene catalyzed by water-soluble palladium–phosphine complexes in ionic liquid. *J Mol Catal A Chem* 264:17–21
61. Mastrolilli P, Nobile CF, Paolillo R, Suranna GP (2004) Catalytic Pauson–Khand reaction in ionic liquids. *J Mol Catal A Chem* 214:103–106
62. Williams DBG, Ajam M, Ranwell A (2007) High rate and highly selective vinyl acetate hydroformylation in ionic liquids as solvent or cosolvent. *Organometallics* 26:4692–4695
63. Klingshirn MA, Rogers RD, Shaughnessy KH (2005) Palladium-catalyzed hydroesterification of styrene derivatives in the presence of ionic liquids. *J Organomet Chem* 690:3620–3626
64. Corma A, García H, Leyva A (2005) Palladium catalyzed cycloisomerization of 2,2-diallylmalonates in imidazolium ionic liquids. *J Organomet Chem* 690:3529–3534
65. Scariot M, Silva DO, Scholten JD, Machado G, Teixeira SR, Novak MA, Ebeling G, Dupont J (2008) Cobalt nanocubes in ionic liquids: synthesis and properties. *Angew Chem Int Ed* 47:9075–9078
66. Xiao C-X, Cai Z-P, Wang T, Kou Y, Yan N (2008) Aqueous-phase Fischer–Tropsch synthesis with a ruthenium nanocluster catalyst. *Angew Chem Int Ed* 47:746–749
67. Xiao Y, Geng S, Hirouyuki A, Tsunehiro T, Xi C, Yuan Y, Gabor L, Yuan K, Paul JD, Yan N (2013) *Chem Eur J* 19:1227–1234
68. Cacchi S, Fabrizi G, Goggiamani A (2004) The palladium-catalyzed hydroarylation of propargylic alcohols in room temperature ionic liquids. *J Mol Catal A Chem* 214:57–64
69. Hubbard CD, Illner P, van Eldik R (2011) Understanding chemical reaction mechanisms in ionic liquids: successes and challenges. *Chem Soc Rev* 40:272–290

Metal Nanoparticle Synthesis in Ionic Liquids

Christoph Janiak

Abstract The synthesis of metal nanoparticles (M-NPs) in ionic liquids (ILs) can start from metals, metal salts, metal complexes, and in particular metal carbonyls and can be carried out by chemical reduction, thermolysis, photochemical, microwave irradiation, sonochemical/ultrasound-induced decomposition, electroreduction, or gas-phase synthesis, including sputtering, plasma/glow-discharge electrolysis, physical vapor deposition, or electron beam and γ -irradiation. Metal carbonyls, $M_x(CO)_y$, are commercially available and elegant precursors because the metal atoms are already in the zerovalent oxidation state for M-NPs so that no reduction is necessary. The thermal decomposition of metal complexes, including metal carbonyls in ILs by microwave irradiation, provides a fast and low-energy access to M-NPs. The reason is an excellent absorption efficiency of ILs for microwave energy due to their high ionic charge, high polarity, and high dielectric constant. Ionic liquids allow for the stabilization of M-NPs without the need of additional stabilizers, surfactants, or capping ligands because of the electrostatic and steric properties inherent to ILs. From the IL dispersion, the M-NPs can be deposited on various surfaces, including graphene derivatives and nanotubes. The formation of intermetallic MM' -nanoalloys in ILs has just begun to be explored. Examples for $M(M')$ -NP/IL dispersions in catalytic reactions (C–C coupling, methanol synthesis, hydrogenation) are noted.

Keywords Catalysis · Ionic liquid · Metal nanoparticle · Stabilization · Synthesis

C. Janiak (✉)

Institut für Anorganische Chemie und Strukturchemie, Heinrich-Heine-Universität Düsseldorf,
Universitätsstrasse 1, D-40225 Düsseldorf, Germany
e-mail: janiak@uni-duesseldorf.de

Contents

1	Introduction	18
2	Ionic Liquids (ILs)	19
3	Metal Nanoparticles and Ionic Liquids	20
4	Synthesis of Metal Nanoparticles in Ionic Liquids	21
4.1	Chemical Reduction	28
4.2	Photochemical Reduction	33
4.3	Sonochemical (Ultrasound) Reduction	34
4.4	Electro(chemical) Reduction	34
4.5	Gas-Phase Synthesis	35
4.6	Metal Nanoparticles from Zerovalent Metal Precursors	38
5	Conclusions	47
	References	48

1 Introduction

Metal nanoparticles (M-NPs) are of interest for new technologies [1]. The terms “nanoparticles,” “nanophase clusters,” “nanocrystals,” and “(nano-)colloids” are often used with a similar connotation. Here we use the word nanoparticles as a generic term. For applications, it is important to synthesize M-NPs with defined size and small-size distribution in a controlled and reproducible manner [2–6]. A chemical “bottom-up” approach prepares M-NPs by reduction of metal salts or the photolytic, sonolytic, or thermal decomposition of metal–organic precursors [7]. The synthesis conditions such as temperature, solvent, and reducing and stabilizing agent can influence the size, size distribution, and shape of metal nanoparticles [8].

Nanoparticles have a high surface-to-bulk atom ratio and a high surface energy which dominates their properties [9]. A high surface area is, for example, beneficial in (heterogeneous) catalysis [10–16]. Therefore, small M-NPs need to be stabilized; otherwise they will combine to thermodynamically favored larger particles via agglomeration (Fig. 1).

Agglomeration of small particles is based on the principles of Ostwald ripening [17, 18] which is a thermodynamically driven spontaneous process and occurs because larger particles are more energetically favored than smaller ones. Coordinatively, unsaturated surface atoms of a particle are in a higher energy state than well-ordered and fully coordinated atoms in the bulk. The lower the surface area with respect to the bulk volume, the lower the energy state of a particle. A small metal nanoparticle tries to lower its overall energy by detaching atoms from the surface. The atoms then diffuse through the solution and attach to the surface of a larger particle. Thereby, larger particles grow at the expense of smaller particles (Fig. 2).

Small metal nanoparticles can be stabilized by coordination of surface capping ligands, polymers, or surfactants which form a protective electrostatic and/or steric layer to prevent agglomeration (Fig. 1) [19–22]. Metal nanoparticles in ionic liquids (ILs) do not require additional stabilizers. The electrostatic and steric properties of

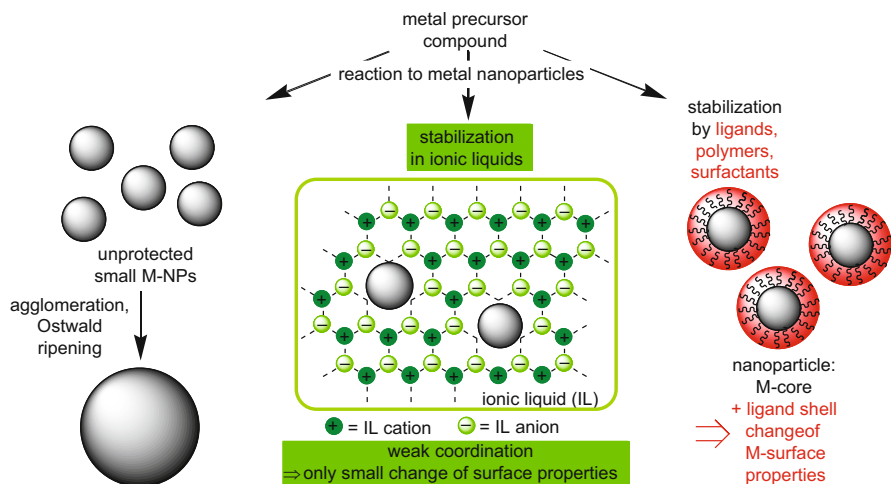


Fig. 1 Metal nanoparticles (M-NP) will agglomerate to larger particles (*left*) unless prevented by electronic and steric stabilization in ionic liquids (*middle*) or through protective stabilizers (*right*)

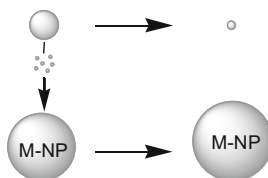


Fig. 2 Schematic presentation of Ostwald ripening

ionic liquids can stabilize M-NPs without capping ligands, polymers, or surfactants (Fig. 1). ILs stabilize metal nanoparticles through their ionic nature [23], high polarity, high dielectric constant, and supramolecular network (cf. Fig. 4) [24–31].

2 Ionic Liquids (ILs)

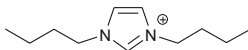
By definition, ionic liquids are salts with a melting point below 100°C. Typically, ILs are even liquid at room temperature (RT-ILs). For this, they consist of conformationally flexible and weakly coordinating inorganic or organic cations and anions with small lattice enthalpies so that the liquid state is thermodynamically favored [32–36]. Examples of nonfunctionalized IL cations and anions are shown in Fig. 3, and functionalized IL cations in Fig. 5 [12, 43]. ILs have a high charge density, high polarity, and high dielectric constant and form a supramolecular network [28]. Ionic liquids (ILs) have become interesting alternatives to traditional aqueous or organic solvents [44, 45]. Over the last years, they have

Cations:

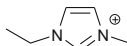
[BMIm]⁺ = 1-*n*-butyl-3-methyl-imidazolium ([BMI]⁺, [C₄mim]⁺)



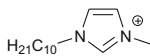
[BBIm]⁺ = 1,3-di-*n*-butyl-imidazolium



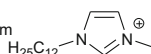
[EMIm]⁺ = 1-ethyl-3-methyl-imidazolium



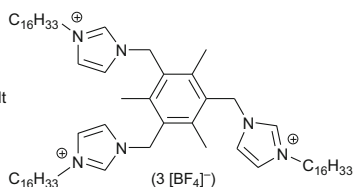
[C₁₀MIm]⁺ = 1-*n*-decyl-3-methylimidazolium



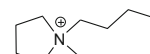
[C₁₂MIm]⁺ = 1-*n*-dodecyl-3-methyl-imidazolium



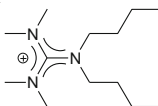
[tris-Im]⁺ = tris-imidazolium salt



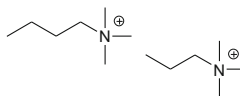
[BMPy]⁺ = 1-butyl-1-methyl-pyrrolidinium



[Guan]⁺ = 1,1-dibutyl-2,2,3,3-tetramethyl-guanidinium



[BTMA]⁺ = *n*-butyl-tri-methyl-ammonium



[Me₃PrN]⁺ = trimethyl-*n*-propyl-ammonium



[TBA]⁺ = tetra-*n*-butyl-ammonium, ^{*n*}Bu₄N⁺

[TBP]⁺ = tetra-*n*-butyl-phosphonium, ^{*n*}Bu₄P⁺

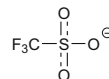
Anions:

Chloride, Cl⁻

tetrafluoroborat, [BF₄]⁻

hexafluorophosphate, [PF₆]⁻

trifluoromethylsulfonate, triflate, [TfO]⁻
(trifluoromethanesulfonate) (TfMS)

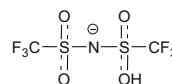


ethylsulfate (ES), EtSO₄⁻

methylsulfonate (MS), MeSO₃⁻

trifluoroacetate, [TFA]⁻, F₃C-CO₂⁻

bis(trifluoromethylsulfonyl)amide, [Tf₂N]⁻
(*N*-bis(trifluoromethanesulfonyl)imide)
(TFSA)



[citrate]⁻ =



Fig. 3 Cations and anions of nonfunctionalized ILs. For functionalized IL cations see Fig. 5. The abbreviations given in the literature vary

been introduced into solution chemistry and intensively investigated as a new liquid medium [46, 47].

3 Metal Nanoparticles and Ionic Liquids

The preparation of advanced functional materials, including metal nanoparticles, in ILs through ionothermal synthesis, appears highly promising [14, 25, 48–55]. Nanoparticles and ionic liquids go more and more together for materials chemistry [27, 56]. ILs have excellent solvent properties, such as negligible vapor pressure, high thermal stability, high ionic conductivity, a broad liquid-state temperature

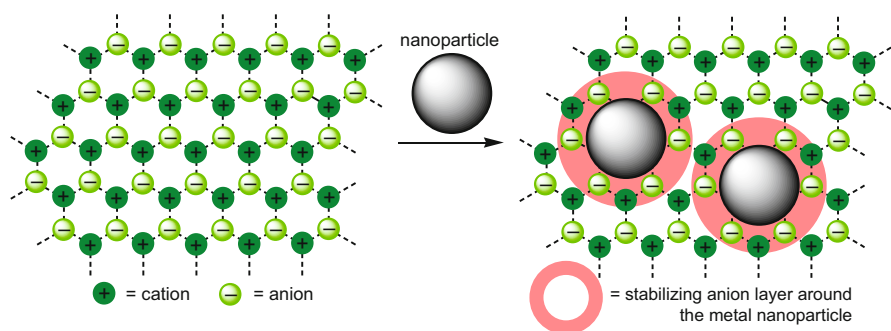


Fig. 4 Schematic network structure in ionic liquids and metal nanoparticles in the IL network. Formation of an anion layer around the M-NPs is suggested for the *electrostatic* and *steric* (= *electrosteric*) stabilization

range, and the ability to dissolve a variety of materials [57, 58]. The combination of undirected Coulomb forces and directed hydrogen bonds leads to a high attraction of the IL building units. This induces the (high) viscosity, negligible vapor pressure, and three-dimensional network in ILs. Figure 4 suggests how the IL network could provide the needed *electrostatic* and *steric* (= *electrosteric*) stabilization through the formation of an ion layer around metal nanoparticles [24, 26, 27]. The type of this ion layer, IL-anion or IL-cation, is still a matter of some discussion [27, 37].

ILs provide an electrostatic protection for M-NPs according to DLVO (Derjaguin–Landau–Verwey–Overbeek) theory [59–65] which predicts that the IL-anions should be the primary source of stabilization for the electrophilic metal nanoparticles [59].

Thiol- [38–40], ether- [41], carboxylic acid- [37], amino- [37, 42], hydroxyl- [39, 66, 67], or nitrile- [68–70] functionalized imidazolium cations can stabilize metal NPs even more efficiently through the added functional group (Fig. 5). The OH-functionalized IL [HOEMIm][Tf₂N] gave smaller Pd-NPs with diameter 4.0 ± 0.6 nm compared with Pd-NPs isolated from the nonfunctionalized IL [BMIm][Tf₂N] with diameter 6.2 ± 1.1 nm (cf. Table 1) [67]. The donor atom of the functional group on the cation can attach to the metal nanoparticle like a stabilizing capping ligand possibly together with parallel coordination of the imidazolium plane (Fig. 6) [17, 37, 41, 111–113].

4 Synthesis of Metal Nanoparticles in Ionic Liquids

Metal nanoparticles are obtained in ionic liquids from metal salts by either one of the following ways [114]: (1) chemical reduction [71, 76, 78, 79, 81, 104, 115–118], (2) photochemical reduction [119, 120], or (3) electroreduction/electrodeposition [121–123]. Compounds with zerovalent metal atoms, such as metal carbonyls

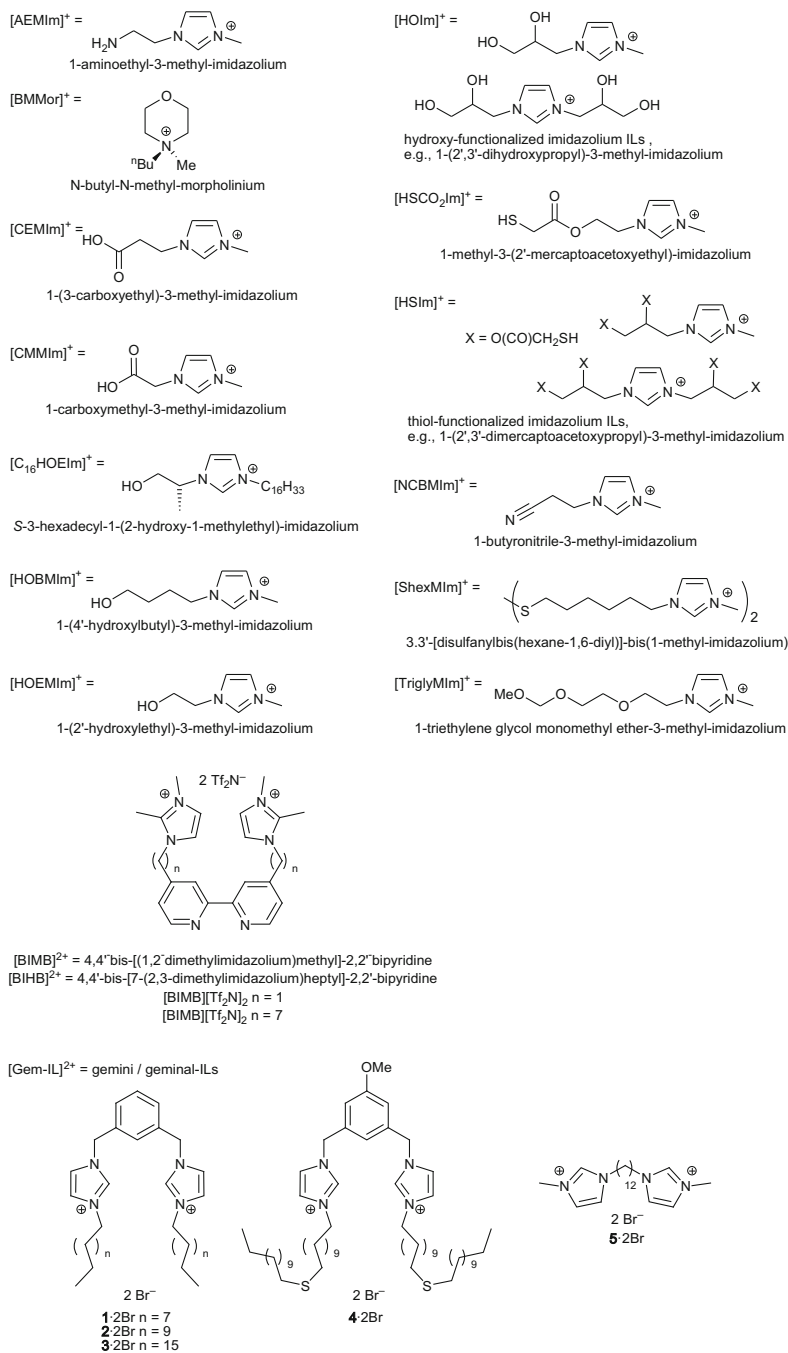


Fig. 5 Examples of functionalized imidazolium cations [37–42]

Table 1 M-NPs prepared by chemical reduction in ILs*

Metal	Metal salt precursor	Reducing agent	Ionic liquid ^a	M-NP average diameter \pm standard deviation (nm)	References
<i>Monometallic, group 9 (Rh, Ir)</i>					
Rh	RhCl ₃ ·3H ₂ O	H ₂ , 75°C and 4 bar	[BMIm][PF ₆]	2.0–2.5	[71]
	[Rh(COD)- μ -Cl] ₂ ^b	H ₂ + laser radiation	[BMIm][PF ₆]	7.2 \pm 1.3	[72]
	RhCl ₃	NaBH ₄	[BMIm][Tf ₂ N]/[BIMB][Tf ₂ N] ₂ or [BIHB][Tf ₂ N] ₂	1–3	[73]
Ir	[Ir(COD)Cl] ₂ ^b	H ₂ , 75°C, and 4 bar	[BMIm][BF ₄], [BMIm][PF ₆], [BMIm][TfO ⁻]	2–3	[74, 75]
	[Ir(COD) ₂ BF ₄], [Ir(COD)Cl] ₂ ^b	H ₂	[1-alkyl-3-methyl-im][BF ₄]	Irregular 1.9 \pm 0.4, 3.6 \pm 0.9	[76]
<i>Group 10 (Pd, Pt)</i>					
Pd	H ₂ PdCl ₄	NaBH ₄	[HSCO ₂ Im][Cl]	Nanowires	[40]
	H ₂ PdCl ₄	NaBH ₄	[Guan][Br]/Vulcan-72 carbon	~2.8	[77]
	PdCl ₂	H ₂ + laser radiation	[BMIm][PF ₆]	4.2 \pm 0.8	[72]
	Pd(acac) ₂	H ₂	[BMIm][PF ₆]	10 \pm 0.2	[78]
	Pd(acac) ₂	Imidazolium ILs, thermal, see text	[BMIm][PF ₆], [HOBMIm][Tf ₂ N]	5, 10, catalysts for selected acetylene hydrogenation	[78]
	Pd(OAc) ₂ or PdCl ₂	Imidazolium ILs, ultrasound, see text	[BBIm][Br], [BBIm][BF ₄]	20, catalyst for Heck reactions	[79, 80]
	Pd(OAc) ₂	[BMIm][Tf ₂ N], thermal	[BMIm][Tf ₂ N]/PPh ₃	~1, catalyst for Heck reactions	[80, 81]
Pd(OAc) ₂		Imidazolium ILs, thermal, see text	[HOEMIm][TfO]	2.4 \pm 0.5	[67]
			[HOEMIm][TFA]	2.3 \pm 0.4	
			[HOEMIm][BF ₄]	3.3 \pm 0.6	
			[HOEMIm][PF ₆]	3.1 \pm 0.7	
			[HOEMIm][Tf ₂ N]	4.0 \pm 0.6	
	[BMIm][Tf ₂ N]		6.2 \pm 1.1		

(continued)

Table 1 (continued)

Metal	Metal salt precursor	Reducing agent	Ionic liquid ^a	M-NP average diameter \pm standard deviation (nm)	References
Pt	Pd(OAc) ₂		[TBA][Br]/[TBA][OAc]	3.3 \pm 1.2, catalyst for Heck arylations	[80, 82, 83]
	Pd(OAc) ₂		[BtMA][Tf ₂ N]	Catalyst for Heck cross-coupling	[80, 84]
	Pd(OAc) ₂	Imidazolium IL, thermal, see text	[NCBMIm][Tf ₂ N]	7.3 \pm 2.2	[85]
	Pd ₂ (dba) ₃ ^c	H ₂ , 3 atm	[tris-Im][BF ₄], see Fig. 3	Catalyst for Suzuki cross-coupling	[80, 86]
	Bis(benzothiazolylidene carbene)PdI ₂		[TBA][Br]/[TBA][OAc]	Catalyst for Heck arylations	[82]
	Na ₂ Pt(OH) ₆	NaBH ₄	[HSIm][A] or [HOIm][A], A = Cl ⁻ or HS-(CH ₂) ₃ -SO ₃ ⁻	3.2 \pm 1.1, 2.2 \pm 0.2, 2.0 \pm 0.1	[39]
	H ₂ PtCl ₆	NaBH ₄	[CMMIm][Cl], [AEMIm][Br]	2.5	[37]
	PtO ₂	H ₂	[BMIm][BF ₄], [BMIm][PF ₆]	2–3	[87]
	Pt ₂ (dba) ₃ ^c	H ₂ , 75°C, 4 atm	[BMIm][PF ₆]	2.0–2.5	[88]
	(MeCp)PtMe ₃	Imidazolium ILs, MWI, hv, thermal, see text	[BMIm][BF ₄], [BtMA][Tf ₂ N]	1.5 \pm 0.5, see text; catalyst for hydrosilylation	[89]
<i>Group 11 (Cu, Ag, Au)</i>					
Cu	Cu(OAc) ₂ ·H ₂ O	H ₂ NNH ₂ ·H ₂ O (hydrate)	[BMIm][BF ₄]	Spherical; PVP, 80–130; PVA, 260	[90]
			[BMIm][PF ₆]	Cubic, PVP: 160 \pm 14; catalyst in click reaction	
			Each w. 1% PVP or PVA as stabilizer ^d		
	Cu(I)-amidinate, {[MeC(N ⁺ Pr) ₂]Cu} ₂	Imidazolium IL, thermal, see text	[BMIm][BF ₄]	11 \pm 6	[189]

Ag	AgBF ₄	H ₂ , 85°C, 4 atm	[BMIm][BF ₄]	2.8 ± 0.8	[91]
		BIm as scavenger, see text	[BMIm][PF ₆] [BMIm][TfO] [BTMA][Tf ₂ N] [BMIm][BF ₄]	4.4 ± 1.3 8.7 ± 3.4 26.1 ± 6.4	
	AgBF ₄	H ₂	[BMPy][TfO] with TX-100/ cyclohexane as reverse micellar system	~9 (DLS) ~11 (DLS), both ~3 from TEM	[92]
	AgBF ₄	[BMIm][BH ₄], 1-MeIm as scavenger	[BMIm][Tf ₂ N] in microfluidic reactor	3.73 ± 0.77	[93]
	Ag ₂ CO ₃	Me ₂ NCHO (DMF)	[Me ₂ NH ₂][Me ₂ NCO ₂] with small amounts of DMF	2–14	[94]
Au	AgNO ₃	Tween 85	[BMIm][PF ₆]	3–10	[95]
	HAuCl ₄	Na ₃ citrate/NaBH ₄ , Na ₃ citrate, ascorbic acid	[EMIm][EtSO ₄]	9.4 3.9 nanorods	[96]
	HAuCl ₄	Ascorbic acid	[BMIm][C ₁₂ H ₂₅ OSO ₃] (lauryl sulfate)	20–50	[97]
	HAuCl ₄	Na ₃ citrate	[CMMIm][Cl], [AEMIm][Br]	23–98	[37]
	HAuCl ₄ ·3H ₂ O	H ₂ NNH ₂ ·H ₂ O (hydrate) zinc monohydrate)	[TriglyMIm][MeSO ₃]	~7.5	[41]
	HAuCl ₄	NaBH ₄	[ShexMIm][Cl]	5.0	[38]
	HAuCl ₄	NaBH ₄	[HSIm][A] or [HOIm][A], A = Cl ⁻ or HS-(CH ₂) ₃ -SO ₃ ⁻	3.5 ± 0.7, 3.1 ± 0.5, 2.0 ± 0.1	[39]
	HAuCl ₄	NaBH ₄	[CMMIm][Cl], [AEMIm][Br]	3.5	[37]
	HAuCl ₄ [C ₁₆ HOEIm]/AuCl ₄ from [C ₁₆ HOEIm]Br and HAuCl ₄	NaBH ₄	CHCl ₃ /H ₂ O, [C ₁₆ HOEIm][Br]	6.0 ± 1.4	[98]

(continued)

Table 1 (continued)

Metal	Metal salt precursor	Reducing agent	Ionic liquid ^a	M-NP average diameter \pm standard deviation (nm)	References
	HAuCl ₄	NaBH ₄	[Gem-IL][Br] ₂ 1-2Br to 4-2Br, see Fig. 5	3: 8.8 \pm 2.2 4: 5.3 \pm 2.4	[99]
	HAuCl ₄	NaBH ₄	[BMIm][BF ₄] in microfluidic reactor	4.38 \pm 0.53	[100]
	HAuCl ₄	NaBH ₄	[BMIm][PF ₆]	4.8 \pm 0.7 (5.3 \pm 0.8 after 2 weeks)	[101]
	HAuCl ₄	NaBH ₄	[BMIm][PF ₆]/[AEMIm][PF ₆]	4.3 \pm 0.8	[101]
	HAuCl ₄	NaBH ₄	[C ₁₂ MIm][Br]	8.2 \pm 3.5, stable for at least 8 months	[102]
	HAuCl ₄	NaBH ₄	[Gem-IL][Br] ₂ 5-2Br, see Fig. 5	10.1 \pm 4.2	[102]
	HAuCl ₄	[BMIm][BH ₄], 1-MeIm as scavenger	[BMIm][Tf ₂ N] in microfluidic reactor	4.28 \pm 0.84	[93]
	HAuCl ₄ ·3H ₂ O	NaBH ₄ , cellulose	[BMIm][Cl]	9.7 \pm 2.7	[103]
	HAuCl ₄	Cellulose, see text	[BMIm][Cl]	300–800	[104]
	HAuCl ₄ ·3H ₂ O	Glycerol	[EMIm][TfO], [EMIm][MeSO ₃], [EMIm][EtSO ₄]	5–7, low temperature 5–7, aggregate at higher temperature	[105]
	HAuBr ₄	Me ₂ NCHO (DMF)	[Me ₂ NH ₂][Me ₂ NCO ₂] with small amounts of DMF	15–20, polydisperse 2–4	[94]
	Au(CO)Cl	Imidazolium ILs, thermal, MWI, hv, see text	[BMIm][BF ₄]	1.8 \pm 0.4, 4.1 \pm 0.7	[106]
	KAuCl ₄	[BMIm][BF ₄] thermal, see text	[BMIm][BF ₄]	1.1 \pm 0.2	[106]

HAuCl ₄ · 4H ₂ O	[Me ₃ NC ₂ H ₄ OH] [Zn _n Cl _{2n+1}], thermal	[Me ₃ NC ₂ H ₄ OH] [Zn _n Cl _{2n+1}]	135°C: 35 ± 12, 140°C: 30 ± 4, 145°C: 24 ± 3	[107]
HAuCl ₄ · 3H ₂ O,	[BMIm][BF ₄], ultra- sound, see text	[BMIm][BF ₄]/MWCNT ^e	10.3 ± 1.5	[108]
KAuCl ₄	SnCl ₂	[BMIm][BF ₄]	2.6–200	[109]
AuCl ₃ · 3H ₂ O	[TBP][citrate]	[TBP][citrate]	15–20	[110]
Zn(II)-amidinate, [Me(C(N ⁱ Pr) ₂] ₂ Zn	Imidazolium IL, ther- mal, see text	[BMIm][BF ₄]	3 ± 6	[189]
<i>Bimetallic</i>				
Pd-Au 3:1	K ₂ PdCl ₄ , HAuCl ₄	[BMIm][PF ₆]	5.3 ± 3.0	[101]
β-CuZn or γ-Cu ₃ Zn	Cu(I)- and Zn(II)- amidinate, {[Me(C (N ⁱ Pr) ₂] ₂ Cu] ₂ , [Me(C(N ⁱ Pr) ₂] ₂ Zn	[BMIm][PF ₆] [BMIm][PF ₆]/[AEMIm][PF ₆] [BMIm][BF ₄]	3.6 ± 0.7 β-CuZn: 51 ± 29, pre-catalyst for MeOH formation from syngas, γ-Cu ₃ Zn: 48 ± 12	[101] [189]

*This Table is largely reprinted from Z. Naturforsch., 2013, 68b, 1059–1089. Copyright Verlag der Zeitschrift für Naturforschung, Tübingen 2013

^aFor nonfunctionalized ILs, see Fig. 3; for functionalized ILs, see Fig. 5

^bCOD 1,5-cyclooctadiene, COT 1,3,5-cyclooctatriene

^c*dba* bis-dibenzylidene acetone

^dPVP polyvinyl pyrrolidone, PVA polyvinyl alcohol

^eMWCNT multiwalled carbon nanotube

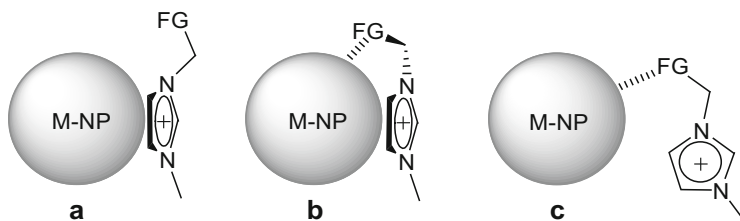


Fig. 6 Possible coordination modes of imidazolium cations with functional groups (FG) to metal nanoparticles [111]

$M_x(CO)_y$ [24, 117, 124, 125] or $[Ru(COD)(COT)]$ (see Sect. 4.6) [91, 126], give metal nanoparticles by thermal, photolytic, or chemical decomposition. Extra stabilizing molecules or organic solvents are not needed in ILs but are added in some cases [19, 24, 27, 65, 127].

4.1 Chemical Reduction

Table 1 compiles metal nanoparticles which have been obtained from the reduction of metal salts and complexes in ionic liquids. Frequent reducing agents are H_2 gas, sodium citrate, ascorbic acid, and imidazolium cations of ILs, $NaBH_4$, or $SnCl_2$.

The synthesis of M-NPs by reduction is carried out in batch reactions using glass flasks, but also microfluidic reactors have been reported for the fabrication of metal nanoparticles of cobalt, copper, platinum, palladium, gold, silver, and core-shell particles [93].

Noble metal nanoparticles, such as Pd- or Ir-NPs, can be synthesized in the presence of imidazolium ILs from metal salts without an added reducing agent [78, 81, 85, 128]. Pd-*N*-heterocyclic carbene complexes may form as intermediates preceding the formation of Pd-NPs (Fig. 7) [79, 80, 128]. Imidazolium salts are precursors for stable carbenes and mild reducing agents [129].

Thermal reduction/decomposition of $Pd(OAc)_2$ to black Pd-NP dispersion in hydroxyl-functionalized ILs with the 1-(2'-hydroxyethyl)-3-methylimidazolium $[HOEMIm]^+$ cation and nonfunctionalized control IL argued against the alcohol group in the $[HOEMIm]^+$ cation as reductant according to unchanged 1H NMR spectra [67]. The influence of anions on the decomposition rate of $Pd(OAc)_2$ was given in the order $[Tf_2N]^- > [PF_6]^- > [BF_4]^- > [OTf]^- > [TFA]^-$.

Decomposition of the organometallic Pt(IV) precursor $(MeCp)PtMe_3$ in the ILs $[BMIm][BF_4]$ and $[BtMA][Tf_2N]$ also does not require a separate reductant and leads to small, crystalline, and longtime stable Pt-nanoparticle (Pt-NP) dispersions (Fig. 8) [89].

The salt $AgBF_4$ can be reduced with H_2 in *n*-butyl-methyl-imidazolium ionic liquids with different anions to yield Ag-NPs which increase in size with the size of

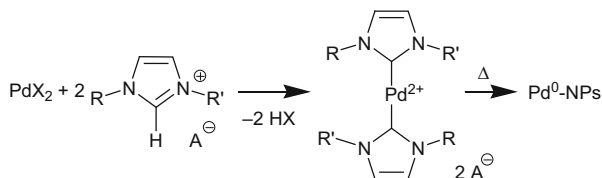


Fig. 7 Pd-carbene formation with imidazolium IL as an intermediate to Pd-NPs [80]

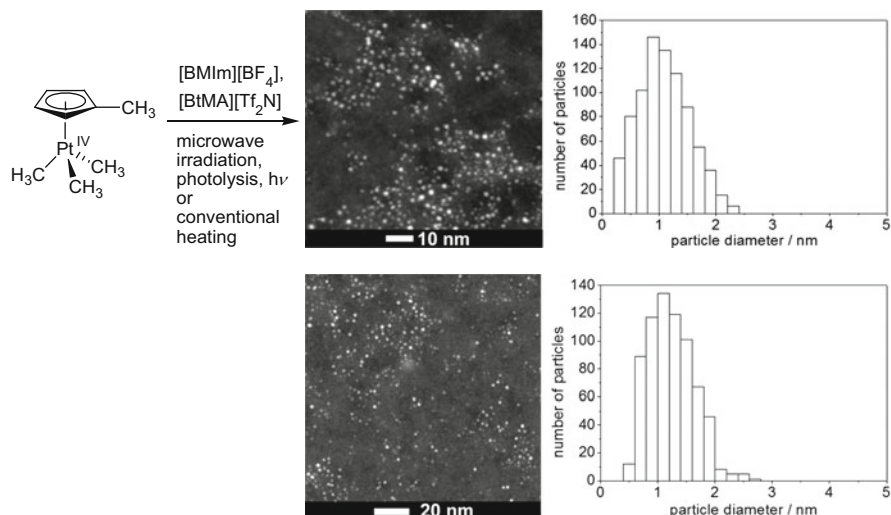


Fig. 8 Decomposition of the air and moisture stable organometallic Pt(IV) precursor (MeCp) PtMe₃ in ILs to well-defined, small, crystalline, and longtime (>10 months) stable Pt-nanocrystals without any additional reducing agents. High-angle annular dark-field-scanning transmission electron microscopy (HAADF-STEM) images with particle diameter distributions in histograms, *top row*: freshly prepared sample with NP diameter distribution $\bar{\phi} 1.1 \pm 0.5$ nm, based on 703 particles; *bottom row*: sample after 331 days, $\bar{\phi} 1.2 \pm 0.4$ nm, based on 518 particles [89]. Reprinted from [89] with permission from the author; © 2012 The Royal Society of Chemistry

the ionic liquid anion (Fig. 9). The acidic HBF₄ side product needs to be scavenged with a base in order not to perturb the ionic liquid matrix. N-Butylimidazole (BIm) was the base of choice because it gave a [BHIm]⁺ cation which closely resembled the [BMIm]⁺ cation (Fig. 9) [115].

Gold nanoparticles are among the best-studied particles in nano- and materials science due to their electronic, optical, thermal, and catalytic properties associated with possible applications in the fields of physics, chemistry, biology, medicine, and materials science [130]. Au-NPs can be reduced from gold salts, e.g., KAuCl₄ or auric acid, HAuCl₄, by citrate which in addition acts as a coordinating ligand (Turkevich route) [131]. This reduction could also be carried out in the IL 1-ethyl-3-methylimidazolium ethyl sulfate [EMIm][EtSO₄] and the Au-NP shape adjusted

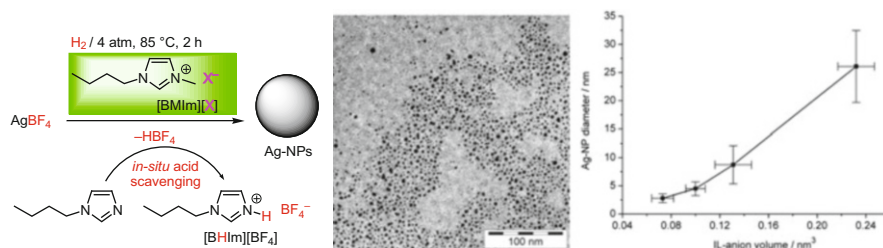


Fig. 9 Formation of Ag-NPs by hydrogen reduction of AgBF_4 with an imidazole scavenging process in $[\text{BMIm}][\text{X}]$. The TEM image shows the Ag-NPs in $[\text{BMIm}][\text{BF}_4]$ ($\text{Ø } 2.8 \pm 0.8 \text{ nm}$). The Ag particle size increases with the size of the X^- anion from $\text{BF}_4^- < \text{PF}_6^- < \text{TfO}^- < \text{Tf}_2\text{N}^-$ [115]. TEM reprinted from [115] with permission from the author; © 2008 American Chemical Society

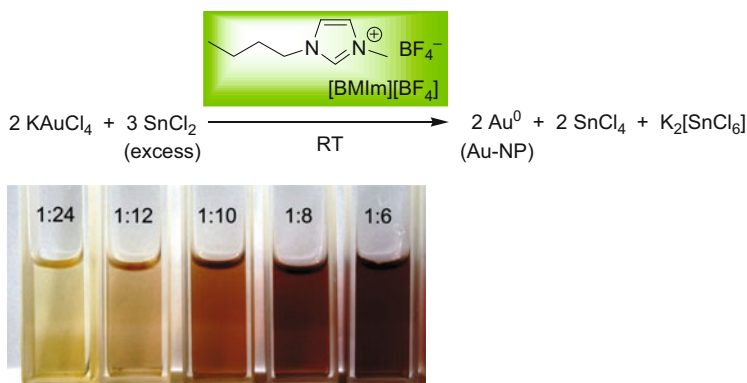


Fig. 10 Selected colors with given molar Au: Sn ratios during the step-by-step Au-NP growth process. The color change represents the transition of Au-NPs from nonmetallic (*white/yellow*) to metallic and crystalline (*red and purple*) particles. Because of the weakly coordinating nature of the IL, the gold nanoparticle growth can be stopped and resumed here reproducibly by the controlled dropwise addition of a KAuCl_4 solution to a mixture of SnCl_2/IL at every different color step, which is size dependent for Au-NPs. Such a stop-and-go nanoparticle growth would not be possible in the presence of strongly coordinating capping ligands [109]. Cuvette picture reprinted from [109] with permission from the author; © 2010 The Royal Society of Chemistry

by addition of a silver salt [96]. Cellulose is a reductant, morphology- and size-directing agent for Au-NPs from HAuCl_4 so that gold nano-plates with a thickness from 300 nm at 110°C to 800 nm at 200°C were synthesized [104]. Variation of the molar Au(III):Sn(II) ratio gave Au-NPs in different sizes in a stepwise, stop-and-go nucleation, nanocrystal growth process. The Au-NP growth could be stopped and resumed at different color steps and sizes from 2.6 to 200 nm (Fig. 10) [109].

Gold nanoparticles are obtained from $\text{Au}(\text{CO})\text{Cl}$ or KAuCl_4 in imidazolium ILs without an added reducing agent. The reductive thermal, photolytic, or microwave-assisted decomposition was carried out in the presence of *n*-butyl-imidazole as a scavenger (Fig. 11). The nanoparticles of about 1–2 nm diameter in $[\text{BMIm}][\text{BF}_4]$

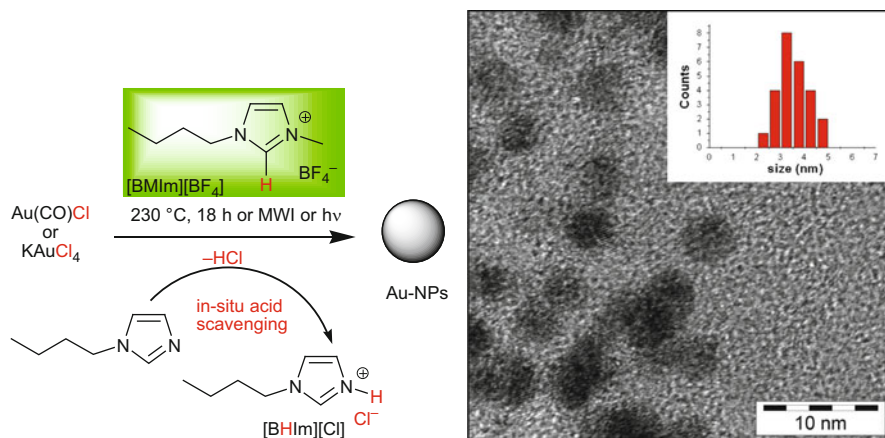


Fig. 11 Formation of Au-NPs (\AA 3.6 ± 0.6 nm from Au(CO)Cl in thermal process) with the imidazole scavenging process in [BMIm][BF₄] (cf. Fig. 9). The TEM picture shows the nanoparticles after 6 weeks of exposure to air [106]. The decomposition of Au(CO)Cl can also proceed by intramolecular reduction under phosgene formation according to $2 \text{ Au(CO)Cl} \rightarrow 2 \text{ Au} + \text{CO} + \text{COCl}_2$ [132]. TEM reprinted from [106] with permission from the author; © 2009 Wiley-VCH

increase in size with the ionic liquid anion in [BMIm][TfO] and [BtMA][Tf₂N] [106].

Small Au-NPs of diameter 1.1 ± 0.2 nm which are formed without any capping ligands or surfactants in the IL [BMIm][BF₄] can be selectively reduced or oxidized (quantized charged). A theoretical density functional theory calculation suggests that the positive or negative cluster charging is accompanied by a switching in the orientation of the ionic shell from anion to cation [133].

NaAuCl₄ and KAuC_N₂ were reduced in [BMIm][PF₆] to gold nanoparticles which were catalysts for the cyclopropanation of alkenes with ethyldiazoacetate to yield cyclopropanecarboxylates. In the IL, the stabilized gold catalysts could be separated and recycled [134].

Carboxylic acid- and amino-functionalized ionic liquids [CMMIm][Cl] and [AEMIm][Br] (cf. Fig. 5) stabilized gold and platinum nanoparticles in an aqueous solution. Smaller Au-NPs (3.5 nm) and Pt-NPs (2.5 nm) were prepared with NaBH₄ as reducing agent. Larger gold nanospheres (23, 42, and 98 nm) were synthesized with trisodium citrate. Simultaneous interactions between imidazolium ions and its functional groups and the metal atoms were proposed for the M-NP stabilization (cf. Fig. 6). The metal nanoparticles could be assembled on multiwalled carbon nanotubes. The imidazolium ring moiety of the ionic liquids might interact with the nanotube π -surface and the functional group with the M-NPs surface (cf. Fig. 6c) [37].

The microwave-induced decomposition of the transition metal amidinates $\{\text{[Me(C(N}^i\text{Pr)}_2\text{)]Cu}\}_2$ and $\{\text{[Me(C(N}^i\text{Pr)}_2\text{)]}_2\text{Zn}\}$ in [BMIm][BF₄] gives copper and zinc nanoparticles which are stable in the absence of capping ligands (surfactants)

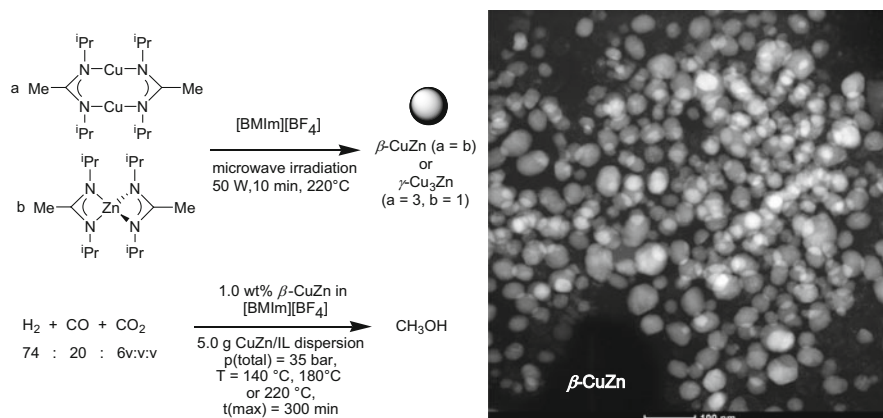


Fig. 12 Microwave-assisted thermal co-decomposition of copper and zinc amidinates to mono-metallic (not shown) and bimetallic Cu/Zn-NPs in IL. The high-angle annular dark-field-scanning TEM (HAADF-STEM) image of a 1.0 wt% β -CuZn dispersion in IL gave a median diameter of 51 ± 29 nm. The β -CuZn/IL dispersion could be employed as precursor for the conversion of syngas to methanol without any catalyst deactivation up to 300 min (5 h) at different temperatures

for more than 6 weeks [189]. Co-decomposition of the two amidinates selectively yields the intermetallic nano-brass phases β -CuZn and γ -Cu₃Zn depending on the chosen molar ratios of the precursors. The bimetallic β -CuZn nanoparticles were precursors to active catalysts for methanol synthesis from synthesis gas $\text{H}_2/\text{CO}/\text{CO}_2$ with a productivity of 10.7 mol(MeOH)/(kg(Cu)-h) (Fig. 12). STEM investigation of the CuZn/[BMIm][BF₄] dispersion after catalytic methanol formation still showed particles in the 50 nm diameter range as before the catalysis. These particles had a high Cu content by energy-dispersive X-ray spectroscopy (EDX). The regions around the particles were amorphous and contained mostly ZnO according to EDX. Also powder X-ray diffraction of the separated particles revealed that only a fraction of the original β -CuZn phase remained with the rest having turned into crystalline Cu-NPs and amorphous ZnO [189].

From ILs metal nanoparticles can also be deposited onto a support.

Rhodium-NPs (<5 nm) on attapulgite (Rh-Atta) were prepared by reducing immobilized Rh^{3+} on Atta in the IL 1,1,3,3-tetramethylguanidinium lactate. Cyclohexene hydrogenation activity of the Rh-Atta composite was much higher than other catalysts with turnover frequencies reaching 2,700 (mol cyclohexene/mol Rh)/h [135]. Uniform Pd nanoparticles on Vulcan XC-72 carbon were synthesized from H_2PdCl_4 and NaBH_4 using G-IL as medium [77].

Hybrids of Au-NP-decorated multiwalled carbon nanotubes (Au-MWCNT) onto poly(ethylene terephthalate) (PET) films were prepared by a sonochemical method from $\text{HAuCl}_4 \cdot 3\text{H}_2\text{O}$ and MWCNT in [BMIm][BF₄] [108]. Au-NPs can also be deposited onto a polytetrafluoroethylene (PTFE, Teflon) surface [106]. Poly(vinylpyrrolidone) (PVP)-stabilized Au-NPs were encapsulated into titania

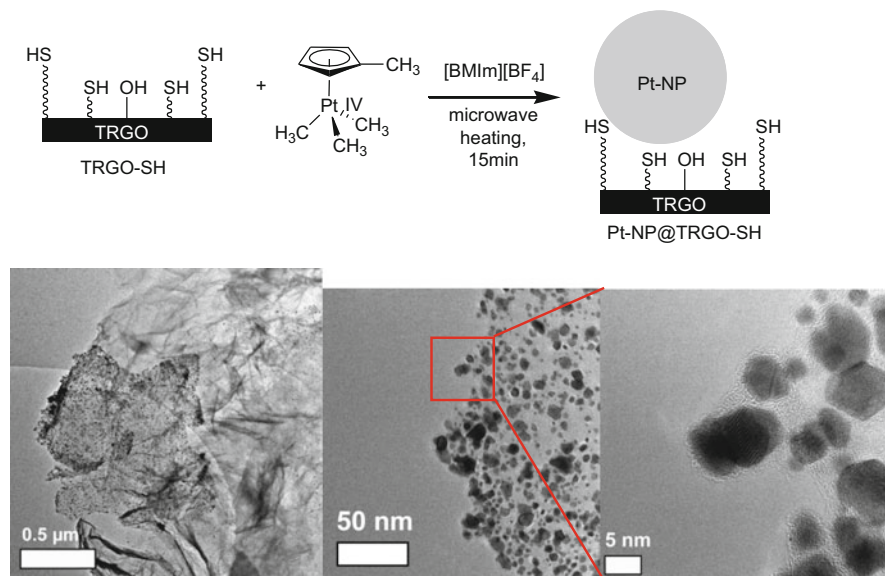


Fig. 13 Schematic presentation of the formation of Pt@TRGO-SH hybrid materials in IL with three magnifications of TEM images. The Pt-NP loading is 3.2 wt% with a median particle diameter of 9 ± 4 nm. Reprinted from [137] with permission from the author; © 2014 Elsevier B.V

xerogels with [BMIm][PF₆] as medium. Then the IL was removed by solvent extraction and the PVP calcinated. The average Au-NP diameter was 8.8 ± 2.5 nm after calcination [136].

Hybrid materials of platinum nanoparticles and thiol-functionalized thermally reduced graphite oxide (TRGO-SH) were synthesized by thermal decomposition of the organometallic precursor (MeCp)PtMe₃ in dispersions of TRGO-SH in [BMIm][BF₄] under microwave heating conditions (Fig. 13) [137]. Thiol groups on TRGO assist the deposition of Pt-NPs through a possible dual role of anchor groups and nucleation centers. The IL also helps to exfoliate and separate the graphene sheets in order to increase the surface area and accessibility for deposition of Pt-NPs [137].

4.2 Photochemical Reduction

UV photolysis of (MeCp)PtMe₃ in [BMIm][BF₄] and [BtMA][Tf₂N] yielded Pt-NPs of 1.1 ± 0.5 nm diameter (1 day old) or 1.2 ± 0.4 nm (aged 331 days) (Fig. 8). Complete decomposition was verified by ¹H-NMR spectroscopy through the absence of the characteristic signals from the Pt-Me groups of (MeCp)PtMe₃ [89].

Irradiation of AgClO_4 with a high-pressure mercury lamp in a mixture of an IL, water, Tween 20 (polyoxyethylene sorbitan monolaurate), and benzoin as photo-activator gave Ag-NPs with average diameters of 8.9 and 4.9 nm in water/[BMIm][BF_4] and water/[OMIm][BF_4] (1-octyl-3-methylimidazolium) microemulsions, respectively [138].

UV irradiation of $\text{HAuCl}_4 \cdot 4\text{H}_2\text{O}$ in a [BMIm][BF_4]/acetone mixture (ratio 10:1) turned the acetone into a free radical which reduced Au(III) to Au nanosheets of about 4 μm length and 60 nm thickness [119]. UV irradiation of HAuCl_4 in 1-decyl-3-methyl-imidazolium chloride/water gave differently shaped nanorods with lengths between 100 and 1,000 nm [120]. Photolysis of $\text{Au}(\text{CO})\text{Cl}$ in [BMIm][BF_4] (cf. Fig. 11) yielded Au-NPs with large diameters of 61 ± 43 nm [106].

4.3 Sonochemical (Ultrasound) Reduction

Ultrasound irradiation of $\text{Pd}(\text{OAc})_2$ or PdCl_2 in [BBIm][Br] or [BBIm][BF_4] for 1 h yielded nearly spherical Pd-NPs with a diameter of 20 nm. The formation of a Pd–biscarbene intermediate and its subsequent sonolytic conversion to Pd nanoparticles (cf. Fig. 7) was established by NMR/MS and TEM analyses [79].

Au-NP-decorated MWCNT-hybrids were prepared by the ionic liquid-assisted sonication onto PET films. Sonication of a $\text{HAuCl}_4 \cdot 3\text{H}_2\text{O}$, MWCNT, and [BMIm][BF_4] mixture for 60 s gave Au-NPs with narrow size distribution of 10.3 ± 1.5 nm decorated onto the surface of ionic liquid-wrapped MWCNTs [108]. Ultrasound was also used for the synthesis of ionic-liquid-functionalized multiwalled carbon nanotubes decorated with highly dispersed Au nanoparticles from $\text{HAuCl}_4 \cdot 3\text{H}_2\text{O}$ in the presence of 1-(3-aminopropyl)-3-methylimidazolium bromide and dicyclohexylcarbodiimide in DMF solution [139].

4.4 Electro(chemical) Reduction

Ionic liquids are conducting and have a wide electrochemical window of up to 7 V which makes them nearly inert in electrolytic processes. A clean route to prepare metal nanoparticles in ionic liquids is electroreduction with electrons as the only metal-reducing agent (see also Sects. 4.5 and 4.5.2). However, the size of the metal nanoparticles from electroreduction is often above the 100 nm definition limit for nanoparticles.

The technique of pulsed electrodeposition (PED) [140, 141] was used to deposit nanocrystalline Ni [142], Pd [143], Cu [144], Fe [145], Cr [146], and other metals with normal potentials $E^\circ > 0$ V as well as nanoalloys $\text{Ni}_x\text{Fe}_{1-x}$ and $\text{Ni}_x\text{Cu}_{1-x}$ [147] from aqueous electrolytes. Less-noble metals like Al, Mg, and W and their alloys cannot be electrodeposited from aqueous electrolytes but from ionic liquids [140, 141]. Table 2 provides an overview on nanostructured metals which were electrodeposited from ILs.

Table 2 Nano-metals by electrodeposition in ILs

Metal	Metal precursor	Ionic liquid ^a	Size and remarks	References
<i>Monometallic</i>				
Fe	FeCl ₃ , anhydrous	[BMIm][Cl]	40–160 nm by variation of the DC-current density	[148]
Pd	Pd-foil	[BMMor][BF ₄]	Nearly 0.5 nm size control with 2.0 ± 0.1, 2.2 ± 0.3, 2.4 ± 0.3, 2.9 ± 0.3, 3.5 ± 0.5, 3.9 ± 0.6, and 4.5 ± 0.9 nm; particle size increased with a decrease in the current density and an increase in temperature and electrolysis duration	[149]
Cu	CuCl	[BMIm][PF ₆]	10 nm, at electrode potential of –1.8 V	[150]
Ag	Ag(TfO)	[EMIm][TfO]	Nanowires 3 μm long and 200 nm wide	[151]
Ag@TiO ₂	AgBF ₄	[BMIm][BF ₄]	Dendritic network	[152]
Au@PANI	HAuCl ₄ ·3H ₂ O	[EMIm][Tos]/CF ₃ COOH	500–800 nm Au-NPs distributed in polyaniline (PANI) matrix	[153]
Au@graphene	HAuCl ₄	[BMIm][PF ₆]	10 nm Au-NPs by simultaneous reduction of graphite oxide and HAuCl ₄ at –2.0 V	[154]
Al	AlCl ₃ , anhydrous	[EMIm][Cl]	Crystallite sizes from 10 to 133 nm with aromatic and aliphatic carboxylic acid additives and by temperature variation	[148]
<i>Bimetallic</i>				
Al _x Mn _{1–x}	MnCl ₂	[BMIm][Cl]/AlCl ₃	25	[148]
Al _x In _{1–x}	InCl ₃	[BMIm][Cl]/AlCl ₃	25	[148]

^aFor nonfunctionalized ILs, see Fig. 3; for functionalized ILs, see Fig. 5

4.5 Gas-Phase Synthesis

Gas-phase synthesis can be divided in gas-phase condensation and flame pyrolysis and is very effective for high purity nanoparticle products. In gas-phase condensation, the metal is vaporized from heated crucibles by electron or laser beam evaporation or sputtering and condensed here onto an ionic liquid. When a precursor compound is decomposed, the process is called chemical vapor condensation or

chemical vapor synthesis. In flame pyrolysis, the gaseous or liquid precursors are decomposed by a combustion reaction [155]. The negligible vapor pressure of ILs allows to use them in methods requiring vacuum conditions. For metal nanoparticle synthesis, such methods are magnetron sputtering onto ILs, plasma reduction in ILs, physical vapor deposition onto ILs, and electron beam and γ -irradiation to ILs [34].

4.5.1 Magnetron Sputtering

The sputtering of clusters or atoms onto ILs to give nanoparticles is possible for all elements that can be ejected from a target by Ar^+ and N_2^+ plasma ion bombardment. Thus, Au, Ag, Pt, and other M-NPs with diameters of less than 10 nm were prepared by magnetron sputtering. The surface tension and viscosity of the IL are important factors for the nanoparticle growth and stabilization [34].

Indium nanoparticles were obtained by sputter deposition of indium into [BMIm][BF₄], [EMIm][BF₄], [(1-allyl)MIm][BF₄], and [(1-allyl)EIm][BF₄]. The In-NP surface was covered by an amorphous In₂O₃ layer as In/In₂O₃ core-shell particles. The size of the In core was tunable from ca. 8 to 20 nm by choice of the IL [156].

Platinum nanoparticles were produced by Pt sputtering onto [Me₃PrN][Tf₂N] with mean particle diameters of 2.3–2.4 nm independent of sputtering time [157].

Gold nanoparticles of 1–4 nm size were prepared by sputter deposition of the metal onto the surface of [BMIm][BF₄] [158] and [BMIm][PF₆] [159]. In the latter, the size of Au nanoparticles was increased from 2.6 to 4.8 nm by heat treatment at 373 K [159]. Au-NPs of 3–5 nm diameter were obtained by sputtering onto several imidazolium ILs [160].

4.5.2 Plasma Deposition Method, Glow-Discharge (Plasma) Electrolysis

A plasma is a gas which is partially ionized, becomes electrically conductive, and has collective behavior. Plasma deposition is also called glow-discharge electrolysis (GDE) [34], plasma electrochemical deposition (PECD) [140, 141, 155], or gas-liquid interfacial discharge plasma (GLIDP) [161]. It is an electrochemical technique in which the discharge is initiated in the gas between a metal electrode and a solution by applying a high voltage. In ionic liquid glow-discharge electrolysis (IL-GDE), the discharge is initiated in the gas between the metal electrode and the ionic liquid solution. The plasma is regarded as an electrode because of the deposition of the materials at the interface of ionic liquid and plasma. In IL-GDE the precursor material is dissolved in the IL and is reduced with free electrons from the plasma [155, 162]. Table 3 lists metal nanoparticles which were obtained by IL-GDE.

Table 3 Nanoparticles by plasma deposition method (glow-discharge plasma electrolysis) in ILs

Metal	Metal precursor	Ionic liquid ^a	Average particle diameter \pm standard deviation/nm	References
Pd	PdCl ₂	[BMIm][BF ₄]	32.7	[163]
Cu	Cu(TfO) ₂	[BMPy][TfO]	~40, deposited on gold surface	[164]
	Cu	[EMIm][Tf ₂ N]	~11	[165]
	Cu	[BMPy][Tf ₂ N]	~26	[165]
Ag	AgNO ₃ /Ag(TfO)	[BMIm][TfO]	~8–30	[155, 166]
	Ag(TfO)	[EMIm][TfO]	20	[155, 164]
	AgBF ₄	[BMIm][BF ₄], [BMIm][PF ₆]	<100, at glassy carbon electrode	[167]
Au	HAuCl ₄	[BMIm][BF ₄]	~2; as Au-NP-DNA encapsulated SWNTs ^b	[161]
	HAuCl ₄ ·4H ₂ O	[BMIm][BF ₄]	1.7 \pm 0.8, in presence of PVP ^c	[168]
Al	AlCl ₃	[BMPy][Tf ₂ N]	~34, 20–64, deposited on gold surface	[164]
Ge	GeCl ₂ dioxane	[EMIm][Tf ₂ N]	<50	[169]

^aFor nonfunctionalized ILs, see Fig. 3; for functionalized ILs, see Fig. 5

^bSWNTs single-walled carbon nanotubes

^cPVP polyvinylpyrrolidone

4.5.3 Physical Vapor Deposition Method

Physical vapor deposition uses laser beam evaporation of the metal and condensation onto an ionic liquid under vacuum. It offers an easy and fast method for the preparation of stable metal and metal-oxide particles. The use of nonvolatile ILs avoids the otherwise needed freezing of the solvent as well as additional stabilizers [170].

Evaporation of elemental Cu powder under high vacuum (10^{-6} Torr) onto the surface of [BMIm][PF₆] or [BMIm][Tf₂N] generated Cu nanoparticles with an average diameter of 3 nm. Cu metal was also vaporized into an IL dispersion of ZnO to give Cu-NPs with ~3.5 nm diameter on or near the ZnO surface [170]. Gas-phase deposition gave Au-NPs whose average diameter (\varnothing) depended on the IL: [BMIm][BF₄] \varnothing 7 nm, [BMIm][Tf₂N] \varnothing 4 nm, [BMPy][Tf₂N] \varnothing 20–40 nm, [BMIm][DCA] (DCA = dicyanamide) initial \varnothing 10 nm, later 40–80 nm, and [*P*₆₆₆₁₄][DCA] (*P*₆₆₆₁₄ = trisheptyltetradecylphosphonium) \varnothing 50 nm [170].

4.5.4 Electron Beam and γ -Irradiation

Very strong electron beam and γ -irradiation of an IL with a dissolved metal salt yield solvated reducing electrons and/or radicals which generate the metal nanoparticles [34].

Accelerator electron beam and γ -irradiation of NaAuCl₄·2H₂O gave Au-NPs at 6 and 20 kGy in [BMIm][Tf₂N]. From accelerator electron beam irradiation, spherical Au nanoparticles were formed with a mean diameter of 7.6 ± 1.5 nm at 6 kGy irradiation and of 26.4 ± 3.7 nm at 20 kGy. The γ -irradiation gave smaller

Au-NPs with 2.9 ± 0.3 nm and 10.7 ± 1.7 nm at 6 kGy and 20 kGy, respectively, in [BMIm][Tf₂N]. It was emphasized that the prepared Au-NPs were stable without the need for a coordinating additive for more than 3 months [171]. A low-energy electron beam irradiation was used to synthesize 122 nm Au-NPs from NaAuCl₄·2H₂O in [BMIm][Tf₂N] [172].

4.6 Metal Nanoparticles from Zerovalent Metal Precursors

4.6.1 Metal Nanoparticles from Metal Carbonyls, M_x(CO)_y

The binary metal carbonyls Cr(CO)₆, Mo(CO)₆, W(CO)₆, Mn₂(CO)₁₀, Re₂(CO)₁₀, Fe(CO)₅, Fe₂(CO)₉, Fe₃(CO)₁₂, Ru₃(CO)₁₂, Os₃(CO)₁₂, Co₂(CO)₈, Co₄(CO)₁₂, Rh₄(CO)₁₂, Rh₆(CO)₁₆, Ir₄(CO)₁₂, and Ni(CO)₄ are commercially available from Aldrich, ABCR, or Acros. Fe(CO)₅ and Ni(CO)₄ are industrially produced on a multiton scale [173]. Most metal carbonyls M_x(CO)_y are easily purified and handled, even if care should be exerted for the possible liberation of poisonous CO. The metal carbonyls contain the metal atoms already in the zerovalent oxidation state, and a reducing agent is not needed for M-NP synthesis. The side product CO is removed through the gas phase. Thus, contamination from by- or decomposition products is greatly reduced. Hence, metal carbonyls were already long used for the preparation of M-NPs but without ILs. Much of the work on Fe- or Co-NPs from M_x(CO)_y dealt with magnetic NPs [174].

Metal nanoparticles were reproducibly obtained by conventional thermal decomposition (180–250°C, 6–12 h), by UV photolysis (1,000 W, 15 min), or by easy, rapid (few minutes), and energy-saving (as low as 10 W) microwave irradiation (MWI) under an argon atmosphere from their metal carbonyl precursors M_x(CO)_y in ILs (Fig. 14, Table 4). The M-NP synthesis in IL from M_x(CO)_y again does not require any additional stabilizers, surfactants, or capping molecules to give long-term stable M-NP/IL dispersions [30, 31].

Ionic liquids have a significant absorption efficiency for microwave energy because of their high ionic charge, high polarity, and high dielectric constant and, thus, are attractive media for microwave reactions [35]. Microwave heating is extremely rapid. The low-frequency energy source of microwaves is remarkably adaptable to many types of chemical reactions [179]. Microwave radiation can interact directly with the reaction components. The reactant mixture absorbs the microwave energy and localized superheating occurs resulting in fast and efficient heating times [180, 181]. The use of microwaves is a rapid way to heat reactants compared with conventional thermal heating. Any presumptions about abnormal “microwave effects” [182–184] have been proven wrong in the meantime [185, 186]. Microwaves are also an “instant on/instant off” energy source which reduces the risk of overheating reactions [179, 180].

Complete M_x(CO)_y decomposition from the short 3–10-min microwave irradiation was verified by Raman or IR spectroscopy through the absence of (metal)

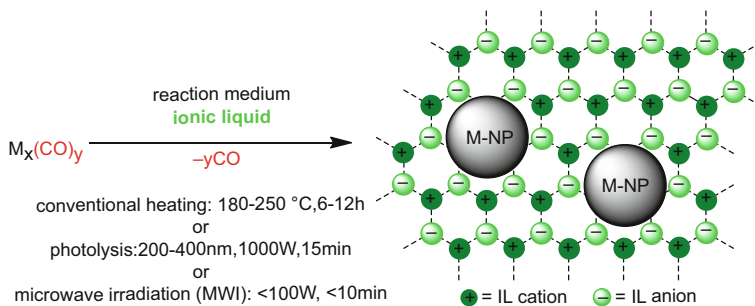


Fig. 14 Schematic presentation for the formation of M-NPs from $M_x(CO)_y$ /IL dispersions by conventional thermal heating, photolysis, or microwave-induced heating

carbonyl bands around $2,000\text{ cm}^{-1}$ (Fig. 15) [30, 31, 111, 117]. For W- and Rh-NPs, it was shown that the diameter increases with the molecular volume of the ionic liquid anion (similar to Ag-NPs, cf. Fig. 9) [124].

Examples of TEM pictures of metal nanoparticles obtained by microwave irradiation or UV photolysis from their metal carbonyl precursors $M_x(CO)_y$ in [BMIm][BF₄] are given in Fig. 16 [117].

The synthesis of Co-NPs and Mn-NPs from $Co_2(CO)_8$ and $Mn_2(CO)_{10}$, respectively, in the functionalized IL 1-(3-carboxyethyl)-3-methyl-imidazolium tetrafluoroborate [CEMIm][BF₄] yields smaller and better separated particles ($1.6 \pm 0.3\text{ nm}$ and $4.3 \pm 1.0\text{ nm}$, respectively) than in the nonfunctionalized IL [BMIm][BF₄] ($5.1 \pm 0.39\text{ nm}$ and $\sim 29 \pm 12\text{ nm}$, respectively) (see Table 4) under the same conditions which is an indication of a rather strong interaction of the IL-carboxy group with the nanoparticles [111].

4.6.2 Metal Nanoparticles from Zerovalent Metal Precursors Other Than $M_x(CO)_y$

Other organometallic compounds with zerovalent metal atoms are [Ru(COD)(COT)] and [Ni(COD)₂] (COD = 1,5-cyclooctadiene, COT = 1,3,5-cyclooctatriene). Hydrogen as a reagent was used to hydrogenate the ligands COD and COT to cyclooctane and thereby dissociate them from the Ru(0) or Ni(0) atom [91, 118, 126, 187]. [Ru(COD)(COT)] and [Ni(COD)₂] were dissolved in imidazolium ILs and the mixture heated with 4 bar of hydrogen under different conditions to obtain the metal nanoparticles (Table 5).

Ruthenium nanoparticles from [Ru(COD)(COT)]/H₂ in various 1-alkyl-3-methyl-imidazolium ionic liquids showed a relationship between the Ru-NP diameter and the size of IL nonpolar domains [188]. This suggested that the size of the nanoparticles is governed by the degree of self-organization of the imidazolium ionic liquid in which they are generated: the more structured the ionic liquid, the

Table 4 Examples of M-NPs prepared from metal carbonyls in ILs.*

Metal	Metal carbonyl precursor	Ionic liquid ^a	M-NP average diameter \pm standard deviation (nm)	Remarks	References
Cr	Cr(CO) ₆	[BMIm][BF ₄], [BMIm][TiO], [BMIm][Tf ₂ N]	$\leq 1.5 \pm 0.3$, MWI, thermal ^b 4.4 ± 1.0 , hv ^b	c,d,e,f	[117, 124]
Mo	Mo(CO) ₆	[BMIm][BF ₄], [BMIm][TiO], [BMIm][Tf ₂ N]	$\sim 1-2$, MWI, hv ^b $\leq 1.5 \pm 0.3$, thermal ^b	c,d,e,f	[117, 124]
W	W(CO) ₆	[BMIm][BF ₄], [BMIm][TiO], [BMIm][Tf ₂ N]	3.1 ± 0.8 , MWI ^b < 1 , hv ^b	c,d,e,f, see Fig. 15	[117, 124]
Mn	Mn ₂ CO ₁₀	[BMIm][BF ₄]	$\leq 1.5 \pm 0.3$, thermal ^b 12.4 ± 3 , MWI < 1 , hv	c,d,e	[111, 117]
Re	Re ₂ CO ₁₀	[CEMIm][BF ₄] [BMIm][BF ₄]	28.6 ± 11.5 , MWI 4.3 ± 1.0 , MWI 2.4 ± 0.9 , MWI	See text c,d,e; see Fig. 16	[111] [117]
Fe	Fe ₂ (CO) ₉	[BMIm][BF ₄]	< 1 , hv 8.6 ± 3.2 , MWI ^b 7.0 ± 3.1 , hv ^b	c,d,e,f	[24, 117]
Ru	Ru ₃ (CO) ₁₂	[BMIm][BF ₄]	5.2 ± 1.6 , thermal ^b 1.6 ± 0.3 , MWI ^b 2.0 ± 0.5 , hv ^b 1.6 ± 0.4 , thermal ^b 2.2 ± 0.4 , MWI	c,d,e,f, see Fig. 16, hydrogenation catalyst, Fig. 18	[24, 117]
Os	Os ₃ (CO) ₁₂	[BMIm][BF ₄]	0.7 ± 0.2 , MWI ^b 2.0 ± 1.0 , hv ^b 2.5 ± 0.4 , thermal ^b	Ru-NPs deposited on TRGO, see text, Fig. 19 c,d,e,f	[175] [24, 117]
Co	Co ₂ (CO) ₈	[BMIm][BF ₄], [BMIm][TiO], [BMIm][Tf ₂ N] [CEMIm][BF ₄]	5.1 ± 0.9 , MWI ^b 8.1 ± 2.5 , hv ^b 14 ± 8 , thermal ^b 1.6 ± 0.3 , MWI	c,d,e,f	[24, 117]
				See text	[111]

Co ₂ (CO) ₈	[C ₄ MIm][Tf ₂ N]	7.7, thermal at 150°C	Fischer–Tropsch catalyst giving olefins, oxygenates, and paraffins (C ₇ –C ₃₀), reusable at least three times	[176]
Co ₂ (CO) ₈	[C ₁₀ MIm][Tf ₂ N]	53 ± 22, thermal at 150°C	Co-NPs with cubic shape together with Co-NPs of irregular shape	[177]
Rh ₆ (CO) ₁₆	[BMIm][BF ₄], [BMIm][TfO], [BMIm][Tf ₂ N]	1.7 ± 0.3, MWI ^b 1.9 ± 0.3, hv ^b 3.5 ± 0.8, thermal ^b 2.8 ± 0.5	c,d,e,f, hydrogenation catalyst	[24, 117]
Rh	[BMIm][BF ₄]	2.1 ± 0.5	Rh-NPs deposited on TRGO, see text, Fig. 19	[175]
Ir	[BMIm][BF ₄], [BMIm][TfO], [BMIm][Tf ₂ N]	0.8 ± 0.2, MWI ^b 1.4 ± 0.3, hv ^b 1.1 ± 0.2, thermal ^b	Rh-NPs deposited on Teflon-coated stirring bar, see text, Fig. 20	[178]
Ir	[BMIm][BF ₄]	0.8 ± 0.2, MWI ^b 1.4 ± 0.3, hv ^b 1.1 ± 0.2, thermal ^b	c,d,e,f, see Fig. 15, hydrogenation catalyst	[24, 117]

*Table reprinted from Z. Naturforsch., 2013, 68b, 1059–1089. Copyright Verlag der Zeitschrift für Naturforschung, Tübingen 2013

^aFor nonfunctionalized ILs, see Fig. 3; for functionalized ILs, see Fig. 5

^bIn [BMIm][BF₄]

^cMedian diameters and standard deviations are from TEM measurements

^dMicrowave decomposition of metal carbonyls with 10 W for 3–10 min

^ePhotolytic decomposition of metal carbonyls with a 1000 W Hg lamp (200–450 nm wavelength) for 15 min

^fThermal decomposition of metal carbonyls from 6 to 12 h with 180–230°C depending on the metal carbonyl

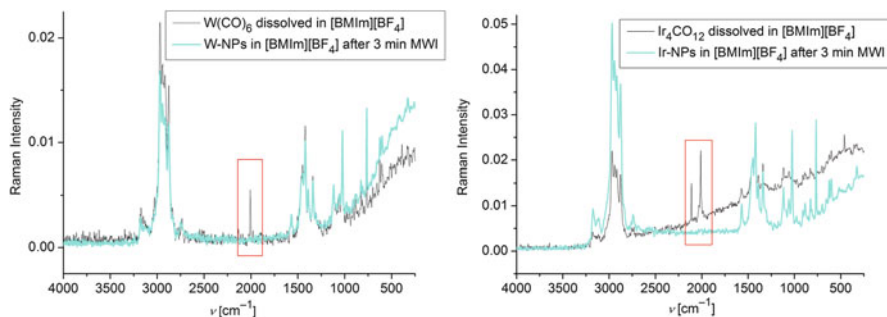


Fig. 15 Raman–Fourier-transform spectra of $\text{W}(\text{CO})_6$ and $\text{Ir}_4(\text{CO})_{12}$ in $[\text{BMIm}][\text{BF}_4]$ before and after 3 min 10 W microwave irradiation (MWI). *Red boxes* highlight the indicative metal carbonyl bands [117]. Adapted from [117] with permission from the author; © 2010 Wiley-VCH

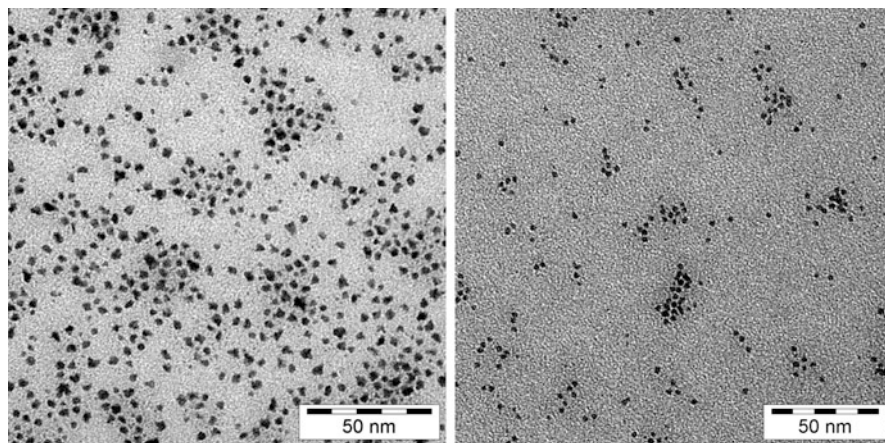


Fig. 16 TEM photographs. *Left:* Re-NPs from $\text{Re}_2(\text{CO})_{10}$ by MWI in $[\text{BMIm}][\text{BF}_4]$, $\varnothing 2.4 \pm 0.9$ nm. *Right:* Ru-NPs from $\text{Ru}_3(\text{CO})_{12}$ by photolysis in $[\text{BMIm}][\text{BF}_4]$, $\varnothing 2.0 \pm 0.5$ nm (cf. Table 4) [117]. Reprinted from [117] with permission from the author; © 2010 Wiley-VCH

smaller the size [91]. The stabilization of Ru-NPs in imidazolium ILs is further related to the presence of surface hydrides and their confinement in nonpolar domains due to the continuous 3-D network of ionic channels [191].

Very small (ca. 1.2 nm) and stable Ru-NPs were obtained from $[\text{Ru}(\text{COD})(\text{COT})]/\text{H}_2$ in the imidazolium ILs $[\text{C}_x\text{MIm}][\text{Tf}_2\text{N}]$ ($\text{C}_x = \text{C}_n\text{H}_{2n+1}$ where $n = 2, 4, 6, 8, 10$) in the presence of amine ligands (1-octylamine, 1-hexadecylamine) which act as coordinating ligands [192].

$\text{Ni}(\text{COD})_2$ also decomposes thermally in 1-alkyl-3-methylimidazolium bis(trifluoromethylsulfonyl)amide ionic liquids [118] or in $[\text{BMIm}][\text{BF}_4]$ under microwave heating to Ni nanoparticles [193]. Thermal co-decomposition of $[\text{Ni}(\text{COD})_2]$ and GaCp^* in $[\text{BMIm}][\text{BF}_4]$ in 1:1 or 1:3 molar ratio gave the stable nanoalloys NiGa and Ni_3Ga , respectively (Fig. 17) [193].

Table 5 Examples of M-NPs prepared in ILs from zerovalent metal precursors other than $M_x(CO)_y$

Metal	Metal precursor ^b	IL ^a	M-NP diameter \pm standard deviation (nm)	References	
Ru	[Ru(COD)(COT)]	[BMIm][Tf ₂ N]	0.9–2.4	[91]	
		[BMIm][Tf ₂ N] w. H ₂ O or 1-octylamine (OA)	H ₂ O: ~2 nm NPs grouped in circular aggregates of 20–30 nm; OA with OA/Ru > 0.1: 1.1 \pm 0.3	[126]	
			25°C, stirring	0°C, no stirring	[188]
			2.4 \pm 0.3	2.3 \pm 0.6	
			2.3 \pm 0.3	1.1 \pm 0.2	
				1.9 \pm 0.6	
			3.6 \pm 1.6	2.3 \pm 0.8	
			Sponge-like superstruct., >100–150		
			2.3 \pm 0.6	2.0 \pm 0.6	
			2.4 \pm 0.3	1.8 \pm 0.5	
Ni	[Ni(COD) ₂]	[BMIm][PF ₆], [BMIm][TfO]	2.6 \pm 0.4	[187]	
		[C ₄ MIm][Tf ₂ N]	4.9 \pm 0.9 to 5.9 \pm 1.4	[118]	
		[BMIm][BF ₄]	10 \pm 4	[193]	
<i>Bimetallic</i>					
NiGa or Ni ₃ Ga	[Ni(COD) ₂], GaCp* ^d	[BMIm][BF ₄]	NiGa: 14 \pm 9, semihydrogenation catalyst; see Fig. 17; Ni ₃ Ga: 17 \pm 8	[193]	

^aFor nonfunctionalized ILs, see Fig. 3; for functionalized ILs, see Fig. 5^bCOD 1,5-cyclooctadiene, COT 1,3,5-cyclooctatriene^c[BMMIm]⁺ 1-butyl-2,3-dimethyl-imidazolium^dCp* pentamethylcyclopentadienyl

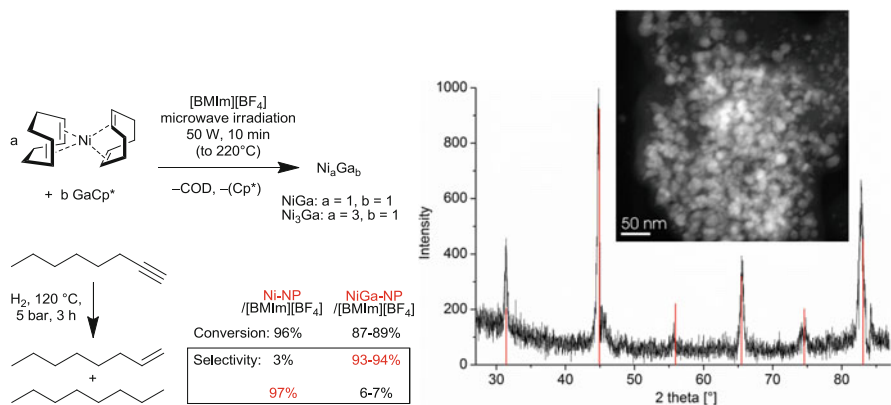


Fig. 17 Microwave-assisted thermal co-decomposition of [Ni(COD)₂] and GaCp* to bimetallic Ni/Ga-NPs in IL. The high-angle annular dark-field-scanning TEM (HAADF-STEM) image of a 1.0 wt% NiGa dispersion in IL gives diameters between 7 and 29 nm (average 14 ± 9 nm). PXRD provides evidence for NiGa as the single crystalline component with reference data in red taken from ICSD No: 103854 (NiGa). The slightly broadened reflections suggest crystallite domain sizes of 21 ± 10 nm as calculated with the Scherrer equation [190]. The NiGa/IL dispersion could be employed for the catalytic semihydrogenation of 1-octyne or diphenylacetylene (tolan, not depicted) to 1-octene or diphenylethylene in about 90% yield and with up to 94 or 87% selectivity, while Ni-NPs under the same conditions yield the alkanes in 97 or 78% selectivity, respectively [193]

4.6.3 Catalytic Applications of Metal Nanoparticles Derived from M_x(CO)_y

Nonfunctional ionic liquids contain only weakly coordinating cations and anions (see Fig. 3) which bind less strongly to the M-NP surface than coordinating capping or protective ligands. Hence, metal nanoparticles in ILs should be effective catalysts, and a number of catalytic reactions have successfully been carried out in ILs [12, 194]. Nonvolatile ILs fit into the context of “green catalysis” [195] which requires that catalysts be designed for easy separation from the reaction products and multi-time efficient reuse [35, 196, 197]. The miscibility of ILs with organic substrates can be designed to allow for phase separation and decantation [197] or removal of volatile products by distillation in vacuum. At the same time, the IL is able to retain the M-NPs for catalyst reuse and recycling. It was already demonstrated that M-NP/IL systems were quite easily recyclable and reusable for several times without significant catalytic deactivation [24]. In hydrogenation reactions with Rh- or Ru-NP/IL systems, the catalytic activity did not decrease upon repeated reuse [117, 124]. The catalytic properties (activity and selectivity) put dispersed M-NPs closer to heterogeneous (multisite, surface-like) than to homogeneous (single-site) catalysts [198, 199].

The hydrogenation of internal alkynes with Pd-NPs at 25°C under 1 bar of hydrogen yields Z-alkenes with up to 98% selectivity. At higher hydrogen pressure

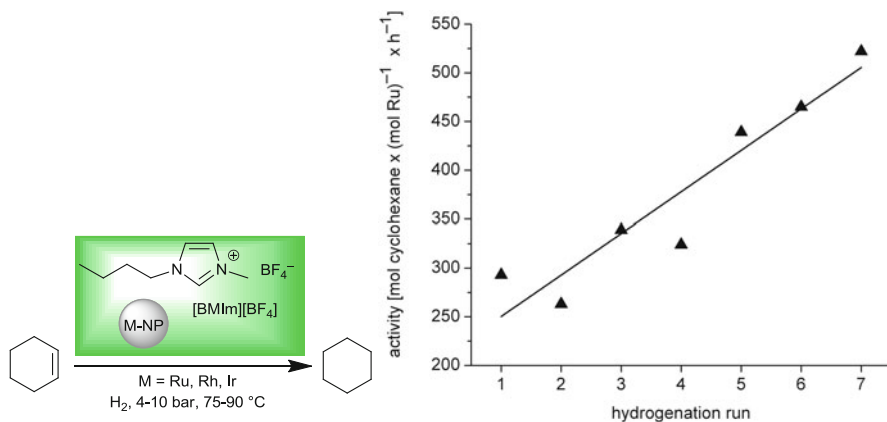


Fig. 18 Hydrogenation of cyclohexene to cyclohexane with Ru-, Rh-, or Ir-NP/IL. Activity even increases over seven runs with the same Ru-NP/[BMIm][BF₄] catalyst at 90°C, 10 bar H₂ pressure. Conversion was intentionally stopped at 95% as thereafter the decrease in cyclohexene concentration lowered the reaction rate [117]. Rh- and Ir-NP/[BMIm][BF₄] gave activities of 1,900 mol cyclohexane × (mol Ir)⁻¹ × h⁻¹ and 380 mol cyclohexane × (mol Rh)⁻¹ × h⁻¹ for quantitative conversion at 4 bar H₂ pressure and 75°C [124]

(4 bar), alkanes were exclusively obtained without detection of any alkenes. TOF values reached 1,282 h⁻¹ with good recyclability of the system and no loss of activity for at least four runs [85].

Ru-, Rh-, and Ir-NP/[BMIm][BF₄] dispersions were active catalysts in the organic-solvent-free hydrogenation of cyclohexene or benzene to cyclohexane (Fig. 18) [30, 31, 117]. Also, a remarkable partial hydrogenation of benzene to cyclohexene with Ru-NP/[BMIm][PF₆] has been reported [187].

Ruthenium or rhodium nanoparticles could be supported on thermally reduced graphite oxide (TRGO, “graphene”) with small and uniform particle sizes (Ru 2.2 ± 0.4 nm and Rh 2.8 ± 0.5 nm) from Ru₃(CO)₁₂ and Rh₆(CO)₁₆, respectively, through microwave irradiation of a M_x(CO)_y/TRGO/[BMIm][BF₄] mixture (Fig. 19). The hybrid materials Rh-NP@TRGO and Ru-NP@TRGO were directly catalytically active in hydrogenation reactions. The recyclable M-NP@TRGO nanocomposites gave a complete conversion of cyclohexene or benzene to cyclohexane under organic-solvent-free conditions (50–75°C, 4 bar H₂) with reproducible and steady activities of 1,570 mol cyclohexene × (mol Ru)⁻¹ × h⁻¹ and 310 mol benzene × (mol Rh)⁻¹ × h⁻¹ (Fig. 19) [175].

Rhodium nanoparticles could be deposited onto a standard Teflon-coated magnetic stirring bar which is present during microwave decomposition of Rh₆(CO)₁₆ in [BMIm][BF₄]. Such metal nanoparticle deposits were not easy to remove from the Teflon surface by simple washing with organic solvents. The barely visible Rh-NP@stirring bar deposits (32 μg or less Rh metal,

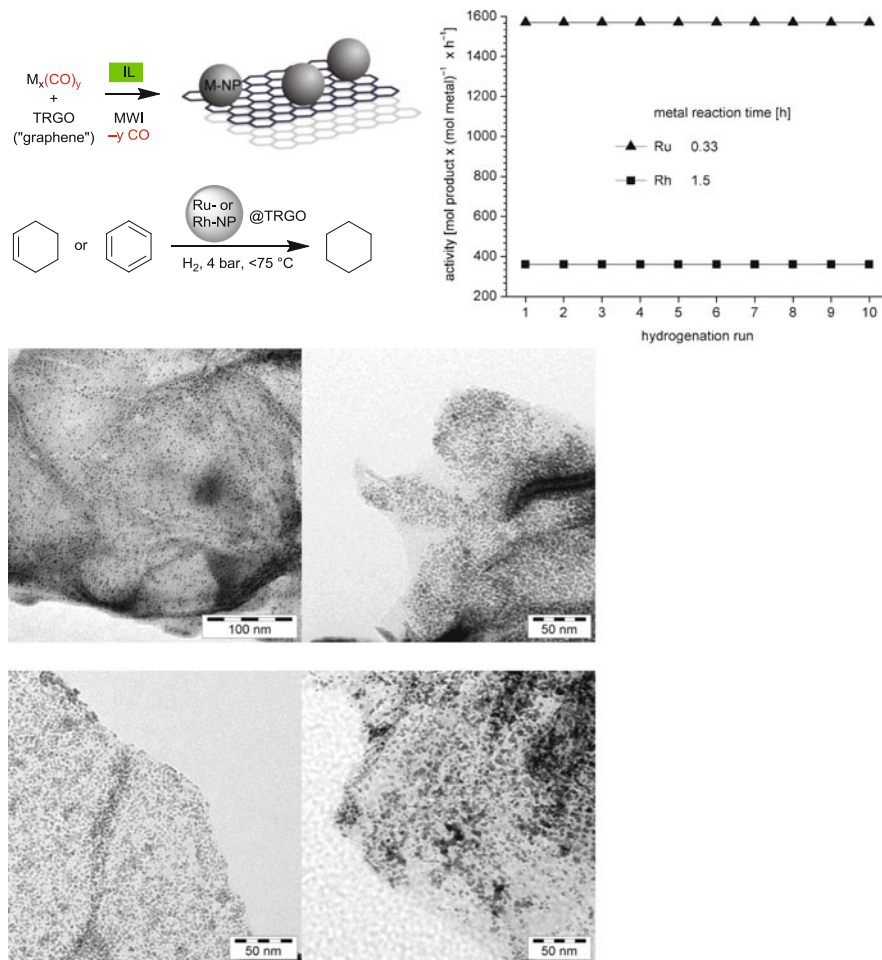


Fig. 19 Scheme for the synthesis of transition metal nanoparticles on thermally reduced graphite oxide (TRGO) in ILs by microwave treatment and the use of Ru- and Rh@TRGO for hydrogenation catalysis with activities for cyclohexene hydrogenation over 10 consecutive runs. TEM images *top row*: Ru-NP@TRGO before (*left*) and after (*right*) 10 hydrogenation runs; *bottom row*: Rh-NP@TRGO before (*left*) and after (*right*) 10 hydrogenation runs [175]. Reprinted in part from [175] with permission from the author; © 2010 Elsevier Ltd

$\text{\AA} 2.1 \pm 0.5$ nm, on a 20×6 mm magnetic stirring bar) could act as an easy-to-handle and reusable catalyst in organic-solvent-free hydrogenation reactions with quantitative conversion and very high turnover frequencies of up to $32,800 \text{ mol cyclohexene} \times (\text{mol Rh})^{-1} \times \text{h}^{-1}$ (Fig. 20) [178].

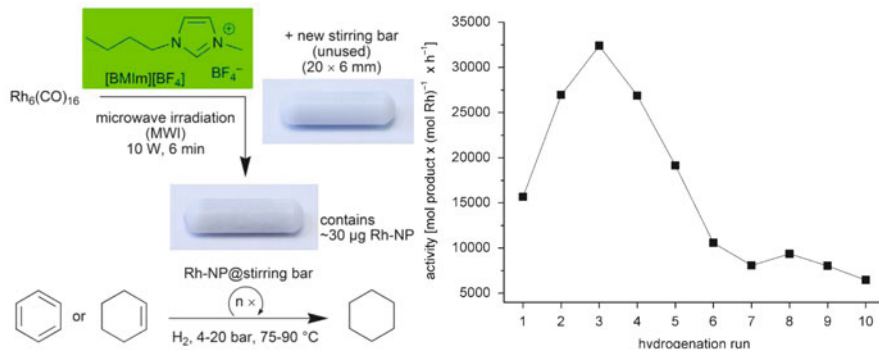


Fig. 20 Rh-NP deposition on a Teflon-coated magnetic stirring bar from an IL dispersion and the use of Rh-NP@stirring bar in hydrogenation catalysis with high activities [178]. Reprinted in part from [178] with permission from the author; © 2010 Elsevier Ltd

5 Conclusions

In this review, it is shown that ionic liquids are remarkable and excellent media for the synthesis and stabilization of metal nanoparticles (M-NPs) without the need of additional coordinating ligands, polymers, or surfactants. The stabilization of metal nanoparticles in ILs can be attributed to electrostatic and steric effects from the Coulomb network properties of ILs which prevent M-NP agglomeration. Various chemical synthesis methods of metal nanoparticles in ILs allow for the design of M-NP shapes and sizes. The synthesis of M-NPs can proceed by chemical, photochemical, sonochemical, and electroreduction as well as gas-phase deposition methods. A microwave-induced thermal decomposition of metal carbonyls $M_x(CO)_y$ in ILs provides an especially rapid and energy-saving access to M-NPs because of the significant absorption efficiency of ILs for microwave energy due to their high ionic charge, high polarity, and high dielectric constant. Metal carbonyls present attractive synthons for M-NPs as they are readily commercially available and contain the metal atoms already in the required zerovalent oxidation state needed. No reducing agent is necessary for metal carbonyls. The only side product is CO which is removed through the gas phase and avoids contaminations of the M-NP/IL dispersion. From the IL dispersion, the M-NPs can be deposited on various surfaces, such as nanotubes and thermally reduced graphite oxide (TRGO). The formation of bimetallic MM'-NPs in ILs has just been started, e.g., with intermetallic Cu/Zn-nanobrass and Ni/Ga nanoalloy phases. M-NP/IL dispersions have been successfully employed in organic-solvent-free catalytic reactions with multiple recycling of the M-NP catalyst.

Acknowledgment Our work was supported by the Deutsche Forschungsgemeinschaft through grant Ja466/17-1.

References

1. Yu S-H, MacGillivray LR, Janiak C (2012) *CrystEngComm* 14:7531–7534
2. Lu AH, Salabas EL, Schüth F (2007) *Angew Chem Int Ed* 46:1222–1244
3. Gedanken A (2004) *Ultrason Sonochem* 11:47–55
4. Rao CNR, Vivekchand SRC, Biswas K, Govindaraj A (2007) *Dalton Trans* 3728–3749
5. Mastai Y, Gedanken A (2004) In: Rao CNR, Müller A, Cheetham AK (eds) *Chemistry of Nanomaterials*, I. Wiley-VCH, Weinheim, p 113
6. Park J, Joo J, Kwon SG, Jang Y, Hyeon T (2007) *Angew Chem Int Ed* 46:4630–4660
7. Peng Z, Yang H (2009) *Nano Today* 4:143–164
8. An K, Alayoglu S, Ewers T, Somorjai GA (2012) *J Colloid Interface Sci* 373:1–13
9. Kim M, Phan VN, Lee K (2012) *CrystEngComm* 14:7535–7548
10. Scholten JD, Leal BC, Dupont J (2012) *ACS Catal* 2:184–200
11. Yan N, Xiao C, Kou Y (2010) *Coord Chem Rev* 254:1179–1218
12. Pârvulescu VI, Hardacre C (2007) *Chem Rev* 107:2615–2665
13. Welther A, Jacobi von Wangelin A (2013) *Curr Org Chem* 17:326–335
14. Campbell PS, Prechtl MHG, Santini CC, Haumesser PH (2013) *Curr Org Chem* 17:414–429
15. Guerrero M, Than Chau NT, Noël S, Denicourt-Nowicki A, Hapiot F, Roucoux A, Monflier E, Philippot K (2013) *Curr Org Chem* 17:364–399
16. Scholten JD (2013) *Curr Org Chem* 17:348–363
17. Ostwald W (1901) *Z Phys Chem* 37:385
18. Ostwald W (1896) *Lehrbuch der Allgemeinen Chemie*, vol 2. Part 1. Wilhelm Engelmann, Leipzig
19. Bönemann H, Richards RM (2001) *Eur J Inorg Chem* 2455–2480
20. Astruc D, Lu F, Aranzas JR (2005) *Angew Chem Int Ed* 44:7852–7872
21. Pan C, Pelzer K, Philippot K, Chaudret B, Dassenoy F, Lecante P, Casanove M-J (2001) *J Am Chem Soc* 123:7584–7593
22. Aiken JD III, Finke RG (1999) *J Am Chem Soc* 121:8803–8810
23. Ueno K, Tokuda H, Watanabe M (2010) *Phys Chem Chem Phys* 12:1649–1658
24. Krämer J, Redel E, Thomann R, Janiak C (2008) *Organometallics* 27:1976–1978
25. Dupont J, Scholten JD (2010) *Chem Soc Rev* 39:1780–1804
26. Dupont J (2004) *J Braz Chem Soc* 15:341–350
27. Neouze M-A (2010) *J Mater Chem* 20:9593–9607
28. Consorti CS, Suarez PAZ, de Souza RF, Burrow RA, Farrar DH, Lough AJ, Loh W, da Silva LHM, Dupont J (2005) *J Phys Chem B* 109:4341–4349
29. Dupont J, Suarez PAZ, de Souza RF, Burrow RA, Kintzinger J-P (2000) *Chem Eur J* 6:2377–2381
30. Vollmer C, Janiak C (2011) *Coord Chem Rev* 255:2039–2057
31. Janiak C (2013) *Z Naturforsch B* 68:1056–1089
32. Weingärtner H (2008) *Angew Chem Int Ed* 47:654–670
33. Xiao D, Rajan JR, Cady A, Li S, Bartsch RA, Quitevis EL (2007) *J Phys Chem B* 111:4669–4677
34. Kuwabata S, Tsuda T, Torimoto T (2010) *J Phys Chem Lett* 1:3177–3188
35. Wasserscheid P, Keim W (2000) *Angew Chem Int Ed* 39:3772–3789
36. Krossing I, Slattery JM, Daguene C, Dyson PJ, Oleinikova A, Weingärtner H (2006) *J Am Chem Soc* 128:13427–13434
37. Zhang H, Cui H (2009) *Langmuir* 25:2604–2612
38. Itoh H, Naka K, Chujo Y (2004) *J Am Chem Soc* 126:3026–3027
39. Kim K-S, Demberelnyamba D, Lee H (2004) *Langmuir* 20:556–560
40. Gao S, Zhang H, Wang X, Mai W, Peng C, Ge L (2005) *Nanotechnology* 16:1234–1237
41. Schrekker HS, Gelesky MA, Stracke MP, Schrekker CML, Machado G, Teixeira SR, Rubim JC, Dupont J (2007) *J Colloid Interface Sci* 316:189–195

42. Marcilla R, Mecerreyes D, Odriozola I, Pomposo JA, Rodriguez J, Zalakain I, Mondragon I (2007) *Nano* 2:169–173
43. Plechkova NV, Seddon KR (2008) *Chem Soc Rev* 37:123–150
44. Welton T (1999) *Chem Rev* 99:2071–2084
45. Feldmann C (2013) *Z Naturforsch* 68b 1057
46. Hallett JP, Welton T (2011) *Chem Rev* 111:3508–3576
47. Torimoto T, Tsuda T, Okazaki K, Kuwabata S (2010) *Adv Mater* 22:1196–1221
48. Janiak C (2013) *Z Naturforsch* 68b:1059–1089
49. Freudenmann D, Wolf S, Wolff M, Feldmann C (2011) *Angew Chem Int Ed* 50:11050–11060
50. Ahmed E, Breternitz J, Groh MF, Ruck M (2012) *CrystEngComm* 14:4874–4885
51. Ahmed E, Ruck M (2011) *Dalton Trans* 40:9347–9357
52. Groh MF, Müller U, Ahmed E, Rothenberger A, Ruck M (2013) *Z Naturforsch* 68b: 1108–1122
53. Morris RE (2009) *Chem Commun* 2990–2998
54. Parnham ER, Morris RE (2007) *Acc Chem Res* 40:1005–1013
55. Cooper ER, Andrews CD, Wheatley PS, Webb PB, Wormald P, Morris RE (2004) *Nature* 430:1012–1016
56. Rao CNR, Matte HSSR, Voggu R, Govindaraj A (2012) *Dalton Trans* 41:5089–5120
57. Lin Y, Dehnen S (2011) *Inorg Chem* 50:7913–7915
58. Lodge P (2008) *Science* 321:50
59. Verwey EJW, Overbeek JTG (1999) *Theory of the stability of lyophobic colloids*. Dover Publications Mineola, New York, pp 1–218
60. Redel E, Krämer J, Thomann R, Janiak C (2008) *GIT Labor-Fachzeitschrift*, GIT Verlag, Wiley-VCH Weinheim, April issue, 400–403
61. Shipway AN, Katz E, Willner I (2000) *ChemPhysChem* 1:18–25
62. Cassagneau T, Fendler JH (1999) *J Phys Chem B* 103:1789–1793
63. Keating CD, Kovaleski KK, Natan MJ (1998) *J Phys Chem B* 102:9404–9413
64. Kobrak MN, Li H (2010) *Phys Chem Chem Phys* 12:1922–1932
65. Schmid G (2010) *Nanoparticles*, 2nd edn. Wiley-VCH, Weinheim, pp 214–238
66. Branco LC, Rosa NJ, Ramos JJM, Alfonso CAM (2002) *Chem Eur J* 8:3671–3677
67. Yuan X, Yan N, Katsyuba SA, Zvereva E, Kou Y, Dyson PJ (2012) *Phys Chem Chem Phys* 14:6026–6033
68. Zhao D, Fei Z, Scopelliti R, Dyson P (2004) *Inorg Chem* 43:2197–2205
69. Zhao D, Fei Z, Geldbach TJ, Scopelliti R, Dyson P (2004) *J Am Chem Soc* 126:15876–15882
70. Prechtl MHG, Scholten JD, Dupont J (2009) *J Mol Catal A* 313:74–78
71. Fonseca GS, Umpierre AP, Fichtner PFP, Teixeira SR, Dupont J (2003) *Chem Eur J* 9: 3263–3269
72. Gelesky MA, Umpierre AP, Machado G, Correia RRB, Magno WC, Morais J, Ebeling G, Dupont J (2007) *J Am Chem Soc* 127:4588–4589
73. Dykeman RR, Yan N, Scopelliti R, Dyson PJ (2011) *Inorg Chem* 50:717–719
74. Dupont J, Fonseca GS, Umpierre AP, Fichtner PFP, Teixeira SR (2002) *J Am Chem Soc* 124:4228–4229
75. Fonseca GS, Machado G, Teixeira SR, Fecher GH, Morais J, Alves MCM, Dupont J (2006) *J Colloid Interface Sci* 301:193–204
76. Migowski P, Zanchet D, Machado G, Gelesky MA, Teixeira SR, Dupont J (2010) *Phys Chem Chem Phys* 12:6826–6833
77. Zhao X, Hua Y, Liang L, Liu C, Liao J, Xing W (2012) *Int J Hydrogen Energy* 37:51–58
78. Ruta M, Laurency G, Dyson PJ, Kiwi-Minsker L (2008) *J Phys Chem C* 112:17814–17819
79. Deshmukh RR, Rajagopal R, Srinivasan KV (2001) *Chem Commun* 1544–1545
80. Prechtl MHG, Scholten JD, Dupont J (2010) *Molecules* 15:3441–3461
81. Anderson K, Fernández SC, Hardacre C, Marr PC (2004) *Inorg Chem Commun* 7:73–76
82. Caló V, Nacci A, Monopoli A, Laera S, Cioffi N (2003) *J Org Chem* 68:2929–2933
83. Caló V, Nacci A, Monopoli A, Detomaso A, Iliade P (2003) *Organometallics* 22:4193–4197

84. Hassine F, Pucheault M, Vaultier M (2011) *C R Chimie* 14:671–679
85. Venkatesan R, Prechtl MHG, Scholten JD, Pezzi RP, Machado G, Dupont J (2011) *J Mater Chem* 21:3030–3036
86. Planellas M, Pleixats R, Shafir A (2012) *Adv Synth Catal* 354:651–662
87. Scheeren CW, Domingos JB, Machado G, Dupont J (2008) *J Phys Chem C* 112:16463–16469
88. Scheeren CW, Machado G, Dupont J, Fichtner PFP, Texeira SR (2003) *Inorg Chem* 42:4738–4742
89. Marquardt D, Barthel J, Braun M, Ganter C, Janiak C (2012) *CrystEngComm* 14:7607–7615
90. Raut D, Wankhede K, Vaidya V, Bhilare S, Darwatkar N, Deorukhkar A, Trivedi G, Salunkhe M (2009) *Catal Commun* 10:1240–1243
91. Gutel T, Garcia-Anton J, Pelzer K, Philippot K, Santini CC, Chauvin Y, Chaudret B, Basset J-M (2007) *J Mater Chem* 17:3290–3292
92. Setua P, Pramanik R, Sarkar S, Ghatak C, Rao VG, Sarkar N, Das SK (2011) *J Mol Liq* 162:33–37
93. Lazarus LL, Riche CT, Marin BC, Gupta M, Malmstadt N, Brutchey RL (2012) *ACS Appl Mater Interfaces* 4:3077–3083
94. Bhatt AI, Mechler A, Martin LL, Bond AM (2007) *J Mater Chem* 17:2241–2250
95. Dai T, Ge L, Guo R (2009) *J Mater Res* 24:333–341
96. Ryu HR, Sanchez L, Keul HA, Raj A, Bockstaller MR (2008) *Angew Chem Int Ed* 47:7639–7643
97. Obliosca JM, Harvey I, Arellano J, Huang MH, Arco SD (2010) *Mater Lett* 64:1109–1112
98. Bai X, Li X, Zheng L (2010) *Langmuir* 26:12209–12214
99. Casal-Dujat L, Rodrigues M, Yagüe A, Calpena AC, Amabilino DB, González-Linares J, Borrás M, Pérez-García L (2012) *Langmuir* 28:2368–2381
100. Lazarus LL, Yang AS-J, Chu S, Brutchey RL, Malmstadt N (2010) *Lab Chip* 10:3377–3379
101. Dash P, Miller SM, Scott RWJ (2010) *J Mol Catal A Chem* 329:86–95
102. Safavi A, Zeinali S (2010) *Colloids Surfaces A Physicochem Eng Aspects* 362:121–126
103. Li Z, Taubert A (2009) *Molecules* 14:4682–4688
104. Li Z, Friedrich A, Taubert A (2008) *J Mater Chem* 18:1008–1014
105. Khare V, Li Z, Manton A, Ayi AA, Sonkaria S, Voelkl A, Thünemann AF, Taubert A (2010) *J Mater Chem* 20:1332–1339
106. Redel E, Walter M, Thomann R, Vollmer C, Hussein L, Scherer H, Krüger M, Janiak C (2009) *Chem Eur J* 15:10047–10059
107. Huang W, Chen S, Liu Y, Fu H, Wu G (2011) *Nanotechnology* 22:025602
108. Park H, Kim J-S, Choi BG, Jo SM, Kim DY, Hong WH, Jang S-Y (2010) *Carbon* 48:1325–1330
109. Redel E, Walter M, Thomann R, Hussein L, Krüger M, Janiak C (2010) *Chem Commun* 46:1159–1161
110. Dinda E, Rashid MH, Biswas M, Mandal TK (2010) *Langmuir* 26:17568–17580
111. Marquardt D, Xie Z, Taubert A, Thomann R, Janiak C (2011) *Dalton Trans* 40:8290–8293
112. Taubert A (2010) *Top Curr Chem* 290:127–159
113. Liu D-P, Li G-D, Su Y, Chen J-S (2006) *Angew Chem Int Ed* 45:7370–7373
114. Taubert A, Li Z (2007) *Dalton Trans* 723–727
115. Redel E, Thomann R, Janiak C (2008) *Inorg Chem* 47:14–16
116. Ott LS, Finke RG (2006) *Inorg Chem* 45:8382–8393
117. Vollmer C, Redel E, Abu-Shandi K, Thomann R, Manyar H, Hardacre C, Janiak C (2010) *Chem Eur J* 16:3849–3858
118. Migowski P, Machado G, Teixeira SR, Alves MCM, Morais J, Traverse A, Dupont J (2007) *Phys Chem Chem Phys* 9:4814–4821
119. Zhu JM, Shen YH, Xie AJ, Qiu LG, Zhang Q, Zhang XY (2007) *J Phys Chem C* 111:7629–7633
120. Firestone MA, Dietz ML, Seifert S, Trasobares S, Miller DJ, Zaluzec NJ (2005) *Small* 1:754–760

121. Peppler K, Polleth M, Meiss S, Rohnke M, Janek J (2006) *Z Phys Chem* 220:1507–1527
122. Safavi A, Maleki N, Tajabadi F, Farjami E (2007) *Electrochem Commun* 9:1963–1968
123. Kim K, Lang C, Kohl PA (2005) *J Electrochem Soc* 152:E9
124. Redel E, Krämer J, Thomann R, Janiak C (2009) *J Organomet Chem* 694:1069–1075
125. Redel E, Thomann R, Janiak C (2008) *Chem Commun* 1789–1791
126. Salas G, Podgorsek A, Campbell PS, Santini CC, Pádua AAH, Costa Gomes MF, Philippot K, Chaudret B, Turmine M (2011) *Phys Chem Chem Phys* 13:13527–13536
127. Antonietti M, Kuang D, Smarly B, Zhou Y (2004) *Angew Chem Int Ed* 43:4988–4992
128. Scholten JD, Ebeling G, Dupont J (2007) *Dalton Trans* 5554–5560
129. Zhao L, Zhang C, Zhuo L, Zhang Y, Ying JY (2008) *J Am Chem Soc* 130:12586–12587
130. Guo S, Wang E (2007) *Anal Chim Acta* 598:181–192
131. Turkevich J, Stevenson PC, Hillier J (1951) *Discuss Faraday Soc* 11:55–75
132. Ryan TA, Ryan C, Seddon EA, Seddon KR (1996) Phosgene and related carbonyl halides, monograph 24. In: Clark RJH (ed) *Topics in inorganic and general chemistry*. Elsevier, Amsterdam, p 242
133. Mertens SFL, Vollmer C, Held A, Aguirre MH, Walter M, Janiak C, Wandlowski T (2011) *Angew Chem Int Ed* 50:9735–9738
134. Corma A, Domínguez I, Ródenas T, Sabater MJ (2008) *J Catal* 259:26–35
135. Miao S, Liu Z, Zhang Z, Han B, Miao Z, Ding K, An G (2007) *J Phys Chem C* 111: 2185–2190
136. Dash P, Scott RWJ (2011) *Mater Lett* 65:7–9
137. Marquardt D, Beckert F, Penntreau F, Tölle F, Mülhaupt R, Riant O, Hermans S, Bartel J, Janiak C (2014) *Carbon* 66:285–294
138. Harada M, Kimura Y, Saijo K, Ogawa T, Isoda S (2009) *J Colloid Interface Sci* 339:373–381
139. Wang Z, Zhang Q, Kuehner D, Xu X, Ivaska A, Niu L (2008) *Carbon* 46:1687–1692
140. Endres F (2002) *ChemPhysChem* 3:144–154
141. Endres F, MacFarlane D, Abbott A (2008) *Electrodeposition from ionic liquids*. Wiley-VCH, Weinheim
142. Erb U (1994) US patent US 5,352,266
143. Natter H, Krajewski T, Hempelmann R (1996) *Ber Bunsenges Phys Chem* 100:55–64
144. Natter H, Hempelmann R (1996) *J Phys Chem B* 100:19525
145. Natter H, Schmelzer M, Löffler M-S, Krill CE, Fitch A, Hempelmann R (2000) *J Phys Chem B* 104:2467–2476
146. Przenioslo R, Wagner J, Natter H, Hempelmann R, Wagner W (2001) *J Alloys Compounds* 328:259–263
147. Natter H, Schmelzer M, Hempelmann R (1998) *J Mater Res* 13:1186–1197
148. Natter H, Bukowski M, Hempelmann R, Zein El Abedin S, Moustafa EM, Endres F (2006) *Z Phys Chem* 220:1275–1291
149. Cha J-H, Kim K-S, Choi S, Yeon S-H, Lee H, Lee C-S, Shim J-J (2007) *Korean J Chem Eng* 24:1089–1094
150. Yu L, Sun H, He J, Wang D, Jin X, Hu X, Chen GZ (2007) *Electrochem Commun* 9: 1374–1381
151. Zein El Abedin S, Endres F (2009) *Electrochim Acta* 54:5673–5677
152. Roy P, Lynch R, Schmuki P (2009) *Electrochem Commun* 11:1567–1570
153. Wei D, Baral JK, Österbacka R, Ivaska A (2008) *J Mater Chem* 18:1853–1857
154. Fu C, Kuang Y, Huang Z, Wang X, Du N, Chen J, Zhou H (2010) *Chem Phys Lett* 499: 250–253
155. Kareem TA, Kaliani AA (2012) *Ionics* 18:315–327
156. Suzuki T, Okazaki K-I, Suzuki S, Shibayama T, Kuwabata S, Torimoto T (2010) *Chem Mater* 22:5209–5215
157. Tsuda T, Yoshii K, Torimoto T, Kuwabata S (2010) *J Power Sources* 195:5980–5985
158. Hatakeyama Y, Takahashi S, Nishikawa K (2010) *J Phys Chem C* 114:11098–11102

159. Kameyama T, Ohno Y, Kurimoto T, Okazaki K-I, Uematsu T, Kuwabata S, Torimoto T (2010) *Phys Chem Chem Phys* 12:1804–1811
160. Wender H, de Oliveira LF, Migowski P, Feil AF, Lissner E, Pechtl MHG, Teixeira SR, Dupont J (2010) *J Phys Chem C* 114:11764–11768
161. Chen Q, Kaneko T, Hatakeyama R (2011) *Curr Appl Phys* 11:S63–S66
162. Kaneko T, Baba K, Hatakeyama R (2009) *J Appl Phys* 105:103306-1–103306-5
163. Xie Y-B, Liu C-J (2008) *Plasma Processes Polym* 5:239–245
164. Zein El Abedin S, Pölleth M, Meiss SA, Janek J, Endres F (2007) *Green Chem* 9:549–553
165. Brettholle M, Höfft O, Klarhöfer L, Mathes S, Maus-Friedrichs W, Zein El Abedin S, Krischok S, Janek J, Endres F (2010) *Phys Chem Chem Phys* 12:1750–1755
166. Meiss SA, Rohnke M, Kienle L, Zein El Abedin S, Endres F, Janek J (2007) *ChemPhysChem* 8:50–53
167. He P, Liu H, Li Z, Liu Y, Xu X, Li J (2004) *Langmuir* 20:10260–10267
168. Wei Z, Liu C-J (2011) *Mater Lett* 65:353–355
169. Aal AA, Al-Salman R, Al-Zoubi M, Borissenko N, Endres F, Höfft O, Prowald A, Zein El Abedin S (2011) *Electrochim Acta* 56:10295–10305
170. Richter K, Birkner A, Mudring A-V (2010) *Angew Chem Int Ed* 49:2431–2435
171. Tsuda T, Seino S, Kuwabata S (2009) *Chem Commun* 6792–6794
172. Imanishi A, Tamura M, Kuwabata S (2009) *Chem Commun* 1775–1777
173. Kerfoot DGE, Nickel X, Wildermuth E, Stark H, Friedrich G, Ebenhöch FL, Kühborth B, Silver J, Rituper R (2008) Iron compounds. In: Ullmann's encyclopaedia of industrial chemistry, 5th edn. Wiley-VCH, Weinheim
174. Hyeon T (2003) *Chem Commun* 927–934
175. Marquardt D, Vollmer C, Thomann R, Steurer P, Mülhaupt R, Redel E, Janiak C (2011) *Carbon* 49:1326–1332
176. Silva DO, Scholten JD, Gelesky MA, Teixeira SR, Dos Santos ACB, Souza-Aguiar EF, Dupont J (2008) *ChemSusChem* 1:291–294
177. Scariot M, Silva DO, Scholten JD, Machado G, Teixeira SR, Novak MA, Ebeling G, Dupont J (2008) *Angew Chem Int Ed* 47:9075–9078
178. Vollmer C, Schröder M, Thomann Y, Thomann R, Janiak C (2012) *Appl Catal A* 425–426: 178–183
179. Bogdal D (2006) *Microwave-assisted organic synthesis*. Elsevier, New York, pp 47–189
180. Buchachenko AL, Frankevich EL (1993) *Chemical generation and reception of radio- and microwaves*. Wiley-VCH, Weinheim, pp 41–56
181. Ahluwalia VK (2008) *Alternative energy processes in chemical synthesis*. Alpha Science International Ltd, Oxford
182. Berlan J, Giboreau P, Lefeuvre S, Marchand C (1991) *Tetrahedron Lett* 32:2363–2366
183. Langa F, de la Cruz P, de la Hoz A, Diaz-Ortiz A, Diez-Barra E (1997) *Contemp Org Synth* 4:373–386
184. Perreux L, Loupy A (2001) *Tetrahedron* 57:9199–9233
185. Stadler A, Kappe CO (2000) *J Chem Soc Perkin Trans* 2:1363–1368
186. Stadler A, Kappe CO (2001) *Eur J Org Chem* 919–924
187. Silveira ET, Umpierre AP, Rossi LM, Machado G, Morais J, Soares GV, Baumvol IJR, Teixeira SR, Fichtner RFP, Dupont J (2004) *Chem Eur J* 10:3734–3740
188. Gutel T, Santini CC, Philippot K, Padua A, Pelzer K, Chaudret B, Chauvin Y, Basset J-M (2009) *J Mater Chem* 19:3624–3631
189. Schütte K, Meyer H, Gemel C, Barthel J, Fischer RA, Janiak C (2014) *Nanoscale* in press. doi:[10.1039/C3NR05780A](https://doi.org/10.1039/C3NR05780A)
190. Langford JI, Wilson AJC (1978) *J Appl Crystallogr* 11:102–113
191. Campbell PS, Santini CC, Bouchu D, Fenet B, Philippot K, Chaudret B, Pádua AAH, Chauvin Y (2010) *Phys Chem Chem Phys* 12:4217–4223
192. Salas G, Santini CC, Philippot K, Collière V, Chaudret B, Fenet B, Fazzini PF (2011) *Dalton Trans* 40:4660–4668

193. Schütte K, Doddi A, Kroll C, Meyer H, Wiktor C, Gemel C, van Tendeloo G, Fischer RA, Janiak C (2014) *Nanoscale* submitted
194. Sawant AD, Raut DG, Darvatkar NB, Salunkhe MM (2011) *Green Chem Lett Rev* 4:41–54
195. Sheldon RA (2008) *Chem Commun* 3352–3365
196. Wasserscheid P, Welton T (2007) *Ionic liquid in synthesis*, vol 1. Wiley-VCH, Weinheim, pp 325–350
197. van Doorslaer C, Schellekens Y, Mertens P, Binnemanns K, De Vos D (2010) *Phys Chem Chem Phys* 12:1741–1749
198. Astruc D (2007) *Nanoparticles and catalysis*. Wiley-VCH, New York
199. Dupont J, de Souza RF, Suarez PAZ (2002) *Chem Rev* 102:3667–3692

Size Control of Monodisperse Metal Nanocrystals in Ionic Liquids

Pascal Lignier

Abstract During the last decade, a great interest in the preparation of uniform nanocrystals has offered efficient synthetic strategies to precisely engineer metal, metal oxide and alloy at the nanoscale. Due to their physicochemical properties, ionic liquids (ILs) simultaneously demonstrated their potential in different areas such as nanocrystal synthesis, catalysis and energy. As a result, ionic liquids have been employed for the preparation of monodisperse nanocrystals and the control of their size. This chapter highlights the most promising methods for the synthesis of uniform nanocrystals in ionic liquids which act as a solvent, stabiliser, reducing agent and even precursor. As a result, successful preparations of nanoparticles in the presence of ILs are now available for both noble and earth-abundant elements such as gold, platinum, iridium, silver, palladium, ruthenium, rhodium, copper, nickel, cobalt and iron.

The formation mechanisms of these nanocrystals are discussed as well as our mechanistic understanding in conventional organic and aqueous solvents. In addition, the IL approach is compared to leading methods in conventional solvents to make possible the identification of general principles for most metallic elements. By analogy with conventional solvents, these strategies can be adapted to the preparation of semiconductor nanocrystals. These achievements are going to drive the identification of relationships between the nature of ILs components, the physicochemical properties of ILs, the formation of nanocrystals in ILs and the resulting performances of these nano-objects.

P. Lignier (✉)
Laboratoire de Chimie de Coordination, CNRS; LCC, 205 Route de Narbonne, F-31077
Toulouse, France

Université de Toulouse; UPS, INPT; LCC, F-31077 Toulouse, France
e-mail: lignier.pascal@gmail.com

Keywords Alloy · Colloid · Earth-abundant metal · Catalysis · Energy · Gold · Iron oxide · Ligand · Metal oxide · Nanocluster · Nanocrystal · Nanoparticle · Nanostructure · Noble metal · Organometallic · Platinum · Ruthenium · Silver · Surface chemistry · Transition metal

Contents

1	Introduction	56
2	Synthesis of Metal Nanocrystals in Conventional Aqueous and Organic Solvents	57
3	Synthesis of Metal Nanocrystals in Ionic Liquids	60
4	Size Control of Uniform Metal Nanocrystals	64
	4.1 Size Uniformity	64
	4.2 Size Control via the IL Cation	66
	4.3 Size Control via the IL Anion	69
	4.4 Size Control in the Presence of Conventional Stabilisers in ILs	70
5	Conclusions	74
	References	74

1 Introduction

Recently, synthetic strategies have been developed for the synthesis of uniform metal, metal oxide and alloy nanocrystals [1–4]. As a result, bottom-up approaches in the liquid phase now lead to nanocrystals which can adopt uniform size, morphology, structure, composition and to some extent, surface chemistry. In comparison with traditional solvents, ionic liquids (ILs) exhibit a combination of distinctive physicochemical properties which are precisely selected via the subtle choice of their cationic and anionic components. As a consequence, ILs are highly relevant for the synthesis of inorganic and hybrid (inorganic–organic) nano-objects [5–9]. In 2002, Dupont et al. initiated the synthesis of uniform metal nanoparticles in ILs [5]; their work demonstrated that ILs are relevant for the synthesis and use in catalysis of metal nanoparticles as small as 3 nm.

This chapter presents the main synthetic strategies and related mechanisms for controlling the size of metal, metal oxide and alloy nanocrystals in ionic liquids (ILs). Successful preparations of nanoparticles in the presence of ILs are now available for most metallic elements [10, 11]. Interestingly, ILs can act as a solvent, stabiliser, reducing agent or even precursor. The resulting nanocrystals offer different properties (catalytic, electronic optical, magnetic). As a consequence, a wide range of innovative nanomaterials has been prepared in ionic liquids for various applications such as catalysis [12, 13] and energy storage [14]. In this chapter, the IL approach is compared to leading strategies in conventional solvents to make possible the establishment of general principles for the preparation of uniform nanocrystals composed of noble and earth-abundant elements.

2 Synthesis of Metal Nanocrystals in Conventional Aqueous and Organic Solvents

During the last decades, scalable preparations of uniform and sophisticated nanoparticles have been achieved via bottom-up strategies in the liquid phase. The controlled transformation of metal precursors, which are organometallic complexes or metal salts, occurs via thermal decomposition and reduction steps. A large temperature range, i.e. from room temperature up to ~ 380 to 400°C , has been used for these preparations. Conventional reducing agents are dihydrogen, hydrides (e.g. sodium borohydride), polyols (e.g. ethylene glycol, 1,2-hexadecanediol), amines (e.g. hexadecylamine) and monosaccharides (e.g. ascorbic acid) [15].

Whilst metal salts are usually cheaper, organometallic complexes have been outstanding metal precursors to prepare well-defined nanoparticles [16] and investigate their surface reactivity as well as the nature, location and dynamics of the species onto the surface of these nanoparticles in conventional solvents [17]. For example, the η^4 -1,5-cyclooctadiene (COD) and η^6 -1,3,5-cyclooctatriene (COT) ligands can be hydrogenated to cyclooctane during the synthesis of Ru nanoparticles from Ru(COD)(COT) under dihydrogen atmosphere at room temperature (Fig. 1). Due to the dissociation of dihydrogen, hydrides are present on the metal surface. Since alkanes will not significantly interact with the metal surface, hydrides are the only species on this surface [19, 20]. As a consequence, these well-defined nano-objects led to significant advances in our understanding of the surface reactivity of metal nanoparticles [17].

Due to their high surface energy and their high surface-area-to-volume ratio, nanoparticles tend to agglomerate to decrease their surface area and therefore

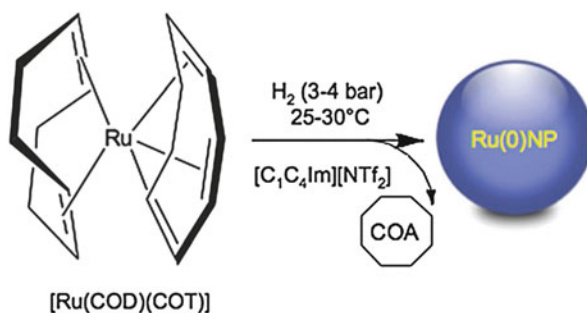


Fig. 1 Synthesis of Ru nanoparticles via the room-temperature decomposition of Ru(COD)(COT) under H₂ atmosphere in conventional solvents or ILs (e.g. [C₁C₄Im][NTf₂]; C₁C₄Im, 1-methyl-3-*n*-butylimidazolium; NTf₂, bis(trifluoromethylsulphonyl)imide) and the associated formation of COA due to the reduction of COD and COT [18]

minimise their total energy. As a consequence, stabilising agents are required to preserve their nanodimensions. The efficient stabilisation of nano-objects originates from the appropriate combination of attractive and repulsive interactions. The attraction between the stabiliser and the nanoparticle surface mainly results from covalent bonding and electrostatic forces. The repulsion between the stabilisers of neighbouring nanoparticles is usually presented as the result of electrostatic and steric effects, as well as their association (electrosteric). For the synthesis of uniform nanoparticles in conventional solvents, different ligands have been extensively employed as stabilising agents. For example, typical ligands are long alkyl chains functionalized with an alcohol, amine, carboxylic acid, phosphine or thiol group. These various ligands can offer different interactions, primarily covalent, with the metal surface. Polymers, such as PVA (polyvinyl alcohol), are also widely used to stabilise nanoparticles (up to ~1 to 3 nm) [21] in conventional solvents. Further functionalisation of the stabiliser introduces complementary properties, e.g. for controlling the selectivity in catalysis or the self-assembly of monodisperse nanocrystals.

The major parameters for the precise synthesis of uniform nanocrystals are the temperature of the reaction medium, the nature and relative concentration of all species (capping agent, metal precursor, reductant, seed, additive) as well as the seed morphology at each reaction time. Since the formation of metal nanoparticles usually involves different organic, inorganic or organometallic species, interactions between these different species can strongly impact the kinetics of formation/evolution of the metal nanoparticles [22]. Understanding secondary reactions and associated intermediates, e.g. the formation and evolution of a complex formed from the metal precursor and an organic additive, is crucial for controlling the final properties of the nanocrystals (Figs. 2 and 3) [4, 23–28]. Furthermore, the preferential adsorption of organic (ligands, polymers, surfactants) or inorganic

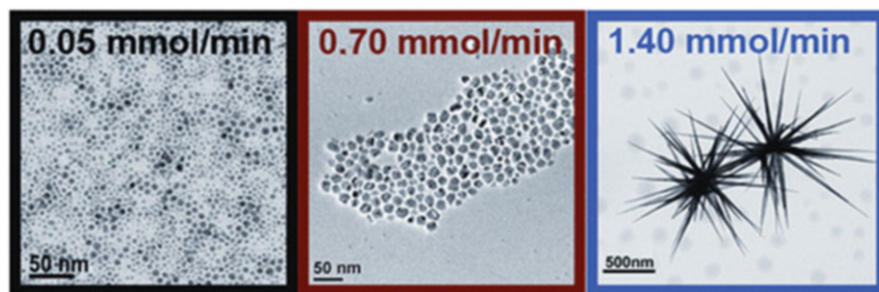


Fig. 2 Cobalt nanocrystals of different sizes and morphologies prepared at 150°C under dihydrogen atmosphere (3 bar) following different addition rates of the metal precursor ($[\text{Co}\{\text{N}(\text{SiMe}_3)_2\}_2(\text{THF})]$) to a solution of conventional ligands (hexadecylamine and lauric acid) at room temperature [23]

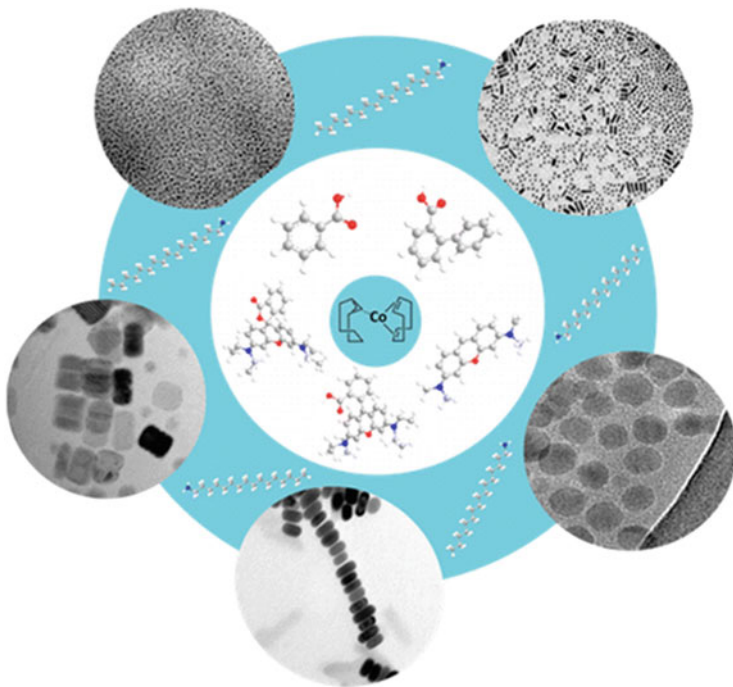


Fig. 3 Size and shape control of cobalt nanocrystals via the amount of free ligands following a reaction between hexadecylamine and a carboxylic acid ligand. Co spheres, rods, discs and hexagonal prisms were prepared via the decomposition of $[\text{Co}(\eta_3\text{-C}_8\text{H}_{13})(\eta_4\text{-C}_8\text{H}_{12})]$ under H_2 (3 bar) at 110–150°C in the presence of ligands e.g. hexadecylamine in association with a rhodamine B derivative [24]

(ions, gases) agents is an advanced strategy for the selective growth or etching of specific facets. This can result in sophisticated nanocrystals via well-controlled nucleation, growth and etching steps [1–4]. Finally, the precise engineering of ligand–nanocrystal interfaces in conventional solvents led to hybrid nanomaterials which exhibit specific properties such as selectivity control in catalysis [17, 29, 30] and air stability [4].

Developed for two decades in aqueous and organic solvents, modern methodologies currently allow the size control of uniform metal nanoparticles. In the next part, the main achievements in the synthesis of these nanoparticles in the presence of ILs are discussed and compared to their preparations in conventional solvents.

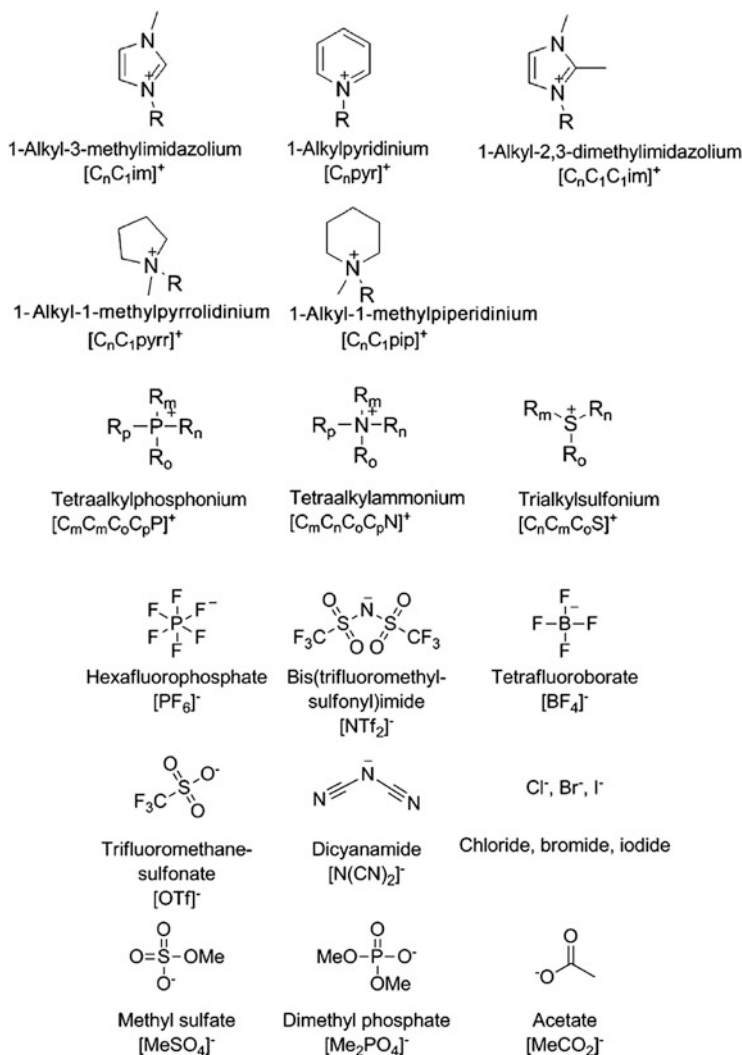


Fig. 4 Cations (*top*) and anions (*bottom*) of ionic liquids (ILs) [31]

3 Synthesis of Metal Nanocrystals in Ionic Liquids

Ionic liquids (ILs) are molten salts (Fig. 4) which combine significant advantages as sustainable solvents: low melting point (from -80 to 100°C), negligible vapour pressure, good thermal stability (e.g. up to 300°C), non-flammability, high miscibility with a wide range of organic and inorganic compounds, hydrophobicity, high ionic conductivity, large liquidus range, high microwave absorption and high electrochemical stability. Their non-volatility avoids exposure to toxic vapours,



Fig. 5 $[C_4C_1Im][PF_6]$; (left) Corey, Pauling, Koltun (CPK) colours; (right) red for polar domains, i.e. the imidazolium ring of the cation and the PF_6^- anion, and green for nonpolar domains, i.e. the side chain of the imidazolium [34]

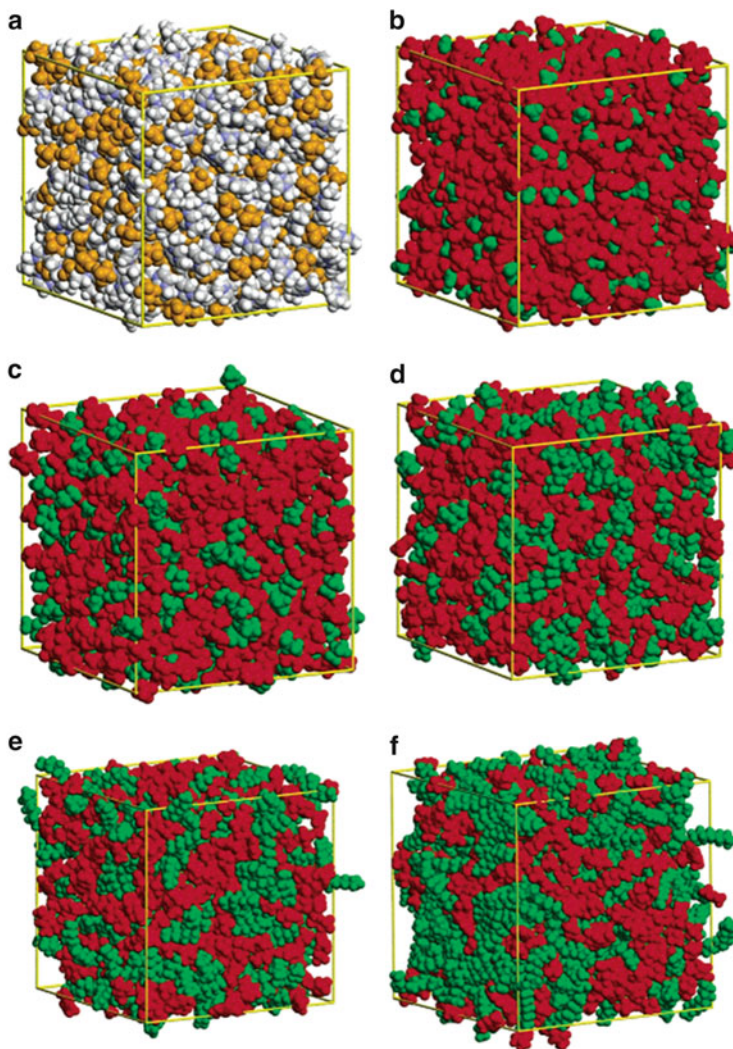


Fig. 6 Simulation boxes of 700 $[C_nC_1Im][PF_6]$ (l is the length of the box sides): (a) $[C_2C_1Im][PF_6]$ CPK colours; (b) $[C_2C_1Im][PF_6]$ red (polar)/green (nonpolar); (c) $[C_4C_1Im][PF_6]$, $l = 49.8$ Å; (d) $[C_6C_1Im][PF_6]$, $l = 52.8$ Å; (e) $[C_8C_1Im][PF_6]$, $l = 54.8$ Å; (f) $[C_{12}C_1Im][PF_6]$, $l = 59.1$ Å [34]

whereas their inherent toxicity, as well as their physicochemical properties, could be controlled by design [32, 33]. Furthermore, their potential recyclability could be a significant advantage.

Ionic liquids, particularly those based on imidazolium cations, can exhibit both polar and nonpolar nanodomains within self-organised three-dimensional networks of non-covalent interactions (Figs. 5 and 6). Charged substances (e.g. metal salts) are preferentially located in polar domains whilst neutral compounds (e.g. metal carbonyls) are within nonpolar domains. Interestingly, these nanodomains may act as dynamic (soft) nanoreactors to engineer nanomaterials since the IL structure depends on easily controllable parameters such as the temperature and the stirring rate.

For example, sub-2 nm Ru metal nanoparticles were prepared in imidazolium and phosphonium ILs from organometallic precursors, such as Ru(COD)(COT) [20] and Ru(2-methylallyl)₂(COD), in the absence of conventional stabilisers [35–37]. In a similar fashion to conventional synthesis [17], organometallic complexes have been remarkable metal precursors to study the surface reactivity of uniform nanoparticles prepared in ILs. In the absence of impurities, these nanoparticles offer unique opportunities for the understanding of the interactions between ILs and the metal surfaces [16].

For example, Santini, Padua et al. achieved such investigations via well-defined Ru metal nanoparticles prepared from Ru(COD)(COT) in [C₁C_nIm][NTf₂] ($2 \leq n \leq 10$) ILs (C₁C_nIm, 1-methyl-3-*n*-alkylimidazolium; NTf₂, bis(trifluoromethylsulphonyl)imide) in the absence of a further stabiliser. These experimental and computational studies concluded that ILs offer a sophisticated and highly dynamic three-dimensional framework of hydrogen bonds, Coulomb and van der Waals forces as well as polar and nonpolar domains. As a consequence, ionic liquids can control the stabilisation of metal nanoparticles within their dynamic nanodomains, mainly via weak interactions (i.e. non-covalent) [38, 39].

For example, isothermal titration calorimetry showed that interactions between the IL and the metal surface are stronger by using [C₁C_nIm]⁺ with longer alkyl chains. This suggests the influence of van der Waals forces. Furthermore, in comparison with [C₁C₄Im][NTf₂], the addition of a methyl group on the C₂ carbon of the [C₁C₄Im]⁺ cation (i.e. [C₁C₁C₄Im][NTf₂]) or, to a lesser extent, the exchange of the imidazolium cation with the *N*-methylpyrrolidinium cation (i.e. [C₁C₄Pyrro][NTf₂]) resulted in weaker hydrogen bonds and therefore a less efficient stabilisation of the Ru nanoparticles.

In addition, Santini and co-workers achieved in situ labelling and spectroscopic studies with these ruthenium nanoparticles in [C₁C₄Im][NTf₂] [40]. Interestingly, hydrides were present on the ruthenium surface, as previously characterised in conventional organic solvents [20], and acted as a stabiliser of the metal nanoparticles. Furthermore, the nanoparticles were in close proximity to the alkyl chains of the imidazolium cations. Finally, the addition of water led to the agglomeration of the Ru nanoparticles. These results suggested that the hydride-covered Ru metal nanoparticles were within the nonpolar domains of the three-dimensional network of [C₁C₄Im][NTf₂] in a similar fashion to organometallic Ru nanoparticles

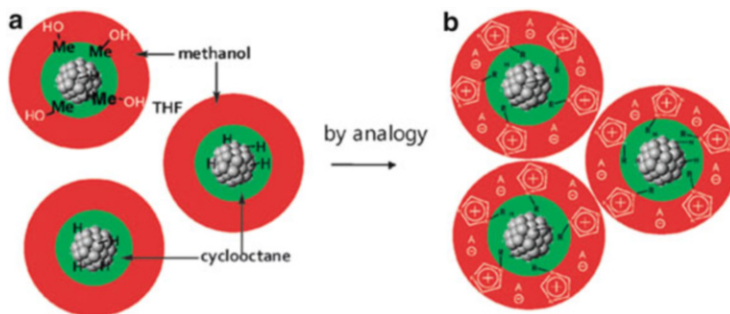


Fig. 7 Stabilisation of ruthenium nanoparticles within nonpolar domains (a) in conventional organic solvents as well as (b) in ILs [40]

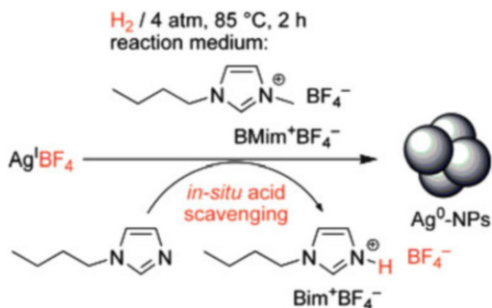
within cyclooctane domains in a mixture of conventional solvents (Fig. 7) [17, 41, 42].

Experimental and computational studies of metal nanoparticles in imidazolium ILs proposed that both cationic and anionic sites of multi-charged $\{[(C_4C_1Im)_x(X)_{x-n}]^{n+}[(C_4C_1Im)_{x-n}(X)_x]^{n-}\}_m$ assemblies (C_4C_1Im , 1-*n*-butyl-3-methylimidazolium cation; X, anion) are located near the metal surface, whereas the alkyl chains could still interact with the surface [10].

IL building blocks usually exhibit weak interactions with metal surfaces. However, stronger ligands can be in situ prepared from ILs. For example, different groups reported the in situ formation of *N*-heterocyclic carbenes (NHC) from imidazolium ILs and the role of these carbenes in the stabilisation of Ir metal nanoparticles [36, 43, 44]. Whilst *N*-heterocyclic carbenes (NHC) were well-known as ligands in ruthenium complexes for olefin metathesis, the ability of carbenes to stabilise metal nanoparticles was first reported in ILs and then in conventional solvents [45], e.g. by using NHC carbenes [46–49].

Conventional stabilisers were also injected in the solution for the synthesis of metal nanocrystals in ILs [50]. Furthermore, highly specific properties resulted from the functionalisation of ILs with conventional reducers [51] or stabilising groups [52]. Both strategies can lead to a stronger stabilisation of metal surfaces via covalent interactions. In addition, conventional reducing agents, such as ascorbate anions, can be the anionic part of imidazolium ILs [53]. Adding conventional stabilisers in ILs is an efficient strategy for the transfer to ILs of advanced methodologies developed in conventional solvents. For example, Hang and co-workers were able to control the size of silver, platinum and iron oxide nanoparticles in $[C_4C_1Im][NTf_2]$ by using oleic acid, oleylamine and cetyltrimethylammonium bromide (CTAB) [50]. In addition, the functionalisation of ILs expands the properties of conventional stabilisers. For example, the incorporation of a hydroxyl group into the IL ethyl chain had a strong impact on the solubility of poly(vinylpyrrolidone) (PVP), an extensively used stabiliser in conventional solvents. As a result, Rh–PVP nanoparticles were homogeneously dispersed in

Fig. 8 Formation and stabilisation of Ag nanoparticles from Ag^+BF_4^- in $[\text{C}_4\text{C}_1\text{Im}][\text{BF}_4^-]$ under dihydrogen atmosphere in the presence of an imidazole [57]



1-(2-hydroxyethyl)-3-methylimidazolium boron tetrafluoride ($[\text{C}_2\text{OHC}_1\text{Im}][\text{BF}_4^-]$) whilst being not soluble in 1-ethyl-3-methylimidazolium boron tetrafluoride ($[\text{C}_2\text{C}_1\text{Im}][\text{BF}_4^-]$) [54]. The efficient stabilisation and dispersion of the Rh–PVP nanoparticles resulted in higher activity, separation and recycling in $[\text{C}_2\text{OHC}_1\text{Im}][\text{BF}_4^-]$ for the selective hydrogenation of styrene to ethylbenzene. Further discussions on the stabilisation of nanocrystals in ILs are available in recent reviews [10, 52, 55].

In addition, the low solubility of dioxygen in ILs [56] can reduce the oxidation rate of sensitive metals such as Fe, Co and Cu. As a consequence, metal oxide nanocrystals could be prepared by controlling the dioxygen diffusion in ILs and associated oxidation of metal nanocrystals. In conventional solvents, this strategy led to sophisticated and highly monodisperse nanocrystals such as hollow metal oxide or metal@metal oxide core-shell nanoparticles prepared from uniform metal nanospheres [4]. The formation of an oxide shell can also limit further oxidation of the metal core [4].

The stability of the metal nanoparticles can also be related to the formation of acidic species, such as HX (X: Cl^- , NO_3^- , BF_4^- , PF_6^- , CF_3SO_3^- anions), which can favour the leaching, i.e. the removal of atoms on the nanocrystal. As a consequence, a proton sponge [43] (e.g. N^1, N^1, N^8, N^8 -tetramethylnaphthalene-1, 8-diamine) or an imidazole was used as a proton scavenger (Fig. 8) [57]. Furthermore, the in situ transformation of ILs can result in the release of nanocrystals' components which are then used in a controlled fashion. For example, the water-assisted formation of F^- from BF_4^- in the presence of a metal precursor (e.g. $\text{Fe}(\text{NO}_3)_3$) led to the well-controlled preparation of iron fluoride (e.g. FeF_3) [58].

4 Size Control of Uniform Metal Nanocrystals

4.1 Size Uniformity

Since the reactivity of metal nanoparticles is related to their size, relevant preparations have to deliver monodisperse nanoparticles which exhibit the optimal

diameter for a specific application, e.g. the use of these nanoparticles as a catalyst in a structure-sensitive reaction [59]. The formation of nanocrystals is usually described using a three-step model: (1) formation of the basic building units of the bulk crystal (monomers) from the precursors; (2) nucleation step, i.e. the formation of crystal seeds (nuclei) from the monomers; and (3) growth step, i.e. the formation of the crystal from the nuclei. The separation of these different steps is an efficient strategy to prepare monodisperse nanocrystals. In addition, the size uniformity is related to the focusing of the size during the growth of the nanocrystals via monomer addition, dissolution, coalescence and “punctuated” growth [60]. As a result, this lead to monodisperse nanocrystals which exhibit a narrow size distribution, i.e. the relative standard deviation of the nanoparticles’ size is below 5–10% [25]. This size uniformity allows nanocrystals to self-assemble in superlattices which can be used as model catalysts [61]. For example, Murray and co-workers investigated the nature of the active sites for CO oxidation by using Au-Fe_xO_y binary superlattices with different densities of catalytic contacts between both components [62].

The final size of monodisperse nanocrystals can be predetermined via the control of nucleation and growth rates. For a given amount of precursor, a low nucleation rate leads to a low concentration of nuclei and consequently in big nanoparticles, whereas smaller nanoparticles are expected at a higher nucleation rate resulting from a higher concentration of nuclei [63]. The separation of the nucleation and growth steps can also be achieved using the controlled addition of monomers on preformed nanocrystals acting as seeds. Since the nucleation on the surface of the preformed nanocrystal is energetically favoured, undesirable nucleation in solution can be avoided [2].

IL nanodomains can be used as a soft template for the facile preparation of nanoparticles which exhibit a relatively narrow size distribution and a size between 1 and 20 nm. Whilst the high surface-area-to-volume ratio of the particles at this scale is relevant for their use as catalysts, their high surface energy favours their agglomeration in the absence of stabilisation. Interestingly, ILs demonstrated their ability to act as efficient stabilising agents for the synthesis, use and storage of nano-objects as small as 1 nm [17].

Recently, in situ transmission electron microscopy (TEM) techniques have been highly useful to investigate the formation mechanisms of metal nanocrystal formation [60]. However, these studies require specific cells to accommodate the volatile solvent within the TEM instrument which operates under high vacuum. Interestingly, Kuwabata and co-workers took advantage of the non-volatility of ILs and achieved similar investigations without a cell, i.e. via a conventional instrument, during the in situ formation of sub-5 nm gold nanocrystals from the reduction of NaAuCl₄ in a mixture of 1-butyl-3-methylimidazolium bis(trifluoromethylsulphonyl)imide [C₄C₁Im][NTf₂] and trimethylpropylammonium bis(trifluoromethylsulphonyl)imide [N_{3,1,1,1}][NTf₂] (volume ratio = 50:50) [64]. Further advantages are the facile deposition of the IL solution onto mesh grids, the superior control of the liquid thickness and a higher resolution due to the absence of window. These studies showed that classical mechanisms of the nanocrystal formation

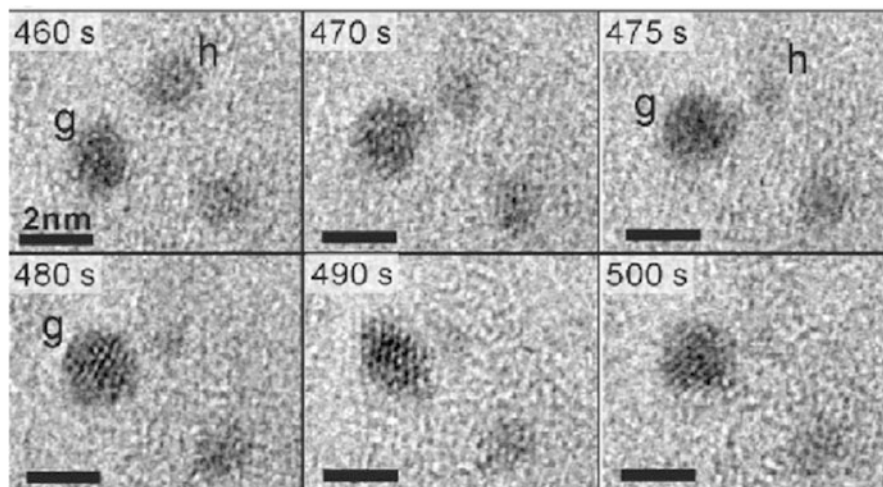


Fig. 9 Sequential disappearance of the particle **h** and associated growth of the particle **g** due to Ostwald ripening [64]

occurred in ILs such as the disappearance of a nanoparticle to feed the growth of a larger (i.e. more stable) nanoparticle via Ostwald ripening (Fig. 9). In addition, the authors observed the sequential formation of a sub-5 nm twinned nanocrystal from the attachment of a multiply twinned nanocrystal to a single-crystalline nanocrystal via rotation, coalescence and relaxation steps (Fig. 10). This sequence also occurs during the oriented attachment of two nanocrystals in conventional solvents [62].

4.2 Size Control via the IL Cation

The nanoparticles' size can depend on the IL cation. Santini and co-workers identified a relationship between the size of Ru metal nanoparticles and the number of carbons (n) of the alkyl chain (C_n) of $[C_nC_1Im][NTf_2]$ (Fig. 11) [65]. Due to its nonpolarity, the organometallic precursor $Ru(COD)(COT)$ was preferentially located within the nonpolar domains of $[C_nC_1Im][NTf_2]$. As a consequence, the nucleation and growth of the Ru metal nanoparticles occurred within these nonpolar reactors under H_2 atmosphere (0.4 MPa), at $0^\circ C$ without stirring or $25^\circ C$ with stirring. Interestingly, in $[C_nC_1Im][NTf_2]$ ILs, longer alkyl chains ($n = 4, 6$ or 8) increased the volume of the nonpolar domains (calculated via molecular dynamics simulation) and therefore the size of the nanoparticles (determined via TEM). However, this relationship was not valid for shortest and longest alkyl chains. This may result from the higher mobility of ruthenium species in $[C_2C_1Im][NTf_2]$ and $[C_{10}C_1Im][NTf_2]$ due to the smaller size of the nonpolar domains for $n = 2$ and the presence of nonpolar channels between the nonpolar domains for $n = 10$. The

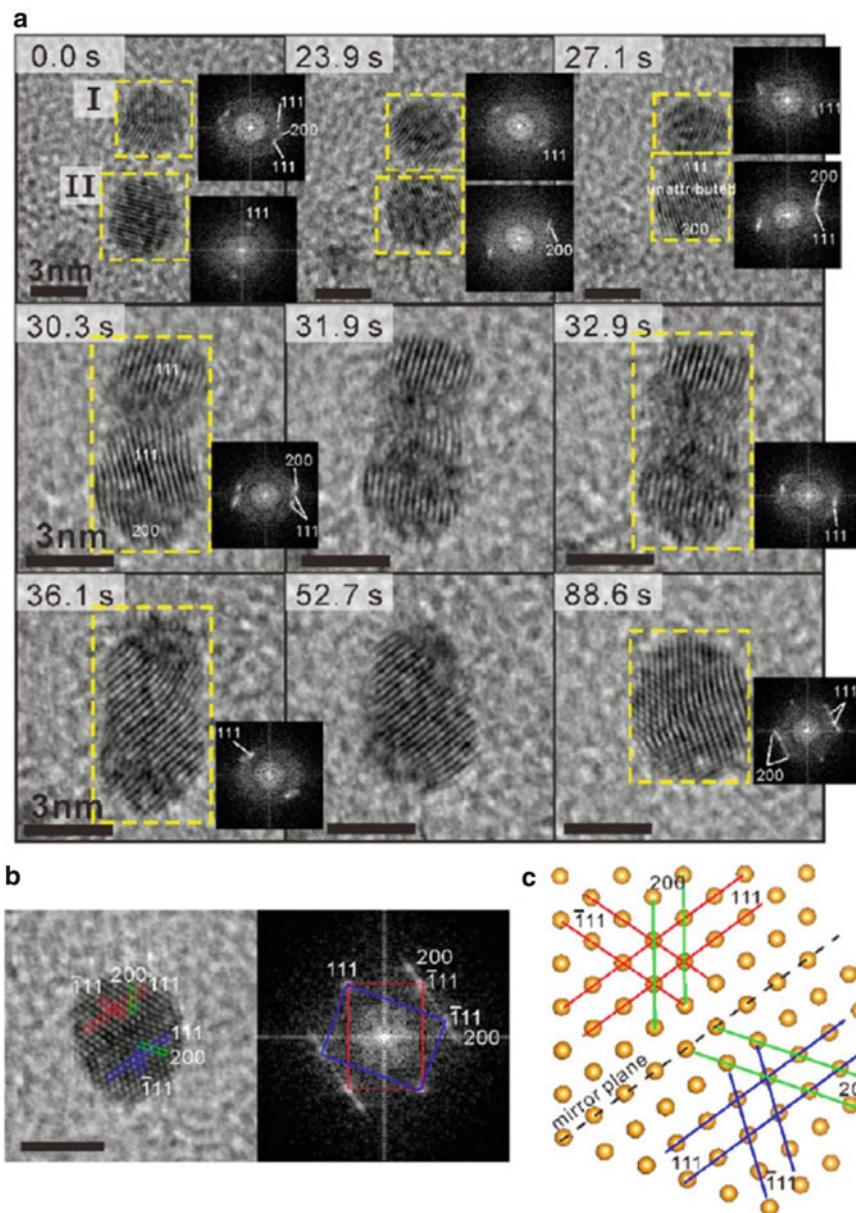


Fig. 10 Sequential formation of a sub-5 nm twinned nanocrystal (B) from the attachment of a multiply twinned (I) nanocrystal and a single-crystalline (II) nanocrystal via rotation, coalescence and relaxation steps. The schema shows the nanocrystal B and specially highlights the twin plane which acts as a (111) mirror plane [64]

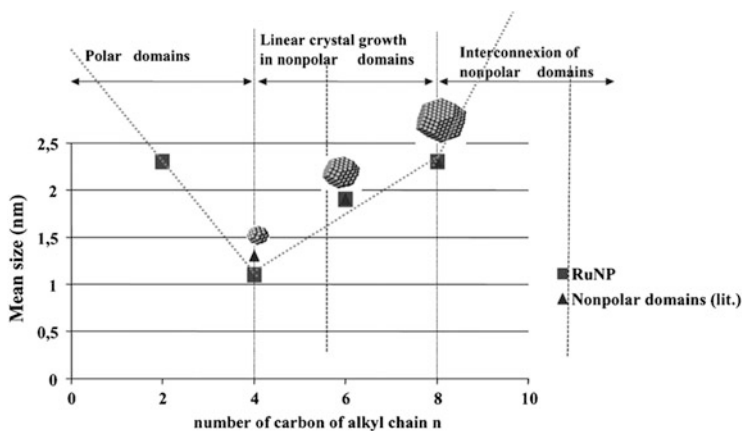


Fig. 11 Size of Ru metal nanoparticles depending on the number of carbons (n) in the alkyl chain (C_n) of $[C_nC_1Im][NTf_2]$ [65]

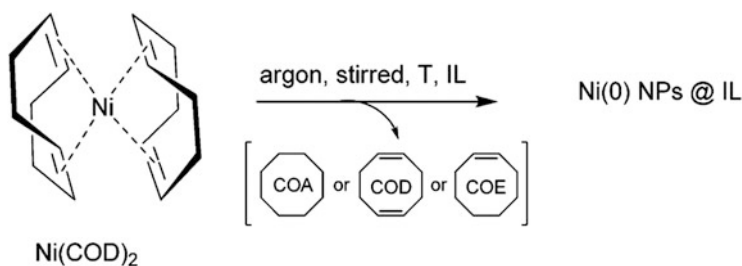


Fig. 12 Ni metal nanoparticles prepared via the room-temperature decomposition of $Ni(COD)_2$ in imidazolium ILs $[C_xC_yC_zIm][NTf_2]$ under inert atmosphere (no dihydrogen was required) [66]

addition of a nonpolar substance in these ILs increased the size of the nonpolar domains and therefore the size of the Ru nanoparticles prepared from $Ru(COD)(COT)$ in these nanodomains. For example, Ru metal nanoparticles of 2.4 ± 0.3 nm were prepared at room temperature in $[C_4C_1Im][NTf_2]$, whereas the addition of cyclooctane (0.5 mol per mole of $Ru(COD)(COT)$) favored the agglomeration of the Ru nanoparticles. This effect of nonpolar compounds in $[C_4C_1Im][NTf_2]$ is similar to previous studies on the synthesis of Ru metal nanoparticles from $Ru(COD)(COT)$ in conventional solvents (i.e. THF/methanol mixtures) [41, 42].

The properties of the alkyl chains also had a strong impact on the size of Ni nanoparticles prepared from $Ni(COD)_2$ in imidazolium ionic liquids [36, 66, 67]. Interestingly, Prechtel, Santini, Dupont and co-workers achieved the room-temperature synthesis of Ni nanoparticles via the auto-decomposition of $Ni(COD)_2$ in the absence of dihydrogen in imidazolium ILs with short alkyl chains (i.e. $[C_2C_1Im][NTf_2]$, $[C_4C_1Im][NTf_2]$ and $[C_4C_4C_1Im][NTf_2]$; $C_4C_4C_1Im$: 1,2-d-*n*-butyl-3-methylimidazolium) (Fig. 12). Whilst sponge-like agglomerates were

obtained in $[\text{C}_2\text{C}_1\text{Im}][\text{NTf}_2]$ and $[\text{C}_4\text{C}_1\text{Im}][\text{NTf}_2]$, well-dispersed metal nanoparticles of 7 ± 2 nm were prepared in $[\text{C}_4\text{C}_4\text{C}_1\text{Im}][\text{NTf}_2]$ at 25°C under inert atmosphere [36]. Mudring and co-workers adapted this facile synthesis for controlling the diameter (d) of monodisperse Ni metal nanoparticles in $[\text{C}_x\text{C}_y\text{C}_z\text{Im}][\text{NTf}_2]$ ILs by using imidazolium cations with longer alkyl chains, e.g. $d = 2.4 \pm 0.8$ nm in $[\text{C}_{12}\text{C}_1\text{Im}][\text{NTf}_2]$, 2.9 ± 0.4 nm in $[\text{C}_{18}\text{C}_1\text{Im}][\text{NTf}_2]$, 4.0 ± 0.5 nm in $[\text{C}_{12}\text{C}_{12}\text{Im}][\text{NTf}_2]$ and 4.4 ± 0.7 nm in $[\text{C}_{12}\text{C}_1\text{C}_{12}\text{Im}][\text{NTf}_2]$. The connexion of two imidazolium cations $[\text{C}_R\text{C}_{12}\text{Im}]^+$ via a hexanediyli linker led to Ni metal nanoparticles of 5.4 ± 1.6 nm, whereas a bridging ether (oxydi-2,1-ethanediyli) resulted in the highest size uniformity ($d = 3.4 \pm 0.2$ nm) obtained in this system.

Similarly to preparations in conventional solvents [16, 24], successful syntheses of nanocrystals have been achieved by using different organometallic complexes such as $\text{Rh}(\text{allyl})_3$ and $\text{Cu}(\text{Mes})$ [4, 51, 68, 69]. Furthermore, promising metal precursors have still to be investigated, e.g. $\text{Co}(\text{COD})(\text{COE})$ (COE: cyclooctadienyli).

4.3 Size Control via the IL Anion

Furthermore, the nanoparticles' size can depend on the IL anion. For example, Janiak and co-workers reported that silver nanoparticles, prepared from AgIX salts (X: BF_4^- , PF_6^- , TfO^- trifluoromethanesulphonate CF_3SO_3^-) in $[\text{C}_4\text{C}_1\text{Im}][\text{Y}]$ ILs at 85°C for 2 h under H_2 (4 atm), were larger with increasing anion (Y) molecular volume. As a result, the size increased from 2.8 to 26.1 nm by using BF_4^- , PF_6^- , CF_3SO_3^- , bis(trifluoromethylsulphonyl)imide or $\text{N}(\text{CF}_3\text{SO}_2)_2^-$ [57].

Taubert et al. prepared gold nanoparticles via the reduction of $\text{HAuCl}_4 \cdot 3\text{H}_2\text{O}$ (65 μmol) in the presence of glycerol (0.2 mmol) as a reducing agent in 1 g $[\text{C}_2\text{C}_1\text{Im}][\text{Y}]$ ILs (Y: ethyl sulphate $\text{C}_2\text{H}_5\text{SO}_4^-$, CF_3SO_3^- , methanesulphonate CH_3SO_3^-) at $120\text{--}180^\circ\text{C}$ for 24 h [70]. As a result, the size of the gold nanoparticles was between ~ 5 and 20 nm depending on both temperature and IL anion [71].

Dupont et al. also proposed that the nanoparticle size was related to the IL anion in the synthesis of Co nanoparticles. The injection of $\text{Co}_2(\text{CO})_8$ (0.05 mmol in 10 mL hexane) into 0.5 mL of IL at 150°C led to diameters of $4.5 + 0.6$ nm in 1-*n*-decyl-3-methylimidazolium tetrafluoroborate ($[\text{C}_{10}\text{C}_1\text{Im}][\text{BF}_4]$) and $7.7 + 1.2$ nm in $[\text{C}_{10}\text{C}_1\text{Im}][\text{NTf}_2]$ [72].

Furthermore, this group obtained Rh nanoparticles of different sizes via the reduction of RhCl_3 at 75°C under hydrogen atmosphere in $[\text{C}_4\text{C}_1\text{Im}]^+$ ILs, i.e. $d = 2.7$ nm and 5 nm with PF_6^- and BF_4^- , respectively [73, 74]. The choice of the precursor was also critical since $[\text{RhCl}(\text{COD})]_2$ in $[\text{C}_4\text{C}_1\text{Im}][\text{PF}_6]$ led to larger and polydisperse Rh nanoparticles ($d = 15$ nm via XRD) [73, 75].

In conclusion, the nature of both anions and cations strongly impacts the physicochemical properties of ILs and therefore the nucleation, growth, stabilisation, dissolution, agglomeration and self-organisation of metal nanoparticles in ILs due to various interactions between the IL and different species

in solution such as the metal precursor. Further investigations are required to understand the relationships between the properties of ILs and the size of the metal nanoparticles.

4.4 *Size Control in the Presence of Conventional Stabilisers in ILs*

The addition of conventional ligands has been used to control the size of monodisperse nanocrystals in ILs. For example, Yang et al. carried out the preparation of uniform metal and metal oxide nanoparticles in $[\text{C}_4\text{C}_1\text{Im}][\text{NTf}_2]$ in the presence of cetyltrimethylammonium bromide (CTAB), oleic acid or oleylamine which are ubiquitous stabilisers in conventional aqueous and organic solvents.

The synthesis of monodisperse Ag nanoparticles was achieved at 160 or 200°C under argon using an excess of a stabilising agent compared to the quantity of a metal precursor (CF_3COOAg) such as the oleic acid–silver trifluoroacetate molar ratio (x) = 3 or 6 [50]. This excess is even much higher once reported to the number of atoms at the surface of the prepared nano-objects. Although the silver salt has a low solubility at room temperature in $[\text{C}_4\text{C}_1\text{Im}][\text{NTf}_2]$, a homogeneous solution was obtained at $\sim 150^\circ\text{C}$ in the presence of both oleic acid (~ 0.50 mmol) and CF_3COOAg in the IL. In addition, metal carboxylate complexes are usually obtained in situ due to the simultaneous presence of various carboxylic acids and metal precursors, such as oleic acid and CF_3COOAg . The low temperature ramp rate (1.5 or 2°C min^{-1}) can lead to the controlled build-up of monomers in solution via the thermal decomposition of silver oleate complexes. This “heating-up” approach, initiated by Hyeon et al., has been extensively used in conventional solvents [4, 25].

At 160°C , silver nanoparticles of 4.1 ± 0.5 nm were prepared at $x=6$ and 6.1 ± 0.8 nm at $x=3$. At 200°C , the increase of the molar ratio x resulted in smaller nanoparticles, i.e. 4.5 ± 0.4 nm at $x=6$ and 5.1 ± 0.7 nm at $x=3$, whilst a higher ratio favoured the uniformity of size at 160 and 200°C . The increase of temperature positively impacted the nanoparticle yields. In addition, higher yields were obtained following the increase of x at 160 and 200°C . As a result, the highest yield ($\sim 70\%$) was reported at $x=6$ and 200°C . As shown on Fig. 13, the self-assembly of these Ag nanoparticles in a two-dimensional superlattice reflected their monodispersity. It is worth mentioning that the nanoparticles can be efficiently separated from $[\text{C}_4\text{C}_1\text{Im}][\text{NTf}_2]$ via a simple settling step as demonstrated by UV and TGA studies. Furthermore, oleic acid-capped nanocrystals can be efficiently dispersed in nonpolar conventional solvents.

For the synthesis of Pt metal nanocrystals, Yang et al. selected a different strategy which has been widely employed for the facile preparation of well-defined nanocrystals in conventional polyol solvents [2, 77]. In their work in $[\text{C}_4\text{C}_1\text{Im}][\text{NTf}_2]$ (5 mL), 1,2-hexanediol (0.34 mmol) was used as a reducing agent in

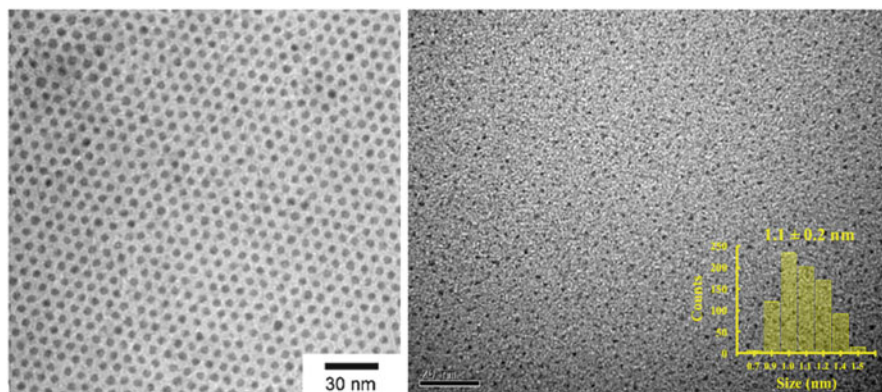


Fig. 13 TEM images of (*left*) oleic acid-capped silver nanoparticles prepared in $[\text{C}_4\text{C}_1\text{Im}][\text{NTf}_2]$ at silver trifluoroacetate–oleic acid molar ratio of 1:6 at 200°C [50]; (*right*) $[\text{C}_{10}\text{C}_1\text{Im}][\text{MPS}]-\text{Au}_{25}$ clusters prepared from MPS– Au_{25} clusters and $[\text{C}_{10}\text{C}_1\text{Im}][\text{Cl}]$ in CH_3CN ; MPS: (3-mercaptopropyl)sulphonate [76]

the presence of a conventional combination of ligands, i.e. oleic acid (~ 0.13 mmol) and oleylamine (0.09 mmol). As discussed herein, these ligands can be involved in molecular complexes formed from the metal precursor [4, 23–26]. As a result, metallic Pt nanoparticles of 4.5 ± 0.8 nm were prepared at 230°C under argon via the reduction of $\text{Pt}(\text{acac})_2$ (0.07 mmol). The simultaneous presence of both ligands was important since the absence of oleic acid in this system led to irregularly shaped nanoparticles, whereas the absence of oleylamine resulted in agglomerates obtained from 5 nm nanoparticles.

The group of Bockstaller prepared gold nanoparticles of different sizes in $[\text{C}_2\text{C}_1\text{Im}][\text{C}_2\text{H}_5\text{SO}_4]$ via the control of the nucleation rate [78]. As discussed herein, larger nanoparticles can be obtained at lower nucleation rates, e.g. under milder reducing conditions. The reduction of HAuCl_4 by citrate ions resulted in 9.4 ± 3 nm. In the presence of CTAB (cetyltrimethylammonium bromide), using a stronger reducing agent, i.e. NaBH_4 , led to smaller nanoparticles: 6.5 ± 2.1 nm at 25°C and 3.9 ± 1.6 nm at 0°C, the size being inversely proportional to the quantity of NaBH_4 .

Yang et al. reported the synthesis of iron oxide nanospheres from the thermal decomposition of a metal carbonyl precursor in an imidazolium IL [79]. The transformation of $\text{Fe}(\text{CO})_5$ (0.25 mmol) was achieved under argon atmosphere in the colourless $[\text{C}_4\text{C}_1\text{Im}][\text{NTf}_2]$ (5 mL). The solution turned black at 150–160°C and oleic acid (0.38 mmol) was then injected at 165°C. Then, the reaction medium was heated up to 280°C and kept at this temperature for 1 h. For an oleic acid-to- $\text{Fe}(\text{CO})_5$ molar ratio of 1.5 and a $\text{Fe}(\text{CO})_5$ concentration of 0.05 M, this method resulted in the synthesis of 10.6 ± 1.6 nm iron oxide nanoparticles. As discussed herein, the efficient separation of the nanoparticles from the IL occurred via a simple settling step. This allowed the facile reuse of $[\text{C}_4\text{C}_1\text{Im}][\text{NTf}_2]$ at recycling

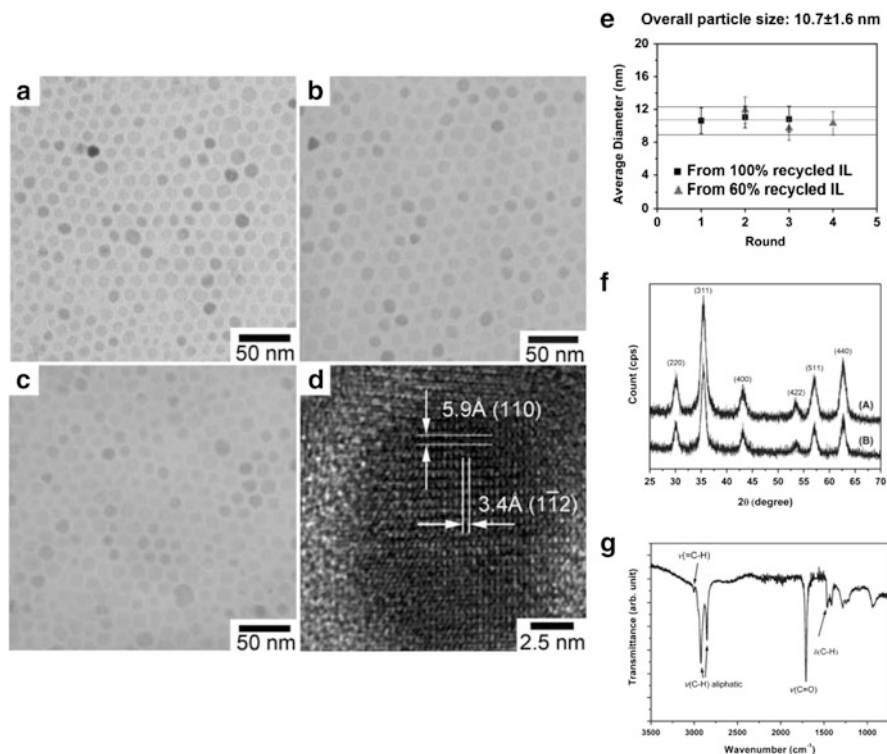


Fig. 14 TEM images of iron oxide nanoparticles prepared (a) in freshly made, (b) second-use, (c) third-use recycled [C₄C₁Im][NTf₂] 100% (v/v), (oleic acid–Fe(CO)₅ molar ratio = 1.5, [Fe(CO)₅] = 0.05 M; (d) HRTEM image of a nanoparticle; (e) average size and distribution of iron oxide nanoparticles prepared in recycled [C₄C₁Im][NTf₂] (square, 100% (v/v), triangle, 60% (v/v)); (f) X-ray diffractograms of nanoparticles prepared in (a) freshly made and (b) 60% (v/v) recycled [C₄C₁Im][NTf₂]; (g) FTIR spectrum of the iron oxide nanoparticles [79]

ratio of 60 or 100% (v/v), at least two times, for the synthesis of monodisperse iron oxide nanoparticles which self-assembled in superlattices and had the same size than nanoparticles prepared in fresh [C₄C₁Im][NTf₂] (Fig. 14e). HRTEM image showed a single-crystalline particle (Fig. 14d). FTIR spectroscopy, which is an efficient technique to probe the surface of the nanoparticles [17], showed that the iron oxide nanoparticles exhibited typical carboxylic C=O and C–H bands. Since no band was assigned to the IL, only oleic acid was present at the surface. In addition, similar X-ray diffractograms were obtained for nanoparticles prepared in fresh or recycled (60% (v/v)) [C₄C₁Im][NTf₂] (Fig. 14f). FTIR and TGA studies of fresh and recycled [C₄C₁Im][NTf₂] showed no significant evolution of the IL properties after four runs in despite of a slight change of the solution colour.

In conventional solvents, the “polyol” approach has frequently used 1,2-hexanediol in combination with oleic acid and oleylamine, as discussed

herein for the synthesis of metal nanocrystals. In $[\text{C}_4\text{C}_1\text{Im}][\text{NTf}_2]$ (5 mL), the “polyol” strategy led to 8 ± 1 nm iron oxide nanoparticles from $[\text{Fe}(\text{CO})_5]$ (0.25 mmol) in the presence of oleic acid (0.2 mmol), oleylamine (0.03 mmol) and 1,2-hexanediol (0.34 mmol) [79]. Studies of the magnetic properties, via SQUID, showed that these 8 nm superparamagnetic particles exhibited a coercivity of 360 Oe at 5 K and a saturation magnetisation (M_s) of $\sim 50 \text{ emu.g}^{-1}$ at 5 K. Using a similar protocol, further studies showed that the reaction temperature (270°C to 288°C) was a key point for controlling the size of iron nanospheres in the sub-10 nm range in $[\text{C}_4\text{C}_1\text{Im}][\text{NTf}_2]$ [80].

Recently, the preparation of atomically defined nano-objects, especially gold nanoclusters, has been highly investigated [81, 82]. Lee et al. exploited these advances and achieved the synthesis of MPS-capped Au_{25} nanoclusters (MPS: 3-mercaptopropyl)sulphonate) showed on the Fig. 13. Then, the association between the sulphonate site of MPS and the cationic site of $[\text{C}_{10}\text{C}_1\text{Im}]$ led to the synthesis of $[\text{C}_{10}\text{C}_1\text{Im}][\text{MPS}]-\text{Au}_{25}$ clusters from MPS-capped Au_{25} and $[\text{C}_{10}\text{C}_1\text{Im}][\text{Cl}]$ in CH_3CN [76].

The addition of conventional stabilisers in ILs has been an efficient strategy for the transfer to ILs of advanced methodologies developed in conventional solvents. The size control of metal nanocrystals has also been achieved in modified ILs [52, 83]. For example, in $[\text{C}_2\text{OHC}_1\text{Im}]$ ILs, the nature of the IL anion impacted the nanoparticles’ size following the functionalisation of the ethyl chain with a hydroxyl group [83]. In these functionalized $[\text{C}_2\text{OHC}_1\text{Im}]$ ILs, the oxidation of the metal nanoparticles also depended on the IL anion.

Whilst the synthesis of multimetallic nanocrystals has been widely explored in conventional solvents, only a few preparations have been reported in ILs. For example, Santini et al. achieved the synthesis of Ru@Cu nanoparticles via the one-pot decomposition of $\text{Ru}(\text{COD})(\text{COT})$ and mesitylcopper (CuMes) in $[\text{C}_1\text{C}_4\text{Im}][\text{NTf}_2]$ under H_2 (0.9 MPa) at 100°C for 4 h [69]. The formation of monometallic nanoparticles being significantly faster from $\text{Ru}(\text{COD})(\text{COT})$, Ru nanoparticles were first obtained. Then, the controlled decomposition of CuMes allowed the preferential deposition of copper onto these Ru cores as demonstrated via a combination of techniques, i.e. electron energy loss spectroscopy (EELS), X-ray photoelectron spectroscopy (XPS), X-ray Auger electron spectroscopy, electron-dispersive X-ray (EDX) and HRTEM. The composition of these monodisperse Ru@Cu nanoparticles was controlled via the molar ratios of the metal precursors. Higher $\text{CuMes}/\text{Ru}(\text{COD})(\text{COT})$ molar ratios (x) led to larger nanoparticles; their size is 1.8 nm for $x = 0.005$ and 3.4 nm for $x = 10$. In addition, the hydrogenation of benzene was used as a complementary tool to study the surface of the Ru@Cu nanoparticles since monometallic Cu are not active unlike the Ru nanoparticles.

5 Conclusions

Over the last decade, significant advances for the efficient synthesis of uniform nanocrystals have occurred simultaneously with the development of ionic liquids. As a result, precise preparations of uniform metal, metal oxide and alloy nanocrystals have been achieved by exploiting ILs properties. This chapter presented the most promising strategies to engineer uniform nanocrystals via recent achievements in the size control of these monodisperse nano-objects in the presence of ionic liquids which play the role of solvent, stabiliser, reducing agent and even precursor.

For example, the selection of specific IL anions or cations has been an efficient strategy for controlling the size of monodisperse nanocrystals via a combination of non-covalent interactions. Further approaches for the efficient size control, stabilisation and use of uniform nanocrystals are the injection of traditional stabilising agents in ILs as well as the *in situ* delivery of conventional stabilisers formed *in operando* from ILs. In addition, ILs were functionalized with specific reducers or stabilising groups to offer an even more subtle control. *In situ* HRTEM studies highlighted that the formation of nanocrystals can occur in ILs similarly than in conventional solvents.

These achievements are going to drive the identification of relationships between the nature of ILs components, the physicochemical properties of ILs, the formation of nano-objects in ILs and the resulting properties of these nano-objects in ILs. Furthermore, the transfer of methods from conventional solvents to ILs could result in even more sophisticated design of nanocrystals as building blocks of functional systems in the areas of catalysis and energy. By analogy with conventional solvents, these strategies can be suitable for the preparation of semiconductor nanocrystals [84]. Finally, it would be potentially relevant to investigate the presence and role of intermediate species during the formation and evolution of nanocrystals.

References

1. Yu Y, Zhang Q, Yao Q et al (2014) Architectural design of heterogeneous metallic nanocrystals – principles and processes. *Acc Chem Res* 47:3530–3540. doi:[10.1021/ar5002704](https://doi.org/10.1021/ar5002704)
2. Xia Y, Xiong Y, Lim B, Skrabalak SE (2009) Shape-controlled synthesis of metal nanocrystals: simple chemistry meets complex physics? *Angew Chem Int Ed* 48:60–103. doi:[10.1002/anie.200802248](https://doi.org/10.1002/anie.200802248)
3. Buck MR, Schaak RE (2013) Emerging strategies for the total synthesis of inorganic nanostructures. *Angew Chem Int Ed* 52:6154–6178. doi:[10.1002/anie.201207240](https://doi.org/10.1002/anie.201207240)
4. Lignier P, Bellabarba R, Tooze RP (2012) Scalable strategies for the synthesis of well-defined copper metal and oxide nanocrystals. *Chem Soc Rev* 41:1708–1720. doi:[10.1039/C1CS15223H](https://doi.org/10.1039/C1CS15223H)

5. Dupont J, Fonseca GS, Umpierre AP et al (2002) Transition-metal nanoparticles in imidazolium ionic liquids: recyclable catalysts for biphasic hydrogenation reactions. *J Am Chem Soc* 124:4228–4229. doi:[10.1021/ja025818u](https://doi.org/10.1021/ja025818u)
6. Zhou Y, Antonietti M (2003) Synthesis of very small TiO₂ nanocrystals in a room-temperature ionic liquid and their self-assembly toward mesoporous spherical aggregates. *J Am Chem Soc* 125:14960–14961. doi:[10.1021/ja0380998](https://doi.org/10.1021/ja0380998)
7. Zhou Y, Schattka JH, Antonietti M (2004) Room-temperature ionic liquids as template to monolithic mesoporous silica with wormlike pores via a sol–gel nanocasting technique. *Nano Lett* 4:477–481. doi:[10.1021/nl025861f](https://doi.org/10.1021/nl025861f)
8. Zhou Y, Antonietti M (2004) A series of highly ordered, super-microporous, lamellar silicas prepared by nanocasting with ionic liquids. *Chem Mater* 16:544–550. doi:[10.1021/cm034442w](https://doi.org/10.1021/cm034442w)
9. Parnham ER, Morris RE (2007) Ionothermal synthesis of zeolites, metal–organic frameworks, and inorganic–organic hybrids. *Acc Chem Res* 40:1005–1013. doi:[10.1021/ar700025k](https://doi.org/10.1021/ar700025k)
10. Dupont J, Scholten JD (2010) On the structural and surface properties of transition-metal nanoparticles in ionic liquids. *Chem Soc Rev* 39:1780–1804. doi:[10.1039/B822551F](https://doi.org/10.1039/B822551F)
11. Vollmer C, Janiak C (2011) Naked metal nanoparticles from metal carbonyls in ionic liquids: easy synthesis and stabilization. *Coord Chem Rev* 255:2039–2057. doi:[10.1016/j.ccr.2011.03.005](https://doi.org/10.1016/j.ccr.2011.03.005)
12. Scholten JD, Leal BC, Dupont J (2011) Transition metal nanoparticle catalysis in ionic liquids. *ACS Catal* 2:184–200. doi:[10.1021/cs200525e](https://doi.org/10.1021/cs200525e)
13. Zhang P, Wu T, Han B (2014) Preparation of catalytic materials using ionic liquids as the media and functional components. *Adv Mater* 26:6810–6827. doi:[10.1002/adma.201305448](https://doi.org/10.1002/adma.201305448)
14. Gebresilassie Eshetu G, Armand M, Scrosati B, Passerini S (2014) Energy storage materials synthesized from ionic liquids. *Angew Chem Int Ed* 53:13342–13359. doi:[10.1002/anie.201405910](https://doi.org/10.1002/anie.201405910)
15. Niu Z, Li Y (2013) Removal and utilization of capping agents in nanocatalysis. *Chem Mater* 26:72–83. doi:[10.1021/cm4022479](https://doi.org/10.1021/cm4022479)
16. Amiens C, Chaudret B, Ciuculescu-Pradines D et al (2013) Organometallic approach for the synthesis of nanostructures. *New J Chem* 37:3374. doi:[10.1039/c3nj00650f](https://doi.org/10.1039/c3nj00650f)
17. Philippot K, Lignier P, Chaudret B (2014) Organometallic ruthenium nanoparticles and catalysis. In: Dixneuf PH, Bruneau C (eds) *Ruthenium in catalysis*. Springer, Heidelberg, pp 319–370
18. Salas G, Podgoršek A, Campbell PS et al (2011) Ruthenium nanoparticles in ionic liquids: structural and stability effects of polar solutes. *Phys Chem Chem Phys* 13:13527. doi:[10.1039/c1cp20623k](https://doi.org/10.1039/c1cp20623k)
19. Pery T, Pelzer K, Buntkowsky G et al (2005) Direct NMR evidence for the presence of mobile surface hydrides on ruthenium nanoparticles. *Chemphyschem* 6:605–607. doi:[10.1002/cphc.200400621](https://doi.org/10.1002/cphc.200400621)
20. García-Antón J, Axet MR, Jansat S et al (2008) Reactions of olefins with ruthenium hydride nanoparticles: NMR characterization, hydride titration, and room-temperature C–C bond activation. *Angew Chem Int Ed* 47:2074–2078. doi:[10.1002/anie.200704763](https://doi.org/10.1002/anie.200704763)
21. Lignier P, Comotti M, Schüth F et al (2009) Effect of the titania morphology on the Au/TiO₂-catalyzed aerobic epoxidation of stilbene. *Catal Today* 141:355–360. doi:[10.1016/j.cattod.2008.04.032](https://doi.org/10.1016/j.cattod.2008.04.032)
22. Lignier P, Bellabarba R, Tooze RP et al (2011) Facile synthesis of branched ruthenium nanocrystals and their use in catalysis. *Cryst Growth Des* 12:939–942. doi:[10.1021/cg201408h](https://doi.org/10.1021/cg201408h)
23. Liakakos N, Cormary B, Li X et al (2012) The big impact of a small detail: cobalt nanocrystal polymorphism as a result of precursor addition rate during stock solution preparation. *J Am Chem Soc* 134:17922–17931. doi:[10.1021/ja304487b](https://doi.org/10.1021/ja304487b)
24. Comesaña-Hermo M, Estivill R, Ciuculescu D et al (2014) Effect of a side reaction involving structural changes of the surfactants on the shape control of cobalt nanoparticles. *Langmuir* 30:4474–4482. doi:[10.1021/la5005165](https://doi.org/10.1021/la5005165)

25. Park J, Joo J, Kwon SG et al (2007) Synthesis of monodisperse spherical nanocrystals. *Angew Chem Int Ed* 46:4630–4660. doi:[10.1002/anie.200603148](https://doi.org/10.1002/anie.200603148)
26. Ortiz N, Skrabalak SE (2014) On the dual roles of ligands in the synthesis of colloidal metal nanostructures. *Langmuir* 30:6649–6659. doi:[10.1021/la404539p](https://doi.org/10.1021/la404539p)
27. Cademartiri L, Kitaev V (2011) On the nature and importance of the transition between molecules and nanocrystals: towards a chemistry of “nanoscale perfection”. *Nanoscale* 3:3435–3446. doi:[10.1039/C1NR10365B](https://doi.org/10.1039/C1NR10365B)
28. Mourdikoudis S, Liz-Marzán LM (2013) Oleylamine in nanoparticle synthesis. *Chem Mater* 25:1465–1476. doi:[10.1021/cm4000476](https://doi.org/10.1021/cm4000476)
29. Wu Y, Wang D, Li Y (2014) Nanocrystals from solutions: catalysts. *Chem Soc Rev* 43:2112–2124. doi:[10.1039/C3CS60221D](https://doi.org/10.1039/C3CS60221D)
30. Chng LL, Erathodiyil N, Ying JY (2013) Nanostructured catalysts for organic transformations. *Acc Chem Res* 46:1825–1837. doi:[10.1021/ar300197s](https://doi.org/10.1021/ar300197s)
31. Niedermeyer H, Hallett JP, Villar-Garcia IJ et al (2012) Mixtures of ionic liquids. *Chem Soc Rev* 41:7780. doi:[10.1039/c2cs35177c](https://doi.org/10.1039/c2cs35177c)
32. Egorova KS, Ananikov VP (2014) Toxicity of ionic liquids: eco(cyto)activity as complicated, but unavoidable parameter for task-specific optimization. *ChemSusChem* 7:336–360. doi:[10.1002/cssc.201300459](https://doi.org/10.1002/cssc.201300459)
33. Paternò A, D’Anna F, Musumarra G et al (2014) A multivariate insight into ionic liquids toxicities. *RSC Adv* 4:23985. doi:[10.1039/c4ra03230f](https://doi.org/10.1039/c4ra03230f)
34. Canongia Lopes JNA, Pádua AAH (2006) Nanostructural organization in ionic liquids. *J Phys Chem B* 110:3330–3335. doi:[10.1021/jp056006y](https://doi.org/10.1021/jp056006y)
35. Prechtl MHG, Scariot M, Scholten JD et al (2008) Nanoscale Ru(0) particles: arene hydrogenation catalysts in imidazolium ionic liquids. *Inorg Chem* 47:8995–9001. doi:[10.1021/ic801014f](https://doi.org/10.1021/ic801014f)
36. Prechtl MHG, Campbell PS, Scholten JD et al (2010) Imidazolium ionic liquids as promoters and stabilising agents for the preparation of metal(0) nanoparticles by reduction and decomposition of organometallic complexes. *Nanoscale* 2:2601–2606. doi:[10.1039/CONR00574F](https://doi.org/10.1039/CONR00574F)
37. Luska KL, Moores A (2012) Ruthenium nanoparticle catalysts stabilized in phosphonium and imidazolium ionic liquids: dependence of catalyst stability and activity on the ionicity of the ionic liquid. *Green Chem* 14:1736. doi:[10.1039/c2gc35241a](https://doi.org/10.1039/c2gc35241a)
38. Santos LMNBF, Canongia Lopes JN, Coutinho JAP et al (2006) Ionic liquids: first direct determination of their cohesive energy. *J Am Chem Soc* 129:284–285. doi:[10.1021/ja067427b](https://doi.org/10.1021/ja067427b)
39. Podgoršek A, Pensado AS, Santini CC et al (2013) Interaction energies of ionic liquids with metallic nanoparticles: solvation and stabilization effects. *J Phys Chem C* 117:3537–3547. doi:[10.1021/jp309064u](https://doi.org/10.1021/jp309064u)
40. Campbell PS, Santini CC, Bouchu D et al (2010) A novel stabilisation model for ruthenium nanoparticles in imidazolium ionic liquids: in situ spectroscopic and labelling evidence. *Phys Chem Chem Phys* 12:4217–4223. doi:[10.1039/B925329G](https://doi.org/10.1039/B925329G)
41. Vidoni O, Philippot K, Amiens C et al (1999) Novel, spongelike ruthenium particles of controllable size stabilized only by organic solvents. *Angew Chem Int Ed* 38:3736–3738. doi:[10.1002/\(SICI\)1521-3773\(19991216\)38:24<3736::AID-ANIE3736>3.0.CO;2-E](https://doi.org/10.1002/(SICI)1521-3773(19991216)38:24<3736::AID-ANIE3736>3.0.CO;2-E)
42. Pelzer K, Vidoni O, Philippot K et al (2003) Organometallic synthesis of size-controlled polycrystalline ruthenium nanoparticles in the presence of alcohols. *Adv Funct Mater* 13:118–126. doi:[10.1002/adfm.200390017](https://doi.org/10.1002/adfm.200390017)
43. Ott LS, Cline ML, Deetlefs M et al (2005) Nanoclusters in ionic liquids: evidence for N-heterocyclic carbene formation from imidazolium-based ionic liquids detected by ²H NMR. *J Am Chem Soc* 127:5758–5759. doi:[10.1021/ja0423320](https://doi.org/10.1021/ja0423320)
44. Scholten JD, Ebeling G, Dupont J (2007) On the involvement of NHC carbenes in catalytic reactions by iridium complexes, nanoparticle and bulk metal dispersed in imidazolium ionic liquids. *Dalton Trans* 5554–5560. doi:[10.1039/B707888A](https://doi.org/10.1039/B707888A)
45. Chen W, Davies JR, Ghosh D et al (2006) Carbene-functionalized ruthenium nanoparticles. *Chem Mater* 18:5253–5259. doi:[10.1021/cm061595l](https://doi.org/10.1021/cm061595l)

46. Vignolle J, Tilley TD (2009) N-Heterocyclic carbene-stabilized gold nanoparticles and their assembly into 3D superlattices. *Chem Commun* 7230. doi:10.1039/b913884f
47. Lara P, Rivada-Wheelaghan O, Conejero S et al (2011) Ruthenium nanoparticles stabilized by N-heterocyclic carbenes: ligand location and influence on reactivity. *Angew Chem Int Ed* 50:12080–12084. doi:10.1002/anie.201106348
48. Baquero EA, Tricard S, Flores JC et al (2014) Highly stable water-soluble platinum nanoparticles stabilized by hydrophilic N-heterocyclic carbenes. *Angew Chem* 126:13436–13440. doi:10.1002/ange.201407758
49. Ling X, Roland S, Pileni M-P (2015) Supracrystals of N-heterocyclic carbene-coated Au nanocrystals. *Chem Mater* 27:414–423. doi:10.1021/cm502714s
50. Wang Y, Yang H (2006) Oleic acid as the capping agent in the synthesis of noble metal nanoparticles in imidazolium-based ionic liquids. *Chem Commun* 2545–2547. doi:10.1039/B604269D
51. Darwich W, Gedig C, Srour H et al (2013) Single step synthesis of metallic nanoparticles using dihydroxyl functionalized ionic liquids as reductive agent. *RSC Adv* 3:20324. doi:10.1039/c3ra43909g
52. Luska KL, Moores A (2012) Functionalized ionic liquids for the synthesis of metal nanoparticles and their application in catalysis. *ChemCatChem* 4:1534–1546. doi:10.1002/cctc.201100366
53. Dinda E, Si S, Kotal A, Mandal TK (2008) Novel ascorbic acid based ionic liquids for the in situ synthesis of quasi-spherical and anisotropic gold nanostructures in aqueous medium. *Chem Eur J* 14:5528–5537. doi:10.1002/chem.200800006
54. Yang X, Yan N, Fei Z et al (2008) Biphasic hydrogenation over PVP stabilized Rh nanoparticles in hydroxyl functionalized ionic liquids. *Inorg Chem* 47:7444–7446. doi:10.1021/ic8009145
55. Neouze M-A (2010) About the interactions between nanoparticles and imidazolium moieties: emergence of original hybrid materials. *J Mater Chem* 20:9593. doi:10.1039/c0jm00616e
56. Anthony JL, Anderson JL, Maginn EJ, Brennecke JF (2005) Anion effects on gas solubility in ionic liquids. *J Phys Chem B* 109:6366–6374. doi:10.1021/jp0464041
57. Redel E, Thomann R, Janiak C (2008) First correlation of nanoparticle size-dependent formation with the ionic liquid anion molecular volume. *Inorg Chem* 47:14–16. doi:10.1021/ic702071w
58. Li C, Gu L, Tsukimoto S et al (2010) Low-temperature ionic-liquid-based synthesis of nanostructured iron-based fluoride cathodes for lithium batteries. *Adv Mater* 22:3650–3654. doi:10.1002/adma.201000535
59. Van Santen RA (2009) Complementary structure sensitive and insensitive catalytic relationships. *Acc Chem Res* 42:57–66. doi:10.1021/ar800022m
60. Zheng H, Smith RK, Jun Y et al (2009) Observation of single colloidal platinum nanocrystal growth trajectories. *Science* 324:1309–1312. doi:10.1126/science.1172104
61. Yamada Y, Tsung C-K, Huang W et al (2011) Nanocrystal bilayer for tandem catalysis. *Nat Chem* 3:372–376. doi:10.1038/nchem.1018
62. Kang Y, Ye X, Chen J et al (2013) Engineering catalytic contacts and thermal stability: gold/iron oxide binary nanocrystal superlattices for CO oxidation. *J Am Chem Soc* 135:1499–1505. doi:10.1021/ja310427u
63. Shevchenko EV, Talapin DV, Schnablegger H et al (2003) Study of nucleation and growth in the organometallic synthesis of magnetic alloy nanocrystals: the role of nucleation rate in size control of CoPt₃ nanocrystals. *J Am Chem Soc* 125:9090–9101. doi:10.1021/ja029937I
64. Uematsu T, Baba M, Oshima Y et al (2014) Atomic resolution imaging of gold nanoparticle generation and growth in ionic liquids. *J Am Chem Soc* 136:13789–13797. doi:10.1021/ja506724w
65. Gutel T, Santini CC, Philippot K et al (2009) Organized 3D-alkyl imidazolium ionic liquids could be used to control the size of in situ generated ruthenium nanoparticles? *J Mater Chem* 19:3624. doi:10.1039/b821659b

66. Yang M, Campbell PS, Santini CC, Mudring A-V (2014) Small nickel nanoparticle arrays from long chain imidazolium ionic liquids. *Nanoscale* 6:3367. doi:[10.1039/c3nr05048c](https://doi.org/10.1039/c3nr05048c)
67. Migowski P, Machado G, Texeira SR et al (2007) Synthesis and characterization of nickel nanoparticles dispersed in imidazolium ionic liquids. *Phys Chem Chem Phys* 9:4814. doi:[10.1039/b703979d](https://doi.org/10.1039/b703979d)
68. Stratton SA, Luska KL, Moores A (2012) Rhodium nanoparticles stabilized with phosphine functionalized imidazolium ionic liquids as recyclable arene hydrogenation catalysts. *Catal Today* 183:96–100. doi:[10.1016/j.cattod.2011.09.016](https://doi.org/10.1016/j.cattod.2011.09.016)
69. Arquillière PP, Helgadottir IS, Santini CC et al (2013) Bimetallic Ru–Cu nanoparticles synthesized in ionic liquids: kinetically controlled size and structure. *Top Catal* 56:1192–1198. doi:[10.1007/s11244-013-0085-3](https://doi.org/10.1007/s11244-013-0085-3)
70. Khare V, Li Z, Manton A et al (2010) Strong anion effects on gold nanoparticle formation in ionic liquids. *J Mater Chem* 20:1332. doi:[10.1039/b917467b](https://doi.org/10.1039/b917467b)
71. Krämer J, Redel E, Thomann R, Janiak C (2008) Use of ionic liquids for the synthesis of iron, ruthenium, and osmium nanoparticles from their metal carbonyl precursors. *Organometallics* 27:1976–1978. doi:[10.1021/om800056z](https://doi.org/10.1021/om800056z)
72. Silva DO, Scholten JD, Gelesky MA et al (2008) Catalytic gas-to-liquid processing using cobalt nanoparticles dispersed in imidazolium ionic liquids. *ChemSusChem* 1:291–294. doi:[10.1002/cssc.200800022](https://doi.org/10.1002/cssc.200800022)
73. Bruss AJ, Gelesky MA, Machado G, Dupont J (2006) Rh(0) nanoparticles as catalyst precursors for the solventless hydroformylation of olefins. *J Mol Catal A Chem* 252:212–218. doi:[10.1016/j.molcata.2006.02.063](https://doi.org/10.1016/j.molcata.2006.02.063)
74. Fonseca GS, Umpierre AP, Fichtner PFP et al (2003) The use of imidazolium ionic liquids for the formation and stabilization of Ir⁰ and Rh⁰ nanoparticles: efficient catalysts for the hydrogenation of arenes. *Chem Eur J* 9:3263–3269. doi:[10.1002/chem.200304753](https://doi.org/10.1002/chem.200304753)
75. Gelesky MA, Umpierre AP, Machado G et al (2005) Laser-induced fragmentation of transition metal nanoparticles in ionic liquids. *J Am Chem Soc* 127:4588–4589. doi:[10.1021/ja042711t](https://doi.org/10.1021/ja042711t)
76. Kwak K, Kumar SS, Pyo K, Lee D (2013) Ionic liquid of a gold nanocluster: a versatile matrix for electrochemical biosensors. *ACS Nano* 8:671–679. doi:[10.1021/nn4053217](https://doi.org/10.1021/nn4053217)
77. Yu F, Xu X, Baddeley CJ et al (2014) Surface ligand mediated growth of CuPt nanorods. *CrystEngComm* 16:1714–1723. doi:[10.1039/C3CE41524D](https://doi.org/10.1039/C3CE41524D)
78. Ryu HJ, Sanchez L, Keul HA et al (2008) Imidazolium-based ionic liquids as efficient shape-regulating solvents for the synthesis of gold nanorods. *Angew Chem Int Ed* 47:7639–7643. doi:[10.1002/anie.200802185](https://doi.org/10.1002/anie.200802185)
79. Wang Y, Maksimuk S, Shen R, Yang H (2007) Synthesis of iron oxide nanoparticles using a freshly-made or recycled imidazolium-based ionic liquid. *Green Chem* 9:1051–1056. doi:[10.1039/B618933D](https://doi.org/10.1039/B618933D)
80. Wang Y, Yang H (2009) Synthesis of iron oxide nanorods and nanocubes in an imidazolium ionic liquid. *Chem Eng J* 147:71–78. doi:[10.1016/j.cej.2008.11.043](https://doi.org/10.1016/j.cej.2008.11.043)
81. Jin R, Zhu Y, Qian H (2011) Quantum-sized gold nanoclusters: bridging the gap between organometallics and nanocrystals. *Chem Eur J* 17:6584–6593. doi:[10.1002/chem.201002390](https://doi.org/10.1002/chem.201002390)
82. Negishi Y, Nakazaki T, Malola S et al (2014) A critical size for emergence of nonbulk electronic and geometric structures in dodecanethiolate-protected Au clusters. *J Am Chem Soc* 137:1206–1212. doi:[10.1021/ja5109968](https://doi.org/10.1021/ja5109968)
83. Yuan X, Yan N, Katsyuba SA et al (2012) A remarkable anion effect on palladium nanoparticle formation and stabilization in hydroxyl-functionalized ionic liquids. *Phys Chem Chem Phys* 14:6026. doi:[10.1039/c2cp23931k](https://doi.org/10.1039/c2cp23931k)
84. Biswas K, Rao CNR (2007) Use of ionic liquids in the synthesis of nanocrystals and nanorods of semiconducting metal chalcogenides. *Chem Eur J* 13:6123–6129. doi:[10.1002/chem.200601733](https://doi.org/10.1002/chem.200601733)

Structural Features and Properties of Metal Complexes in Ionic Liquids: Application in Alkylation Reactions

Cinzia Chiappe, Tiziana Ghilardi, and Christian Silvio Pomelli

Abstract Metal-containing ionic liquids (ILs) represent a promising sub-class of “charged” liquids which increase the tunability of ILs combining the properties of common organic salts with magnetic, photophysical/optical or catalytic properties of the incorporated metal salts. In ILs lacking of coordinating groups on cation dissolution of metal salts is generally associated with the coordination of the metal cation with IL anion(s). Here we report on the anionic speciation of metals in ILs having either highly or poorly coordinating anions and we discuss some peculiar properties of these systems in the light of their structural features.

Keywords Alkylation reactions · Ionic liquids · Metal speciation · Transition metals

Contents

1	Introduction	80
2	Solvation of Metal Salts in Ionic Liquids	81
3	Coordination Structure of Transition Metal Salts in Ionic Liquids	83
3.1	Coordination Structure and Physico-Chemical Properties	86
4	Application of Halometallates in Synthesis: Alkylation Reactions	87
5	Conclusions	91
	References	91

Abbreviations

[bmim] ⁺	1-Butyl-3-methylimidazolium
[C ₃ mpip] ⁺	<i>N,N</i> -propylmethylpiperidinium
[C ₄ mpyr] ⁺	<i>N,N</i> -butylmethylpyrrolidinium

[emim] ⁺	1-Ethyl-3-methylimidazolium
[Et ₃ NH] ⁺	Triethylammonium
[omim] ⁺	1-Octyl-3-methylimidazolium
[Tf ₂ N] ⁻	bis(Trifluoromethanesulfonyl)imide
ILs	Ionic liquids

1 Introduction

Ionic liquids (ILs) are a relatively recent class of ionic compounds which have many potentialities in synthesis, (bio)catalysis, separation processes, electrochemistry as well as in material sciences and for the development of new electrical and electrochemical devices [1]. Usually constituted by an organic cation and a polyatomic anion, ILs are characterized by melting points near or below room temperature. ILs have also a negligible vapour pressure, a high thermal stability, a nonflammable nature [2] and a good solvent power. Since cations and anions can exert practically all types of interactions with solutes (coulombic interactions, hydrogen bonding, π - π stacking), ILs can solubilize a large variety of organic, inorganic compounds and polymeric materials. Moreover, their physico-chemical properties, such as melting temperature and hydrophilicity/hydrophobicity, can be simply tuned by changing the structure of the cations and anions: for instance, ILs can be designed to make them immiscible in water or in certain organic solvents [3]. The incorporation of specific functional groups into the chemical structure of constituent ions can be used to confer a desired chemical or physical property on the resulting ILs, commonly defined task-specific ionic liquids. It is noteworthy that these peculiar features can be transferred also onto solid surfaces through the formation of self-assembled monolayers of properly functionalized ILs.

Metal-containing ILs represent a promising sub-class of “charged” liquids which combine the properties of the common ILs with magnetic, photophysical/optical or catalytic properties of the merged metal salts [4, 5]. ILs that contain salts of palladium, ruthenium, platinum, gold, aluminium (but also iron, nickel, zinc or copper) have been used with success in catalysis. The use of ILs in catalysis is generally related to their ability to dissolve at least small amounts of metal salts, often favouring the formation of transient “active” species and, contemporaneously, avoiding the leaching of the metal salt during product extraction. This latter feature increases indeed the possibility of recycling the catalyst, and many excellent accounts and reviews have already been published on this topic [6–10].

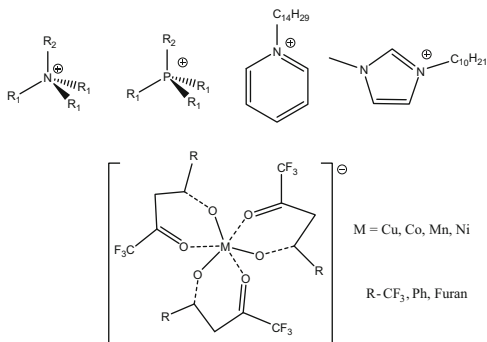
Moreover, the ability of ILs to dissolve ions (in particular, large amounts of metal salts) is of great interest also in other fields of chemistry, such as electrochemistry and material sciences: ILs that contain metal salts are used in batteries, photovoltaic cells and in electrical devices or sensors. Metallic materials having specific characteristics (thin films, nanostructures and others) can be obtained by electrodeposition of metal salts dissolved in appropriate ILs [11]. Of course the addition of metal salts to common ILs modifies the physico-chemical properties of

where the step (0) is practically independent by the IL nature, whereas step (1) and (2) are related to the transfer of the salt in solution and subsequent possible coordination reactions (for instance, the coordination of a further anion). Since the formation of bond between a metal centre and a small mono-dentate anion to give a charged complex typically gives a (negative) energy ranging from -50 to -100 kcal mol $^{-1}$, while the dissolution of a neutral salt, M(X), in an IL gives a positive excess free energy of about 25 – 50 kcal mol $^{-1}$ and the extent of solute polarization energy by an unfunctionalized IL is considerably lower, about 1 – 10 kcal mol $^{-1}$, it is possible to deduce that the driving force for solubilization of a metal salt in an IL is the formation of the charged complex in solution, arising from an “addition reaction.”

Since in a pure IL we expect to find the formed charged complex of the metal solvated by the IL cation (generally a mono charged species) the metal complexes with a single negative charge should be preferred for electrostatic reasons. This aspect, together with the coordination properties of the anion (mono- bi- or polydentate species), determines the coordination number (see below), which must be coherent also with the coordination number of the metal ion.

A remarkable point to be stressed is that calculations show that the stability of mixed complexes is usually much lower than that of the homocomplexes [4], in particular when the ligands differ in denticity, geometry, or type of bonding. This observation can support some experimental data showing that the solubility of transition metal salts in ILs sharing the same anion is significantly higher than that in ILs having a different anion. Metal triflates, acetates, nitrates, and bis(trifluoromethanesulfonyl)imides ($[\text{Tf}_2\text{N}]^-$) show indeed a high solubility in ILs possessing the corresponding anion, and they are characterized by a low dissolution ability in ILs bearing a different anion (for example, metal bis(trifluoromethanesulfonyl)imides are poorly soluble in $[\text{bmim}][\text{NO}_3]$) [4].

Chlorometallate ILs are easily obtained via direct mixing of a metal chloride with an organic chloride salt and the physico-chemical properties, as well as their Lewis acidity and catalytic ability, depend on both the nature of the merged metal salt and the ratio of the metal chloride to organic chloride salt. However, mixed complexes can be present in solution and their formation, even as transient species, may be determinant for some specific applications of the metal. Tetrahedral mixed tetrahaloaluminates (III), tetrahaloferrates (III), and tetrahalogallates(III) (for example, $[\text{AlCl}_3\text{Br}]^-$, $[\text{FeCl}_3\text{Br}]^-$, $[\text{GaCl}_3\text{Br}]^-$) can be obtained by dissolution of the corresponding trichlorides (MCl_3) in the proper halide ILs; however, complex stability strongly depends on halide nature. The ^{27}Al NMR spectra show indeed that $[\text{AlCl}_3\text{Br}]^-$ anion is the dominant species in the $[\text{C}_8\text{mim}]\text{Br}-\text{AlCl}_3$ sample, whereas the $[\text{C}_8\text{mim}]\text{I}-\text{AlCl}_3$ mixture is characterized by three peaks corresponding to $[\text{AlCl}_4]^-$, the dominant anion, $[\text{AlCl}_3\text{I}]^-$ and $[\text{AlCl}_2\text{I}_2]^-$, respectively [14]. On the other hand, tetrahedral mixed complexes including halides and pseudohalides (such as NCS^-) have been reported for aluminium(III) and iron(III), $[(\text{MCl}_3)\text{NCS}]^-$ where $\text{M} = \text{Al(III)}$ or Fe(III) [15]. Actually, also mixed complexes involving anions with significantly different shapes and dimensions, such as bis(trifluoromethanesulfonyl)imide and chloride, have been reported, at least as transient species. In particular, it has been shown that even if the addition of AlCl_3 to pyrrolidinium, piperidinium or imidazolium bis(trifluoromethanesulfonyl)imides ($[\text{C}_4\text{mpyr}][\text{Tf}_2\text{N}]$, $[\text{C}_3\text{mpip}][\text{Tf}_2\text{N}]$,

Fig. 1 ILs with metal chelate anions

and [bmim][Tf₂N]) gives, depending on composition and temperature, phase separation due to the formation of Al(Tf₂N)₃ (lower phase) and the homocomplex [AlCl₄][−] (upper phase), these species arise from the disproportionation of the initially formed mixed complexes, [AlCl_{*x*}(Tf₂N)_{4−*x*}][−] (where *x* may be 3 or 4) [16, 17]. These transient species present relevant properties, as shown by the fact that while aluminium deposition doesn't occur with [AlCl₄][−] in chloroaluminated ILs, this process can be performed in the above reported mixtures and the mixed complex [AlCl₃(Tf₂N)][−] has been proposed as the electroactive aluminium-containing species. A similar behaviour has been attributed to [AlCl₂(Tf₂N)₂][−] [18].

Finally, it is necessary to mention that hydrophobic ILs composed of simple organic cations (ammonium, phosphonium, pyridinium and imidazolium) having as counteranion chelate anions of monovalent transition metal (Mn, Co, Ni, Cu) have been recently prepared, characterized and used as catalysts in oxidation reactions [19] (Fig. 1).

3 Coordination Structure of Transition Metal Salts in Ionic Liquids

It is well known that in the case of halometallates the coordination chemistry of the anion and, consequently, the Lewis acidity of the resulting IL can be modified by tuning the ratio of metal chloride to organic chloride (generally expressed as mole fraction of metal chloride, χ_{MCl_x}).

Equations (1–3) show the acid–base reactions that occur when an organic chloride salt (IL = [cat]Cl) and AlCl₃ are mixed.



When χ_{AlCl_3} is 0.5, $[\text{AlCl}_4]^-$ is practically the sole anionic species present in solution; however, in systems with $\chi_{\text{AlCl}_3} > 0.5$ multinuclear chloroaluminate anions are formed which are in equilibrium each other. In the presence of an excess of organic chloride salt ($\chi_{\text{AlCl}_3} < 0.5$) the resulting ILs are Lewis basic systems becoming neutral at $\chi_{\text{AlCl}_3} = 0.5$ and Lewis acidic at $\chi_{\text{AlCl}_3} > 0.5$ [20]. The tunable and variable acidity of these salts is therefore determined by the molar fraction of the Lewis acid, a parameter that strongly affects also all the physico-chemical and thermal properties of the resulting melts. Anionic speciation based on analogous equilibria has been reported also for many other chlorometallate systems, such as chloroferrate(III), chloroindanate(III) and chlorogallate(III).

On the other hand, the existence of several anions and equilibria has been reported also for systems arising by the addition of Me(II) salts (ZnCl_2 , CuCl_2 , SnCl_2 and FeCl_2) to organic chloride salts although, at least for some of these metals, the nature of the predominant species is still the object of debate. On the basis of fast atom bombardment mass spectra (FAB-MS) of the ZnCl_2 -[emim]Cl mixtures it was reported [21] the formation of the ZnCl_3^- ion under basic conditions (excess of chloride anion), a result subsequently confirmed [22] by Lecocq et al. through NMR and MS analyses. On the contrary, an anion speciation based exclusively on Cl^- , $[\text{ZnCl}_4]^{2-}$, $[\text{Zn}_2\text{Cl}_6]^{2-}$, $[\text{Zn}_3\text{Cl}_8]^{2-}$ and $[\text{Zn}_4\text{Cl}_{10}]^{2-}$ anions has been reported in a more recent investigation [23], whereas the Raman spectra of proper mixtures of [bmim]Cl and ZnCl_2 appeared to suggest the presence of $[\text{ZnCl}_4]^{2-}$ as the main ionic species at $\chi_{\text{ZnCl}_2} < 0.3$ [24]. A different speciation has been proposed for dissolution of SnCl_2 in chloride-based ILs [25]. In this case, when the anionic speciation of the resulting chlorostannate(II) liquids has been investigated in both solid and liquid states, no evidence was collected for the existence of $[\text{SnCl}_4]^{2-}$ within the entire range of χ_{SnCl_2} , although such anion was reported [26] in the literature for chlorostannate(II) organic salts crystallized from organic solvents. Both liquid and solid systems contained $[\text{SnCl}_3]^-$ in equilibrium with Cl^- , when χ_{SnCl_2} was < 0.50 , $[\text{SnCl}_3]^-$ in equilibrium with $[\text{Sn}_2\text{Cl}_5]^-$, when χ_{SnCl_2} was > 0.50 , and only $[\text{SnCl}_3]^-$ when $\chi_{\text{SnCl}_2} = 0.5$.

Finally, in the case of CuCl_2 in [bmim]Cl the presence under specific conditions of the trigonal and deformed tetrahedral copper(II) chloride coordination complexes, $[\text{CuCl}_3]^-$ and $[\text{CuCl}_4]^{2-}$ respectively, has been proposed on the basis of both experimental (XPS, UV-Vis and EPR) and DFT calculations [27].

Although the above reported examples are related to metal salts in ILs having strongly coordinating anions, anionic speciation can occur also in weakly coordinating ILs, such as bis(trifluoromethylsulfonyl)imide-based ILs. This "innocent" anion can act as a monodentate ligand coordinating the metal directly through either an N or O atom or as a bidentate ligand chelating the metal ion via O, O or O, N atoms to give stable six-membered chelate rings. The coordination via two oxygen atoms, each placed on a different sulfonyl group, assures, however, a remarkable flexibility due to some structural features of this anion and, therefore, it should be preferred. In particular, this kind of coordination guarantees the fact that: (1) the rotation of the CF_3SO_2 moieties around the N-S bonds allows to modify distance and relative orientation of

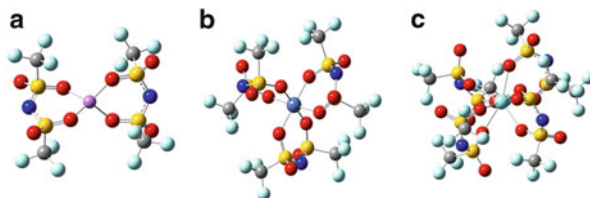


Fig. 2 (a) $[\text{Li}(\text{Tf}_2\text{N})_2]^-$; (b) $[\text{Ni}(\text{Tf}_2\text{N})_3]^-$; (c) $[\text{Y}(\text{Tf}_2\text{N})_4]^-$ complexes. In all complexes the ligands ($[\text{Tf}_2\text{N}]^-$) are in *trans* conformation and the CF_3 groups are arranged to form a sort of belt, probably due to an interligand dispersive interaction

the two chelating oxygen atoms thus favouring the adoption of the preferred coordination geometry of the metal cation; (2) the presence of 2 equiv. oxygen atoms on each sulfonyl group adds further geometrical flexibility; and (3) free rotation of the CF_3 groups can reduce the steric hindering in the coordination complex.

Furthermore, considering that each metal cation is characterized by a peculiar charge (M) and a preferred coordination number (N), and that in common bis(trifluoromethylsulfonyl)imide-based ILs the dissolution of single charged species should be favoured with respect to uncharged or multicharged species [28], since bis(trifluoromethylsulfonyl)imide is a mono charged anion and a bivalent ligand, coordination complexes of the type $[\text{M}^{+M}(\text{Tf}_2\text{N})_{N/2}]^{-1}$ should be the most stable. This is the situation characterizing single charged metals in tetrahedral coordination complexes, typical example (Li(I)), double charged metals in octahedral coordination complexes, typical examples Ni(II), Co(II), Zn(II), Cu(II) and so on, or triple charged metals in square antiprism coordination complexes, typical example Y(III). In Fig. 2, an optimized structure for each of the above-mentioned coordination complexes $[\text{M}^{+M}(\text{Tf}_2\text{N})_{N/2}]^{-1}$ is reported.

The stability of these coordination complexes with respect to the neutral salts determines the chemical and electrochemical behaviour of these solutions as well as their surface properties. The coordination of the metal cation with the IL anion and the interaction of the arising complex with the counteranion (IL cation) strongly affects the metal ion distribution inside the IL and at the IL/air surface [12, 27, 29] thus determining the IL properties in the bulk and at the interface.

X-ray photoelectron spectroscopy (XPS), a technique able to provide information about elemental and chemical state of a sample, has been employed in the last years not only to investigate the surface of solid materials, including metals and metal compounds, but also of metal-containing ILs [12]. Since the species present in ILs are highly mobile in comparison with solid ionic compounds, the surfaces show phenomena such as surface segregation and enrichment, preferential orientation, and others in much larger extent than crystalline or amorphous solids. In the case of “pure” ILs surface often presents peculiar characteristics, such as the enrichment of the cation alkyl chains at the expense of the polar cation head groups and the anions. It is noteworthy that the enhancement effect depends on alkyl chain length and anion size, and more in particular, it is most evident for the smallest anions and least pronounced for the largest anions [30, 31]. On these bases, it is reasonable to expect that systems constituted by metal ions dissolved in ionic

liquids, because of the larger number of chemical species present in such ionic mixtures, may be characterized by structural differences between bulk and surface. In fact, the presence of complexation equilibria can lead to the simultaneous existence of several anions having different size and therefore affinity toward the liquid/gas interface. It is noteworthy that in these systems, slight variations in IL/metal ratio can dramatically change the surface composition with important consequence when ILs are used for surface processes, for example in the ILs chemistry on supported materials (supported IL phase, SILP).

3.1 Coordination Structure and Physico-Chemical Properties

Addition of metal halides (AlCl_3 , ZnCl_2 , FeCl_3 and so on) to organic chlorides gives ILs whose physico-chemical properties are determined by anion speciation. The effect of anionic composition on melting point, glass transition temperature, viscosity, and conductivity has long been recognized. In the case of 1-methyl-3-ethylimidazolium chloride/aluminium trichloride ($[\text{emim}]\text{Cl}/\text{AlCl}_3$) viscosity remains practically constant at values significantly lower than the starting IL, until the amount of $[\text{emim}]\text{Cl}$ is below 50 mol%, however, when $[\text{emim}]\text{Cl}$ exceed 50 mol%, the absolute viscosity begins to increase [2]. This increase in viscosity, which is related to the increase in chloride ion concentration, has been attributed to hydrogen bonding between chloride ion and imidazolium cation. The formation of the metal complexes ($[\text{emim}]\text{Cl}$ below 50 mol%) therefore decreases, at least in this case, the viscosity reducing the hydrogen bond ability of the anion and the Coulombic forces inside the IL, as a consequence of the lower charge density of the Al_nCl_m^- anions. Moreover, on the basis of a more recent investigation in which density, viscosity and conductivity of 1-butyl-3-methylimidazolium and 1-hydrogen-3-methylimidazolium chloroaluminates, $[\text{bmim}]\text{Cl}-\text{AlCl}_3$ and $[\text{Hmim}]\text{Cl}-\text{AlCl}_3$, have been determined varying the molar composition in the temperature range 293.15–343.15 K, it has been inferred [32] that not only the hydrogen bonding but also the structural geometry of the formed complexes and cation/anion interaction have a significant effect on the physico-chemical properties of these liquids. An analogous behaviour of viscosity, i.e. high viscosity values in the case of very basic compositions (excess of chloride) and a dramatic decrease with increasing Lewis acid concentration, was observed also in the case of chlorostannates(II) (the investigated system was $[\text{omim}]\text{Cl}-\text{SnCl}_2$), the minimum viscosity value for this system being at $\chi_{\text{SnCl}_2} = 0.5$ [25].

Furthermore, it is noteworthy that for this class of metal-containing ILs (imidazolium chlorometallates) an interesting and not predictable correlation has been found between chlorometallate compositions, i.e. anion speciation, and Lewis acidity using the Gutmann acceptor number [33].

Although the mixtures of metal salts in ILs bearing weakly coordinating anions have been scarcely investigated, it is nevertheless known to researchers working in ILs chemistry that the unwanted presence in bis(trifluoromethylsulfonyl)imide-based ILs of even small amounts of LiTf_2N , arising from the metathesis reaction,

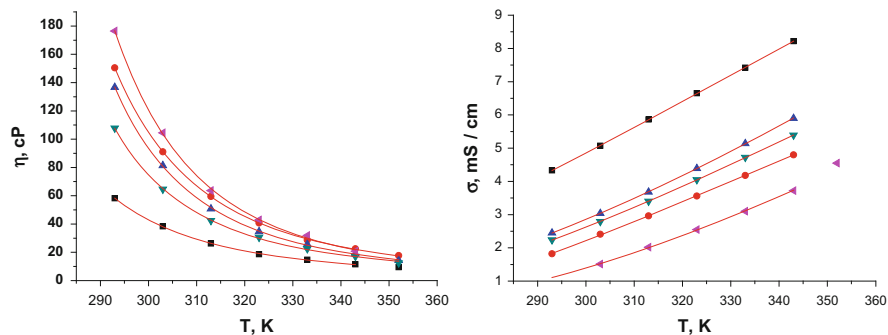


Fig. 3 Temperature dependence of viscosity and conductivity for [bmim][Tf₂N] (black square); [bmim][Tf₂N]/Co(Tf₂N)₂ (red circle); [bmim][Tf₂N]/Cu(Tf₂N)₂ (blue triangle); [bmim][Tf₂N]/Ni(Tf₂N)₂ (green inverted triangle) and [bmim][Tf₂N]/Al(Tf₂N)₃ (pink right-pointing triangle). At 0.1 mol fraction of Me(Tf₂N)_n

dramatically decreases the melting temperature of the resulting IL and modifies its physico-chemical properties (viscosity, conductivity, hydrophobicity, polarity and so on). Generally, the presence of the metal salt increases viscosity and decreases conductivity with respect to the pure IL and the entity of the effect is determined by the metal cation nature. In contrast with chloride-based ILs, the interaction between cations and anions in organic bis(trifluoromethylsulfonyl)imide is very low and probably moderately affected by the formation of the metal complexes which can, however, modify the packing ability of the system and the “holes” availability. Fig. 3 illustrates the temperature dependence of viscosity and conductivity for some [bmim][Tf₂N]-Me(Tf₂N)_n (Me = Cu, Co, Al, Ni) mixtures, at $\chi_{\text{Me}(\text{Tf}_2\text{N})_n} = 0.1$.¹

It is noteworthy that both these properties are strongly affected by the temperature; however, while viscosities of the investigated [bmim][Tf₂N]-Me(Tf₂N)_n (Me = Cu, Co, Al, Ni) mixtures at relatively high temperatures (340–350 K) converge towards the values of the pure IL, conductivities remain parallel and always significantly lower than the pure IL.

4 Application of Halometallates in Synthesis: Alkylation Reactions

Since the earlier development of chloroaluminate ILs in the 1960s, halometallates have been largely used as replacements for conventional acid catalysts for many different applications [34]. In particular, as a consequence of the industrial interest, the petroleum industry has been by far the largest applicant of this kind of ILs; alkylations of arenes (Friedel–Crafts reaction) and alkanes (in particular, of isobutane with 2-butene for the production of high-octane gasoline) have been widely

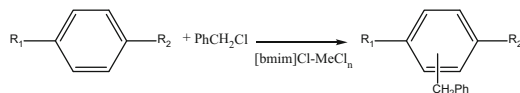
¹ Unpublished results from this laboratory.

investigated (from 2005 more than 50 patents have been published on alkylation with chloroaluminate-based ILs!). The high potential of ILs as alkylating catalysts is best expressed by the fact that an industrial alkylation plant in China is now running with an IL as catalyst [35] and the use of ILs was also studied by several companies (e.g. by the IFP in a pilot plan) although specific details have been not reported up to now.

Wilkes first reported [36] the Friedel–Crafts reactions of aromatic substrates, such as benzene, toluene, chlorobenzene and nitrobenzene in [emim]Cl–AlCl₃: with the exception of nitrobenzene the aromatic substrates were efficiently alkylated. Subsequently, chloroaluminate ILs have been extensively tested as solvents and catalysts for alkylation of other aromatic systems, such as naphthalene and anthracene [37, 38] and, more recently, also other halometallate-based ILs have been investigated [38] for the same reaction.



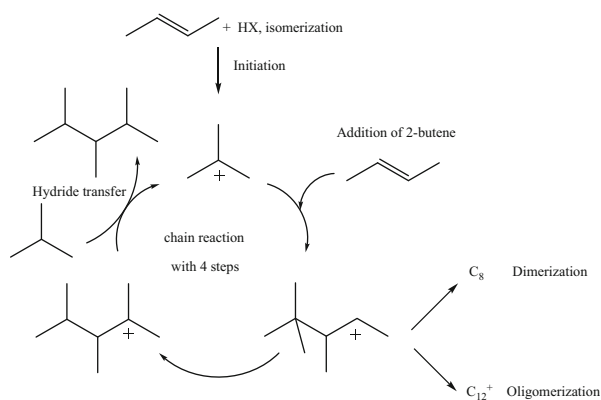
In particular, in 2006 Yin et al. [39] reported the syntheses of diphenylmethane and its derivatives through Friedel–Crafts benzylation of benzene and derivatives with benzyl chloride through the use, for the first time, of the moisture-stable [bmim]Cl/ZnCl₂, [bmim]Cl/FeCl₃, and [bmim]Cl/FeCl₂ systems as solvents and catalysts. Easy separation of the reaction products, increased reaction rates with respect to conventional molecular solvents, and high selectivity towards monoalkylated products were obtained in these media under specific conditions.



Recently, also the moisture-stable chloroindanate ILs have been used [40] as versatile catalysts for the reaction of phenols with alkenes, obtaining high conversions to alkylated phenols with high selectivities. However, the supposition that moisture-stable chlorometallates can always substitute chloroaluminate-based ILs does not found a general agreement from the literature. Indeed, their lower Lewis acidities have been reported to be an important detrimental factor in some reactions: for example, in the case of anthracene alkylation [38], it has been stressed that [emim]Cl/AlCl₃ gave the best results in terms of both yield (74.5%) and selectivity (82.9%).

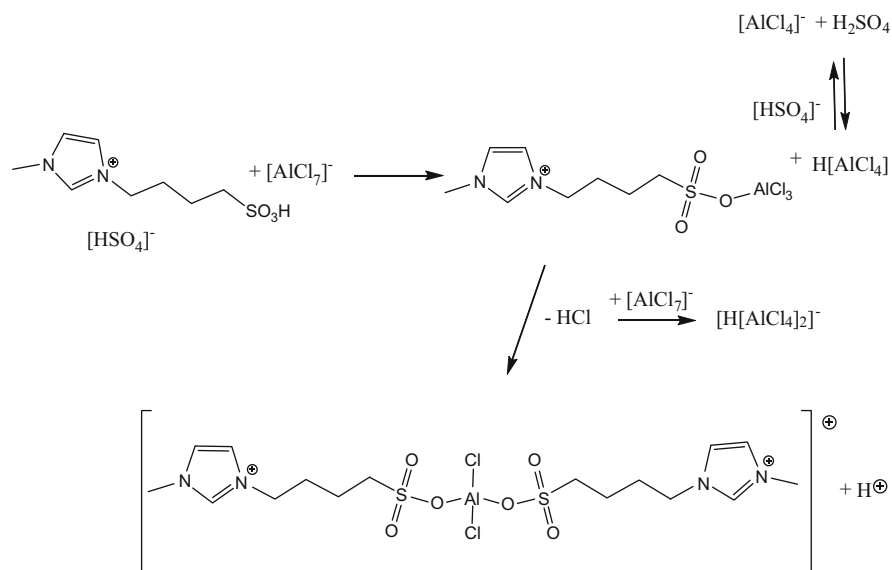
Inspired by the outstanding strong Lewis acidity of chloroaluminate ILs, Chauvin et al. firstly investigated the use of [bmim]Cl–AlCl₃ as catalysts in another important refinery process, the isobutane alkylation with light alkenes to obtain branched alkanes [41]. Despite the fact that the alkylate products obtained in chloroaluminate-based ILs alone were characterized by a relatively low content of octane components and a low trimethylpentane/dimethylhexane ratio [41], also

other chloroaluminate systems have been studied [14, 42–44] as catalysts for this reaction. It is noteworthy that, according to the accepted mechanism, in this case strong Brønsted acids are the catalytic species which can be generated from the interaction between a strong Lewis acid and a Brønsted acid; in the case of [bmim]Cl–AlCl₃ they arise from the interaction of Lewis acidic chloroaluminates ([Al₂Cl₇][−] or [Al₃Cl₁₀][−]) with HCl. Acidic protons are indeed inherently present in halogenoaluminate ILs due to the reaction of AlCl₃ with the IL cation or traces of water, if the preparation is done in a not very dry atmosphere. Since acidity is a crucial parameter in alkylation, which can be controlled by the molar fraction of the Lewis acid and the addition of “electron donating substances”, various additives including metal chlorides, organosulfur compounds and *tert*-butyl halides, were investigated to improve the catalytic performance of the chloroaluminate ILs in this reaction [42–45].



In this context, interesting results have been recently obtained by addition of acid cation exchange resins (dry or with small amount of water) or 1-(4-sulfobutyl)-3-methylimidazolium hydrogensulfate ([[(HO₃Sbu)mim][HSO₄]]) to the catalytic medium, 1-octyl-3-methylimidazolium bromide–aluminium chloride, [omim]Br–AlCl₃. Under optimized conditions, a content of desired trimethylpentanes (up to 64%) and thus an octane number (RON up to 96) comparable or higher than that with H₂SO₄ [46] were obtained. First of all, it is noteworthy that [omim]Br–AlCl₃ was chosen because the anionic species formed, [AlCl₃Br][−] or [Al₂Cl₆Br][−], show higher Lewis acidity compared to complexes containing only chloride as halogenide. Furthermore, a Brønsted acid able to give highly acidic protons was added. In particular, in the case of 1-(4-sulfobutyl)-3-methylimidazolium hydrogensulfate ([[(HO₃Sbu)mim][HSO₄]]), the reaction of the Lewis acidic haloaluminate with the sulfonic group of the functionalized IL leads to a dimeric structure generating superacid protons which can react with either the hydrogensulfate or the [Al₂Cl₇][−] anion species. The Lewis acid is able to react with hydrogensulfate to give HCl and another highly acidic proton. On the other

hand, HCl interacts with the $[\text{Al}_2\text{Cl}_7]^-$ anion leading to $\text{H}[\text{AlCl}_4]$ which is regarded as a superacid.



Thus, on the basis of these latter results the possibility to control the Brønsted acidity by forming superacidic IL species or superacidic species in ILs, via protic additives, appears a particularly promising approach to obtain high yields and selectivities in isobutane alkylation. However, the efficiency of this reaction is also determined by reaction conditions (temperature, stirring, paraffin/olefin ratio and residence parameters). Recent kinetic studies, carried out in reactors with and without stirring, have shown [47] that the biphasic alkylation of light olefins with *i*-paraffins using chloroaluminate ILs as catalysts is an extremely fast reaction, leading to a low effectiveness factor of the IL catalyst. In a well-mixed reactor the effective reaction rate is determined by the size of the interphase and of the characteristic length of the diffusion in the IL phase, the thickness of an IL film or the diameter of the IL droplets dispersed in the organic phase [48].

Although chloroaluminate ILs are the most investigated systems for this reaction, recently also chlorogallate ILs have been tested [49]. These latter ILs are more resistant to hydrolysis than the analogous chloroaluminate ones and are characterized by a Lewis acidity comparable or slightly higher than those of chloroaluminate ILs having analogous compositions. In particular, a series of triethylammonium-based chlorogallate ILs with a variety of Lewis acidity have been applied to isobutane alkylation. The triethylammonium chloride–gallium trichloride ($[\text{Et}_3\text{NH}]\text{Cl}-\text{GaCl}_3$) with $\chi_{\text{GaCl}_3} = 0.65$ displayed a potential catalytic activity and the addition of CuCl (5% mol) dramatically enhanced the alkylation reaction; also in this case, up to 70.1% C8 selectivity and 91.3 RON were achieved under selected conditions (0.5 MPa, 900 r min^{-1} , 15 min, 288 K).

5 Conclusions

Ionic liquids containing metal salts represent a fascinating world in the ILs universe that can open up new possibilities in important areas such as catalysis, electrochemistry and material science. The physico-chemical properties of the included metals and the structural organization of the ionic systems arising from the interaction between the “appropriate IL” and the metal salt can give new materials, catalysts and solvents. Bulk and surface properties of ILs containing a metal cation can be substantially modified changing IL anion (more or less coordinating anions can give ILs having completely different properties and abilities) and IL/metal salt ratio, although also the IL cation, in particular when functionalized, can contribute to this purpose.

References

1. Plechkova NV, Seddon KR (2008) Applications of ionic liquids in the chemical industry. *Chem Soc Rev* 37:123
2. Wasserscheid P, Welton T (2008) *Ionic liquids in synthesis*, 2nd edn. Wiley-VCH, Weinheim
3. Chiappe C, Pieraccini D (2005) Ionic liquids: solvents properties and organic reactivity. *J Phys Org Chem* 18:275
4. Chiappe C, Malvaldi M (2010) High concentrated solutions of metal cations in ionic liquids: current status and future challenges. *Phys Chem Chem Phys* 12:11191
5. Binnemans K (2007) Lanthanides and actinides in ionic liquids. *Chem Rev* 107:2592
6. Dupont J, de Souza RF, Suarez PAZ (2002) Ionic liquid (molten salt) phase organometallic catalysis. *Chem Rev* 102:3667
7. Wasserscheid P, Keim W (2000) Ionic liquids-new “Solutions” for transition metal catalysis. *Angew Chem* 39:3772
8. Pârulescu VI, Hardacre C (2007) Catalysis in ionic liquids. *Chem Rev* 107:2615
9. Lee JW, Jang HB, Shin JY, Chun YY, Song CE, Lee S (2010) Toward understanding the origin of positive effects of the ionic liquids on catalysis: formation of more reactive catalysis and stabilization of reactive intermediates and transition. *Acc Chem Res* 43:985
10. Dyson PJ, Geldbach TJ (2005) Metal catalysed reactions in ionic liquids. Springer, Dordrecht
11. Endres F, Abbott AP, MacFarlane DR (2008) *Electrodeposition from ionic liquids*. Wiley-VCH, Weinheim
12. Chiappe C, Pomelli CS, Bardi U, Caporali S (2012) Interface properties of ionic liquids containing metal ions: features and possibilities. *Phys Chem Chem Phys* 14:5045
13. Di Francesco F, Calisi N, Creatini M, Melai B, Salvo P, Chiappe C (2011) Water sorption by anhydrous ionic liquids. *Green Chem* 13:1712
14. Yoo K, Namboodiri VV, Varma RS, Smirniotis PG (2004) Ionic liquid-catalyzed alkylation of isobutane with 2-butene. *J Catal* 222:511
15. Algra G, Balt S (1983) Reversible substitution reactions of tetrahedral tetrahaloferrates(III) with thiocyanate. *Inorg Chim Acta* 75:179
16. Rodopoulos T, Smith L, Horne MD, Rütther T (2010) Speciation of aluminium in mixtures of the ionic liquids [C3mpip][NTf2] and [C4mpyr][NTf2] with AlCl3: an electrochemical and NMR spectroscopy study. *Chem Eur J* 16:3815
17. Eiden P, Liu Q, El Abedin SZ, Endres F, Krossing I (2009) An experimental study of the aluminium species present in mixtures of AlCl3 with the ionic liquids [BMP][Tf2N] and [EMIm][Tf2N]. *Chem Eur J* 15:3426

18. Rocher NM, Izgorodina EI, R  ther T, Forsyth M, MacFarlane DR, Rodopoulos T, Horne MD, Bond AM (2009) Aluminium speciation in 1-butyl-1-methylpyrrolidinium bis(trifluoromethylsulfonyl)amide/AlCl₃ mixtures. *Chem Eur J* 15:3435
19. Zhang P, Gong Y, Lv Y, Guo Y, Wang Y, Wang C, Li H (2012) Ionic liquids with metal chelate anions. *Chem Commun* 48:2334
20. Piao LY, Fu X, Yang YL, Tao GH, Kou Y (2004) Alkylation of diphenyl oxide with α -dodecene catalyzed by ionic liquids. *Catal Today* 93:301
21. Hsiu S, Huang J-F, Sun I-W, Yuan C-H, Shiea J (2002) Lewis acidity dependency of the electrochemical window of zinc chloride-1-ethyl-3-methylimidazolium chloride ionic liquids. *Electrochim Acta* 47:4367
22. Lecocq V, Graille A, Santini CC, Baudouin A, Chauvin Y, Basset JM, Arzel L, Bouchu D, Fenet B (2005) Synthesis and characterization of ionic liquids based upon 1-butyl-2,3-dimethylimidazolium chloride/ZnCl₂. *New J Chem* 29:700
23. Estager J, Nockemann P, Seddon KR, Swad  ba-Kwa  sny M, Tyrrell S (2011) Validation of speciation techniques: a study of chlorozincate(II) ionic liquids. *Inorg Chem* 50:5258
24. Alves MB, Santos VO, Soares VCD, Suarez AZ, Rubin JC (2008) Raman spectroscopy of ionic liquids derived from 1-*n*-butyl-3-methylimidazolium chloride and niobium chloride or zinc chloride mixtures. *J Raman Spectrosc* 39:1388
25. Currie M, Estager J, Licence P, Men S, Nockemann P, Seddon KR, Swad  ba-Kwa  sny M, Terrade C (2013) Chlorostannate(II) ionic liquids: speciation, Lewis acidity, and oxidative stability. *Inorg Chem*. doi:10.1021/ic300241p
26. Yin RZ, Yo CH (1998) Structural and optical properties of the (CnH_{2n} + 1NH₃)₂SnCl₄ (n = 2, 4, 6, 8, and 10) System. *Bull Korean Chem Soc* 19:947
27. Caporali S, Chiappe C, Ghilardi T, Pomelli CS, Pinzino C (2012) Coordination environment of highly concentrated solutions of Cu(II) in ionic liquids through a multidisciplinary approach. *Chemphyschem* 14:1885
28. Chiappe C, Pomelli CS (2013) Computational studies on organic reactivity in ionic liquids. *Phys Chem Chem Phys* 15:412
29. Chiappe C, Malvaldi M, Melai B, Fantini S, Bardi U, Caporali S (2010) An unusual common ion effect promotes dissolution of metal salts in room-temperature ionic liquids: a strategy to obtain ionic liquids having organic–inorganic mixed cation. *Green Chem* 12:77
30. Kolbeck C, Cramer T, Lovelock KRJ, Paape N, Schulz PS, Wasserscheid P, Maier F, Steinr  ck HP (2009) Influence of different anions on the surface composition of ionic liquids studied using ARXS. *J Phys Chem B* 113:8682
31. Maier F, Cremer T, Kolbeck C, Lovelock KRJ, Paape N, Schulz PS, Wasserscheid P, Steinr  ck HP (2010) *Phys Chem Chem Phys* 12:1905
32. Zheng Y, Dong K, Wang Q, Zhang J, Lu X (2013) Density, viscosity and conductivity of Lewis acid 1-butyl- and 1-hydrogen-3-methylimidazolium chloroaluminate ionic liquids. *J Chem Eng Data*. doi:10.1021/je3004904
33. Estager J, Oliferenko AA, Seddon KR, Swad  ba-Kwa  sny M (2010) Chlorometallate(III) ionic liquids as Lewis acidic catalysts: a quantitative study of acceptor properties. *Dalton Trans* 39:11375
34. Welton T (2004) Ionic liquids in catalysis. *Coord Chem Rev* 248:2459
35. Liu Z, Zhang R, Xu C, Xia R (2006) *Oil Gas J* 104:52
36. Boon JA, Levisky JA, Pflug JL, Wilkes JS (1986) Friedel-Crafts reactions in ambient-temperature molten salts. *J Org Chem* 51:480
37. Blanco CG, Banciella DC, Gonz  lez Azp  roz MD (2006) Alkylation of naphthalene using three different ionic liquids. *J Mol Catal A* 253:203
38. Chen M, Luo Y, Li G, He M, Xie J, Li H, Yuan X (2009) Alkylation of anthracene to 2-isopropylanthracene catalyzed by Lewis acid ionic liquids. *Korean J Chem Eng* 26:1563
39. Yin D, Li C, Tao L, Yu N, Hu S, Yin D (2006) Synthesis of diphenylmethane derivatives in Lewis acidic ionic liquids. *J Mol Catal A* 245:260
40. Gunaratne HQN, Lotz TJ, Seddon KR (2010) Chloroindanate(III) ionic liquids as catalysts for the alkylation of phenols and catechol with alkene. *New J Chem* 34:1821

41. Chauvin Y, Hirschauer A, Olivier H (1994) Alkylation of isobutane with 2-butene using 1-butyl-3-methylimidazoliumchloride aluminium-chloride molten-salts as catalysts. *J Mol Catal* 92:3508
42. Zhang J, Huang CP, Chen BH, Li JW, Li YX (2008) Alkylation of isobutane and butane using chloroaluminate imidazolium ionic liquid. *Korean J Chem Eng* 25:982
43. Liu Y, Hu RS, Xu CM, Su HQ (2008) Alkylation of isobutane with 2-butene using composite ionic liquid catalysts. *Appl Catal A Gen* 346:189
44. Huang CP, Liu ZC, Xu CM, Chen BH, Liu YF (2004) Effects of additives on the properties of chloroaluminate ionic liquid catalyst for alkylation of isobutene and butane. *Appl Catal A Gen* 277:41
45. Aschauer S, Schilder L, Korth W, Fritschi S, Jess A (2011) Liquid-phase isobutane/butane-alkylation using promoted Lewis-acidic IL-catalysts. *Catal Lett* 141:1405–1419
46. Bui TLT, Korth W, Aschauer S, Jess A (2009) Alkylation of isobutane with 2-butene using ionic liquids as catalyst. *Green Chem* 11:1961
47. Aschauer SJ, Jess A (2012) Effective and intrinsic kinetics of the two-phase alkylation of i-paraffins with olefins using chloroaluminate ionic liquids as catalyst. *Ind Eng Chem Res* 51:16288
48. Schilder L, Maass S, Jess A (2013) Effective and intrinsic kinetics of liquid-phase isobutane/2-butene alkylation catalyzed by chloroaluminate ionic liquids. *Ind Eng Chem Res* 52:1877
49. Qi XX, Ying ZG, Zhong CJ (2012) Chlorogallate(III) ionic liquids: synthesis, acidity, determination and their catalytic performances for isobutene alkylation. *Sci China Chem* 55:1547

Ionic Liquids in Transition Metal-Catalyzed Hydroformylation Reactions

Bernhard Rieger, Andriy Plikhta, and Dante A. Castillo-Molina

Abstract The latest state of the art in ionic liquid-based hydroformylation is reviewed in detail in this chapter. This multiphase homogenous catalytic system represents a promising strategy in order to reduce catalyst leaching during product separation and achieve the desired ratio of linear-to-branched aldehyde with a high catalytic activity and yield. A series of different catalytic systems, ionic liquids (ILs), and ligands together with their application in the hydroformylation of a variety of alkenes is presented. The features of those ILs derived from their composition and their interactions with substrates and catalysts are also discussed. In addition, recent studies on the catalyst distribution in the bulk and on the surface of ILs are summarized. Herein, the properties of the ligands show an impact in the activity and selectivity of the reaction. Moreover, not only Co and Rh complexes can be applied in the hydroformylation in ILs but also Pt and Ru complexes. On the other hand, the uses of CO₂ as chemical C¹ feedstock or *sc*CO₂ as carrier for the reagents and products in the hydroformylation reaction are commented. Catalytic processes where supported ionic liquid phases (SILPs) and nanocatalysts intervened complement this work.

Keywords Alkenes, Hydroformylation, Ionic liquids, *sc*CO₂, SILP

Contents

1	Introduction	99
2	Properties and Effects of ILs in Hydroformylation	101
3	Structure, Properties, and Application of Ligands in ILs-Based Hydroformylation	111
4	Ionic Liquid-Supported Hydroformylation in <i>sc</i> CO ₂	118
5	Supported Ionic Liquid Phase (SILP) Hydroformylation	121

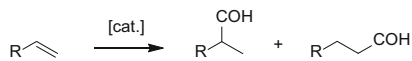
5.1	SILP Catalysts for Hydroformylation of Nonfunctionalized Linear Alkenes in Batch Reactors	121
5.2	SILP Catalysts for Hydroformylation of Different Substrates in Batch and in Continuous-Flow Reactors	125
6	Nanoparticles in Oxo Processes	131
7	Pt-Based Hydroformylation	131
8	Ru-Based Hydroformylation	132
9	Concluding Remarks	134
	Appendix	134
	References	140

Abbreviations

[4-mbpy][Cl]	1- <i>N-n</i> -Butyl-4-methylpyridinium chloride
[b((MeOSi) ₃ p)im][Cl]	1-Butyl-3-[3-(trimethoxysilyl)propyl]imidazolium chloride
[bdmim][PF ₆]	1,2-Dimethyl-3-butylimidazolium hexafluorophosphate
[bmim][BF ₄]	1- <i>n</i> -Butyl-3-methylimidazolium tetrafluoroborate
[bmim][Cl]	1- <i>n</i> -Butyl-3-methylimidazolium chloride
[bmim][Co(CO) ₄]	1- <i>n</i> -Butyl-3-methylimidazolium tetracarbonylcobaltate
[bmim][<i>n</i> -C ₁₂ H ₂₅ OSO ₃]	1- <i>n</i> -Butyl-3-methylimidazolium <i>n</i> -dodecylsulfate
[bmim][<i>n</i> -C ₈ H ₁₇ OSO ₃]	1- <i>n</i> -Butyl-3-methylimidazolium <i>n</i> -octylsulfate
[bmim][<i>p</i> -C ₆ H ₄ SO ₃]	1- <i>n</i> -Butyl-3-methylimidazolium <i>para</i> -toluenesulfonate
[bmim][PF ₆]	1- <i>n</i> -Butyl-3-methylimidazolium hexafluorophosphate
[bmim][Tf ₂ N]	1- <i>n</i> -Butyl-3-methylimidazolium bis(trifluoromethylsulfonyl)imide
[bmim][TfO]	1- <i>n</i> -Butyl-3-methylimidazolium trifluoromethanesulfonate
[bpy][BF ₄]	<i>N-n</i> -Butylpyridinium tetrafluoroborate
[bpy][Tf ₂ N]	<i>N-n</i> -Butylpyridinium bis(trifluoromethylsulfonyl)imide
[daim][An]	1,3-Dialkylimidazolium anion
[emim][C ₂ H ₅ OSO ₃]	1-Ethyl-3-methylimidazolium ethylsulfate
[emim][TfO]	1-Ethyl-3-methylimidazolium trifluoromethanesulfonate
[emmim][TfO]	1-Ethyl-2,3-dimethylimidazolium trifluoromethanesulfonate
[hmim][Tf ₂ N]	1- <i>n</i> -Hexyl-3-methylimidazolium bis(trifluoromethylsulfonyl)imide
[hmim][TfO]	1- <i>n</i> -Hexyl-3-methylimidazolium trifluoromethanesulfonate
[mbmim][TfO]	1-(2-Methyl- <i>n</i> -butyl)-3-methylimidazolium trifluoromethanesulfonate
[mg][Co(CO) ₄]	<i>N</i> -Methyl-guanidinium tetracarbonylcobaltate
[mtr][Co(CO) ₄]	1-Methyl-triazolium tetracarbonylcobaltate

[NBnEt ₃][Tf ₂ N]	<i>N</i> -Benzyltriethylammonium bis(trifluoromethylsulfonyl)imide
[NBu ₄][BF ₄]	Tetra- <i>n</i> -butylammonium tetrafluoroborate
[NEt ₄][Tf ₂ N]	Tetraethylammonium bis(trifluoromethylsulfo-nyl)imide
[NOC ₃ Me][Tf ₂ N]	<i>N</i> -Methyltri- <i>n</i> -octylammonium bis(trifluoromethylsulfonyl)imide
[omim][Tf ₂ N]	1- <i>n</i> -Octyl-3-methylimidazolium bis(trifluoromethylsulfonyl)imide
[omim][TfO]	1- <i>n</i> -Octyl-3-methylimidazolium trifluoromethanesulfonate
[P(C ₄ H ₉) ₃ (C ₁₄ H ₂₉)][DBS]	Tri(<i>n</i> -butyl)- <i>n</i> -tetradecylphosphonium dodecylbenzenesulfonate
[P(C ₄ H ₉) ₃ (C ₂ H ₅)][DEP]	Tri(<i>n</i> -butyl)ethylphosphonium diethylphosphate
[P(C ₆ H ₁₃) ₃ (C ₁₄ H ₂₉)][Cl]	Tri(<i>n</i> -hexyl)- <i>n</i> -tetradecylphosphonium chloride
[P(C ₆ H ₁₃) ₃ (C ₁₄ H ₂₉)][DCA]	Tri(<i>n</i> -hexyl)- <i>n</i> -tetradecylphosphonium dicyanamide
[P(C ₆ H ₁₃) ₃ (C ₁₄ H ₂₉)][Tf ₂ N]	Tri(<i>n</i> -hexyl)- <i>n</i> -tetradecylphosphonium bis(tri-fluoromethylsulfonyl)imide
[PEmim][PF ₆]	1-(2'-Piperid-1'-yl-ethyl)-3-methylimidazolium hexafluorophosphate
[PEmmim][PF ₆]	1-(2'-Piperid-1'-yl-ethyl)-2-methyl-3-methylimidazolium hexafluorophosphate
[prmim][TPPMS]	1- <i>n</i> -Propyl-3-methylimidazolium triphenyl-phosphine-3-monosulfonate
[prmim] ₂ [TPPDS]	1- <i>n</i> -Propyl-3-methylimidazolium triphenyl-phosphine-3,3'-disulfonate
[tmg][Co(CO) ₄]	<i>N,N</i> -Tetramethyl-guanidinium tetracarbonylcobaltate
[tmim][TfO]	1,2,3-Trimethylimidazolium trifluoromethanesulfonate
2-(DPP-C ₆ H ₄)-[mmim][BF ₄]	2-Diphenylphosphinophenylene-1,3-dimethylimidazolium tetrafluoroborate
2-DPP-[mbim][PF ₆]	1- <i>n</i> -Butyl-2-diphenylphosphino-3-methylimidazolium hexafluorophosphate
2-DPP-[PEmmim][PF ₆]	1-(2'-Piperid-1'-yl-ethyl)-2-diphenylphosphino-3-methylimidazolium hexafluorophosphate
bim(B(C ₆ H ₅) ₃)	(3- <i>n</i> -Butylimidazole)triphenylboron
Co	Cobalt
CO	Carbonyl or carbon monoxide
COD	Cycloocta-1,5-diene
DPP-Cobaltocene	1,1'-Bis(diphenylphosphino)cobaltocenium hexafluorophosphate
DPPiPr-Cobaltocene	1,1'-Bis(diphenylphosphino)- <i>iso</i> -propylcobaltocenium hexafluorophosphate

EDX	Energy-dispersive X-ray spectroscopy
FTIR	Fourier transform infrared spectroscopy
ILCs	Ionic liquid crystals
IR	Infrared
m.p.	Melting point
MAS	Magic angle spinning
MCILs	Metal-containing ionic liquids
MCM-41	Mesoporous silica nanoparticles
NHCs	<i>N</i> -heterocyclic carbenes
nm	Nanometer
NMR	Nuclear magnetic resonance
NORBOS-Cs ₃	Tricesium 3,4-dimethyl-2,5,6-tris(<i>p</i> -sulfonato-phenyl)-1-phosphanorbornadiene
NPs	Nanoparticles
OPGPP	Octylpolyethyleneglycol-phenylene-phosphite
P	Phosphorus
PEG	Polyethylene glycol
PFILs	Phosphine-functionalized phosphonium ILs
PGMILs	Polyether guanidinium methanesulfonates ILs
POP-Xantphos-2 [mmim][PF ₆]	Phenoxaphosphino-modified Xantphos
ppb	Parts per billion
Pt	Platinum
PTSA	<i>para</i> -Toluene sulfonic acid
Rh	Rhodium
Rh(CO) ₂ (acac)	(Acetylacetonato)dicarbonylrhodium(I)
rt	Room temperature
Ru	Ruthenium
scCO ₂	Supercritical carbon dioxide
SCF	Supercritical fluid
SEM	Scanning electron microscopy
SILP	Supported ionic liquid phase
TEM	Transmission electron microscopy
<i>T_g</i>	Glass-transition temperature
TMGL	1,1,3,3-Tetramethylguanidinium lactate
TOF	Turn over frequency
TOMAC	Trioctylmethylammonium chloride
TON	Turn over number
TPP, PPh ₃	Triphenylphosphine
TPPDS	Disodium triphenylphosphine-3,3'-disulfonate
TPPMS	Sodium triphenylphosphine-3-monosulfonate
TPPTI	Tri(1,2-dimethyl-3- <i>n</i> -butyl-imidazolium)triphenylphosphine-3,3',3''-trisulfonate
TPPTS	Trisodium triphenylphosphine-3,3',3''-trisulfonate
XRD	X-ray diffractometry



Scheme 1 Typical hydroformylation of an alkene

1 Introduction

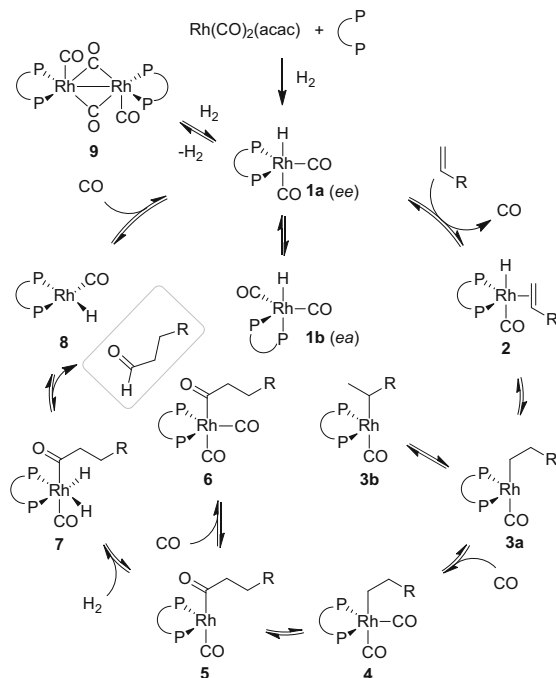
Hydroformylation, also known as oxo process or oxo synthesis, is the most powerful synthetic industrial tool where an alkene is converted in a highly valuable aldehyde through a homogeneous procedure [1]. During this process, a new C–C bond is formed using CO and H₂ as reagents, which affords a linear and a branched product with the use of a transition metal catalyst as depicted in Scheme 1.

Since its discovery in 1938 by Otto Roelen, the hydroformylation reaction has been conducted under diverse conditions and/or reaction media in order to achieve the desired ratio of linear-to-branched aldehyde and the highest catalytic activities and yields with a low catalyst leaching [2]. Accordingly, the first hydroformylation reactions in a homogeneous medium were reported using Co catalysts. Later on, Rh complexes were introduced as catalysts in the reaction and most of the reports in the last decades are related to this metal due to the remarkable activity of Rh [3].

Consecutively, further ligand-modified Rh and Co catalysts were proposed and showed an improvement in the reaction. However, the separation of the products from the reaction mixture was always an important subject during the development of new procedures in hydroformylation. In this regard, an aqueous biphasic hydroformylation process was established for the first time by Ruhrchemie with the purpose of overcoming expensive recycling cycles [4]. This technical breakthrough has been commercially used since 1984 and facilitated the separation of catalyst and products by decantation. Several examples of aqueous hydroformylation reactions with multiphase systems have since then been reported in the literature [5–10].

The mechanism of hydroformylation in a biphasic medium is analogous to that in organic solvents, as exemplified in Scheme 2. In addition, high-pressure IR and NMR studies have confirmed that the catalytic active Rh complexes are present in a dynamic equatorial–equatorial (*ee*) and equatorial–apical (*ea*) equilibrium (**1a** and **1b**) [12]. On the other hand, the decay in the catalytic activity is often associated with the dimerization of the catalytic active species (**9**). However, an increase in the partial hydrogen pressure shifts the equilibrium to the monomer site, and a reduction of both ligand and catalyst concentration also leads to an increase in catalytic activity [13]. Moreover, the oxo process is often accompanied by different side reactions such as double-bond isomerization, hydrogenation of unsaturated substrates to saturated species, or reduction of the formed aldehydes to alcohols.

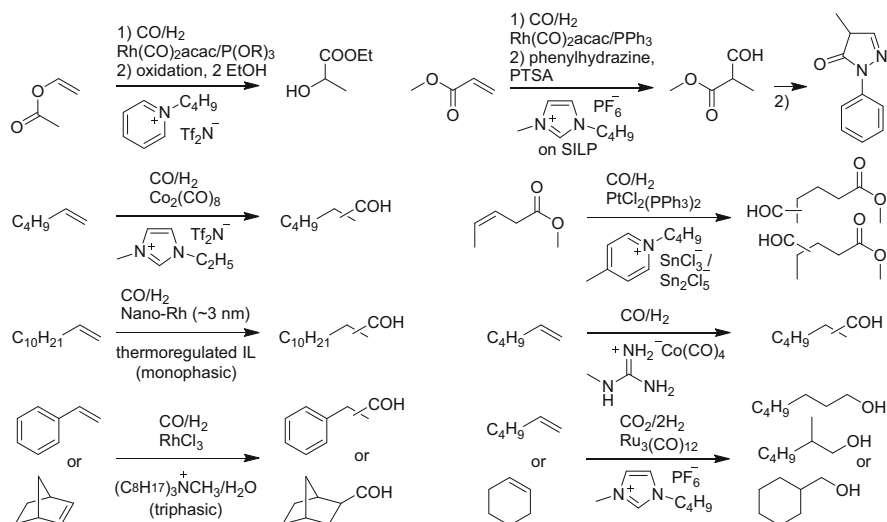
Scheme 2 General hydroformylation mechanism using bidentate phosphine ligands [11]



Due to the low solubility of higher alkenes, the aqueous biphasic hydroformylation is limited to C_2 – C_5 olefins (Scheme 2) [14]. The industrial conversion of higher olefins to aldehydes is mainly based on cobalt catalyst and is applicable under rather harsh conditions [15]. Therefore, ILs were seen as alternative solvents in order to overcome the limitations of the water-based biphasic oxo synthesis [16].

ILs can better dissolve organic substrates and, in consequence, increase the reaction rates. Their use as solvents in catalysis is well documented for other catalytic reactions [17–21]. The possibility of using ILs in biphasic oxo processes was shown as an example by Chauvin on the Rh-catalyzed hydroformylation of 1-pentene in $[\text{bmim}][\text{PF}_6/\text{BF}_4]$ in the presence of PPh_3 , TPPMS, and TPPTS in 1995 [22]. The non-nucleophilic $[\text{PF}_6]$, $[\text{SbF}_6]$, $[\text{BF}_4]$, and $[\text{CuCl}_2]$ counterions were chosen for the first studies, due to their availability and relative stability. Nevertheless, an earlier report on the hydroformylation in molten chlorostannates by Parshall in 1972 can be found in the literature [23].

Up to date a range of substrates have been tested in ionic liquid-supported hydroformylation. These include linear C_2 – C_{16} , cyclic unsaturated hydrocarbons, and unsaturated esters like methyl acrylate [24], norbornene [25], styrene [25, 26], methyl-3-pentenoate [27, 28], vinyl acetate [29, 30], vinyl naphthalene [31], and dimethyl itaconate [32]. An overview of the different catalytic systems is presented in Scheme 3. Herein, it is important to remark that some of the substrates tested in ionic liquid-based hydroformylation afford not only aldehydes but also alcohols [33–35] or heterocycles [24] due to the subsequent hydrogenation or cyclization.



Scheme 3 The variety of hydroformylation approaches

This chapter is organized in an easy-to-understand form. Reports on the use of Rh and Co as catalytic centers are presented at first as most of the studies are focused on those metals. Within this section, the properties, effects, and performance of ILs and ligands in different catalytic systems are described. Additionally, the development and latest results on the use of *sc*CO₂ and SILP in multiphasic ionic liquid-based hydroformylation catalysis are also summarized. Subsequently, the less explored homogeneous hydroformylation with Pt and Ru in ILs is reviewed. Hydroformylation with Ru complexes has been investigated in recent years due to the recent concerns on the efficient use of CO₂ as C¹ feedstock in industrial processes. A summary of Rh- and Co-based hydroformylations in ILs excluding those systems using *sc*CO₂ and SILP is presented by the end of this chapter (Appendix, Table 3).

2 Properties and Effects of ILs in Hydroformylation

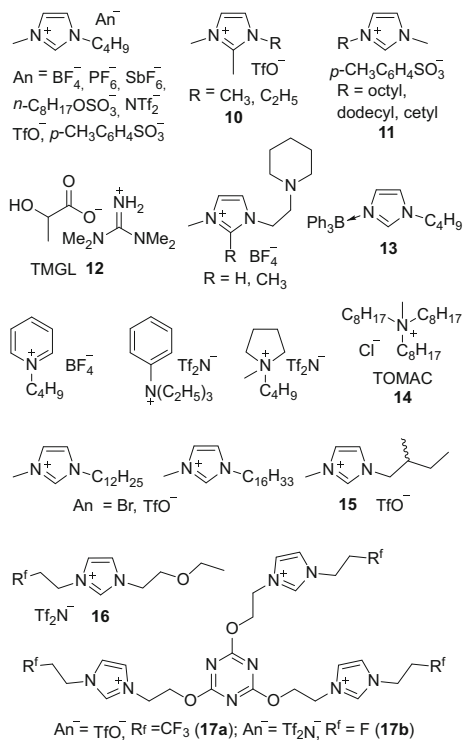
Liquid organic salts below 100°C, defined as ionic liquids (ILs), are promising non-conventional green solvents, which attract more and more interest for industrial homogeneous multiphasic applications. They are constituted by a wide range of asymmetric organic cations such as imidazolium, pyridinium, morpholinium, ammonium, or phosphonium as well as by inorganic or organic anions like halogenides, perfluorinated borates and phosphates, sulfonates, carbonates, and carboxylates. Their physicochemical properties are related to those cations and anions. Solubility, stability, thermomorphic behavior, density, viscosity, and

polarity are key physicochemical features of ILs. On the other hand, their recyclability, cost, and toxicity have to be considered before applying them in catalysis, especially for industrial purposes. Herein, their decomposition pathways and toxicities [67] remain as issues to be studied in detail. Some of the advantages of using ILs in catalysis are their negligibly low vapor pressure, relatively high thermal stability, task-specific structure variability, and ability to immobilize the catalyst.

The progress on the ILs-based hydroformylation covering the period from 1972 to 2008 has been reviewed by Dyson and Geldbach [13] as well as in publications from Haumann and Riisager [68, 69] to the full extent. The interest on its industrial application is reflected by the number of patents reported from 1993 to 2009 [36, 70–81]. The first studies in this field were focused on the following subjects: catalyst retention and recyclability in multiphase ionic liquid systems, examination of parameters influencing catalytic activity, selectivity and substrate solubility, search for new molecular architectures of liquid organic salts, and new feedstocks.

The development of ILs has been marked by important achievements. For instance, Wasserscheid et al. investigated the hydroformylation of methyl-3-pentenoate as a model technical feedstock in 1999. This substrate did not form biphasic reaction mixtures with [bmim][PF₆], but a TOF of 180 h⁻¹ was achieved [27]. Herein, the catalyst could be easily reused after simple product distillation from the monophasic reaction mixture. Later on, Dupont applied xanthene-modified phosphines to the hydroformylation of high olefins (C₈–C₁₈) in [bmim][PF₆] and [bmim][BF₄] and raised the question about the structural organization of ILs [60]. Consecutively, Olivier-Bourbigou reported the first systematic solubility screening of alkenes in ILs and discussed the dependence of the catalytic activity as a function of 1-hexene solubility in various ILs [44]. Further, the series of useful ionic liquid anions in hydroformylation was expanded to [CF₃SO₃], [CF₃CO₂], and [Tf₂N]. Similarly, Wasserscheid proposed the application of the ionic liquid [bmim][*n*-C₈H₁₇SO₄] as a halogen-free and hydrolytically stable ionic medium for hydroformylation of high olefins and, therefore, opened a discussion on the green aspects of the ILs-based catalysis [47]. In addition, Raubenheimer extended the ILs library with new molecular architectures and tested these ILs in 1-hexene and 1-decene hydroformylation [62]. Notably, a similar activity but a higher tendency toward alkene isomerization in comparison with conventional organic solvents was observed. Following this tendency, Shreeve presented in 2004 a new family of triazine-based polyfluorinated triquarternary liquid salts [59]. The catalysis based on those high viscous ionic compounds (**17a, b**, Fig. 1) gave almost full conversion for 1-octene within 19 h at 80°C and 69 bar. The range of novel ILs was hereafter expanded with high viscous ammonium ILs tagged with polyether tails by Jin in 2004 [64]. These asymmetric ammonium salts were investigated in the thermoregulated hydroformylation of 1-tetradecene. Furthermore, Williams found that imidazolium- and ammonium-type ILs gave markedly higher *n/iso* ratios for branched aldehydes (>99:1) in the monophasic reaction of vinyl acetate compared to those obtained in organic solvents [30]. A promoting effect of ILs on the catalytic activity has been also reported by several authors [30, 37, 68]. Interestingly, the

Fig. 1 Examples of ILs applied in hydroformylation



blending of two different ILs and the addition of organic solvents enhance the reaction rates and selectivities [30].

Solubility of gaseous substrates like CO, CO₂, H₂, and C₂–C₄ olefins in ionic liquid media during hydroformylation is an important issue, which should be clearly understood in order to perform the catalysis effectively. The actual collected experimental data allow to outline some correlation trends in solubility, but, due to the application of different methodologies and techniques, not all data is reliable and, in some cases, appears to be even contradictory [82].

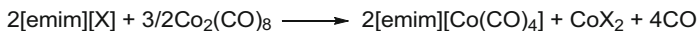
Generally, the solubility of CO and H₂ gases in ILs is substantially lower than in common organic solvents [13]. For [bmim]-containing ILs, H₂ solubility increases in the order [PF₆] < [BF₄] < [SbF₆] ≈ [CF₃CO₂] < [Tf₂N] [82] and, for 1-alkyl-3-methylimidazolium cations, seems to be largely independent of alkyl chain length [83]. Pyridinium-based ILs solubilize H₂ slightly better than those based on imidazolium. The highest H₂ solubility was found for the phosphonium-based ionic liquid [P(C₆H₁₃)₃(C₁₄H₂₉)] [PF₃(C₂F₅)₃]. A diminution in the temperature raises the H₂ solubility in [(C₄H₉)N(CH₃)₃] [Tf₂N], [bmim] [Tf₂N], and [emim] [Tf₂N], but the inverse temperature effect is observed for [bmim] [PF₆], [hmim] [Tf₂N], [bmim] [MeSO₄], and [bmim] [Tf₂N] [82]. In addition, the CO solubility rises in the anion order [BF₄] < [PF₆] < [SbF₆] < [CF₃CO₂] < [Tf₂N] for [bmim]-based ILs and in the order [mmim] < [emim] < [bmim] < [hmim] < [omim] for

cations with the same anion as determined by ^{13}C NMR, which indicates anion and alkyl chain length dependences [68, 84]. A contrary effect was only observed for [bmim][CH_3SO_4].

Solubility of gaseous unsaturated hydrocarbons in ILs commonly improves with increasing the olefin chain length $\text{C}_2\text{H}_4 < \text{C}_3\text{H}_6 < \text{C}_4\text{H}_8$. Regarding the influence of the IL anions, solubility of alkenes ascends regularly in the order $[\text{BF}_4] < [\text{PF}_6] < [\text{CF}_3\text{SO}_3] < [\text{CF}_3\text{CO}_2] < [\text{Tf}_2\text{N}]$ as well as with alkyl chain length of the substituents in imidazolium cations [82]. For phosphonium-containing ILs, the solubility rises in the order $[\text{P}(\text{C}_4\text{H}_9)_3(\text{C}_{14}\text{H}_{29})][\text{DBS}] < [\text{P}(\text{C}_4\text{H}_9)_3(\text{C}_2\text{H}_5)][\text{DEP}] < [\text{P}(\text{C}_6\text{H}_{13})_3(\text{C}_{14}\text{H}_{29})][\text{DCA}] < [\text{P}(\text{C}_6\text{H}_{13})_3(\text{C}_{14}\text{H}_{29})][\text{Cl}] < [\text{P}(\text{C}_6\text{H}_{13})_3(\text{C}_{14}\text{H}_{29})][\text{Tf}_2\text{N}]$ [85]. Pyrrolidinium-based ILs solubilize ethylene better than the ammonium-containing ILs.

Normally, when the catalytic conversion of substrates is conducted in an ionic liquid as the supporting solvent, the TOFs of the catalysts are affected because only the gaseous reagents initially dissolved in the ionic liquid substrate are available for the catalytic active species, and, once consumed, the solubilization of further gas into the ionic liquid occurs slowly [86]. Mass transfer limitations have been recognized since first reports on biphasic hydroformylations. As an example, a different reactivity was observed for alkenes in water-based biphasic media. While the hydroformylation of lower olefins based on water-soluble sulfonated monodentate phosphines is running with acceptable rates, the poorly water-soluble higher olefins can be hydroformylated with a rather low activity due to mass transfer limitations [68, 86, 87]. Therefore, several solutions have been suggested to increase the reaction rates of higher alkenes in aqueous-phase catalytic conversions, such as addition of conventional surfactants [87]. In ILs, an increase in the olefin chain length from 1-hexene to 1-decene causes a drop in catalytic activity from $1,155 \text{ h}^{-1}$ to 22.1 h^{-1} , as observed for the oxo synthesis using a bidentate Rh complex in [bmim][$p\text{-CH}_3\text{C}_6\text{H}_4\text{SO}_3$] [88]. By hydroformylation of higher olefins in [Rmim][$p\text{-CH}_3\text{C}_6\text{H}_4\text{SO}_3$] (**11**, Fig. 1), Lin et al. reported that the activities are strongly dependent on the ionic liquid cation [45]. When the chain length of an alkyl substituent in an imidazolium fragment was comparable with that of an olefinic substrate, the reaction rates evidently accelerated. This confirms a strong influence of the solubility of high alkenes in imidazolium alkylsulfonates on the reaction rates.

An important improvement in the development of ILs for hydroformylation was the incorporation of a catalytic active metal core in the architecture of ILs, which represented another promising approach [25]. One of the first works in this field was addressed to simplify the standard operating procedures of catalyst preparation by eliminating any activation or synthetic steps. Thus, it was found that mixing RhCl_3 and $[(\text{C}_8\text{H}_{17})_3\text{NCH}_3][\text{Cl}]$ (TOMAC; **14**, Fig. 1) led to the formation of $[(\text{C}_8\text{H}_{17})_3\text{NCH}_3][\text{RhCl}_4]$. This ammonium salt, which contains an anionic RhCl_4 moiety, catalyzes effectively the hydroformylation of styrene, norbornene, and tetradecene under triphasic conditions at 80°C without detectable loss of activity (Appendix, Table 3). The catalytic active species could not be fully characterized due to isolation difficulties, but the formation of rhodium carbonyl complexes



Scheme 4 Reaction of $\text{Co}_2(\text{CO})_8$ with ethylmethylimidazolium-based ILs

during the reaction was evidenced by the appearance of two sharp signals ($2,063\text{ cm}^{-1}$ and $1,988\text{ cm}^{-1}$) in the carbonyl region of IR spectra. Interestingly, addition of water was indispensable for the reaction. Such positive “on water” effect has been also reported by other authors [89].

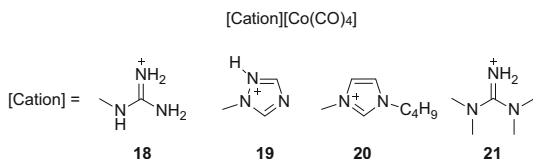
The cobalt-based ionic liquid system $\text{Co}_2(\text{CO})_8/\text{pyridine}/[\text{bmim}][\text{Tf}_2\text{N}]$ appeared to be active in the hydroformylation of 1-hexene at 130°C and 100 bar CO/H_2 pressure reaching a TOF of 110 h^{-1} with a selectivity of 78% for *n*-heptanal [42]. This hydroformylation reaction took place only in ILs which contain non-coordinating anions ($[\text{Tf}_2\text{N}]$ or $[\text{PF}_6]$). Hence, no conversion occurs in the case of $[\text{emim}][\text{CH}_3\text{SO}_3]$, $[\text{emim}][p\text{-CH}_3\text{C}_6\text{H}_4\text{SO}_3]$, and $[\text{bmim}][p\text{-CH}_3\text{C}_6\text{H}_4\text{SO}_3]$. Based on the fact that the reactivity of $\text{Co}_2(\text{CO})_8$ with pyridine produces the ionic pair $[\text{Co}^{2+}(\text{Py})_6][\text{Co}(\text{CO})_4]_2$, Olivier-Bourbigou proposed a putative mechanism for the reaction of $\text{Co}_2(\text{CO})_8$ with ILs, which leads to the formation of the anionic fragment $[\text{Co}(\text{CO})_4]$ as indicated by IR analysis (Scheme 4). This reaction only takes place with the most coordinating anions and seems to be related with the observed catalytic results. Additionally, it was assumed that the catalytic active cobalt complex $[\text{HCo}(\text{CO})_4]$ is generated under high pressure and temperatures, but tends to dimerize into $\text{Co}_2(\text{CO})_8$ or undergoes an acid–base neutralization by pyridine forming $[\text{PyH}][\text{Co}(\text{CO})_4]$ under normal conditions. The $[\text{HCo}(\text{CO})_4]$ complex can be regenerated again by increasing the temperature and pressure. The use of pyridine effectively prevents the cobalt leaching to the 100–150 ppm level.

Further catalytically active metal-containing ILs (MCILs) for hydroformylation reactions were reported by Rieger et al. in 2011 (Fig. 2) [43].

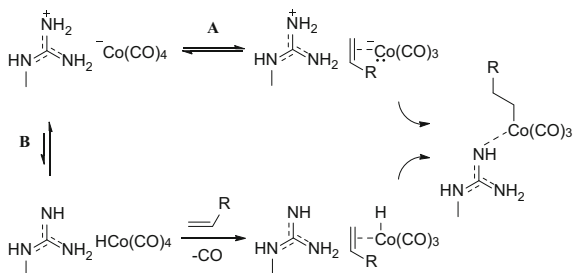
These new MCILs were able to convert 1-hexene to *n*-heptanal with 47% selectivity at 120°C and 30 bar (mixture of 20 bar H_2 and 10 bar CO). Interestingly, only protic steric unhindered metal-containing ILs (**18**, **19**) showed a good performance toward olefin conversion, while zero activity was detected for the aprotic and protic bulky MCILs (**20**, **21**). Herein, in the context of the acid–base reaction discussed above for pyridine, the cation–anion interaction forming $[\text{HCo}(\text{CO})_4]$ is not ruled out for guanidinium carbonylcobaltates (Scheme 5, **B**). However, it was also concluded that $[\text{HCo}(\text{CO})_4]$ is not the active species in this case and hydroformylation occurs via cooperative ligand–metal interactions in the case of protic MCILs (Scheme 5, **A**).

Based on investigations of structural organization of common dialkylimidazolium salts, Dupont et al. described such salts as hydrogen-bonded polymeric supramolecules of the type $[(\text{daim})_x[\text{An}]_{x-n}]^{n+}[(\text{daim})_{x-n}[\text{An}]_x]^{n-}$ [90]. The introduction of guest molecules into ILs environments causes a disruption of the hydrogen bond network and, in some cases, induces the nanostructured reorganization and creation of polar and nonpolar regions. Substantially, electrostatic, hydrogen bonding, and π -stacking interactions between the ionic liquid and guest

Fig. 2 Cobalt-containing ILs reported by Rieger et al.



Scheme 5 Possible insertion pathways of an olefin in a cobalt-containing ionic liquid



substrates take place forming “inclusion complexes” as a result of the supramolecular organization [91]. The ionic media can have a considerable influence on the molecular reactivity and selectivity of the organometallic catalytic species and reaction mechanisms. By consecutive dilution, ILs take the shape of triple ion aggregates and contact ion pairs to a considerable degree, whereas solvent-separated ion pairs in the infinitely diluted state are formed (Fig. 3).

In the last years, investigation on the surface and interface properties of ILs at the molecular level has also gained significant interest with the purpose to assess their mass transfer characteristics, thermic behavior, surface tension, and wettability. Numerous non-vacuum and ultrahigh vacuum spectroscopic and scattering techniques have been applied in order to examine in detail their surfaces [92]. The chemical composition in upper and boundary layers can differ from that in the bulk, due to the non-isotropic environment.

Steinrück and Wasserscheid studied, for the first time, the topologic distribution of Rh complexes and their surface activity in [emim][C₂H₅SO₄], [emim][C₈H₁₇SO₄], [bmim][C₈H₁₇SO₄], [emim][Tf₂N], and [emim][PF₃(C₂F₅)₃] [93]. Steinrück et al. reported on ionic liquid interfaces and related bulk properties and studied chemical reactions and the dissolution of transition metal complexes in situ using X-ray photoelectron spectroscopy (XPS) technique [92]. Analyses of the near-surface region (7–9 nm) at 0° emission angle and of the topmost surface layer (1–1.5 nm) at the 80° emission angle were performed. A surface enrichment with Rh by addition of TPPTS to the dissolved [Rh(CO)₂(acac)] in both [emim][C₂H₅SO₄] and [bmim][C₈H₁₇SO₄] was observed. Moreover, the orientation of the formed Rh–TPPTS complex in the topmost IL layer was also deduced out from the XPS experiments. Herein, the SO₃ groups and P atoms are preferentially pointed toward the ionic liquid bulk (Fig. 4).

Additionally, the hydroformylation reaction can be successfully monitored by common analytic techniques, such as high-pressure IR [94] or NMR [12]. Reliable

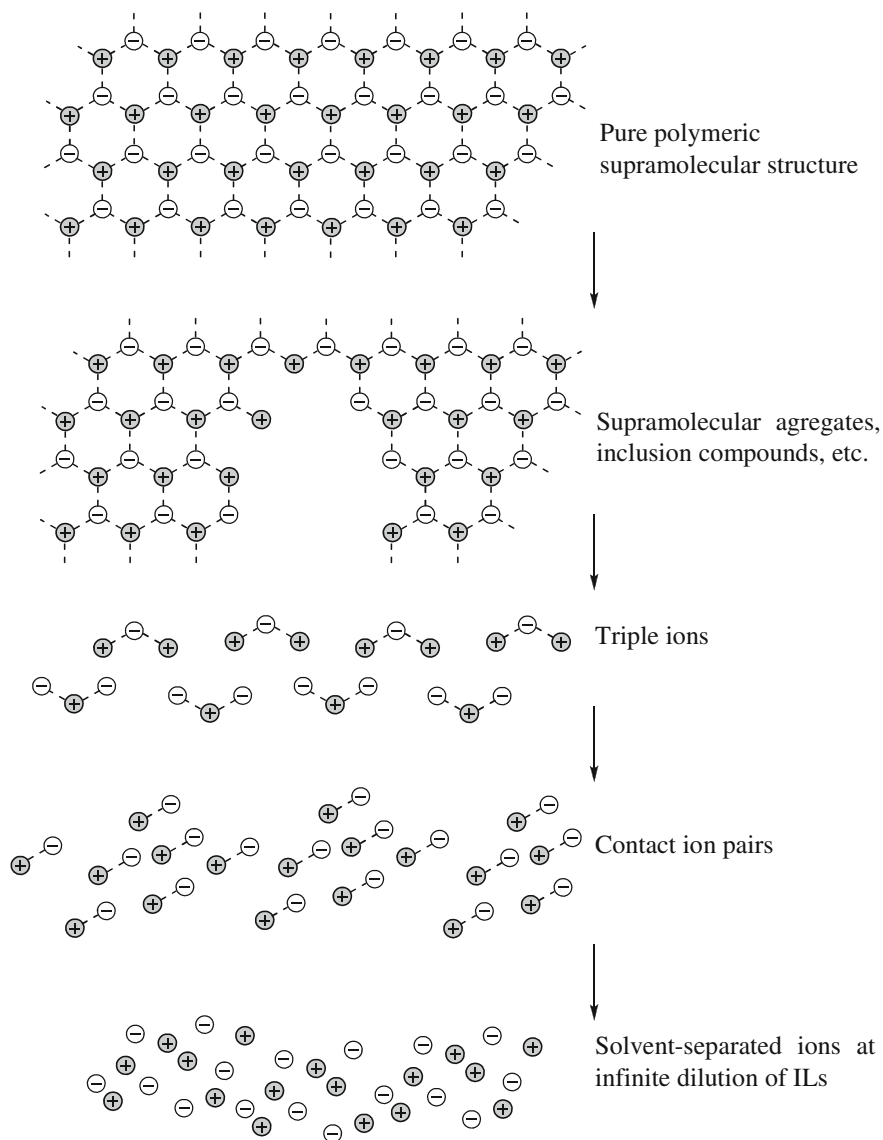
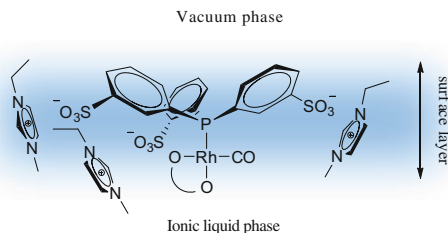


Fig. 3 Simplified two-dimensional model of the structural organization of 1,3-dialkylimidazolium ILs (reproduced from [90])

information about the ionic liquid-immobilized catalyst can be also obtained by direct analysis of reaction mixtures using electrospray ionization ion trap spectrometry, as reported by Dyson and Zhang [37, 95].

In general, the state of matter of most common ILs is mainly due to the dissymmetry of the cationic fragments at standard conditions. Nevertheless, it is

Fig. 4 Surface orientation of a Rh–TPPTS complex in ILs (reproduced from [92])



important to note that symmetric solid organic salts can also be applied in biphasic hydroformylation of olefins by setting their melting point using supercritical CO₂ (scCO₂) or even low-to-moderate CO₂ pressures. As an example, Leitner et al. showed that the prototypical hydroformylation of 2-vinylnaphthalene in [NBu₄][BF₄] is possible by inducing its melting point depression with CO₂ [31]. Thus, the melting point of [NBu₄][BF₄] can be significantly lowered from 156°C to 36°C at 150 bar, whereas [NEt₄][CF₃SO₃] (m.p. 102°C) turns to the liquid state already at 20°C at 35 bar CO₂. This methodology has the potential to expand the number of organic melts by using easy accessible and cheaper symmetric ionic salts as an alternative to ILs.

Another parameter that can be adjusted in order to modify the physical properties of some ionic liquid systems is the temperature. The modulation of this condition opens a new spectrum of possibilities in the application of ILs in catalysis [96]. For instance, numerous concepts that considered the thermomorphic phase behavior of solvents and thermoregulated phase separation of catalysts have been developed in the recent years [96]. The method of thermoregulated multicomponent solvent systems is particularly promising to overcome the mass transport limitations between nonpolar substrates and the polar catalyst-containing phase. This is beneficial for the achievement of a high reactivity, efficient separation, recovery, and recycling of the catalyst [96, 97]. This process contemplates the temperature-dependent miscibility gap of eligible solvent mixtures (Fig. 5). Herein, a system switches from biphasic form under normal conditions to a homogenous liquid by increasing the temperature, and the latter can be again separated by cooling. The point of transition from the biphasic system into the homogeneous state is defined as upper critical solution temperature (UCST). These smart solvents are particularly useful uppermost for industrial homogeneous catalytic applications and, in principle, can be implemented within existing facilities [98].

Incidentally, the combination of ILs with some solvents shows the inverse miscibility effect, which means that a transformation from monophasic to biphasic form passing through the point of lower critical solution temperature (LCST) can be observed by heating [96].

Typical examples of thermoregulated ILs are quaternary ammonium alkane sulfonate salts tailed with various polyether chains (IL_{PEG_x}, $x = 350, 550, 750$; 24, Fig. 7) [63, 64]. Such non-fluorinated ILs are environmentally friendly and allow easy catalyst separation by decantation without observable activity loss over 7 h. Hydroformylation of 1-dodecene catalyzed by Rh–TPPTS was performed

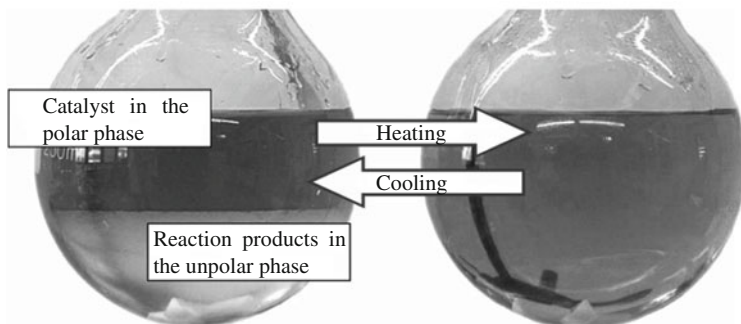


Fig. 5 Functional principle of temperature-controlled multicomponent solvent systems: simple phase separation before or after catalytic conversion (*left*) and reaction under monophasic conditions (*right*) (reproduced from [96])

in a IL_{PEG750}/toluene/*n*-heptane solvent mixture (miscibility point 108°C) with 97% conversion and a TOF of 295 h⁻¹ at 110°C (see Appendix, Table 3). Conducting the reaction at 90°C under biphasic conditions results in much lower conversion (21%) and activity (TOF = 65 h⁻¹), which shows mass transport limitations taking place under biphasic conditions. In addition, the improved conversion values and activities in the temperature range from 100 to 110°C indicate that this thermomorphic system changes from biphasic to monophasic. Products from this reaction were obtained by simple phase separation, while the Rh catalyst was retained in the IL phase with a leaching of less than 1%. PEG-derivatized ammonium methanesulfonates (**22**, **24**, Fig. 7) were also studied in a “ligand-free” hydroformylation of 1-octene using Rh nanoparticles (~1.3–2.1 nm) [53, 54]. Both of them showed thermoregulated phase transition properties, high activities, and retention of Rh NPs with low metal leaching (0.3%) (Fig. 6).

On the other hand, an oxo synthesis performed in ionic liquid crystals (ILCs) was reported recently by Wang [55]. The novel *N*-alkylcaprolactam-based ILCs (**27a**, **b**; Fig. 7) hydroformylate 1-octene with lower conversion compared to common imidazolium-based ILCs **26**. It was shown that the lamellar mesophase and the anion and chain length of the substituents of the cation have a strong impact on the TOF and regioselectivity.

The room temperature-solidifiable polyether guanidinium methanesulfonates ILs (PGMILs; **25**, Fig. 7) possess an advantage in the Rh-catalyzed biphasic hydroformylation of C₈–C₁₄ olefins being long-term highly active (TON = 31188 after 35 runs), selective, and thermal and chemical stable [61]. The glass-transition temperature (*T_g*) of PGMILs can be modulated by changing the polyethyleneglycol chain length (for *n* = 16, 22, and 42 are *T_g* = 23.8, 37.9, and 50.2°C, respectively). Therefore, some PGMILs can solidify at room temperature, which effectively simplifies the separation of catalyst from the product.

Other types of thermoregulated ILs are long alkyl chain imidazolium halogenides and triflates. They can be used as “micellar promoters” by combining

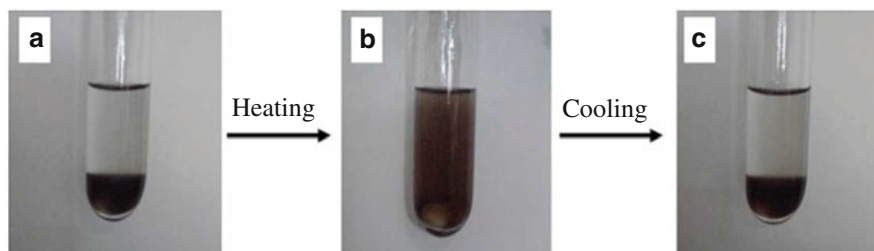


Fig. 6 Visualization of the thermomorphic behavior of PEG-derivatized ammonium methanesulfonates containing Rh nanoparticles ($\sim 1.3\text{--}2.1$ nm): (a) room temperature, (b) miscibility temperature, and (c) phase separation at room temperature (reproduced from [53])

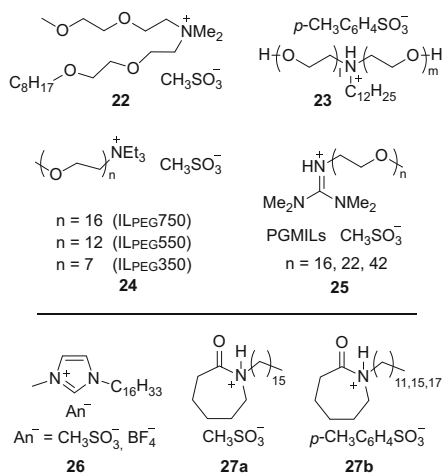


Fig. 7 Thermoregulated systems: PEG-derivatized ammonium-based ILs (*upper section*) and ionic liquid crystals (ILCs, *lower section*)

them with α -cyclodextrins in thermoregulated microemulsions under hydroformylation conditions [66]. The supramolecular interactions of the imidazolium salts favor the micellization at high temperatures, whereas at lower temperatures, the complexation of benzimidazolium cations by α -cyclodextrins leads to destabilization of micelles (Fig. 8). Such thermoregulated switch is a valuable element for organometallic catalysis. The decantation times can be substantially decreased and a perfect phase separation can be achieved in such α -cyclodextrins-containing mixtures.

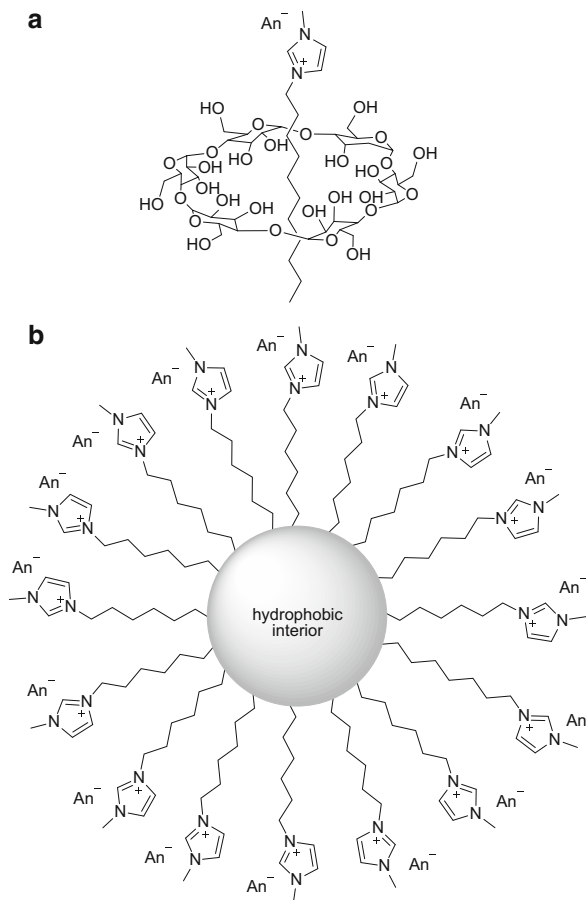
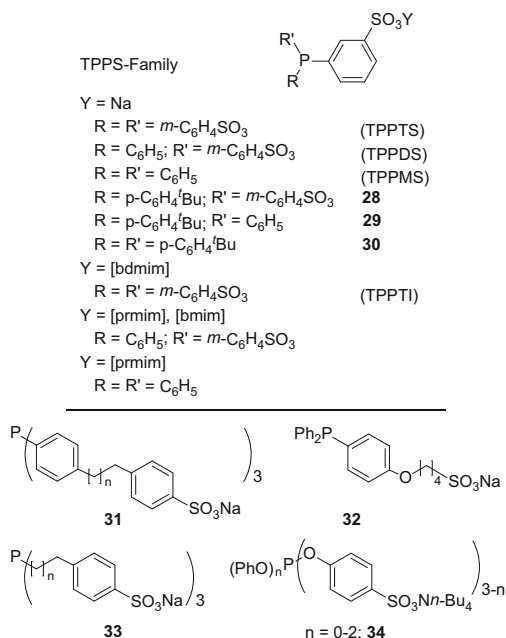


Fig. 8 Self-organizations in imidazolium- α -cyclodextrin systems: (a) [Rmim][An]- α -cyclodextrin complex at low and (b) micelle formation at elevated temperatures [66]

3 Structure, Properties, and Application of Ligands in ILs-Based Hydroformylation

The nature of the ligand structure plays also an essential role in hydroformylation and affects important catalyst properties such as activity, selectivity, stability, and solubility. The latter is crucial in catalytic systems where a catalyst separation and/or recycling step is included. In search for more selective and effective catalysts, a large spectrum of ligands for ionic liquid-supported hydroformylation processes has been designed and tested in the last decades. Nowadays, they can be classified by their physicochemical properties (solubility in organic solvents, water, or in both), their ionic character (ionic and nonionic), or their complexation mode (mono- or bidentate). Herein, PPh_3 has been used very often as a model ligand, due

Fig. 9 Monodentate sulfonated phosphine ligands used in ionic liquid-based hydroformylations

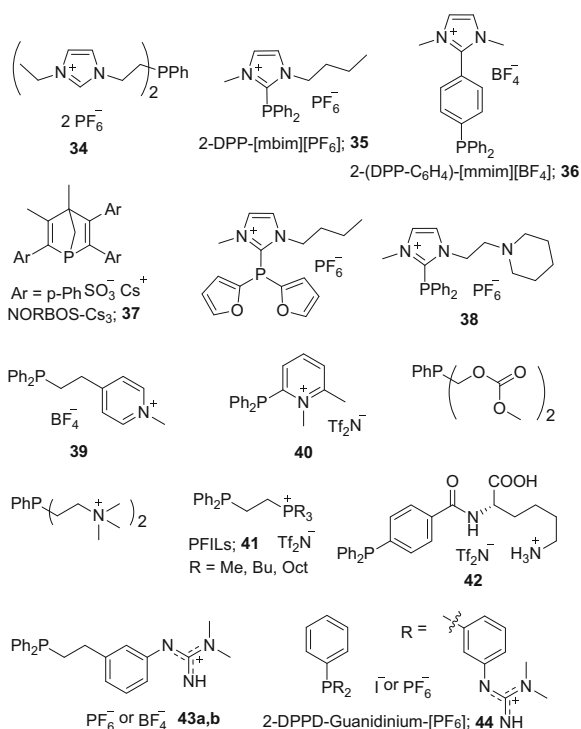


to its availability; it was one of the first ligands used in ionic liquid-containing biphasic hydroformylation reactions. However, although acceptable reaction rates and low-to-moderate selectivities and *n/iso* ratios were obtained, it was observed that a large amount of the Rh catalyst passed into the organic layer during the course of the biphasic hydroformylation reaction [48]. This effect produced a considerable loss of the catalyst during product separation.

The functionalization of PPh₃ with ionic groups showed an improvement in the immobilization of the catalysts in the ionic liquid layer and, therefore, a decrease of the catalyst leaching [99, 100]. Accordingly, several derivatives of sulfonated PPh₃ have been investigated in recent decades (Fig. 9) and their corresponding Rh complexes are reported to be soluble in ILs and water [38]. In some of the cases, their solubility in ionic liquid media can be increased by addition of small amounts of water to the reaction mixture [39]. As an example, the use of (3-sodium sulfonatophenyl)diphenylphosphine (TPPMS), bis(3-sodium sulfonatophenyl)phenylphosphine (TPPDS), and tri(3-sodium sulfonatophenyl)phosphine (TPPTS) under biphasic conditions has been reported by Beller et al. [13, 68, 87].

In order to understand the influence of the sulfonated PPh₃ ligands on the surface composition of Rh-containing ionic liquid solutions, Wasserscheid et al. have conducted ARXRD spectroscopic studies using a Rh–TPPTS complex in [emim][C₂H₅OSO₃] [93]. The results of this study indicated that the nature of the ligand affects the distribution of the catalytic active species at the interface of the ionic liquid. Thus, the Rh–TPPTS complex displays a high surface activity, while the TPPTS-free catalytic system using [Rh(CO)₂(acac)] as precursor showed Rh

Fig. 10 Monodentate phosphine ligands used in ionic liquid-based hydroformylations

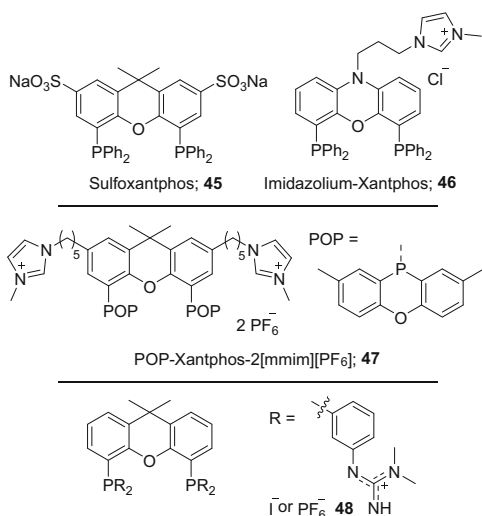


depletion from the ionic liquid surface. In this context, it is important to mention that the influence of new ligands on ionic liquid-based oxo synthesis is often compared in the literature with reaction mixtures where only $[\text{Rh}(\text{CO})_2(\text{acac})]$ is present. For this catalyst precursor in the absence of added ligands (so-called ligand-free conditions), TOF values up to $1,315 \text{ h}^{-1}$ (for 1-hexene and 1-decene) but low *n/iso* ratios (0.5–1.0) and a high metal leaching have been reported depending on substrate, ionic liquid, and reaction conditions [26, 39].

Following the list of monodentate sulfonated phosphines depicted in Fig. 9, a range of amphiphilic or tenside phosphines has also been developed and successfully applied in catalysis [38, 87, 101–103]. Hydroformylation reactions with bis(3-sodium sulfonatophenyl)(4-*tert*-butylphenyl)phosphine (**28**), phenyl(3-sodium sulfonatophenyl)(4-*tert*-butylphenyl)phosphine (**29**), and bis-(4-*tert*-butylphenyl)(3-sodium sulfonatophenyl) phosphine (**30**) in [bmim][PF₆], [bmim][BF₄], and [bmim][*n*-C₁₂H₂₅OSO₃] have shown relatively high reaction rates and higher *n/iso* ratios for 1-hexene in comparison with those obtained with TPPDS and TPPTS [38]. In addition, the complexes of hydrotropic TPPTS and TPPDS showed not to be suitable for catalytic conversion of 1-hexene to heptanal in hydrophobic [bmim][PF₆].

Further monodentate phosphines for hydroformylation in ILs are presented in Fig. 10. Special attention should be paid to the phosphonium-functionalized

Fig. 11 Bidentate phosphine ligands used in ionic liquid-based hydroformylations

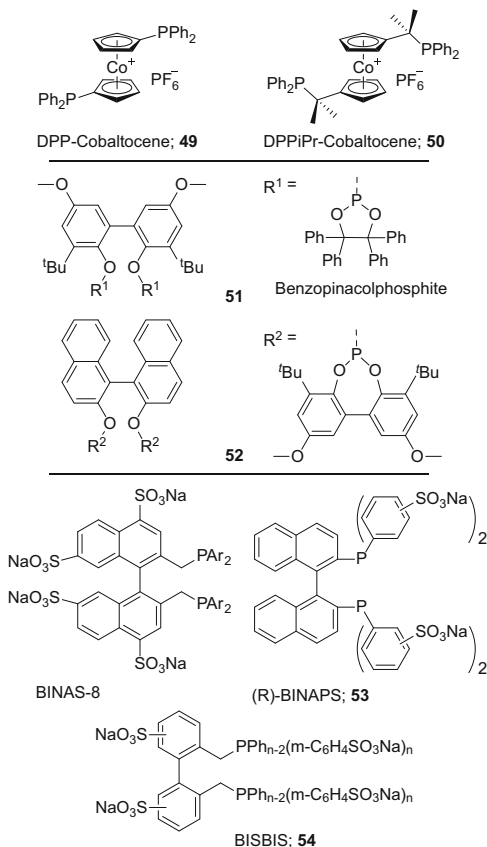


monodentate phosphines (PFILs) **41**, which were found to be effective stabilizing agents for high alkene hydroformylation [51]. The alkene solubility and selectivity in hydroformylation have been enhanced varying the length of the P-alkyl chains. Such phosphonium-derivatized ligands appeared to be more catalytically active and selective in comparison with TPP-based systems (Appendix, Table 3) [104].

A new family of monodentate 2-imidazolium-functionalized phosphines (**35** and **38**, Fig. 10) was applied in the hydroformylation of 1-octene by Stelzer [49] and Liu et al. [58]. According to the authors, the close proximity of the positive charge of the imidazolium moiety to the phosphorus atom significantly enhances the catalytic activity of the catalyst in biphasic 1-octene hydroformylation.

In general, the hydroformylation in the presence of monodentate phosphines provides rather low *n/iso* ratios [13] in comparison to bidentate ligands. Therefore, further investigations have been focused on the development of suitable bidentate ligands for hydroformylation in ILs. From all bidentate ligands reported in the literature, the Xantphos family is one of the most effective in hydroformylation reactions because they give very high activities and *n/iso* selectivities. For instance, catalytic reactions based on the dicationic phenoxaphosphino-modified Xantphos ligand shown in Fig. 11 (POP-Xantphos-2[mmim][PF₆], **47**) displayed one of the highest activities and selectivities for 1-octene with TOF up to 10,100 h⁻¹, high *n/iso* ratio (40–50), low rhodium leaching (<5 ppb), and poor ligand loss (<100 ppb P) [40, 41]. On the other hand, the monocationic imidazolium-xantphos **46** hydroformylated 1-octene in a continuous-flow process in [omim][NTf₂] affording high yields and *n/iso* ratios up to 53 (Appendix, Table 3) [100]. Additionally, a catalyst based on sulfonated xantphos (**45**) converted completely 1-octene in [bmim][PF₆] within 24 h, but showed a TOF of 41 h⁻¹, whereas the selectivity was up to 42 with a 1:5 (Rh:L) ratio [60, 105].

Fig. 12 Other examples of bidentate phosphine ligands used in ionic liquid-based hydroformylation



The guanidinium-modified xantphos (**48**, Fig. 11) has been used in the hydroformylation of 1-octene in [bmim][PF₆] giving good *n/iso* values (20/1) and low rhodium leaching (less than 0.07%). Surprisingly, an increase in the conversion after every reuse of the catalytic mixture was observed. This effect was attributed to the preformation time of the active catalytic species [48]. Moreover, a guanidinium-containing ligand based on PPh₃ (**43**, Fig. 10) was also prepared. Both ligands can be obtained through a simple and efficient methodology and represent an excellent way to immobilize the catalyst.

Ionic bidentate electron-poor phosphines containing a cobaltocenium framework have been tested in the rhodium-catalyzed hydroformylation of 1-octene in [bmim][PF₆] (**49** and **50**, Fig. 12) [46]. The catalysts based on these ligands afforded *n*-nonanal with remarkably high catalytic activity and selectivity. Further rhodium complexes containing phosphines with electron-withdrawing groups (**35**, Fig. 10) have also been reported to show a significantly high TOF [49, 106, 107] and, in some cases, high *n/iso* ratios [108]. The reason for such performance is the low electron density on phosphorus atoms which causes an increase in the π -back bonding between the Rh atom and the phosphine in the catalytic species. This

produces the weakening of π -back donation from an occupied metal d -orbital to the π^* -orbital of a CO ligand and facilitates the substitution of the CO ligands by alkenes. The degree of π -back bonding in metal carbonyl complexes and the hydroformylation rate can be assessed with the stretching frequency of the CO ligands in IR [109, 110].

The incorporation of an aliphatic spacer between the phosphorus atoms and the electron-withdrawing cobaltocenium moieties resulted in a significant diminution of the catalytic activity and selectivity (**50**, Fig. 12). A similar insulation effect was observed by Brauer et al. in the catalytic activity of DPP-[mbim][PF₆] (**35**) (TOF = 552 h⁻¹) and 2-(DPP-C₆H₄)-[mmim][BF₄] (**36**) (51 h⁻¹) in the biphasic hydroformylation of 1-octene in [bmim][PF₆] due to the presence of a *para*-phenylene bridge. This conclusion is also in good agreement with the results reported by Leitner et al. [111] and Erkey et al. [109], where the insulation effects of oxygen and methylene spacer were indicated. Herein, the introduction of ionic fragments such as sulfonate, phosphonate, and guanidinium at the *para*- or *meta*-position to phosphorus in arylphosphines does not lead to a significant change in the electronic and steric properties of phosphine ligands, according to IR and NMR studies [48, 112].

The use of bidentate ligands with biphenyl or binaphthyl backbones in ionic liquid-based hydroformylations is also reported in the literature (Fig. 12). For instance, a BISBIS-containing catalyst gave up to 95% conversion in the hydroformylation of 1-octene in *N*-alkylimidazolium sulfonates (**54**, Fig. 12) with high TOF (1,055 h⁻¹) and *n/iso* values (17.9) [88]. The selectivity in this case is determined by the steric effects of the ligand and the P–metal–P angles [13, 113]. Overall, bidentate phosphines with large bite angles promote high *n/iso* ratios. For instance, high selectivities (66.5:1) were achieved in the hydroformylation of 1-hexene with the very flexible ligand BISBIS, which has a wide bite angle (124.8°).

Inter- and intramolecular interactions taking place in the catalytic environment have a strong impact in the performance and stability of the catalysts. The rhodium leaching is a substantial problem to overcome considering the high metal costs and complicity of the catalyst recovering. It can be caused by ligand dissociation followed by formation of tetracarbonyl rhodium hydrides [114] as well as by a range of other undesirable side reactions, leading to catalyst decomposition, such as metal reduction, ligand degradation, or oxidation. The metal leaching can be significantly decreased by the equipping of phosphine ligands with cationic (guanidinium, imidazolium, phosphonium [51], ammonium, pyridinium) or anionic (sulfonates) functionalities. Such designed ligands are a powerful tool for the retention of active catalytic species in ionic liquid matrices [44, 48].

Furthermore, the ligand loading affects the activity of the catalytic systems. Thus, it was observed that reactions with a Rh:L ratio (1:3) have a slightly higher TOF (up to 75 min⁻¹) in comparison to systems with a Rh:L ratio of 1:10 (TOF = 70 min⁻¹), while an overload (Rh:L = 1:100) causes a drop in the catalytic activity (TOF = 30 min⁻¹) in [bmim][PF₆]. In all cases, the *n/iso* ratios remained unchanged. On the other hand, a high amount of added phosphine prevents significantly metal leaching, which stays below the detection limit [39].

In addition to the known advantages in the catalyst recyclability and stability, ILs can also participate as ligands when they are used as reaction medium. Formation of *N*-heterocyclic carbene (NHC) Rh complexes can take place during the catalysis in imidazolium-based ILs in accordance with several reports about the room temperature C–H activation at the C²/C⁴ position of imidazolium cations. Hence, NHC-mediated hydroformylation became an intensive research area since 1997. However, the first investigations on mono- and bidentate NHCs-supported Rh and Co hydroformylations were conducted mainly in organic solvents (benzene, toluene, and dichloromethane) [115–118]. Evidences for the complexation of Rh with carbenes in ionic liquid-supported oxo synthesis have been reported more intensively in recent years [37, 119]. For instance, the formation of transient carbene species in the ILs-supported hydroformylation of 1-octene was first observed by Dupont et al. [119]. Based on D/H exchange experiments, it was concluded that NHCs derived from imidazolium moieties are produced in typical [bmim]-based catalytic systems. Moreover, phosphine ligands play an essential role in the creation of carbene species, and the presence of weak bases, such as methanol, favors the complexation. The formed Rh–NHC complexes do not cause any significant changes in the catalytic activity or selectivity, and the NHCs can be easily displaced by other substrates present in the reaction mixture.

Regarding the catalyst decomposition pathways, three different cases can be mentioned: the well-studied oxidative addition of the P–C bond on the rhodium center, the aryl migration from one phosphine to Rh, and the hydrolytic cleavage of water-soluble ligands [103, 120]. Furthermore, a very small amount of oxygen or peroxide in the reagent feed system over long flow periods can lead to phosphine oxidation with the subsequent ligand cleavage from the rhodium atom. This results in a dramatic decrease of linear-to-branched aldehyde ratios as well as in metal loss, especially in a continuous-flow process. In order to overcome this problem, a cheaper phosphine was added as a sacrificial oxygen scavenger. However, this has not shown to be very effective in preserving the carrying ligand from oxidation and it could negatively affect the *n/iso* ratio [100]. Therefore, the development of alternative oxygen-resistant ligands is still an important research area in industrial hydroformylation.

The interactions of a ligand with an ionic liquid have a remarkable impact on the rate and selectivity in oxo synthesis. For example, significant catalytic activity increase after addition of a salt to a reaction mixture containing surface active water-soluble phosphines was observed by Basset [121]. This “salt effect” was proposed to be an expression of the self-associations on tenside phosphines studied by Hanson (31 and 33) in 1995 [103]. The expected exchange between Na and [mbmim] in a TPPMS/[mbmim][TfO] mixture and the formation of hydrogen bonds between the SO₃[−] groups and [mbmim] were observed while studying IL–ligand interactions [26]. Therein, a 2D-NMR study confirmed that the sulfonated phosphine tended to form an 1:1 “inclusion complex” with [mbmim][TfO] due to supramolecular interactions, while the neutral TPP is π -stacked to the imidazolium moiety of the ionic liquid framework [26]. The same fact was reflected in a molecular dynamic simulation of biphasic systems, which indicated the presence

of π -interactions between aromatic and alkene groups and the [mbim] moiety [122]. The formation of such “inclusion complexes” may cause a drop in activity and in linear-to-branched ratio for 1-decene, as proposed by different authors [26]. On the other hand, an induction of stereoselectivity by optically pure ionic liquid **15** has been noted in certain reactions. Herein, a chiral environment around the rhodium core can be created through the strong intermolecular interactions between TPPTS and chiral imidazolium ions. At the same time, it is not ruled out that the solvation of other solutes by optic active ILs fragments or formation of asymmetric NHC–Rh complexes can be the reason for the transmission of the chiral information.

Another important side effect is the reduction of Rh(I) to Rh(0), which takes place in reductive hydroformylation environments and results in nanoparticles (NPs) formation [51]. The latest is not always accompanied by a color change in the reaction mixture. Thus, the PPh_3 -containing catalyst solutions turn from an orange to a dark brown color under CO/H_2 pressure at elevated temperatures (indicating the formation of a high concentration Rh NPs and their macro agglomerates), while the reaction mixtures based on phosphonium-functionalized phosphines (**41**, Fig. 10) containing NPs in the size range ~ 2 –10 nm remained orange throughout recycling experiments. Modification of the ligand structure or the Rh:L ratio can diminish the size and concentration of NPs.

4 Ionic Liquid-Supported Hydroformylation in $sc\text{CO}_2$

Hydroformylation of alkenes was one of the first catalytic reactions investigated in $sc\text{CO}_2$ due to its industrial importance. The conception of using $sc\text{CO}_2$ in the hydroformylation of alkenes came as a solution for the high energy-consuming distillations to separate the desired products from the catalyst in the reaction medium [123–127]. Moreover, such distillations have to be often carried out above the decomposition temperature from the catalyst.

Due to the sharp changes in solubilities of dissolved species with density of the supercritical medium, $sc\text{CO}_2$ was seen as a solvent for hydroformylation that would facilitate such separations by easy pressure alterations to control fluid density and, in turn, catalyst or product solubility. Additionally, $sc\text{CO}_2$ is an environmentally friendly solvent which is totally miscible with permanent gases (e.g., H_2 and CO). Therefore, there are not major problems related to interfacial gas transport.

One of the first studies on the use of $sc\text{CO}_2$ in hydroformylation was reported by Rathke et al. in the late 1980s [128]. Their research can be considered the first systematic study with the aim of understanding the equilibrium and dynamic processes in the hydroformylation of propylene in $sc\text{CO}_2$ catalyzed by a dicobalt octacarbonyl complex. Sometime later, several methods were described in the literature involving changes in the temperature and/or pressure in the $sc\text{CO}_2$ -based hydroformylation reactors to separate the products from the catalyst.

However, a separation procedure that occurs under the reaction conditions was more desirable, so that it could be adapted for use in flow systems.

Cole-Hamilton et al. proposed at first a solution by introducing a highly active catalyst which was poorly soluble in *scCO*₂ [129]. The products could be removed by fluxing them into a second autoclave at low temperature and decompressing the system. Nevertheless, a catalyst decomposition was detected after several cycles due to the low solubility of the ligand in *scCO*₂. Therefore, a new strategy to immobilize the catalyst was searched.

ILs were seen as a solution for these processes due to their poor solubility in *scCO*₂ (as a result of their ionic character and negligible vapor pressure) and the high solubility of *scCO*₂ in certain ILs, as observed by Brennecke et al. [130]. In addition, the ability of CO₂ to induce liquid/liquid phase separations of ILs and organics has also been studied and it depends on the solubility of CO₂ in the ionic liquid and the hydrogen bonding interactions between the latest and organics [130–132]. Therefore, pure organic compounds could be extracted from the catalyst-containing ionic liquid phase by using *scCO*₂. There are further remarkable properties of *scCO*₂-ionic liquid systems: they remain biphasic even at high operating pressures, and the presence of *scCO*₂ decreases the viscosity of the original ILs, enhancing the mass transfer and solubility of permanent gases in the liquid phase (the high-pressure phase equilibria of CO₂ and ionic liquids have been studied by Scurto et al. see: [133]). This reduction of potential mass transfer barriers can lead to increased reaction rates and selectivities. Additional studies about the interactions of CO₂ or *scCO*₂ in ILs and their effects have been published elsewhere [134–137].

Preliminary studies using triarylphosphite ligands for the hydroformylation of 1-hexene in a batch system with *scCO*₂/[bmim][PF₆] mixtures showed an improvement in the selectivity (84%), the *n/iso* ratio (6.1), and the reaction rate in comparison to reactions in the absence of *scCO*₂ [138]. A semicontinuous operation using 1-hexene or 1-nonene as substrates showed a decrease in the selectivity and reactivity after three runs with reuse of the catalytic medium due to degradation of the catalyst by [PF₆] from the reaction medium. In similar conditions, TPPTS gave low yields as a result of their poor solubility in the biphasic system. An exchange of sodium for [bmim] increased the catalyst reactivity (TON = 160–320 h⁻¹), and rhodium leaching was not observed, but the *n/iso* ratio fell slowly after 9 runs (3.7 to 2.5). This was due to ligand oxidation as a result of the handling steps required for the semicontinuous process.

Cole-Hamilton et al. reported the first continuous-flow process with immobilization of the catalyst in ILs and extraction with *scCO*₂ [139]. This process showed that the catalyst was stable during 30 h due to the lack of ligand oxidation. A general design of the applied system for the hydroformylation is depicted in Fig. 13. This consists of two separated vessels. On the first one, an ionic catalyst is immobilized in the ionic liquid in a stirred reactor. The desired alkene, CO/H₂, and *scCO*₂ are introduced continuously at determined rate, coming from separated feeds. The reaction takes place under homogeneous conditions. The expected products and *scCO*₂ are transferred to a second vessel where they are subject to product

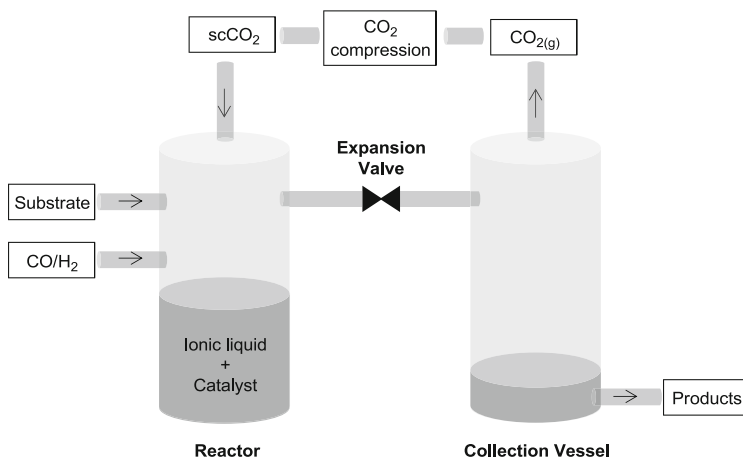


Fig. 13 General representation of a continuous-flow system for hydroformylation in the presence of ILs and using $scCO_2$ as the transport vector

separation from the gases by simple expansion. The desired products precipitate immediately due to the poor solvating capacity of the expanded CO_2 under ambient conditions. The catalyst and the ionic liquid stay in the reactor and CO_2 can be recycled.

The ligand $[pr\text{mim}]_2[\text{TPPDS}]$ was tested at first in the continuous-flow hydroformylation of 1-octene using $[\text{bmim}][\text{PF}_6]$ as ionic liquid and $\text{Rh}_2(\text{OAc})_4$ as catalyst precursor [139]. The catalyst showed a high stability during 30 h due to the lack of phosphine oxidation and a good *n/iso* ratio (3.8). The rhodium content in the recovered products was <1 ppm. However, the low conversion (10%) and reaction rate ($\text{TOF} = 5\text{--}10 \text{ h}^{-1}$) stimulated the search for optimized reaction conditions.

The partitioning of the alkenes was considered to be the rate determining factor in the biphasic system. Therefore, an ionic liquid which is able to solubilize a large amount of nonpolar substrates was envisioned to overcome the mass transport limitation. The effects of anions and alkyl groups from the ILs in the solubility of 1-octene were studied. An enhancement on the solubility was observed by increasing the alkyl chain length in the 1-position of 1-alkyl-3-methylimidazolium moiety and by changing $[\text{PF}_6]$ for $[\text{Tf}_2\text{N}]$. In this manner, $[\text{omim}][\text{Tf}_2\text{N}]$ showed the best results in the hydroformylation of 1-dodecene catalyzed by $[\text{Rh}_2(\text{OAc})_4]/[\text{pr}\text{mim}][\text{TPPMS}]$ with a high conversion (up to 87%) and TON ($>1,000$) [52, 138]. Additional optimization tests were conducted with this system. An increment in the TOF of the hydroformylation of 1-octene was noted with higher substrate flow rates, although the percentage of aldehyde in the recovered solution decreased [138]. Accordingly, a TOF of more than 500 h^{-1} was achieved. Furthermore, this value was not affected by the use of other substrates. Similar growth in the TOF was observed as the CO/H_2 partial pressure was increased up to a saturation limit. This result was interpreted as a shift in the equilibrium partitioning of substrate toward the ionic liquid phase. When the system reached the highest CO/H_2 partial pressure,

the solvating properties of *sc*CO₂ decreased with a subsequent undesirable accumulation of the substrate in the reactor. However, the poor solvating properties of *sc*CO₂ at high CO/H₂ partial pressures were beneficial to prevent rhodium leaching as most of it stayed in the ionic liquid. The content of rhodium in the product during steady-state operation was <0.1 ppm.

A more specific study to understand the kinetics, phase behavior, and mass transport in biphasic reaction systems for hydroformylation has also been reported by Scurto et al. using 1-octene/[Rh(CO)₂(acac)]/PPh₃ in [hmim][Tf₂N]/*sc*CO₂ as model system [140].

Ultimately, Cole-Hamilton et al. showed that the selectivity in the hydroformylation of 1-octene can be improved (*n/iso* ratio = 40) by the use of the imidazolium–xantphos ligand (**46**, Fig. 11) [52].

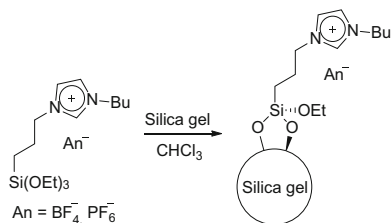
5 Supported Ionic Liquid Phase (SILP) Hydroformylation

As noted in the previous section, catalyst immobilization in an ionic liquid for hydroformylation has been a well-established method for the separation of the corresponding aldehydes from the reaction mixture with minimal catalyst losses. Although the use of *sc*CO₂ showed a very low proportion of catalyst leaching during continuous-flow processes, an easier to handle catalytic system would be more attractive for the industry. In this case, the great majority of industrial catalysts are in solid form due to the ease of catalyst separation and the possibility to use a fixed-bed reactor. On the other hand, the use of large amounts of ILs in an industrial hydroformylation process is not desirable from an economic and environmental point of view. Additionally, the liquid–liquid biphasic catalysis does not make use of all available ionic liquid and catalyst dissolved in it. Due to the slow mass transfer to ionic liquid, a fast catalytic reaction is limited by the concentration of an alkene in the bulk ionic liquid phase, and the reaction occurs mostly at the interface or at the diffusion layer rather than in the whole ionic liquid phase. Therefore, a good catalytic system would consist in an ionic liquid phase of the same size as the alkene diffusion layer. Herein, new approaches to immobilize the catalyst and separate it from the reaction media were envisioned [141–146].

5.1 SILP Catalysts for Hydroformylation of Nonfunctionalized Linear Alkenes in Batch Reactors

Mehnert et al. reported the first immobilized ionic liquid media on the surface of a support material (SILP) [147]. Accordingly, a silica gel surface was modified with a monolayer of ionic liquid fragments, which were covalently attached using alkoxysilane groups as depicted in Scheme 6.

Scheme 6 Surface attachment of an ionic liquid monolayer to silica gel



Further amount of non-covalently attached ionic liquid could be added to the modified silica gel and this afforded a multiple layer of free ionic liquid on the support. All those layers served as the homogeneous reaction media in which a catalyst could be dissolved. For instance, a Rh-based catalyst precursor and a ligand could be mixed in an organic solvent and added to a previously modified silica gel. After removal of the solvent, the silica gel-supported catalyst was ready to be used in hydroformylation. Some examples of hydroformylation of alkenes using this procedure are shown in Table 1. The first results in catalysis from those supported catalysts in the hydroformylation of 1-hexene in a batch reactor showed an enhanced activity, probably due to the higher concentration of the catalyst on the surface in comparison to the biphasic systems. However, the catalyst leaching was similar in both systems [147, 154]. A low aldehyde concentration was necessary to be kept during the reaction in order to avoid the catalyst loss.

Other supports have also been used for the preparation of SILP catalysts for hydroformylation in a batch reactor. For instance, Yuan et al. reported an SILP catalyst prepared from a mesoporous material with well-order periodic structures (MCM-41) [149, 150]. This support was impregnated with a mixture of a Rh–TPPTS complex and a halogen-free ionic liquid (TMGL; **12**, Fig. 1) to afford an active (TOF up to 389 h^{-1}) and low regioselective (n/i ratio up to 3.5) catalyst in the hydroformylation of 1-hexene. This regioselectivity was slightly higher in comparison to published results for monodentate rhodium catalysts. In the case of 1-octene, 1-decene, and 1-dodecene, lower TOF and selectivities were obtained. The hexagonal array of MCM-41 was not disturbed after treatment with the ionic liquid/Rh complex mixture, but the surface area, pore volume, and pore size were smaller, as indicated by XRD and N_2 adsorption measurements. This implied that most of the ionic liquid and Rh complex were located in the inner channels of the support. FTIR and ^{31}P NMR experiments of the TGML–TPPTS–Rh-supported catalyst showed the presence of the active hydroformylation species [149, 150]. The catalytic activity of this catalyst depended on the type of ionic liquid and its loading. TMGL was advantageous in the reaction in comparison with [bmim][PF₆] and [bmim][BF₄]. The latest gave the lowest regioselectivities. This SILP catalyst was active even after eleven cycles without losing its catalytic performance.

Further studies on the physicochemical and thermodynamic properties of ionic liquid-containing mesoporous materials have been reported recently by Romanos et al. [155]. In addition, a complete characterization of SILP materials applying

Table 1 Examples of hydroformylation of alkenes using SILP

Substrate	Ligand	Reaction medium	Conversion/yield (%)	<i>n</i> / <i>iso</i>	TOF (h ⁻¹)	References
Propene	2-DPPD-guanidinium-PF ₆ (44)	[bmim][PF ₆]	—/—	0.9	21	[104]
Propene	NORBOS-Cs ₃ (37)	[bmim][PF ₆]	—/—	2	88	[104]
Propene	Sulfoxantphos (45)	[bmim][PF ₆]	—/—	23	37	[105]
Propene	Sulfoxantphos (45)	[bmim][<i>n</i> -C ₈ H ₁₇ OSO ₃]	—/—	19	18	[105]
1-Butene	Sulfoxantphos (45)	[bmim][<i>n</i> -C ₈ H ₁₇ OSO ₃]	32/—	— ^a	564	[148]
1-Hexene	TPPTI	[bmim][BF ₄] ^b	—/33	2.4	3,900	[147]
1-Hexene	TPPTS	[bmim][BF ₄] ^b	—/40	2.4	3,360	[147]
1-Hexene	TPPTI	[bmim][PF ₆] ^b	—/46	2.4	3,600	[147]
1-Hexene	TPPTS	TGML ^c	36/—	3.5	270	[149, 150]
1-Octene	TPPTS	TGML ^c	39/—	1.6	195	[150]
1-Octene	NORBOS-Cs ₃ (37)	[bmim][PF ₆]	—/—	2.6	44	[104]
1-Octene	[primim][TPPMS]	[omim][NTf ₂]	42/—	3	500–800	[86, 151]
1-Decene	TPPTS	TGML ^c	18/—	1.3	74	[150]
1-Dodecene	TPPTS	TGML ^c	15/—	1.5	55	[150]
Styrene	TPPMS	[b((MeOSi) ₃ p)im][Cl]	100/97	1:32	—	[152]
4-Methoxystyrene	TPPMS	[b((MeOSi) ₃ p)im][Cl]	100/97	1:31	—	[152]
4-Methylstyrene	TPPMS	[b((MeOSi) ₃ p)im][Cl]	99/96	1:28	—	[152]
4-Fluorostyrene	TPPMS	[b((MeOSi) ₃ p)im][Cl]	100/95	1:23	—	[152]
3-Bromostyrene	TPPMS	[b((MeOSi) ₃ p)im][Cl]	74/71	1:31	—	[152]
2-Chlorostyrene	TPPMS	[b((MeOSi) ₃ p)im][Cl]	84/77	1:10	—	[152]
3-Chlorostyrene	TPPMS	[b((MeOSi) ₃ p)im][Cl]	99/97	1:50	—	[152]
4-Chlorostyrene	TPPMS	[b((MeOSi) ₃ p)im][Cl]	98/95	1:30	—	[152]
3-Nitrostyrene	TPPMS	[b((MeOSi) ₃ p)im][Cl]	100/100	—	—	[152]
2-Vinylnaphthalene	TPPMS	[b((MeOSi) ₃ p)im][Cl]	85/83	1:34	—	[152]
Prop-2-en-1-ol	PPh ₃	[bmim][PF ₆]	99/90	20	—	[153]

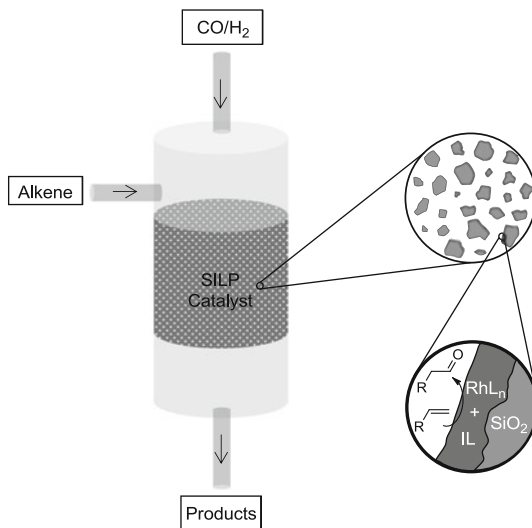
(continued)

Table 1 (continued)

Substrate	Ligand	Reaction medium	Conversion/yield (%)	<i>n</i> / <i>iso</i>	TOF (h ⁻¹)	References
But-3-en-2-ol	PPh ₃	[bmim][PF ₆]	100/90	36	–	[153]
2-Methylprop-2-en-1-ol	PPh ₃	[bmim][PF ₆]	76/93	100	–	[153]
(E)-But-2-en-1-ol	PPh ₃	[bmim][PF ₆]	75/85	5	–	[153]
2-Methylbut-3-en-2-ol	PPh ₃	[bmim][PF ₆]	94/92	42	–	[153]

^a*n*-pentanal yield: 97%^bUsing previously modified silica gel^cMCM-41 as support

Fig. 14 Schematic representation of a continuous-flow fixed-bed reactor with an SILP catalyst



diverse analytical and spectroscopic techniques from different porous supports can be found in the literature [156].

5.2 SILP Catalysts for Hydroformylation of Different Substrates in Batch and in Continuous-Flow Reactors

5.2.1 Propene

Fehrmann et al. reported the first SILP catalytic system without chemical modification of the supporting material surface for a continuous gas-phase fixed-bed hydroformylation process (Fig. 14) [105]. Hence, silica gel was impregnated with a nonionic organic solvent/ionic liquid mixture containing a ligand (sulfoxantphos; **45**, Fig. 11) and $[\text{Rh}(\text{CO})_2(\text{acac})]$ as catalyst precursors followed by subsequent removal of the nonionic organic solvent. This procedure can be carried out with the use of a rotary evaporator although a new scalable preparation method for SILP catalyst has been recently reported [157]. In addition, Fehrmann et al. used for the first time a halogen-free ionic liquid ($[\text{bmim}][n\text{-C}_8\text{H}_{17}\text{OSO}_3]$) in SILP systems. As indicated in Table 1, the hydroformylation of propene exhibited a moderate TOF at steady state with selectivity for the linear product up to 96% during typically 3–4 h. The regioselectivity depended on the amount of catalyst precursor. Additionally, the catalyst performance was strongly influenced by the catalyst composition. Low activities were obtained for catalysts with low ligand to rhodium ratios and a prolonged use of the catalyst resulted in a decrease in catalytic activity and selectivity. Moreover, the catalytic activity decreased with increase of ionic liquid

loading, and this supports the conclusion that the catalysts were operating with a mass transfer limitation.

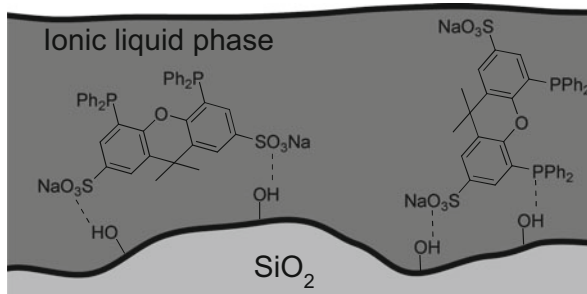
2-DPPD-guanidinium-PF₆ and NORBOS-Cs₃ (**44** and **37**, respectively, Fig. 10) were also tested as ligands in the continuous gas-phase hydroformylation of propene [104]. A two-phase catalyst preparation procedure was conducted with those ligands due to the better reproducibility of the kinetic results. TOF up to 88 h⁻¹ was obtained with NORBOS-Cs₃ at steady state typically 4–5 h after initial catalyst preformation. Despite of the larger catalytic activity, the best *n/iso* ratio obtained with this ligand was 2.8. This result is in the range for Rh-monophosphine ligands in hydroformylation. The modified 2-DTPPD ligand afforded a lower *n/iso* ratio and catalytic activity.

As noted above, the catalytic activity decreased in systems with a covalently anchored ionic liquid, where catalyst leaching was detected, or in some with physisorbed catalyst precursors [105, 147]. Wasserscheid et al. observed that a more stable SILP catalyst for the hydroformylation of propene could be prepared by a high-temperature pretreatment of the silica gel used as supporting material [158, 159]. This process afforded a dehydroxylated silica gel without inducing structural changes. Nevertheless, the catalyst performance and stability was still influenced by the catalyst composition, and a large excess of ligand was still necessary to prepare long durable catalysts. Therefore, a dependence of the catalytic activity and the ligand degradation was established. The optimal Rh:L ratio was found to be around 10. To further understand this process, FTIR spectroscopy of the SILP catalyst with different amounts of sulfoxantphos (**45**, Fig. 10) was used to detect the catalytic species under reaction conditions. As expected, signals corresponding to Rh complexes related to those reported for homogeneous hydroformylation were observed confirming that the catalysis in the supported ionic liquid layer is homogeneous. In addition, the amount of those species corresponded to the amount of ligand and hydroxyl groups in the silica gel. As observed by MAS ³¹P NMR spectroscopy, part of the ligand was irreversibly attached to the surface before and during catalysis. Therefore, those acidic groups on the silica gel surface affected the long-term stability of SILP Rh–phosphine catalysts and a large excess of phosphine ligand was necessary to compensate for some detrimental surface reactions.

FTIR and MAS NMR in situ studies were also conducted by Bell et al. using the catalytic SILP system [Rh(CO)₂(acac)]/sulfoxantphos/[bmim][*n*-C₈H₁₇OSO₃] for the hydroformylation of propene [160]. Accordingly, it was proposed that the active Rh complexes are attached to the silica gel surface by interactions of the sulfonate groups of the ligand with silanol groups of the support (Fig. 15). Interactions between the phosphine groups and the silica gel surface are also possible but undesirable, because they reduce the number of active Rh species. Therefore, it was suggested that the task of the ionic liquid film on the silica gel support is to decrease the negative interactions between the ligand and the silanol groups. Herein, an optimal amount of ionic liquid is necessary to achieve the best results in hydroformylation.

Supplementary kinetic studies on the continuous gas-phase hydroformylation of propene using SILP catalysts have been also reported [159, 161, 162]. Accordingly,

Fig. 15 Proposed interactions of sulfoxantphos with the silanol groups of silica gel in an SILP catalyst



the activation energy of the catalytic SILP system sulfoxantphos/[bmim][*n*-C₈H₁₇OSO₃] was determined to be $63.3 \pm 2.1 \text{ kJ mol}^{-1}$, and the reaction was found to be first order with respect to propene partial pressure. These data were similar to those obtained for rhodium-catalyzed hydroformylations using sulfonated ligands in homogeneous media. Therefore, this comparison provided additional proof that an SILP catalyst behaves as a homogeneous catalyst. Furthermore, it was found that a slightly decreased in catalytic activity of the SILP catalyst prepared under enhanced conditions was due to the formation of high boiling side products which dissolve in the ionic liquid layer and lowered the effective catalyst concentration. However, those by-products could easily be removed from the catalyst by a vacuum procedure, after which the initial activity could be regained. Following this procedure, the catalytic system Rh-sulfoxantphos/[bmim][*n*-C₈H₁₇OSO₃] showed to be active for more than 700 h without decomposition. Additional kinetic studies were reported by Bell [163].

5.2.2 1-Butene

Further substrates have also been tested using the Rh-sulfoxantphos complex in [bmim][*n*-C₈H₁₇OSO₃] and supported in silica gel. 1-Butene showed a significantly higher activity and selectivity than propene, as depicted in Table 1 [148]. This improvement on activity was related to an enhanced solubility of 1-butene in the SILP system, as determined by magnetic suspension balance measurements. The reaction order on 1-butene and activation energy were similar to those observed for propene. The selectivity was not affected by the 1-butene pressure or the catalyst loading, but the temperature had a small influence on it. The reaction rate showed first-order dependency in rhodium concentration. The syngas composition affected the reaction in accordance with the accepted hydroformylation mechanism. The reaction kinetics was also studied in a gradient-free loop reactor (Berty reactor) [164]. This type of reactor has a circulating flow which has an order of magnitude higher than the previous system, and the outlet concentration is representative for the concentration inside the catalyst bed. Therefore, the resulting kinetic data obtained from this type of reactor have smaller errors. Accordingly, the kinetic

information was similar to that previously found. Additionally, the catalytic system was operated under no mass transport limitations.

As pure 1-butene is not a very attractive substrate for industrial hydroformylation due to its high price, a new catalytic system for the hydroformylation of an industrial C₄ feedstock was envisioned. For instance, raffinate I (a mixture containing 1-butene, *cis*-2-butene, *trans*-2-butene, isobutene, and butanes) was seen as a possible substrate. Herein, a complex that would be able to catalyze not only the hydroformylation reaction but also the isomerization of *cis*-2-butene and *trans*-2-butene to 1-butene was conceived. Wasserscheid et al. showed that an SILP–Rh complex formed with a benzopinacolphosphite ligand (**51**, Fig. 12) could be successfully applied in a continuous gas-phase hydroformylation of raffinate I [165]. This reaction gave an excellent regioselectivity toward *n*-pentanal (up to 99.5%) with no formation of 3-methylbutan-1-al, and the 2-butenes were hydroformylated after isomerization to give *n*-pentanal. The high content of isobutene (43%) did not affect the reaction. The success of this catalytic system was due to the high stability of the catalyst achieved through the combination of a drying procedure for the substrate and the use of an acid scavenger to avoid ligand decomposition. Under optimized reaction conditions, the TOF reached 3,600 h⁻¹ and the selectivity toward *n*-pentanal remained above 99% after at least 30 days time-on-stream. Moreover, a space–time yield of 850 kg_{*n*-pentanal} m⁻³ h⁻¹ could be maintained for at least 10 h time-on-stream. Catalyst leaching was not detected by analyzing the product with coupled plasma atomic emission spectrometry. Kinetic investigations of the catalytic system indicated that the reaction is influenced by H₂ and CO partial pressures like in a homogeneous hydroformylation reaction, with activation energy of 41 kJ mol⁻¹. The hydroformylation of a C₄ feedstock with a lower amount of 1-butene/2-butenes (70% *n*-butane) has shown to give a lower selectivity on *n*-pentanal (93.2%) with the use of a bidentate phosphite similar to those shown in Fig. 12, but with a still industrially acceptable space–time yield of 100 kg_{*n*-pentanal} m⁻³ h⁻¹ [166]. A related patent application can be also found in the literature [167].

5.2.3 Ethylene

Ethylene is one of the substrates for hydroformylation where the SILP technology has just been recently applied. An SILP catalyst prepared by impregnating [Rh(CO)₂(acac)] and TPPTS–Cs₃ on silica gel for the hydroformylation of ethylene was reported by Fehrmann et al. [168]. This catalyst showed good activity in the continuous-flow gas-phase hydroformylation of ethylene giving TOF above 800 h⁻¹. The supported catalyst was also characterized by physical adsorption of nitrogen, SEM-EDX, and FTIR. The content of ionic liquid in the pores of the solid support had a strong influence on the catalytic activity, and it was suggested that the deactivation of the catalyst could be due to the redistribution of the catalyst-containing ionic liquid on the support surface.

5.2.4 Vinylarenes

As observed above, most of the research about SILP catalysts has been focused on the synthesis of linear aldehydes through the hydroformylation of alkenes due to the importance of the products in the manufacture of detergents and other widespread substances. Nevertheless, branched aldehydes could also be of interest for the chemical industry [169]. Consequently, Blum et al. reported the first synthesis of branched aldehydes starting from vinylarenes using an entrapped Rh complex in a sol-gel matrix [152]. The SILP catalyst was prepared by mixing $[\text{Rh}(\text{COD})\text{Cl}]_2$ and TPPMS in the presence of $[\text{b}((\text{MeOSi})_3\text{p})\text{im}][\text{Cl}]$ and $\text{Si}(\text{OMe})_4$, and this mixture was aged at room temperature. The molar ratio ionic liquid/ $\text{Si}(\text{OMe})_4$ was between 1/20 and 1/30. No Rh was detected in the solvents used to prepare the SILP catalyst, which indicates that the resulting ceramic material contained all catalyst precursors. In addition, washings with *n*-heptane and CH_2Cl_2 after hydroformylation of vinylarenes did not show catalyst loss for four consecutive runs.

The sol-gel-supported catalyst was applied to the hydroformylation of different substituted vinylarenes as well as to 2-vinylnaphthalene in a batch reactor giving high conversions and branched aldehyde yields (Table 1). No electronic effects due to the substituents in the substrates were observed. However, the steric effects related to the *ortho* position substitution caused a reduction in the reaction rate and the selectivity. High syngas pressures were beneficial for the increase of the selectivity in the reaction. The hydroformylation proceeded well in solvents like alkanes and toluene, but it gave lower selectivities in 1,2-dichloroethane, and hydrogenation of the starting material was detected in THF. The same catalytic system was later used together with a separately engaged base in a one-pot, multistep reaction which included hydroformylation of vinylarenes, base-promoted condensation of the corresponding aldehyde with reactive methylene compounds (malononitrile or ethyl cyanoacetate), and hydrogenation of the formed unsaturated products [56].

The use of water as a solvent was also reported for this supported catalyst [170]. Hence, a microemulsion of a vinylarene in water with a surfactant was performed and the entrapped catalyst was added to give the desired branched aldehydes. The hydroformylation of styrene showed a TON of $1,666 \text{ h}^{-1}$ with excellent selectivity (branched aldehyde yield: 99%). Nevertheless, 4-methylstyrene, 4-fluorostyrene, 4-chlorostyrene, and 2-vinylnaphthalene did not show better results as those previously reported.

5.2.5 Allylic Alcohols

Hydroformylation of allylic alcohols is an important step toward the synthesis of 1,4-butanediol in the chemical industry. However, this synthetic route has some challenges as diverse side reactions can be found for unsaturated alcohols under hydroformylation conditions. Herein, a novel approach for the regioselective

hydroformylation of allylic alcohols in a batch reactor was reported by Bhanage et al. with the use of an SILP catalyst in water [153]. As observed in Table 1, a series of allylic alcohols was tested in a hydroformylation reaction where the catalyst precursors ($\text{HRhCO}(\text{PPh}_3)_3/\text{PPh}_3$) were previously impregnated in an ionic liquid film on silica gel. An excess of PPh_3 was necessary to get high conversions and regioselectivities, and a higher catalyst loading increased the reaction rate without altering the regio- and chemoselectivity. The latest was affected by the temperature. The catalyst could be used until five times without any loss in activity and selectivity.

5.2.6 1-Octene

The gained experiences on propene were also applied in the hydroformylation of 1-octene by Riisager et al. [104]. A continuous-flow two-phase hydroformylation from 1-octene using an SILP catalyst with NORBOS- Cs_3 (37, Fig. 10) as ligand indicated a TOF of 44 h^{-1} and a *n/iso* ratio of 2.6. Rhodium leaching was not detectable.

One of the disadvantages of SILP catalyst in the hydroformylation of liquid substrates is the possible solubility of the supported ionic liquid in the liquid substrate or product depending on their polarity. When this solubility is high, losses of the ionic liquid layer could be detected in continuous-flow hydroformylation processes. In addition, problems related to the gas solubility of reagents in the substrate and in ionic liquid layer can be still present. As discussed above, this is an important factor in hydroformylation because the reaction rates depend on the solubilities of such gaseous reagents in the ILs. Therefore, a hybrid process for the hydroformylation of liquid alkenes was proposed by Cole-Hamilton et al. [86, 151]. Based on previous reports on the use of supercritical fluids for transporting substrates across SILP catalysts, a catalytic system involving flowing the substrate, CO , H_2 , and products using *sc* CO_2 as the mobile phase for the hydroformylation of 1-octene was developed. The employed SILP catalyst contained $[\text{Rh}(\text{CO})_2(\text{acac})]$ and $[\text{prmim}][\text{TPPMS}]$ in $[\text{omim}][\text{Tf}_2\text{N}]$ and showed high hydroformylation activities (rates up to 800 h^{-1}) with a low catalyst leaching (from 2–4 ppm at the beginning to 0.5 ppm later) and a high stability (at least 40 h). The reaction rate had a limited dependence on the film thickness (ionic liquid loading) at constant catalyst loading. This suggested that diffusion is no longer limiting the reaction rate and all catalytic active species can reach the reactants. The reaction was mainly affected by the substrate flow rate and the CO_2 pressure.

6 Nanoparticles in Oxo Processes

Nanoparticles were reported as an active catalyst in oxo synthesis of olefins according to the works published recently (Appendix, Table 3) [171–175]. The ionic matrices are able to retain the nano-sized particles [54] and prevent their agglomeration to some extent [171]. Using thermoregulated ILs, a good recyclability of the nanocatalysts by simple phase separation can be achieved, while the catalytic process is driven under monophasic conditions [53, 54]. The stability and activity of NPs in imidazolium-based ILs is mainly determined by the nature of the substrates or products and the coordinative strength of the aggregates with the metal surface. The chemoselectivity and activity are strongly influenced by nanoparticles size. While the 1.5–5-nm-scaled rhodium was highly active and selective in ILs-supported hydroformylation, the large-sized Rh cores (>15 nm) produce only small amounts of aldehydes with low selectivity similar to Rh/C heterogeneous-driven processes. The TEM, XRD, IR, and NMR experiments gave evidence on the Rh NP catalyst degradation. Herein, catalytic active carbonyl species are formed under reaction conditions [53, 171, 176]. Thus, it was concluded that the Rh NPs served as a reservoir for active catalyst [172, 175]. The coexistence of NPs with mononuclear species in the hydroformylation mixtures is evident, but their role and impact in active catalyst formation in hydroformylation mediated by organometallic Rh(I) compounds has not yet been fully clarified and remains as a subject of intensive research.

7 Pt-Based Hydroformylation

Due to the high activity of Rh complexes in the hydroformylation reaction, demand growth of this metal and increasing prices have been observed in the last years. Therefore, alternative transition metal catalysts have become more desirable [177].

In addition to Rh and Co catalysts, phosphine-containing platinum complexes have been reported to catalyze the hydroformylation of alkenes in the presence of chlorostannate ILs. The Lewis acidity and anionic speciation of those ILs have been recently studied in detail [178]. As a first example in the literature, a method for the hydroformylation of ethylene using a low-melting tetraalkylammonium salt ($[(C_2H_5)_4N][SnCl_3]$) and a platinum complex ($PtCl_2$) as catalyst precursor was presented by Parshall in 1972 [23]. Herein, a 65% combined conversion of propionaldehyde and 2-methyl-2-pentenal was obtained under harsher conditions (90°C and 400 atm). Although more data on the catalytic activity was not presented, this seminal work was extended to other substrates by Wasserscheid et al. [28]. Accordingly, the hydroformylation of methyl-3-pentenoate and 1-octene with $(PPh_3)_2PtCl_2$ was conducted in slightly Lewis-acidic chlorostannate ILs, which were prepared by mixing $SnCl_2$ and an ionic liquid ($[bmim][Cl]$ or $[4-mbp][Cl]$). For the first substrate, an enhancement of catalyst lifetime and activity in the ionic liquid was observed in comparison with similar reactions in

CH_2Cl_2 . However, a low conversion of methyl-3-pentenoate was observed in the presence of both ILs. Methylpentanoate was also detected, which indicates that hydrogenation of the product occurs simultaneously.

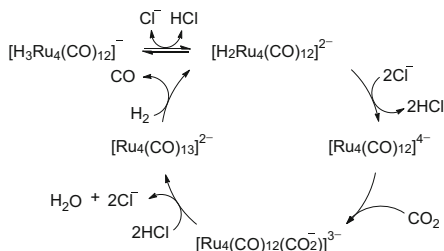
In the case of 1-octene, a biphasic reaction took place with each of the chlorostannate ILs. Therefore, the isolation of the catalyst was conducted by simple phase separation. A maximum conversion of 22% was obtained with [bmim][Cl]/ SnCl_2 and a high selectivity of 96% was achieved. Herein, the hydrogenation activity of the catalyst was higher as in methyl-3-pentenoate. The highest ratio hydroformylation to hydrogenation was obtained at low temperatures and high syngas pressures. It is important to mention that hydroformylation of styrene under similar conditions has been also tested. However, the formed platinum complexes have been practically inactive in imidazolium-type ILs [179]. NMR mechanistic investigations on the formation of catalytic precursors in chlorostannate ILs were first reported by Kollár et al. [180]. Additional reports can also be found in the literature [181, 182].

8 Ru-Based Hydroformylation

A different reaction mechanism has been proposed for the hydroformylation of alkenes using ruthenium clusters as catalytic precursors and CO_2 as educt. During the search for new environmentally friendly alternatives for the hydroformylation, CO_2 has been found to be a good nontoxic reagent to produce alcohols and/or aldehydes. The first tests on hydroformylation with CO_2 as carbon source in ILs were reported by Tominaga et al. [33]. His previous work on the hydroformylation of alkenes using metal halides and multinuclear ruthenium complexes as catalyst precursors [183] prompted him to look for alternative polar solvents to *N*-methyl-2-pyrrolidone (NMP), which has a high boiling point and, therefore, complicates the isolation of hydroformylation products. In addition, terminal alkenes in NMP afforded the corresponding alkanes due to the reduction of the educt before the hydrogenation took place. Herein, ILs were seen as an alternative solvent to overcome those difficulties. Accordingly, a biphasic system would reduce the undesired alkene hydrogenation and improve the chemoselectivity toward hydroformylation. Moreover, the catalytic species could remain in the ionic liquid layer with the possibility of reusing it several times. Hydroformylation with CO_2 using the most effective catalyst precursors ($\text{H}_4\text{Ru}_4(\text{CO})_{12}$ or $\text{Ru}_3(\text{CO})_{12}$) consists of two steps: conversion of CO_2 to CO via a reverse water–gas shift reaction and subsequent reaction of the latest with alkenes through a hydroformylation mechanism. For the first step, tetranuclear ruthenium species have been detected in the reaction medium, and these are assumed to be responsible for the reduction of CO_2 to CO, as depicted in Scheme 7 [34, 184].

A key step in the mechanism requires the successive elimination of the coordinated hydrogens in the hydride complex $[\text{H}_2\text{Ru}_4(\text{CO})_{12}]$, which is promoted by the chloride anions from the corresponding ionic liquid. Subsequent nucleophilic attack of protons to tetranuclear ruthenium $[\text{Ru}_4(\text{CO})_{12}(\text{CO}_2^-)]$ converts CO_2 to

Scheme 7 Ruthenium-catalyzed reduction of CO₂ to CO



CO. According to investigations followed by Tominaga, the halide anions are sufficiently strong to abstract a proton from metal hydride complexes in nonaqueous solvents. Therefore, the reaction rate depends on the proton affinity of such anions. This is supported by the observed effect of anions: the yield of hydroformylation increases in the order $\text{Cl} > \text{Br} > \text{I}$.

For the second step of the hydroformylation of alkenes with CO₂ catalyzed by ruthenium complexes, the reactivity of CO with cyclohexene in the presence of metal halides has been studied to determine the possible mechanism [34]. The observations by electrospray ionization mass spectrometry suggested that this step is catalyzed by a combination of mono- and tetranuclear ruthenium complexes ($[\text{RuCl}_3(\text{CO})_3]$ and $[\text{H}_3\text{Ru}_4(\text{CO})_{12}]$). Moreover, $[(\text{cyclohexene})\text{RuCl}_2(\text{CO})_3]$ was also observed in the reaction solution. As a sequel, this step involves the coordination of substrates to the mononuclear species, followed by insertion of CO and the hydrogen donation from the tetranuclear species. These observations can be extrapolated to the reactions in ILs. Table 2 shows some examples of hydroformylation of alkenes with CO₂ using multinuclear ruthenium complexes and different ILs.

The seminal investigations conducted by Tominaga et al. have been used to develop a new strategy for the hydroaminomethylation of olefins. Srivastava et al. reported the first example of a one-pot protocol which includes the hydroformylation of alkenes and a subsequent reductive amination which leads to secondary and tertiary amines with good yields [186]. This reaction was carried out in the presence of $\text{Ru}_3(\text{CO})_{12}$, CO₂, and an ionic liquid (benzyltriethylammonium chloride).

Recently, Porcheddu has demonstrated that formic acid can be used as feedstock in the hydroformylation of alkenes [187]. This procedure avoids all the safety issues related to the use and management of gaseous reagents and facilitates the performance of small-scale reactions. However, the reactions have to be conducted in two separated reaction chambers to obtain good yields. The production of CO₂ and H₂ is done in one of the chambers in the presence of a small amount of sodium formate and lithium chloride. The second chamber contains the desired educt and a mixture of ILs ($[\text{bmim}][\text{Cl}]/[\text{bmim}][\text{Tf}_2\text{N}]$) to accomplish the hydroformylation. Both chambers contain $\text{Ru}_3(\text{CO})_{12}$ as catalyst precursor and heated at the same temperature. Several alkenes were reported to afford the corresponding alcohol through this procedure with high regioselectivity. Some examples are (conversion; yield; *n*/*iso* ratio): 1-hexene (95; 74; 85/15), 2-methyl-1-hexene (95; 71; 100/0), vinylcyclohexane (94; 81; 82/18), and α -methylstyrene (97; 71; 100/0).

Table 2 CO₂ hydroformylation of alkenes using Ru₃(CO)₁₂ as catalyst precursor^a

Substrate	Reaction medium	Conversion/yield ^b	References
1-Hexene	[bmim][Cl]/toluene	97/84, 0, 11	[33, 35]
1-Hexene	[bmim][BF ₄]/toluene	96/63, 0, 26	[33]
1-Hexene	[bmim][PF ₆]/toluene	95/3, 0, 86	[33]
1-Hexene	[bmim][Cl]/[bmim][NTf ₂] ^c	94/82, 0, 9	[185]
1-Hexene	[bmim][Cl]/[bmim][BF ₄] ^c	95/71, 0, 9	[185]
1-Hexene	[bmim][Cl]/[bmim][PF ₆] ^c	94/50, 0, 7	[185]
Cyclohexene	[bmim][Cl]/toluene	80/76, 0, 3	[35]
α-Methylstyrene	[bmim][Cl]/toluene	78/50, 0, 22	[35]
α-Methylstyrene	[bmim][Cl]/benzene	88/62, 2, 22	[35]
Styrene	[bmim][Cl]/toluene	100/47, 0, 49	[35]
Styrene	[bmim][Cl]/benzene	100/60, 0, 38	[35]

^a $p(\text{CO}_2/\text{H}_2)$ [bar] = 40/40 and T [°C] = 140°C, unless noted

^bAlcohol, aldehyde, and alkane, respectively

^c T [°C] = 160°C

9 Concluding Remarks

Although the use of ionic liquid for immobilization of the catalyst is the most viable method for hydroformylations where high *n/iso* ratios and yields with a low catalyst leaching are desirable, modifications to the catalytic systems still need to be conducted in order to afford better results. For instance, a rigorous model-based reactor for such processes has to be developed. In this regard, new reactor concepts for the hydroformylation of long chain linear alkenes have been proposed by Sundmacher et al. recently [188, 189]. In addition, a reduction in the catalyst leaching with the application of nanofiltration membranes to a continuous homogeneous hydroformylation has been reported by Subramaniam et al. [190]. His pioneering work has shown a high efficiency in the retention of Rh complexes in the reaction medium. Moreover, CO₂ can be also used as a switchable water additive to allow homogeneous hydroformylation to take place in a monophasic form and to separate the products in a biphasic version [191]. This new technique presented by Jessop et al. does not suffer from the traditional mass transfer limitations because the reaction is conducted in a monophasic medium.

As noticed by Leitner et al., the right combination of immobilization techniques with modern engineering solutions will cope the still remaining challenges in hydroformylation [192].

Appendix

Table 3 Summary of Rh- and Co-based hydroformylations in ILs

Substrate	Catalyst precursor/ligand	Reaction medium	$p(\text{CO}/\text{H}_2)$ [bar]/T (°C)	Conversion/ yield	TOF (h^{-1})	$[n]_{\text{D}20}^a$	Cat. recycle. (times)	References
Ethylene	Rh(PPH_3)Cl/ PPH_3 (Rh/L = 1/10)	[bmim][BF ₄], [hmim][BF ₄], [omim][BF ₄], [bpim][BF ₄], [bdim][BF ₄], [bmim][PF ₆]	20/100	71.4–98.2	1,123–10,627	–	6	[36, 37]
1-Pentene	[Rh(CO) ₂ (acac)]/ PPH_3 , TPPTS, TPPMS (Rh/L = 1/3–10)	[bmim][TsO], [bmim][AcO], [bmim][SCN], [bmim][HSO ₄]	20–40/80	/16–99	59–333	2.8–3.9	–	[22]
1-Hexene	[Rh(CO) ₂ (acac)]/ 28 , 29 , 30 (Rh/L = 1/5)	[bmim][BF ₄], [emim][BF ₄], [bmim][PF ₆]	15/100	58.5–87.3	117–174	2.6–3.9	–	[38]
	[Rh(CO) ₂ (acac)]/–	[bmim][PF ₆]	41.4/100	–	2–21	0.5–1.5	5	[39]
	[Rh(CO) ₂ (acac)]/TPP,	[bmim][BF ₄]	41.4/100	–	4–14	1.9–2.6	3–10	[39]
	TPPTS, TPPTI (Rh/L = 1/10)	[bmim][PF ₆]	–	–	23–70	1.8–2.6	1–10	
	[Rh(CO) ₂ (acac)]/POP-xanthophos-2[mmim][PF ₆]	[bdmim][PF ₆]	60/100	49–89/–	3–37	2.2–2.6	1–7	
	(47) (Rh/L = 1/4)	[bmim][PF ₆]	–	–	4,000–8,900	54–58	1–9	[40, 41]
	Co ₂ (CO) ₈ /pyridine, substituted pyridines	[bmim][PF ₆] [bmim][TF ₂ N] [bmpyr][TT ₂ N]	100/130	66–90/–	47–260	1.8–2.1	–	[42]
	[mtr][Co(CO) ₄] (19) [mg][Co(CO) ₄] (18)	–	(10/20)/120	27–87	–	43 ^b	3	[43]
	[Rh(CO) ₂ (acac)]/ 33 (Rh/L = 1/4–1/10)	[bmim][BF ₄], [bmim][PF ₆]	20/80	42–96/74–96	60–240	2.6–12.6	2	[44]

(continued)

Table 3 (continued)

Substrate	Catalyst precursor/ligand	Reaction medium	$p(\text{CO}/\text{H}_2)$ [bar]/T (°C)	Conversion/ yield	TOF (h^{-1})	$[\eta/\text{ISO}]^a$	Cat. recycle. (times)	References
1-Octene, 1-decene, 1-dodecene	$[\text{Rh}(\text{CO})_2(\text{acac})]/\text{TPPTS}$ (Rh/L = 1/6–1/10)	$[\text{bmim}][\text{TsO}]$, $[\text{omim}][\text{TsO}]$, $[\text{dodmim}][\text{TsO}]$, $[\text{cmim}][\text{TsO}]$ (11)	30/100	59.3–98.7/–	654–2,181	2.8– 15.6	9	[45]
1-Octene	$[\text{Rh}(\text{CO})_2(\text{acac})]/\text{TPP}$, TPPTS, DPPE, DPPF, 49 , 50 (Rh/L = 1/2)	$[\text{bmim}][\text{PF}_6]$	10/100	–	35–828	2.6– 16.2	–	[46]
	$[\text{Rh}(\text{CO})_2(\text{acac})]/\mathbf{31}$ (Rh/L = 1/2)	$[\text{bmim}][\text{BF}_4]$, $[\text{bmim}][\text{PF}_6]$, $[\text{bmim}][\text{t}-\text{C}_8\text{H}_{17}\text{OSO}_3]$, $[\text{bmim}][\text{t}-\text{C}_8\text{H}_{17}\text{OSO}_3]$ + cyclohexane	28/100	–/–	276–892	2.0–2.9	–	[47]
	$[\text{Rh}(\text{CO})_2(\text{acac})]/\text{TPP}$, TPPTS, 48 , 43a , b (Rh/L = 1/2)	$[\text{bmim}][\text{PF}_6]$	30/100	7.7–69.1/–	15–680	1.7– 21.3	10	[48]
	$[\text{Rh}(\text{CO})_2(\text{acac})]/\text{DPP-}$ $[\text{mbim}][\text{PF}_6]$ (35), 2-(DPP- C_6H_4)- $[\text{mmim}]$ $[\text{BF}_4]$ (36) (Rh/L = 1/2)	$[\text{bmim}][\text{PF}_6]$	30/100	–	51–552	1.1–2.8	–	[49]
	$[\text{Rh}(\text{CO})_2(\text{acac})]/\text{POP-}$ xantphos-2- $[\text{mmim}][\text{PF}_6]$ 47 (Rh/L = 1/4)	$[\text{bmim}][\text{PF}_6]$	60/100	40/–	1,200– 10,100 (6,200)	1.9–45 (44)	1–13	[40]
	$[\text{Rh}(\text{CO})_2(\text{acac})]/\mathbf{34}$ (Rh/L = 1/2)	$[\text{bmim}][\text{PF}_6]$	30/100	–	32	2.8	–	[50]
	$[\text{Rh}(\text{CO})_2(\text{acac})]/\text{PFIL } \mathbf{37}$, 38 , 39 (Rh/L = 1/2, 4, 8)	PFIL 41 (acts as IL)	10–40/ 50– 100	57–100/–	–	1.8–3.7	1–5	[51]

[Rh(CO) ₂ (acac)]/ imidazolium-xantphos (46) (Rh/L = 1/2)	[omim][TF ₂ N]	60–94 100	–	8–53	–	[52]
Rh NP's (1.3–2.4 nm)/–	IL-PEG750 (22)	20–50/ 80– 120	32–100/24– 99	0.8–1.6	5	[53]
Rh NP's (2.1 nm)/–	IL-PEG750 (22)	30–60/ 70– 100	40–99/22– 91	1.2–4.7	8	[54]
[(TPP) ₃ RhCl]/TPP	<i>N</i> -alkylcaprolactam-based ILC's (27a, b), [C ₁₆ mim] [TfO][BF ₄] (26) [bmim][PF ₆]	40/105	67–98/– 74–969	0.3–5	–	[55]
[Rh(CO) ₂ (acac)]/ sulfoxantphos (45) (Rh/L = 1/4)	[bmim][TF ₂ N], [bmim][TF ₂ N] + MeOH	10, (5/10), (16/4)/ 100	63–68/36– 39	382–411	6–7	–
[Rh(CO) ₂ (acac)]/ 42 (Rh/L = 1/10)	[bmim][TF ₂ N], [bmim][TF ₂ N] + MeOH	120/80	98/–	–	2.7–2.9	17
[(2-DPP-[mbim][PF ₆]) ₂ Rh (Cl ₄)]/ 38 (Rh/L = 1/6)	[bmim][BF ₄] [PEmim][BF ₄]	40/120	96–98/–	613–866	2.8	2
[Rh(CO) ₂ (acac)]/ 40 (Rh/L = 1/4 1/20)	17a, 17b, 16	69/80	12–60/–	20–207	1.2–19	2
[Rh(CO) ₂ (acac)]/xantphos, sulfoxantphos (45) (Rh/L = 1/1–1/5)	[bmim][PF ₆] [bmim][PF ₆] + H ₂ O [bmim][BF ₄]	15.2– 50.6/ 80– 100	18–99/–	15–245	1.7– 14.8	–
RhCl ₃ •3H ₂ O/TPPTS	[Me(EO) ₁₆ TMG]Oms (25)	50	85/–	193	2.0	35

(continued)

Table 3 (continued)

Substrate	Catalyst precursor/ligand	Reaction medium	$p(\text{CO}/\text{H}_2)$ [bar]/T (°C)	Conversion/ yield	TOF (h^{-1})	$[n]_{\text{iso}}^a$	Cat. recycle. (times)	References
1-Decene	[Rh(CO) ₂ (acac)]/–	[bmim][TfO]	50/80	–	1,315	0.5	–	[26]
	[Rh(CO) ₂ (acac)]/TPP, TPPMS, TPPTS (Rh/L = 1/5.25)	[emim][TfO] [bmim][TfO] [mbmim][TfO] [hmim][TfO] [omim][TfO]	50/80	58–62/– 88–89/– 97–99/– 97–100/– 98–99/–	400–760 530–960 925–1,300 910–1,045 1,225– 1,260	2.1–2.8 2.2–2.8 1.8–2.7 1.4–2.7 1.2–2.7	–	[26]
1-Hexene, 1-dodecene	Rh(PPH ₃)Cl, [RhCOD (2-menthyl-4,7- dimethylindenyl)]	10, 13	80/140– 155	68–100/40– 82	–	0.4–2.1	–	[62]
1-Dodecene	RhCl ₃ •H ₂ O/TPPTS, 55 (Rh/L = 1/3–30)	IL-PEG-750 (24)	50/110	90–98/74– 96	230–298	–	8	[63]
1-Decene	RhCl ₃ •3H ₂ O/TPPTS	[Me(EO) ₁₆ TMG]Oms (25)	50	95/–	180	2.3	4	[61]
1-Dodecene				86/–	160	2.4	5	
1-Tetradecene				94/–	150	2.3	6	
	RhCl ₃ /PPH ₃ , TPPTS, OPGPP (Rh/L = 1/15)	23	50.6/105	17–95/16– 94	16–95	0.2–3.9	3	[64]
1-Tetradecene, norbornene, styrene	[(C ₈ H ₁₇) ₃ NCH ₃][RhCl ₄]	–	(45/45)/ 60–80	54–100	–	4/96–1/ 99 ^b	5	[25]
Methyl-3-pentenoate	[Rh(CO) ₂ (acac)]/PPH ₃ , 52 (Rh/L = 1/4)	[bmim][PF ₆]	10/110	–	107–180	0.1–1.0	10	[65]
Styrene, allyl- substituted aromatics	[Rh(CO) ₂ (acac)]/TPPTS (Rh/L = 1/5)	[C ₁₂ mim][Br]	50/80	38–100/–	–	2.7–5.2	3	[66]
	α-cyclodextrin	[C ₆ mim][Br] [C ₁₂ mim][TfO]						

2-Vinylnaphthalene	[Rh(CO) ₂ (acac)]/TPPTS (Rh/L = 1/5)	[NBu ₄][BF ₄]	40/75	100/98	20/80 ^b	–	[31]
Vinyl acetate	[Rh(CO) ₂ (acac)]/tris(2,4-di- <i>tert</i> -butylphenyl)phosphite (Rh/L = 1/3)	[bmim][Tf ₂ N] [NOC ₃ Me][Tf ₂ N] [NBuEt ₃][Tf ₂ N] [C ₄ Py][Tf ₂ N]	20–71/ 85– 100	–/–	5/95–1/ 99 ^b	2	[30]
Vinyl acetate, styrene	[Rh(CO) ₂ (acac)]/BINAP, BINAPS (53) (Rh/L = 1/ 3)	[bmim][BF ₄], [bmim][BF ₄] + toluene	20/60	28.2–55.2/–	–	6	[32]
Methyl acrylate and other unsaturated esters	[Rh(CO) ₂ (acac)]/PPh ₃ /SILP (Rh/L = 1/10)	[bmim][PF ₆]	40/60	64–98/–	5/95–0/ 100 ^b	>1	[24]

^aMolar ratio of linear-to-branched aldehyde

^bExpressed in %

References

1. Franke R, Selent D, Börner A (2012) *Chem Rev* 112:5675–5732
2. Cornils B, Herrmann WA, Rasch M (1994) *Angew Chem Int Ed* 33:2144–2163
3. Magna L, Harry S, Faraj A, Olivier-Bourbigou H (2013) *Oil Gas Sci Technol Rev IFP Energies Nouvelles* 68:415–428
4. Kohlpaintner CW, Fischer RW, Cornils B (2001) *Appl Catal A* 221:219–225
5. Ungvary F (2002) *Coord Chem Rev* 228:61–82
6. Ungvary F (2005) *Coord Chem Rev* 249:2946–2961
7. Ungvary F (2007) *Coord Chem Rev* 251:2072–2086
8. Ungvary F (2007) *Coord Chem Rev* 251:2087–2102
9. Marteel AE, Davies JA, Olson WW, Abraham MA (2003) *Annu Rev Env Resour* 28:401–428
10. Joo F, Papp E, Katho A (1998) *Top Catal* 5:113–124
11. Deshpande RM, Kelkar AA, Sharma A, Julcour-Lebigue C, Delmas H (2011) *Chem Eng Sci* 66:1631–1639
12. Silva SM, Bronger RPJ, Freixa Z, Dupont J, van Leeuwen P (2003) *New J Chem* 27:1294–1296
13. Dyson P, Tilmann G (2005) *Catalysis by metal complexes*, vol 29. Springer, The Netherlands, p 246
14. Werner S, Haumann M, Wasserscheid P (2010) *Annu Rev Chem Biomol* 1:203–230
15. Dümbgen G, Neubauer D (1969) *Chem Ing Tech* 41:974–980
16. Obrecht L, Kamer PCJ, Laan W (2013) *Catal Sci Technol* 3:541–551
17. Wasserscheid P (2003) *Chem Unserer Zeit* 37:52–63
18. Davis JH (2004) *Chem Lett* 33:1072–1077
19. Welton T (2004) *Coord Chem Rev* 248:2459–2477
20. Plechkova NV, Seddon KR (2008) *Chem Soc Rev* 37:123–150
21. Dupont J, Consorti CS, Spencer J (2000) *J Braz Chem Soc* 11:337–344
22. Chauvin Y, Musmann L, Olivier H (1995) *Angew Chem Int Ed* 34:2698–2700
23. Parshall GW (1972) *J Am Chem Soc* 94:8716–8719
24. Panda AG, Bhor MD, Jagtap SR, Bhanage BM (2008) *Appl Catal A-Gen* 347:142–147
25. Paganelli S, Perosa A, Selva M (2007) *Adv Synth Catal* 349:1858–1862
26. Leclercq L, Suisse I, Agbossou-Niedercorn F (2008) *Chem Commun* 311–313
27. Keim W, Vogt D, Waffenschmidt H, Wasserscheid P (1999) *J Catal* 186:481–484
28. Wasserscheid P, Waffenschmidt H (2000) *J Mol Catal A Chem* 164:61–67
29. Dabbawala AA, Bajaj HC, Rao GVS, Abdi SHR (2012) *Appl Catal A-Gen* 419–420:185–193
30. Williams DBG, Ajam M, Ranwell A (2007) *Organometallics* 26:4692–4695
31. Scurto AM, Leitner W (2006) *Chem Commun* 3681–3683
32. Deng C, Ou G, She J, Yuan Y (2007) *J Mol Catal A: Chem* 270:76–82
33. Tominaga K, Sasaki Y (2004) *Chem Lett* 33:14–15
34. Tominaga K-i, Sasaki Y (2004) *J Mol Catal A Chem* 220:159–165
35. K-i T, Sasaki Y (2004) *Stud. Surf Sci Catal* 153:227–232
36. Chauvin Y, Olivier H, Musmann L (1997) EP776880-A
37. Diao Y, Li J, Wang L, Yang P, Yan R, Jiang L, Zhang H, Zhang S (2013) *Catal Today* 200:54–62
38. Peng Q, Deng C, Yang Y, Dai M, Yuan Y (2007) *React Kinet Catal Lett* 90:53–60
39. Mehnert CP, Cook RA, Dispenziere NC, Mozeleski EJ (2004) *Polyhedron* 23:2679–2688
40. Bronger RPJ, Silva SM, Kamer PCJ, van Leeuwen P (2004) *Dalton Trans*: 1590–1596
41. Bronger RPJ, Silva SM, Kamer PCJ, van Leeuwen P (2002) *Chem Commun* 3044–3045
42. Magna L, Harry S, Proriol D, Saussine L, Olivier-Bourbigou H (2007) *Oil Gas Sci Technol* 62:775–780
43. Dengler JE, Doroodian A, Rieger B (2011) *J Organomet Chem* 696:3831–3835
44. Favre F, Olivier-Bourbigou H, Commereuc D, Saussine L (2001) *Chem Commun* 1360–1361
45. Lin Q, Jiang W, Fu H, Chen H, Li X (2007) *Appl Catal A Gen* 328:83–97

46. Brasse CC, Englert U, Salzer A, Waffenschmidt H, Wasserscheid P (2000) *Organometallics* 19:3818–3823
47. Wasserscheid P, van Hal R, Bosmann A (2002) *Green Chem* 4:400–404
48. Wasserscheid P, Waffenschmidt H, Machnitzki P, Kottsieper KW, Stelzer O (2001) *Chem Commun* 451–452
49. Brauer DJ, Kottsieper KW, Liek C, Stelzer O, Waffenschmidt H, Wasserscheid P (2001) *J Organomet Chem* 630:177–184
50. Kottsieper KW, Stelzer O, Wasserscheid P (2001) *J Mol Catal A Chem* 175:285–288
51. Laska KL, Demmans KZ, Stratton SA, Moores A (2012) *Dalton Trans* 41:13533–13540
52. Webb PB, Kunene TE, Cole-Hamilton DJ (2005) *Green Chem* 7:373–379
53. Xu Y, Wang Y, Zeng Y, Jiang J, Jin Z (2012) *Catal Lett* 142:914–919
54. Zeng Y, Wang Y, Xu Y, Song Y, Zhao J, Jiang J, Jin Z (2012) *Chinese J Catal* 33:402–406
55. Yang J, Li F-F, Zhang J, Li J, Wang W-X (2010) *Helv Chim Acta* 93:1653–1660
56. Hamza K, Schumann H, Blum J (2009) *Eur J Org Chem* 1502–1505
57. Jin X, Zhao K, Kong F, Cui F, Yang D (2013) *Catal Lett* 143:839–843
58. Chen S-J, Wang Y-Y, Yao W-M, Zhao X-L, Vo-Thanh G, Liu Y (2013) *J Mol Catal A: Chem* 378:293–298
59. Omotowa BA, Shreeve JM (2004) *Organometallics* 23:783–791
60. Dupont J, Silva SM, de Souza RF (2001) *Catal Lett* 77:131–133
61. Jin X, Yang D, Xu X, Yang Z (2012) *Chem Commun* 48:9017–9019
62. Stenzel O, Raubenheimer HG, Esterhuysen C (2002) *J Chem Soc Dalton* 1132–1138
63. Tan B, Jiang J, Wang Y, Wei L, Chen D, Jin Z (2008) *Appl Organomet Chem* 22:620–623
64. Kong FZ, Jiang JY, Jin ZL (2004) *Catal Lett* 96:63–65
65. Sharma A, Lebigue CJ, Deshpande RM, Kelkar AA, Delmas H (2010) *Ind Eng Chem Res* 49:10698–10706
66. Leclercq L, Lacour M, Sanon SH, Schmitzer AR (2009) *Chem-Eur J* 15:6327–6331
67. Frade RF, Afonso CA (2010) *Hum Exp Toxicol* 29:1038–1054
68. Haumann M, Riisager A (2008) *Chem Rev* 108:1474–1497
69. Welton T (1999) *Chem Rev* 99:2071–2083
70. Briggs JR, Maher JM, Harrison AM (1993) US5225387-A
71. Keim W, Waffenschmidt H, Wasserscheid P (2000) DE19901524-A1
72. Valkenberg M, Sauvage E, Castro-Moriera CP, Hoelderich WF (2000) WO 0132308A
73. Bahrman H, Bohnen H (2000) EP1177163-B1
74. Favre F, Commereuc D, Olivier-Bourbigou H (2002) US6617474; EP1241156-A1
75. Favre F, Commereuc D, Olivier-Bourbigou H, Saussine L (2002) EP1182187-A1
76. Hillebrand G, Hirschauer A, Commereuc D, Olivier-Bourbigou H, Saussine L (2004) EP1106595-A
77. Bohnen H, Herwig J, Hoff D, Van Hal R, Wasserscheid P, Hal RV (2004) EP1400504-A1
78. Magna L, Olivier-Bourbigou H, Saussine L, Kruger-Tissot V, Kruger TV (2003) EP1352889-A1
79. Magna L, Harry S, Olivier BH, Saussine L (2008) FR2903686-A1; FR2903686-B1
80. Magna L, Saussine L, Proriol D, Olivier-Bourbigou H (2008) FR2903687-A1; WO2008006951-A1
81. Francio G, Klankermayer J, Leitner W, Schmitkamp M, Dianjun C (2009) DE102007040333-A1
82. Lei Z, Dai C, Chen B (2013) *Chem Rev* doi:10.1021/cr300497a
83. Dyson PJ, Laurenczy G, Andre Ohlin C, Vallance J, Welton T (2003) *Chem Commun* 2418–2419
84. Kumelán J, Pérez-Salado Kamps Á, Tuma D, Maurer G (2007) *Fluid Phase Equilib* 260:3–8
85. Ferguson L, Scovazzo P (2007) *Ind Eng Chem Res* 46:1369–1374
86. Hintermair U, Zhao G, Santini CC, Muldoon MJ, Cole-Hamilton DJ (2007) *Chem Commun* 1462–1464
87. Cornlis B, Herrmann WA (1998) *Aqueous-phase organometallic catalysis*. Wiley-VCH, Weinheim

88. Lin Q, Fu H, Jiang W, Chen H, Li X (2007) *J Chem Res S* 216–220
89. You H, Wang Y, Zhao X, Chen S, Liu Y (2013) *Organometallics* 32:2698–2704
90. Dupont J (2004) *J Braz Chem Soc* 15:341–350
91. Leclercq L, Schmitzer AR (2009) *Supramol Chem* 21:245–263
92. Steinrueck H-P (2012) *Phys Chem Chem Phys* 14:5010–5029
93. Kolbeck C, Paape N, Cremer T, Schulz PS, Maier F, Steinrueck H-P, Wasserscheid P (2010) *Chem Eur J* 16:12083–12087
94. Diebolt O, van Leeuwen PWNM, Kamer PCJ (2012) *Acs Catalysis* 2:2357–2370
95. Dyson PJ, McIndoe JS, Zhao DB (2003) *Chem Commun* 508–509
96. Behr A, Wintzer A (2011) *Chem Ing Tech* 83:1356–1370
97. Wang YH, Jiang JY, Jin ZL (2004) *Catal Surv Asia* 8:119–126
98. Hugel H, Nobis M (2008) *Top Organomet Chem* 23:1–17
99. Wasserscheid P, Waffenschmidt H (2002) *ACS Symp Ser* 818:373–386
100. Kunene TE, Webb PB, Cole-Hamilton DJ (2011) *Green Chem* 13:1476–1481
101. Buhling A, Kamer PCJ, van Leeuwen PWNM (1995) *J Mol Catal A Chem* 98:69–80
102. Hanson BE (1999) *Coord Chem Rev* 185–186:795–807
103. Beller M, Cornils B, Frohning CD, Kohlpaintner CW (1995) *J Mol Catal A Chem* 104:17–85
104. Riisager A, Eriksen KM, Wasserscheid P, Fehrmann R (2003) *Catal Lett* 90:149–153
105. Riisager A, Wasserscheid P, van Hal R, Fehrmann R (2003) *J Catal* 219:452–455
106. Unruh JD, Christenson JR (1982) *J Mol Catal* 14:19
107. Moser WR, Papite CJ, Brannon DA, Duwell RA (1987) *J Mol Catal* 41:271
108. Magee MP, Luo W, Hersh WH (2001) *Organometallics* 21:362–372
109. Erkey C, Palo DR, Haji S (2002) *Fuel Chem Div Prepr* 47:144
110. Azouri M, Andrieu J, Picquet M, Richard P, Hanquet B, Tkatchenko I (2007) *Eur J Inorg Chem* 4877–4883
111. Kainz S, Koch D, Leitner W, Baumann W (1997) *Angew Chem Int Ed Engl* 36:1628–1630
112. Machnitzki P, Tepper M, Wenz K, Stelzer O, Herdtweck E (2000) *J Organomet Chem* 602:158–169
113. Casey CP, Whiteker GT, Melville MG, Petrovich LM, Gavney JA, Powell DR (1992) *J Am Chem Soc* 114:5535–5543
114. Riisager A, Fehrmann R, Haumann M, Wasserscheid P (2006) *Eur J Inorg Chem* 2006:695–706
115. Veige AS (2008) *Polyhedron* 27:3177–3189
116. Gil W, Boczon K, Trzeciak AM, Ziolkowski JJ, Garcia-Verdugo E, Luis SV, Sans V (2009) *J Mol Catal A Chem* 309:131–136
117. Gil W, Trzeciak AM (2011) *Coord Chem Rev* 255:473–483
118. Velazquez HD, Verpoort F (2012) *Chem Soc Rev* 41:7032–7060
119. Scholten JD, Dupont J (2008) *Organometallics* 27:4439–4442
120. Herrmann WA, Kohlpaintner CW (1993) *Angew Chem Int Ed Eng* 32:1524–1544
121. Ding H, Hanson BE (1994) *J Chem Soc Chem Commun* 2747
122. Sieffert N, Wipff G (2007) *J Phys Chem B* 111:4951–4962
123. Leitner W (2002) *Acc Chem Res* 35:746–756
124. Leitner W (2003) *Chem Unserer Zeit* 37:32–38
125. Osuna AB, Serbanovic A, Nunes da Ponte M, Matsubara H, Ryu I, Dupont J (2006) *Fluid Extraction*. In: Afonso CAM, Crespo JG (eds) *Green separation processes: fundamentals and applications*. Weinheim, Wiley, pp 207–218
126. Niessen HG, Woelk K (2007) *Top Curr Chem* 276:69–110
127. Pitter S, Dinjus E, Ionescu C, Maniut C, Makarczyk P, Patcas F (2008) *Top Organomet Chem* 23:109–147
128. Rathke JW, Klingler RJ, Krause TR (1991) *Organometallics* 10:1350–1355
129. Sellin MF, Cole-Hamilton DJ (2000) *J Chem Soc Dalton* 1681–1683
130. Blanchard LA, Hancu D, Beckman EJ, Brennecke JF (1999) *Nature* 399:28–29
131. Scurto AM, Aki SNVK, Brennecke JF (2002) *J Am Chem Soc* 124:10276–10277

132. Mellein BR, Brennecke JF (2007) *J Phys Chem B* 111:4837–4843
133. Ren W, Sensenich B, Scurto AM (2010) *J Chem Thermodyn* 42:305–311
134. Blanchard LA, Gu Z, Brennecke JF (2001) *J Phys Chem B* 105:2437–2444
135. Anthony JL, Maginn EJ, Brennecke JF (2002) *J Phys Chem B* 106:7315–7320
136. Cadena C, Anthony JL, Shah JK, Morrow TI, Brennecke JF, Maginn EJ (2004) *J Am Chem Soc* 126:5300–5308
137. Scurto AM, Hutchenson K, Subramaniam B (2009) Gas-expanded liquids: fundamentals and applications. In: Scurto AM, Hutchenson K, Subramaniam B (eds) *Gas-expanded liquids and near-critical media: green chemistry and engineering*. American Chemical Society, Washington, DC, pp 3–37
138. Webb PB, Sellin MF, Kunene TE, Williamson S, Slawin AMZ, Cole-Hamilton DJ (2003) *J Am Chem Soc* 125:15577–15588
139. Sellin MF, Webb PB, Cole-Hamilton DJ (2001) *Chem Commun* 781–782
140. Ahosseini A, Ren W, Scurto AM (2009) *Ind Eng Chem Res* 48:4254–4265
141. Cole-Hamilton DJ (2003) *Science* 299:1702–1706
142. Riisager A, Fehrmann R, Haumann M, Wasserscheid P (2006) *Top Catal* 40:91–102
143. Li H, Bhadury PS, Song B, Yang S (2012) *RSC Adv* 2:12525–12551
144. Tundo P, Perosa A (2007) *Chem Soc Rev* 36:532–550
145. Hagiwara H (2012) *Heterocycles* 85:281–297
146. Van Doorslaer C, Wahlen J, Mertens P, Binnemans K, De Vos D (2010) *Dalton Trans* 39:8377–8390
147. Mehnert CP, Cook RA, Dispenziere NC, Afeworki M (2002) *J Am Chem Soc* 124:12932–12933
148. Haumann M, Dentler K, Joni J, Riisager A, Wasserscheid P (2007) *Adv Synth Catal* 349:425–431
149. Yang Y, Lin HQ, Deng CX, She JR, Yuan YZ (2005) *Chem Lett* 34:220–221
150. Yang Y, Deng CX, Yuan YZ (2005) *J Catal* 232:108–116
151. Hintermair U, Gong Z, Serbanovic A, Muldoon MJ, Santini CC, Cole-Hamilton DJ (2010) *Dalton Trans* 39:8501–8510
152. Hamza K, Blum J (2007) *Eur J Org Chem* 4706–4710
153. Panda AG, Jagtap SR, Nandurkar NS, Bhanage BM (2008) *Ind Eng Chem Res* 47:969–972
154. Mehnert CP (2004) *Chem Eur J* 11:50–56
155. Vangeli OC, Romanos GE, Beltsios KG, Fokas D, Kouvelos EP, Stefanopoulos KL, Kanellopoulos NK (2010) *J Phys Chem B* 114:6480–6491
156. Lemus J, Palomar J, Gilarranz MA, Rodriguez JJ (2011) *Adsorption* 17:561–571
157. Werner S, Szesni N, Kaiser M, Haumann M, Wasserscheid P (2012) *Chem Eng Technol* 35:1962–1967
158. Riisager A, Fehrmann R, Flicker S, van Hal R, Haumann M, Wasserscheid P (2005) *Angew Chem Int Edit* 44:815–819
159. Riisager A, Fehrmann R, Haumann M, Wasserscheid P (2006) *Eur J Inorg Chem* 695–706
160. Shylesh S, Hanna D, Werner S, Bell AT (2012) *ACS Catal* 2:487–493
161. Riisager A, Fehrmann R, Haumann M, Gorle BSK, Wasserscheid P (2005) *Ind Eng Chem Res* 44:9853–9859
162. Riisager A, Fehrmann R, Haumann M, Wasserscheid P (2008) *Catalytic SILP Materials*. In: Leitner W, Hölscher M (eds) *Regulated systems for multiphase catalysis*. Springer, Berlin Heidelberg, pp 149–161
163. Hanna DG, Shylesh S, Werner S, Bell AT (2012) *J Catal* 292:166–172
164. Haumann M, Jakuttis M, Werner S, Wasserscheid P (2009) *J Catal* 263:321–327
165. Jakuttis M, Schoenweiz A, Werner S, Franke R, Wiese K-D, Haumann M, Wasserscheid P (2011) *Angew Chem Int Edit* 50:4492–4495
166. Haumann M, Jakuttis M, Franke R, Schoenweiz A, Wasserscheid P (2011) *Chemcatchem* 3:1822–1827

167. Franke R, Brausch N, Fridag D, Christiansen A, Becker M, Wasserscheid P, Haumann M, Jakuttis M, Werner S, Schoenweiz A (2012) DE102010041821-A1; WO2012041846-A1
168. Ha HNT, Duc DT, Dao TV, Le MT, Riisager A, Fehrmann R (2012) *Catal Commun* 25:136–141
169. Clarke ML (2005) *Curr Org Chem* 9:701–718
170. Nairoukh Z, Blum J (2012) *J Mol Catal A Chem* 358:129–133
171. Migowski P, Dupont J (2007) *Chem Eur J* 13:32–39
172. Yuan Y, Yan N, Dyson PJ (2012) *ACS Catal* 2:1057–1069
173. Han D, Li X, Zhang H, Liu Z, Li J, Li C (2006) *J Catal* 243:318–328
174. Han D, Li X, Zhang H, Liu Z, Hu G, Li C (2008) *J Mol Catal A Chem* 283:15–22
175. Axet MR, Castillón S, Claver C, Philippot K, Lecante P, Chaudret B (2008) *Eur J Inorg Chem* 2008:3460–3466
176. Bruss AJ, Gelesky MA, Machado G, Dupont J (2006) *J Mol Catal A Chem* 252:212–218
177. Pospech J, Fleischer I, Franke R, Buchholz S, Beller M (2013) *Angew Chem Int Ed* 52:2852–2872
178. Currie M, Estager J, Licence P, Men S, Nockemann P, Seddon KR, Swadźba-Kwaśny M, Terrade C (2012) *Inorg Chem* 52:1710–1721
179. Petocz G, Rangits G, Shaw M, de Bod H, Williams DBG, Kollar L (2009) *J Organomet Chem* 694:219–222
180. Rangits G, Petocz G, Berente Z, Kollar L (2003) *Inorg Chim Acta* 353:301–305
181. Rangits G, Berente Z, Kegl T, Kollar L (2005) *J Coord Chem* 58:869–874
182. Illner P, Zahl A, Puchta R, van Eikema HN, Wasserscheid P, van Eldik R (2005) *J Organomet Chem* 690:3567–3576
183. Tominaga K-I, Sasaki Y (2000) *Catal Commun* 1:1–3
184. Tominaga K-I, Sasaki Y, Hagihara K, Watanabe T, Saito M (1994) *Chem Lett* 23:1391–1394
185. Tominaga K (2006) *Catal Today* 115:70–72
186. Srivastava VK, Eilbracht P (2009) *Catal Commun* 10:1791–1795
187. Mura MG, Luca LD, Giacomelli G, Porcheddu A (2012) *Adv Synth Catal* 354:3180–3186
188. Peschel A, Hentschel B, Freund H, Sundmacher K (2012) *Chem Eng J* 188:126–141
189. Peschel A, Hentschel B, Freund H, Sundmacher K (2011) In: 21st European symposium on computer aided process engineering, vol 29. pp 1246–1250
190. Fang J, Jana R, Tunge JA, Subramaniam B (2011) *Appl Catal A Gen* 393:294–301
191. Mercer SM, Robert T, Dixon DV, Jessop PG (2012) *Catal Sci Technol* 2:1315–1318
192. Hintermair U, Francio G, Leitner W (2011) *Chem Commun* 47:3691–3701

ILs in Transition Metal-Catalysed Alkoxy- and Aminocarbonylation

Rita Skoda-Földes

Abstract The use of carbon monoxide as a carbonyl source for the preparation of aldehydes, ketones and carboxylic acid derivatives in homogeneous catalytic reactions is a valuable tool in the synthesis of fine chemicals. Amongst immobilising agents for carbonylation catalysts, the application of ILs drew particular attention. Besides enabling catalyst reuse, the ionic liquid may influence the structure of catalysts or catalyst precursors, may affect the chemoselectivity of the reaction or may be capable of solubilising special substrates. The present chapter is intended to summarise the research carried out in the past 15 years involving carbonylation reactions of alkenes/alkynes and aryl/alkenyl halides in the presence of various nucleophiles, such as alcohols, water, amines and thiols.

Keywords Alkenes · Aryl halides · Carbon monoxide · Nucleophiles

Contents

1	Introduction	146
2	Carbonylation of Alkenes and Alkynes	146
2.1	Alkoxy carbonylation	147
2.2	Hydroxy carbonylation	150
2.3	Aminocarbonylation	151
3	Carbonylation of Aryl or Alkenyl Halides	152
3.1	Alkoxy carbonylation	152
3.2	Hydroxy carbonylation	155
3.3	Aminocarbonylation	156
3.4	Thiocarbonylation	159
4	Concluding Remarks	159
	References	159

1 Introduction

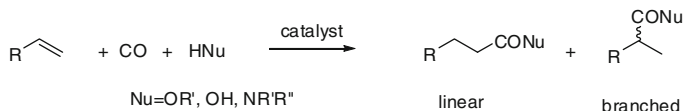
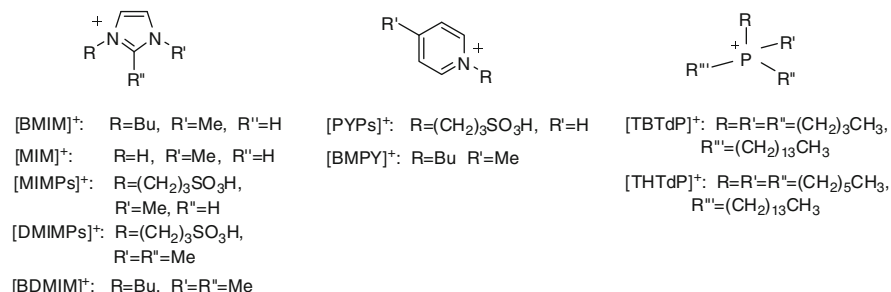
By homogeneous catalytic methods, carbon monoxide can be introduced directly into a number of different sites in an organic molecule leading to the synthesis of carbonyl compounds and carboxylic acid derivatives. In many cases, instead of a multi-step synthesis, the targeted product can be obtained in a single selective catalytic step, resulting in a substantially higher overall yield. As a consequence, transition metal-catalysed carbonylation reactions have become a useful tool for the preparation of bulk and fine chemicals as well as intermediates for organic synthesis [1, 2].

The common drawback of all homogeneous catalytic reactions, the difficulties in phase separation and recovery and reuse of the catalysts, raised the application of various alternative solvents [3]. Amongst these systems, the use of ILs drew particular attention due to their many advantageous properties, such as a very wide liquid range, negligible vapour pressure, ability to stabilise metal complexes, great variability of the structure of cation and anion. At the same time, the lower solubility of CO in ILs than in conventional solvents [4] necessitates the use of relatively high pressures in many cases.

Although hydroformylation was the most thoroughly explored transition metal-catalysed carbonylation reaction in ILs, other carbonylations – especially those based on palladium catalyst precursors – such as alkoxy- and aminocarbonylation of alkenes and aryl halides have also been investigated [5, 6]. This chapter is intended to review briefly the progress of research since the first report on alkoxy carbonylation carried out in ILs by Dupont in 1998 [7].

2 Carbonylation of Alkenes and Alkynes

In this reaction an unsaturated hydrocarbon is reacted with CO and a nucleophile (alcohol (alkoxy carbonylation), water (hydroxy carbonylation) or an amine (amino carbonylation)) to produce the corresponding carboxylic acid derivatives (Scheme 1) [8]. Of the catalytic systems investigated, phosphine–palladium complexes, promoted with a strong protic acid, have received particular attention. In these procedures, valuable carboxylic acids, such as linear fatty acids or branched 2-arylpropanoic acids (the latter used as nonsteroidal anti-inflammatory agents (ibuprofen, naproxen and ketoprofen)), can be obtained. As a consequence, a significant research effort has been devoted to find adequate catalyst recycling methods [9] to facilitate large-scale applications. Amongst immobilisation methodologies, the use of ILs can be particularly interesting. Besides enabling catalyst reuse, the presence of an IL in the reaction mixture may have other important consequences. It may influence the structure of catalysts or catalyst precursors, and may affect the chemoselectivity of the reaction. Also, the IL may be capable of solubilising special substrates, such as cellulose, or it can play the role of not only the solvent but also the acidic promoter.

**Scheme 1** Carbonylation of alkenes**Fig. 1** Cations of some ILs used in the carbonylation reactions

2.1 Alkoxy-carbonylation

The first example for alkoxy-carbonylation (also called hydroalkoxy-carbonylation or hydroesterification) of alkenes in ILs was published by Dupont in 1998 [7]. Starting from styrene, very high regioselectivities in the branched products, 2-arylpropionic esters (>99.5%), were obtained using a catalytic system composed of PdCl₂(PhCN)₂, (+)-neomenthyl-diphenylphosphine and *p*-toluenesulphonic acid (TsOH) under mild reaction conditions (10 bar and 70°C). The reactions were performed in a two-phase system composed of [BMIM][BF₄] (Fig. 1) and isopropanol/cyclohexane. Although a chiral phosphine ligand was used, the degree of asymmetric induction was low (<5%).

The products could easily be separated by decantation, but the ionic phase could not simply be recycled since the palladium catalyst was decomposed after the catalytic reaction. At the same time, atomic absorption analysis of the two phases of the reaction mixture obtained at low conversion (<35% after 3 h) indicated that more than 95% of the Pd was still retained in the ionic phase. In accordance with this, the recovered ionic solution obtained at low conversions could be reused giving 60% conversion of styrene after 20 h.

Shaughnessy et al. carried out a detailed investigation of alkoxy-carbonylation of styrene derivatives in a range of ionic liquid media [10]. The PPh₃/Pd/TsOH catalyst system gave high linear to branched ratios (3–5) that were relatively independent of reaction conditions. An excess of the PPh₃ ligand was necessary to prevent catalyst decomposition. The reversed regioselectivity obtained in this study was explained by the different mechanistic pathways that might take place in the IL/methanol and IL/isopropanol/cyclohexane [7] systems. It was assumed that the use of the IL solvent alone made the cationic pathway, resulting in linear esters, more favourable.

Upon recycling the IL/catalyst solution, ester yields remained constant through the first two runs with near complete conversion of styrene. After that, a gradual decline was observed, but product yields remained greater than 50% until the sixth cycle. PPh_3 was added in each cycle to account for leaching losses.

A detailed investigation of the effect of IL structure and the choice of phosphine ligands on the same reaction was carried out by Kollár et al. [11, 12]. Alkoxy carbonylation of styrene was performed in a number of imidazolium-based ILs in the presence of either $(\text{Pd}(\text{PPh}_3)_2\text{Cl}_2)$ or in situ systems obtained from $\text{Pd}(\text{PPh}_3)_2\text{Cl}_2$ and bidentate phosphine ligands. The reactions were carried out in the absence of an acidic promoter at 100°C and under 100 bar CO pressure. An enhanced oligomerisation/polymerisation of styrene, compared to similar reactions in organic solvents, was observed, especially in $[\text{BMIM}][\text{PF}_6]$, possibly due to the formation of HF in the presence of trace amounts of water.

Styrene conversion and regioselectivity of alkoxy carbonylation were found to be greatly dependent on the choice of the alcohol reaction partner, added ligand and the ionic liquid solvent. The use of bidentate phosphines uniformly led to lower conversions. The highest regioselectivities towards the branched ester were observed with $\text{PdCl}_2(\text{PPh}_3)_2$, whilst the linear regioisomer was the prevailing product in the presence of DPPF (DPPF: 1,1'-bis(diphenylphosphino) ferrocene) as the added ligand. However, the branched/linear ratio was also greatly influenced by the choice of the IL. The use of the $\text{Pd}(\text{PPh}_3)\text{Cl}_2$ catalyst led to moderate branched selectivities in imidazolium ILs with butyl, dodecyl or 4-cyanopropyl substituents. On the other hand, the introduction of an acetyl or benzyl group resulted in the exclusive formation of branched esters.

The application of the $[\text{BF}_4]^-$ counterion seemed to enhance branched selectivity compared to $[\text{PF}_6]^-$ even in the presence of bidentate ligands. The great difference in the regioselectivity of the reaction in the two types of ILs was attributed to the formation of different catalytic species. According to ^{31}P NMR experiments, monodentate and bidentate mode of coordination of bidentate phosphines was observed in $[\text{BMIM}][\text{BF}_4]$ and $[\text{BMIM}][\text{PF}_6]$, respectively. Recycling of the ionic liquid containing the catalytically active species led to a 10–25% decrease in the activity in the first three runs, even if some additional phosphine was added.

Ammonium and phosphonium salts were also proved to be suitable media for the alkoxy carbonylation of styrene [13]. Using the $\text{PdCl}_2/\text{PPh}_3/\text{CuCl}_2$ system at 50 bar CO pressure and 110°C , almost complete conversion and acceptable regioselectivity, 74–78% towards the branched regioisomer, could be reached. The reaction in the presence of ammonium salts showed strong dependence of the regioselectivity on the halide counterion (bromide or chloride). Improved reaction rate and lower regioselectivity were observed with the $\text{PdCl}_2/\text{PPh}_3/\text{CuCl}_2\text{-NBu}_4\text{Br}$ system. The chloride–bromide exchange in the coordination sphere of palladium was proved by ^{31}P NMR.

Brønsted acidic ILs were employed not only as solvents but also as acid promoters [14]. The catalytic activity was almost in agreement with the

acidity order of the ILs ($[\text{MIMPs}][\text{HSO}_4] > [\text{MIMPs}][\text{BF}_4] > [\text{PYPs}][\text{TsO}] > [\text{MIMPs}][\text{TsO}] > [\text{DMIMPs}][\text{TsO}] > [\text{MIMPs}][\text{H}_2\text{PO}_4] > [\text{MIM}][\text{TsO}]$, Fig. 1). In the alkoxy-carbonylation of 1-hexene better conversion, higher linear/branched ratio and more efficient recycling were achieved, compared to the reaction of styrene. Both UV-vis measurements, carried out to determine the partition coefficients of the PPh_3 -Pd complex in the organic phase and IL-methanol phase, and ICP measurements showed a higher Pd loss in the case of styrene, which may be related to the different coordinative abilities of the reactants to the Pd species.

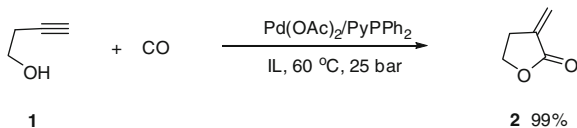
During alkoxy-carbonylations, the use of longer chain alcohols led to varying results depending on the reaction conditions. Excellent conversions, exceeding even that of the carbonylation with ethanol, were obtained with benzyl or *n*-octyl alcohol [11]. At the same time, alkoxy-carbonylation with bulky alcohols was less facile (with isopropanol [14]) or did not take place at all (with *tert*-butanol [11]).

Screening of ethylene alkoxy-carbonylation with *n*-propanol by $\text{Pd}(\text{OAc})_2/\text{PPh}_3/\text{methanesulphonic acid}$ in BMIM ionic liquids revealed that the success of the reaction greatly depended on the choice of the anion [15]. No reaction occurred with $[\text{BMIM}][\text{OAc}]$ and $[\text{BMIM}][(\text{MeO})_2\text{PO}_2]$, in $[\text{BMIM}][\text{NTf}_2]$ the products were obtained in moderate yield, whilst in $[\text{BMIM}][\text{MeSO}_3]$ essentially full conversion was observed.

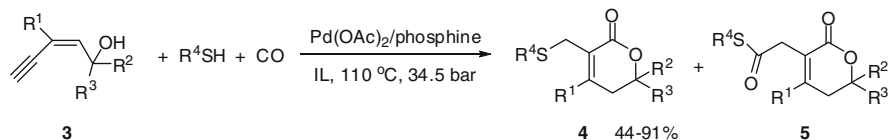
Based on these results, alkoxy-carbonylation of ethylene with cellulose was carried out in $[\text{BMIM}][\text{MeSO}_3]$. Maximum substitution of cellulose, with a degree of 1–2, was obtained in the presence of $\text{Pd}(\text{OAc})_2/\text{PPh}_3$ at 100°C and 55 bar pressure (ethylene/CO = 1:1). The use of either lower or higher temperatures led to worse results, because of slow reaction and catalyst deactivation, respectively.

Intramolecular alkoxy-carbonylations, leading to *exo*- α -methylene γ -lactones [16] and δ -lactones [17], were carried out effectively in ILs. The carbonylation of 3-butyne-1-ol (**1**, Scheme 2) was performed in the presence of a cationic palladium complex formed from $\text{Pd}(\text{OAc})_2$ and 2-(diphenylphosphino)pyridine (PyPPh_2) dissolved in $[\text{BMIM}][\text{BF}_4]$ or $[\text{BMIM}][\text{PF}_6]$ [16]. However, a significant drop in the yield of **2** was observed (from 99% in the first run to 85% and 37% in the first and second recharges) using the same IL-catalyst solutions.

A dramatic effect of ILs was noticed in the palladium-catalysed reaction of enynols (**3**, Scheme 3) with thiols [17]. Carbonylation in THF led to double carbonylated products (**5**) via a cyclocarbonylation-thiocarbonylation reaction sequence. In ILs monocarbonylated 6-membered ring lactones (**4**) were obtained in high yields. Although in the latter reactions the thioether derivatives (**4**) were the main products, the selectivity of the reaction was affected by the choice of both the catalyst precursor and the ionic liquid. For example, the system of $\text{Pd}(\text{OAc})_2/\text{PPh}_3/[\text{BMIM}][\text{NTf}_2]$ gave **4** as a sole product in excellent yield, whilst the use of bidentate phosphines, as well as the $\text{Pd}(\text{OAc})_2/\text{PPh}_3/[\text{BMIM}][\text{BF}_4]$ system, provided a mixture of **4** and **5**.



Scheme 2 Carbonylation of 3-butyn-1-ol (1)



Scheme 3 Carbonylation of enynols (3)

2.2 Hydroxycarbonylation

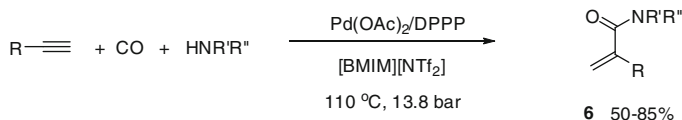
An extensive investigation of hydroxycarbonylation of styrene and other alkenes in an IL/heptane two-phase system was carried out by Lapidus et al. [18].

Similarly to the alkoxy carbonylation reaction, complexes with bidentate phosphines were less active than PdCl₂(PPh₃)₂ [19]. An acid promoter was a necessary component of the catalytic system. In weakly acidic media, branched and linear products were formed in nearly equal amounts, whilst with an increase in the concentration of HCl the branched/linear ratio increased.

Both the conversion of styrene and the yield of acids depended on the pressure in the range of 10–70 bar in a nearly linear fashion [18]. The experimental results suggested that the nature of the catalytic system changed at temperatures higher than 120–130 °C, when palladium metal precipitation could be observed together with a dramatic increase in the hydrogenating ability of the catalyst.

[Bu₄N]Br was found to be an ideal medium to stabilise palladium catalysts in the absence of phosphine ligands. With palladium acetate precursor, products were obtained in even higher yields than with PdCl₂(PPh₃)₂ [20]. Formation of a nanosized suspension of palladium metal was proved by TEM measurements in [Bu₄N]Br [21]. The presence of the bromide anion seemed to be essential to stabilise palladium nanoparticles. Whilst ligand-free palladium was retained in the melts of [Bu₄N]Br and [BMIM]Br, the precipitation of palladium black was observed in [Bu₄N]Cl, [BMIM]Cl, [BMIM][BF₄] and [MIM][PF₆] [20]. At the same time, the PdCl₂(PPh₃)₂-TsOH-[Bu₄N]Cl catalytic system was proved to be equally efficient. So phosphine ligands and chloride anions seem to have an ambiguous effect on the catalyst activity, depending on the molten salt nature. Phosphine can replace CO in the coordination sphere of palladium and thus it hampers the formation of an acyl-Pd complex. However, [Bu₄N]Cl and [BMIM]⁺-containing ILs stabilise palladium less efficiently; therefore, PPh₃ is needed to avoid precipitation of palladium black.

The nature of IL anions was also found to influence the regioselectivity of styrene carbonylation to a substantial extent [22]. In [NBu₄]Cl and [BMIM]Cl,



Scheme 4 Aminocarbonylation of alkynes

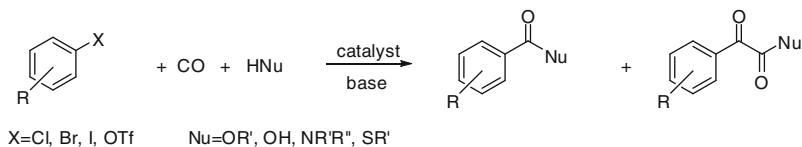
the branched/linear ratio was between 6 and 10 depending on the reaction conditions, whilst hydroxycarbonylations carried out in the analogous bromides resulted in the formation of approximately equimolar amounts of the regioisomeric products. In order to explain the anion-dependence of regioselectivity, the mechanism of migratory insertion of styrene to the palladium–hydrogen bond was studied using the B3LYP method of density functional theory. In the absence of PPh_3 , chlorine ligand was found to decrease substantially the stability of the intermediate carbonyl complex compared to the bromide analogue.

The Pd(OAc)_2 –acid promoter– $[\text{Bu}_4\text{N}]\text{Br}$ catalytic system was found to be suitable for the production of higher fatty acids from aliphatic olefins [19, 21]. The reactivity of the substrates decreased as the number of substituents at the double bond increased. In the reaction of dodecene-1, the application of an excess of phosphine ligands was found to be beneficial [21]. Although conversion decreased, the presence of phosphines could completely suppress the migration of the double bond in the olefin and lowered the yield of the corresponding isomeric acids. As an additional advantage, the linear/branched ratio also increased.

An efficient recycling of the $\text{PdCl}_2(\text{PPh}_3)_2$ – TsOH – $[\text{Bu}_4\text{N}]\text{Br}$ mixture was achieved, with only a small loss of activity or selectivity to acids [18]. In the hydroxycarbonylation of dodecene-1, it was demonstrated that the activity of the catalyst could be sustained with the addition of another portion of TsOH after the sixth run, to compensate the gradual washout of the acidic promoter from the reaction mixture [21].

2.3 Aminocarbonylation

Aminocarbonylation of alkynes with various primary and secondary amines was shown to proceed efficiently in $[\text{BMIM}][\text{NTf}_2]$ under mild conditions (13.8 bar, 110°C). The reaction was regioselective, affording α -methylene amides (**6**, Scheme 4) in good yields. In this IL, even catalyst recycling was performed without any significant loss of activity after five runs. The use of $[\text{BMIM}][\text{PF}_6]$ led to lower conversion and in $[\text{BMIM}][\text{BF}_4]$ the product was obtained only in traces. The choice of the palladium precursor was also a crucial point: both $\text{Pd}(\text{CH}_3\text{CN})_2\text{Cl}_2$ and $\text{Pd(OAc)}_2/\text{PPh}_3$ demonstrated poor catalytic activity, but in the presence of $\text{Pd(OAc)}_2/\text{DPPP}$ (DPPP: 1,3-bis(diphenylphosphino)propane), terminal alkynes with diverse structure could be converted to acrylamides efficiently. Carbonylation of internal alkynes was less facile [23].



Scheme 5 Carbonylation of aryl halides

3 Carbonylation of Aryl or Alkenyl Halides

When aromatic halides are treated with an appropriate nucleophile in a carbon monoxide atmosphere in the presence of a catalytic amount of a palladium complex, the leaving group is formally replaced by the nucleophile with incorporation of one or two molecules of carbon monoxide (Scheme 5) [24–27]. In ILs, carbonylations were carried out in the presence of both phosphine-free palladium catalysts and phosphine–palladium complexes. In the latter case a high P/Pd ratio had to be used to perform efficient catalyst recycling. In most reactions, relatively high CO pressures (above 5 bar) were used, resulting in the formation of a considerable amount of double carbonylated products, especially in aminocarbonylation reactions. Phosphonium ILs were found to be especially suitable solvents that made it possible to carry out carbonylations under mild conditions leading to selective monocarbonylation.

3.1 Alkoxy carbonylation

The first examples for palladium-catalysed mono- and double carbonylation of aryl halides in ILs were reported by Tanaka in 2001 [28]. A considerable enhancement in the rate of alkoxy carbonylation of bromobenzene was observed in [BMIM][BF₄] and [BMIM][PF₆] compared to the reactions carried out using the alcohol reagent as solvent. Even *tert*-butyl alcohol, which participates reluctantly in the carbonylation reaction, gave the corresponding ester in an acceptable yield. The use of the IL solvent seemed to suppress double carbonylation. Under 29 bar CO pressure, selective monocarbonylation took place, and the ketoester products were formed only in 5–6% even at elevated pressure (147 bar). An efficient recycling of the catalyst could be achieved only by the increase of the PPh₃/Pd(OAc)₂ ratio from 4 to 20, and the IL–catalyst mixture exhibited catalytic activity even in the seventh run (25% yield). At low PPh₃/Pd ratio, the formation of metallic palladium was observed both in alcohol or IL solvents.

The water-soluble Pd–TPPTS (TPPTS: triphenylphosphine-3,3',3''-trisulphonic acid trisodium salt) complex was effective in alkoxy carbonylation of iodobenzene in [BMIM][OTf] and [BMIM][BF₄] [29]. At 150°C and 30 bar CO pressure, TOFs as high as 1938 and 1660 h⁻¹ were achieved, respectively. Although the catalyst showed similar activity in dioxane or THF, the use of ILs made it possible to

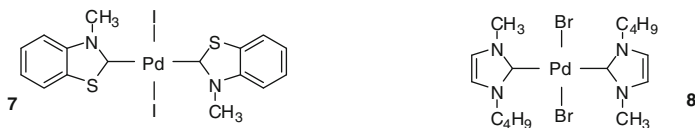


Fig. 2 Palladium–carbene catalysts used in the alkoxy-carbonylation of aryl halides

recover and recycle the catalyst. Only a small loss of activity was observed during the first ten runs. Optimal results were obtained with catalysts with a P/Pd ratio of 4. Lower concentrations of TPPTS led to the formation of inactive palladium black, whilst at higher P/Pd ratios catalytic activity decreased, probably due to the coordination of TPPTS that led to the formation of stable complexes.

Butoxycarbonylation of aryl halides was carried out in $[\text{Bu}_4\text{N}]\text{Br}$ melt in the presence of a Pd–benzothiazole carbene catalyst (**7**, Fig. 2) developed by Calò et al. [30]. Iodobenzene could be carbonylated efficiently at atmospheric pressure, whilst for other substrates (4-bromoacetophenone, bromobenzene) the use of somewhat higher pressure (8 bar) and the addition of phosphine ligands were necessary to obtain optimal results. The palladium–carbene catalyst could be recycled and only a small loss of activity was observed after six runs.

The presence of $[\text{Bu}_4\text{N}]\text{Br}$ was shown to exert a beneficial effect on the carbonylation of bromobenzene even in the presence of an organic solvent. This phenomenon was attributed to the stabilisation of the 14-electron, underligated $\text{L}_2\text{Pd}(0)$ complex, obtained by the reduction of **7**, in the form of a stable and catalytically active 16-electron complex $[\text{L}_2\text{PdBr}]^- [\text{R}_4\text{N}]^+$. This assumption is supported by the fact that ILs with poorly coordinating anions, such as $[\text{OTf}]^-$ or $[\text{BF}_4]^-$, were proved to be unsuitable solvents for the carbonylation. Also, the activating effect of other halides, changing in the order: $\text{Cl}^- \sim \text{I}^- < \text{Br}^-$, was explained by the different coordinating power of the anions. The I^- ion is less coordinating than the Br^- , whilst Cl^- is too coordinating towards palladium, and slows down the successive CO insertion process. ILs with imidazolium cations were proved to be less effective than ammonium salts. It was assumed that the planar $[\text{BMIM}]^+$ cation, by binding the anion tightly, rendered the latter less available for palladium and hindered the formation of $[\text{L}_2\text{PdBr}]^-$.

A catalyst stabilisation and rate enhancing effect of $[\text{Bu}_4\text{N}]\text{Cl}$ was reported by Trzeciak in methoxycarbonylation of iodobenzene [31]. According to ^1H NMR investigations of $\text{PdCl}_2(\text{COD})$ and $[\text{Bu}_4\text{N}]\text{Cl}$ mixtures, a partial removal of cyclooctadiene from the coordination sphere of palladium was observed in the presence of increasing amounts of the ammonium salt. It was proposed that $[\text{Bu}_4\text{N}]\text{Cl}$ participated in the reaction only as an agent facilitating breaking of Pd–C bonds. In the molten salt, ionic palladium complexes were thought to be stabilised by electrostatic interactions of cationic $[\text{Pd}_2\text{Cl}_2(\text{COD})_2]^{2+}$, $[\text{Bu}_4\text{N}]^+$ and anionic $[\text{PdCl}_4]^{2-}$, X^- species. In contrast to $[\text{Bu}_4\text{N}]\text{Cl}$, $[\text{BMIM}]\text{Cl}$ was shown to have an inhibiting effect on carbonylation.

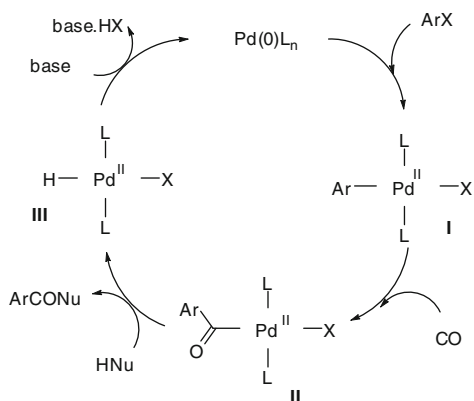
Another explanation for the high activity of these systems can be the reduction of $\text{PdCl}_2(\text{COD})$ to colloidal $\text{Pd}(0)$ under carbonylation conditions [32]. Tetrabutylammonium salts can stabilise the Pd colloid by a double layer of ions surrounding the metal colloid crystallite, which prevents aggregation and inactivation. XRD studies of the reaction mixture have indeed revealed the presence of $\text{Pd}(0)$ nanoparticles. The assumption that these nanoparticles were responsible for the catalytic activity was supported by the fact that $\text{PdCl}_2(\text{COD})$ and a preformed Pd/PVP (PVP: *N*-polyvinylpyrrolidone) colloid exerted similar catalytic activity in molten salts as reaction media.

Not only molten salts with tetraalkylammonium ions, but also pyridinium ILs were shown to increase the yield of ester products in methoxycarbonylations carried out in the presence of preformed Pd colloids [33]. The best results were obtained with catalytic systems with $[\text{Bu}_4\text{N}]\text{X}$ ($\text{X} = \text{Cl}, \text{Br}, \text{I}$). However, during the recycling experiments, a more significant decrease in the catalytic activity was observed here than in the reactions carried out in pyridinium ILs. Imidazolium type ILs with non-coordinating anions gave only slightly worse results. On the contrary, [BMIM] halides were found to inhibit the reaction, probably via formation of stable carbenes in the presence of $[\text{BMIM}]^+$ on the surface of the Pd colloid.

This assumption was supported by several observations [34]. (1) A preformed palladium–carbene catalyst **8** (Fig. 2) presented much lower activity in methoxycarbonylation than other precursors, such as $\text{PdCl}_2(\text{COD})$, $\text{PdCl}_2(\text{P}(\text{OPh})_3)_2$, or complexes obtained by the reaction of $\text{PdCl}_2(\text{COD})$ with [BMIM]Cl or [BMPY]Cl (Fig. 1). (2) The presence of [BMIM]Cl was shown to result in the decomposition of aryl–palladium complexes (**I**, Scheme 6), intermediates in carbonylation reactions, using both phosphine-free systems and complexes with phosphite ligands. (3) No inhibiting effect of imidazolium halides with C-2 methyl group (such as [BDMIM], Fig. 1) was observed.

In the report of McNulty [35], phosphonium salts (e.g. [THTdP]Br, Fig. 1) were shown to be highly effective solvents in alkoxy carbonylation of aryl iodides/bromides and vinyl bromides. The reactions could be carried out under mild conditions (1 bar CO, 60°C) and good or acceptable yields were obtained even using secondary or tertiary alcohols as nucleophiles. The most striking feature was the superiority of the bromide-containing medium over ILs with other anions. It was assumed that the great difference of the results obtained in ILs with chloride and bromide anions was not consistent simply with the involvement of an anionic $[\text{L}_2\text{PdX}]^-$ species. Control experiments carried out in the absence of a nucleophile showed the presence of carboxylic acid bromides possibly formed from acyl–palladium complexes (**II**, Scheme 6). So in the presence of an excess of bromide ions, another path involving $\text{ArC}(\text{O})\text{Br}$ intermediates, alternative to the generally accepted catalytic cycle, might be operating.

Scheme 6 General mechanism for the carbonylation of aryl halides

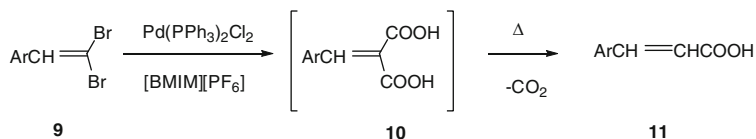


3.2 Hydroxycarbonylation

Hydroxycarbonylations of iodobenzene and bromobenzene were carried out by Hayashi et al. in ionic liquid media ([BMIM][PF₆], [BMIM][BF₄] and [CH₃(C₈H₁₇)₃N]Cl) under conditions similar to alkoxy carbonylation [28], but using water as the nucleophile [36]. Exceptionally high catalytic activity was observed in [BMIM][PF₆]. As this IL is not miscible with water, the catalyst–IL mixture could be recycled, after separation of the product by aqueous extraction. The problem concerning the accumulation of triethylammonium salt in the catalytic system that hindered catalyst reuse in alkoxy carbonylation [28, 30] was solved here, as the salt of Et₃N could be removed together with the product at the end of each run. As a result, the activity of the catalyst species was sustainable to allow recycling several times without a significant decrease in the yield. The reaction of bromobenzene in [BMIM][PF₆] catalysed by a higher amount of palladium acetate also allowed recycling but chlorobenzene could not be converted at all under similar conditions.

The use of a phosphonium salt as reaction medium made it possible to carry out hydroxycarbonylation of aryl and vinyl bromides under mild conditions (1 bar CO, 60°C) in the presence of a Pd(OAc)₂/DPPF catalytic system [35].

Isomeric vinyl bromides (*E/Z* ≥ 5:1) were carbonylated in good yields to the corresponding α,β -unsaturated carboxylic acids with excellent *E/Z* stereoselectivity (up to 99:1) in [BMIM][PF₆] under 10 bar of CO in the presence of 3 mol% Pd(PPh₃)₄ [37]. When PdCl₂(PPh₃)₂ was used as precursor, the IL–catalyst mixture could be recycled, but the reactions had to be carried out under harsher conditions (20 bar of CO, 5 mol% catalyst, at 100°C). The yields were higher in the second and third runs than that in the first run with better *E/Z* molar ratios. A side reaction of self-coupling of the substrates was also observed under these conditions. Vinyl dibromides (**9**, Scheme 7) afforded only monoacids **11**. It was supposed that the substrates were initially carbonylated to the corresponding diacids **10** that were easily decarboxylated under the relatively harsh conditions, to form the monoacids **11** in modest stereoselectivity.



Scheme 7 Hydroxycarbonylation of vinyl dibromides (**9**)

Arylacetic acids were obtained starting from benzyl chloride derivatives in the presence of 1–2 mol% PdCl₂(PPh₃)₂, with NaOH as the base instead of Et₃N [36]. However, a greater drop in product yields was observed in recycling experiments than in the reactions of aryl halides. The carbonylation was not completely selective and some side-products, such as benzyl alcohol (by hydrolysis) and toluene (by reduction with some metal hydride generated through possible water–gas shift reaction), were formed simultaneously.

Similarly to alkoxy-carbonylations, a beneficial effect of the use of tetrabutylammonium salts was observed during hydroxycarbonylation of benzyl halides [38]. Interestingly, the order of efficiency of various molten salts and ionic liquids as reaction medium was somewhat different ([NBu₄]Cl ≫ [NBu₄]Br > [NBu₄]I > [BMIM]Cl > [BMIM]Br ≫ [BMIM][PF₆] ~ [BMIM][BF₄]) from that observed during alkoxy-carbonylation [33] of aryl halides. The reactions were carried out under phosphine-free conditions and, as another advantage, in the absence of a base. Similar to the results of Hayashi [36], carbonylation of benzyl chloride and its reduction to toluene were found to be competing reactions. Upon pressure decrease from 50 to 5 bar, carbonylation was suppressed whilst toluene formation increased.

3.3 Aminocarbonylation

The first example for aminocarbonylation in ILs was reported by Tanaka [28]. Iodobenzene was converted into a mixture of mono- and double carbonylated products (see Scheme 5) in [BMIM][BF₄] and [BMIM][PF₆] solvents in the presence of Pd(OAc)₂/4PPh₃. Contrary to the alkoxy-carbonylation reactions, the use of ILs did not alter the selectivity of the reaction. At 40 bar CO pressure double carbonylation was the prevailing reaction, and the α-ketoamide was obtained with 58% selectivity even at 5 bar. As another difference, at lower pressure the use of ILs resulted in lower conversion, compared to the reaction carried out in the amine nucleophile as solvent. The catalyst/IL mixture could be recycled only if a fresh supplement of 4 equiv. of PPh₃, relative to Pd, was added in each cycle.

Carboxamides could be prepared in good yields in ILs even at atmospheric CO pressure starting from steroidal alkenyl iodides and secondary amines [39]. The use of ILs with non-coordinating anions ([BF₄][−] or [PF₆][−]) was essential, the presence of imidazolium halides destroyed catalytic activity rapidly. [Bu₄N]Br was a suitable solvent but its solubility properties made impossible product separation via

extraction. High activity of palladium catalysts with either PPh_3 or DPPBA (DPPBA: 4-(diphenylphosphino)-benzoic acid) ligands was observed. The use of the water-soluble ligand, TPPTS, led to lower conversions.

The efficiency of catalyst recovery and recycling depended greatly on the choice of the phosphine ligand. In the case of catalysts with PPh_3 , a considerable loss of both Pd and phosphine was observed. The $\text{Pd}(\text{OAc})_2/\text{DPPBA}$ system was proved to be a highly efficient catalyst with no leaching of the phosphine upon recycling. This also means that completely phosphane-free products could be obtained by simple extraction. In order to avoid the formation of inactive palladium–carbonyl complexes and drop of activity upon reuse, carbonylations had to be carried out in the presence of catalysts with relatively high P/Pd ratio (6 for PPh_3 and 10 for DPPBA both in $[\text{BMIM}][\text{BF}_4]$ and in $[\text{BMIM}][\text{PF}_6]$ solvents). It should be mentioned that a further increase in the P/Pd ratio led to a decrease in the yield of the product. Under optimal conditions, 94% conversion could be achieved after the fifth run in $[\text{BMIM}][\text{BF}_4]$ that turned out to be a more suitable solvent than $[\text{BMIM}][\text{PF}_6]$.

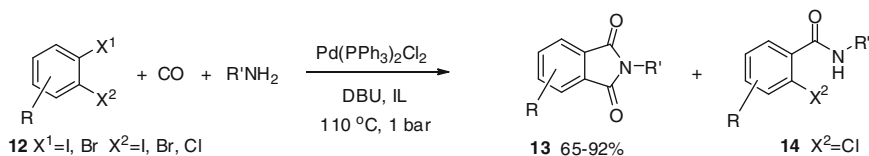
At the same time, the results show that the catalyst/IL systems should be fine-tuned for each particular aminocarbonylation reaction when using nucleophiles of diverse structure. The replacement of the amine nucleophile by an amino acid ester was shown to affect strongly the outcome of the reactions [40–43]. In recycling experiments, satisfactory results were achieved even in the presence of the $\text{Pd}(\text{OAc})_2 + 2\text{PPh}_3$ system, used normally in conventional solvents. $[\text{BMIM}][\text{PF}_6]$ turned out to be a superior reaction medium compared to $[\text{BMIM}][\text{BF}_4]$. Besides, optimal results in $[\text{BMIM}][\text{PF}_6]$ were obtained with catalysts with P/Pd = 4 ratio using either PPh_3 or DPPBA as the phosphine ligand.

Whilst carboxamides were found as single products during carbonylation of iodo-alkenes, the formation of α -ketoamides, via double carbon monoxide insertion, was favoured with iodo-arenes especially at higher CO pressure [41].

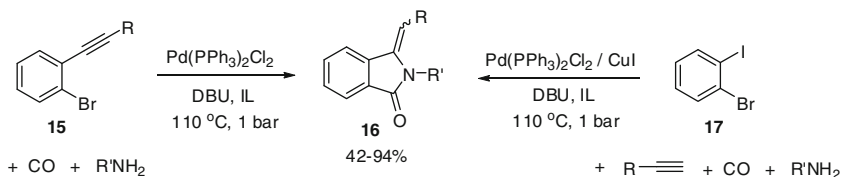
A low pressure microflow system was developed by Fukuyama and Ryu [44] for palladium-catalysed multiphase carbonylation reactions in an IL. Carrying out the reactions at various CO pressures (20 and 15 bar), the yields of α -ketoamides were higher in the case of the microflow system than in a batch reaction. The superior efficiency of the microflow reactor was attributed to the occurrence of an alternate liquid (IL + substrate)–gas (CO) plug flow that provided a large specific interfacial area between the CO and the liquid phase and facilitated the diffusion of CO into the thin IL plugs.

Aryl bromides were carbonylated efficiently using Et_2NH as the nucleophile in phosphonium ILs. In the presence of $\text{Pd}(\text{OAc})_2/\text{DPPF}$, excellent results were obtained under mild conditions (1 bar, 60°C) affording the amide products in 81–85% yield in 6–8 h [35].

Preformed Pd-nanoparticles stabilised by the phosphonium IL $[\text{TBTdP}][\text{DBS}]$ (Fig. 1) were used for the aminocarbonylation of various aryl halides [45]. Both electron-rich and electron-poor aryl iodides were successfully transformed into the corresponding amides in moderate to high yields under 12 bar CO pressure, at 130°C in the presence of K_2CO_3 as the base. In most cases, the catalytic activity in $[\text{TBTdP}][\text{DBS}]$ was higher compared to imidazolium-based ILs. The recycled catalyst demonstrated sustained activity. After five runs, TEM and XPS studies of



Scheme 8 Carbonylation of dihaloarenes (**12**)



Scheme 9 Synthesis of 3-methyleneisoindolin-1-ones (**16**)

the nano-Pd(0) catalyst demonstrated that both particle size and oxidation state of palladium have essentially remained unchanged. In the phosphonium ionic liquid, displaying increased stability towards thermal and chemical degradation, aminocarbonylation of less reactive substrates such as aryl chlorides and bromides could be carried out, to generate the corresponding amides in 25–47% and 50–77% yields, respectively. In these reactions, a strong base (KOTBu) and a relatively high temperature (150°C) were employed to enhance catalyst activity. Based on mercury poisoning tests, the authors excluded the possibility of residual homogeneous palladium catalyst initiating the aminocarbonylation reaction.

A similar ionic liquid, [THTdP]Br (Fig. 1), was shown to be an efficient medium for the synthesis of phthalimides (**13**, Scheme 8) from different dihaloarenes (**12**) [46]. Under optimised reaction conditions, a wide variety of amines reacted readily with dibromobenzene affording good yields of products **13**. Both bromo- and iodoarenes with different substituents could be used as substrates. At the same time, the reaction of 1-bromo-2-chlorobenzene and allylamine afforded only the monocarbonylated product (**14**, R' = C₃H₅), in 77% yield after 24 h.

Under the same reaction conditions, 1-halo-2-alkynylbenzenes (**15**, Scheme 9) were converted to substituted 3-methyleneisoindolin-1-ones (**16**) via a carbonylation–intramolecular hydroamination reaction sequence [47]. The results revealed that the bromide-containing media showed the greatest efficiency, ILs with [NTf₂][−] and [PF₆][−] anions were not effective. Both aromatic and the aliphatic amines showed good reactivity, and consistently provided the (*Z*)-isomer of **16** as the main product. *tert*-Butylamine afforded lower yields of the target products (41%), possibly because of the bulkiness of the *tert*-butyl group.

The 3-methyleneisoindolin-1-ones (**16**) could also be synthesised by the one-pot Sonogashira coupling–carbonylation–hydroamination reaction of **17**, alkynes and amines, in the presence of the PdCl₂(PPh₃)₂/CuI/DBU catalyst system.

Photo-induced atom transfer carbonylation (ATC) reactions of alkyl iodides and amines to produce amides were also carried out using ILs, such as [BMIM][PF₆] and [BMIM][NTf₂], as reaction media in the presence of a catalytic amount of a Pd–carbene complex [48].

3.4 Thiocarbonylation

Alper reported the first examples for palladium-catalysed thiocarbonylation of aryl iodides with thiols in phosphonium ionic liquids [49]. ILs consisting of the [THTdP]⁺ cation with a range of common anions were screened for the carbonylation reaction of iodobenzene and thiophenol. ILs with Br[−], [NTf₂][−] and [PF₆][−] anions gave uniformly good results, but the use of the latter IL enabled easier separation of the product. Pd(OAc)₂/4PPh₃ was the most effective catalyst system for the formation of the corresponding thioester in 91% yield at 100°C and 14 bar CO pressure. Under similar conditions, a great variety of aryl iodides were converted to the products using both aromatic and aliphatic thiols as reaction partners.

4 Concluding Remarks

As the above examples show, the use of ILs serves as a promising methodology to improve carbonylation reactions. ILs enhance catalytic activity, stabilise catalytic species, make catalyst recycling and product separation easier. However, a lot more research remains to be done. Just to mention a few topics: the possibility of fine-tuning the IL structure has not been exploited to its full extent. Despite the efforts made until now, the nature of the catalytically active species and the effect of ILs on their structure are not entirely understood in most reactions. In the case of alkenes, the development of the enantioselective version of carbonylation is a great challenge, too.

References

1. Grigg R, Mutton SP (2010) Pd-catalysed carbonylations: versatile technology for discovery and process chemists. *Tetrahedron* 66:5515–5548
2. Kollár L (2008) *Modern carbonylation methods*. Wiley, Weinheim
3. Liu S, Xiao J (2007) Toward green catalytic synthesis—transition metal-catalyzed reactions in non-conventional media. *J Mol Catal A* 270:1–43
4. Ohlin C A, Dyson P J, Laurenczy G (2004) Carbon monoxide solubility in ionic liquids: determination, predictions and relevance to hydroformylation. *Chem Commun* 1070–1071
5. Consorti CS, Dupont J (2008) Catalytic carbonylations in ionic liquids. In: Kollár L (ed) *Modern carbonylation methods*. Wiley, Weinheim

6. Petz A, Kollár L (2010) Activation of 'small molecules' by P-ligand – platinum metal complexes in ionic liquids. *Curr Org Chem* 14:1185–1194
7. Zim D, de Souza RF, Dupont J, Monteiro AL (1998) Regioselective synthesis of 2-arylpropionic esters by palladium-catalyzed hydroesterification of styrene derivatives in molten salt media. *Tetrahedron Lett* 39:7071–7074
8. Brennführer A, Neumann H, Beller M (2009) Palladium-catalyzed carbonylation reactions of alkenes and alkynes. *ChemCatChem* 1:28–41
9. de Pater JJM, Deelman BJ, Elsevier CJ, van Koten G (2006) Multiphase systems for the recycling of alkoxy carbonylation catalysts. *Adv Synth Catal* 348:1447–1458
10. Klingshirn MA, Rogers RD, Shaughnessy KH (2005) Palladium-catalyzed hydroesterification of styrene derivatives in the presence of ionic liquids. *J Organomet Chem* 690:3620–3626
11. Rangits G, Kollár L (2005) Palladium-catalysed hydroalkoxycarbonylation of styrene in [BMIM][BF₄] and [BMIM][PF₆] ionic liquids. *J Mol Catal A* 242:156–160
12. Rangits G, Kollár L (2006) Palladium catalysed hydrothoxycarbonylation in imidazolium-based ionic liquids. *J Mol Catal A* 246:59–64
13. Balázs A, Benedek C, Törös S (2006) Application of molten salts in hydroalkoxycarbonylation of styrene. *J Mol Catal A* 244:105–109
14. Yang J, Zhou H, Lu X, Yuan Y (2010) Brønsted acidic ionic liquid as an efficient and recyclable promoter for hydroesterification of olefins catalyzed by a triphenylphosphine–palladium complex. *Catal Commun* 11:1200–1204
15. Osichow A, Mecking S (2010) Alkoxy carbonylation of ethylene with cellulose in ionic liquids. *Chem Commun* 46(4980):4981
16. Consorti CS, Ebeling G, Dupont J (2002) Carbonylation of alkynols catalyzed by Pd(II)/2-PyPPh₂ dissolved in organic solvents and in ionic liquids: a facile entry to α -methylene γ - and δ -lactones. *Tetrahedron Lett* 43:753–755
17. Cao H, Xiao WJ, Alper H (2007) Dramatic effects of ionic liquids on the palladium-catalyzed cyclocarbonylation of enynols with thiols. *J Org Chem* 72:8562–8564
18. Lapidus AL, Eliseev OL, Stepin NN, Bondarenko TN (2004) Carboxylation of styrene in the N(C₄H₉)₄Br–heptane system. *Russ Chem Bull* 53:2564–2567
19. Lapidus AL, Eliseev OL (2010) Catalytic carbonylation in ionic liquids. *Sol Fuel Chem* 44:197–202
20. Lapidus A, Eliseev O, Bondarenko T, Stepin N (2006) Palladium catalysed hydroxycarbonylation of 1-phenylethanol in molten salt media. *J Mol Catal A* 252:245–251
21. Lapidus AL, Eliseev OL, Bondarenko TN, Chaub NH (2010) Manufacture of C₁₃ higher fatty acids from their esters by carbonylation of dodecene-1 in ionic liquid medium. *Petrol Chem* 50:442–449
22. Lapidus AL, Eliseev OL, Zvyagintsev NV, Kondrat'ev LT (2011) Regioselectivity of styrene carbonylation in the presence of palladium(II) complexes. *Russ J Phys Chem A* 85:786–791
23. Li Y, Alper H, Yu Z (2006) Palladium-catalyzed regioselective aminocarbonylation of alkynes in the ionic liquid [bmim][Tf₂N]. *Org Lett* 8:5199–5201
24. Skoda-Földes R, Kollár L (2002) Synthetic applications of palladium catalysed carbonylation of organic halides. *Curr Org Chem* 6:1097–1119
25. Boyarskii VP (2008) Catalytic systems for carbonylation of aryl halides. *Russ J Gen Chem* 78:1742–1753
26. Barnard CFJ (2008) Palladium-catalyzed carbonylations – a reaction come of age. *Organometallics* 27:5402–5422
27. Brennführer A, Neumann H, Beller M (2009) Palladium-catalyzed carbonylation reactions of aryl halides and related compounds. *Angew Chem Int Ed* 48:4114–4133
28. Mizushima E, Hayashi T, Tanaka M (2001) Palladium-catalysed carbonylation of aryl halides in ionic liquid media: high catalyst stability and significant rate-enhancement in alkoxy carbonylation. *Green Chem* 3:76–79
29. Lin Q, Yang C, Jiang W, Chen H, Li X (2007) Carbonylation of iodobenzene catalyzed by water-soluble palladium–phosphine complexes in ionic liquid. *J Mol Catal A* 264:17–21

30. Calò V, Giannoccaro P, Nacci A, Monopoli A (2002) Pd-benzothiazole carbene catalyzed carbonylation of aryl halides in ionic liquids. *J Organomet Chem* 645:152–157
31. Trzeciak A M, Wojtków W, Ziółkowski JJ (2003) Catalytic activity of palladium complexes, PdCl₂(COD) and PdCl₂(P(OPh)₃)₂, in methoxycarbonylation of iodobenzene. *Inorg Chem Commun* 6:823–826
32. Trzeciak AM, Ziółkowski JJ (2005) Structural and mechanistic studies of Pd-catalyzed C C bond formation: the case of carbonylation and Heck reaction. *Coord Chem Rev* 249:2308–2322
33. Wojtków W, Trzeciak AM, Choukroun R, Pellegatta JL (2004) Pd colloid-catalyzed methoxycarbonylation of iodobenzene in ionic liquids. *J Mol Catal A* 224:81–86
34. Zawartka W, Trzeciak AM, Ziółkowski JJ, Lis T, Ciunik Z, Pernak J (2006) Methoxycarbonylation of iodobenzene in ionic liquids. A case of inhibiting effect of imidazolium halides. *Adv Synth Catal* 348:1689–1698
35. McNulty J, Nair JJ, Robertson A (2007) Efficient carbonylation reactions in phosphonium salt ionic liquids: anionic effects. *Org Lett* 9:4575–4578
36. Mizushima E, Hayashi T, Tanaka M (2004) Environmentally benign carbonylation reaction: palladium-catalyzed hydroxycarbonylation of aryl halides and benzyl chloride derivatives in ionic liquid media. *Top Catal* 29:163–166
37. Zhao X, Alper H, Yu Z (2006) Stereoselective hydroxycarbonylation of vinyl bromides to α , β -unsaturated carboxylic acids in the ionic liquid [BMIM]PF₆. *J Org Chem* 71:3988–3990
38. Lapidus AL, Eliseev OL, Bondarenko TN, Chau NH, Kazantsev RV (2009) Exceptionally simple catalytic system for the carbonylation of benzyl halides. *Mendeleev Commun* 19:256–257
39. Skoda-Földes R, Takács E, Horváth J, Tuba Z, Kollár L (2003) Palladium-catalysed aminocarbonylation of steroidal 17-iodo-androst-16-ene derivatives in *N, N'*-dialkyl-imidazolium-type ionic liquids. *Green Chem* 5:643–645
40. Müller E, Péczely G, Skoda-Földes R, Takács E, Kokotos G, Bellis E, Kollár L (2005) Homogeneous catalytic aminocarbonylation of iodoalkenes and iodobenzene with amino acid esters under conventional conditions and in ionic liquids. *Tetrahedron* 61:797–802
41. Takács E, Skoda-Földes R, Ács P, Müller E, Kokotos G, Kollár L (2006) Prolinates as secondary amines in aminocarbonylation: synthesis of *N*-acylated prolينات. *Lett Org Chem* 3:62–67
42. Skoda-Földes R (2007) Palladium-catalysed aminocarbonylation of 17-iodo-5 α -androst-16-ene with L-amino acid esters in ionic liquids. *React Kinet Catal Lett* 90:159–165
43. Takács E, Skoda-Földes R (2009) Investigation of the effect of the ligand/palladium ratio on the catalytic activity of reusable palladium/phosphine/ionic liquid systems in aminocarbonylation of 17-iodo-androst-16-ene with amino acid ester nucleophiles. *Lett Org Chem* 6:448–452
44. Rahman MT, Fukuyama T, Kamata N, Sato M, Ryu I (2006) Low pressure Pd-catalyzed carbonylation in an ionic liquid using a multiphase microflow system. *Chem Commun* 2236–2238
45. Zhu Y, Chuazhao L, Biying AO, Sudarmadji M, Chen A, Tuan DT, Seayad AM (2011) Stabilized well-dispersed Pd(0) nanoparticles for aminocarbonylation of aryl halides. *Dalton Trans* 40:9320–9325
46. Cao H, Alper H (2010) Palladium-catalyzed double carbonylation reactions of o-dihaloarenes with amines in phosphonium salt ionic liquids. *Org Lett* 12:4126–4129
47. Cao H, McNamee L, Alper H (2008) Syntheses of substituted 3-methyleneisindolin-1-ones by a palladium-catalyzed Sonogashira coupling-carbonylation-hydroamination sequence in phosphonium salt-based ionic liquids. *Org Lett* 10:5281–5284
48. Fukuyama T, Inouye T, Ryu I (2007) Atom transfer carbonylation using ionic liquids as reaction media. *J Organomet Chem* 692:685–690
49. Cao H, McNamee L, Alper H (2008) Palladium-catalyzed thiocarbonylation of iodoarenes with thiols in phosphonium salt ionic liquids. *J Org Chem* 73:3530–3534

Metal-Catalyzed Oxidation of C–X (X = S, O) in Ionic Liquids

Andreia A. Rosatella and Carlos A.M. Afonso

Abstract Ionic liquids (ILs) have attracted the scientific community due to several advantages compared with traditional solvents such as their low volatility and high ability to dissolve different organic and inorganic compounds, among other advantages. Transition metals can be toxic compounds; however, this issue can be minimized when used in catalytic amounts which also allows reaction efficiency and selectivity increases. The combination of metal catalysis with the use of ILs can be a powerful tool for several organic reactions, taking advantage of the most attractive property of the ILs, which is the possibility of an easier recycling of the catalytic system, increasing the greenness of the process. The application of ILs in metal-catalyzed oxidation reactions of alcohols and sulfides is discussed in this chapter.

Keywords Alcohols · Green chemistry · Ionic liquids · Oxidation · Sulfides

Contents

1	Introduction	164
2	Oxidation of Sulfides	164
3	Oxidation of Alcohols	174
4	Conclusions	182
	References	182

1 Introduction

Oxidation reactions are an important subject in organic synthesis. Different metals have been reported as catalyst for this type of reaction, but in some cases still a stoichiometric amount of the metal is necessary for higher efficiency of the reaction. It is a challenge to developed greener catalytic oxidation reactions, where the oxidant gives no waste as by-product(s), the catalyst is used in a small amount and can be reused, reaction conditions near room temperature and atmospheric pressure and the solvent can be reused, and ideally can be biodegradable. Ionic liquids (ILs) have attracted the scientific community due to several advantages compared with traditional solvents, such as their low volatility and high ability to dissolve different organic and inorganic compounds, among other advantages [1]. Although several advantages can be attributed to these new solvents, other important issues have to be taken into account, for example their toxicity and biodegradability. After using the IL, it is necessary the remediation of the wastes that can became a problem, since the majority of the reported ILs are not biodegradable, or their toxicity is not well known. The viscosity of the IL can also be a problem, since these solvents can have high viscosities at room temperature. But this problem can be minimized by the fact that the IL physical properties can be tuned by changing the cation and/or anion. In this chapter the oxidation of sulfones and alcohols in ILs is discussed. In Fig. 1 the structure of all cations and anions in the ILs described in this chapter is presented.

2 Oxidation of Sulfides

Sulfur-containing compounds (S-compounds) present in fuel can be converted into sulfur oxides (SO_x) during combustion of car engines. This can lead to serious environmental problems, such as acid rains and air pollution. On the other hand, SO_x can also reduce the efficiency of engine catalytic converters promoting the emissions of CO, NO_x , also with serious environmental outcome. To avoid this contamination, governments all over the world are reducing the limit of S-compounds present in diesel. In this way the production of ultra low sulfur diesel (ULSD) has become a major task for refineries. The most used process to reduce S-compounds from diesel is the hydrodesulfurization (HDS) that uses high temperatures and high pressures [2]. This method can remove S-compounds such as thiols and sulfides efficiently, but it is not so effective for more hindered ones such as dibenzothiophene (DBT), benzothiophene (BT), and their derivatives. For this reason different strategies for deep desulfurization have been developed, such as extraction adsorption, oxidation, and biodesulfurization [2]. The extraction process extractive desulfurization (EDS) was reported using polar solvents, such as dimethyl sulfoxide (DMSO), acetonitrile, and dimethylformamide (DMF), but the selectivity of the extraction is difficult to achieve, since diesel possesses different

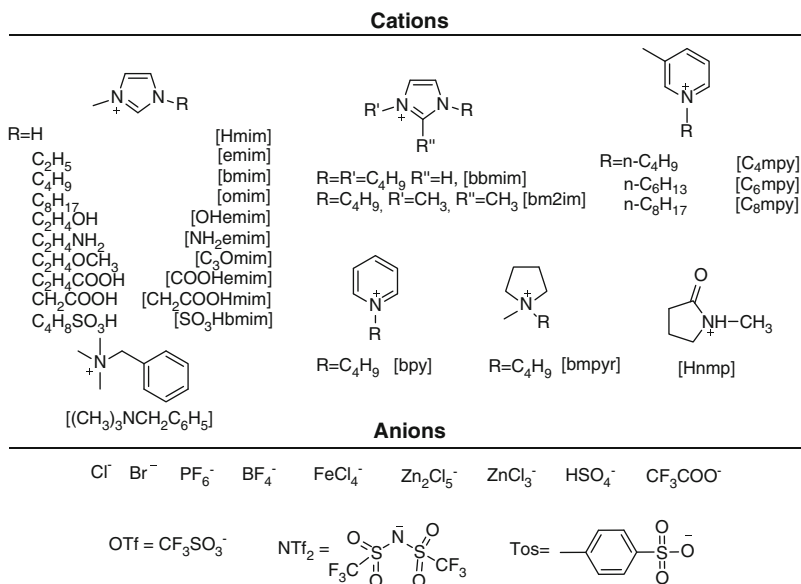


Fig. 1 Structure of all cations and anions present in the ILs described in this chapter

aromatic compounds with similar polarity [2]. In a way to avoid the use of volatile organic solvents and improve the extraction selectivity, ILs have been reported as efficient extractors of S-compounds from diesel. The use of ILs as extractors of S-compounds from diesel was first reported in 2001 [3], and since then different ILs were reported, including Fe- and Cu-containing ILs [4, 5]. Although good extraction values for aromatic S-compounds could be achieved, the selectivity is still an open issue, due to the cross-solubility of aromatic compounds present in diesel. In the search for ULSD, researchers have accomplished the extraction process with oxidation (extraction and oxidative desulfurization, EODS), where S-compounds are extracted to the IL phase and then are oxidized (Fig. 2). Since the S-compounds are consumed by oxidation, the equilibrium is displaced to the IL phase, increasing the extraction efficiency.

Taking advantage of the group experience in vanadium complexes, Correia et al. [6] characterized different vanadium complexes based on the structure VO (X-acac)₂ (where X = Cl, Me, or Et, Fig. 3) and tested their catalytic activity for the oxidation of sulfur compounds (S-compounds) from model oil (*n*-octane), at room temperature. Since vanadium complexes are soluble in different ILs, the authors tested the oxidation catalysis with ILs based on imidazolium and pyridinium cations, in combination with OTf, NTf₂, BF₄, and PF₆ anions. They observed that when ILs based on NTf₂ and PF₆ (least coordinating anions) were used, the catalytic activity for the oxidation was higher. The best O/S ratio [O-oxidant (H₂O₂), S-sulfur compounds] obtained in this study was 4, when DBT, 4, 6-DMDBT, and BT were used as substrates. The highest conversion values

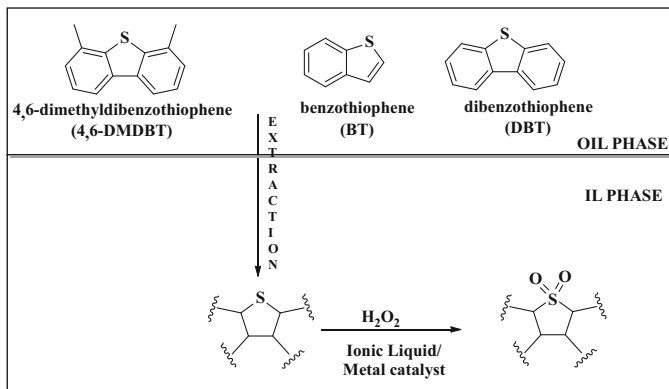


Fig. 2 General scheme for the EODS process, using ILs as extractors for S-compounds from model oil, H_2O_2 as oxidant, and different metals as catalysts

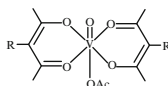


Fig. 3 Vanadium-based catalyst used for the oxidation of S-compounds (catalyst 1: $\text{R} = \text{H}$, 2: $\text{R} = \text{Cl}$, 3: $\text{R} = \text{CH}_3$, 4: $\text{R} = \text{CH}_2\text{CH}_3$)

obtained in 2 h of reaction, using $[\text{bmim}]\text{NTf}_2$, were 96% – DBT, 92% – 4,6-DMDBT, and 100% – BT. The authors emphasized that the use of this type of catalysts in more environmental friendly ILs could be an attractive alternative to the HDS method.

In 2009 was reported the EODS using V_2O_5 as catalyst for the oxidation step in combination with different ILs [7]. The ILs water immiscible $[\text{omim}]\text{BF}_4$, $[\text{bmim}]\text{PF}_6$, and $[\text{omim}]\text{PF}_6$ were less efficient than the water miscible $[\text{bmim}]\text{BF}_4$, which maybe due to the formation of triphasic systems. In the optimized conditions $[\text{IL}/\text{oil} = 1:5$ (volume ratio), $\text{DBT}/\text{catalyst} = 20$ (molar ratio), $\text{O}/\text{S} = 6$ (molar ratio)], at 30°C for 4 h, it was possible to remove 98.7% of DBT from the model oil (*n*-octane), and the IL/catalyst phase could be recycled seven times without loss of activity. Different aromatic S-compounds were also tested, and under optimized conditions was possible to remove 98.7%, 79.4%, and 40.4% of DBT, BT, and 4,6-DMDBT, respectively. The authors justify the less efficient removal of 4,6-DMDBT by the highest steric hindrance of the compound. The proposed mechanism involves peroxovanadium $\text{VO}(\text{O}_2)^{2-}$ as the active species in the oxidation reaction transferring the active oxygen to the S atom.

In the same year (2009) the oxidation and extraction of DBT from model oil (*n*-octane) using ZnCl_2 -based ILs was reported [8]. ILs based on $[(\text{CH}_3)_3\text{NCH}_2\text{C}_6\text{H}_5]\text{Cl}$ in combination with different proportions of ZnCl_2 were tested, and the authors concluded that the extraction efficiency depends on the Lewis acidity and viscosity of the IL. They observed that the extraction ability

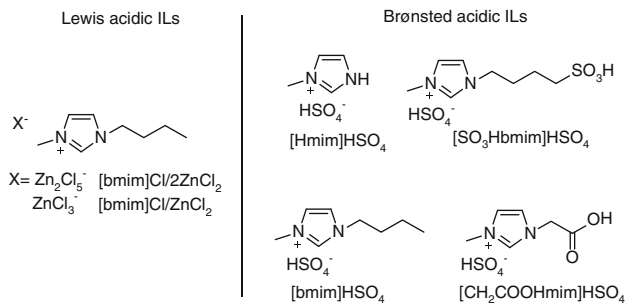


Fig. 4 Lewis and Brønsted acidic ILs used for the EODS process, reported by Chen and his group [10]

increases with the increase in Lewis acidity and the decrease in viscosity. In this way the authors have chosen [(CH₃)₃NCH₂C₆H₅]Cl·2ZnCl₂ as the best IL studied. After the process optimization, the best extraction efficiency was observed for an IL/oil ratio of 1:5 and O/S ratio of 6. Under these conditions, at 30°C for 30 min, it was possible to extract 94% of the S-compounds present on the model oil (*n*-octane). It was also possible to recycle the IL six times without a significant decrease in activity. The extraction mechanism was proposed based on literature results [9] that showed the importance of the pi-complexation between the lone pair electrons on organosulfur compounds and the unoccupied orbital on transition metal ions. After extraction, the oxidation reaction occurs in the IL phase, where H₂O₂ and acetic acid are present, forming the peracetic acid (CH₃COOOH) that the authors claim to be the active oxidant of the reaction.

Chen and his group have reported Zn-based ILs as extractant and catalyst for the EODS process [10]. Lewis and Brønsted acidic ILs (Fig. 4) were tested as extractors and also as catalysts for the EODS process using H₂O₂ as oxidant. The authors claim that the IL acidity strongly influence the extraction and catalyst activity, being the most efficient [bmim]Cl/2ZnCl₂ and [bmim]HSO₄. It was also observed that besides the anion effect, the cation is also an important issue for the extraction efficiency. The optimization of the process was performed by testing different temperatures, O/S, and IL/oil ratios. The results have shown that for higher temperatures compiled with longer reaction times, the oxidant (H₂O₂) degradation enlarges, decreasing the efficiency of the process. The optimal temperatures observed were: 90°C for [bmim]Cl/2ZnCl₂ and 60°C for [bmim]HSO₄. Although the EODS process is sensitive to small changes in the O/S ratio, the same does not happen with IL/oil ratio, since the increase of oil phase from 1 to 5 the extraction efficiency variation is less than 10%. It was possible to recycle the two ILs for at least six times without loss of efficiency. The decrease in the extraction efficiency on the next cycles can be due to the accumulation of oxidative product in the IL phase. To extract these products from the IL, it was re-extracted with tetrachloromethane, and the final products were isolated. The authors tested this process with real commercial diesel fuel and also coke diesel fuel (with higher S-content), and observed that the EODS was less effective than with the model diesel. Furthermore

the S-content extracted from the coke diesel fuel was much lower than the one extracted from the commercial diesel fuel. This means that this EODS process is less efficient for diesel with high S-content. The authors suggest a process where the oxidative extraction using this ILs could be applied after HDS treatment.

Yan et al. [11] reported the extraction and catalytic oxidative desulfurization process using ILs as extracting agents and different Fenton-like reagents such as CoCl_2 , CuCl_2 , NiCl_2 , MnCl_2 , CrCl_3 , and FeCl_3 as catalysts, using H_2O_2 as oxidant. The results showed that the extraction of DBT from model diesel (*n*-octane) with ILs was improved when H_2O_2 was added to the IL/oil system, nevertheless a better improvement was observed when a catalyst was added to the system (extractive catalytic oxidation desulfurization). All the catalysts tested showed extraction values lower than 50%, except for Fenton reagent ($\text{Fe}^{2+}/\text{H}_2\text{O}_2$) and Fenton-like reagent ($\text{Fe}^{3+}/\text{H}_2\text{O}_2$) that could remove up to 96% of the DBT from the model oil. Different ILs were tested, and the more hydrophobic ones formed three phases EODS system, although the biphasic systems were more efficient. In this way $[\text{bmim}]\text{BF}_4$, anhydrous FeCl_3 , and aqueous H_2O_2 were chosen for further EODS optimization. The optimum O/S molar ratio was 6:1, and the optimum temperature was 30°C, due to the decomposition of the oxidant at higher temperatures. The catalyst/DBT ratio was also studied, and if the catalyst excess is high it is possible that FeCl_3 promote the H_2O_2 decomposition, decreasing the efficiency of the DBT extraction. On the other hand, if the catalyst amount is too low, the extraction is also compromised, so it was chosen a 1:1 ratio of catalyst/DBT. Under these conditions and when H_2O_2 was added in four different batches during 4 h (to avoid the oxidant self-decomposition), the DBT extraction from the model oil could reach 99%. When different S-containing substrates were tested, the extraction efficiency was higher for DBT (DBT (96.1%) > BT (76.6%) > 4,6-DMDBT (32.6%)). The authors explained these results by the chemical hindrance, that is higher for 4,6-DMDBT, and also by the lower Nernst partition coefficient of 4,6-DMDBT in comparison with DBT and BT, being more difficult to extract this compound from the oil to the IL phase where the oxidation occurs. The IL/catalyst was recycled for at least five times without considerable loss of efficiency, although the authors reported that the accumulation of the oxidative products in the IL phase was responsible for the loss of efficiency in further cycles. The catalytic oxidation mechanism of DBT with Fenton-like reagent was explained by the authors due to the formation of hydroxyl radicals that are strong oxidants.

In the same year the same group reported the use of $[\text{bmim}]\text{Cl}/\text{FeCl}_3$ as efficient extractor/catalyst for the EODS process [12]. The authors observed that in the presence of anhydrous FeCl_3 and the oxidant (H_2O_2), the extraction of S-compounds (DBT) from the model diesel was only 55%, although when $[\text{bmim}]\text{Cl}$ was added to the system the extraction could reach 99%. The ILs $[\text{omim}]\text{Cl}/\text{FeCl}_3$ and $\text{Et}_3\text{NHCl}/\text{FeCl}_3$ were also tested. Although $[\text{omim}]\text{Cl}/\text{FeCl}_3$ provided higher extraction capability for EDS (68%) than $[\text{bmim}]\text{Cl}/\text{FeCl}_3$ (66%), when the oxidant was added (EODS process), this last IL could remove almost completely the DBT present in the model oil (99%) in comparison with the 87%

achieved with [omim]Cl/FeCl₃. The authors explained this difference by the steric hindrance of the alkyl chain interfering with the oxidation reaction. Under the optimized conditions (IL = [bmim]Cl/FeCl₃; oil/IL = 3 (mass ratio); O/S = 3 (molar ratio); temperature 30°C, for 10 min), it was possible to remove DBT, 4,6-DMDBT, and BT in 99.2%, 90.3%, and 75.9%, respectively, from the three different model oils. Actual diesel was also tested, and the extraction efficiency dropped to 71%. It was possible to recycle the IL at least six runs, although in the last one only 90% of DBT was extracted from the model oil. However when the oxidized compounds were removed from the IL after each cycle, it was possible to recycle the IL nine times with the efficiency drop from 99.2% to only 98.6%.

The same authors reported in 2012 a similar study of EODS using ILs based on the triethylammonium cation [13], in combination with metal salts: ZnCl₂, CoCl₂, SnCl₂, CrCl₃, and FeCl₃. These ILs were tested as catalysts and extractor solvents for the extraction of DBT from model oil (*n*-octane). The best extraction result was obtained for the IL [Et₃NHCl]FeCl₃ that under the optimized conditions (30°C, 5 min, O/S = 6, V(IL)/V(oil) = 2/5) could extract 97.1% of the model substrate. In this study the authors also tested different substrates and the extraction decreased in the order: DBT > BT > 4,6-DMDBT. A similar result was obtained in the previous work [11], although the EODS efficiency was improved, since the S-removal from the model oil was 82.5%, 86.9%, and 97.1% for DBT, BT, and 4,6-DMDBT, respectively. It was possible to recycle the IL for at least four times. To justify the loss of efficiency of the IL by the accumulation of the oxidized S-compounds in the IL phase, the authors have re-extracted the IL with tetrachloromethane after each cycle. In this way it was possible to recycle the IL for ten cycles, without loss of efficiency. No IL contamination was observed in the model oil after EODS. By this process it was possible to decrease the S-content of pre hydro-treated gasoline from 150 to 15 mg/L, although two rounds of reactions were required.

1-*n*-Butyl-3-methylimidazolium chloride in combination with different metal chloride salts (MCl₂) were reported as Lewis acidic ILs for the EDS and the EODS process [14]. When the metal was Zn, Fe, Sn, and Co, the EODS was more efficient than EDS, as expected, although for the metals Cu and Mg, the extraction results of EODS were lower than EDS. The authors explained this result by the addition of the oxidant (H₂O₂) on the IL phase which enforces DBT to return to the oil phase, and the possibility that these two ILs ([bmim]Cl/MgCl₂ and [bmim]Cl/CuCl₂) accelerate the oxidant degradation, reducing the oxidative power. In this way [bmim]Cl/ZnCl₂ was chosen to be the best IL to proceed with further optimization reactions. It was observed that the extraction efficiency increased with the Lewis acidity of the IL ([bmim]Cl/*x*ZnCl₂), being the best catalyst, the one with higher amount of ZnCl₂. The higher efficiency of [bmim]Cl/3ZnCl₂ was also explained by the formation of more complex anions such as Zn₂Cl₅⁻ and Zn₃Cl₇⁻, and the possibility to have ZnCl₂ in solution will improve somehow the oxidative reaction. The optimum conditions for this process were achieved using [bmim]Cl/3ZnCl₂ as catalyst and extractor, with a O/S ratio of 8 and IL/oil ratio of 1:2 (mass ratios), and reaction temperature of 45°C, for 3 h. Under these conditions it was possible to

extract 99.9% of DBT from the model oil (*n*-octane). The IL was recycled seven times without loss of efficiency, although after some cycles the oxidized S-compounds accumulated on the IL were re-extracted from the IL with tetrachloromethane and obtained as white solid. The experiment of the EODS with real diesel resulted in a much lower efficiency, even when the O/S ratio increases to 60, the extraction is 63.5%. After five runs of EODS, it was possible to remove 90.6% of the S-content in the real diesel.

Three different dialkyl-pyridinium tetrachloroferrate ILs were tested as extractors and catalyst for the EODS process [15]. The EDS results showed that the efficiency of S-removal from the model oil (*n*-octane) decreased in this order: $[\text{C}_8\text{mpy}]\text{FeCl}_4 > [\text{C}_6\text{mpy}]\text{FeCl}_4 > [\text{C}_4\text{mpy}]\text{FeCl}_4$. When the oxidant was added to the process, the effect of the cation alkyl chain almost disappears, and it was observed an S-removal of 100% with $[\text{C}_8\text{mpy}]\text{FeCl}_4$ and $[\text{C}_4\text{mpy}]\text{FeCl}_4$ after 20 min reaction. The authors denote that the EODS efficiency was determined by the catalysis of the Lewis acid anion. After optimization of the EODS process, it was possible to remove 100% of S-compounds from the model oil at 25°C for 30 min with a mass ratio of IL/oil 1:5 and O/S of 6. The authors also studied the S-content of the initial oil model (500 and 1,000 ppm of DBT in *n*-octane) and observed that at higher temperatures the initial S-content affected the S-extraction, but the same does not happen when the reaction was performed at room temperatures. It was observed that the IL/oil ratio did not affect the EODS performance, and after two cycles of recycling the IL the EODS efficiency decreased from 100% to 90%. The authors explained this result by the saturation of the IL with the oxidized S-compounds, which could be re-extracted from the IL with tetrachloromethane.

Different Brønsted acidic ILs based on pyrrolidonium and imidazolium cations were tested for the EODS of thiophene in model oil (*n*-octane), being the best $[\text{Hnmp}]\text{BF}_4$ (*N*-methyl-pyrrolidonium tetrafluoroborate), that could extract 99.4% in the optimal conditions (Fig. 5) [16]. Commercial catalysts based on tungsten, vanadium, and molybdenum were tested, and tungsten catalysts could remove higher amount of thiophene from the model oil, especially ammonium tungstate. The authors justify this result by the formation of peroxy-species derived by the catalyst and the oxidant. Aromatic sulfur-containing compounds are the most difficult to remove from real diesel, and thus the authors have tested the oxidation of thiophene and derivatives (Table 1). It was observed that the oxidation product of thiophene (1,2-dioxide) was unstable, and consequent reactions lead to benzaldehyde, benzoic acid, and sulfuric acid. When the substitution of thiophene was increased, the stability of the oxidized product also increased, being possible their isolation. Using ammonium tungstate in a ratio of 25 (sulfur/catalyst), $[\text{Hnmp}]\text{BF}_4$ as solvent, for a reaction time of 5 h, at 60°C, with a molar ratio of O/S of 10, it was possible to completely remove each substrate from the model oil (experiments were done with six different model oils for each substrate). Based on $^1\text{H-NMR}$, FT-IR, and electrochemical studies, it was demonstrated that the thiophene aromaticity decreases when this is dissolved in the $[\text{Hnmp}]\text{BF}_4$, due to polarization induced by the IL, and also by the hydrogen bonding present between the substrate and the IL.

Fig. 5 Structure of the ILs used for the EODS of thiophene and derivatives

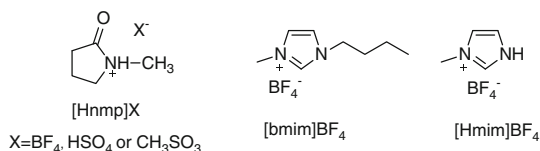


Table 1 Reaction conditions: temperature = 60°C, 20 mL model oil of thiophene in *n*-octane, [Hnmp]BF₄ (4 g), ammonium tungstate as catalyst, S/W = 25 (molar ratio), O/S = 10 (molar ratio, oxidant H₂O₂)

Substrate	Product	Conversion (%)	Yield (%)
		93.5	87.6
		92.5	90.3
		98.2	96.5

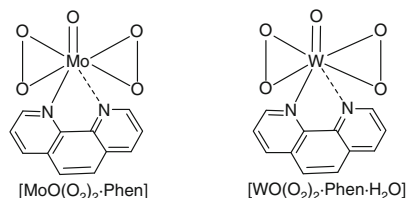
The authors claimed that this distortion on the thiophene structure favors the oxidation reaction catalyzed by the ammonium tungstate.

In 2001 it was reported the use of a halogen-free IL ([SO₃Hbmim]Tos) in the EODS process using Na₂WO₄ as catalyst [17]. DBT dissolved in *n*-tetradecane was used as model oil. Although the extraction efficiency increased with the temperature, the EODS optimal temperature was determined taking into account that aromatic compounds (such as toluene) can be oxidized at temperatures over 50°C in the same oxidative conditions, thus the temperature chosen for further studies was 50°C. In the optimal conditions, it was possible to remove 99.4% of DBT from the model oil, and it was possible to recycle the IL with the catalyst, for at least five times, without loss of efficiency, and without the need to re-extract the oxidized S-compounds. The authors proposed a mechanism involving the formation of unstable peroxytungstate species that are somehow stabilized in the IL and have the capability to oxidize the extracted DBT in the IL phase.

Using [bmim]BF₄ as extracting agent, Song et al. [18] reported the use of polyoxometals (POMs) as catalysts for the EODS process. Different POMs were tested, being Na₇H₂EuW₁₀O₃₆ (EuW₁₀) and Na₇H₂LaW₁₀O₃₆ (LaW₁₀) capable of removing 100% of DBT in less than 12 min, at 70°C. The optimized conditions for EODS were: molar ratio of H₂O₂/DBT/LaW₁₀, 500:100:5 at 30°C, for 25 min. It was possible to recycle the IL/catalyst for at least ten times without significant loss of extractive efficiency. After that, the oxidized S-compounds were re-extracted with chloroform from the IL, and the FT-IR spectrum of the recycled [bmim]BF₄ showed no changes from the freshly IL. An interesting result that the authors didn't tested would be another round of recycling cycles using the recycled IL/catalyst.

The combination of two catalysts based on molybdenum and tungsten with different ILs was studied for the EODS process (Fig. 6) [19]. Similar results were

Fig. 6 Reported catalysts for the EODS process, using [bmim]BF₄ as extractor



obtained with ILs [omim] and [bmim] with both anions PF₆ and BF₄ (93–98.6% extraction for EODS process). It was interesting to observe that [omim]BF₄ was more efficient for EDS process than [bmim]BF₄, although when the catalyst/oxidant is added, [bmim]BF₄ could remove a higher amount of S-compounds from the model oil than [omim]BF₄. In the optimized conditions (IL = [bmim]BF₄; DBT/catalyst = 25 (molar ratio); O/S = 10 (molar ratio); oil/IL = 5:2 (volume ratio); at 70°C, for 3 h) it was possible to extract 98.6% and 93% with [WO(O₂)₂-Phen·H₂O] and [MoO(O₂)₂-Phen], respectively. It was possible to recycle the catalyst/IL five times with the two catalysts with a slight decrease in the catalytic activity.

Peroxophosphomolybdates based on three different cations (Q₃(PO₄[MoO(O₂)₂]₄) (Q = [(C₄H₉)₄N], [C₁₄H₂₉N(CH₃)₃], and [C₁₆H₃₃NC₅H₅])) with different alkyl chains were tested as catalyst for the EODS in combination with different ILs [20]. The results have shown that the best catalyst was the peroxophosphomolybdates with the shorter alkyl chain ([[(C₄H₉)₄N]₃PO₄[MoO(O₂)₂]₄), although in the absence of the IL the most efficient catalyst was the longer chain. This result is explained by the steric hindrance of the long alkyl chain that prevents the access of the catalytic active species to the sulfur atom in the IL. Different ILs were tested under the optimized conditions (Table 2), being the best [bmim]BF₄ that could remove up to 97% of DBT from the model oil (*n*-octane). Different substrates were tested, and the order of reactivity in the EODS system was DBT > 4,6-DMDBT > BT (45.8, 90.2, and 98.8, respectively). It was possible to recycle the catalytic system for four runs, with the efficient decrease of 97.3–95.9%.

The same ILs were studied for the EODS process using as catalysts different commercially available molybdic and tungstic compounds [21, 46]. When molybdic salts were used [21] the best catalytic system was obtained with the combination [bmim]BF₄ and Na₂MoO₄ (Table 2) although very good DBT extraction (92.6–99.0%) was also possible to obtain with the other Mo-species catalysts tested. When other substrates were tested, the reactivity order in the EODS system was DBT > 4,6-DMDBT > BT, as reported in the previous work [20]. It was also possible to recycle the catalytic system five times, with a decrease in efficiency from 99% to 90%, which maybe due to the accumulation of the oxidized S-compounds retained in the IL phase. The authors also observed that Mo catalysts could be leached into the oil phase during the EODS process, leading to the loss of activity of the catalytic system during the recycling runs.

A similar study was performed using alkylammonium decatungstate as catalysts [22]. From the different catalyst tested ([[(CH₃)₄N]₄W₁₀O₃₂, [(C₂H₅)₃N(C₇H₇)₄W₁₀O₃₂,

Table 2 EODS process using different ILs

Ionic liquid	Sulfur removal (%) ^a	Sulfur removal (%) ^b	Sulfur removal (%) ^c	
	[(C ₄ H ₉) ₄ N] ₃ PO ₄ [MoO(O ₂) ₂] ₄	Na ₂ MoO ₄	H ₃ PW ₁₂ O ₄₀	
[bmim]BF ₄	97.3	99.0	98.2	Biphasic system
[omim]BF ₄	83.2	67.6	64.7	Triphasic system
[bmim]PF ₆	90.7	69.8	98.0	Triphasic system
[omim]PF ₆	94.5	77.8	63.5	Triphasic system
[omim]CF ₃ COO	67.6	37.4	–	Biphasic system

^a[(C₄H₉)₄N]₃[PO₄[MoO(O₂)₂]₄] as catalyst, reaction conditions: oil/IL = 5 (volume ratio); O/S/catalyst = 200:100:1; at 70°C for 3 h [20]

^bNa₂MoO₄ as catalyst, reaction conditions: oil/IL = 5 (volume ratio); O/S = 4; S/catalyst = 20; at 70°C for 3 h [21]

^cH₃PW₁₂O₄₀·14H₂O as catalyst, reaction conditions: oil/IL = 5 (volume ratio); O/S/catalyst = 300:100:1 (molar ratio); at 30°C for 1 h [46]

and [(C₄H₉)₄N]₄W₁₀O₃₂), the tetrabutylammonium decatungstate [(C₄H₉)₄N]₄W₁₀O₃₂ was chosen as the best catalyst for the oxidation step, using [bmim]PF₆ as extractor solvent for the EODS process. Therefore starting from 1000 ppm of DBT dissolved in the model oil it was possible to extract 98% of DBT (reaction conditions: 60°C, for 0.5 h, O/S = 3 (molar rate); S/catalyst = 100 (molar rate)). It was possible to recycle the catalytic system for six cycles, although in the last run the extraction efficiency was only 83%, and longer reaction time was needed (1 h). The authors reported that 0.7% of the catalyst was leached into the oil phase.

Important values must be considered in the EODS process, such as the ratios IL/oil and oxidant/S-compounds (O/S), temperature, and time reaction. The volume ratio of the IL vs. model oil (IL/oil ratio) used indicates the extraction efficiency, lower this rate, more efficient is the extraction. The usual oxidant in this process is the aqueous H₂O₂, considered environment friendly since the only by-product is water. Usually the S-removal efficiency increases when the O/S molar ratio also increases, although when the amount of the oxidant is too high, the IL phase can be diluted losing some extraction capability, thus decreasing the S-removal efficiency [10, 14]. On the other hand, stoichiometrically 2 mol of oxidant is consumed per mol of S-compound (when S-compounds are oxidized to sulfones), although 2:1 molar ratio O/S is not sufficient to achieve a good EODS efficiency. This result is justified by the self-destruction of the oxidant in the different reaction conditions, thus a molar ratio O/S higher than 2 is always required [20]. The H₂O₂ self-destruction is also a determinant effect in the reaction temperature selection. Usually the efficiency of EODS increases with the temperature, although when H₂O₂ is used this effect is only observed for short time reaction, and after a period of time the efficiency starts to decrease, due to the degradation of the oxidant [7]. On the other hand, if the temperature is too low, the viscosity of the IL determines the EODS efficiency [8]. The choice of the catalyst is also important, and several Lewis acids were tested for the oxidation step of the EODS. When iron is used, the formation of a Fenton-like reagent is possible, forming hydroxyl radicals that are strong oxidizers.

In this case it is possible that the metal ions can also consume hydroxyl radicals increasing the H_2O_2 degradation [15, 23].

Besides very efficient methods reported for the oxidation of more demanding substrates such as 4,6-DMDBT, DBT, and BT by different catalysts immobilized in ILs and using H_2O_2 as oxidant, the overall process of desulfurization of diesel still requires more combined feasible methods for the removal of the oxidized products from the system (IL or diesel).

3 Oxidation of Alcohols

The oxidation of alcohols to the correspondent ketone, aldehyde, or carboxylic acid is a fundamental transformation in organic chemistry, since carbonyl groups are essential constituents of chemical platform, pharmaceuticals, and other important chemicals. In this section the oxidation of alcohols using ILs in combination with metal catalysts will be discussed.

In 2007 [24] the oxidation of *sec*-alcohols using as catalyst copper(II) acetylacetonate ($\text{Cu}(\text{acac})_2$, Fig. 7, catalyst 1) was reported. Four different ILs were tested as solvents ($[\text{bmim}]\text{PF}_6$, $[\text{bmim}]\text{BF}_4$, $[\text{emim}]\text{CF}_3\text{COO}$, and $[\text{bpy}]\text{PF}_6$), and it was observed that when ILs based on PF_6 anions were used, the reaction rate was faster than with BF_4 -based ILs. Imidazolium-based ILs were also better for this reaction than pyridinium ones. Therefore $[\text{bmim}]\text{PF}_6$ was chosen as solvent for further reaction optimization. In the optimized conditions, using *t*-BuOOH as oxidant, different substrates were tested. Good yields were obtained for aromatic alcohols (91–94%), although aliphatic alcohols were converted in moderate yields (58–66%). It was possible to recycle the IL/catalyst system for at least five times, although the efficiency dropped from 91% to 84% in the last run. These reactions were performed at room temperature for 5 h, although the same group have reported [25] that the reaction time could be improved when a different catalyst/IL system was used (Fig. 7). The oxidation of primary and secondary alcohols (into acids and ketones, respectively) was reported, using an amino acid Schiff base copper ligand catalyst (Fig. 7, catalyst 2). The efficiency of this new catalyst could be improved when $[\text{bmim}]\text{BF}_4$ was used as solvent. Other oxidants were also tested, such H_2O_2 and NaClO , but the results demonstrated that *t*-BuOOH showed to be optimal for this reaction system. The results obtained for secondary alcohols were similar as the one obtained in the previous work [24], although in reduced reaction time. This oxidation system was also not so efficient for aliphatic alcohols (30–63% yields). The catalytic system could be recycled at least five times, with an yield of 83% in the last cycle.

The continuation of research for greener oxidation of alcohols in ILs by metal catalysts was reported in 2012 by Han group [26]. The authors used salicylic amino acid Schiff base manganese ligand as catalyst (Fig. 7, catalyst 3), and H_2O_2 was shown to be the best oxidant, when $[\text{bmim}]\text{BF}_4$ was used as a solvent. After optimization, different substrates were tested. Good yields were obtained for

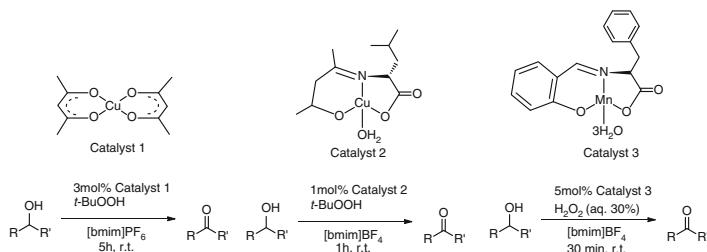
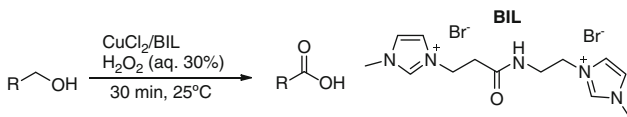


Fig. 7 Catalysts and reaction conditions reported by Han group (catalyst 1 [24], catalyst 2 [25], catalyst 3 [26])

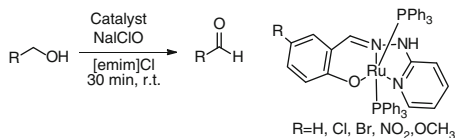
aromatic alcohols (88–94% yield), although for aliphatic alcohols the reaction system was not so effective (48–62% yield). The catalytic system could be recycled at least four times with a drop of efficiency from 94% yield to 82% in the last run.

With the purpose of direct oxidation of aliphatic and aromatic primary alcohols to carboxylic acids, Kumar et al. [27] reported a novel catalytic system based on CuCl_2 and a bifunctional IL (Scheme 1). The ILs [COOHemim]Br and [NH₂emim]Br were tested in combination with CuCl_2 leading to no reaction, or the formation of the respective aldehyde, in the presence or absence of additional organic solvents. The optimized conditions were achieved when CuCl_2/BIL was used as catalyst, and H_2O_2 as oxidant, at room temperature (Scheme 1). Good to very good yields (88–99%) were achieved for aromatic alcohols with reaction times near 30 min. The authors observed that when electron-donating groups were present in the aromatic nucleus, the reaction was accelerated, although when electron-withdrawing groups were present the reaction was retarded. The oxidation of aliphatic alcohols required longer reaction time (near 4 h), but yields over 84% could be achieved. It was possible to recycle the catalyst for five runs without any significant loss of catalytic activity (99–91% yields in the last run). The chemoselectivity of this reaction was studied, when benzyl alcohol and 1-octanol were allowed to react in the presence of CuCl_2/BIL catalyst. Benzoic acid was formed in 78% yield and 1-octanoic acid in 22% yield. The authors explained this result by the higher acidity of the α -CH unit in the benzyl alcohol.

In 2011 [28] the synthesis of different ruthenium triphenylphosphine complexes containing *N*-(2-pyridyl)-*N'*-(5-sub-salicylidene) hydrazine (Scheme 2) was reported. These catalysts were used for the oxidation of primary and secondary alcohols, to the correspondent aldehyde and ketone, respectively. Five different catalyst were tested ($\text{R} = \text{H}, \text{Cl}, \text{Br}, \text{NO}_2, \text{OCH}_3$, Scheme 2), and similar oxidation yields were obtained for the five catalyst, although the authors observed that catalytic activity slightly decreases with increase in bulkiness of the substituents, due to steric hindrance. When [emim]Cl was used as solvent, and NaClO as oxidant, it was possible to obtain yields over 86% for aromatic and allylic primary alcohols. Good yields (over 70%) were also obtained for aliphatic primary alcohols. The IL/catalyst system was recycled seven times, but the catalytic efficiency decreased during the recycle runs, from 90% to 80% yield. As active specie of



Scheme 1 Reaction conditions and catalyst structure for the oxidation of aliphatic and aromatic primary alcohols

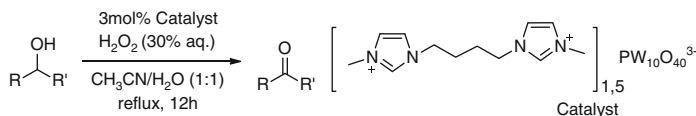


Scheme 2 Ruthenium(II)-based complexes as catalyst for the oxidation of primary alcohols, using [emim]Cl as solvent and NaClO as oxidant

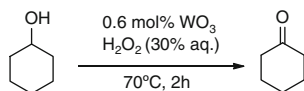
the catalytic oxidation, the authors proposed the valent ruthenium-oxo species formed by the oxidant (NaClO).

Using RuCl_3 as catalyst, Dullius et al. [29] have reported the oxidation of several alcohols using [bmim] BF_4 as solvent. It was observed that the selectivity of cyclohexanol oxidation was increased to 100% when the IL was used as solvent, instead of toluene. In the optimized conditions (1 mol% of RuCl_3 , 100°C and 7 atm of oxygen) different fluorinated ILs were tested, although no improvement in the reaction efficiency was achieved. It should be noted that [bmim] PF_6 was not stable under reaction conditions. It was possible to obtain up to 80% yield for the oxidation of aliphatic *sec*-alcohols, but lower yield was obtained for primary aromatic alcohols (<47%). This catalytic system was not efficient for allylic alcohols that didn't react. Although the catalytic system RuCl_3 /[bmim] BF_4 could be reused, the authors didn't refer the number of cycles possible.

An heterogeneous system was reported using a hybrid catalyst involving dicationic IL and W-containing heteropolyanion, based on tungsten-bearing Keggin-structured heteropolyacids (Scheme 3) [30]. Using this catalyst in combination with different polar solvents, including DMSO, acetonitrile, and water, resulted in moderate conversions. Although when a mixture of acetonitrile/water (1:1) was used, the best conversion and selectivity were obtained (benzyl alcohol conversion and selectivity, 92.3% and 98.2%, respectively). The oxidation of benzyl alcohol in this liquid–solid heterogeneous system resulted the formation of an insoluble product that was easily isolated from the reaction medium. In these conditions the authors also tested catalysts bearing different mono-cations, based on imidazolium, pyridinium, and ammonium salts that resulted in a homogeneous catalysis, although with good conversion and selectivity. The authors excluded these catalysts due to the difficulty of recovering the catalyst from the reaction system. Cyclohexanol, 1-phenylethyl alcohol, benzhydrol, and 1-octanol were tested as substrates providing high conversion and selectivity results, except for 1-octanol that was only possible to obtain 7.4% conversion. The catalyst was reused



Scheme 3 Oxidation of alcohols using an hybrid catalyst involving dicationic IL and W-containing heteropolyanion



Scheme 4 Oxidation of cyclohexanol using as catalyst tungsten oxide

for at least six runs although with a small loss of catalytic activity, since the conversion drop from 92% to 84% in the last run. The decrease observed in the catalyst activity may be due to some leaching of the catalyst observed in the first run, when fresh catalyst was used.

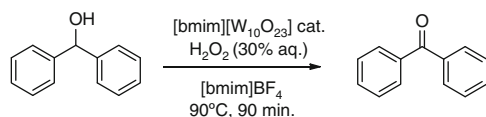
The oxidation of cyclohexanol to cyclohexanone was studied in 2011 by Sundmacher et al. [31] using tungsten oxide as catalyst and H_2O_2 as oxidant (Scheme 4). The authors compared the efficiency of the oxidation between organic solvents and ILs. Traditional polar solvents resulted in conversions under 50%, although ILs (based on imidazolium cation and chloride as anion) resulted in conversions over 70%. A study was made based on the theory of COSMO-RS, which demonstrated that solvents polarities can be ordered as acetone, 2-propanol, methanol, and [HOemim]Cl, being the last the most polar one. This study justified the order of reactivity for the tested solvents, being the most polar, the most efficient. ILs with different alkyl chains were also tested, and it was observed that lipophilic ILs (higher chain) were the most efficient ones, and in the case of [omim]Cl it was possible to achieve 100% conversion with 100% of selectivity to cyclohexanone. Although it is a good result, no further substrates were tested by the authors under these conditions. Later, the same group has reported the oxidation of different aromatic alcohols to the respective aldehydes, using tungsten oxide and H_2O_2 as oxidant; however, in this work toluene was used as co-solvent in combination with [omim]Cl [32]. After an optimization, where different ILs and organic solvents were tested, it was possible to achieve good conversions for different aromatic alcohols (Table 3).

Kumar et al. [33] have studied the oxidation of biphenyl carbinol to benzophenone, in ILs. Initially sodium tungstate and sodium molybdate were tested as catalyst, using [bmim]BF₄ as solvent, although only 34% and 40% yield, respectively, were achieved. The authors explained this result by the low solubility of the inorganic salts in the IL, and also the known effect of ammonium salts to affect the catalytic activity of these salts [33]. In order to increase the reaction efficiency, the authors developed a new catalyst where sodium was replaced by another cation. 1-methyl-3-butylimidazolium decatungstate [bmim]₄[W₁₀O₂₃] was slightly soluble

Table 3 Oxidation of several aromatic alcohols, using tungsten oxide as catalyst, in a toluene/[omim]Cl mixture

Substrate	Product	Time (h)	Conversion	Selectivity
		6	100	98
		12	96	95
		12	95	94
		10	94	93
		6	94	96
		12	92	92

Reaction conditions: aromatic alcohol (1 g), hydrogen peroxide (30 wt.%, 2 g), ILs (0.2 g)/toluene (10 g), and tungsten oxide (0.01 g) were mixed for a period of time, at 90°C

**Scheme 5** Biphenyl carbinol oxidation, using [bmim]BF₄ as solvent and [bmim][W₁₀O₂₃] as catalyst

in the IL [bmim]BF₄, but with the addition of the oxidant (aq. H₂O₂), only one phase was observed, which maybe due to the formation of peroxometalate complex [33]. Under the optimized conditions (Scheme 5), it was possible to oxidize biphenyl carbinol to benzophenone in 96% yield, and recycle the catalytic system for at least five cycles. Different substrates were tested, and this oxidation method was shown to be efficient for secondary aliphatic alcohols, but not to aliphatic primary alcohols, where no reaction occurs. To illustrate this selectivity the authors tested the method to the substrate 1-phenyl-1,2-diethanol and was obtained phenylhydroxymethyl ketone as major product (92% yield). Aromatic primary alcohols resulted in the respective aldehyde with very good yields (up to 96% yield).

Also in 2005 a similar work was reported, in which the catalyst was based on phosphotungstate complex (Fig. 8) [34]. The oxidation reaction was performed in [bmim]BF₄, at 90°C, for different reaction times (2–4 h). Different secondary alcohols were tested with good yields (86–98% yield). For benzyl alcohol it was possible to stop the oxidation in the respective aldehyde when only 2 equiv. of H₂O₂ was added for 8 h. In addition, the corresponding acid was formed when higher amount of H₂O₂ was added (4 equiv.), and larger reaction time was used.

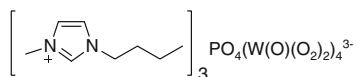
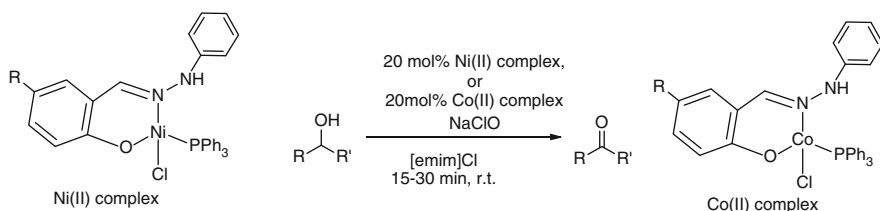


Fig. 8 Structure of the tungstate-based catalyst (tris(imidazolium)-tetrakis (diperoxotungsto) phosphate (3[−])) reported for the oxidation of alcohols



Scheme 6 Oxidation of alcohols using [emim]Cl as solvent, NaClO as oxidant, and catalysts based on Ni(II)[36] and Co(II) [35] complexes

In 2010 the use of catalysts based on nickel and cobalt for oxidation of alcohols was reported (Scheme 6) [35, 36]. For Ni(II) or Co(II) complexes it was observed that the catalytic activity decreased with increase in bulkiness of the substituents. It was observed that good yields could be obtained at room temperature. Under optimized conditions different substrates were tested (primary and secondary, aromatic and aliphatic alcohols). When Ni(II) complexes were used, it was possible to obtain good to very good yields (60–96%). With Co(II) complexes as catalysts was also possible to oxidize all the tested substrates in good to very good yields (71–94%).

Methyltrioxorhenium (MTO) is a well-known catalyst used in several oxidation reactions [37]. In a way to improve the immobilization of MTO in ILs, Saladino et al. [38] reported the synthesis of catalysts based on the heterogenization of MTO on poly(4-vinylpyridine) and poly(4-vinylpyridine N-oxide) (Fig. 9). The oxidation of alcohols and hydrocarbons was tested, using H₂O₂ as oxidant in [bmim]PF₆. For the alcohols biphenyl carbinol and 1-phenylethanol, similar results were obtained when MTO and the other catalysts were used (Scheme 7). The authors observed that MTO was not entirely retained in the IL, being loss during the recycling experiences, although it was possible to recycle the catalyst V with similar selectivity and reactivity.

Using Mn (salen) as catalyst and PhI(OAc)₂ as oxidant (Scheme 8), Li et al. [39] reported the oxidation of several secondary alcohols. The authors observed that oxidation reaction was faster when the IL [bmim]PF₆ was used as solvent in combination with dichloromethane as co-solvent. The yield of aromatic alcohols was good (88–99% yields), although aliphatic alcohols resulted in very low yields (24–59% yields). Primary alcohols were also tested under the reaction conditions, and depending on the substrate it was possible to obtain the respective acid or aldehyde in moderate yields (22–60% yields). It was possible to recycle the catalytic

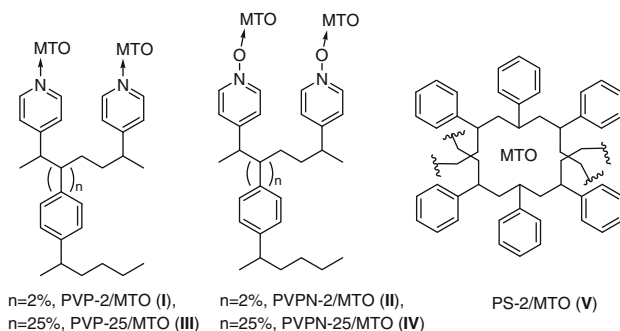
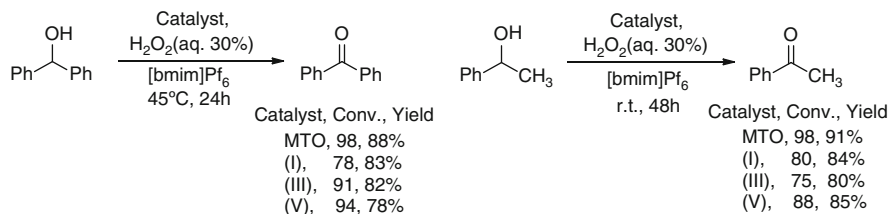
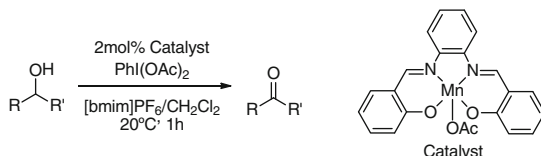


Fig. 9 Structure of the catalysts based on the heterogenization of MTO on poly(4-vinylpyridine) and poly(4-vinylpyridine N-oxide)



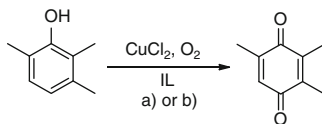
Scheme 7 Reaction conditions for the oxidation of alcohols with different catalysts



Scheme 8 Reaction conditions for the oxidation of alcohols, using Mn(salen) as catalyst

system five times, although with some decrease in the activity (from 99% to ~80% yield in the last run).

Trimethyl-1,4-benzoquinone (TMBQ) is an important intermediate for the production of vitamin E. TMBQ is obtained from the oxidation of 2,3,6-trimethylphenol (TMP), in a two-steps reaction (*para*-sulfonation of TMP followed by oxidation of MnO_2). The search for more efficient one-step oxidation of TMP to TMBQ has been investigated. In 2004 the use of ILs in this oxidation reaction was reported [40]. Sun et al. reported the use of catalytic amounts of CuCl_2 in $[\text{bmim}]\text{Cl}$ using *n*-butanol as co-solvent and molecular oxygen as oxidant. Under these conditions it was possible to obtain 100% conversion, with 94% selectivity for the desired product. The authors also isolated the catalytic active species as red cubic crystals in which the X-ray showed to be the 1-*n*-butyl-3-methylimidazolium oxotetracuprate. Further studies [41] have shown that ILs based on 1,3-dialkyl imidazolium chloride resulted in a better selectivity than $[\text{Hmim}]\text{Cl}$ (82% vs. 94% selectivity for $[\text{Hmim}]\text{Cl}$ and $[\text{bmim}]$



Scheme 9 Oxidation of 2,3,6-trimethylphenol, using ILs as solvents and CuCl_2 as catalyst. Reaction conditions: (a) $[\text{bmim}]\text{Cl}/\text{CuCl}_2$ (1:1), 2 mL of *n*-BuOH, 10 bar O_2 , at 60°C for 5 h [40, 41] and (b) $[\text{bmim}]\text{BF}_4/\text{CuCl}_2$ (5:1), O_2 , at 80°C , for 1 h [44]

Cl, respectively). No significant effect was observed for ILs based on 1-*H*-3-alkylpyridinium chloride and 1-alkyl-3-alkylpyridinium chloride; although the observed selectivity with pyridinium ILs was lower than imidazolium-based ILs. Different copper salts were tested as catalyst and was observed that chloride salts are more active than bromide, acetate, or nitrate. The authors claimed that the chloride ion has an important role in the oxidation mechanism. On the other hand, copper(II) chloride was more active than copper(I) chloride, and no significant difference was observed when anhydrous copper(II) chloride was used. In 1989 have been reported that nitrogen compounds can enhance the catalytic activity of copper(II) chloride [42, 43], so the authors have tested other N-containing compounds instead of ILs. For 1-methyl-imidazole the selectivity decreased to 84%. When the proportion of the catalyst/N-containing compounds was increased to 1:3, no product was observed, meaning that when copper(II) chloride is full coordinated with these N-compounds its activity is inhibited. In the optimized conditions (Scheme 9a) was possible to obtain TMBQ in 98% yield.

In 2008 was reported the IL $[\text{bmim}]\text{BF}_4$ as co-catalyst for the oxidation of 2,3,6-trimethylphenol (TMP) (Scheme 9b) [44]. The use of $[\text{bmim}]\text{BF}_4$ in combination with CuCl_2 resulted into better results than traditional solvents. The authors explained this observation by higher solubility of the catalyst and substrate in the IL media, and also due to the positive cooperation of $[\text{bmim}]\text{BF}_4$ and CuCl_2 , since it was already reported that nitrogen compounds can enhance the catalytic activity of copper(II) chloride [42, 43]. Another advantage of using ILs is that no side products were observed, in opposition of what was observed when organic solvents were used. Under the optimized conditions was possible to obtain up to 88.6% selectivity for TMBQ.

A continuation of this study in 2009 by the same authors reported the effect of the IL used and also the recyclability of the IL/catalyst [45]. Imidazolium and ammonium ILs were tested for the TMP oxidation under atmospheric oxygen, and it was observed that the anion effect can influence the reaction selectivity. For neutral anions, such as BF_4^- , good selectivities were obtained (over 94%), although for stronger acidic ILs, with anions such as HSO_4^- and H_2PO_4^- , the selectivity decreased up to 80%. This anion effect was confirmed when a screening was made with ammonium ILs possessing anions with different acidity. The nitrogen-containing precursors of the ILs were also tested as co-catalysts, namely imidazole and pyridine. It was observed that when ILs were used the selectivity was up to 90%, whereas for imidazole or pyridine the selectivity was above 64%.

The authors explained these results by the positive cooperation of the ILs and CuCl_2 , possibly via formation of oxotetracuprate as an active species for the oxidation reaction. The IL could be reused for at least five runs without significant loss of activity (decrease from 96% to 92% in the selectivity).

4 Conclusions

Ionic liquids (ILs) have been successfully applied as reaction media, promoting agent, and anchoring catalyst for different oxidation systems, such as sulfides and alcohols. In case of sulfide oxidation for desulfurization of diesel, the ILs also play an important role in removing the oxidized product from the diesel. The combination of ILs as efficient extracting catalyst and reaction media with air oxidant is expected to be more explored in near future for different functional group oxidations.

Acknowledgments The authors acknowledge Foundation for Science and Technology (FCT) and FEDER for financial support (SFRH/BPD/75045/2010, ERA-CHEM/0001/2008 and PEst-OE/SAU/UI4013/2011).

References

1. Sheldon R (2001) Catalytic reactions in ionic liquids. *Chem Commun* (23):2399
2. Kulkarni PS, Afonso CAM (2010) Deep desulfurization of diesel fuel using ionic liquids: current status and future challenges. *Green Chem* 12(7):1139
3. Bosmann A, Datsevich L, Jess A, Lauter A, Schmitz C, Wasserscheid P (2001) Deep desulfurization of diesel fuel by extraction with ionic liquids. *Chem Commun* (23):2494
4. Ko NH, Lee JS, Huh ES, Lee H, Jung KD, Kim HS, Cheong M (2008) Extractive desulfurization using Fe-containing ionic liquids. *Energy Fuel* 22(3):1687
5. Huang C, Chen B, Zhang J, Liu Z, Li Y (2004) Desulfurization of gasoline by extraction with new ionic liquids. *Energy Fuel* 18(6):1862
6. Mota A, Butenko N, Hallett JP, Correia I (2012) Application of (VO)-O-IV(acac)(2) type complexes in the desulfurization of fuels with ionic liquids. *Catal Today* 196(1):119
7. Xu D, Zhu W, Li H, Zhang J, Zou F, Shi H, Yan Y (2009) Oxidative desulfurization of fuels catalyzed by V_2O_5 in ionic liquids at room temperature. *Energy Fuel* 23(12):5929
8. Li FT, Liu RH, Wen JH, Zhao DS, Sun ZM, Liu Y (2009) Desulfurization of dibenzothiophene by chemical oxidation and solvent extraction with $\text{Me}_3\text{NCH}_2\text{C}_6\text{H}_5\text{Cl}\cdot 2\text{ZnCl}_2$ ionic liquid. *Green Chem* 11(6):883
9. Zhang S, Zhang Q, Zhang ZC (2004) Extractive desulfurization and denitrogenation of fuels using ionic liquids. *Ind Eng Chem Res* 43(2):614
10. Yu GR, Zhao JJ, Song DD, Asumana C, Zhang XY, Chen XC (2011) Deep oxidative desulfurization of diesel fuels by acidic ionic liquids. *Ind Eng Chem Res* 50(20):11690
11. Zhang J, Zhu W, Li H, Jiang W, Jiang Y, Huang W, Yan Y (2009) Deep oxidative desulfurization of fuels by Fenton-like reagent in ionic liquids. *Green Chem* 11(11):1801
12. Li H, Zhu W, Wang Y, Zhang J, Lu J, Yan Y (2009) Deep oxidative desulfurization of fuels in redox ionic liquids based on iron chloride. *Green Chem* 11(6):810
13. Zhu WS, Zhang JT, Li HM, Chao YH, Jiang W, Yin S, Liu H (2012) Fenton-like ionic liquids/ H_2O_2 system: one-pot extraction combined with oxidation desulfurization of fuel. *RSC Adv* 2(2):658

14. Chen XC, Song DD, Asumana C, Yu GR (2012) Deep oxidative desulfurization of diesel fuels by Lewis acidic ionic liquids based on 1-n-butyl-3-methylimidazolium metal chloride. *J Mol Catal A Chem* 359:8
15. Nie Y, Dong YX, Bai L, Dong HF, Zhang XP (2013) Fast oxidative desulfurization of fuel oil using dialkylpyridinium tetrachloroferrates ionic liquids. *Fuel* 103:997
16. Zhang BY, Jiang ZX, Li J, Zhang YN, Lin F, Liu Y, Li C (2012) Catalytic oxidation of thiophene and its derivatives via dual activation for ultra-deep desulfurization of fuels. *J Catal* 287:5
17. Liu D, Gui JZ, Ding JF, Ma JJ, Lee J, Sun ZL (2011) Oxidation of dibenzothiophene catalyzed by Na_2WO_4 in a halogen-free ionic liquid. *React Kinet Mech Catal* 104(1):111
18. Xu JH, Zhao S, Chen W, Wang M, Song YF (2012) Highly efficient extraction and oxidative desulfurization system using $\text{Na}_7\text{H}_2\text{LaW}_{10}\text{O}_{36}\cdot 32\text{H}_2\text{O}$ in bmim BF_4 at room temperature. *Chem Eur J* 18(15):4775
19. Zhu W, Li H, Jiang X, Yan Y, Lu J, Xia J (2007) Oxidative desulfurization of fuels catalyzed by peroxotungsten and peroxomolybdenum complexes in ionic liquids. *Energy Fuel* 21(5):2514
20. He L, Li H, Zhu W, Guo J, Jiang X, Lu J, Yan Y (2008) Deep oxidative desulfurization of fuels using peroxophosphomolybdate catalysts in ionic liquids. *Ind Eng Chem Res* 47(18):6890
21. Zhu W, Li H, Jiang X, Yan Y, Lu J, He L, Xia J (2008) Commercially available molybdic compound-catalyzed ultra-deep desulfurization of fuels in ionic liquids. *Green Chem* 10(6):641
22. Li H, Jiang X, Zhu W, Lu J, Shu H, Yan Y (2009) Deep oxidative desulfurization of fuel oils catalyzed by decatungstates in the ionic liquid of [Bmim]PF₆. *Ind Eng Chem Res* 48(19):9034
23. Jiang Y, Zhu W, Li H, Yin S, Liu H, Xie Q (2011) Oxidative desulfurization of fuels catalyzed by Fenton-like ionic liquids at room temperature. *ChemSusChem* 4(3):399
24. Liu C, Han JY, Wang JA (2007) A simple, efficient and recyclable copper(II) acetylacetonate catalytic system for oxidation of sec-alcohols in ionic liquid. *Synlett* (4):643
25. Rong M, Liu C, Han J, Sheng W, Zhang Y, Wang H (2008) Catalytic oxidation of alcohols by a novel copper Schiff base ligand derived from acetylacetonate and L-leucine in ionic liquids. *Catal Lett* 125(1–2):52
26. Rong M, Wang J, Shen Y, Han J (2012) Catalytic oxidation of alcohols by a novel manganese Schiff base ligand derived from salicylaldehyde and 1-phenylalanine in ionic liquids. *Catal Commun* 20:51
27. Karthikeyan P, Aswar SA, Muskawar PN, Bhagat PR, Kumar SS (2012) A novel CuCl_2/BIL catalyst for direct oxidation of alcohol to acid at ambient temperature. *Catal Commun* 26:189
28. Ramakrishna D, Bhat BR (2011) Green conversion of alcohols to carbonyls catalyzed by novel ruthenium-Schiff base-triphenylphosphine complexes. *Inorg Chem Commun* 14(1):155
29. de Souza RF, Dupont J, Dullius JED (2006) Aerobic, catalytic oxidation of alcohols in ionic liquids. *J Braz Chem Soc* 17(1):48
30. Leng Y, Zhao P, Zhang M, Chen G, Wang J (2012) A dicationic ionic liquid-modified phosphotungstate hybrid catalyst for the heterogeneous oxidation of alcohols with H_2O_2 . *Sci China Chem* 55(9):1796
31. Chen L, Zhou T, Chen L, Ye Y, Qi Z, Freund H, Sundmacher K (2011) Selective oxidation of cyclohexanol to cyclohexanone in the ionic liquid 1-octyl-3-methylimidazolium chloride. *Chem Commun* 47(33):9354
32. Chen L, Chen L, Ye Y, Qi Z, Freund H, Sundmacher K (2012) Co-solvent intensification effect on aromatic alcohol oxidation. *Catal Commun* 28:143
33. Chhikara BS, Tehlan S, Kumar A (2005) 1-Methyl-3-butylimidazolium decatungstate in ionic liquid: an efficient catalyst for the oxidation of alcohols. *Synlett* (1):63
34. Chhikara BS, Chandra R, Tandon V (2005) Oxidation of alcohols with hydrogen peroxide catalyzed by a new imidazolium ion based phosphotungstate complex in ionic liquid. *J Catal* 230(2):436

35. Ramakrishna D, Bhat BR (2010) Cobalt complexes in [EMIM]Cl – a catalyst for oxidation of alcohols to carbonyls. *Inorg Chem Commun* 13(1):195
36. Ramakrishna D, Bhat BR, Karvembu R (2010) Catalytic oxidation of alcohols by nickel(II) Schiff base complexes containing triphenylphosphine in ionic liquid: an attempt towards green oxidation process. *Catal Commun* 11(5):498
37. Kühn FE, Scherbaum A, Herrmann WA (2004) Methyltrioxorhenium and its applications in olefin oxidation, metathesis and aldehyde olefination. *J Organomet Chem* 689(24):4149
38. Bianchini G, Crucianelli M, Angelis FD, Neri V, Saladino R (2005) Highly efficient C–H insertion reactions of hydrogen peroxide catalyzed by homogeneous and heterogeneous methyltrioxorhenium systems in ionic liquids. *Tetrahedron Lett* 46(14):2427
39. Li JW, Sun W, Xu LW, Xia CG, Wang HW (2004) Room temperature ionic liquid: a powerful additive of Mn(salen) catalyzed oxidation of sec-alcohols. *Chin Chem Lett* 15(12):1437
40. Sun H, Harms K, Sundermeyer J (2004) Aerobic oxidation of 2,3,6-trimethylphenol to trimethyl-1,4-benzoquinone with copper(II) chloride as catalyst in ionic liquid and structure of the active species. *J Am Chem Soc* 126(31):9550
41. Sun H, Li X, Sundermeyer J (2005) Aerobic oxidation of phenol to quinone with copper chloride as catalyst in ionic liquid. *J Mol Catal A Chem* 240(1–2):119
42. Takehira K, Shimizu M, Watanabe Y, Orita H, Hayakawa T (1989) A novel oxygenation of 2,3,6-trimethylphenol to trimethyl-para-benzoquinone by dioxygen with copper(II) chloride amine hydrochloride catalyst. *Tetrahedron Lett* 30(48):6691
43. Bodnar Z, Mallat T, Baiker A (1996) Oxidation of 2,3,6-trimethylphenol to trimethyl-1,4-benzoquinone with catalytic amount of CuCl₂. *J Mol Catal A Chem* 110(1):55
44. Guan W, Wang C, Yun X, Hu X, Wang Y, Li H (2008) A mild and efficient oxidation of 2,3,6-trimethylphenol to trimethyl-1,4-benzoquinone in ionic liquids. *Catal Commun* 9(10):1979
45. Wang C, Guan W, Xie P, Yun X, Li H, Hu X, Wang Y (2009) Effects of ionic liquids on the oxidation of 2,3,6-trimethylphenol to trimethyl-1,4-benzoquinone under atmospheric oxygen. *Catal Commun* 10(5):725
46. Li H, He L, Lu J, Zhu W, Jiang X, Wang Y, Yan Y (2009) Deep oxidative desulfurization of fuels catalyzed by phosphotungstic acid in ionic liquids at room temperature. *Energy Fuel* 23(3):1354

Epoxidation of Olefins with Molecular Catalysts in Ionic Liquids

Christian J. Münchmeyer, Lilian R. Graser, Iulius I.E. Markovits, Mirza Cokoja, and Fritz E. Kühn

Abstract This review gives a summary of the epoxidation of various olefins catalyzed by different transition metal complexes, as well as by metal-free compounds in ionic liquid media. A comparison of the most active systems for different olefins is presented, and the effect of the ionic liquid solvents on the catalytic activity and catalyst reusability is discussed.

Keywords Ionic liquid · Epoxidation · Transition metals · Metal free · Olefins · Homogenous catalysis · Heterogeneous catalysis

Contents

1	Molecular Catalysts	186
1.1	Transition Metals	186
1.2	Metal-Free Catalysts	215
2	Enzymatic Catalysts	218
3	Heterogeneous Catalysts	222
3.1	Group VI Metals (Mo, W)	222
3.2	Group VII Metals (Mn, Re)	226
4	Conclusion	229
	References	230

Christian J. Münchmeyer, Lilian Graser, and Iulius I.E. Markovits have equally contributed to the manuscript.

C.J. Münchmeyer, L.R. Graser, I.E. Markovits, M. Cokoja, and F.E. Kühn (✉)
Catalysis Research Center, Technische Universität München, Ernst-Otto-Fischer-Straße 1,
D-85747 Garching bei München, Germany
e-mail: fritz.kuehn@ch.tum.de

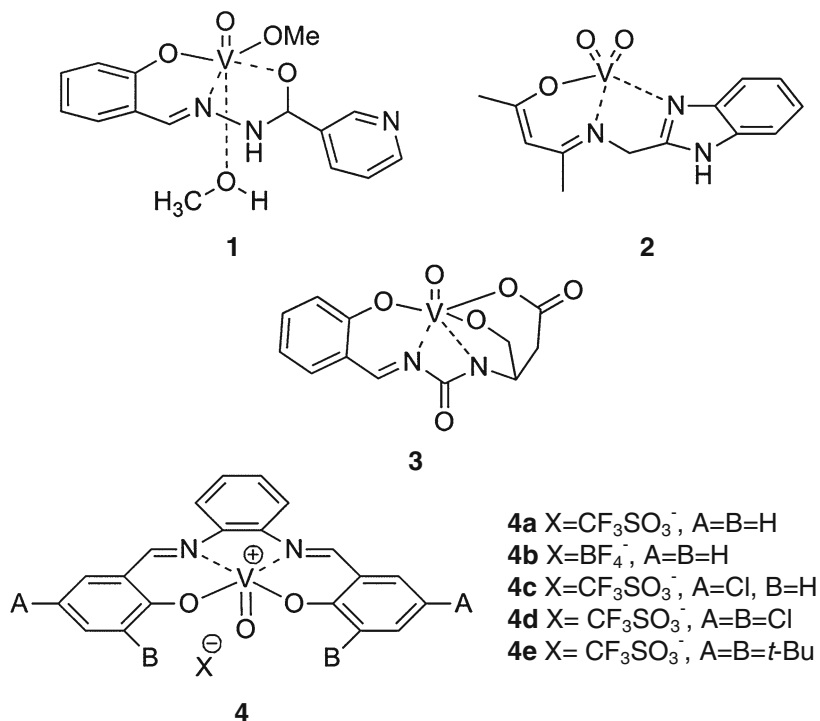


Fig. 1 Vanadium complexes reported by Conte et al. [2]

1 Molecular Catalysts

1.1 Transition Metals

1.1.1 Group V Metals (V)

Among the transition metals, vanadium is one of the most abundant elements in sea water soils and freshwater. Vanadium peroxides are known to be effective oxidants for different organic and inorganic substrates such as alkanes, alcohols, alkenes, and sulfites [1]. These catalytic or stoichiometric oxidation reactions use hydrogen peroxide under mild conditions with good product yields and selectivities.

Conte et al. [2] reported the synthesis of several new vanadium complexes (Fig. 1). The catalytic performance was tested for the epoxidation of cyclooctene as model substrate, with hydrogen peroxide as oxidant in [bmim]PF₆ and acetonitrile; yields up to 25% were obtained for complex **4a** after 4 h at room temperature (Table 1).

Table 1 Epoxidation of cyclooctene with V(V) complexes

Entry	Complex	Solvent	Time (h) ^a	Yield (%) ^b
1	1	CH ₃ CN	24	7
2	1	[bmim]PF ₆	5	20
3	2	CH ₃ CN	24	0
4	2	[bmim]PF ₆	5	8
5	3	CH ₃ CN	24	33
6	3	[bmim]PF ₆	4	15
7	4a	CH ₃ CN	5	53
8	4a	[bmim]PF ₆	4	25

Reaction conditions: cyclooctene 0.5 mmol, H₂O₂ 0.05 mmol, V(V)-catalyst 0.005 mmol, room temperature, solvent 1 mL

^aAt complete consumption of peroxide

^bBased on H₂O₂

However, the epoxide yields were significantly better (53%, 5 h) in acetonitrile and trifluoroethanol. Varying temperature and polarity of the ionic liquid from hydrophobic to hydrophilic led to significant lower yields of epoxide [2].

1.1.2 Group VI Metals (Mo, W)

Molybdenum

In 2009 Valente et al. [3] described a dioxomolybdenum(VI) complex containing an anionic *N,O* oxazoline ligand (Fig. 2). The investigation of different solvents, including ionic liquids, for the epoxidation of *trans*- β -methylstyrene revealed a higher solubility of the Mo(VI) complex in the more polar solvent [bmpy]BF₄ matched with [bmpy]PF₆ (31% conversion in [bmpy]BF₄ vs. 1% after 24 h in [bmpy]PF₆). Only the desired epoxide was obtained when using IL as solvent concluding in a selectivity of 100%. In their studies concerning the recyclability of the system it was shown that the catalyst leaches out of the IL when using [bmpy]BF₄.

Kühn et al. [4] applied four different Mo(VI) catalysts **6–9** in ionic liquids for the oxidation of *cis*-cyclooctene (Fig. 3). The catalytic reactions were performed at room temperature whereas most groups test their systems at 55°C. With a concentration of 1 mol% and within 1 h reaction time quantitative yields were obtained with **6** and **7**. The loading of catalyst **6** can be reduced to a concentration of 0.05 mol% which results in a commanding turnover frequency of >44,000 h⁻¹. Experiments on the recyclability of the systems revealed a minor loss of activity after three runs (third run: 80% conversion).

Compound **8** in [bmim]NTf₂ gave a moderate yield of 43% after 24 h reaction time and a TOF of around 110 h⁻¹ [5].

Fig. 2 Dioxomolybdenum (VI) complex with chiral tetradentate oxazoline ligand

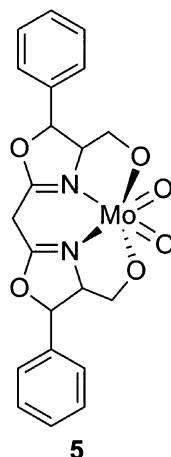
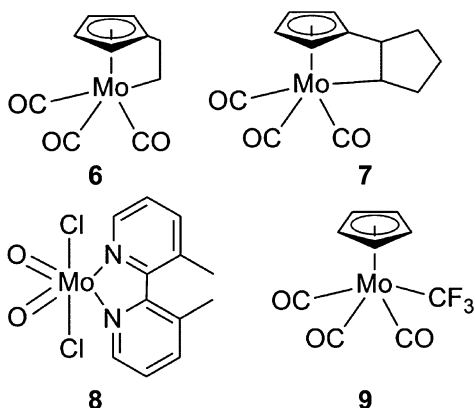


Fig. 3 Investigated molybdenum compounds



Recently the fluorinated organomolybdenum complex **9** was studied. A considerably slower reaction time (93% conversion after 24 h) was accepted for the possibility to reuse the catalyst for at least eight runs without any loss of activity [6].

Furthermore a series of $[\text{MoO}_2\text{X}_2\text{L}_2]$ ($\text{L} = 4,4'$ -bis-methoxycarbonyl-2,2'-bipyridine, 5,5'-bis-methoxycarbonyl-2,2'-bipyridine, 4,4'-bis-ethoxycarbonyl-2,2'-bipyridine, 5,5'-bis-ethoxycarbonyl-2,2'-bipyridine) were tested by the same group in 2010 in different room temperature ionic liquids for the epoxidation of *cis*-cyclooctene with TBHP. The authors stated that the activity of the employed compounds is approximately four times higher in RTILs than in dichloromethane [7].

Abrantes et al. [8] studied an amino acid-functionalized CpMo-complex **10** for the epoxidation of *trans*- β -methylstyrene in $[\text{bmim}]\text{BF}_4$ (Fig. 4). The authors chose room temperature and a catalyst concentration of 1 mol% as their standard conditions using TBHP as oxidant. The complex was well soluble in the IL, without

Fig. 4 Amino-acid functionalized MoCp-complex

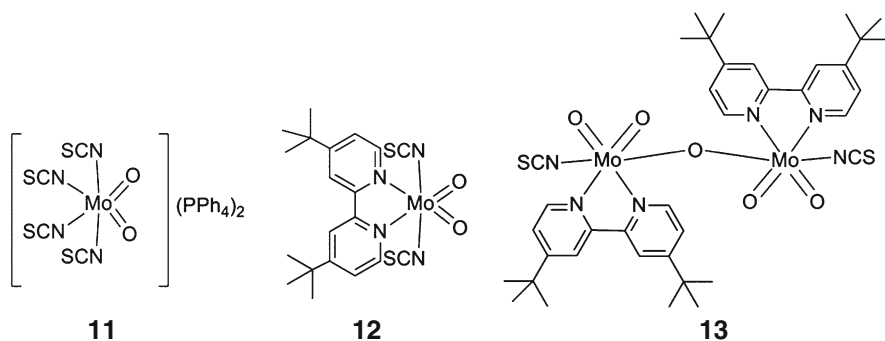
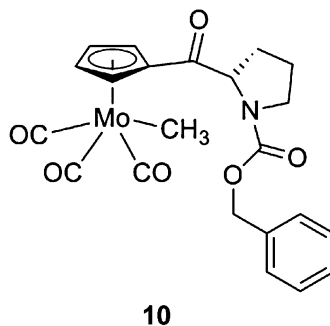


Fig. 5 Thiocyanatodioxomolybdenum complexes for the epoxidation of olefins

Table 2 Catalytic results of **11–13** in ILs

Entry	Catalyst	Solvent	Selectivity (%)	Yield (%)	TOF (h ⁻¹)
1	11	[Bmpy]BF ₄	54 (92)	67 (74)	97 (50)
2	12	[Bmpy]BF ₄	83 (88)	74 (78)	57 (56)
3	13	[Bmpy]BF ₄	93 (94)	85 (86)	62 (31)

Reaction conditions: substrate: cyclooctene = 1:1.5, $T = 55^{\circ}\text{C}$, $t = 24$ h, oxidant: TBHP, 1 mol% catalyst, values in parenthesis – results of second run

any color change of the organic phase during reaction time. Indeed the obtained yield was lower than in aprotic solvent ([bmim]BF₄: 41% conversion, MeCN: 77%), with no significant improvement of the ee, which was independent from the solvent used below 5%.

The effect of an ionic liquid on the catalytic performance of thiocyanatodioxomolybdenum(VI) complexes was studied by Pillinger et al. [9]. The authors synthesized and characterized three different compounds **11–13** (Fig. 5) and noted the poor solubility of complex **11** in the IL.

This fact explains the lower yield compared to complex **12** and **13** in the same solvent (Table 2). The kinetic profile of the epoxidation of *cis*-cyclooctene using

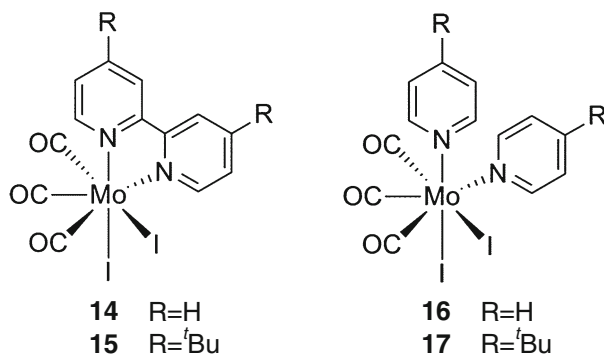


Fig. 6 Catalyst precursors used by Pillinger et al. [9]

Table 3 Conversion of methyl oleate

Entry	Catalyst	Conversion (%)
1	14	72
2	15	78
3	16	25
4	17	37

Reaction conditions: $T = 75^{\circ}\text{C}$, $t = 24$ h, Mo:MO:TBHP = 1:100:152

TBHP in decane was interestingly practically congruent with the one using TBHP in water although in a comparison of the two runs a loss in activity is revealed.

The same group used Molybdenum(II) diiodo-Tricarbonyl complexes containing nitrogen donor ligands as precursors for the epoxidation of methyl oleate in 2012 [10].

The authors utilized four different compounds (Fig. 6) in a molar ratio of catalyst: substrate: oxidant = 1:100:152 and were able to achieve conversion of 80% with a yield of 9,10-epoxystearate (MES) up to 71%.

A sizeable difference in reaction rate was observed, which is attributed to the different solubility of the complexes. Complex **16** appeared to be the least soluble decelerating the overall reaction rate by a slower in situ formation of the active species (Table 3).

By adding complex **14** to [bmim]BF₄ the authors investigated the potential of recycling the catalytic system. They obtained 86% MES after 24 h at 75°C and were able to separate the reaction products by adding *n*-hexane. After treating the IL at 40°C under vacuum for 1 h a second batch run was initiated and showed a similar activity of the catalytic system.

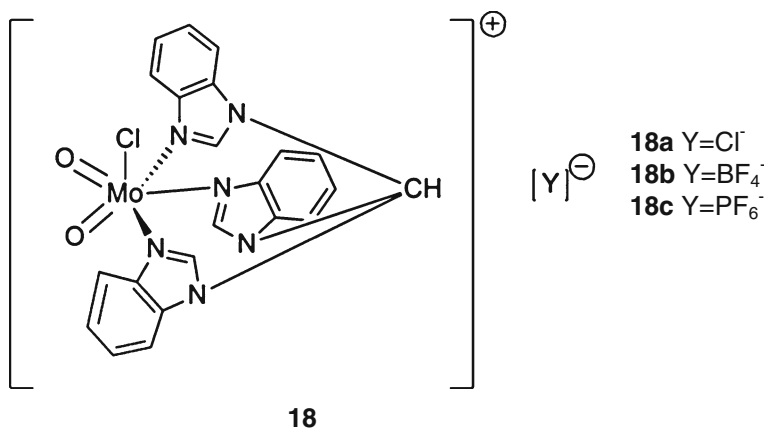
A technical mixture of methyl oleate and methyl linoleate was epoxidized by Wang and co-workers [11]. They used MoO(O₂)₂ · 2QOH (QOH = 8-quinolinol) in [bmim]BF₄, [hydremim]BF₄ and [bmim]PF₆.

The obtained conversions, selectivities, and turnover-frequencies of the ionic liquids that were tested are shown in Table 4. Entry 2 and 3 show that for [bmim]BF₄ and [hydremim]BF₄ the highest activities for the probed substrate mixture were

Table 4 Epoxidation of methyl oleate and methyl linoleate catalyzed by MoO(O₂)₂ 2QOH

Entry	Solvent	Conversion %		Selectivity (%)	TON (TOF)
		Methyl oleate	Methyl linoleate		
1	No solvent	55	31	90	3,690 (1,845)
2	[bmim]BF ₄	92	78	93	7,812 (3,906)
3	[bmim]PF ₆	75	44	94	5,358 (2,679)
4	[hydemim]BF ₄	96	89	95	8,740 (4,370)
5	CH ₃ CN	85	63	92	6,624 (3,312)
6	30% CH ₃ CN/70% [hydemim]BF ₄	94	84	95	8,360 (4,180)
7	C ₂ H ₅ OH	81	45	93	5,580 (2,790)
8	30% C ₂ H ₅ OH/70% [hydemim]BF ₄	90	74	95	7,695 (3,848)

Reaction conditions: $T = 30^{\circ}\text{C}$, $t = 2$ h, oxidant: H₂O₂, 0.01 mol% catalyst, co-catalyst: NaHCO₃

**Fig. 7** Cationic molybdenum complexes

achieved. The addition of [hydemim]BF₄ (Entry 6) to an organic solvent approved the positive effect of the ionic liquid concerning the activity of the Mo-catalyst and maybe subscribed to the polar character of the BF₄⁻ anion.

It can be seen that both the conversion and the selectivity to the corresponding epoxide increased when the ionic liquid was involved. The Mo(VI)-containing IL phase of the catalytic system could be eagerly recycled and reused for at least five runs without any loss of selectivity and only a minor drop of conversion (methyl oleate: 87% and methyl linoleate: 82% after fifth run).

Gonçalves et al. [12] described in 2010 the catalytic olefin epoxidation with different cationic molybdenum(VI) *cis*-dioxo complexes comprising weakly coordinating anions **18a–18c** (Fig. 7).

The compounds were tested at 55°C with TBHP as oxidant in different solvents, including DCE, [bmim]BF₄, [bmpy]BF₄, [bmim]PF₆, and [bmpy]PF₆. When using DCE as a solvent the authors obtained conversion between 61% and 98% within

Table 5 Epoxidation of *cis*-cyclooctene catalyzed by **18a–18c**

Entry	Solvent	Catalyst	Conversion (%)	TOF (h ⁻¹)
1	DCE	18a	96	201
2		18b	98	168
3		18c	61	69
4	[bmim]BF ₄	18a	78 (70)	76
5		18b	75 (60)	91
6		18c	40 (23)	15
7	[bmpy]BF ₄	18a	80 (71)	64
8		18b	81 (59)	102
9		18c	40 (13)	15
10	[bmim]PF ₆	18a	91 (89)	142
11		18b	45 (11)	67
12		18c	42 (11)	22
13	[bmpy]PF ₆	18a	94 (87)	163
14		18b	51 (11)	73
15		18c	40 (17)	19

Values in parentheses are cyclooctene conversions at 24 h for the second runs

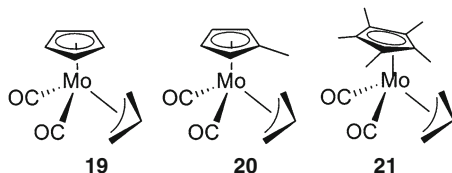
24 h and a selectivity of 100%. Independent of the used solvent complex **18c** is less soluble than **18a** and **18b** resulting in the lowest conversion. Table 5 shows the results of the catalytic reactions. Knowing that in contrast to compound **18c**, **18a** could be completely dissolved in all ILs while **18b** showed good solubility only in BF₄-type ILs it can be concluded that the different solubility of the catalyst is the most important factor concerning the activity. Due to the fact that the upper organic phase stayed colorless while the IL phase was yellow (indicating the active species being formed) the authors defined the reaction as heterogeneous.

Two consecutive 24 h runs at 55°C were done after extracting the IL/catalyst phase with *n*-hexane to test the recyclability of the three systems. ICP-AES analyses for Mo showed that no more than 1% of the catalyst was lost during the extraction. Furthermore the authors compared the use of different oxidants for the oxidation of cyclooctene. The authors proclaim that the coordinating abilities of water lead to a less active catalytic species resulting in a significantly faster reaction rate when applying water-free oxidants (TBHP in decane, UHP).

An interesting feature is the fact that the authors did not observe any diol-formation when applying aqueous TBHP or H₂O₂. To explore the substrate scope the catalytic system **18a**/[bmim]PF₆/TBHP was used. After a reaction time of 24 h the following olefin conversions were obtained: cyclooctene (91%), norbornene (55%), cyclohexene (37%), and styrene ≈ α -pinene (15%).

The same group reported in 2010 about the synthesis and characterization of complexes Cp'Mo(CO)₂(η^3 -C₃H₅) (Cp' = η^5 -C₅H₄Me **20**, = η^5 -C₅Me₅ **21** (Fig. 8) [13].

Compounds **19–21** were utilized as catalyst precursors for the epoxidation of *cis*-cyclooctene with TBHP (in *n*-decane at 55°C). The obtained results using **19** as catalyst are shown in Table 6. The kinetic profile of the catalytic reaction without

Fig. 8 Cp*Mo dicarbonyl η^3 -allyl compounds**Table 6** Olefin epoxidation at 55°C using complex **19** as catalyst

Entry	Substrate	Oxidant	Solvent	TOF	Conversion (%)	Selectivity (%)
1	<i>cis</i> -cyclooctene	TBHP aq.	None	97	99	100
2		H ₂ O ₂ aq.	None	<1	27	100
3		TBHP (decane)	None	310	100	100
4			DCE	361	100	100
5			[bmim]BF ₄	156	94	100
6			[bmpy]PF ₆	108	93	100
7	1-octene	TBHP (decane)	DCE	6	51	100
8	<i>trans</i> -2-octene	TBHP (decane)	DCE	81	89	100
9	Cyclododecene	TBHP (decane)	DCE	188	92	100
10	(R)-(+)-limonene	TBHP (decane)	DCE	289	100	70

Reaction conditions: $T = 55^\circ\text{C}$, $t = 24$ h, catalyst concentration = 1 mol%

any cosolvent and in [bmim]BF₄ appeared to be quite similar although the reactions performed in ILs are significantly slower than those involving a single liquid phase.

Royo et al. [14] reported in 2011 about dioxomolybdenum(VI) complexes containing chiral oxazolines for the epoxidation of olefins in ionic liquids. The compounds are shown in Fig. 9 and contain bis(oxazoline) **23** and the oxazoliny-pyridine **24** ligand, respectively, while **22** is a bimetallic system.

All three compounds were tested at 55°C for the epoxidation of *cis*-cyclooctene and gave moderate to good yields (Table 7). Compound **22** led to the exclusive formation of *trans*-1,2-(R)-limonene when tested in [bmpy]NTf₂ while the mono-metallic complexes **23** and **24** were not able to introduce diastereoselectivity.

It is noteworthy that the induction of diastereoselectivity was gone when an imidazolium-based ionic liquid was used as solvent. The authors state that this is due to the in situ formation of a Mo-NHC carbene complex.

The catalytic system involving **22** in [bmim]PF₆/CH₂Cl₂ allowed the recycling of the catalyst for at least five consecutive runs.

Commercially available molybdenum(VI) compounds were tested for the epoxidation of olefins in [bmim]PF₆ by Galindo et al. [15]. They chose 1 mmol scale reactions, employing an 1.5 eq. excess of oxidant and 60°C as their standard conditions. The results of their tests are summarized in Table 8.

It can be seen that the epoxide yield is strongly dependent on the solvent and its ability to solve all of the reaction components. Furthermore it can be noticed that the use of aqueous hydrogen peroxide resulted in ring opening hydrolysis of the

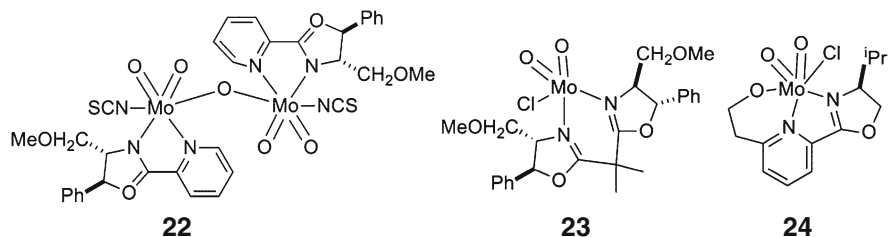


Fig. 9 Oxazoline-substituted Mo-complexes

Table 7 Cyclooctene epoxidation catalyzed by compounds **22–24**

Entry	Catalyst	Solvent	Conversion (%)	Epoxide yield (%)
1	22	[bmipy]NTf ₂ /CH ₂ Cl ₂	81	81
2	23	[bmipy]NTf ₂ /CH ₂ Cl ₂	98	98
3	24	[bmipy]NTf ₂ /CH ₂ Cl ₂	87	87
4	22	CH ₂ Cl ₂	100	100
5	23	CH ₂ Cl ₂	94	85

Reaction conditions: substrate: oxidant = 1:1.5, catalyst concentration: 2.5 mol%, $T = 55^\circ\text{C}$, $t = 1$ h, 1 mL of [bmipy]NTf₂ and 1.5 mL CH₂Cl₂

Table 8 Epoxidation of *cis*-cyclooctene in several solvents employing Mo(VI) complexes

Entry	Solvent	Precatalyst	Oxidant	Conversion (%)	Yield (%)
1	[bmim]PF ₆		UHP	<5	<5
2	[bmim]PF ₆	(NH ₄) ₂ Mo ₂ O ₇	UHP	>90	>90
3	[bmim]PF ₆	MoO ₃	UHP	>90	>90
4	[bmim]PF ₆	MoO ₃	H ₂ O ₂	0	0
5	[bmim]PF ₆	[Mo(O)(O ₂) ₂ (bipy)]	UHP	>90	>90
6	MeOH	(NH ₄) ₂ Mo ₂ O ₇	UHP	0	0
7	MeOH	MoO ₃	UHP	1	1
8	H ₂ O	(NH ₄) ₂ Mo ₂ O ₇	UHP	0	0
9	H ₂ O	MoO ₃	UHP	<5	<5
10	H ₂ O	MoO ₃	H ₂ O ₂	<5	<5
11	Cl ₂ CH ₂	(NH ₄) ₂ Mo ₂ O ₇	UHP	0	0

epoxide. The authors advertise Entry 3 as the optimal system with a cheap and commercially available catalyst and UHP as oxidant. Meanwhile they admit the long reaction time and high temperatures compared to optimal examples of Mo-catalyzed epoxidation.

The reaction systems shown in Entry 3 and 5 were used to investigate the recyclability in the ionic liquid. Already after two runs a decline in yield was observed.

In two subsequent publications Galindos group further investigated the influence of *N*-donor bases on the olefin epoxidation with oxodiperoxomolybdenum compounds using hydrogen peroxide as oxidant [16, 17].

Table 9 Oxidation of *cis*-cyclooctene

Entry	Base additive	Solvent	Conversion (%)	Yield (%)	Selectivity (%)
1	None	Cl ₃ CH	17	1	6
2		[bmim]PF ₆	29	9	31
3		[omim]PF ₆	38	25	66
4		[ddmim]PF ₆	40	40	100
5	Pyridine	[omim]PF ₆	29	29	100
6		[ddmim]PF ₆	49	49	100
7	4-Picoline	[bmim]PF ₆	31	18	58
8		[omim]PF ₆	54	54	100
9		[ddmim]PF ₆	46	46	100
10	2,2'-Bipyridine	[bmim]PF ₆	18	5	28
11		[ddmim]PF ₆	19	1	5
12	Pyrazole	Cl ₃ CH	16	3	19
13		[omim]PF ₆	63	63	100
14		[ddmim]PF ₆	73	73	100
15	3-Methylpyrazole	[omim]PF ₆	62	62	100
16		[ddmim]PF ₆	78	78	100
17	3,5-Dimethylpyrazole	Cl ₃ CH	23	8	35
18		[omim]PF ₆	84	84	100
19		[odmim]PF ₆	99	99	100

Reaction conditions: catalyst concentration 2.5 mol%, catalyst precursor: [Mo(O)(O₂)₂(H₂O)_n], base additive: 0.10 mmol, oxidant: 30% aqueous H₂O₂, substrate:oxidant = 1:3, *T* = 60°C, *t* = 2 h

Table 10 Molybdenum catalyst epoxidation of olefins

Entry	Substrate	Conversion (%)	Yield (%)
1	1-Octene	<1 (2)	<1 (2)
2	<i>trans</i> -2-octene	5 (20)	5 (20)
3	Styrene	60	4
4	Allyl amine	0	0
5	Cyclohexen-1-ol	66	34

Reaction conditions: catalyst concentration 2.5 mol%, catalyst precursor: [Mo(O)(O₂)₂(H₂O)_n], 3,5-dimethylpyrazole: 0.10 mmol, oxidant: 30% aqueous H₂O₂, substrate:oxidant = 1:3, *T* = 60°C, *t* = 2 h (18 h)

The authors showed that hydrolysis of the epoxide product can be limited by the addition of coordinating base species and by tuning the IL media to limit the availability of water. It was also shown that *N*-heterocyclic base species undergo favorable oxidation under the applied reaction conditions while pyrazoles resist the oxidation and even enhance the catalytic activity. Some results are summarized in Table 9.

They were able to recycle the catalytic system containing 3,5 dimethylpyrazole (Entry 18) for ten cycles without any loss of activity. It needs to be noted that the system is only suitable for activated substrates such as *cis*-cyclooctene. Experiments with more demanding substrates such as 1-octene, styrene, or allyl amine resulted in very poor yields (Table 10).

Table 11 Epoxidation of olefins catalyzed by [bmim]₃PW₁₂O₄₀

Entry	Substrate	Solvent	Yield (%)	Selectivity (%)	TON
1	<i>cis</i> -Cyclooctene	[bmim]PF ₆	87	99	289
2	Cyclohexene	[bmim]PF ₆	36	80	121
3	1-Octene	[bmim]PF ₆	12	86	40
4	<i>trans</i> -2-Octene	[bmim]PF ₆	37	94	125
5	2-Methyl-2-heptene	[bmim]PF ₆	67	89	223
6	Styrene	[bmim]PF ₆	9	32	31
7	<i>trans</i> - β -methylstyrene	[bmim]PF ₆	22	67	74
8	<i>cis</i> -Cyclooctene	[bmim]NTf ₂	82	94	274
9	<i>cis</i> -Cyclooctene	[bmim]BF ₄	Trace	12	<1
10	<i>cis</i> -Cyclooctene	CH ₃ CN	1	77	3
11	<i>cis</i> -Cyclooctene	CH ₃ OH	Trace	40	1
12	<i>cis</i> -Cyclooctene	CH ₂ Cl ₂	Trace	75	1

Reaction conditions: $T = 60^\circ\text{C}$, $t = 1$ h, cat:sub:ox = 3:100:150

Tungsten

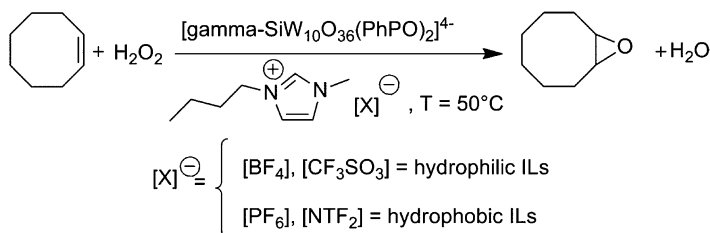
Polyoxometalates (POMs) are a large family of bulky clusters of transition metal oxide anions. In recent years, they have been utilized for a diversity of applications in catalysis, electronics, optics, medicine, and biology [18]. It is also well known that POM catalysts are widely used for organic oxidations [19], a typical example being the Venturello–Ishii $\{\text{PO}_4[\text{WO}(\text{O}_2)_2]_4\}_3^-$ catalyst for the epoxidation of olefins.

In 2007 the group of Jincai Zhao investigated the influence of ionic liquids as an activator for the epoxidation of olefins catalyzed by polyoxotungstate [20]. When exploiting [bmim]PF₆ as solvent for the epoxidation reaction the authors observed a significant enhancement of activity (289 times TOF) and selectivity (1.3 times) compared to that of traditional organic solvents (e.g., CH₂Cl₂). They tested several ionic liquids (Table 11) and could evidence that the counter ion of the ionic liquid plays a crucial role in the epoxidation of olefin.

Comparing Entry 1 with Entry 9 it can be seen that a change of the counterion from PF₆⁻ to BF₄⁻ reduced the TOF and the selectivity for cyclooctene oxide dramatically. Via in situ ³¹P-NMR spectroscopy the authors could reveal the fast formation of the active peroxotungstate $[\text{PO}_4\{\text{W}(\text{O})(\text{O}_2)_4\}_3]^{3-}$ (Venturello complex) in presence of [bmim]PF₆.

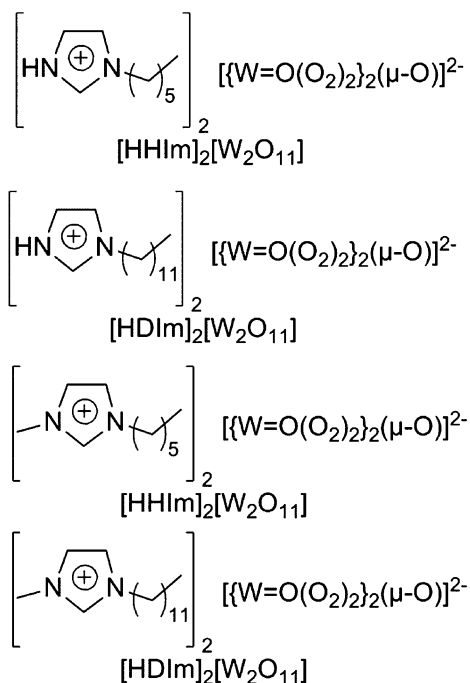
Bonchio and co-workers [21] used microwave irradiation to enhance the activity of $[\gamma\text{-SiW}_{10}\text{O}_{36}(\text{PhPO})_2]^{4-}$ for catalytic epoxidation of olefins in ionic liquids. The authors screened several ILs to optimize the recycling and the catalytic efficiency (Scheme 1) and furthermore tested the influence of continuous microwave irradiation. In hydrophobic ILs quantitative conversion and selective epoxidation were obtained.

They also screened the influence of water within the substrate/IL/oxidant multiphase system and ascertained a decreasing TOF with a rising water content. The results gained by the implementation of microwave irradiation into the catalytic



Scheme 1 Catalytic epoxidation of cyclooctene with H_2O_2

Fig. 10 The anion $[\text{W}_2\text{O}_{11}]^{2-}$ functionalized catalysts



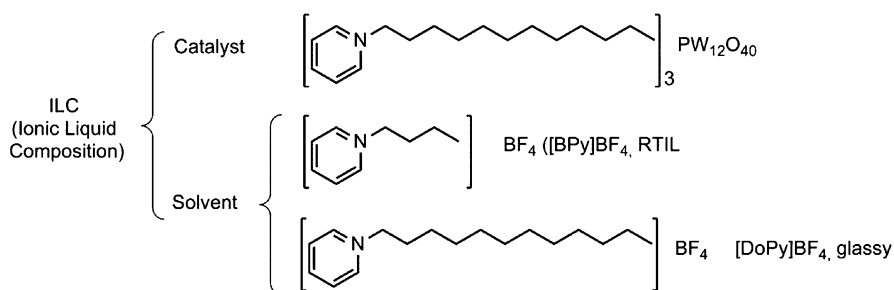
system are noteworthy – quantitative epoxidation of cyclooctene occurred within 1 min incrementing the TOF value by 35 times to ca $7,500 \text{ mol mol}_{\text{Cat}}^{-1} \text{ h}^{-1}$. The substrate scope for the microwave-assisted protocol resulted in moderate to good yields (1-octene 54% in 3 h, E-2-octene 99% in 45 min).

Hou and co-workers [22] synthesized and characterized four polyoxometalate anion-functionalized catalysts (Fig. 10). The epoxidation of *cis*-cyclooctene was chosen as model reaction and 30% aqueous H_2O_2 solution was used as oxidant. The authors were able to show a close relation between the length of the alkyl chain on the imidazolium cation and the reaction rate.

Table 12 Epoxidation of cyclooctene with four different polyoxometallate catalysts

Entry	Solvent	[HHIm] ₂ [W ₂ O ₁₁]	[HDIIm] ₂ [W ₂ O ₁₁]	[HMIIm] ₂ [W ₂ O ₁₁]	[DMIIm] ₂ [W ₂ O ₁₁]
1	None	24	66	39	41
2	H ₂ O	16	65	13	28
3	EtOAc	42	54	14	20
4	CH ₂ Cl ₂	55	79	5	52
5	CH ₃ CN	59	97	13	29
6	CH ₃ OH	66	100	4	46
7	CH ₃ OH–H ₂ O	54	100	26	100

Reaction conditions: catalyst concentration: 2 mol%, Cat:Sub:Ox = 2:100:150, $T = 60^\circ\text{C}$, $t = 4$ h

**Fig. 11** The compositions of the amphipathic ionic liquid mixture

[Hdim]₂[W₂O₁₁] can be regarded as a reaction-induced phase-separation catalyst and proved to be the most active catalyst (Table 12). A noteworthy fact is that the catalytic system switched the reaction mixture from triphase to emulsion, then to a biphasic system, and at the end of the reaction all the catalysts self-precipitated from the reaction medium. This feature makes it possible to recycle the catalyst via decantation.

In 2009 Lui et al. [23] designed an amphipathic ionic liquid system to allocate a convenient reaction medium for both hydrophobic and hydrophilic molecules (Fig. 11). The catalytic system was designed for alkene epoxidation using H₂O₂ as oxidant. The phosphotungstate functionalized ionic liquid [dopy]₃[PW₁₂O₄₀] was used as a catalyst, dissolved in the amphipathic ionic liquid mixture of [dpy]BF₄ and [dopy]BF₄.

Under optimized conditions (80°C, 1 h, 1 mol% catalyst, 7.5 mmol H₂O₂) the authors reported a conversion of 88% for the epoxidation of *cis*-cyclooctene with 95% selectivity towards the epoxide. Additionally the group explored the substrate scope of the system (Table 13).

They achieved moderate to good conversions for more demanding substrate but a significant lower selectivity to epoxides. After six consecutive runs the authors report no observable decomposition of the catalyst and a conversion of 84% in run six for cyclooctene.

Table 13 Epoxidation of different olefins in the ILC with H₂O₂ and UHP as oxidant

Entry	Substrate	H ₂ O ₂ as oxidant		UHP as oxidant	
		Conversion (%)	Selectivity (%)	Conversion (%)	Selectivity (%)
1	<i>cis</i> -Cyclooctene	88	98	97	99
2	Cyclohexene	80	56	90	57
3	Norbornene	76	34	91	87
4	Styrene	66	29	63	29
5	4-Chlorostyrene	49	46	56	86
6	4-Bromostyrene	44	52	53	89
7	4-Methylstyrene	63	10	77	24
8	Ethyl cinnemate	<5	–	<5	–
9	1-Octene	10	21	22	100
10	1-Dodecene	7	30	8	98

Döring et al. [24] synthesized several penta- and hexaalkylated guanidinium-based ionic liquids and tested these as solvents for the epoxidation of cyclooctene. They used hydrogen peroxide as oxidant and the Venturello complex, [C₈H₁₇]₃N(CH₃)₃[PO₄{WO(O₂)₂}₄], as catalyst. They reported moderate to good epoxide yields in the range between 13% and 79% depending on the substituents on the guanidinium moiety. Furthermore, the miscibility of the anion of ionic liquid with water played for this system an important role. It was possible to use the system for three consecutive runs. Additionally the group synthesized new guanidinium phosphotungstates containing the PW₁₂O₄₀³⁻ anion and tested these compounds as catalyst in guanidinium-based ionic liquids as well as in acetonitrile. Compared with their ammonium-based analog ([NR₄][PW₁₂O₄₀]) the guanidinium-based catalyst showed a significant higher activity.

1.1.3 Group VII Metals (Mn, Re)

Manganese

Song and Roh [25] reported the first use of an imidazolium-based ionic liquid, [bmim]PF₆, as reaction media for the epoxidation of alkenes using a Jacobsen-type Mn-salen **25** as catalyst and NaOCl as oxidant, at 0°C and an pH 13. To prevent solidification a mixture of CH₂Cl₂ and IL was used in a ratio of 4:1. Good to excellent yields and ee's were obtained under these conditions with conversion at ca. 70–80% and selectivity above 84%. Although the catalytic system could be recycled for five times a significant loss of activity was observed for 2,2-dimethylchromene with a drop in yield (ee) from 86 (96)% for the first run to 53 (88)% for the fifth [25] (Fig. 12).

Li and Xia [26] reported the epoxidation of alkenes with a Mn-porphyrin system **26** in a [bmim]PF₆-CH₂Cl₂ mixture (3:1) at room temperature. They investigated the influence of the oxidation agent, the substituents on the porphyrin ring and the amount of organic solvent added to the reaction mixture on the catalytic

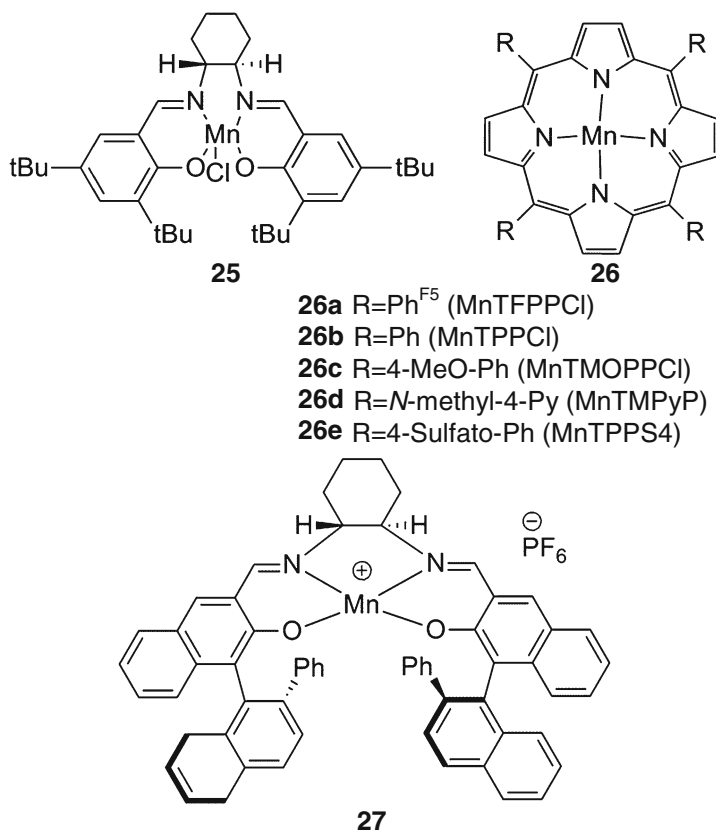


Fig. 12 Jacobsen-type chiral Mn catalysts **25**, Mn-porphyrin system **26**, Katsuki-type Mn catalyst **27**

performance. An increase in conversion of styrene of about 15% from 81% to 95% was achieved when $\text{PhI}(\text{OAc})_2$ was used instead of PhIO , more significantly the selectivity towards the epoxide increased from 46% to 85%. Comparing **26a**, **26b**, and **26c** a slight trend in favor of the fluorinated rest can be concluded from the epoxidation results, also a decrease in volume of organic solvent benefits the catalysis [26–28].

El-Hiti et al. [29] performed an intensive study on the concentration dependence of the oxidation agent as well as catalyst amount and a comparison of the most used ionic liquids for these types of reaction $[\text{bmim}]\text{PF}_6$ and $[\text{bmim}]\text{BF}_4$. The catalyst used was a Katsuki-type Mn-salen complex **27** with 4-phenyl pyridine *N*-oxide as axial ligand, NaOCl as oxidant and similar reaction conditions to those used by Song and Roh et al. The best results (conversion 99%, selectivity 99%, ee 95%) were obtained in a $[\text{bmim}]\text{PF}_6\text{-CH}_2\text{Cl}_2$ mixture (2:3, v/v) at 0°C with a catalyst concentration of 2.5 mol% after 2 h reaction time [29]. A straightforward system was reported by Chan et al. [30] with tetramethyl ammonium hydrogen carbonate

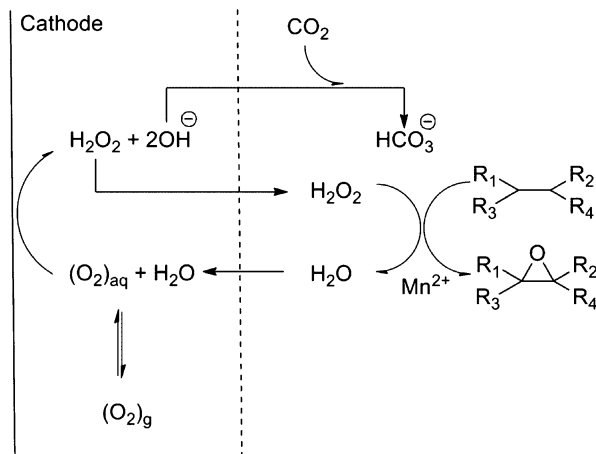


Fig. 13 Indirect electrochemical assisted epoxidation of olefins

and $MnSO_4$ in $[bmim]BF_4$ using hydrogen peroxide as oxidant. Conversions of 99% are achieved for styrene and 1,2-dihydro naphthalene with excellent selectivity at room temperature and 2 h reaction time. The recycling experiments have shown that a constant addition of $MnSO_4$ and/or Me_4NHCO_3 keeps the yield of styrene oxide at 95%; however without addition of $MnSO_4$ a yield of 45% is reported after the third run and only 10% after the fourth [30].

The same group performed an indirect approach generating hydrogen peroxide through electrolysis in alkaline media established by sodium hydroxide at first followed by the epoxidation of several olefins with $MnSO_4$ in $[bdmim]BF_4$, in a continuous flow of carbon dioxide for the second step (Fig. 13). After 4 h reaction time, conversions up to 99% with selectivities for 1,2 dihydronaphthalene and styrene of 83% are achieved. Although this was one of the first examples where epoxidation of alkenes was performed indirectly with O_2 in an ionic liquid, recycling experiments have proven to be difficult since Mn^{2+} species hinders the electrolysis. When the Mn^{2+} cation was removed completely by the addition of Na_2CO_3 after each cycle, the reaction mixture could be reused for five times with a conversions of 83% for the first and 85% for the fifth run [31]. In 2008, Han et al. disclosed the epoxidation of styrene using hydrogen peroxide, $MnSO_4$, and KOH under CO_2 pressure, similar to the reports of Chan et al. After 4 h at $40^\circ C$ a conversion of 95% with a yield of 69% could be achieved [32]. In 2005, Chen et al. reported the synthesis of a new type of complex tagged with imidazolium-based side chains **28**, attempting to increase the solubility of the complex and therefore the active species (Fig. 14).

The epoxidation of chalcones with *m*-chloroperoxybenzoic acid (*m*-CPBA) as oxidant and *N*-methylmorpholine *N*-oxide (NMO) as co-catalyst using catalyst **28** has yielded conversions above 90%, without a significant loss of activity even after five runs in CH_3CN [33]. A similar approach was made by Lu et al. (2007) tagging a

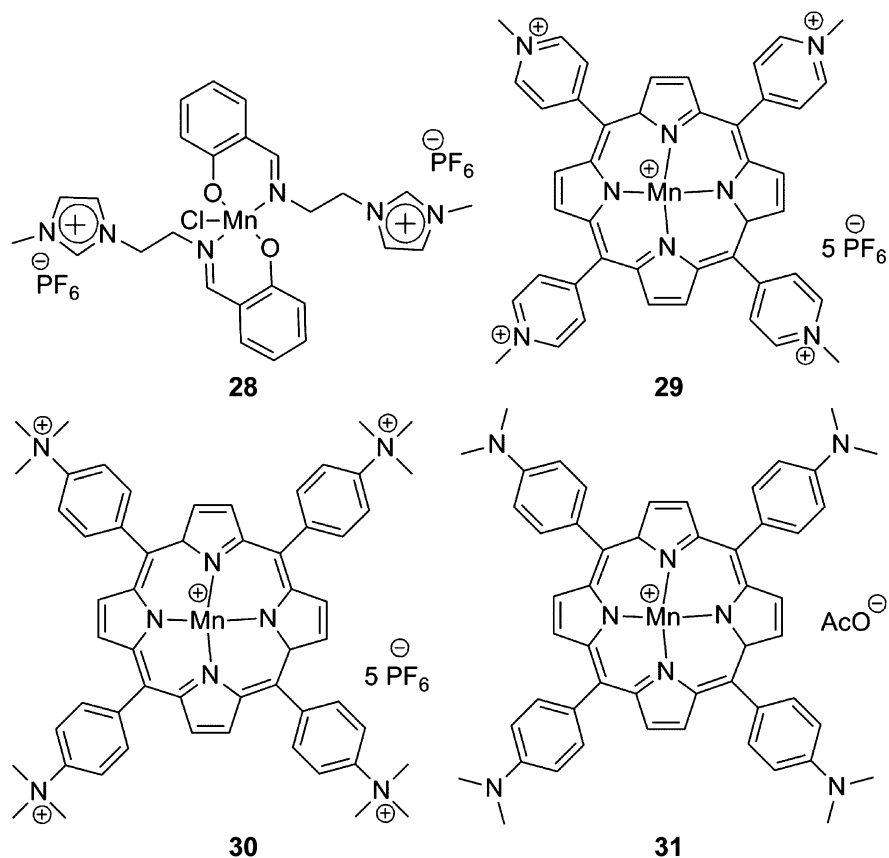
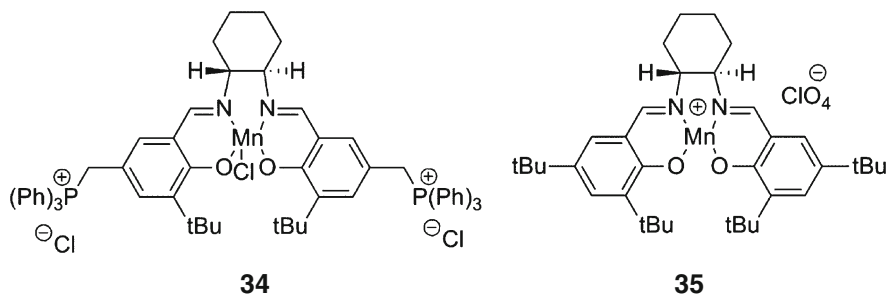
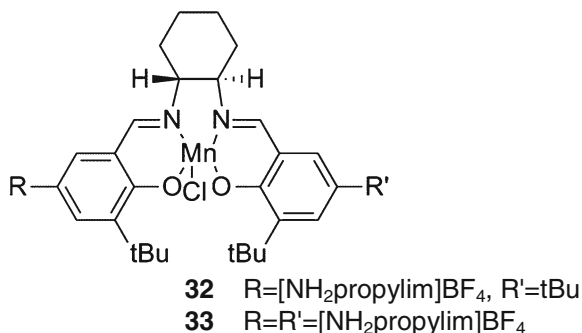


Fig. 14 Ionic Mn-catalysts

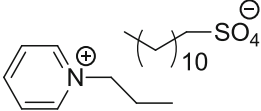
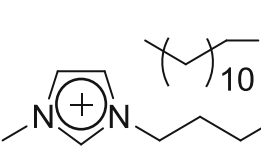
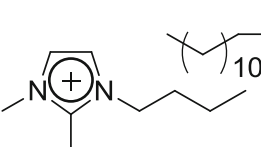
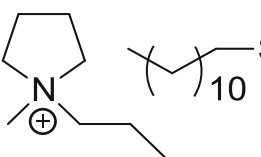
Mn porphyrin catalysts **29** with a pyridium-PF₆ based ionic liquid, dissolving the catalyst directly in [bpy]BF₄ as reaction media without any organic solvent. The catalytic runs were carried out at 30°C with PhIO as oxidation agent with a catalyst loading of 0.4 mol%. By comparison with previous reports the conversion of styrene to styrene oxide increases up to 96% even with a significant reduction in the catalyst concentration. The only drawback of this system is that after five recycling runs almost no styrene oxide is formed only the corresponding aldehyde with a conversion of 71% [34]. Similar results were obtained using catalyst **29**, **30**, and **31** in a [bmim]BF₄ and/or [bzmIm]BF₄ solvent mixture by the group of Liu et al. (2007), Liu et al. (2008) and Cai et al (2008). [35–37]. In the same year Bernardo-Gusmao et al. [38] reported the selective epoxidation of limonene using catalyst **25** in [bmim]BF₄ with moderate results with a conversion of 74% and diastereomeric excess of 74%. However similar results are obtained in organic solvent with a smaller amount of catalyst [38] (Fig. 15).

Fig. 15 Ionic Jacobsen-type Mn complexes**Fig. 16** Ionic Jacobsen-type Mn complexes

Simultaneously, Yin et al. [39] reported the synthesis of a new type of Jacobsen-type Mn-catalysts where the ionic liquid is anchored directly on the salen ligand without any axial ligand on Mn. The amino functionalized ionic liquid was also tested as solvent acting as axial ligand for the epoxidation of styrene. Under the same condition using a m-CPBA/NMO at 0°C 98–99% yield of styrene oxide was obtained for catalysts **32** and **33**, without any loss of activity after the tenth run, whereas using [NH₂propylim]BF₄ as solvent/axial ligand the first run yielded 75% styrene oxide and only 38% after the third cycle [39] (Fig. 16).

A detailed screening of the influence of the ionic liquid and different oxygen sources was performed by Friere et al. (2010). The 1,3-dialkylimidazolium ionic liquids provided good epoxide yields with good ee's. Additionally, an increase in the alkyl chain on the cation led to decrease in the enantiomeric excess and, on the other hand the substitution of the acidic proton in the 2-position of the imidazolium ring facilitated an increase in ee. [bmim]PF₆ using NaOCl as oxidant has proven to be the best system for the Jacobsen catalyst **25** although greener oxidants such as H₂O₂ and UHP have shown lower yields but similar ee's. Compared to **25**, the newly synthesized catalysts **34** and **35** have shown pronounced deficits in activity with 49% and 53% compared to a yield of 96%; however, similar ee's are obtained with Urea-H₂O₂ as oxidant [40]. NaIO₄ was used by the group of Tangestaninejad et al. [41] in [bmim]BF₄ as oxidation agent with several Mn-propyhrin complexes,

Table 14 Comparison of the different ionic liquids used by Wong et al. for the epoxidation of 1-octene

Entry	Ionic liquids	Conversion (%)	Yield (%)
1		65	63
2		74	69
3		84	77
4		100	94

Reaction conditions: 1 g (ionic liquid), NaHCO₃ (150 mg), H₂O (0.38 mL), 1-octene (2.5 mmol), Mn(OAc)₂, (0.04 M in water), peracetic acid (3.4 equiv.), 30 min

with yields greater than 99% in excellent selectivities [41]. A simpler and more efficient way for the epoxidation of linear alkenes was reported by Wong et al. [42] with Mn(OAc)₂ as catalyst and peracetic acid as oxygen source. Despite the simple system, good to excellent conversions were obtained for aliphatic mono- or di-alkenes, the latter ones being fully epoxidized. Table 14 presents the results obtained for the four different ionic liquids used for the epoxidation of 1-octene. The same experiment was performed in water without any addition of ionic liquid which has shown no conversion of 1-octene.

Recycling the systems has shown stable conversions of 1-octene even after nine runs. However after four runs manganese oxide and sodium acetate had to be filtered off with subsequent addition of fresh Mn(OAc)₂ [42] (Fig. 17).

Jacobsen-type chiral catalysts **36** and **37** were reported by Tang and Wu et al. (2011) as good catalysts for the epoxidation of 6-chloro-dimethylchromene in [bmim]PF₆ as solvent with NaOCl as oxidation agent. Yields up to 93%, ee 94% were achieved at 0°C and good recyclability even after six runs was proclaimed [43]. Pyrrolidinium-based ionic liquids such as [mopyrro]NTf₂ used as solvent for

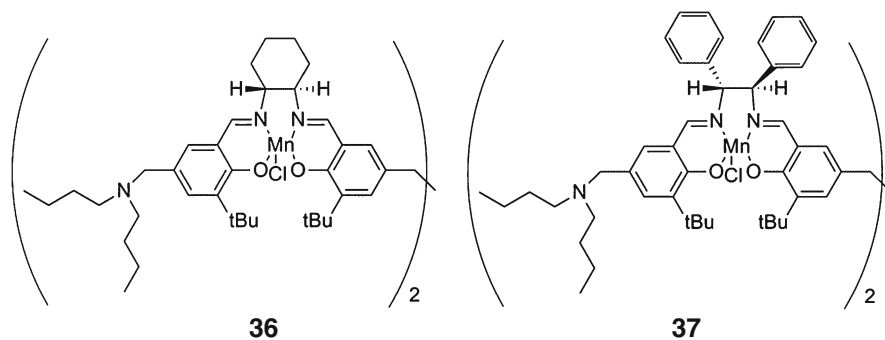


Fig. 17 Dimeric Jacobsen-type complexes

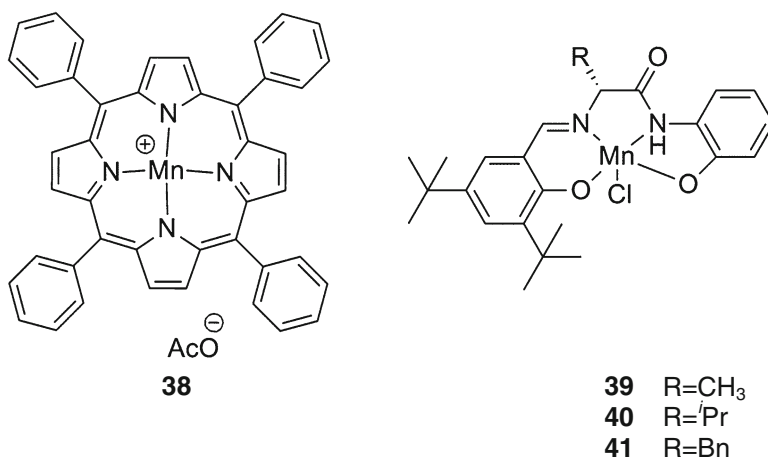


Fig. 18 Mn-TPPPOAc and Mn Chiral Schiff-base complex

the epoxidation of styrene with hydrogen peroxide as oxygen source by Androletti and Draye et al. under ultrasound, with a $\alpha\beta$ -bis-binaphthyl-strapped Mn porphyrin catalysts, which showed moderate activity towards epoxidation [44]. However, using an ionic Mn-porphyrin **37**, good to excellent results were obtained for several alkenes [45] (Fig. 18).

Cheng et al. [46] reported the synthesis and the application of complex **38** for the asymmetric epoxidation of chromenes in a (L-1-ethyl-3-(1-hydroxy-2-propanyl)imidazolium bromide-CH₂Cl₂) mixture. As expected increasing the size of the chiral information, yields (ee) from 89% (88%) for **39** to yields up to 98% (95%) were obtained for 6-chloro-2,2'-dimethylchromene with **41**, using NaClO as oxygen source and pyridine *N*-oxide as axial ligand [46]. Zhang et al. [47] performed an extensive study on the epoxidation of unfunctionalized olefins using catalyst **25** and electro-generated NaClO in a [bmim]X (X = BF₄ or PF₆) - NaCl/NaOH/H₂O mixture. The data summarized in Table 15 concludes that the addition of organic

Table 15 Electrochemical epoxidation of unfunctionalized olefins

Entry	Olefin	Media ^a	Yield % (ee %)
1	Styrene	I	80 (94)
2		II	54 (79)
3		III	72 (92)
4		IV	61 (81)
5	α -Methylstyrene	I	78 (86)
6		II	67 (75)
7		III	68 (82)
8		IV	70 (79)
9	Indene	I	85 (89)
10		II	50 (79)
11		III	77 (83)
12		IV	79 (72)

Reaction conditions: substrate, 2 mmol; catalyst, 0.2 mmol, 10 mol%. ^aMedia (I) [bmim]PF₆-NaCl/NaOH/H₂O; (II) [bmim]BF₄-NaCl/NaOH/H₂O; (III) [bmim]PF₆/CH₂Cl₂-NaCl/NaOH/H₂O; (IV) [bmim]BF₄/CH₂Cl₂-NaCl/NaOH/H₂O

solvent has a significant effect on the yield of epoxide with a decrease of 5–10% for the [bmim]PF₆ and a slight increase for [bmim]BF₄. This could be attributed to the solubility of the substrates in the ionic liquid-aqueous solution. Additionally, using an axial ligand such as NH₄OAc showed a decrease in activity in all four reaction media [48].

In 2013 Abdi et al. reported the use of four macrocyclic Jacobsen-type-salen **25** as catalysts for the epoxidation of olefins in different organic carbonates as solvents with UHP as oxygen source. One experiment was performed in a [bmim]PF₆-MeOH mixture with yields for styrene of 99% (31%). However, the reaction time for dimethyl carbonate or propylene carbonate methanol mixture was significantly lower at 6 to 7 h, compared to 12 h for the ionic liquid:MeOH mixture [49].

Rhenium

In 2000, Abu-Omar and Owens reported the first successful application of ILs as solvent for the MTO-catalyzed epoxidation of olefins [50]. In this work, several different olefinic substrates were oxidized at room temperature (RT) to their corresponding epoxides applying 2 mol% MTO as catalyst, 2.0 equiv. UHP as oxidant and [emim]BF₄ as solvent (Table 16). The yields range from fair (in the case of 1-decene, Entry 9) to excellent. The poor conversion of 1-decene is ascribed to the low solubility in the ionic liquid. However, the advantage of this MTO/UHP-system becomes apparent when applying aqueous H₂O₂ to 1-Phenylcyclohexene, which results in a ring opening and diol formation. The advantages of this oxidation system are (1) the excellent solubility of MTO and UHP in the IL, resulting in a homogeneous solution; (2) the oxidation solution is practically water-free, thus the formation of diols is significantly reduced; (3) leftover reactants, if any, and

Table 16 Epoxidation of several olefinic substrates with MTO in [emim]BF₄^a

Entry	Substrate	Conversion (%)	Yield (%)
1	Cyclohexene	>95	>99
2	1-Methylcyclohexene	>95	>95
3	1-Phenylcyclohexene	>95	>95
4	2-Cyclohexen-1-ol	>99	>95
5	Styrene	95	>95
6	<i>trans</i> - β -methylstyrene	>95	>95
7	Cyclooctene	>95	>95
8	1,5-Cyclooctadien	>99	>85 ^b
9	1-Decene	46 ^c	>99

^aReaction conditions: 0.5 mol substrate, 2.0 equiv. UHP, 2 mol% MTO, RT, 8 h

^bThis yield represents the diepoxide; only 1.0 equiv. UHP were used

^cThis conversion was obtained after 72 h

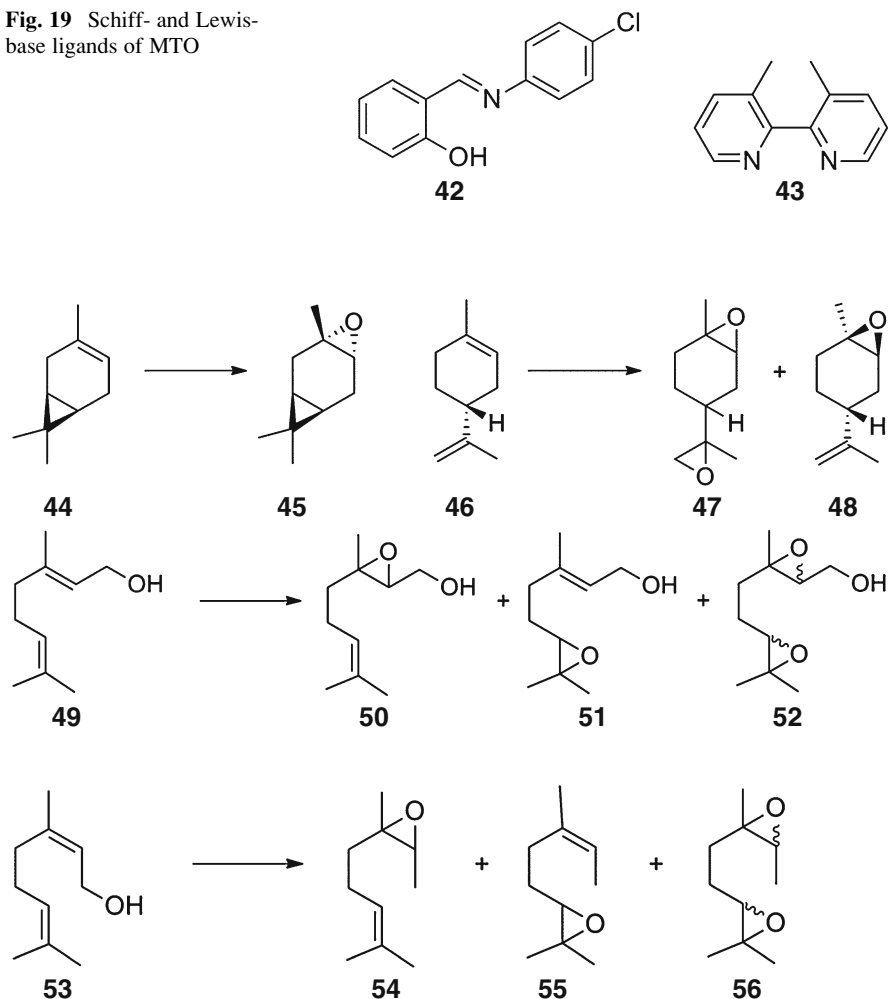
products are easily separated from the oxidation solution by extraction with an immiscible solvent; and (4) most of the epoxidation rates are at least comparable to previously published data.

Further studies of the kinetics and thermodynamic of the reaction of MTO with hydrogen peroxide in different ionic liquids have been done by the same group [51]. Additionally, the rate constants for the oxygen atom transfer from the monoperoxo and bisperoxorhenium complexes of MTO to olefins have been investigated by means of UV/Vis and NMR spectroscopy [52].

Qiao and Yokoyama gained comparable results for the epoxidation of styrene under the same conditions by only using 1.1 equiv of UHP and 2 h reaction time (94.8% conversion; 93.4% yield of epoxide) with [bmim]BF₄ as solvent [53]. A detailed screening of several ionic liquids has shown that [bmim]BF₄ was the most suitable under these reaction conditions. The optimization of the reaction parameters showed that 1.1 equiv. of UHP is the optimal oxidant/substrate ratio. Besides, it was observed that halogen impurities in the IL have a major effect on the epoxidation outcome. ILs with lower chloride concentrations gave a better performance with respect to the yield of styrene oxide. The negative influence of halides towards the epoxidation of olefins with MTO is already known in literature. Halides are oxidized by MTO to the corresponding hypohalous acids, which can catalyze the disproportionation of hydrogen peroxide [54, 55]. Recycling experiments were done, with a yield of 78% styrene epoxide after the second run. It is noteworthy that with the recycling procedure used, only 58% of the IL could be recovered.

The first report of H₂O₂-promoted epoxidation with MTO carried out in ILs was by Herrmann et al. [5]. In this work, cyclooctene was oxidized in four different water-equilibrated ILs, namely [bmim]BF₄, [bmim]PF₆, [bmim]NTf₂, and [omim]NTf₂, with Schiff- and Lewis-base adducts of MTO and ligands **42** and **43** (Fig. 19) as catalyst. The MTO adducts have shown higher yields of cyclooctene oxide compared to MTO in any of the IL used, however without any addition of solvent only diol formation was observed. In all cases, the MTO/**42** system led to higher yields than MTO/**43**. The highest activity of both systems was observed when applying ionic liquid [bmim]PF₆ as solvent.

Fig. 19 Schiff- and Lewis-base ligands of MTO



Scheme 2 MTO-catalyzed epoxidation of monoterpenes

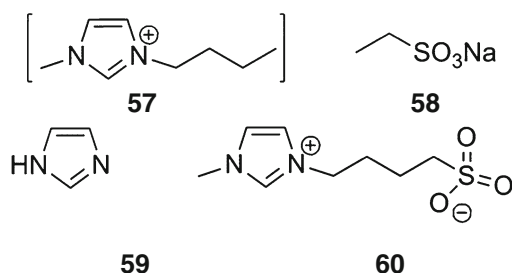
In 2009, Saladino et al. [56] published an efficient catalytic epoxidation system of monoterpenes with MTO. In this work, MTO (5.0 mol%) was applied as catalyst for the conversion of monoterpenes such as 1(S)-(+)-3-carene **44**, 1(R)-(+)-limonene **46**, geraniol **49**, and nerol **53** to their corresponding epoxides, using UHP as oxidant and [bmim]BF₄ and [bmim]PF₆ as solvents (Scheme 2).

The epoxidation of **44** with MTO in ILs resulted in **45** as the only product and was more selective than in CH₂Cl₂ (only 75% yield) (Table 17). Moreover, the TON and TOF values of [bmim]BF₄ and CH₂Cl₂ are the same. The oxidation of **46** with MTO gave the bis-peroxide **47** as major product (88% yield). Interestingly, with CH₂Cl₂ as solvent, the ratio is inverted (13% yield for **47**). The oxidation of allylic monoterpenes **49** and **53** proceeded selectively at the more electron-rich 6,7-double bond.

Table 17 Oxidation of monoterpenes with MTO using UHP as oxidant^a

Entry	Substrate	Solvent	Temp (°C)	Time (h)	Product(s)	Conversion (%)	Yield (%)
1	44	[bmim]BF ₄	RT	1	45	98	98
2		[bmim]PF ₆	RT	2		98	98
3	46	[bmim]BF ₄	RT	2	47 (48)	98	88 (10)
4	49	[bmim]BF ₄	20	1	50 (51) [53]	95	8 (38) [50]
5		[bmim]BF ₄	10	2	50 (51)	92	6 (86)
6	53	[bmim]BF ₄	20	1	54 (55) [57]	98	6 (39) [54]
7		[bmim]BF ₄	10	2	54 (55) [57]	98	6 (91) [3]

^aReaction conditions: 1.0 mmol substrate, 2.0 equiv. UHP, 5 mol% MTO, 1–2 h

Fig. 20 Structures of the additives**Table 18** Epoxidation of different olefins with MTO and A4 as additive^a

Entry	Substrate	Time (h)	Conversion (%)	Selectivity (%)
1	Cyclohexene	6	99	92.70 ^b
2	Styrene	12	60	69.13 ^b
3	1-Decene	12	30	97.85 ^b
4	1,2-Dihydronaphthalene	2	96	85.80 ^b
5	1-Phenylcyclohexene	7	99	61.54 ^b
6	α -Methylstyrene	7	95	86.85 ^b

^aReaction conditions: 5.0 mmol substrate, 2.0 equiv. H₂O₂ (30 wt%), 1 mol% MTO, 1 mol% MBSIB, 7.0 mL MeOH, 0°C

^bNo additive was added

Michel et al. [57] investigated the influence of additives, oxidants, and solvents on the epoxidation of α -pinene with MTO as catalyst. Dichloromethane has proven to be the best solvent, while the investigated IL [bmim]PF₆ was not suitable for the tested olefins.

In 2011, Zhang et al. [58] applied several additives (10:1 ratio with MTO) in the MTO-catalyzed epoxidation of cyclohexene (Fig. 20).

The additive **60** turned out to be the best choice, but was inferior to the MTO-pyridine system with respect to the epoxide selectivity [59]. In all cases, the selectivity increased, when **60** was used as additive. The highest increase was observed, when styrene was used as a substrate (Table 18). Furthermore, after full conversion of cyclohexene (Entry 1), a fresh batch of substrate and oxidant was

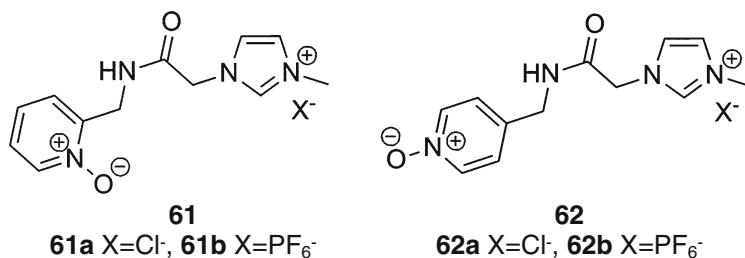
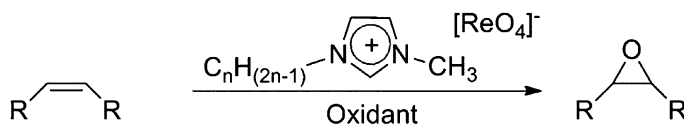


Fig. 21 The structures of the used additives



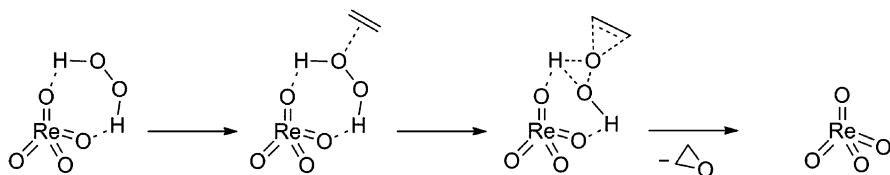
Scheme 3 Epoxidation of olefins with perrhenate containing ionic liquids

added to the reaction mixture and a new run was taken. This recycling procedure could be repeated for four times with only a small decrease in selectivity (99.1% conversion and 75.1% selectivity after fifth run).

In 2013, the same group tagged pyridine *N*-Oxide via an amide linker to an imidazolium moiety (Fig. 21) [60]. The pyridine *N*-oxide functionalized imidazolium salts were used in a ratio of 1:1 (ligand:catalyst) in the MTO-catalyzed epoxidation of olefins in MeOH as solvent and H₂O₂ as oxygen source. The addition of the ligands to the reaction mixture had a significant impact on the selectivity of the epoxidation reaction, with an increase from 13 % to 86 % for styrene oxide. However, a slight decrease in conversion was observed with addition of the ligands. The substitution patterns on the pyridine moiety have shown no influence on the activity or the selectivity. Interestingly, catalytic runs in ionic liquids with chloride as anion have performed better as those with PF₆⁻.

Water- and air-stable perrhenate ILs were first reported in 2010 by Yang et al. with the synthesis of several *N*-alkyl pyridinium perrhenates [61]. The same group reported the synthesis of imidazolium-based perrhenate ionic liquids [62]. The authors describe the synthesis of these ionic liquids, their thermodynamic and physicochemical properties. In this work, the physicochemical properties of several different 1-methyl-3-alkyl substituted imidazolium perrhenates were examined, but no application in the epoxidation of olefins was mentioned.

Very recently Kühn et al. [63] reported the epoxidation of olefins mediated by perrhenates in ILs, conversions and selectivities of 99% were reported for cyclooctene (Scheme 3). Furthermore, the mechanism of the reaction was investigated by in-situ Raman, FT-IR, and NMR spectroscopy and corroborated by DFT calculations. It could be shown that the epoxidation occurs via an outer-sphere activation of H₂O₂ by the formation of hydrogen bonds between perrhenate



Scheme 4 Calculated reaction pathway of direct epoxidation via hydrogen bonding

and the hydrogen peroxide, which makes it susceptible to an attack from the olefin (Scheme 4). Additionally, these ionic liquids could be recycled for at least 8 times without any significant loss of activity (yield cyclooctene 98–99%).

1.1.4 Group VIII Metals (Fe, Ru)

Iron

In 2002, Chauhan et al. [64] described the epoxidation of several alkenes with the sodium salt iron (III) porphyrin catalyst $\text{Cl}_8\text{TPPS}_4\text{Fe(III)}$ in a biphasic mixture of ionic liquid and dichloromethane. The yields of the corresponding epoxide ranged from fair to good (Table 19). In case of styrene and cyclooctene, the reaction was also run in homogeneous solution of water/acetonitrile (1:1: v/v). The yields were inferior compared to the yield obtained with the biphasic dichloromethane/IL system (17% in case of styrene and 21% in case of cyclooctene). The biphasic system allowed the recycling of the catalyst and showed comparable results even after 4–5 runs (62% yield after fifth run).

In 2012, the same group used two different iron (III) porphyrin catalysts for the epoxidation of guggulsterone **63** in $[\text{bmim}]\text{BF}_4$ and H_2O_2 as oxidizing agent (Scheme 5) [65]. With the complex $\text{Cl}_8\text{TPPS}_4\text{Fe(III)}$ in 2 mL ionic liquid **64** could be obtained after 3 h reaction time, whereas with the catalyst $\text{Cl}_8\text{TTPPF}_e(\text{III})\text{Cl}$ in 15 mL dichloromethane, only 16.1% of **64** could be obtained after the same time.

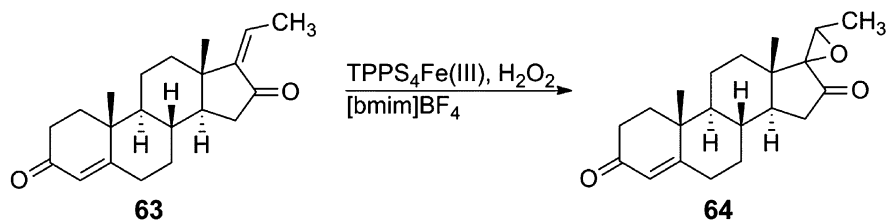
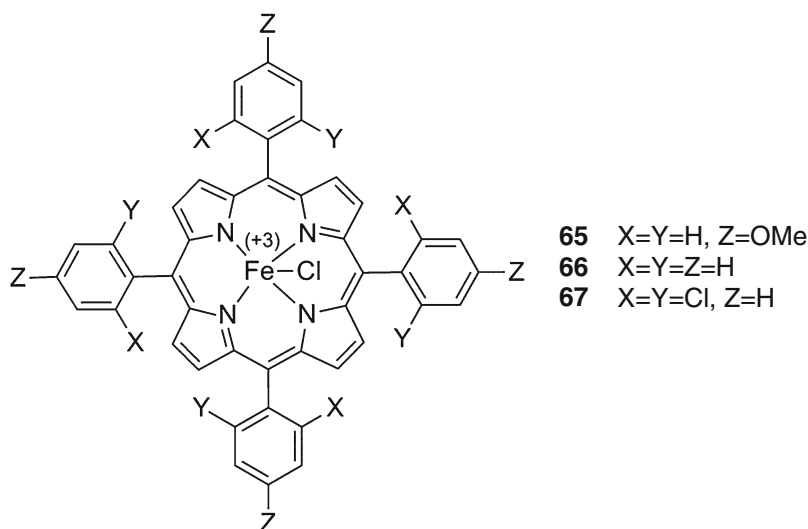
The epoxidation of substrates with both electron-rich and electron-deficient double bonds utilizing different iron (III) catalysts was reported by the same group in 2011 [66]. They used different *meso*-tetraarylporphyrin iron(III) chlorides [TAPFe(III)Cl] (Fig. 22) in different imidazolium ionic liquids $[\text{bmim}][\text{X}]$ ($\text{X} = \text{Br}, \text{BF}_4, \text{PF}_6$ and OAc) and H_2O_2 or PhIO as oxidizing agent.

With latter, only the electron-rich olefins were epoxidized (**70** and **73**), whereas with H_2O_2 a mixture of both were obtained with the electron-poor epoxide as major product (**69** and **72**). When the reaction was carried out in ionic liquids, a significant increase in the yield could be observed compared to organic solvents such as dichloromethane or acetonitrile. This might be due to the better stabilization of highly ionic iron (III) porphyrin intermediates. In all cases, catalyst **65** gave the best

Table 19 Alkene epoxidation with hydrogen peroxide catalyzed by 1 under a nitrogen atmosphere in dichloromethane/[bmim]Br^a

Entry	Substrate	Yield (%), time (h)
1	Styrene	74 (4)
2	<i>p</i> -Chlorostyrene	70 (5)
3	Cyclohexene	42 (5)
4	<i>cis</i> -Cyclooctene	81 (4)

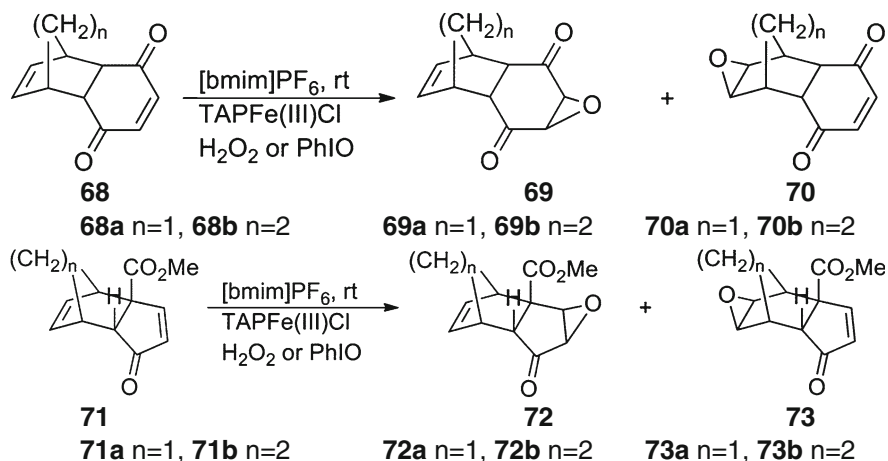
^aReaction conditions: 125.0 mmol substrate, 1.0 equiv. H₂O₂ (30 wt%), 1 mol% Cl₈TPPS₄Fe(III), 2.0 mL [bmim]Br, 5.0 mL dichloromethane, RT, 4–5 h reaction time, under nitrogen atmosphere

**Scheme 5** Epoxidation of guggulsterone with iron (III) porphyrin catalyst in [bmim]BF₄**Fig. 22** Structure of the used iron (III) porphyrin catalysts

results. For the epoxidation of **69a** the best results were obtained with [bmim]OAc as ionic liquid (Scheme 6).

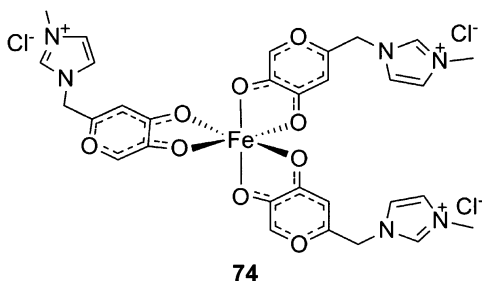
In 2012, Neto et al. [67] used a ionically tagged imidazolium-based iron(III) complex (Fig. 23) for the epoxidation of alkenes in ionic liquids with air and hydrogen peroxide.

The air oxidation of methyl oleate with **74** in the corresponding ionic liquids [bmim][X] (X = BF₄, PF₆ and NTF₂) afforded the epoxide in good yields



Scheme 6 Epoxidation of substrates with H_2O_2 or PhIO catalyzed by TAPF(III)Cl in IL

Fig. 23 Structure of the ionically tagged iron(III) complex



(80%, 81%, and 83%, respectively) as the exclusive product. It is noteworthy that when the reaction is carried out in the absence of any IL, good yields of epoxide were obtained (88%). When the reactions were turned out at 70°C a decomposition of $[\text{bmim}]\text{PF}_6$ was observed; the system turned black. Reactions without the presence of oxygen gave no conversion. The best epoxide yield could be obtained at a temperature of 90°C . The epoxidation of different oils and oleic acid resulted in good to excellent yields (79–89%). However, substrates such as styrene, methylacrylate cyclohexene and others gave no conversion. The oxidation method works good for biomass derivatives, especially for biodiesel, oils, and fatty acids.

When hydrogen peroxide was used as oxidizing agent, methyl oleate oxide was obtained in good yields (68% for $[\text{emim}]\text{BF}_4$, 81% for $[\text{emim}]\text{PF}_6$ and 81% for $[\text{emim}]\text{NTf}_2$, respectively). The reactions were run at 30°C . However, with water as solvent a yield of 80% epoxide could be obtained. Recycling experiments with H_2O_2 resulted in a drastically decrease in the yield (3% yield after fifth run). Because no leaching could be detected by means of ICP-AES analysis, the authors see the catalyst deactivation as reason for the low yield. On the other hand, recycling experiments with air as the oxidizing agent gave no loss of activity, even after ten cycles (Fig. 24).

Fig. 24 Epoxidation of olefins with complex **75**

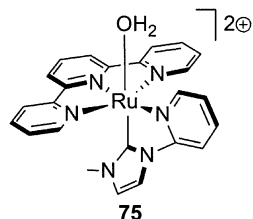


Table 20 Epoxidation of olefins with Ru-NHC complex **75**

Entry	Substrate	Conversion (%)		Selectivity (%)	
		IL: CH ₂ Cl ₂	CH ₂ Cl ₂	IL: CH ₂ Cl ₂	CH ₂ Cl ₂
1	Styrene	62	99.9	57	61
2	<i>trans</i> - β -methyl styrene	99.9	–	99.9	–
3	<i>cis</i> - β -methyl styrene	99.9	81	99 ^a	94 ^a
4	Cyclooctene	99.9	99.9	99.9	94
5	1-Octene	45	98	98	80
6	1-Methyl cyclohexene	90	–	59	–
7	4-Vinyl cyclohexene	73	99	93 ^b	97 ^b

Reaction conditions: substrate 50 mM, catalyst 0.5 mM, PhI(OAc)₂ 100 mM, solvent 2 mL, room temperature, 24 h

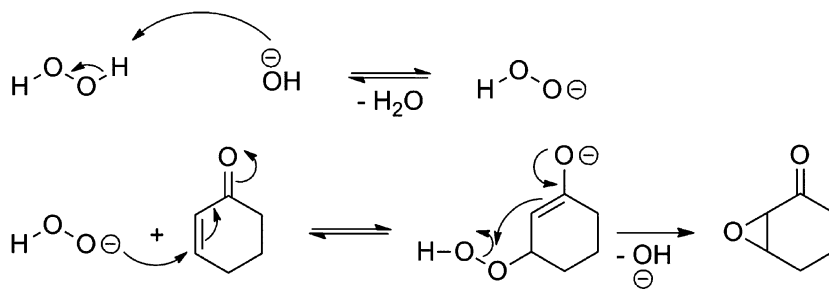
^aSpecific for *cis*-epoxide

^bEpoxidation exclusively at the cyclohexene ring

Ruthenium

Although ruthenium complexes have been widely applied in the homogenous catalysis, only one example of epoxidation of olefins in ionic liquids has been reported to date. Romero and Rodriguez et al. (2011) have synthesized NHC-Ru complex **75** and used it for the epoxidation of aliphatic and cyclic alkenes at room temperature in a [bmim]PF₆:CH₂Cl₂ solvent mixture, with PhI(OAc)₂ as oxygen source.

As can be seen in table 20 for styrene, 1-octene and 4-vinyl cyclohexene (Entry 1, 5 and 7) epoxide yields decrease when as solvent mixture containing ionic liquid is utilized. Yet, selectivities towards epoxide formation were slightly better in the ionic liquid organic solvent mixture, for all tested substrates with exception of 4-vinyl cyclohexene. When cyclooctene is used as substrate a beneficial impact of using a solvent mixture containing IL on conversion and selectivity to the epoxide can be proclaimed (table 20, Entry 4). Additionally the authors were able to reuse the catalytic system for ten runs achieving consistent conversions and yields up to 98% whereas when using CH₂Cl₂ for the recycling experiment the conversion drops to 35% in the second run [68].



Scheme 7 Reaction mechanism for the nucleophilic epoxidation of electron-deficient olefins

1.2 Metal-Free Catalysts

1.2.1 Nucleophilic Epoxidation of Electron-Deficient Olefins

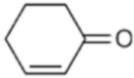
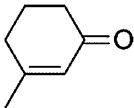
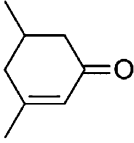
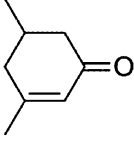
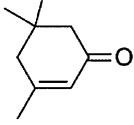
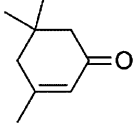
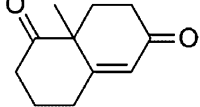
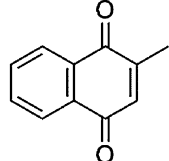
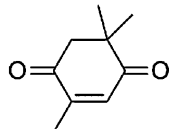
The epoxides of α,β -unsaturated carbonyl compounds are widely applied as intermediates in pharmaceutical and fine chemicals. The reaction requires strong alkaline conditions. First, the nucleophilic oxidant (peroxide anion) is generated using a strong base such as NaOH. After the conjugated addition to the olefin a carbanion is formed as an intermediate. A hydroxide anion then acts as a leaving group and the epoxide is formed (Scheme 7). It has to be mentioned that the substrate scope is limited to electron-poor olefins which implies that an industrial application is unlikely.

The first example of metal-free epoxidation of olefins carried out in ionic liquids was reported in 2002, by Bortolini et al. [69]. In this work, electrophilic alkenes of vitamin K structure were oxidized to their corresponding epoxides with a NaOH/ H_2O_2 -system in [bmim] BF_4 and [bmim] PF_6 as solvents. Almost quantitative conversions were obtained with the less hindered substrates. For sterically more demanding substrates either a longer reaction time or a larger excess of H_2O_2 was needed to complete the reaction. One year later, the same group extended the substrate scope and also screened several other ionic liquids [70]. The results are shown in Table 21. The best results were obtained with [bmim] CF_3SO_3 . It was observed that with longer reaction times, [bmim] BF_4 becomes unstable.

The epoxidation reactions of electron-deficient α,β -unsaturated carbonyl compounds were investigated by Yang et al. [71]. In this work, olefins were oxidized in an IL/water biphasic system using NaOH/ H_2O_2 as terminal oxidant. The conversions range from fair to excellent but with an excellent selectivity in all cases. [bmim] PF_6 / H_2O_2 turned out to be the most efficient system. With longer alkyl chains, the conversions decreased. Furthermore, the ionic liquid could be recycled up to eight times, without losing significant activity.

In 2004 Bernini et al. [72] showed a convenient and efficient method for the epoxidation of chromone, isoflavone, and chalcone derivatives using a NaOH/ H_2O_2 -system with [bmim] BF_4 as solvent (Fig. 25). In all cases, the ionic liquid was superior to common organic solvents such as dichloromethane and acetone.

Table 21 Base-catalyzed epoxidation of electrophilic alkenes with H₂O₂ in ionic liquids with different anions [X]^a

Entry	Substrate	Epoxide yield % (time, min)			
		[BF ₄] ⁻	[CF ₃ SO ₃] ⁻	[PF ₆] ⁻	NTF ₂ ⁻
1		98 (5)	99 (5)	98 (5)	99 (5)
2		97 (5)	99 (5)	99 (30)	84 (5) 99 (30)
3		–	97 (30)	25 (30) 99 (90)	22 (30) 47 (90)
4		–	99 (30)	20 (30) 85 (120)	2 (30)
5		Traces (120)	80 (120)	Traces (120)	41 (120)
6		–	40 (30) 81 (300)	6 (30) 15 (300)	7 (300)
7		99 (5)	99 (1)	99 (5)	99 (1)
8		–	99 (1)	99 (60)	99 (60)
9		–	–	90 (15)	–

^aReaction conditions: 1 mmol substrate, 3.0 equiv. H₂O₂ (30 wt%), 2.0 equiv. NaOH, 1 mL ionic liquid, 25°C, addition of 4.0 equiv. water

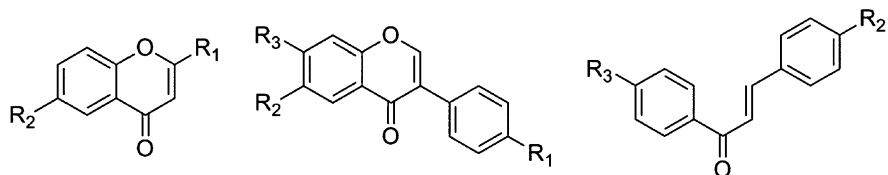


Fig. 25 Epoxidation of chromones, isoflavones, and chalcones

Chan et al. [73] reported about a process for the epoxidation of electrophilic alkenes, where the oxidant H_2O_2 is generated in situ through electrosynthesis from oxygen in an IL/aqueous NaOH mixture. [bmim] BF_4 was chosen as ionic liquid. A number of α,β -unsaturated ketones were oxidized to their corresponding epoxides in fair to excellent yields (65–92%). It was additionally shown that the [bmim] BF_4 /NaOH system could be recycled up to four times, with only little decrease in yield (86% after first run; 80% after fifth run).

Okamoto [74] used in 2006 imidazolium salts as phase transfer catalysts in a liquid–liquid phase system. The authors investigated the structure–activity relationship of the catalysts and their influence on the nucleophilic epoxidation of α,β -unsaturated carbonyl compounds. The two-phase system consisted of an aqueous NaOCl solution and an organic solvent (toluene or dichloromethane). Interestingly, all imidazolium salts exhibited catalytic activity except those who were not substituted at the C2-position. The activity increased with longer alkyl chains at the 1- and 3-positions of the imidazolium ion, presumably due to enhanced solubility in the organic solvent.

Han et al. [32] reported the epoxidation of styrene using carbon dioxide and a KOH/ H_2O_2 -system with different ionic liquids as solvents. Styrene was converted to its epoxide in bad to fair yields. The best result was obtained, when applying [bmim] BF_4 as ionic liquid (95% conversion; 69% yield). [bmim]Cl gave low yields (34%) and [bmim] PF_6 and the remaining ones gave very bad conversion and yields (<2%). In case of [bmim] PF_6 this is explained by the bad miscibility with H_2O_2 . Generally, the yield of [bmim] BF_4 and [bmim]Cl was higher than those obtained with organic solvents such as ethanol and acetonitrile.

Chiral quininium bromide was used as catalyst for the enantioselective epoxidation of chalcones in different ionic liquids by Pal et al. [75]. The authors reported that [bmim] BF_4 is the most convenient solvent at a temperature of -5°C . Several aryl-substituted enones were oxidized to their corresponding epoxides using a KOH/ H_2O_2 -system in excellent yield with fair ee (53–68%) at -5°C .

Bhagat et al. [76] synthesized an imidazolium-based IL **76**, where asparagine is tagged on the imidazolium moiety (Fig. 26). This compound was used as an equimolar additive for the asymmetric epoxidation of α,β -unsaturated ketones in a H_2O_2 /NaOH-system with DMF as solvent. The epoxides were obtained in good to excellent yield with ee's ranging from 80% to 90%. The system was reusable for up to five times without significant loss of activity.

Fig. 26 Asparagine-tagged imidazolium-based ionic liquid

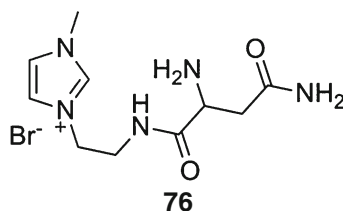


Table 22 Catalytic epoxidation of olefins with [mdhqm]NTf₂

Entry	Substrate	Conversion (%) (TON)	
		MeCN/H ₂ O	(bmim)OTf/H ₂ O (1:1)
1	Cyclohexene	92 (19)	100 (20)
2	1-Phenylcyclohexen	75 (15)	63 (13)
3	Methyltransstilbene	66 (13)	6 (1)
4	Hexen	18 (4)	14 (3)
5	<i>trans</i> -Stilbene	0	0

Reaction conditions: 2.0 equiv. Oxone™, 4.0 equiv. Na₂CO₃, H₂O:solvent 1:1, 0°C, 18 h reaction time

1.2.2 Isoquinoline Systems

In 2008, Welton et al. [77] used several ionic liquids as cosolvents for the catalytic epoxidation of alkenes with Oxone® and *N*-alkyl-3,4-dihydroquinolinium salts. Due to the reported results it can be proclaimed that the ionic liquid has no positive effect on conversions and turnover numbers (Table 22). The best results were obtained with the ionic liquid [bmim]OTf. Interestingly, in hydrophobic ILs such as [emim]NTf₂, the epoxidation does not take place. The mechanism is shown in Fig. 27.

In 2012, Baj et al. [78] reported the epoxidation of alkenes with several *N*-alkyl-3,4-dihydroquinolinium salts with Oxone® and Na₂CO₃. The best results in the epoxidation of cyclohexene and cyclooctene obtained with [hdhmq]NTf₂ were 73% and 58%, respectively. In most cases, the NTf₂⁻ anion was superior to Br⁻ and BF₄⁻.

2 Enzymatic Catalysts

Enzyme-catalyzed epoxidation reactions normally follow the principle of a chemo-enzymatic cascade reaction (Scheme 8). Lipases, such as *Candida antarctica* Lipase B (CALB), catalyze the reaction of carboxylic acids with H₂O₂ to their corresponding peroxy acids (enzymatic reaction). These peracids are capable of

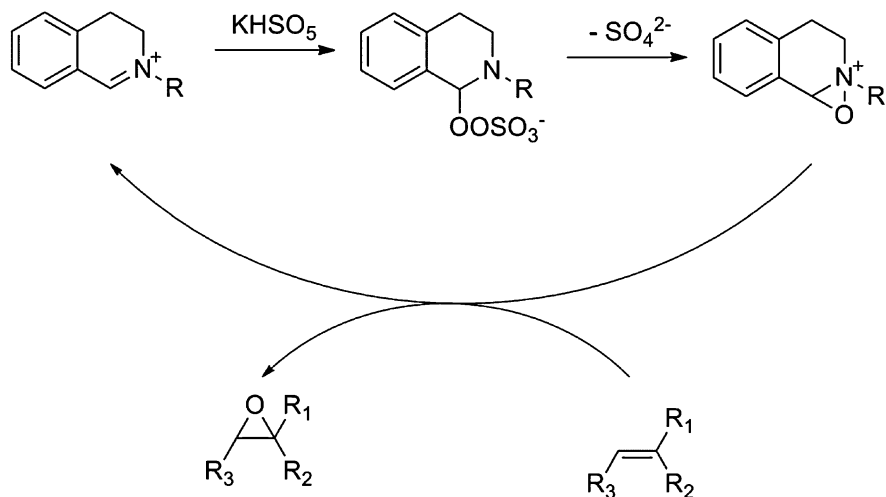
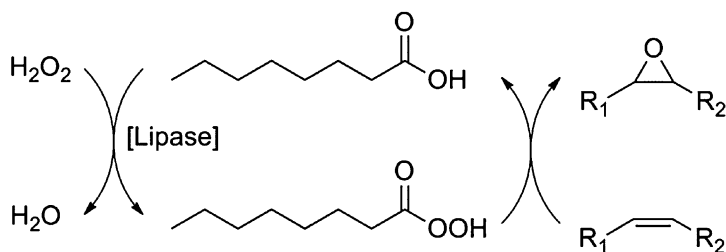


Fig. 27 Mechanism for the epoxydation of olefins with dihydroisoquinolinium salts



Scheme 8 Chemo-enzymatic cascade for the epoxydation of olefins with peracids

oxidizing olefins to epoxides (chemical reaction). Octanoic acid is the common acyl donor.

The first enzymatic epoxydation reaction in ILs was reported in 2000 by Sheldon et al. [79]. In this work, cyclohexene was oxidized by peroctanoic acid, generated in situ from octanoic with H_2O_2 by Novozym 435. With [bmim] BF_4 as solvent, a yield of 83% epoxide was obtained after 24 h compared to 93% in acetonitrile.

The same enzyme (*CALB*) was used in 2007 for the epoxydation of (+)-3-carene [80]. Again, octanoic acid was chosen as acyl donor and H_2O_2 as oxidizing agent. The highest conversions could be obtained when toluene, dichloromethane, and acetonitrile were used (all > 99%) whereas hexane gave the worst performance. When mixtures of dichloromethane:IL (10:1 v/v) were applied, different effects could be observed. With [bmim] BF_4 as IL, no conversion was obtained, whereas with [bmim] PF_6 the conversions to the epoxide were higher than with hexane and lower than with pure dichloromethane. These results might be explained with the higher hydrophilic property of the BF_4^- anion, thus absorbing water from the

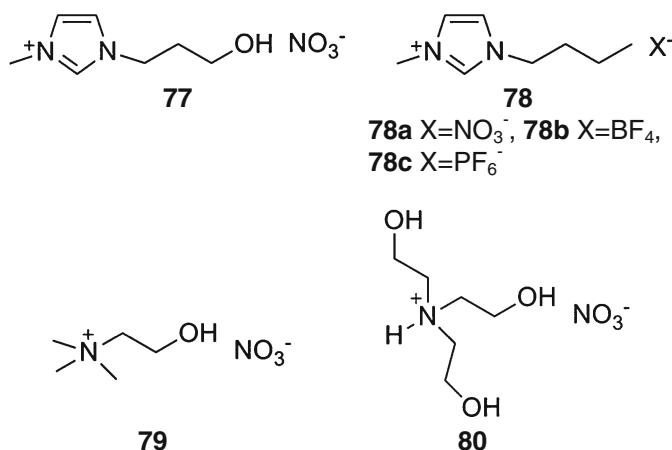


Fig. 28 Structures of the applied ionic liquids

enzyme, which leads to deactivation. Besides, Novozym 435 (CALB immobilized on acrylic resin) could be recycled four times without notable loss of activity (85% conversion after fifth run).

Goswami et al. [81] reported the *CALB*-catalyzed enantioselective epoxidation of styrene derivatives with a chiral ketone and UHP as oxygen source in different solvents. The best result for the epoxidation of 4-hydroxy styrene could be obtained with a mixture of dry dichloromethane and THF (4:1) (75% yield, 57% ee), the worst was obtained with HFIP (40% yield, 51% ee). The ionic liquid [bmim]Br performed and comparable to dry THF (45% yield, 50% ee). Furthermore, the chiral additive and the enzyme could be recovered and used for further runs. There was no significant loss in the activity observed with respect to the yield of the corresponding product 4-hydroxy styrene oxide (66% yield after sixth run).

In 2011, Suarez and Neto [82] applied several hydrophobic and hydrophilic ILs as solvents for the lipase-catalyzed epoxidation of methyl oleate by nine different enzymes. No acyl donor was used in this case. The best result of epoxide yield was obtained with the enzyme from *Aspergillus niger* in [bmim]BF₄ after 1 h reaction time (89%). Interestingly, when the reaction was carried out in the hydrophobic ILs [bmim]PF₆ and [bmim]NTf₂ with the same enzyme, 64% and 67% yield epoxide were obtained after the same time, respectively. However, when the reactions were carried out in hydrophilic medium, a significant increase in diol formation was observed. This should be expected since more water is present in the hydrophilic ILs leading to ring opening of the epoxide.

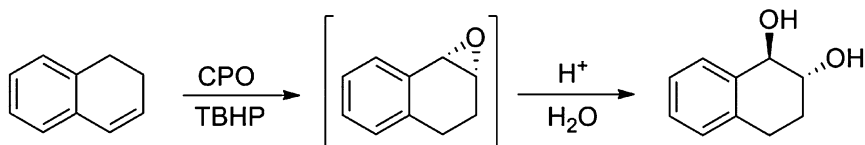
Sheldon and Arends [83] synthesized several ionic liquids with nitrate anions (Fig. 28) and investigated their application as solvents for the lipase-catalyzed epoxidation of different olefins with hydrogen peroxide as oxidant and octanoic acid as acyl donor. Nitrate was chosen because it is stable under oxidative conditions, nonpoisonous, neutral, biocompatible, and cheap.

Table 23 CalB-catalyzed epoxidation of olefins in ionic liquids^a

Entry	Substrate	Yield epoxide (%), used IL				
		77	78b	78c	79	80
1	Cyclohexene	71 86 ^b	62 73 ^b	56	79 ^b	56 ^b
2	Cyclooctene	69	46	38	–	–
3	Styrene	44	40	41	–	–

^aReaction conditions: 1.48 mmol substrate, 1.7 equiv. H₂O₂ (50%), 10 mg Novozym 435, 0.2 mmol octanoic acid, 1.0 mL IL, RT, 24 h reaction time

^bExperiments at 50°C for 5 h

**Scheme 9** CPO-catalyzed epoxidation of 1,2-dihydronaphthalene

The best results could be obtained with the hydrogen bond donating ionic liquid 77 as solvent (Table 23). Styren was the most demanding substrate with a yield of 44%.

A lipase-catalyzed epoxidation of citronellol with UHP as oxidant and octanoic acid as acyl donor was reported by da Silva et al. [84]. The best results were obtained with chloroform and dichloromethane as solvents (both > 99% conversion). When mixtures of chloroform/[bmim][X] (where X = BF₄, SCN, Cl) were used in a ratio of 9:1 (v/v), no conversion was observed. With the more hydrophobic ionic liquid [bmim]PF₆, the epoxide was obtained in moderate yields of 33% after 24 h reaction time. Mixtures of MTBE/[bmim][X], where X = Cl and PF₆ (9:1, v/v) showed moderate degrees of conversion, 38% and 31%, respectively. These were superior to those obtained with pure MTBE. The same enhancement was observed when mixtures of *n*-hexane/[bmim]BF₄ were applied (31% yield with mixture compared to 24% with pure hexane).

The first epoxidation of olefins with chloroperoxidase (CPO) and ILs as cosolvent was first reported in 2004 by Sanfilippo et al. [85]. In this work, 1,2-dihydronaphthalene was transformed to its corresponding epoxide catalyzed by chloroperoxidase from *C. fumago* in a homogenous reaction media formed by citrate buffer containing 10% (v/v) of several hydrophilic ionic liquids, namely [mmim]MeSO₄, [bmim]MeSO₄, [bmim]Cl, and [bmim]BF₄ using TBHP as terminal oxidant (Scheme 9). Due to the fast hydrolytic ring opening in the aqueous medium the product is recovered as (1R,2R)-(+)-dihydroxytetrahydronaphthalene.

The enzyme showed no activity and no conversion after 24 h in pure ionic liquid. In the buffered biphasic mixtures epoxidation activity was observed for all ILs except [bmim]BF₄. With [bmim]Cl the formation of the 1,2-halohydrin was observed. The best results were obtained with [mmim]MeSO₄ and [bmim]MeSO₄ as cosolvent in 10% (v/v) (Table 24).

Table 24 Epoxidation of 1,2-dihydronaphthalene with CPO in different media

Entry	Co-solvent	Conversion (%)	ee Product (%)
1	None	48	85
2	[mmim]MeSO ₄	43	73
3	[bmim]MeSO ₄	42	77

Reaction conditions: 0.092 mmol substrate, 1.5 equiv. TBHP, enzyme (800 U)10% IL (v/v), citrate buffer 0.1 N (pH 5), 1,200 rpm, RT, 3 h reaction time

Jiang et al. [86] reported in 2010 the CPO-catalyzed asymmetric epoxidation of 3-chloropropene with TBHP as oxidizing agent in phosphate-buffered solutions. The best result was obtained when a mixture of [emim]Br/aqueous phosphate buffer (1.6% v/v) was chosen as solvent (88.8% yield; 97.1% ee) after 1 h reaction time. It was superior to the pure phosphate-buffered solution (41.6% yield, 93.9% ee).

3 Heterogeneous Catalysts

3.1 Group VI Metals (Mo, W)

3.1.1 Molybdenum

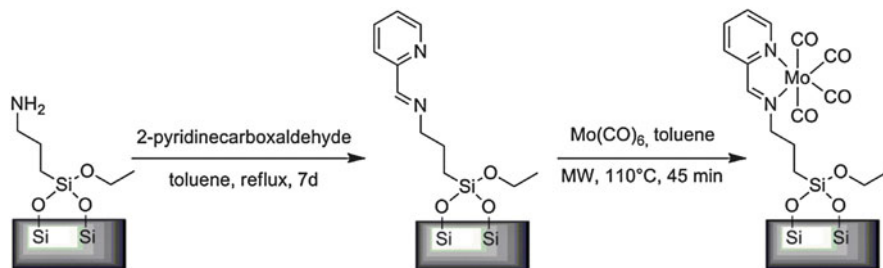
In 2009 Gonçalves et al. reported about the immobilization of molybdenum tetracarbonyl-pyridylimine complexes and their use as catalyst precursors for the epoxidation of cyclooctene [87]. The heterogeneous catalyst was synthesized by the condensation reaction of 2-pyridinecarboxyaldehyde with amino propyl groups that were covalently attached to the ordered mesoporous silica MCM-41 (Scheme 10).

The ligand-silica material was then microwave-assisted heated with Mo(CO)₆ in toluene at 110°C. The authors utilized the compound as precursor for the epoxidation of cyclooctene in solventless conditions and in [bmim]BF₄ and compared the results with the conversions achieved with a homogenous analog compound.

Cyclooctene, TBHP and the catalyst precursor in the ionic liquid formed a biphasic system and the conversion was slower than that observed without cosolvent (Table 25, Entry 1 and 2), but the authors were able to run the system for at least five consecutive runs without any effect on the activity.

As can be seen in Table 25, the epoxidation of cyclooctene using MCM-41-pyim/Mo as catalyst is a lot slower than the one observed for its homogenous analog.

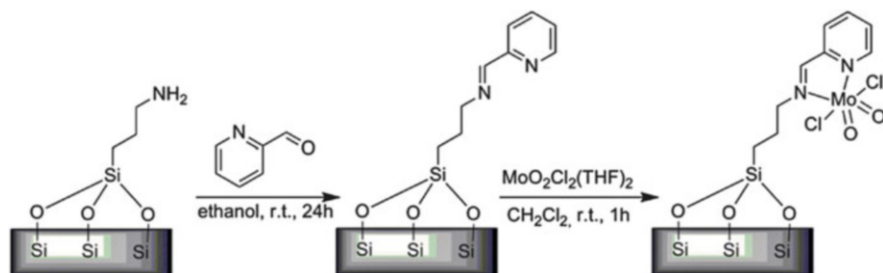
The group affiliated this to the presumption that some metal sites are inaccessible to the reagents and therefore the number of active sites might be smaller than for the free complex. When using [bmim]BF₄ as cosolvent for the MCM-41-pyim/Mo-system the authors were able to recycle the reaction system three times without lowering the cyclooctene oxide selectivity.



Scheme 10 Synthesis of MCM-41-pyim/Mo

Table 25 Cyclooctene epoxidation with TBHP

Entry	Sample	Solvent	Conversion (%)
1	<i>cis</i> -[Mo(CO) ₄ (pyim)]	No solvent	100
2	<i>cis</i> -[Mo(CO) ₄ (pyim)]	[bmim]BF ₄	100
3	MCM-41-pyim/Mo	No solvent	36
4	MCM-41-pyim/Mo	[bmim]BF ₄	22



Scheme 11 Synthesis of the MTS-pym/Mo

The same group compared the activity of a dichlorodioxomolybdenum(VI)-pyridylimine complex when attached to a micelle-templated silica (MTS) with the compound being immobilized in an ionic liquid.

Through a condensation reaction of 2-pyridinecarboxaldehyde with either 3-aminopropyl groups attached to MTS or *n*-propylamine the authors were able to gain the *N*-(*n*-propyl)-2-pyridylmethanimine (pyim) ligand or its immobilized analog (pyim-MTS) (Scheme 11) [88]. The treatment of the solvent adduct $\text{MoO}_2\text{Cl}_2(\text{THF})_2$ with the immobilized or the free ligand in dichloromethane resulted in the requested catalyst precursors.

When the complex $\text{MoO}_2\text{Cl}_2(\text{pyim})$ was used for the epoxidation reaction a TOF of $1,855 \text{ mol mol}_{\text{Cat}}^{-1} \text{ h}^{-1}$ was obtained (93% conversion within 10 min) while the reaction in [bmim]BF₄ was with an epoxide yield of 96% after 24 h significantly slower although the overall yield was higher than with the immobilized catalyst (85% in 24 h). By applying the MTS-pyim/Mo compound in the epoxidation of cyclooctene at different temperatures a temperature-dependent leaching of the active species was verified.

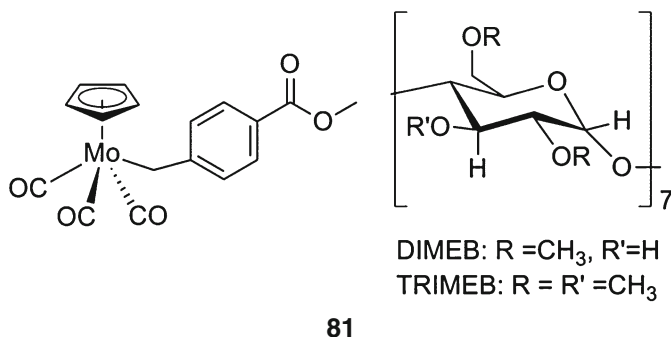


Fig. 29 Mo-Cp compound and cyclodextrins

Table 26 Epoxidation of cyclooctene under different conditions

Entry	Catalyst	Oxidant	Solvents	Yield (%)
1	81	TBHP (decane)	No solvent	100
2		TBHP aq.	No solvent	95
3			H ₂ O/hexane	80
4			IL/hexane	9
5		H ₂ O ₂	H ₂ O/hexane	78
6	81@DIMEB	TBHP (decane)	No solvent	96
7		TBHP aq.	No solvent	97
8			H ₂ O/hexane	87
9			IL/hexane	9
10		H ₂ O ₂	H ₂ O/hexane	13
11	81@TRIMEB	TBHP (decane)	No solvent	100
12		TBHP aq.	No solvent	88
13			H ₂ O/hexane	83
14			IL/hexane	8
15		H ₂ O ₂	H ₂ O/hexane	81

Reaction conditions: $T = 55^{\circ}\text{C}$, substrate = *cis*-cyclooctene, $t = 24$ h

In a recent report Gonçalves et al. described an ester-substituted cyclopentadienyl molybdenum tricarbonyl complex that is shown in Fig. 29 [89].

By mixing a solution of **81** in CH₂Cl₂ with equimolar amounts heptakis(2,6-di-*O*-methyl)- β -cyclodextrin **81@DIMEB** or heptakis(2,3,6-tri-*O*-methyl)- β -cyclodextrin **81@TRIMEB** the compound was encapsulated in the cyclodextrins.

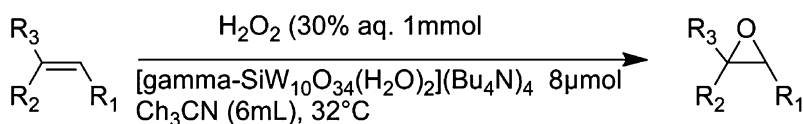
The authors tested all three substances for olefin epoxidation using *cis*-cyclooctene as model substrate. They checked different oxidants (TBHP in water and in decane, aqueous hydrogen peroxide) and several solvents with the aim of facilitating the recycling of the catalytic system. The results of these catalytic experiments are summarized in Table 26.

It can be seen that the yields are poor when an ionic liquid containing solvent mixture (Entry 4, 9 and 14) is used. The authors give no explanation for this observation.

Table 27 Epoxidation of olefins with H₂O₂

Entry	Substrate	Time (h)	Yield (%)
1	<i>cis</i> -2-octene	3	>99
2	<i>trans</i> -2-octene	7	73
3	<i>cis</i> - β -methylstyrene	2	>99
4	Cyclohexene	3	80
5	2-norbornene	2,5	80
6	Cycloheptene	2	>99
7	Cyclooctene	1	>99
8	Geraniol	4	95
9	4-methyl-3-penten-2-ol	4	90
10	(<i>z</i>)-3-methyl-3-penten-2-ol	4	90

Reaction conditions: catalyst concentration: 1 mol%, $T = 30^\circ\text{C}$, CH₃CN (0.5 mL)

**Scheme 12** Epoxidation of alkenes promoted by silicadecatungstate and aqueous H₂O₂

3.1.2 Tungsten

In 2004 Mizuno et al. [90] reported about the immobilization of the dinuclear peroxotungstate $[\{\text{W}(=\text{O})(\text{O})_2(\text{H}_2\text{O})\}_2(\mu\text{-O})]^{2-}$ on dihydroimidazolium-based ionic liquid-modified SiO₂. They applied the material for the epoxidation of olefins using H₂O₂ as oxidant. *Cis*-2-octene, *cis*- β -methylstyrene, and cyclooctene gave the best result (Table 27) with a quantitative conversion and 100% selectivity. The authors were able to recover the catalyst by filtration and reuse it for at three consecutive runs without any loss of activity.

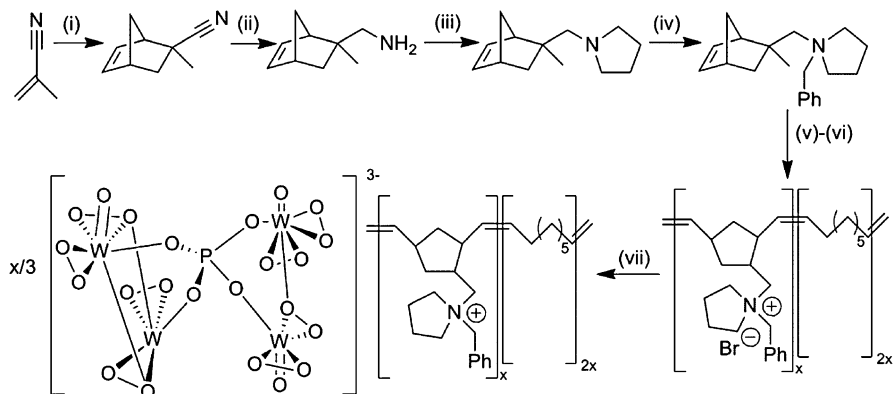
In comparison with the homogenous analog, the heterogenized catalyst did not forfeit in activity and selectivity.

Later, Mizuno [92] successfully immobilized a related silicadecatungstate catalyst on SiO₂ modified with the dihydroimidazolium cation. The compound displayed good to excellent efficiency in the epoxidation of a broad range of olefins and sulfides with a high selectivity to the desired products (Scheme 12).

Moreover the authors were able to separate and recycle the catalyst up to five times with retention of its catalytic activity. The authors used a mixture of acetonitrile and *tert*-butylalcohol as reaction solvent.

It is noteworthy that the gained results concerning stereospecificity and regioselectivity of the heterogeneous catalyst are very similar to those of the homogenous compound under the same reaction conditions.

In a recent report Hardacre and Manyar et al. [91] synthesized a peroxophosphotungstate polymer-immobilized ionic liquid phase catalyst (Scheme 13) and utilized it for the epoxidation of allylic alcohols and alkenes.



Scheme 13 Reagents and conditions: (i) cyclopentadiene, BCl_3 ; (ii) LiAlH_4 , Et_2O ; (iii) 1,4-dibromobutane, K_2CO_3 , MeCN reflux 15 h; (iv) PhCH_2Br , acetone; (v) *cis*-cyclooctene, 2 mol% $[\text{RuCl}_2(\text{PCy})_3]_2-(=\text{CHPh})$, CHCl_3 , 50°C ; (vii) $\text{H}_3[\text{PO}_4\{\text{WO}(\text{O})_2\}_4]_{\text{aq}}$, pyridine, EtOH

The catalyst gave good to excellent conversions for the epoxidation of a range of alcohols and alkenes. The authors were able to recover the catalyst containing polymer by centrifugation and siphoning off the liquid phase and observed only a minor drop in the reaction rate after four cycles.

3.2 Group VII Metals (*Mn*, *Re*)

3.2.1 Manganese

In 2006, Liu et al. reported a heterogeneous approach to the epoxidation of prochiral olefins, using complex **25** as catalyst with *m*-CPBA/NMO as oxygen source. The catalyst was immobilized on an ionic liquid-modified mesoporous silicate MCM-48, additionally $[\text{bmim}]\text{PF}_6$ was used as coating of the inorganic support (Fig. 30).

The catalytic activity towards epoxidation of olefins was tested for several substrates, summarized in Table 28. For the epoxidation of styrene (Table 28, entry 1–4) a significant loss of activity is observed for the silica supported Mn-complexes, compared to the homogenous reaction in dichloromethane. However, a considerable increase in ee's is seen for all substrates for the supported catalysts, for α -methylstyrene from 50 to 99% (Table 28, entry 5 and 6). Additionally, the catalysts could be recycled several times without any significant loss of activity [93].

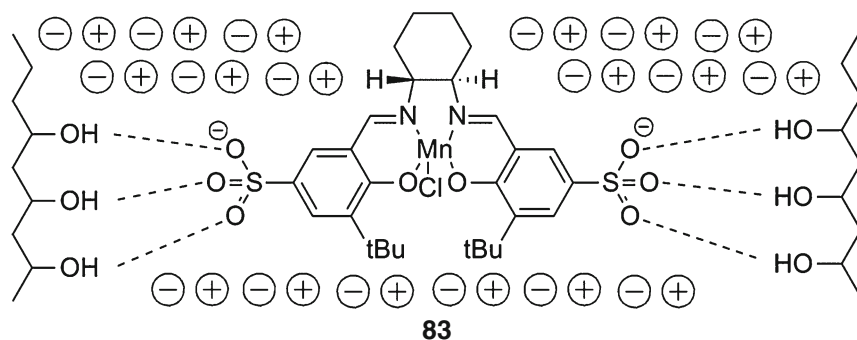
The same group reported the synthesis of a covalently bound Jacobsen-type Mn-catalyst on four different ionic liquid-modified inorganic supports, SBA-15, MCM-48, MCM-41, and SiO_2 . The epoxidation of styrene, α -methylstyrene, and indene, using *m*-CPBA/NMO as oxidant, was performed at 0°C in CH_2Cl_2 , yielded conversions up to 99% with good to excellent ee's after 1 h reaction time.

Table 28 Asymmetric epoxidation of unfunctionalized olefins

Entry	Substrate	Catalyst	Conversion (ee) (%)
1	Styrene	1(a)	99 (48)
2		1(a)/IL ^a -MCM48	50 (41)
3		1(b)	89 (64)
4		1(b)/IL-MCM48	52 (48)
5	α -Methylstyrene	1(a)	99 (50)
6		1(a)/IL-MCM48	99 (99)
7	1-Phenylcyclohexene	1(a)	96 (86)
8		1(a)/IL-MCM48	95 (92)
9		1(b)	89 (78)
10	Indene	1(b)/IL-MCM48	83 (83)
11		1(b)	97 (88)
12		1(b)/IL-MCM48	97 (87)

Reaction conditions: substrate/catalyst/m-CPBA/NMO = 1:0,01:2:5, solvent CH₂Cl₂, 0°C, 2 h

^aIL = [Bmim]PF₆

**Fig. 31** 5,5'-sulfonate functionalized Jacobsen catalyst

performed under same conditions as the previous report, but significant lower yields and ee's are obtained compared to the system used by Tang et al. [47].

3.2.2 Rhenium

The only report on immobilized MTO complexes for the epoxidation was in 2009 by Saladino et al. with polymer-supported MTO catalysts [56]. In this work, MTO was immobilized on poly(4-vinylpyridine) 2% **84** or 25% **85** cross-linked with divinylbenzene or microencapsulated MTO in polystyrene **86** (loading factor 1.0 mmol/g) (Fig. 32). With all catalysts, the substrate **44** was oxidized to its epoxide **45** in [bmim]BF₄ and [bmim]PF₆ in quantitative yield. The catalysts in ionic liquids were more selective and more reactive than in molecular solvents. Catalyst **85** showed the best reactivity with substrate **46** and **53**. In most cases, the

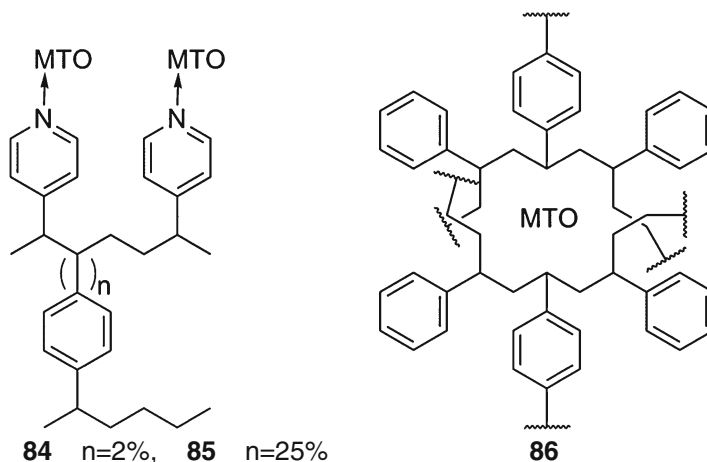


Fig. 32 Immobilized MTO complexes

heterogeneous catalysts showed a higher activity when applied in ionic liquids. In the case of substrate **44**, the catalysts **85** and **86** could be recycled up to three times without significant loss of activity.

4 Conclusion

The epoxidation of olefins with molecular catalysts in organic solvents as well as in ionic liquids is well studied. A wide range of transition metals have found application as homogenous catalysts for the epoxidation of olefins in ionic liquids or supported on different inorganic or organic carrier materials. These catalysts form stable epoxides in good to excellent yields and selectivities. As substrates for the epoxidation reactions a considerable amount of olefins have been used, from cyclic to acyclic/terminal olefins. Also, numerous epoxidation reactions of prochiral olefins have been reported with catalysts carrying chiral information. The rare use of homogenous catalysts in chemical industry is largely due to the high costs of the catalysts and the oxidation agent needed. Taking this into account, reusing these systems for several times appears to make homogenous catalysts in ionic liquids good candidates for sustainable processes, particularly since most of them work at temperatures below 60°C and low pressures. However, experiments answering the question whether ionic liquids allow catalyst recycling for thousands of times, as would be required for most industrially relevant systems are still lacking. Furthermore, the epoxidation of bulk chemicals such as ethylene or propylene is not yet sufficiently tackled.

Only few reports describing the exact role or influence of the ionic liquid during catalysis are available. Understanding the role of the ionic liquid should provide

more information about the “stabilization effect” needed during the epoxidation reaction and help making it possible to “tailor-make” ionic liquids for different reactions/reaction paths. So far, experiments are more or less constrained to “trial-and error” approaches, using a rather quasi-combinatorial approach applying many structurally different ionic liquids.

The epoxidation of olefins with homogeneous catalysts is known for more than 40 years and nearly all aspects of this reaction have been investigated in great detail. The next step in the development – especially in terms of a large-scale applications – most likely is to find molecular catalysts which match or even surpass the activity, stability, reusability, and price of the current industrial “work horses,” such as the titanium silicate TS-1, which is a very active epoxidation catalyst, but also quite active in the catalytic decomposition of the (expensive) oxidant, hydrogen peroxide. Accordingly, quite a challenge lies still ahead in this field of research.

References

1. Conte V, Floris B, Silvagni A (2007) Vanadium-catalyzed oxidation in ionic liquids. In: Kustin K, Pessoa JC, Crans DC (eds) Vanadium: the versatile metal, American Chemical Society, Michigan 28–37
2. Conte V, Fabbianesi F, Floris B et al (2009) Vanadium-catalyzed, microwave-assisted oxidations with H₂O₂ in ionic liquids. *Pure Appl Chem* 81:1265–1277
3. Neves P, Gago S, Pereira CCL et al (2009) Catalytic epoxidation and sulfoxidation activity of a dioxomolybdenum(VI) complex bearing a chiral tetradentate oxazoline ligand. *Catal Lett* 132:94–103
4. Betz D, Raith A, Cokoja M, Kuehn FE (2010) Olefin epoxidation with a new class of ansamolybdenum catalysts in ionic liquids. *ChemSusChem* 3:559–562
5. Betz D, Herrmann WA, Kühn FE (2009) Epoxidation in ionic liquids: a comparison of rhenium(VII) and molybdenum(VI) catalysts. *J Organomet Chem* 694:3320–3324
6. Hauser SA, Cokoja M, Drees M, Kuehn FE (2012) Catalytic olefin epoxidation with a fluorinated organomolybdenum complex. *J Mol Catal A-Chem* 363:237–244
7. Günnyar A, Betz D, Drees M et al (2010) Highly soluble dichloro, dibromo and dimethyl dioxomolybdenum(VI)-bipyridine complexes as catalysts for the epoxidation of olefins. *J Mol Catal A Chem* 331:117–124
8. Abrantes M, Paz FAA, Valente AA et al (2009) Amino acid-functionalized cyclopentadienyl molybdenum tricarbonyl complex and its use in catalytic olefin epoxidation. *J Organomet Chem* 694:1826–1833
9. Monteiro B, Gago S, Neves P et al (2009) Effect of an ionic liquid on the catalytic performance of thiocyanatodioxomolybdenum(VI) complexes for the oxidation of cyclooctene and benzyl alcohol. *Catal Lett* 129:350–357
10. Gamelas C, Neves P, Gomes A et al (2012) Molybdenum(II) diiodo-tricarbonyl complexes containing nitrogen donor ligands as catalyst precursors for the epoxidation of methyl oleate. *Catal Lett* 142:1218–1224
11. Cai S-F, Wang L-S, Fan C-L (2009) Catalytic epoxidation of a technical mixture of methyl oleate and methyl linoleate in ionic liquids using MoO(O₂)₂·2QOH (QOH = 8-quinilinol) as catalyst and NaHCO₃ as co-catalyst. *Molecules* 14:2935–2946
12. Gago S, Balula SS, Figueiredo S et al (2010) Catalytic olefin epoxidation with cationic molybdenum(VI) *cis*-dioxo complexes and ionic liquids. *Appl Catal Gen* 372:67–72

13. Neves P, Pereira CCL, Almeida Paz FA et al (2010) Cyclopentadienyl molybdenum dicarbonyl η^3 -allyl complexes as catalyst precursors for olefin epoxidation. Crystal structures of Cp'Mo(CO)₂(η^3 -C₃H₅) (Cp' = η^5 -C₅H₄Me, η^5 -C₅Me₅). *J Organomet Chem* 695:2311–2319
14. Brito JA, Ladeira S, Teuma E et al (2011) Dioxomolybdenum(VI) complexes containing chiral oxazolines applied in alkenes epoxidation in ionic liquids: a highly diastereoselective catalyst. *Appl Catal A-Gen* 398:88–95
15. Herbert M, Montilla F, Moyano R et al (2009) Olefin epoxidations in the ionic liquid [C4mim][PF₆] catalysed by oxodiperoxomolybdenum species in situ generated from molybdenum trioxide and urea–hydrogen peroxide: the synthesis and molecular structure of [Mo(O)(O₂)₂(4-MepyO)₂] · H₂O. *Polyhedron* 28:3929–3934
16. Herbert M, Alvarez E, Cole-Hamilton DJ et al (2010) Olefin epoxidation by hydrogen peroxide catalysed by molybdenum complexes in ionic liquids and structural characterisation of the proposed intermediate dioxoperoxomolybdenum species. *Chem Commun (Camb)* 46:5933–5935
17. Herbert M, Montilla F, Galindo A et al (2011) Influence of N-donor bases and the solvent in oxodiperoxomolybdenum catalysed olefin epoxidation with hydrogen peroxide in ionic liquids. *Dalton Trans* 40:5210–5219
18. Long D-L, Burkholder E, Cronin L (2007) Polyoxometalate clusters, nanostructures and materials: from self assembly to designer materials and devices. *Chem Soc Rev* 36:105–121
19. Kamata K, Ishimoto R, Hirano T et al (2010) Epoxidation of alkenes with hydrogen peroxide catalyzed by selenium-containing dinuclear peroxotungstate and kinetic, spectroscopic, and theoretical investigation of the mechanism. *Inorg Chem* 49:2471–2478
20. Liu L, Chen C, Hu X et al (2008) A role of ionic liquid as an activator for efficient olefin epoxidation catalyzed by polyoxometalate. *New J Chem* 32:283
21. Berardi S, Bonchio M, Carraro M et al (2007) Fast catalytic epoxidation with H₂O₂ and [γ-SiW(10)O(36)(PhPO)₂](4-) in ionic liquids under microwave irradiation. *J Org Chem* 72:8954–8957
22. Qiao Y, Hou Z, Li H et al (2009) Polyoxometalate-based protic alkyylimidazolium salts as reaction-induced phase-separation catalysts for olefin epoxidation. *Green Chem* 11:1955
23. Wang S-S, Liu W, Wan Q-X, Liu Y (2009) Homogeneous epoxidation of lipophilic alkenes by aqueous hydrogen peroxide: catalysis of a Keggin-type phosphotungstate-functionalized ionic liquid in amphiphatic ionic liquid solution. *Green Chem* 11:1589
24. Ghamati L, Walter O, Arnold U, Doering M (2011) Guanidinium-based phosphotungstates and ionic liquids as catalysts and solvents for the epoxidation of olefins with hydrogen peroxide. *Eur J Inorg Chem* 2011:2756–2762
25. Song CE, Roh EJ (2000) Practical method to recycle a chiral (salen)Mn epoxidation catalyst by using an ionic liquid. *Chem Commun* 10:837–838
26. Li Z, Xia C-G (2003) Epoxidation of olefins catalyzed by manganese(III) porphyrin in a room temperature ionic liquid. *Tetrahedron Lett* 44:2069–2071
27. Li Z (2003) Manganeseporphyrin-catalyzed alkenes epoxidation by iodobenzene diacetate in a room temperature ionic liquid. *Appl Catal Gen* 252:17–21
28. Li Z (2004) Oxidation of hydrocarbons with iodobenzene diacetate catalyzed by manganese(III) porphyrins in a room temperature ionic liquid. *J Mol Catal A Chem* 214:95–101
29. Smith K, Liu S, El-Hiti GA (2004) Use of ionic liquids as solvents for epoxidation reactions catalysed by a chiral Katsuki-type salen complex: enhanced reactivity and recovery of catalyst. *Catal Lett* 98:95–101
30. Tong K-H, Wong K-Y, Chan TH (2003) Manganese/Bicarbonate-catalyzed epoxidation of lipophilic alkenes with hydrogen peroxide in ionic liquids. *Org Lett* 5:3423–3425
31. Ho K-P, Wong K-Y, Chan TH (2006) Indirect catalytic epoxidation with hydrogen peroxide electrogenerated in ionic liquids. *Tetrahedron* 62:6650–6658
32. Song J, Zhang Z, Jiang T et al (2008) Epoxidation of styrene to styrene oxide using carbon dioxide and hydrogen peroxide in ionic liquids. *J Mol Catal A Chem* 279:235–238

33. Peng Y, Cai Y, Song G, Chen J (2005) Ionic liquid-grafted Mn(III)-Schiff base complex: a highly efficient and recyclable catalyst for the epoxidation of chalcones. *Synlett* 2005: 2147–2150
34. Liu Y, Zhang H-J, Lu Y et al (2007) Mild oxidation of styrene and its derivatives catalyzed by ionic manganese porphyrin embedded in a similar structured ionic liquid. *Green Chem* 9:1114
35. Liu Y, Zhang H-J, Wu H-H et al (2007) Oxidation of styrene catalyzed by ionic manganese porphyrin immobilized in ionic liquid. *Chem J Chin Univ-Chin* 28:1523–1527
36. Zhang H-J, Liu Y, Lu Y et al (2008) Epoxidations catalyzed by an ionic manganese(III) porphyrin and characterization of manganese(V, IV)-oxo porphyrin complexes by UV–vis spectrophotometer in ionic liquid solution. *J Mol Catal A Chem* 287:80–86
37. Mang H, Liu Y, Cai Y et al (2008) Epoxidation of styrene and its derivatives catalyzed by a multi-component ionic liquid functionalized with manganese porphyrin. *Chin J Catal* 29:127–133
38. Pinto LD, Dupont J, De Souza RF, Bernardo-Gusmão K (2008) Catalytic asymmetric epoxidation of limonene using manganese Schiff-base complexes immobilized in ionic liquids. *Catal Commun* 9:135–139
39. Tan R, Yin D, Yu N et al (2008) Ionic liquid-functionalized salen Mn(III) complexes as tunable separation catalysts for enantioselective epoxidation of styrene. *J Catal* 255:287–295
40. Teixeira J, Silva AR, Branco LC et al (2010) Asymmetric alkene epoxidation by Mn(III)salen catalyst in ionic liquids. *Inorg Chim Acta* 363:3321–3329
41. Tangestaninejad S, Moghadam M, Mirkhani V et al (2010) Efficient epoxidation of alkenes with sodium periodate catalyzed by manganese porphyrins in ionic liquid: investigation of catalyst reusability. *Inorg Chem Commun* 13:1501–1503
42. Ho K-P, Wong W-L, Lee LYS et al (2010) Manganese acetate in pyrrolidinium ionic liquid as a robust and efficient catalytic system for epoxidation of aliphatic terminal alkenes. *Chem Asian J* 5:1970–1973
43. Chen L, Cheng F, Jia L et al (2011) Asymmetric epoxidation of olefins using novel chiral dinuclear Mn(III)-salen complexes with inherent phase-transfer capability in ionic liquids. *Chirality* 23:69–75
44. Chatel G, Goux-Henry C, Mirabaud A et al (2012) H₂O₂/NaHCO₃-mediated enantioselective epoxidation of olefins in NTF2-based ionic liquids and under ultrasound. *J Catal* 291:127–132
45. Chatel G, Goux-Henry C, Kardos N et al (2012) Ultrasound and ionic liquid: an efficient combination to tune the mechanism of alkenes epoxidation. *Ultrasound Sonochem* 19:390–394
46. Chen L, Wei J, Tang N, Cheng F (2012) Asymmetric epoxidation of chromenes using manganese(III) complexes with novel chiral salen-like schiff base ligands. *Catal Lett* 142: 486–491
47. Zhang Z, Guan F, Huang X et al (2012) New ternary immobilization of chiral sulfonato-(salen) manganese(III) complex for aqueous asymmetric oxidation reactions. *J Mol Catal A-Chem* 363:343–353
48. Zhao R, Tang Y, Wei S et al (2012) Electrosynthesis of sodium hypochlorite in room temperature ionic liquids and in situ electrochemical epoxidation of olefins. *Reac Kinet Mech Cat* 106:37–47
49. Maity NC, Rao GVS, Prathap KJ et al (2013) Organic carbonates as solvents in macrocyclic Mn(III) salen catalyzed asymmetric epoxidation of non-functionalized olefins. *J Mol Catal A Chem* 366:380–389
50. Owens GS, Abu-Omar MM (2000) Methyltrioxorhenium-catalyzed epoxidations in ionic liquids. *Chem Commun* 13:1165–1166
51. Owens GS, Abu-Omar MM (2002) Comparative kinetic investigations in ionic liquids using the MTO/peroxide system. *J Mol Catal A Chem* 187:215–225
52. Owens GS, Durazo A, Abu-Omar MM (2002) Kinetics of MTO-catalyzed olefin epoxidation in ambient temperature ionic liquids: UV/Vis and ²H NMR study. *Chemistry (Weinheim an der Bergstrasse, Germany)* 8:3053–3059

53. Ono F, Qiao K, Tomida D, Yokoyama C (2007) Direct preparation of styrene carbonates from styrene using an ionic-liquid-based one-pot multistep synthetic process. *Appl Catal Gen* 333:107–113
54. Espenson JH, Pestovsky O, Huston P, Staudt S (1994) Organometallic catalysis in aqueous solution: oxygen transfer to bromide. *J Am Chem Soc* 116:2869–2877
55. Hansen PJ, Espenson JH (1995) Oxidation of chloride ions by hydrogen peroxide, catalyzed by methylrhenium trioxide. *Inorg Chem* 34:5839–5844
56. Saladino R, Bernini R, Neri V, Crestini C (2009) A novel and efficient catalytic epoxidation of monoterpenes by homogeneous and heterogeneous methyltrioxorhenium in ionic liquids. *Appl Catal Gen* 360:171–176
57. Michel T, Betz D, Cokoja M et al (2011) Epoxidation of alpha-pinene catalyzed by methyltrioxorhenium(VII): influence of additives, oxidants and solvents. *J Mol Catal A-Chem* 340:9–14
58. Yang R, Zhang Y, Zhao J (2011) Methyltrioxorhenium-catalyzed epoxidation of alkenes with hydrogen peroxide as an oxidant and 1-methyl-3-(butyl-4-sulfonate) imidazolium betaine as an additive. *Catal Commun* 12:923–926
59. Altmann P, Kühn FE (2009) Methyltrioxorhenium catalysed epoxidations: a comparative study of different N-donor ligands. *J Organomet Chem* 694:4032–4035
60. Zhang Y, Li Z, Cao X, Zhao J (2013) Methyltrioxorhenium-catalyzed epoxidation of olefins with hydrogen peroxide as an oxidant and pyridine N-oxide ionic liquids as additives. *J Mol Catal A-Chem* 366:149–155
61. Fang D-W, Zang S-L, Guan W et al (2010) Study on thermodynamic properties of a new air and water stable ionic liquid based on metal rhenium. *J Chem Thermodyn* 42:860–863
62. Fang DW, Wang H, Yue S et al (2012) Physicochemical properties of air and water stable rhenium ionic liquids. *J Phys Chem B* 116:2513–2519
63. Markovits IIE, Eger WA, Shuang Y, Cokoja M, Münchmeyer CJ, Zhang B, Zhou M-D, Genest A, Mink J, Zhang S-L, Rösch N, Kühn FE (2013) Activation of hydrogen peroxide with ionic liquids: mechanistic studies and application in the epoxidation of olefins. *Chem Eur J* doi:<http://dx.doi.org/10.1002/chem.201203208>
64. Srinivas KA, Kumar A, Chauhan SMS (2002) Epoxidation of alkenes with hydrogen peroxide catalyzed by iron(III) porphyrins in ionic liquids Electronic supplementary information (ESI) available: experimental. *Chem Commun* 20:2456–2457, See <http://www.rsc.org/suppdata/cc/b2/b207072n/>
65. Singhal A, Chauhan SMS (2012) Biomimetic oxidation of guggulsterone with hydrogen peroxide catalyzed by iron(III) porphyrins in ionic liquid. *Catal Commun* 25:28–31
66. Singh PP, Ambika CSMS (2012) Chemoselective epoxidation of electron rich and electron deficient olefins catalyzed by meso-tetraarylporphyrin iron(III) chlorides in imidazolium ionic liquids. *New J Chem* 36:650–655
67. Dos Santos MR, Diniz JR, Arouca AM et al (2012) Ionically tagged iron complex-catalyzed epoxidation of olefins in imidazolium-based ionic liquids. *ChemSusChem* 5:716–726
68. Dakkach M, Fontrodona X, Parella T et al (2011) A Novel carbene ruthenium complex as reusable and selective two-electron catalyst for alkene epoxidation. *Adv Synth Catal* 353: 231–238
69. Bortolini O, Conte V, Chiappe C et al (2002) Epoxidation of electrophilic alkenes in ionic liquids. *Green Chem* 4:94–96
70. Bortolini O, Campestrini S, Conte V et al (2003) Sustainable epoxidation of electron-poor olefins with hydrogen peroxide in ionic liquids and recovery of the products with supercritical CO₂. *Eur J Org Chem* 2003:4804–4809
71. Wang B, Kang Y-R, Yang L-M, Suo J-S (2003) Epoxidation of α , β -unsaturated carbonyl compounds in ionic liquid/water biphasic system under mild conditions. *J Mol Catal A Chem* 203:29–36
72. Bernini R, Mincione E, Coratti A et al (2004) Epoxidation of chromones and flavonoids in ionic liquids. *Tetrahedron* 60:967–971

73. Tang MC-Y, Wong K-Y, Chan TH (2005) Electrosynthesis of hydrogen peroxide in room temperature ionic liquids and in situ epoxidation of alkenes. *Chem Commun (Camb)* 10: 1345–1347
74. Okamoto S, Takano K, Ishikawa T et al (2006) Activity and behavior of imidazolium salts as a phase transfer catalyst for a liquid–liquid phase system. *Tetrahedron Lett* 47:8055–8058
75. Pal R, Dere R, Patil P et al (2009) Immobilization of chiral quininium salt in ionic liquid for enantioselective epoxidation of chalcones. *Lett Org Chem* 6:332–334
76. Karthikeyan P, Arunrao AS, Narayan MP et al (2012) A novel L-asparaginylyl Amido ethyl methyl imidazolium bromide catalyst for heterogeneous epoxidation of alpha, beta-unsaturated ketones. *J Mol Liq* 172:136–139
77. Crosthwaite JM, Farmer VA, Hallett JP, Welton T (2008) Epoxidation of alkenes by OxoneTM using 2-alkyl-3,4-dihydroisoquinolinium salts as catalysts in ionic liquids. *J Mol Catal A Chem* 279:148–152
78. Baj S, Belch M, Gibas M (2012) N-Substituted 3,4-dihydroisoquinolinium ionic liquids as catalysts in alkenes epoxidation reactions. *Appl Catal A-Gen* 433:197–205
79. Lau RM, Van Rantwijk F, Seddon KR, Sheldon RA (2000) Lipase-catalyzed reactions in ionic liquids. *Org Lett* 2:4189–4191
80. Moreira MA, Nascimento MG (2007) Chemo-enzymatic epoxidation of (+)-3-carene. *Catal Commun* 8:2043–2047
81. Sarma K, Goswami A, Goswami BC (2009) Exploration of chiral induction on epoxides in lipase-catalyzed epoxidation of alkenes using (2R,3S,4R,5S)-(–)-2,3:4,6-di-O-isopropylidene-2-keto-l-gulonic acid monohydrate. *Tetrahedron Asymmetry* 20:1295–1300
82. Silva WSD, Lapis AAM, Suarez PAZ, Neto BAD (2011) Enzyme-mediated epoxidation of methyl oleate supported by imidazolium-based ionic liquids. *J Mol Catal B: Enzym* 68:98–103
83. Kotlewska AJ, Van Rantwijk F, Sheldon RA, Arends IWCE (2011) Epoxidation and Baeyer–Villiger oxidation using hydrogen peroxide and a lipase dissolved in ionic liquids. *Green Chem* 13:2154–2160
84. da Silva JMR, da Nascimento MG (2012) Chemoenzymatic epoxidation of citronellol catalyzed by lipases. *Process Biochem* 47:517–522
85. Sanfilippo C, D’Antona N, Nicolosi G (2004) Chloroperoxidase from *Caldariomyces fumago* is active in the presence of an ionic liquid as co-solvent. *Biotechnol Lett* 26:1815–1819
86. Wu J, Liu C, Jiang Y et al (2010) Synthesis of chiral epichlorohydrin by chloroperoxidase-catalyzed epoxidation of 3-chloropropene in the presence of an ionic liquid as co-solvent. *Catal Commun* 11:727–731
87. Gomes AC, Bruno SM, Gago S et al (2011) Epoxidation of cyclooctene using soluble or MCM-41-supported molybdenum tetracarbonyl-pyridylimine complexes as catalyst precursors. *J Organomet Chem* 696:3543–3550
88. Balula SS, Bruno SM, Gomes AC et al (2012) Epoxidation of olefins using a dichlorodioxomolybdenum(VI)-pyridylimine complex as catalyst. *Inorg Chim Acta* 387: 234–239
89. Gomes AC, Bruno SM, Tomé C, et al (2012) Synthesis and characterization of CpMo(CO)₃(CH₂-pC₆H₄-CO₂CH₃) and its inclusion compounds with methylated cyclodextrins. Applications in olefin epoxidation catalysis. *J Organomet Chem*. doi:<http://dx.doi.org/10.1016/j.jorganchem.2012.12.019>
90. Yamaguchi K, Yoshida C, Uchida S, Mizuno N (2005) Peroxotungstate immobilized on ionic liquid-modified silica as a heterogeneous epoxidation catalyst with hydrogen peroxide. *J Am Chem Soc* 127:530–531
91. Doherty S, Knight JG, Ellison JR, Weekes D, Harrington RW, Hardacre C, Manyar H (2012) An efficient recyclable peroxometalate-based polymer-immobilised ionic liquid phase (PIILP) catalyst for hydrogen peroxide-mediated oxidation *Green Chemistry* 14:925–929
92. Kumar A (2007) Epoxidation of alkenes with hydrogen peroxide catalyzed by 1-methyl-3-butylimidazoliumdecatungstate in ionic liquid. *Catal Commun* 8:913–916
93. Lou L-L, Yu K, Ding F et al (2006) An effective approach for the immobilization of chiral Mn(III) salen complexes through a supported ionic liquid phase. *Tetrahedron Lett* 47:6513–6516

94. Lou L, Yu K, Ding F et al (2007) Covalently anchored chiral Mn(III) salen-containing ionic species on mesoporous materials as effective catalysts for asymmetric epoxidation of unfunctionalized olefins. *J Catal* 249:102–110
95. Lou L, Yu Y, Yu K et al (2009) Chiral Mn(III) salen complex immobilized on imidazole-modified mesoporous material via co-condensation method as an effective catalyst for olefin epoxidation. *Sci China Ser B: Chem* 52:1417–1422
96. Wei S, Tang Y, Xu X et al (2011) A new heterogeneous chiral (salen)manganese(III) system for enantioselective epoxidation of non-functionalized olefins. *Appl Organomet Chem* 25:146–153
97. Xu G, Wei S, Fan Y et al (2012) A poly(hydroxyethyl methacrylate)-immobilized chiral manganese(III)salen catalyst for asymmetric epoxidation of alpha-methylstyrene. *Chin J Catal* 33:473–477
98. Huang J, Fu X, Wang G et al (2012) Axially coordinated chiral salen Mn(III) anchored onto azole onium modified ZnPS-PVPA as effective catalysts for asymmetric epoxidation of unfunctionalized olefins. *Dalton Trans* 41:10661–10669

Ionic Liquids in Palladium-Catalyzed Cross-Coupling Reactions

Piero Mastrorilli, Antonio Monopoli, Maria Michela Dell'Anna,
Mario Latronico, Pietro Cotugno, and Angelo Nacci

Abstract This chapter surveys the most significant developments in the field of palladium-catalyzed cross-coupling reactions in ionic liquids. The beneficial effect of the ionic liquids in terms of activity, selectivity, and recyclability is commented for all types of reactions discussed, namely the Heck, Suzuki–Miyaura, Stille, Sonogashira, Ullmann, and Negishi cross-couplings. Insights into the reaction mechanisms reveal that the effect of the ionic liquid on C–C bond forming reactions manifests itself not only in the energy lowering of polar transition states (or intermediates) involved in the catalytic cycles but also, depending on the cases, in the stabilization of palladium nanoparticles, the synthesis of molecular Pd complexes with the IL anions, the enhancement of the chemical reactivity of reactants, and others. The synergistic effect found by using appropriate mixtures of ionic liquids is also discussed.

Keywords C–C bond forming reactions · Cross-coupling reactions · Heck reaction · Ionic liquids · Palladium · Pd nanoparticles

P. Mastrorilli (✉) and M. Latronico
Dipartimento DICATECh del Politecnico di Bari and Istituto CNR-ICCOM, Via Orabona 4,
70125 Bari, Italy
e-mail: p.mastrorilli@poliba.it

A. Monopoli and P. Cotugno
Dipartimento di Chimica dell'Università di Bari, Via Orabona 4, 70125 Bari, Italy

M.M. Dell'Anna
Dipartimento DICATECh del Politecnico di Bari, Via Orabona 4, 70125 Bari, Italy

A. Nacci
Dipartimento di Chimica dell'Università di Bari and Istituto CNR-ICCOM, Via Orabona 4,
70125 Bari, Italy

Contents

1	Introduction	238
2	The Heck Reaction	241
2.1	Tetraalkyl-Ammonium and -Phosphonium Based ILs	242
2.2	Imidazolium and Pyridinium-Based ILs	246
2.3	Heterogeneous Catalysis	249
2.4	Task-Specific ILs	251
2.5	Supported and Layered Ionic Liquids	251
2.6	Heck Coupling in Chiral Ionic Liquids	256
2.7	Ionic Liquid Effect on Activity and Selectivity	258
3	Suzuki–Miyaura Reaction	261
4	The Stille Reaction	267
5	The Sonogashira Coupling	269
6	The Ullmann Homo-Coupling	272
7	The Negishi Reaction	275
8	Conclusions and Outlook	276
	References	276

1 Introduction

During the last 30 years, ionic liquids (ILs) became one of the most interesting and rapidly developing areas of modern physical chemistry, technologies, and engineering [1]. ILs are tunable and multipurpose materials used in a variety of fields including sensors, fuel cells, batteries, plasticizers, lubricants, extractants, synthesis, and catalysis. Their modular physicochemical properties, such as density, viscosity, ionic mobility, hydrophobicity, and miscibility with molecular solvents, associated with a negligible vapor pressure and no-flammability, prompted chemists to test these materials as possible eco-friendly media for synthesis and catalysis as well as for extraction processes.

However, ILs are more than just an alternative “green” reaction media. They differ from molecular solvents by their unique ionic character and their “structure and organization.” For example, the ILs based on the 1,3-dialkylimidazolium cation display a high degree of 3-D structural organization due to the presence of a rigid and planar ring and an extended networks of hydrogen bonds and dispersive forces with polar and nonpolar nanodomains. This structural organization has been exploited for the preparation of a plethora of nanoscale structures, including the synthesis of highly dispersed transition metal nanoparticles (NPs) that may be regarded as soluble forms of heterogeneous catalysts.

Thus, the role of ILs in homogeneous catalysis has more to do with the enhancement of catalytic performances (activity, selectivity) and the possibility of catalyst separation and/or recycling rather than with environmental concerns, which now are rightly regarded only from a mere “historic” point of view. In fact, they can behave as simple innocent solvents, but more often they act as ligands, co-catalysts, and stabilizing agents for both the active species and intermediates of the catalytic cycle.

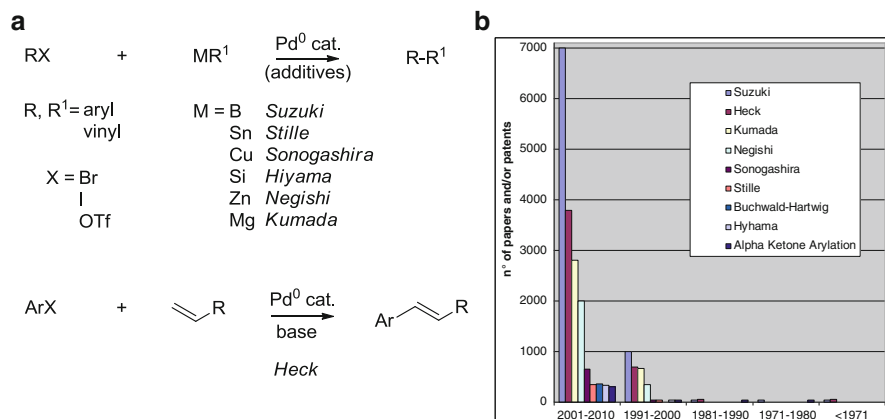


Fig. 1 (a) General scheme for palladium-catalyzed C–C cross coupling reactions; (b) number of publications and patents on C–C cross-coupling reactions over the last four decades

Transition-metal catalyzed carbon–carbon bond formation is certainly the field of catalysis where ILs are considered the most promising alternative to traditional solvents. Over the past 40 years, this branch of organometallic chemistry has emerged as a new powerful tool of organic synthesis enhancing significantly the ability of synthetic organic chemists to assemble complex molecular frameworks and changing the way we think about synthesis (see, for example, [2–4]).

Prominent among these processes are the palladium catalyzed carbon–carbon cross-coupling reactions (Fig. 1a), because the historical, mechanistic, theoretical, and practical aspects of these processes have been widely discussed [5]. The ability of palladium to insert into a variety of carbon–LG bonds (LG = leaving group such as halogen, triflate, and diazonium), its aptitude to give transmetalation with the most common organometallic reagents, and tolerance towards most of the functional groups are the key properties that render this metal the sole capable of promoting such a large number of reactions.

Indeed, palladium is unique in assembling new C–C bonds by a wide array of unsaturated starting materials (aryls, heteroaryls, vinyls, acetylides, etc.), through inter- or intra-molecular processes to yield a myriad of organic compounds having a variety of skeletons and complex molecular architectures, often difficult to be constructed with other synthetic approaches. This newly acquired ability to mold carbon–carbon bonds has opened new opportunities, particularly for total synthesis, broadening the range of industrial applications, which nowadays involves the fields of medicinal chemistry, agriculture, material and polymer sciences, opto-electronics, chemical biology, and nano-technology.

Since from their discovery in the early 1970s, Heck, Suzuki, and Stille reactions, just to cite a few, have become familiar names to the synthetic organic community, with a true outburst of interest in the last decade attested by the extraordinary increment of the number of papers and patents published on these topics (Fig. 1b).

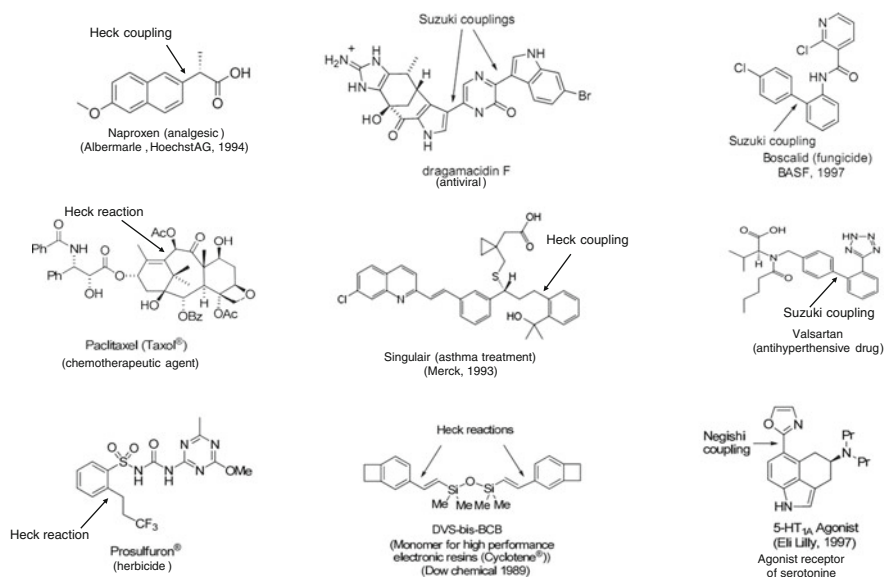


Fig. 2 Some industrial applications of C–C cross-couplings

Heck, Suzuki, and Negishi couplings are considered true milestones in organometallic chemistry, and the Nobel Prize in Chemistry 2010 awarded to their discoverers testifies the importance of these processes mainly due to their impact on the chemical industry. Some widespread antivirals, drugs, pesticides, and products for electronics are nowadays produced on industrial scale by means of these processes. The Heck coupling, for instance, is a key reaction for the production of fine chemicals such as the herbicide Prosulfuron™, the anti-inflammatory Naproxen™ or the anti-asthma Singulair™ on a multi-ton scale per year (Fig. 2).

In general, a cross-coupling is a reaction occurring between an aryl or vinyl halide (or triflate), which is considered the electrophile, and an organometallic reagent as nucleophilic counterpart. Heck coupling represents the exception in which the nucleophile is given by a simple olefin (Fig. 1a).

The R¹ group (Fig. 1a) of the organometallic reagent can be virtually any saturated or unsaturated groups (alkyl, aryl, vinyl, alkynyl, etc.). Most of magnesium, tin, and zinc reagents are sufficiently reactive to undergo transmetalation with palladium without the need for an additive. Boron and silicon reagents, on the other hand, are usually reluctant to trans-metalate in the absence of an activator. As a consequence, Suzuki and Hiyama cross-couplings are typically carried out in the presence of an additive, the role of which is to form a higher-valent, more reactive anionic complex. The generally accepted mechanisms for these processes are reported in Fig. 3. (For mechanistic aspects, see: [6–11].)

A common problem associated with the use of palladium complexes in traditional solvents is the need for ligands that stabilize the metal center and avoid (or at least retard) Pd-black formation. The classical solution, i.e. the addition of an excess

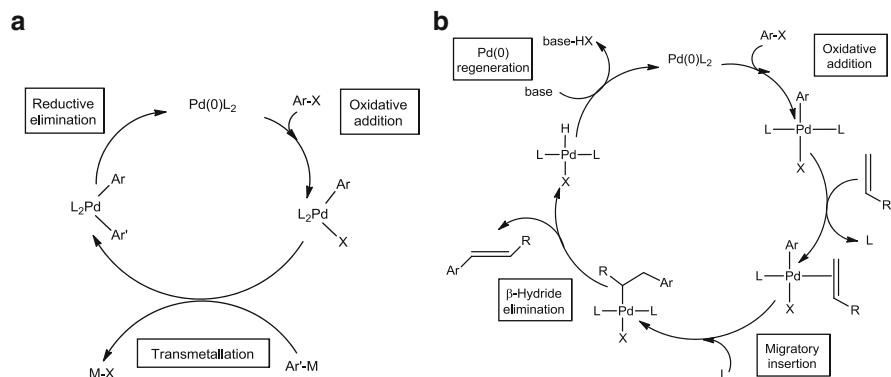


Fig. 3 (a) Generalized mechanism for palladium-catalyzed cross-coupling reactions; (b) The mechanism of the Heck reaction

of phosphanes suffers from the drawback that trivalent P compounds are toxic, expensive, and often sensitive to air.

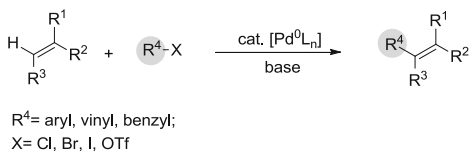
The request of substitutes for phosphanes stimulated the chemists not only to explore new ligands for palladium but also to search for new reaction media which could overcome the need of P-based additives. In this regard, ionic liquids revealed to be a favorable alternative, as their anions can act as stabilizing ligands and, in addition, their use was beneficial in terms of catalyst activity, selectivity, and recyclability [12].

In this chapter the most important achievements in the field of palladium-catalyzed cross-coupling reactions occurring in ILs are surveyed, with an eye to the ways by which the ionic liquids affect the catalytic performances (an exhaustive list of the wide range of Pd-catalyzed cross-couplings reactions in ILs can be found in the following reviews: [13–17]). The material has been subdivided according to the type of C–C bond forming reaction in a chronological approach. The treatment starts with the extensively studied Heck reaction, continues with Suzuki–Miyaura, Sonogashira, and Ullmann cross-couplings, and ends with Negishi reaction.

2 The Heck Reaction

The Heck reaction can be broadly defined as the palladium-catalyzed coupling of alkenyl or aryl (sp^2) halides or triflates with alkenes to yield products which formally derive from the substitution of a hydrogen atom in the alkene (Scheme 1) [18, 19], (Reviews: [20–27]).

To date, the Heck reaction is considered the most powerful method to achieve arylated olefins, substituted dienes, polyenes, and a variety of extended π -systems, many of which are important intermediates in the synthesis of natural product, pharmaceuticals, agrochemicals and in the production of other fine chemicals (see, for example, [28–30]).

Scheme 1 The Heck reaction

The first examples of this reaction were reported independently by Mizoroki [31] and, in an improved form, by Heck [32]. However, the broad applicability of this processes began to be investigated only a decade later by the wider synthetic organic community. In the late 1980s, there was a further resurgence of interest with the asymmetric applications [33], and nowadays this reaction is considered a remarkably robust and efficient tool for carbon–carbon bond formation [13–17], (for reviews on the Heck coupling in ILs, see [34, 35]), particularly for the generation of tertiary and quaternary stereo-centers and for the intramolecular ring formation, still remaining a flourishing area of research.

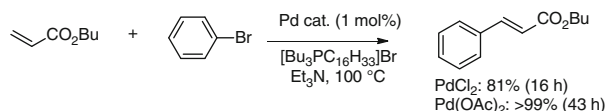
Aryl iodides are the privileged substrates being much more reactive than bromides and chlorides in concordance with the C–X bond energies ($E_{\text{C-X}} = 65, 81, 96$ kcal/mol, for X = I, Br, Cl, respectively). Typically, polar organic solvents (*N,N*-dimethylacetamide, DMA; *N,N*-dimethylformamide, DMF; *N*-methyl-2-pyrrolidone, NMP and others), inorganic (usually K_2CO_3 or NaOAc) or organic (Et_3N) bases and phosphane ligands are employed, with temperature conditions depending on the starting materials (normally above 100°C). Currently, the main goals of researchers in this field are: (1) finding catalytic systems that activate C–Cl bonds or, alternatively; (2) finding alternative substrates endowed with cheaper leaving groups (e.g., anhydride and diazonium); (3) recovery and reuse of the catalysts without loss of activity; (4) development of phosphane-free palladium catalysts.

The first of these objective remains a true challenge of organometallic chemistry, being chloroarenes the most readily available and cheapest starting materials. Unfortunately, they are generally unreactive under the conditions used to couple the corresponding iodides and bromides, and high temperatures (>140°C), expensive and air-sensitive phosphane ligands or sterically hindered amines are usually required for their activation (some examples: [36–42]). From a synthetic standpoint, all these factors are considerable limitations that need to be addressed to apply Heck reaction on an industrial scale [43].

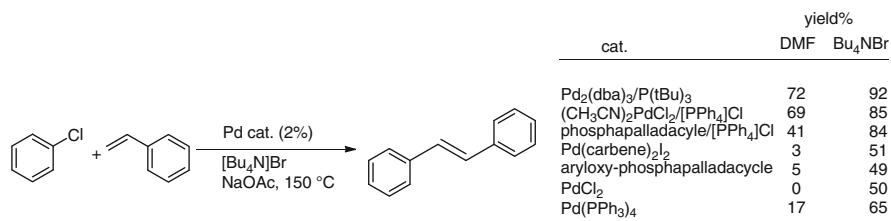
The use of ionic liquids as reaction media is by now considered one of the main solutions proposed to solve these problems. In the following discussion, results are subdivided on the basis of typology of ionic liquid (tetrahedral, planar, task specific, etc.) and on the basis of the kind of catalysis.

2.1 Tetraalkyl-Ammonium and -Phosphonium Based ILs

An ionic liquid was used for the first time in the Heck reaction, solely as an additive, in 1984 by Jeffery [44], in a pioneering work on the palladium-catalyzed vinylation of aryl iodides at room temperature in DMF solvent and NaHCO_3 as the base.



Scheme 2 The first Heck coupling performed entirely in an ionic liquid



Scheme 3 Heck reaction of chlorobenzene with styrene in [Bu₄N]Br

During these investigations, Jeffery found, unexpectedly, that the addition of increasing amounts of tetrabutylammonium chloride exerted a strong activating effect on the catalyst and explained this phenomenon with an efficient solid–liquid phase transfer mechanism promoted by the additive.

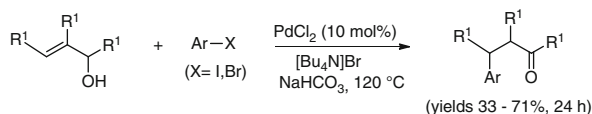
Since then on, a number of Heck reactions were performed by using quaternary ammonium salts as additives under the so-called Jeffery conditions in which, besides the phase transfer agent action, also a stabilizing and activating effect on the active species by the salt was invoked [45–49].

However, the first Heck coupling performed entirely in an ionic liquid was reported by Kaufmann in 1996 [50], who described the synthesis of cinnamic esters carried out coupling bromobenzene with *n*-butyl acrylate in tri-*n*-butylhexadecylphosphonium bromide as solvent, in the presence of Pd(II) salts as catalyst source (Scheme 2).

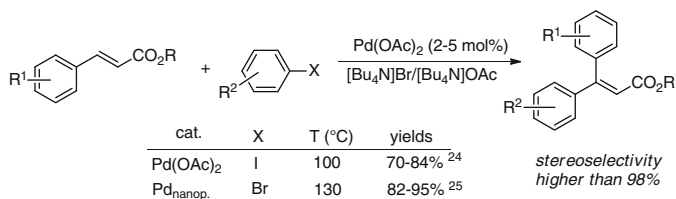
In this pioneering work, palladium acetate was outstanding in terms of both conversions and recyclability. The authors ascribed these good catalytic performances to the stabilizing effect exerted by the phosphonium salt towards the active Pd(0) species formed in situ by reduction of Pd(II) salts. Although this work attracted the attention of many research groups in the world, no attempts were made to disclose the true mechanism operating in this IL medium.

In 1999 Herrmann's group [51, 52] was the first to report the superior performances of tetraalkylammonium ionic liquid media, and particularly of [Bu₄N]Br, in promoting the Heck coupling of reluctant chloroarenes, and this for almost any known catalyst system arising from Pd salts, phosphapalladacycles, Pd(0) or Pd-carbene-type complexes (Scheme 3).

Soon after, Calò's group reported on the Heck arylation of acrylates catalyzed by a Pd-benzothiazole carbene complex in molten [Bu₄N]Br [53], and Muzart et al. investigated, in the same molten salt, the Heck coupling of allyl alcohols to give the β-arylated carbonyl compounds, using PdCl₂ as the catalyst precursor (Scheme 4) [54].



Scheme 4 Heck coupling of allyl alcohols with halobenzenes



Scheme 5 Heck reactions in a [Bu₄N]Br/[Bu₄N]OAc molten mixture

Based on the fundamental results by Reetz [55–58], who described the catalytic activity of palladium nanoparticles stabilized by tetraalkylammonium salts in solution of traditional solvents, the high activity displayed in [Bu₄N]Br was explained with the thermal reduction of the Pd(II) pre-catalyst into extremely active colloids. The reducing agent in this medium is supposed to be the Bu₃N formed by Hoffmann decomposition of the ammonium salt [59]. Noteworthy, neither Pd⁰ complexes nor preformed Pd colloids resulted to actively promote the Heck reaction in [Bu₄N]Br, thus confirming that active species must be formed in situ. This can be interpreted taking into account that the generation of active colloids in these ILs media follows a series of consecutive steps starting with the Pd(II) reduction, fast atoms nucleation and clusters growing driven by the ionic solvent which acts as a protective agent to prevent agglomeration.

In 2002, Cacchi et al. reported that a mixture of [Bu₄N]Br and [Bu₄N]OAc is an excellent medium for promoting the Heck coupling of iodoarenes with high stereoselectivity [60]. Calò et al. extended the same coupling conditions to the less reactive bromoarenes demonstrating that small Pd nanoparticles are the true catalyst of this reaction (Scheme 5) and that [Bu₄N]OAc plays a crucial role for both promoting the rapid (almost instantaneous) thermal reduction of palladium(II) to give stabilized colloids (Fig. 4a), and determining the high degree of the stereoselectivity of the process [61].

The stabilizing effect of the tetraalkylammonium salts [Bu₄N]OAc and [Bu₄N]Br is due to the electrostatic interaction of anions as well as to the steric repulsion of bulky tetraalkylammonium cations present in the surrounding shell of nanoparticle core (Fig. 4b) [62].

The high level of stereochemical control exhibited by this protocol was ascribed to the ability of the acetate to rapidly neutralize, by means of a fast intramolecular elimination (Scheme 6, path a), the palladium hydride intermediate of the Heck cycle inhibiting its readdition to the double bond of the arylated cinnamic ester and causing the *E/Z* isomerization (Scheme 6, path b). The absence of acetate in the

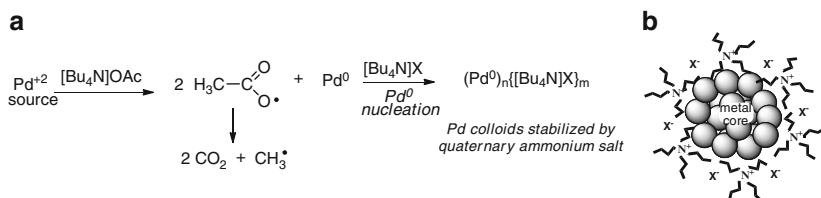
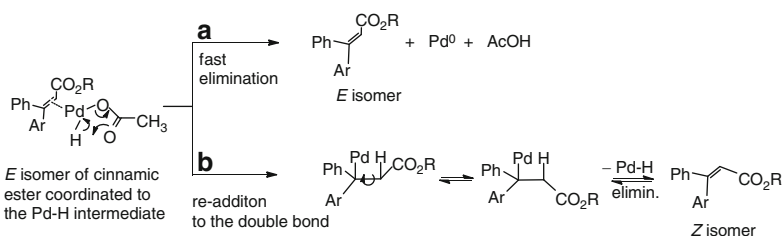


Fig. 4 (a) Pd colloids generated by thermal reduction of Pd(II) source by acetate ions; (b) representation of a Pd nanoparticle stabilized by a surrounding shell of tetraalkylammonium salt ($X = \text{AcO}^-$ or Br^-)



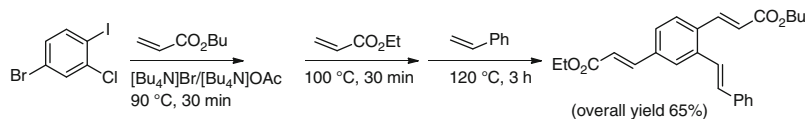
Scheme 6 Isomerization process promoted by palladium hydride Pd-H intermediate of Heck cycle

coordination shell, or the use of other bases, allowed the Pd-H isomerization, leading to a thermodynamic mixture of isomeric olefins.

Similar reaction conditions were employed for the regio-chemical control in the arylation of *n*-butyl methacrylate and α -methylstyrene [63]. In this case, however, a 3:1 mixture of regio-isomers was obtained in favor of the terminal olefins, together with variable amounts of double-arylated products. The terminal olefins were efficiently converted into the thermodynamically more stable internal isomers by using the bulkier tetrabutylammonium pivalate $[\text{Bu}_4\text{N}]^+\text{BuCO}_2^-$ as the base.

In 2005, Trzeciak's group reported an efficient base-free protocol for the Heck reaction in molten $[\text{Bu}_4\text{N}]\text{Br}$. In this study the authors hypothesized that soluble Pd (II) complexes of $[\text{Bu}_4\text{N}]_2[\text{PdX}_3\text{Ph}]$ type were formed by oxidative addition of PhX to Pd(0) (in colloid) and subsequent reaction with $[\text{Bu}_4\text{N}]\text{Br}$ [64]. The $[\text{PdX}_3\text{Ph}]^{2-}$ complexes could be reduced again to Pd⁽⁰⁾L₄ mononuclear species provided that suitable L ligands are present in the system. If not, palladium reduction led to Pd(0) colloids smaller in size than the initial particles.

In 2009, the effectiveness of a mixture of tetraalkylammonium salts has been highlighted by Nacci and coworkers in the ligandless Heck coupling between chloroarenes and deactivated olefins [65]. The catalyst activity was found to strongly depend on the molar ratio of the two ILs partners, $[\text{Bu}_4\text{N}]\text{Br}$ and $[\text{Bu}_4\text{N}]\text{OAc}$. In particular, a ratio of 2:1 in favor of $[\text{Bu}_4\text{N}]\text{Br}$ gave the best results in terms of catalytic performance, resulting in the activation of a wide range of chloroarenes, including the less reactive electron-rich ones (e.g., chloroanisole) as well as of deactivated disubstituted olefins (e.g., cinnamates). The need for greater amounts of



Scheme 7 Triple Heck reaction in ILs

[Bu₄N]Br was explained by admitting that bromide ions, not involved in tight ion pairs, could provide adequate electron density to the Pd⁰ species in place of the electron-rich phosphane ligands, facilitating the oxidative-addition step.

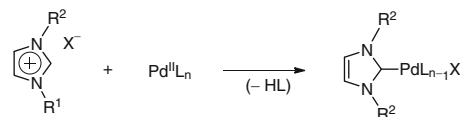
The ability to activate C–Cl bond exhibited by [Bu₄N]Br in the absence of additives has been exploited for the sequential couplings of polyhalobenzenes with different olefins. In this regard, a triple Heck reaction has been reported dealing with the 4-bromo-2-chloro-1-iodobenzene in a one-pot sequential manner, by activating the C–I, C–Br, and C–Cl bonds on the aromatic ring at the three different temperatures of 90 °C, 100 °C and 120 °C, respectively. Unsymmetrical trisubstituted arenes were produced with high reaction rates and high overall yield (Scheme 7) [66].

2.2 Imidazolium and Pyridinium-Based ILs

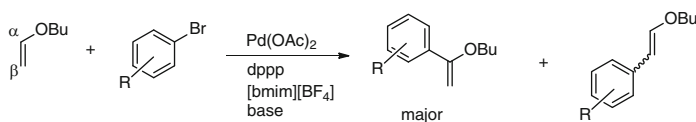
Dialkylimidazolium and alkylpyridinium-based ionic liquids represent the most common RTILs (room temperature ionic liquid) and, even though their performance does not arrive at that of quaternary ammonium molten salts, they have been largely employed in catalysis of the Heck reaction during the last decade.

Basically, the effectiveness of the most common ionic liquids decreases in the order: *tetraalkylammonium* > *imidazolium* > *pyridinium* [52]. Such an order has been related to a better ability of tetraalkylammonium salts to stabilize, by steric effect, the palladium colloids formed during the catalytic process (Fig. 4). Moreover, the bulky alkyl chains of [R₄N]⁺ cations somehow shield the positive charge, thus giving rise to loose ion pairs with the counter-anions. As a consequence, the “almost naked” anions of [R₄N]X salts possess a higher coordinating ability than those of other ILs (not to speak of the same anions in traditional solvents, where they are invariably solvated) thus enabling the formation of very active anionic Pd complexes. This is also the rationale for the detrimental effect observed by replacing a coordinating halide with a poorly coordinating anion in an ionic liquid used as reaction medium for C–C bond forming reactions.

For example, the Heck coupling of iodobenzene with acrylates in hexylpyridinium chloride as the solvent, Et₃N as the base and Pd(OAc)₂ as the catalyst proceeds under mild conditions [67]. When the chloride anions of the IL were replaced by tetrafluoroborate or hexafluorophosphate, the yields in cinnamate dropped dramatically and longer reaction times and higher temperatures were necessary to reach complete conversions.



Scheme 8 Formation of palladium *N*-heterocyclic carbene complexes in imidazolium based ILs



Scheme 9 Arylation of electron-rich α -olefins in an imidazolium IL

To explain the better performances of imidazolium-based ILs in comparison with the pyridinium-based ones, the formation in situ of stable and active palladium *N*-heterocyclic carbene complexes (Pd-NHC) is usually invoked (Scheme 8) [52].

The first extensive investigations on the Heck coupling in imidazolium salts were reported in 2000 by Xiao [68], who showed that, under catalytic conditions, the imidazolium cation can react with palladium acetate affording an *N*-heterocyclic carbene complex via deprotonation of C-2.

Subsequently, Xiao focused the attention on the palladium-catalyzed arylation of electron-rich olefins, such as butyl vinyl ether in an imidazolium IL showing that Pd(OAc)₂ and 1,3-bis-(diphenylphosphanyl)propane (dppp) in [bmim][BF₄] (bmim = 1-*n*-butyl-3-methylimidazolium) form an excellent catalytic system capable of arylating electron-rich olefins at the α -position with no need for any halide scavengers (Scheme 9) [69, 70]. The influence of the IL and some mechanistic details are discussed in a section below (*vide infra*).

As in tetralkylammonium salts, also in imidazolium ones Pd colloids have been recognized in many cases as the true catalytic species operating in Heck reactions. Moreover, it should be noted that carbenes formed by H-abstraction from the imidazolium cations may compete, under certain circumstances, with the aryl halide substrate for the coordination onto the Pd colloid surface, thus inhibiting the reaction (Fig. 5a) [71]. This could be another reason for the worse performance of imidazolium salts with respect to tetraalkylammonium ones.

One of the first reports on Heck reaction with Pd nanoparticles in imidazolium-based ILs was published in 2001 by Srinivasan et al. [72]. In that protocol, iodobenzenes and olefins were reacted under sonication, at ambient temperature (30°C), with considerably reduced reaction times (1.5–3 h). TEM and NMR analyses showed that Pd(OAc)₂ precursor afforded first a palladium bis-carbene complex and then, by further reduction, metal colloids.

Detailed mechanistic insights on the role of Pd colloids in these media were gained by Dupont et al. [73–75] that converted palladacycles pre-catalysts into Pd nanoparticles, by reduction with dimethylallene, and dispersed the obtained nanoparticles into [bmim][PF₆]. This system was then tested in the Heck reaction

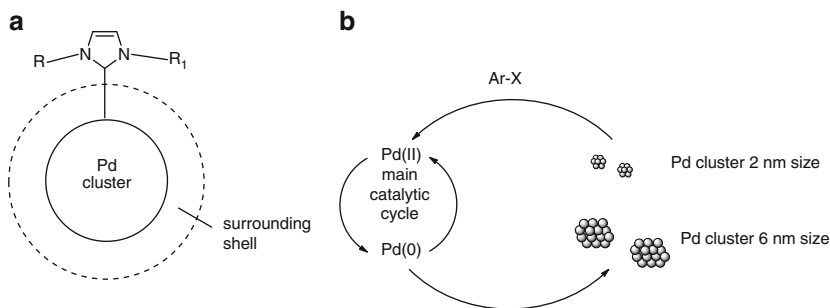
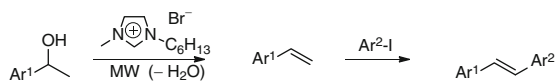


Fig. 5 (a) Carbene-bound Pd nanoparticle surface. (b) The catalytic cycle involving Pd nanoparticles in ILs (adapted from [71])

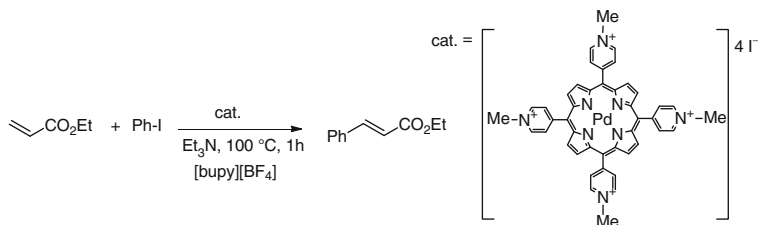


Scheme 10 Synthesis of stilbenoids molecules by dehydrative Heck one pot sequence

with aryl halides and *n*-butyl acrylate. TEM analyses of the Pd-powder in IL revealed the presence of Pd colloids 2 nm in size before catalysis and 6 nm in size after catalysis (Fig. 5b). In addition, the analysis of the organic layer showed that considerable quantities of palladium were leached out into the organic phase indicating that colloids act as reservoir for molecular catalytically active Pd species. On these bases, the authors proposed that the reaction starts with the oxidative addition of the aryl halide on the metal surface, followed by cleavage of this oxidized molecular palladium species from the surface, which enters the catalytic cycle. By using a simple approach based on membrane physical separation, Rothenberg and coworkers reported that ions and Pd atoms detached from the surface of palladium clusters are likely the catalytically active species of the Heck and Suzuki coupling [76, 77].

An intriguing application of ILs to the Heck coupling is the preparation of stilbenoids molecules involving the dehydrative Heck one pot sequence assisted by the ionic liquid [hmim]Br (hmim = *N*-*n*-hexyl-*N'*-methylimidazolium). The method utilizes readily accessible and inexpensive secondary aryl alcohols as in situ source of styrenes and does not require an inert atmosphere. The protocol is an atom-economic, and eco-friendly alternative to the existing multistep approaches as it eliminates the tricky isolation of the styrenes, as well as the protection/deprotection manipulations in the case of hydroxy-substituted stilbenoids (Scheme 10) [78].

Few examples have been reported on the Heck cross-coupling in pyridinium-based ILs, which represent the less efficient IL class in stabilizing the active species when compared to tetraalkylammonium or imidazolium-based ones. However, an interesting application of a tetradentate pincer *N*-ligand based on a porphyrin



Scheme 11 A porphyrin-based Pd catalyst in the Heck reaction

functionalized with four pyridinium tags has been reported (Scheme 11). These catalytic systems efficiently catalyze the Heck reaction of iodobenzenes and ethyl acrylate in [bupy]BF₄ (bupy = *N*-*n*-butylpyridinium) as the solvent and under aerobic conditions [79]. The good performances were accounted for by the authors with the strong cation- $\pi/\pi-\pi$ interaction, and a good “ionophilicity” between the catalyst and the ionic medium.

2.3 Heterogeneous Catalysis

In principle, ionic liquids may be considered an immobilizing phase for the catalyst that could assure the easy separation of the reaction products from the IL phase and a prompt catalyst reuse. However, the main drawback remains the metal leaching during the separation procedures, usually carried out by extraction with organic solvents, that leads to the slow catalyst inactivation.

One of the solutions adopted is the linkage of palladium catalysts to solid supports. In the case of Pd colloids, the support must be capable of anchoring nanoparticles strongly, leaving the active sites well dispersed and easily accessible on their surface. Moreover, the nature of the support can strongly affect the catalyst properties and activities as well as the particle size, structure, and methods of preparation of the composite. To this purpose, charcoal, dendrimers, organic polymers, metal oxides, clays, and silica have been used over the last few years.

Pd/C is one of the typical heterogeneous hydrogenation catalysts, which is commercially available and inexpensive. In 2001, Hagiwara and coworkers [80] tested this supported catalyst in the Heck reaction of a variety of olefins in [bmim][PF₆] as the reaction medium. The reactions proceeded in moderate to satisfactory yields and the catalyst was reused for six times without significant loss of activity. Interestingly, the presence of the Pd species in the ionic liquid before and after the Heck reaction was negligible.

In 2002 Choudary and coworkers [81] reported on the Heck reaction of chloroarenes, including the less reactive electron-rich ones, by using a ligand-free

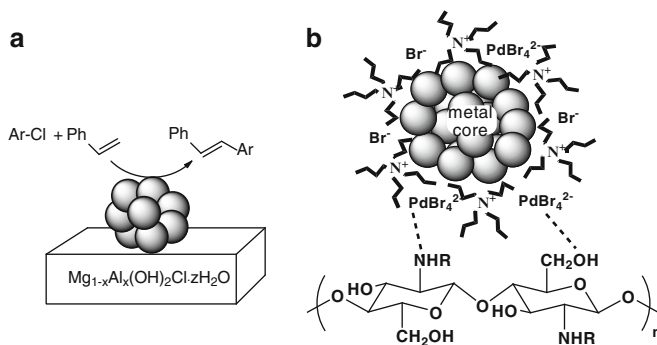


Fig. 6 Pd nanoparticles anchored onto solid supports constituted of (a) Mg–Al layered double hydroxides (LDH-Pd⁰); and (b) chitosan

supported catalyst under microwave irradiation and [Bu₄N]Br as IL. The heterogeneous catalyst was prepared by anchoring Pd nanoparticles on a basic support made up of Mg–Al layered double hydroxides (LDH-Pd⁰, Fig. 6a).

The activity of LDH-Pd⁰ in the Heck olefination of 4-chloroanisole was higher than that of Pd/C, Pd/SiO₂, Pd/Al₂O₃, and polymer supported-PdCl₄²⁻. The catalyst was quantitatively recovered from the reaction mixture by simple filtration and reused for a high number of cycles. Interestingly, mechanistic insights evidenced that the reaction proceeded on the surface of the nanopalladium particles of the heterogeneous catalyst.

In 2004 Calò et al. reported on the use of electro-reduced Pd nanoparticles supported on chitosan (Fig. 6b) as efficient and highly recyclable heterogeneous catalysts for the Heck reaction of iodo-, bromo-, and activated chloro-arenes with *n*-butyl acrylate in tetrabutylammonium-based ILs [82]. Noteworthy, this system was inactive when used in imidazolium-based IL.

Pan et al. used the microwave irradiation for promoting the Pd/C-catalyzed olefination of iodo- and bromo-arenes in [omim][BF₄] (omim = 1-*n*-octyl-3-methylimidazolium), in the absence of phosphane ligand [83]. The catalyst, immobilized into the IL phase, was reused five times with a little loss of activity.

The Heck reaction between bromobenzene and styrene performed in tributylhexylammonium bistriflimide, using ultrafine particles of palladium metal supported onto hydrophilized mesoporous soot as the catalyst, has confirmed the fundamental role of the IL in the catalyst stabilization, also evidencing that the reaction occurs through a “true heterogeneous” mechanism [84].

Mesoporous SiO₂ is a widespread support for metal catalysts, due to its excellent chemical and thermal stability, high porosity, large surface area, and high surface concentration of silanols. Pd nanoparticles have been recently immobilized on silica-based molecular sieves SBA-15 using 1,1,3,3-tetramethylguanidinium lactate (TMGL) as IL [85]. This catalytic system showed an excellent activity and recyclability for the Heck reaction of aryl iodides at 140°C.

2.4 *Task-Specific ILs*

Besides supporting them onto insoluble matrices, another attractive solution to prepare robust catalysts is the covalent tethering of a functional groups to one or both ions of an ordinary ionic liquid that can impart to the resulting salt the ability to work itself as a support. These functionalized ILs are referred to as “task-specific” ionic liquids (TSIL) and are finding an increasing number of applications in synthesis, separation techniques, and catalysis.

Many efforts have been devoted to the functionalization of ionic liquids by incorporating specific groups such as amines, hydroxyls, phosphanes, phosphinites, and nitriles, into the imidazolium ring, with the aim of synthesizing new ionic solvent having a solvo-catalytic behavior [86].

In this context, during the last decade, a plethora of functionalized ionic liquids have been prepared and used for anchoring palladium as chelate or carbene complexes. Table 1 summarizes some of the most representative catalytic systems formed following this approach along with their applications to the Heck coupling.

A large contribution in this field comes from Shreeve’s group (Table 1 [87–92]) who prepared and used several modified TSILs bearing a number of modified imidazolium cations such as 2,2’-monoquateryary diimidazole, *N*-pyrazolyl 2-methylimidazolium, *N*-pyrazolyl 2-methylimidazolium, pincer dication, dicationic imidazolium and triazolium.

Under the Heck coupling conditions all these TSILs were able to give rise to stable and active palladium catalysts acting as carbenes (by H deprotonation in C-2) or *P*- (phosphinite) and *N*-donor ligands. In some case, the TSIL bearing a tetraalkyl-ammonium cation has been found suitable for stabilizing the Pd colloids formed in situ. Interestingly, a series of imidazolium-based ILs *N*-functionalized with diol or glyceryl groups have been used as ligands and solvents for palladium(II)-catalyzed reactions. These compounds present, besides the *N*-heterocyclic donor moiety arising from the imidazolium skeleton, the ethylene glycol group able to act as an excellent chelating ligand.

Particularly intriguing are TSILs bearing basic groups like tertiary amine that render the IL suitable to function as both solvent and proton scavenger (Fig. 7a). An intriguing approach is also the use of mixtures of differently substituted ILs which can exert the functions of ligand, base and reaction medium (Fig. 7b). Comparing results obtained using a single IL with those achieved with their binary mixtures evidences that the mixtures were superior to each single IL tested, thus highlighting a synergistic effect of the ILs [99].

2.5 *Supported and Layered Ionic Liquids*

Materials making use of thin ionic liquid films as support-modifying functional layer open up a variety of new possibilities in heterogeneous catalysis, which range from the tailoring of gas–surface interactions to the immobilization of molecularly

Table 1 Summary of the most relevant protocols using task-specific ionic liquids used in the Heck reaction

Type	Formula	Pd catalyst	Applications	References
2,2'-Monoquaternary diimidazole			Recyclable Heck coupling of iodo- and chloro-arenes with methyl acrylate	[87]
N-Pyrazolyl 2-methyl imidazolium			Recyclable Heck (and Suzuki and Sonogashira) coupling of haloarenes	[88]
N-Pyrazolyl 2-methyl imidazolium			Recyclable Heck coupling of aryl halides	[89, 90]
Pincer dication			Recyclable Heck coupling of iodo- and bromo-benzene	[91]
Dicationic imidazolium and triazolium			Heck reaction	[92]

Imidazolium based phosphinite		A PdL ₂ species is supposed to operate. No NMR evidence of Pd-carbene complex formation	Recyclable Heck coupling of aryl halides (including chlorobenzene) with styrene and butyl acrylate	[93]
Nitrile functionalized imidazolium			Various C–C couplings	[94]
Glyceryl imidazolium		R = Me or (CH ₂) _n CN R ₁ = H, Me	High reaction rates in the Heck coupling of iodobenzene. The reaction yields increased on increasing the alkyl chain on cation	[95]
Diol imidazolium		R = <i>n</i> -octyl, Bu, Me X = Cl, Br	Recyclable Heck coupling of aryl bromides under aerobic condition	[96]
Tetra-alkylammonium			Heck coupling with activated and deactivated iodo, bromo, and chloroarenes	[97]
Brønsted guanidine acid-base			Recyclable Heck reaction of aryl halides with styrene and butyl acrylate	[98]

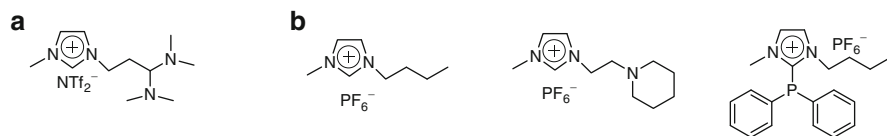


Fig. 7 (a) An example of an ionic liquid bearing basic functionalities. (b) A mixture of monofunctionalized ILs with synergistic effect

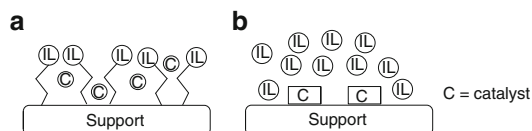


Fig. 8 General scheme for (a) a SILP and (b) a SCILL material

defined reactive sites. In this context, during the last decade the “supported ionic liquid phase (SILP)” [100–102] and “solid catalysts with an ionic liquid layer (SCILL)” materials are the most important developed methodologies [103–105].

Basically, in a supported ionic liquid phase (SILP or SCILL) catalyst system, an ionic liquid film is immobilized on a high-surface area porous solid, and a homogeneous catalyst is dissolved in this supported IL layer (Fig. 8). Typically, there is no direct interaction between the homogeneous catalyst and the support surface, and thus the molecular control over the catalytic activity is well maintained.

The activity and selectivity is affected by the coating in two ways: (1) the IL may have a beneficial effect on the chemical properties of the catalyst (“cocatalytic effect”) or (2) the IL changes the concentrations of reactant and/or intermediate, compared to the uncoated catalyst (“solvent effect”). For example, the selectivity towards the intermediate is favored if this latter is less soluble in the IL than the reactant.

This approach potentially combines the attractive features of homogeneous catalysts with the benefits of heterogeneous catalysts, and the resulting advantages seem to be: (1) an increased surface/volume ratio, (2) an easier diffusion of substrates to the IL-dissolved catalyst, especially of gaseous reagents, (3) the possibility to use highly viscous ILs, (4) small amounts of ILs requested, (5) the opportunity to operate in gas phase or liquid phase reactors, (6) a facile catalyst recovery, (7) the possibility to work under continuous operation. In addition, their low vapour pressure allows the IL films to remain on the catalyst surface under reaction conditions. Moreover, by properly choosing the combination of anion and cation, it is possible a fine tune of the physicochemical properties of the ionic liquids [105]. Some selected examples are reported below.

In 2005 polymeric beads of a PEG-supported IL (PEG = polyethyleneglicol), prepared via the covalent anchoring of an imidazolium salt to a PEG-4000 support,

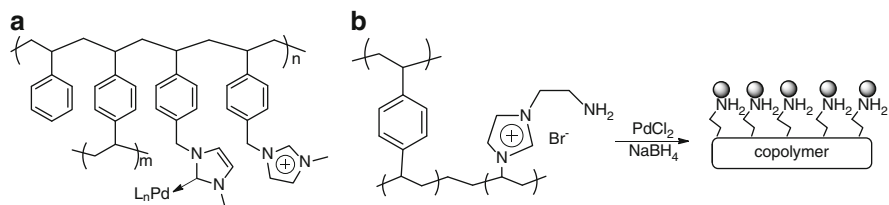


Fig. 9 (a) Gel-supported ionic liquid-like phases (g-SILLP). (b) Pd nanoparticles anchored on a polymeric aminoethyl imidazolium grafted on a cross-linked polydivinylbenzene (PDVB)

were used as a novel reaction medium for the Heck reaction. Using the $\text{Pd}(\text{OAc})_2/[\text{PEGmim}][\text{Cl}]$ system, the Heck coupling of both aryl bromides and activated aryl chlorides with olefins afforded the coupled products in excellent yields, and the catalyst could be recycled five times without deactivation [106].

In 2010, García-Verdugo et al. used a catalytic system in which palladium was immobilized onto gel-supported ionic liquid-like phases (g-SILLPs) based on gel-type polystyrene-divinylbenzene resins (Fig. 9a) [107]. Palladium was initially supported onto the g-SILLPs as Pd–NHC complexes and the microenvironment allowed a controlled release, under the reaction conditions, of the active species to the homogeneous phase. The presence of additional IL-like moieties contributed to stabilize and recapture the palladium species released in solution, rendering the catalyst easily recoverable, reusable and with essentially no Pd leaching at the end of the reaction.

Another intriguing protocol exploits a copolymer obtained from 1-aminoethyl-3-vinylimidazolium bromide grafted on the cross-linked polydivinylbenzene (PDVB), which is used as a support to immobilize palladium nanoparticles (Fig. 9b). The performance of the catalytic system was studied under solvent-free conditions in the Heck arylation of olefins with different aryl iodides demonstrating that the catalyst was very active and stable and could be reused after simple separation [108].

Similarly, an efficient and reusable heterogeneous catalytic assembly of PdCl_2 incorporated into SiO_2 -supported imidazolium ionic liquids (the so-called ionic liquids brushes) has been used in the coupling of aryl iodides with acrylic acid in water as the solvent and under aerobic conditions, giving the desired products in excellent yield without the need for organic co-solvent or other additives (Fig. 10). A 0.5 mol% of Pd was found to be sufficient for Mizoroki-Heck reaction. In addition, the catalyst was easily recovered after reaction and reused at least eight times [109].

Finally, it is noteworthy the recent application of silica supported ionic liquid phases (SILPs) to the Heck couplings. After IL immobilization, palladium nanoparticles 10 nm in size are trapped by hydrogenation in situ of Pd salts. The Heck coupling reaction of iodobenzene and cyclohexyl acrylate is successfully accomplished with competitive TONs and TOFs, and negligible palladium leaching. Separation of the products can be reached at ease, due to the fact that both palladium species and by-products are trapped within the monolithic foams [110].

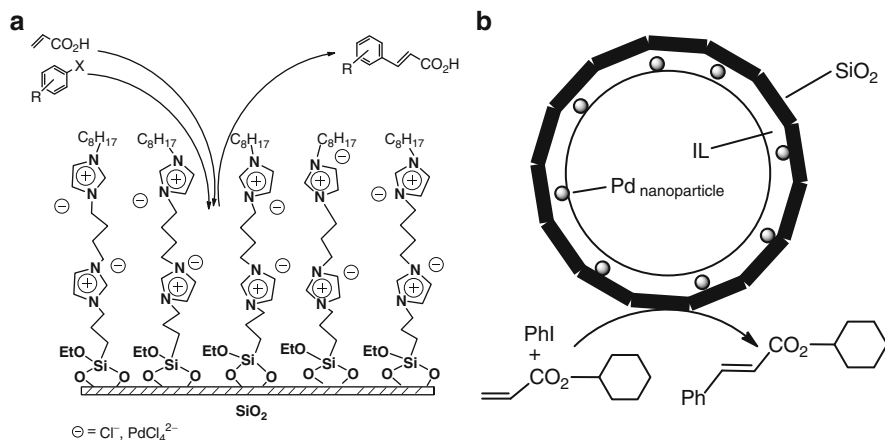


Fig. 10 (a) Imidazolium “ionic liquids brushes” supported on silica in the Heck coupling. (b) Pd nanoparticles in a SILP supported on macroporous silica-based foam

2.6 Heck Coupling in Chiral Ionic Liquids

Chiral ionic liquids (CILs) represent one of the most interesting groups of ionic liquids, and the number of publications dealing with CILs is growing rapidly. Some recent reviews [111, 112] survey the most representative developments and the progress concerning these chiral media.

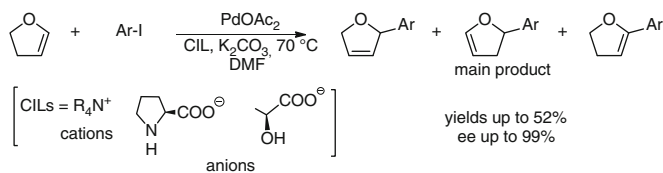
In asymmetric synthesis, it is often believed that CILs can be used as chiral solvents and as sole inducer of chirality due to their polymer-like behavior and potential high degree of organization. However, very few results are reported which demonstrate such potential.

The source of chirality can be provided either on the anion or on the cation, and for economic reasons the synthesis of most of CILs arises directly from natural sources. Representative examples are the use of (–)-menthol and natural aminoacids.

CILs have been applied in metal-free asymmetric catalysis (e.g., aldol condensations, Baylis–Hillman or Michael addition reaction). In the case of metal mediated catalysis, CILs are used mainly in double bond addition reactions as a chirality source or as a “chiral booster” for classic chiral ligands.

There are only few reports about application of CILs in the Heck coupling. Gayet et al. [113] reported on the arylation of 2,3-dihydrofuran (DHF) with iodobenzene catalyzed by a pyridinium CIL with $[\text{PdCl}_4]^{2-}$ as a counterion in $[\text{bmim}][\text{PF}_6]$ medium. Two other examples concern the oxyarylation of 7-benzyloxy-2H-chromene [114], and the arylation of aza-endocyclic acrylate in various imidazolium and pyridinium CILs.[115] However, very low enantiomeric excess ($ee < 5\%$) was observed in all these cases.

In 2011, Trzeciak’s group reported that CILs with stereogenic centers present in the anions are promising co-catalysts for the Heck coupling of dihydrofuran (DHF) with



Scheme 12 Enantioselective Heck arylation of DHF in chiral ionic liquids (CILs)

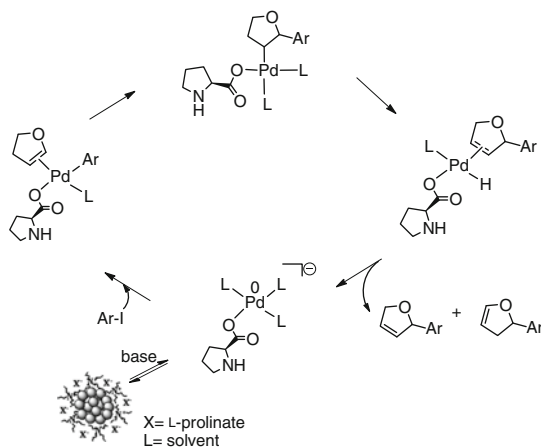


Fig. 11 The proposed mechanism for the asymmetric Heck arylation of DHF (adapted from [117])

iodobenzene, even if with still unsatisfactory *ee* values (up to 17%) [116]. More recently, the same authors found that CILs containing non-chiral quaternary ammonium cations and *L*-prolinate and *L*-lactate anions as chiral inducers allowed the efficient palladium-catalyzed enantioselective Heck arylation of DHF with a series of aryl iodides. With this protocol 2-aryl-2,3-dihydrofurans were achieved as main products in moderate to excellent enantioselectivity (until 99% *ee*) depending on the nature of the CIL and of aryl iodide (Scheme 12) [117].

A number of factors such as the nature of IL ions, the [CIL]:[Pd] molar ratio and the reaction time affect both conversion and selectivity of the coupling. The best results of 52% of yield and 99% *ee* were obtained with tetrabutylammonium *L*-prolinate $[\text{Bu}_4\text{N}][\text{L-PRO}]$ as the CIL in a two-fold excess with respect to $\text{Pd}(\text{OAc})_2$ and in a maximum reaction time of 6 h.

An homogeneous halide-free pathway was proposed as reaction mechanism (Fig. 11) in which Pd(0) nanoparticles (revealed by TEM analyses) act as a source of soluble palladium catalyst species. In addition, the chiral carboxylate anion *L*-prolinate (more basic than lactate) competes more efficiently with I^- for a place in the coordination sphere of palladium and is responsible for the asymmetric induction. The proper selection of the non-chiral cation turned out to be also very important and higher *ee* values were achieved with bulky cations for two reasons: (1) the stabilization of Pd nanoparticles by means of steric interactions with the cations and (2) the influence of the cations on the nucleophilicity of the chiral anion.

2.7 Ionic Liquid Effect on Activity and Selectivity

Based on the results reported hitherto, it is apparent that ionic liquids cannot be considered innocent solvents, but the ionic environment they create may change the course of the reaction in different ways: for example by generating new stable catalysts (e.g., carbene complexes, palladium nanoparticles, or palladium anionic complexes) or by stabilizing intermediates or transition states. The two main evidences of the action of these reaction media are an increase of the reaction rate and/or a better control of the regio- and stereo-selectivity in comparison with “classical” solvents.

The control of regiochemistry is certainly one of the main signs of the ionic liquid effect. To better understand this point, it is worthwhile to recall the well-known dualism of the traditional Heck cycle between “neutral” and “ionic” pathways (Fig. 12). The “neutral” mechanism is characterized by dissociation of one of the coordinating neutral ligand L, while the “ionic” one generates a Pd-cationic species through the dissociation of the (pseudo)halide anion X^- . This double change directly affects the regiochemistry of the Heck reaction. Usually, with monodentate ligands and aryl halides, the neutral pathway dominates, driving the arylation to the β -position of the starting olefin, producing linear alkenes. In contrast, in the presence of low-coordinating anions ($X = \text{tosylate, TsO}$) and chelating bidentate ligands, the ionic pathways prevails, affording branched olefins arising from the regioselective arylation to the α -position.

This is, of course, a simplified view, as several other factors may affect the regioselectivity, primarily the steric and electronic effects on the starting olefins. As a matter of fact, a complete regioselective control is often difficult, especially in the case of electron-rich olefins such as vinyl ethers or enamides.

The environment created by the ionic liquid can be determinant for discriminating between a neutral or an ionic pathway followed by the catalytic system. The two following examples highlight the influence exerted by the nature of both the cation and the anion of the ionic liquid in the type of mechanism and, ultimately, in the regioselectivity of Heck reactions.

In 2005, Xiao et al. [69] reported an elegant regioselective α -arylations of electron-rich olefins, such as enol ethers, enamides, and allyl silanes, by using imidazolium-based ionic liquids in conjunction with Pd-1,3-diphenylphosphanylpropane precatalyst (Scheme 13).

This high degree of regio-control was attributed to the ionic environment created by the IL, which shifts the equilibrium of (1) to the right (Scheme 14) favoring the dissociation of the bromide anion in a classical ionic pathway. This was evidenced by the fact that arylation was notably slowed down by the addition of bromide anions (as $[\text{Bu}_4\text{N}]\text{Br}$) to the reaction mixture. A further confirmation of this hypothesis was given by the addition of hydrogen-donating salts such as $[\text{HNEt}_3][\text{BF}_4]$ that increased both the rate and the selectivity in ionic as well in molecular solvents, presumably by facilitating that dissociation [70].

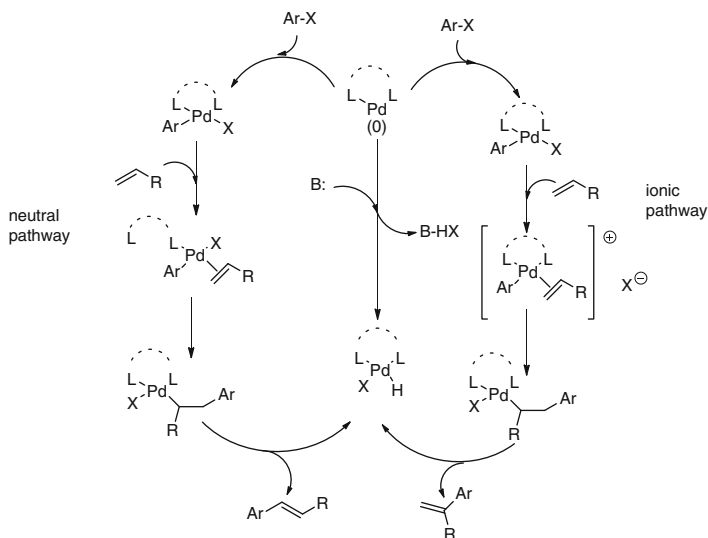
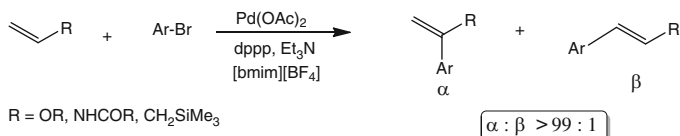
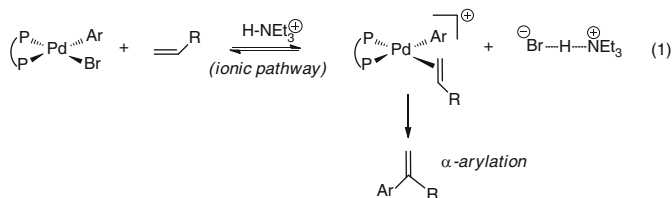


Fig. 12 The proposed neutral and ionic pathways for the Heck reaction

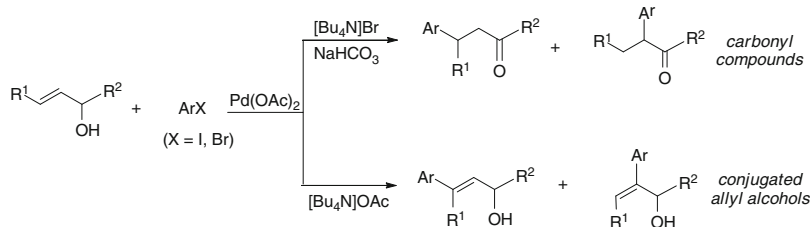


Scheme 13 Regioselective α -arylations of electron-rich olefins

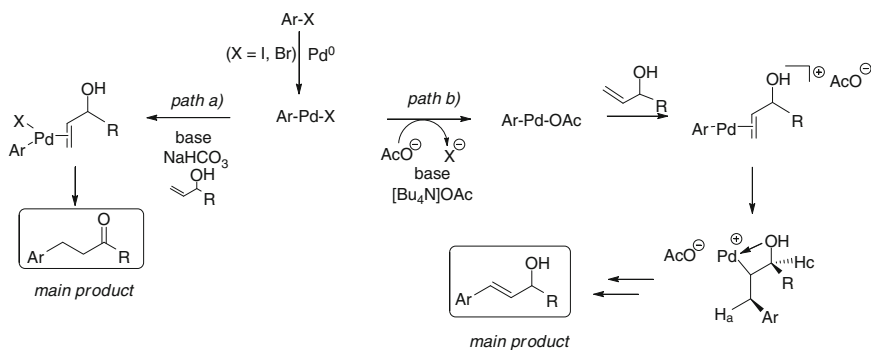


Scheme 14 Regiocontrol of the Heck reaction in ILs by addition of a proton source

In 2007 Nacci and coworkers [118] demonstrated that the regioselectivity of the Heck arylation of allyl alcohols in tetraalkylammonium ionic liquids depends on the nature of the IL anion. In particular, using $[\text{Bu}_4\text{N}]\text{OAc}$ dually as solvent and base, the Heck arylation of allylic alcohols resulted highly selective towards the formation of aromatic conjugated alcohols, while with $[\text{Bu}_4\text{N}]\text{Br}$ as solvent and NaHCO_3 as the base the aromatic carbonyl compounds were selectively obtained (Scheme 15).



Scheme 15 Regioselective arylation of allylic alcohols



Scheme 16 Mechanisms involved in the arylation of allylic alcohols in ILs

It is reasonable that the reaction can follow two different pathways, depending on the nature of the ligand X bonded to palladium before the migratory insertion of the aryl group on the olefinic double bond. The ligand, in turn, depends on the anion which prevails in the reaction medium (Scheme 16). In particular, when $[\text{Bu}_4\text{N}]\text{Br}$ is used as solvent, and a conventional base such as NaHCO_3 is employed, the ligand X is bromide or iodide and the reaction follows the neutral pathway (path *a*).

For steric reasons, the migratory insertion of the aryl group occurs predominantly at the β -position of the alkenol, giving rise to β -arylated carbonyl products. In contrast, when $[\text{Bu}_4\text{N}]\text{OAc}$ is used as the reaction medium, an anionic metathesis probably occurs, and the acetate anion readily dissociates to give a cationic complex. In this case, the migratory insertion on the double bond occurs prevalently to the β -position due to the formation of a chelate structure, which impedes also the hydrogen atom H_c to adopt the *syn*-relationship with Pd, necessary for the β -elimination. Hence, the abstraction of the benzylic hydrogen atom (H_a) remains the only possible pathway.

Besides the influence on the regioselectivity, numerous other factors affect the catalyst activity in ionic liquids which are related to the ability of different types of ionic liquids to generate and/or stabilize several species such as Pd carbenes, Pd nanoparticles, and cationic Pd complexes [14, 15, 119, 120].

Finally, it is worthwhile to outline the existence of an anionic version of the Heck cycle, analogous to that ascertained by Amatore and Jutand for the catalysis by Pd

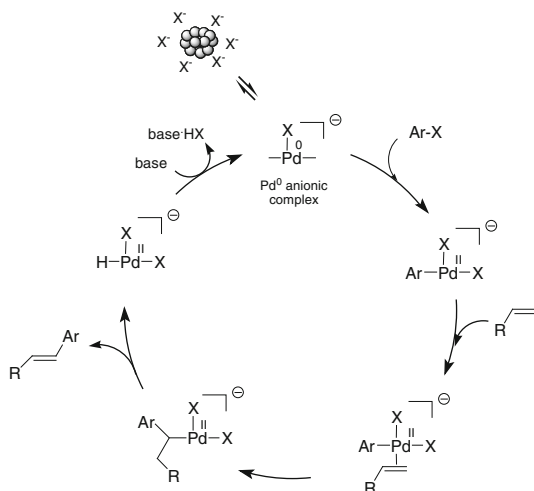


Fig. 13 The “anionic” pathway proposed for the Heck cycle in the presence of halide salts

(OAc)₂/PPh₃ [121, 122] (Fig. 13) that can be invoked also in cross-coupling reactions in ILs. In the case of Pd colloids and in the presence of halides salts, de Vries [123] proposed, based on EXAFS and mass spectrometry experiments, that the role of the salt may be twofold: (1) it stabilizes the colloids, thus preventing their further growth to palladium black; (2) the halide anions act as ligand for palladium in the actual catalytic cycle, which proceeds through anionic intermediates.

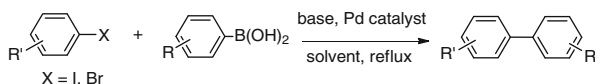
The anionic pathway seems to be preferred in case of most traditional, high temperature Heck reactions carried out with colloids in [Bu₄N]Br [53, 61], while, in case of triflates or other arylating groups bearing non-ligating leaving groups (not halides), the neutral pathway has been often invoked. The anionic pathway is also invoked to explain the higher activity of palladium in activating the less reactive chloroarenes in tetraalkylammonium ILs, for example, in [Bu₄N]Br.

It should be kept in mind, however, that the type of catalytic cycle followed by the system (anionic, neutral, cationic) depends on several factors, including the type of ionic liquid, the substrate, the leaving group, the base, and the metal ligand.

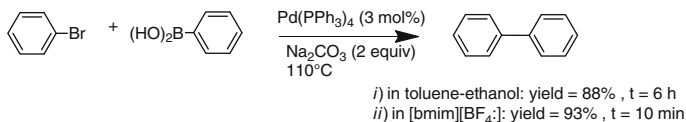
There are still some shadows in the Heck mechanism that have to be highlighted. For example, a Pd(II)/Pd(IV) cycle [124], although not generally accepted, is still being debated and the exact role of the base is still under investigation [125].

3 Suzuki–Miyaura Reaction

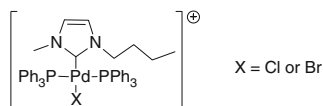
The Suzuki–Miyaura reaction between organoboronic acid and aryl halides [126] is considered the most powerful method for synthesizing the biphenyl skeleton. Particularly in the past decade, the biaryl scaffold has received increased attention



Scheme 17 A typical Suzuki reaction



Scheme 18 The Suzuki reaction performed in organic solvent and in IL



Scheme 19 Phosphine-imidazolylidene palladium complex

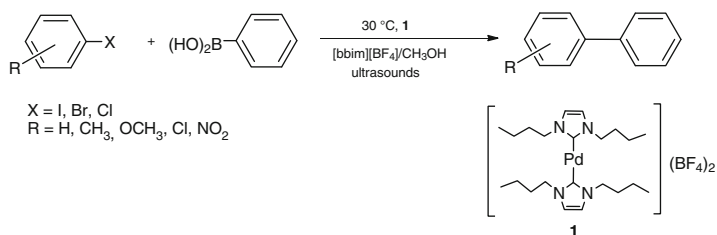
as a privileged structure by the agrochemical and pharmaceutical industries. The core of many types of natural products, advanced materials, polymers, sensors and ligands for asymmetric catalysis contains the biaryl moiety. Consequently, the development of new and efficient methods of synthesizing these structures is crucial to the work of a broad area of organic chemistry.

The Suzuki cross-couplings are typically catalyzed by soluble phosphane palladium complexes in organic solvents, iodo and bromoarenes being the most common reagents (Scheme 17). However, such a protocol suffers from the difficulty in recovering and reusing the expensive homogeneous catalysts.

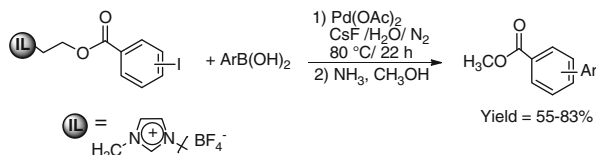
To overcome these drawbacks much work has been devoted to the development of Pd recyclable catalytic systems in ionic liquids [12, 17]. To date, more than a hundred papers can be found in the literature on the Suzuki coupling in ionic liquids media.

In 2000 [127], Welton reported for the first time on the use of ionic liquids in the Suzuki coupling, demonstrating the accelerating effect of the ionic medium. Indeed, the reaction of bromobenzene with phenylboronic acid under original Suzuki conditions (i.e., at 110°C using 3 mol% of Pd(PPh₃)₄ as the catalyst, in the presence of two equivalent Na₂CO₃) led to 88% yield in biphenyl in 6 h in toluene–ethanol [128], while the same reaction in [bmim][BF₄] gave 93% yield of the desired product in only 10 min (Scheme 18). Moreover, the extraction of the product was easy, being carried out with diethyl ether, while the by-product salts were removed by washing with excess water. After reaction workup, the ionic liquid/catalytic system could be reused for three times with no loss of activity and selectivity.

Working under carefully controlled conditions, the same authors detected into the catalytically active solutions a mixed phosphane-imidazolylidene palladium complex (Scheme 19) as the *true* active species for promoting the C–C bond forming reaction [129].



Scheme 20 Suzuki coupling accomplished by the recyclable Pd–biscarbene complex **1**



Scheme 21 Iodobenzoate compound supported onto an IL

In 2002, Srinivasan [130] found palladium-bis(carbene) complexes as the *true* catalyst in the Suzuki coupling at room temperature in [bbim][BF₄] (bbim = 1,3-di-*n*-butylimidazolium), in an interesting protocol carried out under ultrasonic conditions suitable for activating also the poorly reactive chloroarenes and, for improving substrates solubility, in the presence of methanol as co-solvent. The recovered IL could be recycled several times, even though the palladium catalyst progressively deactivated due to the formation of Pd black. Recycling of the catalytic system was possible only when the preformed Pd–biscarbene complex **1** was used as the catalyst (Scheme 20).

The first use of tetrahedral ionic liquids in Suzuki couplings was due to McNulty et al. [131], who employed tetra-*n*-decyltrihexylphosphonium chloride (THPC), in conjunction with Pd₂(dba)₃ (1%) and triphenylphosphane, with the addition of small amounts of toluene (for increasing boronic acid and aryl halide solubility) and water (for increasing the solubility of the potassium phosphate base).

By using mild temperatures (50–70°C) aryl halides, including aryl chlorides, reacted smoothly in THPC and no homo-coupling products were observed. Moreover, the catalytic system was recycled up to five times with negligible loss of activity and selectivity.

Very interesting was the use of ILs to support aromatic substrates and to improve their solubility in water. In 2003, Chan et al. [132] reported a protocol in which the substrate (a iodobenzoate compound) was linked to an imidazolium-based ionic liquid thus becoming water soluble. The Suzuki coupling with phenylboronic acids was accomplished in this mixed IL/H₂O medium and after reaction, cleavage with ammonia/methanol gave biaryl products in good yields and high purities, without the need for chromatographic purification (Scheme 21).

In 2004, Dyson et al. [133] used a series of ionic liquids based on the *N*-butyronitrile pyridinium cation [C₃CNPy]⁺ (Fig. 14a), designed to improve retention of Suzuki and

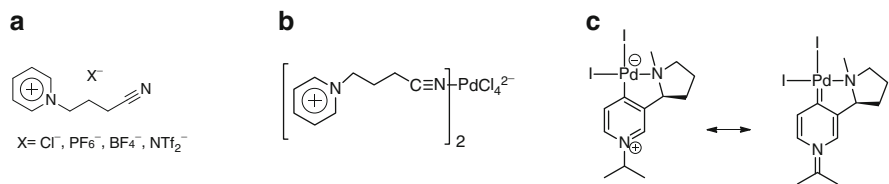
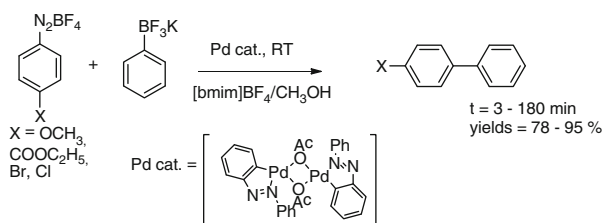
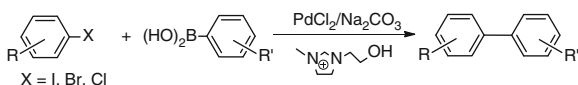


Fig. 14 (a) Nitrile-functionalized pyridinium ionic liquids. (b) The corresponding catalysts formed with PdCl₂. (c) A palladium-pyridylidene *N*-heterocyclic carbene complex



Scheme 22 Coupling of aryldiazonium tetrafluoroborates with organotrifluoroborates in IL



Scheme 23 Suzuki reaction in a hydroxyl-functionalized imidazolium-based ionic liquid

Stille catalysts. Pd-nitrile complexes formed in situ by reaction of [C₃CNPy]X with PdCl₂ (Fig. 13b) showed good activity, and a recyclability considerably superior to those observed in *N*-alkylpyridinium ionic liquids devoid of nitrile functionalities.

Pyridinium based ionic liquids were also used as reagents for palladation in the presence of a base to obtain palladium-pyridylidene *N*-heterocyclic carbene complexes that proved to be active catalysts for Suzuki reactions (Fig. 14c) [134].

A variant of the Suzuki protocol entails the use of aryldiazonium tetrafluoroborates, derived from inexpensive and easily accessible anilines, with organoboronic acids or esters in the absence of base. In this framework, in 2005 Mastrorilli et al. [135] performed successfully the Suzuki coupling between aryldiazonium tetrafluoroborates and organotrifluoroborates in different ILs. High activity and selectivity were shown by catalytic systems comprised of azopalladacycles in [bmim]BF₄/CH₃OH mixtures (Scheme 22).

Remarkable results were obtained in 2009 by Dyson [136] in the Suzuki reaction of aryl chlorides using a hydroxyl-functionalized imidazolium-based ionic liquid. It was demonstrated that the ionic liquid plays a critical role in catalyst/substrate activation directly facilitating the “ligand-free” coupling reactions (Scheme 23).

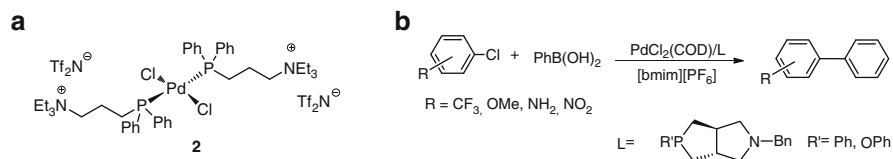


Fig. 15 (a) A triethylammonium-tagged diphenylphosphine palladium(II) complex suitable catalyst for Suzuki coupling in pyrrolidinium IL. (b) Suzuki coupling of chloroarenes in IL catalyzed by a Pd complex bearing an azadioxaphosphabicyclo-octane ligand

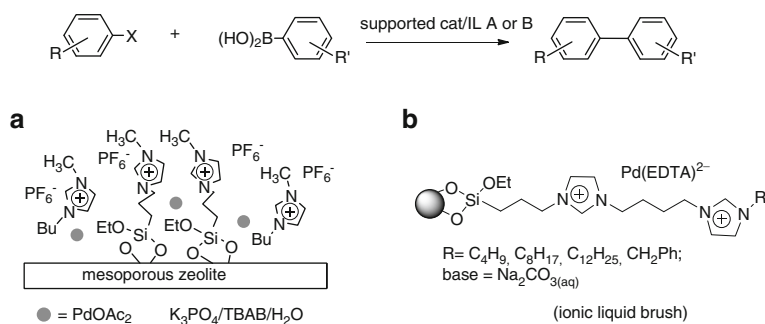
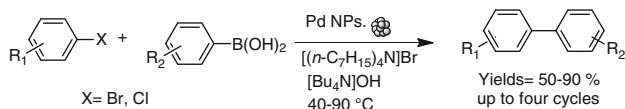


Fig. 16 Supported IL film on mesoporous zeolite (a) and imidazolium “ionic liquid brush” (b) as reaction media for Suzuki coupling

Trombini et al. [137] reported the Suzuki coupling of bromoarenes in good to excellent yields in a pyrrolidinium-based ionic liquid by using the triethylammonium-tagged diphenylphosphane palladium(II) complex **2** (Fig. 15a), and more recently Gómez et al. [138] discussed the use of new azadioxaphosphabicyclo[3.3.0]octane ligands for Suzuki cross-coupling reactions between phenylboronic acid and aryl chlorides bearing either electron-donor or electron-withdrawing substituents, in both organic and ionic liquid solvents (Fig. 15b).

Very intriguing are some recent applications of the supported ILs film (SILP). Two examples concern the use of palladium acetate immobilized in thin ionic liquid layers on the mesopore wall of hierarchical MFI zeolite **A** (Fig. 16) [139] and $[\text{Pd}(\text{EDTA})]^{2-}$ immobilized in an “ionic liquid brush” **B** (Fig. 16) [140]. These reactions were carried out in water under aerobic conditions.

Several reports deal with the use of Pd nanoparticles as catalysts for the Suzuki coupling in ILs. Calò's group [141] was one of the first in using Pd nanocatalysts in these media, demonstrating also in this case the good performance of tetraalkylammonium salts in stabilizing colloids. In particular, it was found that quaternary ammonium salts bearing long alkyl chains, such as tetraheptylammonium bromide in the presence of tetrabutylammonium hydroxide as base afforded remarkable catalyst activity enhancement, permitting the coupling to proceed smoothly under relatively mild conditions (ranging from 40°C for aryl bromides to 90°C for unreactive electron-rich chlorides, Scheme 24). The high activity of the catalytic



Scheme 24 Suzuki coupling in tetraheptylammonium bromide promoted by Pd nanoparticles

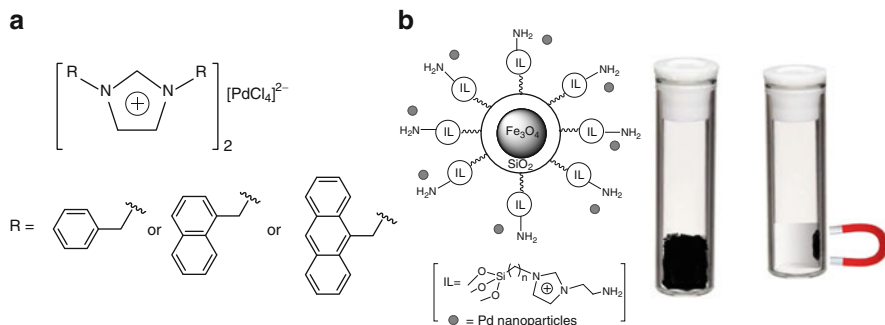


Fig. 17 (a) Tetrachloropalladate salts used as pre-catalyst in the Suzuki coupling carried out in [emim][Tf₂N]. (b) Pd nanoparticles immobilized on a supported imidazolium IL grafted on magnetic Fe₃O₄ covered by SiO₂, which can be separated by means of an external permanent magnet

system was attributed to the nature of both the cation and the anion of the IL as well as of the base, ascribing to the longer alkyl chains of the IL cation the ability to stabilize the nanoparticles, not only by protecting the metal core but also by sterically inhibiting its access. On the other hand, due to its nucleophilicity the bromide anion could act as a cocatalyst, by entering into the metal sphere and forming more active Pd(0) anionic species as already illustrated for the Heck coupling in [Bu₄N]Br [65, 141].

Gómez [142, 143] reported the use of [bmim][PF₆] as efficient immobilizing media for Pd nanoparticles. Since then on, a number of protocols have been reported on the use of Pd colloids in the Suzuki coupling in ILs [144–147]. Two recent selected examples are describe here.

In the first one, tetrachloropalladate salts (obtained from different imidazolium-based salts bearing aromatic moieties) as pre-catalysts (Fig. 17a) are used in Suzuki coupling performed in [emim][Tf₂N] (emim = 1-ethyl-3-methylimidazolium) [148]. TEM analyses demonstrated that under reaction conditions Pd nanoparticles with mean diameter of 6 nm were formed. The catalytic system was active and recyclable with iodo- and bromoarenes but was unactive with the more challenging chloroarenes.

The second example is related to the use of magnetic nanoparticles, promising supports for immobilization of Pd catalysts that are gaining more and more attention in the last years. This methodology is becoming of wide application due to the easy separation of catalyst from the reaction medium by means of an external permanent magnet. In a recent paper, palladium nanoparticles immobilized on

amine functionalized imidazolium ionic liquid grafted on magnetic Fe_3O_4 covered by SiO_2 exhibited high catalytic activity in the Suzuki coupling at room temperature. The catalyst can be separated from the reaction mixture by applying a permanent magnet externally and can be reused for several times without significant loss of activity (Fig. 17b) [149].

4 The Stille Reaction

The Stille cross-coupling [150] is an important palladium-catalyzed reaction between a trialkylorganotin compound and an aryl halide (Scheme 25). Typical alkyl groups on tin are methyls or *n*-butyls: trimethyltin derivatives as by-products are easy to remove but toxic, while tri-*n*-butyltin by-products are less toxic but difficult to take off.

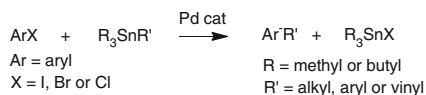
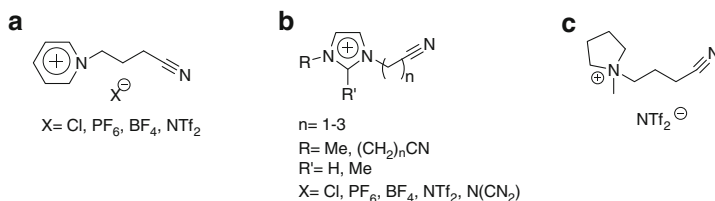
The Stille reaction is generally promoted by palladium complexes in organic solvents, but there are some examples of Stille couplings carried out in ILs.

The first study about the use of ILs in the Stille reaction deals with the catalytic activity of the $\text{PdCl}_2(\text{PhCN})_2/\text{AsPh}_3/\text{CuI}$ system at 90°C for the coupling of aryl iodides and bromides in $[\text{bmim}][\text{BF}_4]$ [151]. The evident advantage of using ILs instead of traditional organic solvents consists in the recyclability up to five runs of the catalyst and solvent.

In subsequent works the Stille coupling in ILs was carried out in the absence of ligands and/or additives. Since 2004, Dyson and coworkers published a series of articles on the use of a variety of nitrile-functionalized ILs for the C–C cross-coupling reactions, including the Stille reaction [94, 133, 152, 153]. In these studies, a series of pyridinium, imidazolium, and pyrrolidinium-based ILs with nitrile side-chains were designed to improve the catalyst retention (Fig. 18).

Interestingly, different types of complexes were obtained using PdCl_2 precursor, depending on the IL anion. In particular, the tetrachloropalladate complex $[\text{C}_3\text{CNpy}]_2[\text{PdCl}_4]$ was formed when the anion was Cl^- , whereas $[\text{PdCl}_2(\text{C}_3\text{CNpy})_2][\text{A}]_2$ species were formed with $\text{A} = \text{PF}_6^-$, BF_4^- , or $\text{N}(\text{SO}_2\text{CF}_3)_2^-$ anions. These palladium complexes showed promising catalytic activity in the cross-coupling of iodobenzene with phenyltri-*n*-butylstannane, with yield ranging from 43% to 63%. The introduction of nitrile functionality in the ionic liquid imparted to these catalytic systems a good recyclability (up to nine runs). Palladium nanoparticles with a mean diameter of 5 nm were identified as the active catalyst [133].

A similar trend was observed with nitrile functionalized imidazolium-based ILs. The coupling between iodobenzene and tri-*n*-butylvinyltin in the presence of $\text{Pd}(\text{OAc})_2$ at 80°C in the ILs depicted in Fig. 18b was found considerably more efficient in terms of activity and recyclability with respect to unfunctionalized imidazolium derivatives [143]. Interestingly, TEM analyses revealed also in this case the formation of palladium nanoparticles of ca. 5 nm in sizes, and colloids isolated from nitrile-functionalized imidazolium $[\text{C}_3\text{CNmim}][\text{BF}_4]$ and from $[\text{bmim}][\text{BF}_4]$ showed different morphologies, with well-separated nanoparticles in the former case in spite of

**Scheme 25** The Stille reaction**Fig. 18** Nitrile-functionalized ILs based on (a) pyridinium (C₃CNpy⁺), (b) imidazolium (RCNIm⁺ or (RCN)₂Im⁺), and (c) pyrrolidinium salts (C₃CNpyr⁺) with several anions

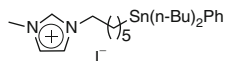
aggregated nanoclusters (up to ca. 30 nm) in the latter one [94]. The presence of a weak interaction between the nitrile group and the palladium nanoparticle surface, exerting a stabilizing effect and preventing aggregation, was proposed to explain these results.

Nitrogen-containing anions such as [NTf₂]⁻ and [N(CN)₂]⁻ were also employed as counterions of the functionalized imidazolium-based ILs. In some cases their use improved the catalyst performance and allowed a higher retention of palladium in the IL. In other cases the presence of [NTf₂]⁻ anion lowered the catalyst performance, presumably due to strong interactions of the anion with the metal center [94].

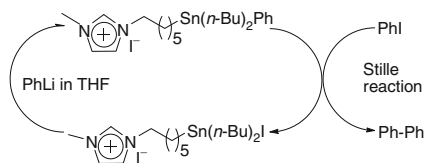
More recent results showed that, besides the promising influence of the nitrile group, ion-pairing effects and the viscosity of the IL play crucial roles in the catalytic performances. In this regard, the good performances obtained in pyrrolidinium-based ILs (Fig. 18c) have been attributed to their comparatively low viscosity [142].

In the framework of Stille coupling in ILs promoted by palladium nanoparticles, important results for activity and recyclability were obtained using tetraalkylammonium salts bearing long alkyl chains, such as tetra-*n*-heptylammonium bromide, in the presence of tetra-*n*-butylammonium hydroxide as base [141]. As in the case of the Suzuki reaction, the process afforded high product yields starting from aryl bromides, as well as simple or activated aryl chlorides. These substrates were in fact successfully converted (yields up to 90%) at 90°C after 16 h reaction, while deactivated electron-rich aryl chlorides turned out to be significantly less reactive and afforded modest yields (10–40%) of biaryls. The high efficiency of the catalytic system can be explained, as in the case of Suzuki reaction, in terms of the nature of the base and of the length of the alkyl chains of the IL cation which can ensure the nanoparticles stabilization.

Another interesting application of the IL system for promoting the Stille reaction deals with the synthesis of ionic liquid supported tin reagents with the aim of recycling the tin compounds (Scheme 26) [154].



Scheme 26 Ionic liquid supported tin reagent



Scheme 27 Stille reaction with IL supported Sn reagent

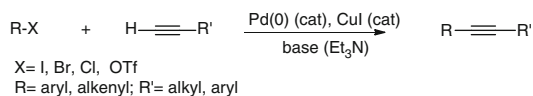
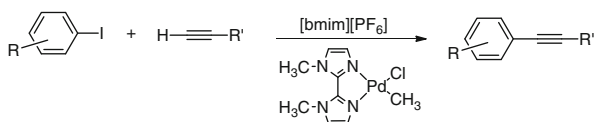
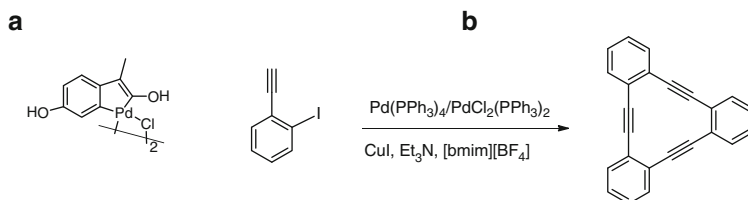
The best results were achieved using iodobenzene as the substrate (the catalytic system was inactive with bromobenzene) in the presence of 5 mol% of $\text{Pd}_2\text{dba}_3 \cdot \text{CHCl}_3$ reaching 98% yield in 112 h at 35°C. At the end of reaction, the products, the remaining starting material and/or side products were extracted by non-ionic liquid miscible organic solvents, while the palladium catalyst and the halogen-tin supported ionic liquid remained in the IL phase. The Stille starting material was regenerated by adding PhLi to this IL phase (Scheme 27).

Unfortunately, the activity of the catalytic system in the second run decreased, and a conversion of 72% was observed after 184 h at 35°C. Poisoning of the palladium catalyst by tin by-products and/or palladium and stannane leaching were presumably responsible for the lowering of the catalytic activity in the recycle, although the authors did not mention such hypothesis.

5 The Sonogashira Coupling

The Sonogashira reaction is known as the most powerful method for the formation of substituted or non-substituted acetylenes and finds applications in the preparation of pharmaceuticals, natural products, liquid crystalline materials, and conducting polymers. Typically, the Sonogashira coupling occurs between an aryl (or vinyl) halide and a terminal alkyne in the presence of a base (generally a tertiary amine), copper(I) salts (usually CuI) as cocatalyst, and palladium with phosphane ligands in organic solvents under inert atmosphere (Scheme 28) [155, 156]. Similar to the Heck coupling, also this process does not require organometallic reagents in stoichiometric amount, being Cu(I) used in catalytic amount. In addition, many copper-free methods have been recently developed.

Since ILs have been successfully used as solvents in many transition metal-catalyzed C–C bond coupling processes, they were also utilized for Sonogashira coupling, but, differently from Heck or Suzuki reactions, less examples have been reported.

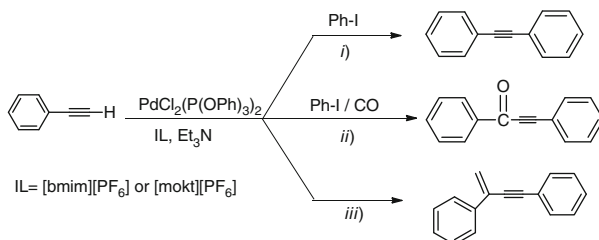
**Scheme 28** The Sonogashira reaction**Scheme 29** Sonogashira reactions in IL**Fig. 19** (a) Carbapalladacycle complex used in the Sonogashira coupling in PEG. (b) Synthesis of annulenes via cyclotrimerization of iodoarylalkyne

The first reports on Sonogashira cross-coupling in ILs appeared in 2002, when Ryu and coworkers developed a copper-free Sonogashira coupling in [bmim][PF₆] in a microflow system by using PdCl₂(PPh₃)₂ as reusable catalyst and diisopropylamine or piperidine as the base [157]. In the same period, the system Pd(OAc)₂/PPh₃/CuI/Et₃N in the same IL was reported to facilitate the coupling of aryl iodides with different alkynes at 80°C with moderate to good yields [158].

In 2004, Alper et al. avoided the use of both copper salts and phosphine ligands, by using a [(bisimidazole)Pd(CH₃)Cl] as catalyst in [bmim][PF₆] [159]. This system proved to be very stable and could be recycled many times without any loss of catalytic activity (Scheme 29).

In 2005, Corma and coworkers reported a comparative study between ionic liquids and polyethylenglycol (PEG) as solvent media for a catalytic system comprising a reusable palladium catalyst to be used in Sonogashira and Suzuki coupling reactions [160]. The carbapalladacycle complex shown in Fig. 19a developed from 4-hydroxyacetophenone oxime and palladium salt was used as pre-catalyst. It was found that PEG gave better results than ILs such as [bmim][PF₆], [bmim]Cl, [bdmim][PF₆] (bdmim = 1,2-dimethyl-3-*n*-butylimidazolium), probably due to the better stability of the Pd complex in PEG than in the ILs tested.

Pan et al. synthesized symmetrical and unsymmetrical tribenzohexadehydro[12]annulene and [12]annulenes via cyclotrimerization of iodoarylalkyne under Sonogashira conditions in [bmim][BF₄] using only 1% of CuI and minimizing homocoupling side reaction (Fig. 19b) [161]. The coupling under the same conditions but in THF as solvent did not occur.



Scheme 30 Various types of phosphito-Pd catalyzed Sonogashira cross-couplings in ILs

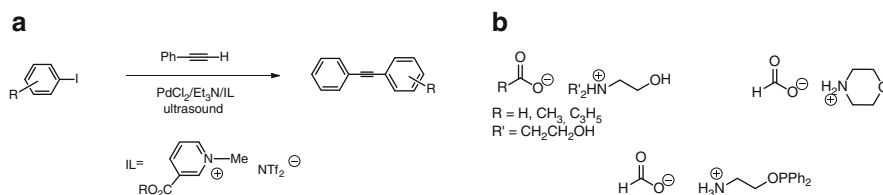


Fig. 20 (a) Sonogashira reaction in a biodegradable ionic liquid derived from nicotinic acid. (b) Ionic liquids based on carboxylate salts

In 2006, Trzeciak et al. [162] reported a simple as well as a carbonylative Sonogashira cross-coupling of terminal alkynes with aryl iodides catalyzed by $\text{PdCl}_2\{\text{P}(\text{OPh})_3\}_2$, in the presence of NEt_3 in $[\text{bmim}][\text{PF}_6]$ or $[\text{mokt}][\text{PF}_6]$ (mokt = 1-methyl-3-octylimidazolium) as ionic liquids (Scheme 30, routes *i* and *ii*). Moreover, in the absence of aryl iodide, the same catalytic system efficiently catalyzed the head-to-tail dimerization of phenylacetylene to 1,3-diphenylacetylene in 85% yield (Scheme 30, route *iii*). More recently, the protocol has been improved by using several triarylphosphito ligands substituted on the phenyl ring [163].

Ryu et al. [164] carried out the carbonylative Sonogashira coupling of iodoarenes in $[\text{bmim}][\text{PF}_6]$ at low pressure in a microflow system as well as the Sonogashira coupling in ionic liquid following a combinatorial approach [165].

In 2007 Picquet and coworkers reported the first catalytic method for the copper-free Sonogashira of unactivated aryl bromides in an ionic liquid. The protocol, developed in $[\text{bmim}][\text{PF}_6]$ at 130°C , uses $[\text{Pd}(\eta^3\text{-C}_3\text{H}_5)\text{Cl}]_2/\text{PPh}_3$ as catalyst in the presence of pyrrolidine as base and permits to couple aryl bromides with phenylacetylene or 1-decyne in good yields [166].

Examples of Sonogashira coupling in pyridinium salts have been recently reported [167, 168]. A copper- and phosphane-free reaction was performed in a biodegradable ionic liquid derived from nicotinic acid, under ultrasonic conditions (Fig. 20a). The system proved to be stable and highly recyclable [168].

A catalytic system based on carboxylate salts, acting as the base, ligand, reducing agent and solvent, has been used for the copper and phosphane-free Sonogashira coupling reaction of aryl iodides and bromides. The authors also introduced a phosphorylated version of one of these ILs showing high efficiency and recyclability under the same conditions (Fig. 19b) [169].

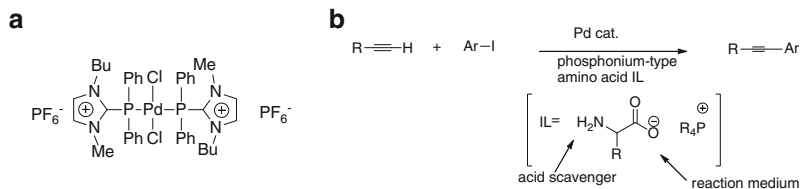


Fig. 21 (a) Sonogashira reaction in a biodegradable ionic liquid derived from nicotinic acid; (b) ionic liquids based on carboxylate salt

A task-specific IL has been reported consisting of a hexafluorophosphate imidazolium Pd-complex (Fig. 21a), which has been used as efficient and recyclable catalyst for the Sonogashira reactions of aryl iodides and aryl bromides with several terminal acetylenes in [bmim]PF₆. No Pd leaching or deactivation was observed even after several runs [170].

Recently, phosphonium amino acid ionic liquids have been found to be useful for the copper-free and amine-free Sonogashira coupling reaction (Fig. 21b). A hydrophobic and lipophobic ionic liquid permitted an easy separation of the product from the catalytic solution, which could be efficiently reused [171].

6 The Ullmann Homo-Coupling

The dimerization of aromatic halides, known as the Ullmann reaction, is a convenient method for the synthesis of biaryls. For a long time, this coupling has been replaced by analogous protocols, such as Suzuki, Stille, and Kumada, due to the need of an excess of copper as promoting agent and the harsh thermal conditions (with temperatures above 200°C).

However, the prevention in the use of stoichiometric amounts of expensive or moisture-sensitive organometallic compounds (i.e., boronic acids, stannanes, Grignard reagents etc.) can make this reaction of particular attraction for industrial applications.

A valuable version of the Ullmann reaction is the palladium-catalyzed homo-coupling of aryl halides under reductive conditions, which makes use of amines, zinc dust, molecular hydrogen, hydroquinone, alcohols, carbon monoxide, ascorbic acid or formic acid salts. However, most of these reducing agents are environmentally unsafe, and hence their replacement with clean and renewable substitutes, together with the use of more eco-friendly solvents, is advisable.

Despite the intrinsic importance of biaryls, only few protocols have been developed in benign solvents such as ionic liquids. The first one was reported by Rothenberg et al. in 2006, who carried out the Ullmann homo-coupling at room temperature in [omim][BF₄] (omim = 1-methyl-3-*n*-octylimidazolium) as ionic liquid under electro-reductive conditions [172]. The catalyst was made up of small Pd colloids (2 nm in size) generated in situ in an electrochemical cell (Pd-anode and Pt-cathode), and the

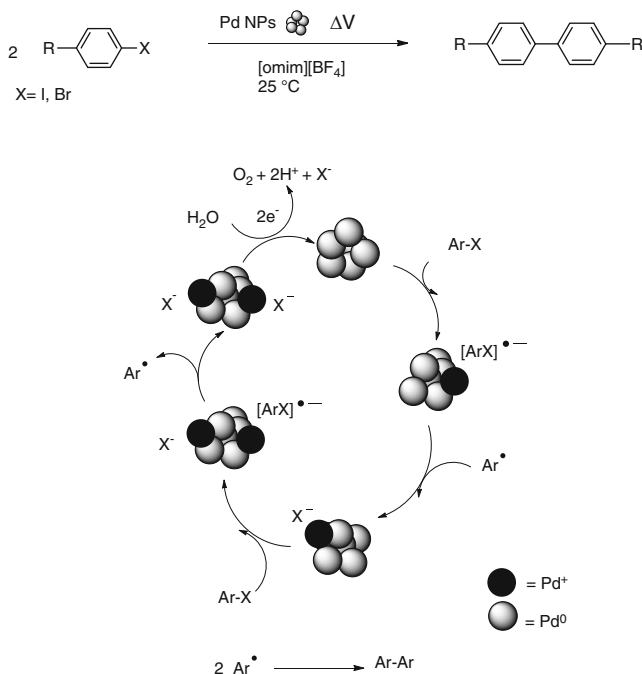
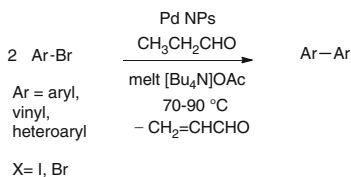


Fig. 22 Proposed catalytic cycle for the electroreductive Pd colloids Sonogashira coupling in [omim][BF₄] (adapted from [172])

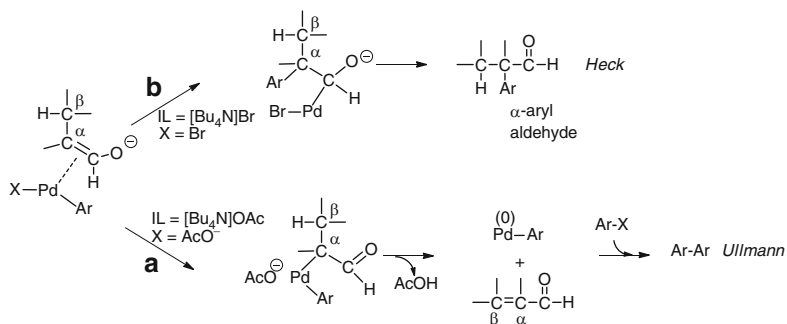


Scheme 31 The Ullmann coupling carried out with aldehydes as reducing agents

reduction was operated by the electric current flowing in the system, without the need for an extra-reagent. Mechanistic insights revealed that catalysis occurs on the Pd clusters surface and that water oxidation closes the catalytic cycle regenerating Pd(0) (Fig. 22).

In 2009, Nacci et al. [173] reported the Ullmann homo-coupling of aryl, vinyl and heteroaryl halides entirely performed in an ionic liquid. For the first time, an aldehyde (propanal) was used as reducing agent and the tetraalkylammonium IL, [Bu₄N]OAc, assumed the multiple role of base, reaction medium and stabilizing ligand for Pd colloid catalyst (Scheme 31).

With this protocol, bromo- and iodo arenes were coupled with good conversions (70–90%) and under relatively mild conditions (70–90°C) to the corresponding symmetrical biaryls in absence of other additives. The reducing equivalent was



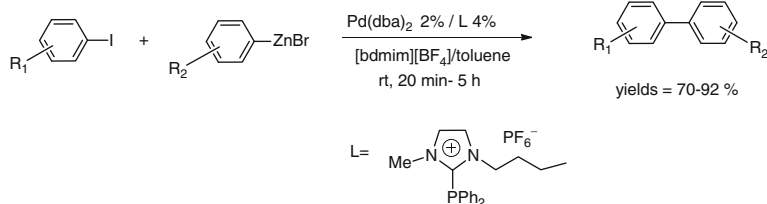
Scheme 32 The anion-dependence of the reaction mechanism (adapted from [173])

furnished by the dehydrogenation of the aldehyde and the advantage of the method was the simple preparation by mixing the substrates and palladium acetate in the IL, followed by the in situ formation of the catalytically active species. With propanal as reductant, the workup was facilitated by evaporation of the volatile by-product (acrolein).

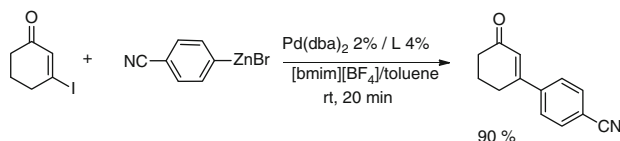
Remarkably, the simple change of the IL anion leads to a dramatic change of the reaction mechanism. In fact, when $[\text{Bu}_4\text{N}]\text{OAc}$ was replaced by $[\text{Bu}_4\text{N}]\text{Br}$ as the ionic solvent, the Heck α -arylation prevailed over the Ullmann homo-coupling. This different behavior can be accounted for on the basis of the different coordinating ability of bromide and acetate anion of the two ionic solvents that would make catalysis to follow two different pathways (Scheme 32). In $[\text{Bu}_4\text{N}]\text{OAc}$ as the solvent, the weaker coordinating acetate ion, rendering the palladium atom cationic in nature, leads to addition of the metal to the more nucleophilic position of the double bond of the enolate ion, that is the α position (path *a*). By contrast, in $[\text{Bu}_4\text{N}]\text{Br}$ the anionic nature of palladium should prevail, and the addition of the metal would occur to the more electrophilic side of the double bond, affording prevalently the Heck product (path *b*).

The Ullmann homo-coupling was also carried out in water under emulsified conditions, using glucose as a clean reductant and $[\text{Bu}_4\text{N}]\text{OH}$ as surfactant. In these studies, both free and supported nanoparticles were employed [174, 175]. In the latter case, the heterogeneous catalyst was made up of Pd colloids on zirconium oxide. Tetrabutylammonium hydroxide in water played the special role of creating a favorable environment for the catalyst. Indeed, in the emulsified mixture generated by the surfactant, reactions presumably occurred in the layer surrounding the nanoparticles surface, where a high concentration of the base OH^- is likely reached, with a corresponding increase of the reaction rate.

Very recently Cheng et al. developed a catalyst system based on Pd nanoparticles suitable to perform the Ullmann reaction of aryl chlorides in an economical and green mixture of IL and super critical CO_2 (scCO_2). The combination of IL and scCO_2 provided superior advantages in terms of product separation, catalyst recycling and reuse of reaction media over traditional organic solvents. In a first protocol [176], they used a Brønsted-acidic imidazolium IL such as 1-butyl-3-(sulfobutyl)-imidazolium



Scheme 33 2-imidazolium-phosphine used as Pd ligand in the Negishi reaction in IL



Scheme 34 Negishi coupling with an alkenyl iodide in IL

hydrogen sulfate $\{\text{bmim}(\text{HSO}_3\text{C}_4)[\text{HSO}_4]\}$, which acts as active hydrogen donor and stabilizing agent for Pd colloids. In a successive method [177] they introduced graphene oxide as support for palladium nanoparticles. This novel support bearing abundant carboxylic, hydroxyl, epoxy and aldehyde groups, replaced efficiently the traditional active hydrogen donor with much enhanced product separation efficiency.

7 The Negishi Reaction

First discovered in 1977, the Negishi coupling is an important nickel or palladium-catalyzed cross-coupling reaction which occurs between an organozinc compound and a variety of organic halides (aryl, vinyl, benzyl, or allyl). Allyl halides provide, in general, superior chemical yields and higher functional group tolerance [178, 179].

The first example of Negishi coupling in ILs was reported in 2000 by Knochel et al. who used a TSIL bearing a diphenylphosphane group in the 2-position of the imidazolium ring as a ligand for palladium (Scheme 33) [180]. The Negishi cross-coupling was carried out in $[\text{bdmim}][\text{BF}_4]/\text{toluene}$ (bdmim = 1-butyl-2,3-dimethylimidazolium) biphasic system and the 2-imidazolium- PPh_2 -Pd complex promoted the reaction at room temperature in short times with high yields.

The same 2-imidazolium- PPh_2 -Pd complex promoted the cross-coupling of 3-iodo-2-cyclohexen-1-one with an arylzinc reagent in $[\text{bmim}][\text{BF}_4]/\text{toluene}$ (Scheme 34) with high yield (90%) in short time (20 min). However, the catalytic activity of the recovered catalytic system decreased significantly after the third cycle. The poor recyclability observed, probably due to zinc contamination effects, discouraged further studies on the use of ILs as solvents for the Negishi reaction.

8 Conclusions and Outlook

In the past decade extraordinary advances in using ILs as the solvent media for catalysis have been reached. Concerning the palladium-catalyzed C–C coupling reactions, it is difficult to draw succinct conclusions on the impact of ILs on the catalyst performances, as the effect of ILs depends on the Pd precursor used, on the presence and nature of a base, and on the reactants. Nevertheless, many strides in the comprehension of the complex interactions between ILs and solute species that can affect their reactivity have been achieved. Although the results presented in this chapter can give an idea on the progress in this field, still much remains to be discovered.

It is commonly accepted that the catalytically active Pd species is determined in many cases by the nature of the ionic liquid, that may also act as a “reservoir” of active species consisting not only of molecular compounds such as Pd-carbenes, Pd-cationic species, anionic complexes such as $[\text{Pd}^0\text{L}_2\text{X}]^-$, but also of small Pd(0) clusters, bigger Pd nanoparticles or colloids. In the case of colloids, it is assumed, and in some instances demonstrated, that the reaction proceeds through the oxidative addition of the aryl halide on the Pd nanoparticle surface, and the oxidized Pd species thus formed are detached from the surface and enter the main catalytic cycle as an active molecular species.

In many cases, the effect of the IL on the reaction outcome can be so large that a simple change of the IL can lead to a radical change of mechanism, as exemplified by results obtained in the regioselective arylation of allyl alcohols, or in the Heck arylation of electron-rich olefins. A remarkably profound impact of the IL type on C–C bond forming reactions is that observed in the coupling of aryl halides with aldehydes, which affords products of Heck cross-coupling when carried out in $[\text{Bu}_4\text{N}]\text{Br}$ and of Ullmann homo-coupling when performed in $[\text{Bu}_4\text{N}]\text{AcO}$.

The research in Pd-catalyzed cross-coupling reactions in ionic liquids is particularly lively nowadays and very recent applications, for example, the task-specific ionic liquids (TSILs), or the supported ionic liquid phase (SILPs or brush ILs) as well as chiral ionic liquids (CILs) can be considered the new horizons of the investigations in this field.

References

1. Angell CA, Ansari Y, Zhao Z (2012) Ionic liquids: past, present and future. *Faraday Discuss* 154:9–27
2. de Mejere A, Diederich F (eds) (2004) *Metal-catalysed cross-coupling reactions*. Wiley, Weinheim, and references therein
3. Nicolaou KC, Bulger PG, Sarlah D (2005) Palladium-catalyzed cross-coupling reactions in total synthesis. *Angew Chem Int Ed* 44:4442–4449
4. Negishi E (2007) Transition metal-catalyzed organometallic reactions that have revolutionized organic synthesis. *Bull Chem Soc Jpn* 80:233–257

5. Corbet JP, Mignani G (2006) Selected patented cross-coupling reaction technologies. *Chem Rev* 106:2651–2710, and references therein
6. Deeth RJ, Smith A, Hii KK, Brown JM (1998) The Heck olefination reaction a DFT study of the elimination pathway. *Tetrahedron Lett* 39:3229–3232
7. Ludwig JM, Strömberg S, Svensson M, Åkermark B (1999) An exploratory study of regiocontrol in the Heck type reaction influence of solvent polarity and bisphosphine ligands. *Organometallics* 18:970–975
8. Amatore C, Jutand A (1999) Mechanistic and kinetic studies of palladium catalytic systems. *J Organomet Chem* 576:254–278
9. von Schenck H, Åkermark B, Svensson M (2003) Electronic control of the regiochemistry in the Heck reaction. *J Am Chem Soc* 125:3503–3508
10. Hills ID, Fu GC (2004) Elucidating reactivity differences in palladium-catalyzed coupling processes: the chemistry of palladium hydrides. *J Am Chem Soc* 126:13178–13179
11. Fristrup P, Le Quement S, Tanner D, Norrby PO (2004) Reactivity and regioselectivity in the Heck reaction: Hammett study of 4-substituted styrenes. *Organometallics* 23:6160–6165
12. Singh R, Sharma M, Mangain R, Rawat DS (2008) Ionic liquids: a versatile medium for palladium-catalyzed reactions. *J Braz Chem Soc* 19:357–379
13. Trzeciak AM, Ziolkowski JJ (2007) The role of ionic liquids in palladium-catalyzed C–C bond-forming reactions. In: Yamamoto K (ed) *Advances organometallic chemistry research*. Nova Science Publishers, New York
14. Bellina F, Chiappe C (2010) The Heck reaction in ionic liquids: progress and challenges. *Molecules* 15:2211–2245
15. Prechtl MHG, Scholten JD, Dupont J (2010) Carbon-carbon cross coupling reactions in ionic liquids catalysed by palladium metal nanoparticles. *Molecules* 15:3441–3461
16. Olivier-Bourbigou H, Magna L, Morvan D (2010) Ionic liquids and catalysis: recent progress from knowledge to applications. *Appl Cat A: Gen* 373:1–56
17. Hallett JP, Welton T (2011) Room-temperature ionic liquids: solvents for synthesis and catalysis 2. *Chem Rev* 111:3508–3576
18. Heck RF (1991) TITOLO? In: Trost BM, Fleming I (eds) *Comprehensive organic synthesis*, vol 4. Pergamon, Oxford
19. Herrmann WA (1996) TITOLO? In: Cornils B, Herrmann WA (eds) *Applied homogeneous catalysis with organometallic compounds*. VCH, Weinheim
20. de Meijere A, Meyer FE (1994) TITOLO? *Angew Chem Int Ed Engl* 33:2379–2411
21. Cabri W, Candiani I (1995) Recent developments and new perspectives in the Heck reaction. *Acc Chem Res* 28:2–7
22. Crisp GT (1998) Variations on a theme – recent developments on the mechanism of the Heck reaction and their implications for synthesis. *Chem Soc Rev* 27:427–436
23. Genet JP, Savignac MJ (1999) Recent developments of palladium(0) catalyzed reactions in aqueous medium. *J Organomet Chem* 576:305–317
24. Whitcombe NJ, Hii KK, Gibson SE (2001) Advances in the Heck chemistry of aryl bromides and chlorides. *Tetrahedron* 57:7449–7476
25. Herrmann WA, Öfele K, Preysing D, Schneider SK (2003) Phospha-palladacycles and N-heterocyclic carbene palladium complexes: efficient catalysts for CC-coupling reactions. *J Organomet Chem* 687:229–248
26. Blaser H-U, Indolese A, Naud F, Nettekoven U, Schnyder A (2004) Industrial R&D on catalytic CC and CN coupling reactions: a personal account on goals, approaches and results. *Adv Synth Catal* 346:1583–1598
27. Christmann U, Vilar R (2005) Monoligated palladium species as catalysts in cross-coupling reactions. *Angew Chem Int Ed* 44:366–374
28. Dominguez B, Iglesia B, de Lera AR (1998) Tetraenylstannanes in the synthesis of retinoic acid and its ring-modified analogues. *J Org Chem* 63:4135–4139
29. Lipshutz BH, Ullman B, Lindsley C, Pecchi S, Buzard DJ, Dickson D (1998) A new bromo trienylne: synthesis of all-E, conjugated tetra-, penta-, and hexaenes common to oxo polyene macrolide antibiotics. *J Org Chem* 63:6092–6093

30. Pinto A, Jia Y, Neuville L, Zhu J (2007) Palladium-catalyzed enantioselective domino Heck–cyanation sequence: development and application to the total synthesis of esermethole and physostigmine. *Chem Eur J* 13:961–967
31. Mizoroki T, Mori K, Ozaki A (1971) Arylation of olefin with aryl iodide catalyzed by palladium. *Bull Chem Soc Jpn* 44:581–581
32. Heck RF, Nolley JP Jr (1972) Palladium-catalyzed vinylic hydrogen substitution reactions with aryl, benzyl, and styryl halides. *J Org Chem* 37:2320–2322
33. Dounay AB, Overman LE (2003) The asymmetric intramolecular Heck reaction in natural product total synthesis. *Chem Rev* 103:2945–2963
34. Beletskaya IP, Cheprakov AV (2000) The Heck reaction as a sharpening stone of palladium catalysis. *Chem Rev* 100:3009–3066
35. Balanta A, Godard C, Claver C (2011) Pd nanoparticles for C–C coupling reactions. *Chem Soc Rev* 40:4973–4985
36. Grasa GA, Viciu MS, Huang J, Nolan SP (2001) Amination reactions of aryl halides with nitrogen-containing reagents mediated by palladium/imidazolium salt systems. *J Org Chem* 66:7729–7737
37. Gstöttma CWK, Böhm VPW, Herdtweck E, Grosche M, Herrmann WA (2002) A defined N-heterocyclic carbene complex for the palladium-catalyzed Suzuki cross-coupling of aryl chlorides at ambient temperatures. *Angew Chem Int Ed* 41:1363–1365
38. Yin J, Rainka MP, Zhang X-X, Buchwald SL (2002) A highly active Suzuki catalyst for the synthesis of sterically hindered biaryls: novel ligand coordination. *J Am Chem Soc* 124:1162–1163
39. Beare NA, Hartwig JF (2002) Palladium-catalyzed arylation of malonates and cyanoesters using sterically hindered trialkyl- and ferrocenyldialkylphosphine ligands. *J Org Chem* 67:541–555
40. Selvakumar K, Zapf A, Beller M (2002) New palladium carbene catalysts for the Heck reaction of aryl chlorides in ionic liquids. *Org Lett* 4:3031–3033
41. Rohlich C, Kohler K (2010) Tetraalkylammonium-free Heck olefination of deactivated chloroarenes by using a macrocyclic catalyst precursor. *Chem Eur J* 16:2363–2365
42. Xu HJ, Zhao YQ, Zhou XF (2011) Palladium-catalyzed Heck reaction of aryl chlorides under mild conditions promoted by organic ionic bases. *J Org Chem* 76:8036–8041k
43. Bader RR, Baumeister P, Blaser HU (1996) Catalysis at Ciba-Geigy. *Chimia* 50:99–105
44. Jeffery T (1984) Palladium-catalysed vinylation of organic halides under solid–liquid phase transfer conditions. *J Chem Soc Chem Commun* 1287–1289
45. Jeffery T (1985) Highly stereospecific palladium-catalysed vinylation of vinylic halides under solid–liquid phase transfer conditions. *Tetrahedron Lett* 26:2667–2669
46. Jeffery T (1996) On the efficiency of the tetralkylammonium salts in the Heck type reactions. *Tetrahedron* 52:10113–10130
47. Beller M, Fischer H, Kühlein K, Reisinger C-P, Herrmann WA (1996) First palladium-catalyzed Heck reactions with efficient colloidal catalyst systems. *J Organomet Chem* 520:257–259
48. Reetz MT, Lohmer G, Schwickardi R (1998) A New catalyst system for the Heck reaction of unreactive aryl halides. *Angew Chem Int Ed Engl* 37:481–483
49. Herrmann WA, Elison M, Fisher J, Köcher C, Artus GRJ (1995) Metal complexes of N-heterocyclic carbenes as new structural principle for catalysts in homogeneous catalysis. *Angew Chem Int Ed Engl* 14:2371–2374
50. Kaufmann D, Nouroozian M, Henze H (1996) Molten salts as an efficient medium for palladium catalyzed C–C coupling reactions. *Synlett* 1091–1092
51. Herrmann WA, Böhm VPW (1999) Heck reaction catalyzed by phospho-palladacycles in non-aqueous ionic liquids. *J Organomet Chem* 572:141–145
52. Böhm VPW, Herrmann WA (2000) Coordination chemistry and mechanisms of metal-catalyzed C–C coupling reactions, part 12 nonaqueous ionic liquids: superior reaction media for the catalytic Heck-vinylation of chloroarenes. *Chem Eur J* 6:1017–1025

53. Calò V, Nacci A, Lopez L, Mannarini N (2000) Heck reaction in ionic liquids catalyzed by a Pd-benzothiazole carbene complex. *Tetrahedron Lett* 41:8973–8976
54. Bouquillon S, Gauchegui B, Estrine B, Hénin F, Muzart J (2001) Heck arylation of allylic alcohols in molten salts. *J Organomet Chem* 634:153–156
55. Reetz MT, Breinbauer R, Wanninger K (1996) Suzuki and Heck reactions catalyzed by preformed palladium clusters and palladium/nickel bimetallic clusters. *Tetrahedron Lett* 37:4499–4502
56. Reetz MT, Lohmer G (1996) Propylene carbonate stabilized nanostructured palladium clusters as catalysts in Heck reactions. *Chem Commun* 1921–1922
57. Reetz MT, Maase M (1999) Redox-controlled size-selective fabrication of nanostructured transition metal colloids. *Adv Mater* 11:773–777
58. Reetz MT, Westermann E (2000) Phosphane-free palladium-catalyzed coupling reactions: the decisive role of Pd nanoparticles. *Angew Chem Int Ed Engl* 39:165–168
59. Trzeciak AM, Ciunik Z, Ziołkowski JJ (2002) Synthesis of palladium benzyl complexes from the reaction of PdCl₂[P(OPh)₃]₂ with benzyl bromide and triethylamine: important intermediates in catalytic carbonylation. *Organometallics* 21:132–137
60. Battistuzzi G, Cacchi S, Fabrizi G (2002) A molten *n*-Bu₄NOAc/*n*-Bu₄NBr mixture as an efficient medium for the stereoselective synthesis of (*E*)- and (*Z*)-3,3-diarylacrylates. *Synlett* 439–442
61. Calò V, Nacci A, Monopoli A, Laera S, Cioffi N (2003) Pd nanoparticles catalyzed stereospecific synthesis of β-aryl cinnamic esters in ionic liquids. *J Org Chem* 68:2929–2933
62. Moreno-Mañas M, Pleixats R (2003) Formation of carbon–carbon bonds under catalysis by transition-metal nanoparticles. *Acc Chem Res* 36:638–643
63. Calò V, Nacci A, Monopoli A, Detomaso A, Iliade P (2003) Pd nanoparticle catalyzed Heck arylation of 1,2-disubstituted alkenes in ionic liquids study on factors affecting the regioselectivity of the coupling process. *Organometallics* 22:4193–4197
64. Gniewek A, Trzeciak AM, Ziołkowski JJ, Kepinski L, Wrzyszczyk J, Tylus W (2005) Pd-PVP colloid as catalyst for Heck and carbonylation reactions: TEM and XPS studies. *J Catal* 229:332–343
65. Calò V, Nacci A, Monopoli A, Cotugno P (2009) Heck reactions with palladium nanoparticles in ionic liquids: coupling of aryl chlorides with deactivated olefins. *Angew Chem Int Ed* 48:6101–6103
66. Cotugno P, Monopoli A, Ciminale F, Cioffi N, Nacci A (2012) Pd nanoparticle catalyzed one-pot sequential Heck and Suzuki couplings of bromo-chloroarenes in ionic liquids and water. *Org Biomol Chem* 10:808–813
67. Carmichael AJ, Earle MJ, Holbrey JD, Mc Cormac PB, Seddon KR (1999) The Heck reaction in ionic liquids: a multiphase catalyst system. *Org Lett* 1:997–1000
68. Xu L, Chen W, Xiao J (2000) Heck reaction in ionic liquids and the in situ identification of N-heterocyclic carbene complexes of palladium. *Organometallics* 19:1123–1127
69. Mo J, Xu L, Xiao J (2005) Ionic liquid promoted, highly regioselective Heck arylation of electron-rich olefins by aryl halides. *J Am Chem Soc* 127:751–760
70. Mo J, Xiao J (2006) The Heck reaction of electron-rich olefins with regiocontrol by hydrogen-bond donors. *Angew Chem Int Ed* 45:4152–4157
71. Wojtkówa W, Trzeciak AM, Choukroun R, Pellegatta JL (2004) Pd colloid-catalyzed methoxycarbonylation of iodobenzene in ionic liquids. *J Mol Catal A: Chem* 224:81–86
72. Deshmukh RR, Rajagopal R, Srinivasan KV (2001) Ultrasound promoted C–C bond formation: Heck reaction at ambient conditions in room temperature ionic liquids. *Chem Commun* 1544–1545
73. Cassol CC, Umpierre AP, Machado G, Wolke SI, Dupont J (2005) The role of Pd nanoparticles in ionic liquid in the Heck reaction. *J Am Chem Soc* 127:3298–3299
74. Consorti CS, Flores FR, Dupont J (2005) Kinetics and mechanistic aspects of the Heck reaction promoted by a CN-palladacycle. *J Am Chem Soc* 127:12054–12065

75. Scholten JD, Leal BC, Dupont J (2012) Transition metal nanoparticle catalysis in ionic liquids. *ACS Catal* 2:184–200
76. Gaikwad AV, Holuigue A, Thathagar MB, ten Elshof JE, Rothenberg G (2007) Ion- and atom-leaching mechanisms from palladium nanoparticles in cross-coupling reactions. *Chem Eur J* 13:6908–6913
77. Thathagar MB, ten Elshof JE, Rothenberg G (2006) Pd nanoclusters in CC coupling reactions: proof of leaching. *Angew Chem Int Ed* 45:2886–2890
78. Kumar R, Shard A, Bharti R, Thopate Y, Sinha AK (2012) Palladium-catalyzed dehydrative heck olefination of secondary aryl alcohols in ionic liquids: towards a waste-free strategy for tandem synthesis of stilbenoids. *Angew Chem Int Ed* 51:2636–2639
79. Wan Q-X, Liu Y (2009) The ionic palladium porphyrin as a highly efficient and recyclable catalyst for the heck reaction in solution under aerobic conditions. *Catal Lett* 128:487–492
80. Hagiwara H, Shimizu Y, Hoshi T, Suzuki T, Ando M, Ohkubo K, Yokoyama C (2001) Heterogeneous heck reaction catalyzed by Pd/C in ionic liquid. *Tetrahedron Lett* 42:4349–4351
81. Choudary BM, Madhi S, Chowdari NS, Kantam ML, Sreedhar B (2002) Layered double hydroxide supported nanopalladium catalyst for Heck-, Suzuki-, Sonogashira-, and stille-type coupling reactions of chloroarenes. *J Am Chem Soc* 124:14127–14136
82. Calò V, Nacci A, Monopoli A, Fornaro A, Sabbatini L, Cioffi N, Ditaranto N (2004) Heck reaction catalyzed by nanosized palladium on chitosan in ionic liquids. *Organometallics* 23:5154–5158
83. Lu X, Xie J, Chen B, Han J, She X, Pan X (2004) Pd/C-catalyzed Heck reaction in ionic liquid accelerated by microwave heating. *Tetrahedron Lett* 45:809–811
84. Kabachii LA, Aslanov YA, Kochev SY, Romanovsky BV, Valetsky PM, Volkov VV, Yatsenko AV, Zakharov VN (2008) Mesoporous soot-supported palladium as a heterogeneous catalyst for the Heck reaction in ionic liquids. *Mendelev Commun* 18:334–335
85. Ma X, Zhou Y, Zhang J, Zhu A, Jiang T, Han B (2008) Solvent-free Heck reaction catalyzed by a recyclable Pd catalyst supported on SBA-15 via an ionic liquid. *Green Chem* 10:59–66
86. Dighe MG, Degani MS (2011) Microwave-assisted ligand-free, base-free Heck reactions in a task-specific imidazolium ionic liquid. *ARKIVOC* xi:189–197
87. Xiao JC, Twamley B, Shreeve JM (2004) An ionic liquid-coordinated palladium complex: a highly efficient and recyclable catalyst for the Heck reaction. *Org Lett* 6:3845–3847
88. Wang R, Piekarski MP, Shreeve J (2006) New types of pyrazolyl-functionalized 2-methylimidazolium-based ionic liquids and their palladium(II) complexes: highly efficient, recyclable catalysts for C–C coupling reactions. *Org Biomol Chem* 4:1878–1886
89. Wang R, Zeng Z, Twamley B, Piekarski MM, Shreeve JM (2007) Synthesis and characterization of pyrazolyl-functionalized imidazolium-based ionic liquids and hemilabile palladium (II) carbene complex catalyzed Heck reaction. *Eur J Org Chem* 655–661
90. Wang R, Twamley B, Shreeve JM (2006) A highly efficient, recyclable catalyst for C–C coupling reactions in ionic liquids: pyrazolyl-functionalized N-heterocyclic carbene complex of palladium(II). *J Org Chem* 71:426–429
91. Jin CM, Twamley B, Shreeve J (2005) Low-melting dialkyl- and bis(polyfluoroalkyl)-substituted 1,1'-methylene-bis(imidazolium) and 1,1'-methylenebis(1,2,4-triazolium) bis(trifluoromethanesulfonyl) amides: ionic liquids leading to bis(N-heterocyclic carbene) complexes of palladium. *Organometallics* 24:3020–3023
92. Wang R, Jin CM, Twamley B, Shreeve JM (2006) Syntheses and characterization of unsymmetric dicationic salts incorporating imidazolium and triazolium functionalities. *Inorg Chem* 45:6396–6403
93. Iranpoor N, Firouzabadi H, Azadi R (2007) An imidazolium-based phosphinite ionic liquid (IL-OPPh₂) as a reusable reaction medium and PdII ligand in Heck reactions of aryl halides with styrene and *n*-butyl acrylate. *Eur J Org Chem* 2197–2201

94. Fei Z, Zhao D, Pieraccini D, Ang WH, Geldbach TJ, Scopelliti R, Chiappe C, Dyson PJ (2007) Development of nitrile-functionalized ionic liquids for C – C coupling reactions: implication of carbene and nanoparticle catalysts. *Organometallics* 26:1588–1598
95. Bellina F, Bertoli A, Melai B, Scalesse F, Signori F, Chiappe C (2009) Synthesis and properties of glycerylimidazolium based ionic liquids: a promising class of task-specific ionic liquids. *Green Chem* 11:622–629
96. Cai Y, Liu Y (2009) Efficient palladium-catalyzed Heck reactions mediated by diol-functionalized imidazolium ionic liquids. *Cat Comm* 10:1390–1393
97. Wang L, Li H, Li P (2008) Task-specific ionic liquid as base, ligand and reaction medium for the palladium-catalyzed Heck reaction. *Tetrahedron* 65:364–368
98. Li S, Li Y, Xie H, Zhang S, Xu J (2006) Bronsted guanidine acid–base ionic liquids: novel reaction media for the palladium catalyzed Heck reaction. *Org Lett* 8:391–394
99. Wan QX, Liu Y, Lu Y, Li M, Wu HH (2008) Palladium-catalyzed Heck reaction in the multi-functionalized ionic liquid compositions. *Catal Lett* 121:331–336
100. Riisager A, Wasserscheid P, Hal R, Fehrmann R (2003) Continuous fixed-bed gas-phase hydroformylation using supported ionic liquid-phase (SILP) Rh catalysts. *J Catal* 219: 452–455
101. Riisager A, Fehrmann R, Haumann M, Wasserscheid P (2006) Supported ionic liquids: versatile reaction and separation media. *Topics Catal* 40:91–102
102. Werner S, Szesni N, Kaiser M, Haumann M, Wasserscheid P (2012) A scalable preparation method for SILP and SCILL ionic liquid thin-film materials. *Chem Eng Technol* 35: 1962–1967
103. Kernchen U, Etzold B, Korth W, Jess A (2007) Solid catalyst with ionic liquid layer (SCILL) – a new concept to improve selectivity illustrated by hydrogenation of cyclooctadiene. *Chem Eng Technol* 30:985–994
104. Steinruck HP, Libuda J, Wasserscheid P, Cremer T, Kolbeck C, Laurin M, Maier F, Sobota M, Schulz PS, Stark M (2011) Surface science and model catalysis with ionic liquid-modified materials. *Adv Mater* 23:2571–2587
105. Sobota M, Happel M, Amende M, Paape N, Wasserscheid P, Laurin M, Libuda J (2011) Ligand effects in SCILL model systems: site-specific interactions with Pt and Pd nanoparticles. *Adv Mater* 23:2617–2621
106. Wan L, Zhang Y, Xie C, Wang Y (2005) PEG-supported imidazolium chloride: a highly efficient and reusable reaction medium for the Heck reaction. *Synlett* 12:1861–1864
107. Burguete MI, García-Verdugo E, García-Villar I, Gelat F, Licence P, Luis SV, Sans V (2010) Pd catalysts immobilized onto gel-supported ionic liquid-like phases (g-SILLPs): a remarkable effect of the nature of the support. *J Catal* 269:150–160
108. Liu G, Hou M, Song J, Jiang T, Fan H, Zhang Z, Han B (2010) Immobilization of Pd nanoparticles with functional ionic liquid grafted onto cross-linked polymer for solvent-free Heck reaction. *Green Chem* 12:65–69
109. Shi X, Han X, Ma W, Fan J, Wei J (2012) A PdCl₂–ionic liquid brush assembly: an efficient and reusable catalyst for Mizoroki–Heck reaction in neat water. *Appl Organom Chem* 26:16–20
110. Brun N, Hesemann P, Laurent G, Sanchez C, Birot M, Deleuze H, Backov R (2013) Macrocellular Pd@ionic liquid@organo-Si(HIPE) heterogeneous catalysts and their use for Heck coupling reactions. *New J Chem* 37:157–168
111. Payagala T, Armstrong DW (2012) Chiral ionic liquids: a compendium of syntheses and applications (2005–2012). *Chirality* 24:17–53
112. Prechtl MHG, Scholten JD, Neto BAD, Dupont J (2009) Application of chiral ionic liquids for asymmetric induction in catalysis. *Curr Org Chem* 13:1259–1277
113. Gayet F, Marty J-D, Lauth de Viguierie N (2008) Palladate salts from ionic liquids as catalysts in the Heck reaction. *ARKIVOC* xvii:61–76
114. Kiss L, Kurtán T, Antus S, Brunner H (2003) Further insight into the mechanism of Heck oxyarylation in the presence of chiral ligands. *ARKIVOC* v:69–76

115. Pastre JC, Génisson Y, Saffon N, Dandurand J, Correia CRD (2010) Synthesis of novel room temperature chiral ionic liquids: application as reaction media for the Heck arylation of aza-endocyclic acrylates. *J Braz Chem Soc* 21:821–836
116. Roszak R, Trzeciak AM, Pernak J, Borucka N (2011) Effect of chiral ionic liquids on palladium-catalyzed Heck arylation of 2,3-dihydrofuran. *Appl Catal A* 148:409–410
117. Morel A, Silarska E, Trzeciak AM, Pernak J (2013) Palladium-catalyzed asymmetric Heck arylation of 2,3-dihydrofuran – effect of prolinic salts. *Dalton Trans* 42:1215–1222
118. Calò V, Nacci A, Monopoli A, Ferola V (2007) Palladium-catalyzed Heck arylations of allyl alcohols in ionic liquids: remarkable base effect on the selectivity. *J Org Chem* 72:2596–2601
119. Lee JW, Shin JY, Chun YS, Jang HB, Song CE, Lee S (2010) Toward understanding the origin of positive effects of ionic liquids on catalysis: formation of more reactive catalysts and stabilization of reactive intermediates and transition states in ionic liquids. *Acc Chem Res* 43:985–994
120. Ruan J, Xiao J (2011) From α -arylation of olefins to acylation with aldehydes: a journey in regiocontrol of the Heck reaction. *Acc Chem Res* 44:614–626
121. Shaw BL (1998) Speculations on new mechanisms for Heck reactions. *New J Chem* 22:77
122. Amatore C, Jutand A (2000) Anionic Pd(0) and Pd(II) intermediates in palladium-catalyzed Heck and cross-coupling reactions. *Acc Chem Res* 33:314–321
123. de Vries J G (2006) A unifying mechanism for all high-temperature Heck reactions. The role of palladium colloids and anionic species. *Dalton Trans* 421–429
124. Shaw BL (1998) Chelating diphosphine–palladium(II) dihalides, outstandingly good catalysts for Heck reactions of aryl halides. *Chem Commun* 1863–1864
125. Phan NTS, Van Der Sluys M, Jones CW (2006) On the nature of the active species in palladium catalyzed Mizoroki–Heck and Suzuki–Miyaura couplings – homogeneous or heterogeneous catalysis, a critical review. *Adv Synth Catal* 348:609–679
126. Miyaura N, Suzuki A (1995) Palladium-catalyzed cross-coupling reactions of organoboron compounds. *Chem Rev* 95:2457–2483
127. Christopher JM, Paul JS, Welton T (2000) Palladium catalysed Suzuki cross-coupling reactions in ambient temperature ionic liquids. *Chem Commun* 1249–1250
128. Miyaura N, Yanagi T, Suzuki A (1981) The palladium-catalyzed cross-coupling reaction of phenylboronic acid with haloarenes in the presence of bases. *Synth Commun* 11:513–519
129. McLachlan F, Mathews CJ, Smith PJ, Welton T (2003) Palladium-catalyzed Suzuki cross-coupling reactions in ambient temperature ionic liquids: evidence for the importance of palladium imidazolylidene complexes. *Organometallics* 22:5350–5357
130. Rajagopal R, Jarikote DV, Srinivasan KV (2002) Ultrasound promoted Suzuki cross-coupling reactions in ionic liquid at ambient conditions. *Chem Commun* 616–617
131. McNulty J, Capretta A, Wilson J, Dyck J, Adjabeng G, Robertson A (2002) Suzuki cross-coupling reactions of aryl halides in phosphonium salt ionic liquid under mild conditions. *Chem Commun* 1986–1987
132. Miao W, Chan TH (2003) Exploration of ionic liquids as soluble supports for organic synthesis demonstration with a Suzuki coupling reaction. *Org Lett* 5:5003–5005
133. Zhao D, Fei Z, Geldbach TJ, Scopelliti R, Dyson PJ (2004) Nitrile-functionalized pyridinium ionic liquids: synthesis, characterization, and their application in carbon–carbon coupling reactions. *J Am Chem Soc* 126:15876–15882
134. Albrecht M, Stoeckli-Evans H (2005) Catalytically active palladium pyridylidene complexes: pyridinium ionic liquids as N-heterocyclic carbene precursors. *Chem Commun* 4705–4707
135. Gallo V, Mastrorilli P, Nobile CF, Paolillo R, Taccardi N (2005) Ionic liquids as reaction media for palladium-catalyzed cross-coupling of Aryldiazonium tetrafluoroborates with potassium organotrifluoroborates. *Eur J Inorg Chem* 582–588
136. Yan N, Yang X, Fei Z, Li Y, Kou Y, Dyson PJ (2009) Solvent-enhanced coupling of sterically hindered reagents and aryl chlorides using functionalized ionic liquids. *Organometallics* 28:937–939

137. Lombardo M, Chiarucci M, Trombini C (2009) A recyclable triethylammonium ion-tagged diphenylphosphine palladium complex for the Suzuki–Miyaura reaction in ionic liquids. *Green Chem* 11:574–579
138. Escarcega-Bobadilla MV, Teuma E, Masdeu-Bulto AM, Gomez M (2011) New bicyclic phosphorous ligands: synthesis, structure and catalytic applications in ionic liquids. *Tetrahedron* 67:421–428
139. Jin M-J, Taher A, Kang H-J, Choi M, Ryoo R (2009) Palladium acetate immobilized in a hierarchical MFI zeolite-supported ionic liquid: a highly active and recyclable catalyst for Suzuki reaction in water. *Green Chem* 11:309–313
140. Wei J-F, Jiao J, Feng J-J, Lv J, Zhang X-R, Shi X-Y, Chen Z-G (2009) PdEDTA held in an ionic liquid brush as a highly efficient and reusable catalyst for Suzuki reactions in water. *J Org Chem* 74:6283–6286
141. Calò V, Nacci A, Monopoli A, Montingelli F (2005) Pd nanoparticles as efficient catalysts for Suzuki and stille coupling reactions of aryl halides in ionic liquids. *J Org Chem* 70: 6040–6044
142. Fernandez F, Cordero B, Durand J, Muller G, Malbosc F, Kihn Y, Teuma E, Gomez M (2007) Palladium catalyzed Suzuki C–C couplings in an ionic liquid: nanoparticles responsible for the catalytic activity. *Dalton Trans* 5572–5581
143. Durand J, Teuma E, Malbosc F, Kihn Y, Gomez M (2008) Palladium nanoparticles immobilized in ionic liquid: an outstanding catalyst for the Suzuki C–C coupling. *Catal Commun* 9:273–275
144. Oda Y, Hirano K, Yoshii K, Kuwabata S, Torimoto T, Miura M (2010) Palladium nanoparticles in ionic liquid by sputter deposition as catalysts for Suzuki–Miyaura coupling in water. *Chem Lett* 39(10):1069–1071
145. Yu Y, Hu T, Chen X, Xu K, Zhang J, Huang J (2012) Pd nanoparticles on a porous ionic copolymer: a highly active and recyclable catalyst for Suzuki–Miyaura reaction under air in water. *Chem Commun* 47:3592–3594
146. Deshmukh KM, Qureshi ZS, Bhatte KD, Venkatesan KA, Srinivasan TG, Rao PRV, Bhanage BM (2012) One-pot electrochemical synthesis of palladium nanoparticles and their application in the Suzuki reaction. *New J Chem* 35:2747–2751
147. Planellas M, Pleixats R, Shafir A (2012) Palladium nanoparticles in Suzuki cross-couplings: tapping into the potential of tris-imidazolium salts for nanoparticle stabilization. *Adv Synt Catal* 354:651–662
148. Song H, Yan N, Fei Z, Kilpin KJ, Scopelliti R, Li X, Dyson PJ (2012) Evaluation of ionic liquid soluble imidazolium tetrachloropalladate pre-catalysts in Suzuki coupling reactions. *Catal Today* 183:172–177
149. Wang J, Xu B, Sun H, Song G (2013) Palladium nanoparticles supported on functional ionic liquid modified magnetic nanoparticles as recyclable catalyst for room temperature Suzuki reaction. *Tetrahedron Lett* 54:238–241
150. Stille JK (1986) The palladium-catalyzed cross-coupling reactions of organotin reagents with organic electrophiles. *Angew Chem Int Ed Engl* 25:508–524
151. Handy ST, Zhang X (2001) Organic synthesis in ionic liquids: the stille coupling. *Org Lett* 3: 233–236
152. Cui YG, Biondi I, Chaubey M, Yang X, Fei ZF, Scopelliti R, Hartinger CG, Li YD, Chiappe C, Dyson PJ (2010) Nitrile-functionalized pyrrolidinium ionic liquids as solvents for cross-coupling reactions involving in situ generated nanoparticle catalyst reservoirs. *Phys Chem Chem Phys* 12:1834–1841
153. Chiappe C, Pieraccini D, Zhao D, Fei Z, Dyson PJ (2006) Remarkable anion and cation effects on stille reactions in functionalised ionic liquids. *Adv Synth Catal* 348:68–74
154. Vitz J, Mac DH, Legoupy S (2007) Ionic liquid supported tin reagents for stille cross coupling reactions. *Green Chem* 9:431–433
155. Sonogashira K (2002) In: Negishi E (ed) *Handbook of organopalladium chemistry for organic synthesis*. Wiley, New York

156. Chinchilla R, Najera C (2007) The Sonogashira reaction: a booming methodology in synthetic organic chemistry. *Chem Rev* 107:874–922
157. Fukuyama T, Shinmen M, Nishitani S, Sato M, Ryu I (2002) A copper-free Sonogashira coupling reaction in ionic liquids and its application to a microflow system for efficient catalyst recycling. *Org Lett* 4:1691–1694
158. Kmentová I, Gotov B, Gajda V, Toma S (2003) The Sonogashira reaction in ionic liquids. *Monatsh Chem* 134:545–547
159. Park B, Alper H (2004) Recyclable Sonogashira coupling reactions in an ionic liquid, effected in the absence of both a copper salt and a phosphine. *Chem Commun* 1306–1307
160. Corma A, Garcia H, Leyva A (2005) Comparison between polyethyleneglycol and imidazolium ionic liquids as solvents for developing a homogeneous and reusable palladium catalytic system for the Suzuki and Sonogashira coupling. *Tetrahedron* 61:9848–9854
161. Li Y, Zhang J, Wang W, Miao Q, She X, Pan X (2005) Efficient synthesis of tribenzohexadecahydro[12]annulene and its derivatives in the ionic liquid. *J Org Chem* 70:3285–3287
162. Sans V, Trzeciak AM, Luis S, Ziolkowski JJ (2006) PdCl₂(P(OPh)₃)₂ catalyzed coupling and carbonylative coupling of phenylacetylenes with aryl iodides in organic solvents and in ionic liquids. *Catal Lett* 109:37–41
163. Blaszczyk I, Trzeciak AM, Ziolkowski JJ (2009) Catalytic activity of Pd(II) complexes with triphenylphosphito ligands in the Sonogashira reaction in ionic liquid media. *Catal Lett* 133: 262–266
164. Rahman MT, Fukuyama T, Kamata N, Sato M, Ryu I (2006) Low pressure Pd-catalyzed carbonylation in an ionic liquid using a multiphase microflow system. *Chem Commun* 2236–2238
165. Rahman MT, Fukuyama T, Ryu I, Suzuki K, Yonemura K, Hughes PF, Nokihara K (2006) High throughput evaluation of the production of substituted acetylenes by the Sonogashira reaction followed by the Mizoroki–Heck reaction in ionic liquids, in situ, using a novel array reactor. *Tetrahedron Lett* 47:2703–2706
166. Hierso J-C, Boudon J, Picquet M, Meunier P (2007) The first catalytic method for Heck alkynylation of unactivated aryl bromides (copper-free Sonogashira) in an ionic liquid: 1 mol-% palladium/triphenylphosphane/pyrrolidine in [BMIM][BF₄] as a simple, inexpensive and recyclable system. *Eur J Org Chem* 583–587
167. de Lima PG, Antunes OAC (2008) Copper-free Sonogashira cross coupling in ionic liquids. *Tetrahedron Lett* 49:2506–2509
168. Harjani JR, Abraham TJ, Gomez AT, Garcia MT, Singer RD, Scammells PJ (2010) Sonogashira coupling reactions in biodegradable ionic liquids derived from nicotinic acid. *Green Chem* 12:650–655
169. Iranpoor N, Firouzabadi H, Ahmadi Y (2012) Carboxylate-based, room-temperature ionic liquids as efficient media for palladium-catalyzed homocoupling and Sonogashira–Hagihara reactions of aryl halides. *Eur J Org Chem* 2:305–311
170. Zhang J, Đaković M, Popović Z, Wu H, Liu Y (2012) A functionalized ionic liquid containing phosphine-ligated palladium complex for the Sonogashira reactions under aerobic and CuI-free conditions. *Catal Commun* 17:160–163
171. Fukuyama T, Rahman MT, Maetani S, Ryu I (2011) Copper-free Sonogashira coupling reaction in phosphonium amino acid ionic liquids. *Chem Lett* 40:1027–1029
172. Pachon LD, Elsevier CJ, Rothenberg G (2006) Electroreductive palladium-catalysed Ullmann reactions in ionic liquids: scope and mechanism. *Adv Synt Catal* 348:1705–1710
173. Calò V, Nacci A, Monopoli A, Cotugno P (2009) Palladium-nanoparticle-catalysed Ullmann reactions in ionic liquids with aldehydes as the reductants: scope and mechanism. *Chem Eur J* 15:1272–1279
174. Monopoli A, Calò V, Ciminale F, Cotugno P, Angelici C, Cioffi N, Nacci A (2010) Glucose as clean and renewable reductant in the Pd-nanoparticles-catalyzed reductive homocoupling of bromo- and chloro-arenes in water. *J Org Chem* 75:3908–3911

175. Monopoli A, Nacci A, Calò V, Ciminale F, Cotugno P, Mangone A, Giannossa LC, Azzone P, Cioffi N (2010) Palladium/zirconium oxide nanocomposite as a highly recyclable catalyst for C–C coupling reactions in water. *Molecules* 15:4511–4525
176. Cheng J, Tang L, Xu J (2010) An economical, green pathway to biaryls: palladium nanoparticles catalyzed Ullmann reaction in ionic liquid/supercritical carbon dioxide system. *Adv Synt Catal* 352:3275–3286
177. Cheng J, Zhang G, Du J, Tang L, Xu J, Li J (2011) New role of graphene oxide as active hydrogen donor in the recyclable palladium nanoparticles catalyzed Ullmann reaction in environmental friendly ionic liquid/supercritical carbon dioxide system. *J Mat Chem* 21: 3485–3494
178. Negishi E, King AO, Okukado N (1977) *J Org Chem* 42:1821–1823
179. Negishi E (1982) Palladium- or nickel-catalyzed cross coupling a new selective method for carbon–carbon bond formation. *Acc Chem Res* 15:340–348
180. Sirieix J, Oberger M, Betzemeier B, Knochel P (2000) Palladium catalyzed cross-couplings of organozincs in ionic liquids. *Synlett* 1613–1615

RTILs in Catalytic Olefin Metathesis Reactions

Cédric Fischmeister and Christian Bruneau

Abstract The homogeneous catalytic olefin metathesis reaction has found a tremendous interest in the past 20 years and multiple applications have now emerged in fine chemical synthesis and polymer chemistry. Immobilization of olefin metathesis (pre)catalysts in room temperature ionic liquids (RTILs) offers the opportunity to recover and in some cases reuse the catalyst and it is also a practical way to reduce the level of metal contaminants in the desired products. This chapter covers the research in this field from the early days with an emphasis on recent results and with a critical look at the origin of catalyst recycling.

Keywords Catalyst immobilization · Ionic liquids · Molybdenum · Olefin metathesis · Ruthenium

Contents

1	Introduction	288
2	Olefin Metathesis in Room Temperature Ionic Liquids	289
2.1	Pioneering Work	289
2.2	Neutral Catalysts	290
2.3	Ionic Catalysts	294
2.4	Ionically Tagged Catalysts	295
2.5	Supported Ionic Liquid Phase and Catalyst	300
3	Conclusion	302
	References	303

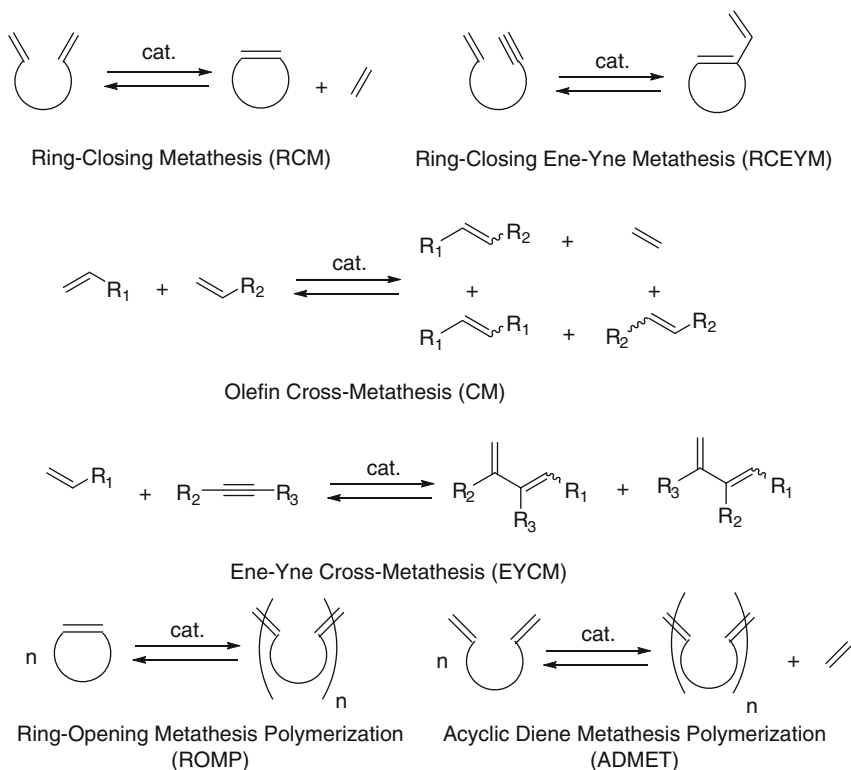
C. Fischmeister and C. Bruneau (✉)

Institut des Sciences Chimiques de Rennes, Organométalliques: Matériaux et Catalyse. UMR 6226-CNRS, Université de Rennes 1, Campus de Beaulieu, 263 avenue du général Leclerc, 35042 Rennes, France

e-mail: christian.bruneau@univ-rennes1.fr

1 Introduction

The transformation of carbon–carbon double bonds by olefin metathesis has known a tremendous growth over the last two decades owing to the continuous development of more efficient, selective and stable catalysts [1–8]. The early proposal of the catalytic mechanism was undoubtedly determining for such a fast and important development ([9]; Y. Chauvin, R. R. Schrock and R. H. Grubbs shared the Nobel Prize 2005 for their major contribution to the development of olefin metathesis [10–12]) making this transformation a recognized and powerful synthetic tool of interest in organic as well as polymer synthesis (Scheme 1) [13–21]. More recently, olefin metathesis has found a growing interest for the transformation of renewables in particular for the production of polymer precursor arising from plant oils [22–26]. Owing to these developments, industrial applications employing olefin metathesis should be expanding in particular for the production of bio-sourced compounds [27]. Thanks to the continuous improvements of catalyst efficiency achieved over the last 20 years, high performances and productivities are now accessible. However, even though low catalyst loadings are possible, at high scale, catalyst or metal separation and recovery are still important issues for several reasons including prevention of product contamination as well as reduction of costs. Furthermore, organometallic species arising from catalyst decomposition may promote undesired side reactions. For these reasons, several strategies have been implemented in order to achieve efficient separation of the catalysts from the reaction products. For example, a variety of ruthenium scavengers or catalysts designed for improved separation by column chromatography have been reported [28]. Many efforts have also been dedicated to catalyst immobilization onto various organic or inorganic supports [29, 30] and Organic Solvent Nanofiltration recently appeared as a new promising process for the separation of ruthenium based catalysts [31–34]. Nevertheless, immobilization of olefin metathesis catalysts in non-conventional reaction media has received most attention over the last 10 years [35, 36]. In particular the use of ionic liquids as reaction media has been extensively described aiming at facilitating catalyst separation from the reaction products and also at recycling or reusing the immobilized catalysts. This last point relied essentially on the admitted “boomerang” or “release and return” mechanism of the Hoveyda type catalysts [37]. However, in the light of recent research showing that this mechanism is not operating [38], it is likely that most of the results based on catalyst recycling were rather due to the formation of a catalyst reservoir in the ionic liquid media that was gradually emptied upon running successive catalytic cycles. In this chapter, we will survey the numerous reports on olefin metathesis in RTILs with an emphasis on recent results that have not been covered by previous reviews on the topic [39, 40].



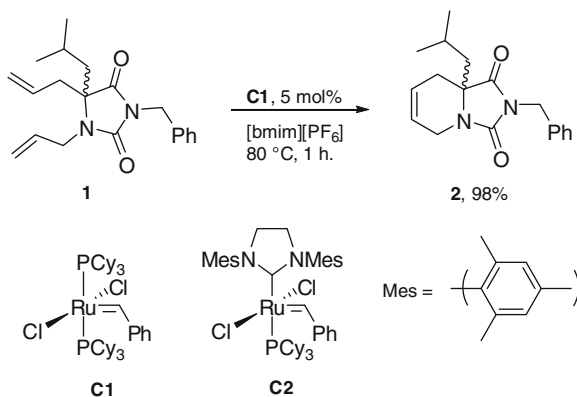
Scheme 1 Some of the olefin metathesis transformations

2 Olefin Metathesis in Room Temperature Ionic Liquids

2.1 Pioneering Work

In the 1990s, the group of Chauvin at the Institut Français du Pétrole (now IFP-Energies Nouvelles) extended the use of organochloroaluminate ionic liquids to a number of catalyzed transformations in particular the dimerization of butenes (Difasol). These ILs were also used for metathesis transformation of short olefins. Thus, using the tungsten precursor $W(OAr)_2Cl_4$ ($ArOH = 2,6$ -diphenylphenol or $2,4,6$ -triphenylphenol) in $[bmim][Cl]/AlCl_3/EtAlCl_2$ ($bmim = 1$ -butyl-3-methyl imidazolium), the self-metathesis of 1-pentene furnished ethylene and 4-octene [41]. Of note, the catalyst was quite soluble in the ionic liquid phase and did not leach into the hydrocarbon phase allowing its reuse after decantation.

Scheme 2 RCM in [bmim]
[PF₆]



2.2 Neutral Catalysts

2.2.1 Ruthenium Based Catalysts

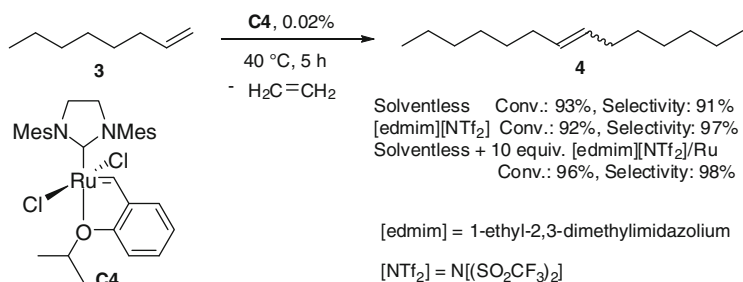
Shortly after Chauvin reported on olefin metathesis in room temperature ionic liquids (RTILs), several groups investigated the olefin metathesis reaction in RTILs employing neutral catalysts. In 2001, Buijsman reported a study on the ruthenium catalyzed RCM of various dienes performed in [bmim] based ionic liquids [42]. It was shown that Grubbs 1st generation **C1** and 2nd generation **C2** were very efficient for the RCM of compound **1** (Scheme 2). In particular, when a 5 mol% catalyst loading of **C1** was used it was shown that following extraction by diethyl ether the residual ruthenium content of the product was 3,200 ppm. For comparison the same reaction conducted in dichloromethane (DCM) furnished a product containing 1,700 ppm of ruthenium after purification by column chromatography. Attempts to reuse catalysts **C1** and **C2** were not successful as conversions dropped down after two cycles even when a high initial catalyst loading of 5 mol% was used.

Microwave activation of olefin metathesis catalysts in RTILs was reported in 2002. Impressive rate enhancements were obtained as the RCM of diethyl diallylmalonate (DEDAM) was completed within 15 s in [bmim][BF₄] even though a rather high catalyst loading of **C2** was employed for this type of reaction [43]. The authors postulated a non-thermal effect as none of the reaction conducted in a domestic microwave-oven exceeded a temperature of 33°C. However another study employing laboratory designed microwave equipment demonstrated that rate enhancement was most certainly due to a thermal microwave effect [44]. So far limited to RCM reactions, self-metathesis transformations of various substrates in RTILs were investigated by the groups of Tang [45] and Williams [46]. Grubbs catalyst **C2** was used for the self-metathesis of styrene in [bmim][PF₆]. The isolated yield of (*E*)-stilbene obtained in [bmim][PF₆] at 45°C with 2.5 mol% of **C2** was slightly better than that of the reaction performed in DCM under identical conditions

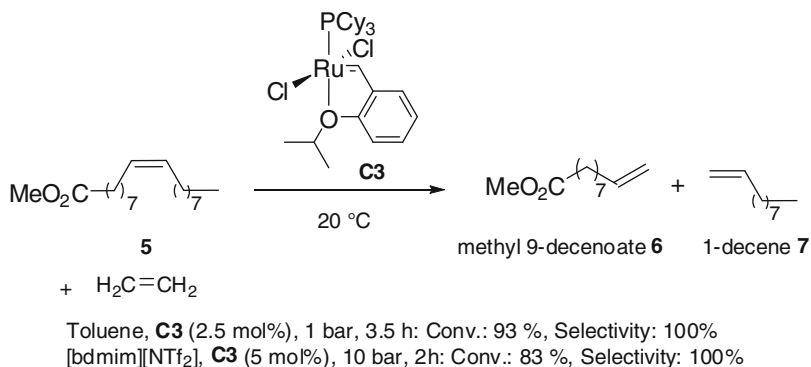
(85% vs. 81%). Following extraction with diethyl ether, the ionic liquid solution could be reused three times with only low loss of productivity. The authors demonstrated that this gradual decrease was due to catalyst leaching in the organic phase. It was also demonstrated that recycling performances dropped upon increasing the reaction temperature and duration as a result of faster catalyst decomposition. Williams studied the self-metathesis of 1-octene **3** using various catalysts and compared the conversion and selectivity of reactions performed without solvents and in ionic liquids (biphasic reaction mixture). First generation Grubbs catalyst **C1** and a related complex bearing a phoban phosphine ligand were evaluated and showed rapid deactivation in both the solventless and ILs reactions. When Grubbs catalyst **C2** was used, high conversions were obtained and interestingly the selectivity for 7-tetradecene **4** was much higher when ILs were used as reaction media. This result was ascribed to secondary metathesis product (SMP) formation resulting from double bond migration occurring under solventless conditions. These side reactions would be inhibited in ILs. The more stable Hoveyda type catalysts **C3** and **C4** have been extensively used in RTILs. Williams used Hoveyda catalyst **C4** for the above-mentioned transformation and found that this catalyst was the most efficient as high conversions and selectivity were reached under both types of reaction conditions although higher selectivity was yet observed in ILs. Furthermore, lower leaching of catalyst into the organic product was measured by ICP with **C4** (2%) whereas 72% of Ru had leached when using the first generation Grubbs catalyst **C1**. This study clearly highlighted the beneficial impact of ILs on the reaction selectivity not only when reactions were conducted in pure ILs but also when ILs were used as additives in solventless reactions (Scheme 3).

2.2.2 Transformation of Renewables in RTILs

Metathesis transformations of renewables in particular fatty acid methyl esters (FAMES) have attracted a strong interest from academia and industry in recent years in particular for the preparation of polymer precursors [22–26]. Ethenolysis of methyl oleate **5** leads to methyl 9-decenoate **6** and 1-decene **7**, two compounds of interest for polymer synthesis [47, 48]. This transformation was investigated in ionic liquids with the aim of reusing the immobilized catalyst [49]. A preliminary catalyst screening in toluene identified catalyst **C3** as the most efficient and selective catalyst whereas **C4** led to large amounts of SMPs resulting from double bond migration. In toluene the best results were obtained at room temperature under 1 bar of ethylene pressure. Under these conditions and using 2.5 mol% of catalyst, the reaction proceeded with 93% conversion and the reaction products were isolated in 93% yield. Higher temperature led to lower selectivity and higher pressure only allowed marginal improvement of the reaction performances (Scheme 4). When the reaction was performed in an ionic liquid media, the same level of performance could be reached provided a higher amount of catalyst and higher ethylene pressure were used. Due to the high initial catalyst loading, **C3** in [bdmim][NTf₂] ([bdmim] = 1-butyl-2,3-dimethylimidazolium) could be reused twice maintaining almost the



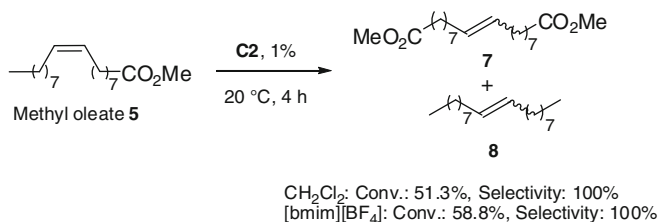
Scheme 3 Self-metathesis of 1-octene



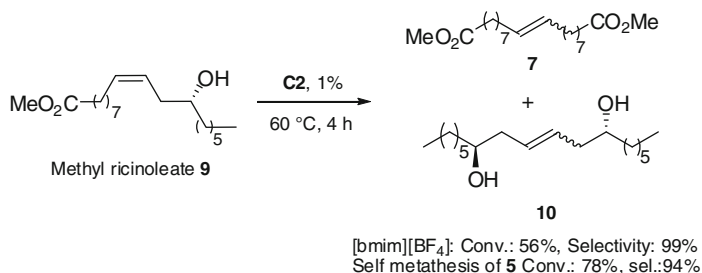
Scheme 4 Ethenolysis of methyl oleate **5** in toluene and [bdmim][NTf₂]

same level of performances but in that case traces of self-metathesis products were detected.

In 2009, the group of B. Marvey in South Africa evaluated the interest of RTILs for the self-metathesis of methyl oleate using the Grubbs 1st and 2nd generation catalysts **C1** and **C2** [50]. First the influence of different counter anions associated to [bmim] was studied. The self-metathesis of methyl oleate **5** was thus conducted in [bmim][PF₆], [bmim][BF₄] and [bmim][NTf₂] using **C1** and **C2** catalysts at 20°C. In all cases the biphasic mixture led to conversions in the range 50–60% after 4 h with full selectivity towards the self-metathesis products **7** and **8** hence no major difference with regards to the counter anions was visible. Increasing the reaction temperature had a beneficial impact on the conversion but the selectivity decreased due to the formation of SMPs. As already reported [49] these side metathesis products were formed in higher amounts using the NHC based second generation catalyst **C2**. The same reaction was repeated in several conventional organic solvents (DCM, dichloroethane, toluene and chlorobenzene) and compared to that performed in the RTIL allowing the best results, namely [bmim][BF₄]. Amongst the organic solvents tested the best result was obtained in DCM but the performance in this solvent was slightly lower than in [bmim][BF₄] hence showing an interest for running this reaction in an ionic liquid media (Scheme 5).



Scheme 5 Solvent comparison for the self-metathesis of methyl oleate **5**

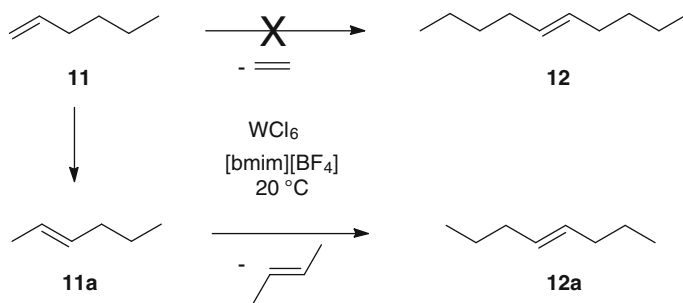


Scheme 6 Self-metathesis of methyl ricinoleate **9**

This synthetic protocol was extended to the self-metathesis of methyl ricinoleate **9**, a FAME arising from the non-edible castor oil [51, 52]. In addition to the catalysts and ionic liquids used in their previous work, Hoveyda catalysts **C3** and **C4** and [bdmim] cations were studied (bdmim = 1-butyl-2,3-dimethyl imidazolium). Catalyst **C4** proved to be a little more efficient than the Grubbs catalyst **C2** for the self-metathesis of methyl oleate **5**. In addition, the use of [bdmim] led to slightly better results than [bmim] cation. However, the self-metathesis of methyl ricinoleate was studied in [bmim][X] RTILs using catalysts **C1** and **C2** at 60°C. The best result was obtained with **C2** catalyst with almost negligible influence of the ionic liquid anion (conv.: 55–58%). The performances were slightly lower than those obtained with methyl oleate under identical conditions (Scheme 6).

2.2.3 Early Transitions Metals

Following the pioneering work by Chauvin (see Sect. 2.1), tungsten catalyzed olefin metathesis in RTILs was investigated by Vasnev [53]. The self-metathesis of 1-hexene **11** catalyzed by WCl₆ (8 mol%) was performed at 20°C in [bmim][PF₆] and [bmim][BF₄] (Scheme 7). In both cases, low conversion was reached (<20%) and the major product was not the expected dec-5-ene **12** but instead oct-4-ene **12a** was obtained due to a preliminary fast isomerization of 1-hexene **11** into 2-hexene **11a**. These results could be slightly improved by using tin promoters in particular SnBu₄. In that case the conversion reached 25% and the reaction led very selectively to



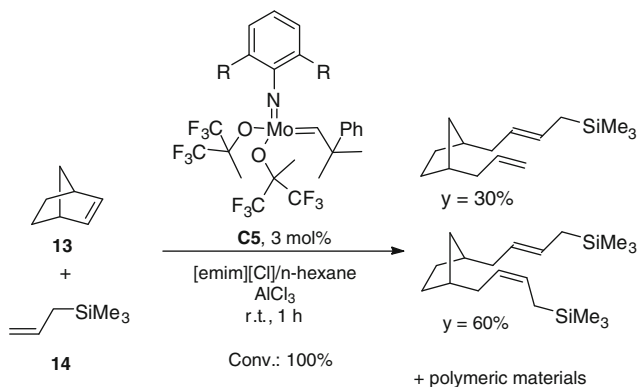
Scheme 7 Tungsten catalyzed self-metathesis of 1-hexene **11**

oct-4-ene **12a**. This catalytic system was recently used for the ethenolysis of 4-octene and 4-pentanol [54]. In both cases, complex reaction mixtures were obtained due to the presence of double bond migration and self-metathesis reactions.

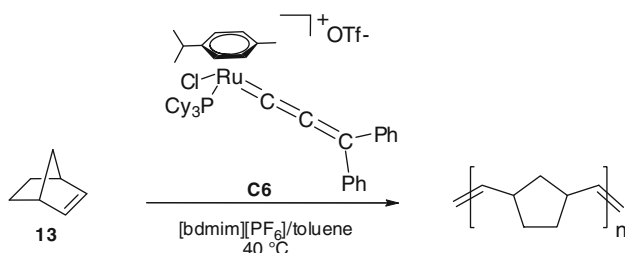
The first generation of Schrock type catalysts are very efficient and selective catalysts in a variety of metathesis reactions [4, 55]. However, due to their higher sensitivity towards moisture and functional groups, their implementation in RTILs media is seldom. An early example of the use of catalyst **C5** was reported in 1999 in a Bayer AG patent [56]. In this example **C5** was used for the ROM-Cross metathesis of norbornene **13** with allyl silane **14** in a biphasic mixture of [emim][Cl] and hexane in the presence of 4 equiv. of AlCl_3 (Scheme 8). In 2007 a second study employing **C5** ($\text{R} = \textit{i}\text{Pr}$) in a RTIL was reported by Bowden [57]. Several RCM and CM reactions were conducted in [bmim][PF₆]. In all cases, excellent yields were obtained when reactions were conducted at 75 °C using a 5 mol% catalyst loading thus showing a similar level of performance as the same reaction performed in DCM at r.t. The ROMP of strained norbornene derivatives was also tested resulting in uncontrolled polymerization. Interestingly, an effective protocol for the separation of the reaction products and the solvent using a tailor-made polydimethylsiloxane (PDMS) thimble was also reported.

2.3 Ionic Catalysts

Cationic ruthenium allenylidene complexes **C6** as olefin metathesis catalysts were disclosed by Dixneuf and Fürstner in 1998 [60]. Due to their ionic character, these complexes are very soluble in classical RTILs. The first report on the use of such catalyst in RTILs came from Bayer in 1999 [56]. It was shown that the RCM of 1,7-octadiene proceeded with modest yield (32%) when performed in [bmim][Cl] in the presence of AlCl_3 and methyl *t*-butyl ether as co-solvent. In 2002 and 2003, better results were reported with this catalyst **C6** by Dixneuf and Bruneau. In particular it was shown that the choice of the ionic liquid anion was very important to control both the reactivity and selectivity of the catalyst in RCM reactions. It was proposed that anion exchange with the complex anion could occur resulting in variations of



Scheme 8 Schrock catalyst in an ionic liquid



Scheme 9 Polymerization of norbornene in ionic liquids

the catalyst properties since it was earlier shown that the reaction outcome was strongly dependent on the catalyst anion [60]. Hence, since the best catalysts were based on OTf or PF₆ anions, the ionic liquids should also contain the same anion [61]. In 2003, the first ROMP in RTILs was reported [62]. Norbornene **13** was polymerized in high yields in a biphasic mixture of [bdmim][PF₆] and toluene and the catalyst immobilized in the ionic liquid phase could be reused four times (Scheme 9). Further studies on polymerization reactions employing **C6** as catalyst were reported by Rooney in 2009. The influence of the counter anion was yet evidenced upon monitoring the σ_{cis} parameter in different solvents as a probe of catalyst efficiency [63].

2.4 Ionically Tagged Catalysts

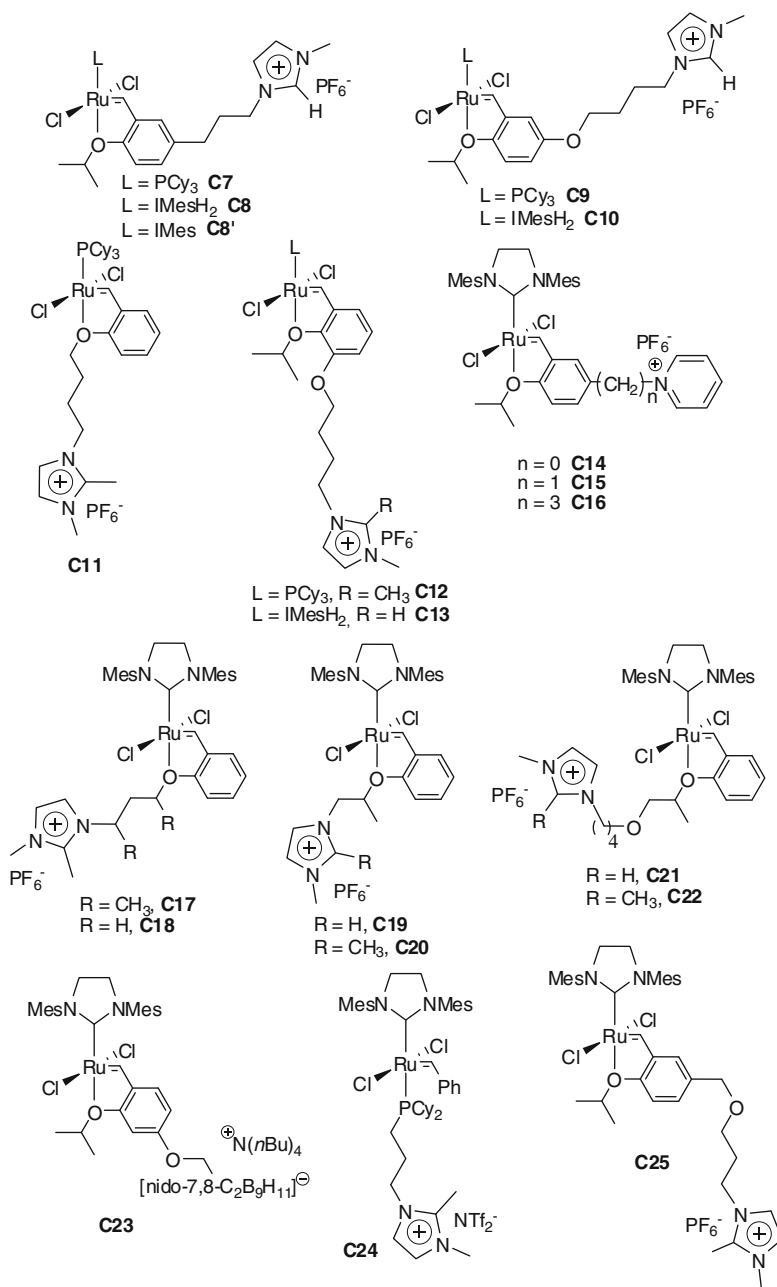
Following the early reports on olefin metathesis in ionic liquids employing neutral and ionic catalysts, it became obvious that efficient immobilization of neutral olefin metathesis catalysts in ILs in view of low leaching and potential recycling would be greatly enhanced by anchorage on an ionic tag. Thus several strategies were

implemented for the introduction of such ionic tags on metathesis catalyst ligands. Most of the research reports deal with the modification of the stable Hoveyda type catalysts (**C7–C23**, **C25**, Scheme 10). Owing to the admitted boomerang mechanism and because of easier synthetic protocols, ionic tags were exclusively introduced on the chelating alkoxy-benzylidene ligand. Grubbs type complexes bearing tagged phosphine were investigated to a lower extent (**C24**, Scheme 10). These catalysts were used under three different types of experimental conditions: in pure RTILs, in monophasic DCM/RTILs mixtures or in biphasic toluene/RTILs conditions.

Two similar types of first generation complexes (**C7** and **C9**) were reported almost simultaneously in 2003 by the groups of Mauduit and Yao [64, 65]. Ligand synthesis from commercially available compounds required eight steps in both cases. The activity and recyclability of catalyst **C7** were evaluated in pure [bmim][PF₆] for the RCM of diallyltosylamide **15** using 2.5 mol% of catalyst. Almost full conversion was reached after 45 min at 60°C and following extraction of the organic product with toluene, the ionic liquid phase containing the **C7** catalyst could be reused up to five times without drop of conversion (Scheme 11). However, when more demanding substrates were used, the possibility to reuse the initial loading of catalyst was reduced. In the same manner, catalyst **C9** was evaluated in the RCM of a longer chain tosylamine substrate leading to 7-membered ring. However, in that case the reaction was performed in a monophasic mixture of DCM and [bmim][PF₆]. Similarly to **C7**, a rather high 5 mol% loading of **C9** could be reused several times before the conversion dropped. These two studies evidenced the superiority of the ionically tagged complexes in terms of reusability. Indeed, complexes **C1** and **C3** were found to be poorly reusable as the result of their fast extraction from the ionic liquid phase.

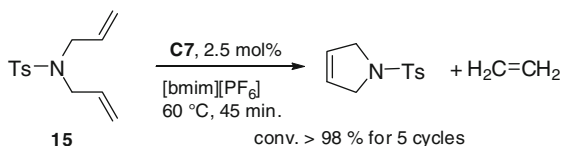
The more reactive second generation of both types of complexes was logically prepared shortly after the first generation with the aim of increasing the stability of the catalysts and improving their performances with sterically demanding substrates [66, 67]. These goals were only partially reached since complex **C8** proved ineffective for the challenging RCM of **18** even under optimized solvent mixture of [bmim][PF₆]/toluene (25/75) whereas it could be reused in the RCM of **16** and **17** (Scheme 12) [68]. Interestingly, when **C8** was used under biphasic conditions, the organic products extracted contained a very low residual amount of ruthenium typically below 22 ppm even though a rather high initial catalyst loading of 5 mol% was used.

Complexes **C11** and **C12** were prepared with the objective of shortening the synthesis of the ionically tagged ligands and to increase the catalyst efficiency in the latter case [69]. Indeed, it was shown by Blechert that substitution at the ortho position of the coordinating ether resulted in higher activity of the catalyst due to the weakening of the Ru–O bond hence facilitating catalyst initiation [70]. However, both catalysts displayed modest activities in [bdmim] or [bmim] based ionic liquids in the RCM of **15** and **16**. As expected, **C12** was more efficient than **C11**, which certainly suffered from low stability resulting from the presence of a O–CH₂ coordinating ether instead of a O–*i*Pr [71]. Due to its faster initiation, **C12** showed a lower reuse capability than **C11**. Catalyst **C13**, the second generation version

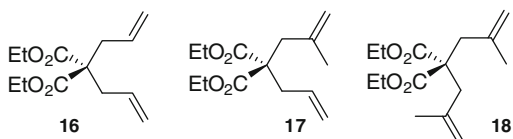


Scheme 10 Ionically tagged-ruthenium based olefin metathesis catalysts

Scheme 11 RCM of diallyltosylamine **15** in [bmim][PF₆]



Scheme 12 Benchmark RCM substrates

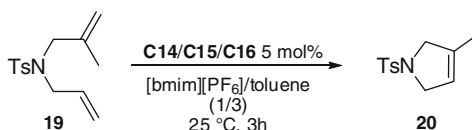


of **C12**, was reported in 2008 by Wakamatsu [72]. As a second generation catalyst, **C13** exhibited a very high activity for the RCM of various dienes in dichloromethane/[bmim][PF₆] mixture. However, its reuse was limited to only four cycles with high yields for the RCM of **16** with a high initial catalyst loading of 5 mol%. In order to take advantage of fast catalyst initiation promoted by electron withdrawing groups [73], Grela and Mauduit prepared complex **C14** bearing a pyridinium ion playing the dual role of ionic tag and initiation booster [74]. As anticipated this catalyst showed better activity than **C4** and **C8** for the RCM of **17** in DCM. The recyclability of this complex was also evaluated in a solvent mixture of toluene and [bmim][PF₆ or BF₄]. As observed with sterically promoted fast initiating complexes **C12** and **C13**, **C14** showed modest recycling properties. In both cases and considering that the boomerang mechanism is operating the authors attributed this lower recyclability to an inhibited recoordination of the ionically tagged ligand. Alternatively, it might also be considered that enhanced initiation results in faster depletion of the catalyst reservoir immobilized in the ionic liquid. Having demonstrated that fast initiating catalyst was not the best suited catalyst, pyridinium tagged complexes **C15** and **C16** were prepared aiming at finding the best compromise between activity and reusability [75, 76]. The propylene bridged pyridinium **C16** displayed similar activity and reusability properties as **C8** hence demonstrating that the nature of the ionic tag was not a determining parameter. **C15** led to the best compromise between activity and recyclability. As shown in Table 1, **C15** allowed the best performances for a series of RCM of the sterically hindered diene **19**. Here also, the metathesis reactions were performed in a biphasic mixture of [bmim][PF₆]/toluene using a high initial catalyst loading (Scheme 13).

Several other ionically tagged olefin metathesis catalysts based on the Hoveyda architecture displaying original linkers between the standard chelating ligand and the ionic tag were reported. As observed with **C11**, complexes **C17** and **C18** confirmed the beneficial role of a branched ether ligand with regards to a linear aliphatic chain [77]. Of note when the RCM of **16** was attempted in a mixture of [bmim][PF₆] and toluene using a reasonable catalyst loading (0.25 mol% of **C17**) the catalyst could be reused only one time without loss of conversion. Complexes **C19–C22** were reported by Lee in 2009. It was demonstrated that non-precarbenic ionic tag (R = CH₃) and ionic liquids ([bdmim]) led to improved recycling performance and lower ruthenium

Table 1 Comparative recycling of **C14–C16** in the RCM of **19**

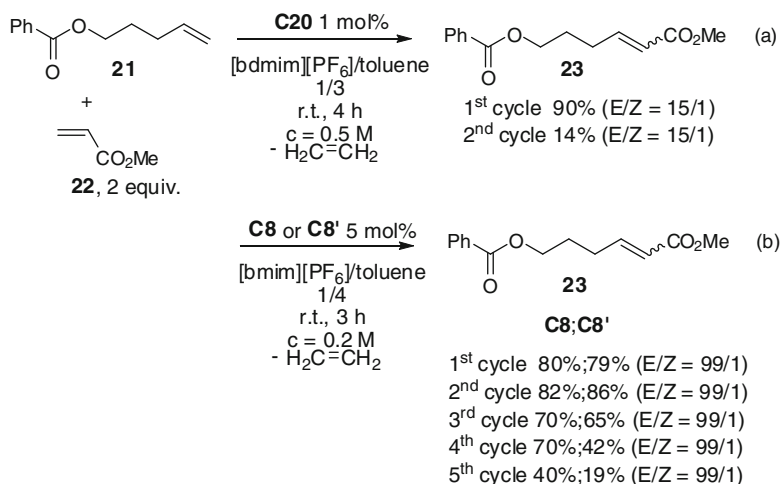
Catalyst	Cycle/conversion (%)					
	1	2	3	4	5	6
C14	>98	95	65	6	–	–
C15	>98	>98	>98	>98	>98	>98
C16	>98	>98	>98	>98	93	91

Scheme 13 RCM of **19** catalyzed by pyridinium tagged catalysts

leaching in the organic phase [78]. **C20** and **C22** were also evaluated in cross-metathesis reactions of ester **21** and methyl acrylate **22** (Scheme 14a). If high conversions were reached, the use of an RTIL media had no influence on the stereoselectivity of the reaction and **23** was obtained as the *E* isomer, which is a general feature in cross-metathesis reactions involving methyl acrylate [25, 79, 80]. In addition poor recycling was achieved with this more demanding reaction since the conversion dropped below 14% upon running a second cycle. Another study on cross-metathesis reaction in ionic liquids employing **C8** and **C8'** led to similar conclusions albeit slightly different results were obtained [81]. Indeed, better performances in terms of catalyst reuse were obtained but in this case an initial catalyst loading of 5 mol% was used (Scheme 14b). Surprisingly, even with this much higher catalyst loading, the efficiency on the first cycle was lower than that reported by Lee with 1 mol% of catalyst **C20**. This difference may find its origin in the nature of the ionic liquid cation ([bdmim] and [bmim]) and in the different concentrations used since higher concentrations are beneficial for cross-metathesis reactions involving methyl acrylate [25]. In both studies, the excess of methyl acrylate necessary for this type of reaction was postulated as responsible for the low reusability of the catalysts.

The original anion (carbollide) tagged complex **C23** was reported in 2007 [82]. This catalyst performed very well on a series of RCM reactions run in DCM. It was also evaluated in [bmim][PF₆] for the RCM of **15**. As reported with other complexes, the high initial loading of 2.5 mol% could be reused up to ten times at 40 °C with only little decrease of the conversion.

Being the archetype of stable precatalyst, the Hoveyda type architecture has been almost exclusively used when catalyst immobilization and recycling were targeted not only in ionic liquids but also for other types of immobilization or heterogenization [5, 29, 30]. Nevertheless, in 2008 Dupont reported the ionically tagged Grubbs type catalyst **C24** [83]. Interestingly, a low initial catalyst loading (0.25 mol%) of this catalyst could be reused several times at 45 °C for the efficient RCM of 1,7-octadiene in biphasic solvent mixtures of toluene and [bmim] based RTILs. These results clearly indicate that careful investigation of both catalyst stability and initiation/propagation mechanism and kinetics in RTILs of the various type of olefin metathesis



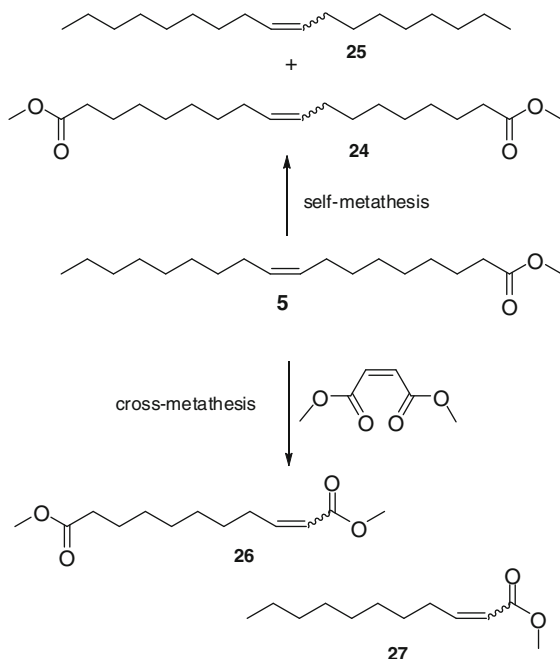
Scheme 14 Cross-metathesis with methyl acrylate in RTILs

catalysts have to be addressed. Surprisingly, it was also shown that the neutral catalyst **C2** could be reused up to four times with this type of biphasic solvent mixture provided extended reaction durations were used. Catalysts **C17** and **C24** were later used for a tandem orthogonal [84] isomerization/metathesis process of trans-3-hexene into a mixture of olefins containing four to seven carbon atoms [85]. In this example, biphasic mixtures of RTILs and toluene were employed with a toluene soluble isomerization catalyst $\text{RuHCl}(\text{CO})(\text{PPh}_3)_3$ and catalysts **C17** and **C24** immobilized in $[\text{bmim}][\text{PF}_6]$. By this means and owing to the poor affinity of olefins for this type of RTIL, the metathesis reaction was slowed with regard to the isomerization reaction hence resulting in a broader olefin distribution.

2.5 Supported Ionic Liquid Phase and Catalyst

Immobilization of olefin metathesis catalysts as supported ionic liquid catalyst (SILC) was described in 2008 by Hagiwara [86]. These catalysts were prepared by mixing a suspension of a porous inorganic solid and a solution of ruthenium catalyst in an ionic liquid dissolved in THF. The SILC was obtained after THF evaporation and diethyl ether washings. The highest loading ($>99\%$, 0.03 mmol g^{-1}) was obtained with Grubbs **C1** catalyst and $[\text{hmim}][\text{PF}_6]$ using alumina as the inorganic support. Lower loadings were obtained with Grubbs **C2** and Hoveyda **C4** catalyst. Attempted immobilization of **C1** performed without IL led to a lower loading of 0.02 mmol g^{-1} . The RCM of **16** was used to evaluate the catalytic efficiency of the SILCatalysts. Modest performances were obtained as the product was isolated in 77% after 2.5 h refluxing in benzene. The reaction did not proceed at all in other solvents in particular in DCM which is a solvent of choice for olefin metathesis

Scheme 15 SILC catalyzed self- and cross-metathesis of methyl oleate



reactions. Finally, the catalytic solid could be reused up to six times with similar yields provided the reaction time was extended from 1 to 2 h. This process was extended to catalyst **C4** and to the synthesis of macrocyclic lactones affording 13- to 18-membered lactones in satisfactory yields [87]. Another original use of a SILC consisted in a continuous flow process as reported in 2010 [88]. Catalyst **C8** was immobilized in [bmim][NTf₂] and supported within the pores of silica with supercritical CO₂ as the flowing medium. This system was applied to the standard RCM of **16** and to the industrially relevant transformation of methyl oleate **5**. Two types of methylenide free transformation were implemented with this process. Thus, the self-metathesis of **5** into the diester **24** (dimethyl 1,18-octadec-9-enedioate) and 9-octadecene **25** as well as the cross-metathesis with dimethyl maleate leading to diester **26** and monoester **27** were carried out (Scheme 15). The self-metathesis of **5** performed very well allowing a cumulative TON as high as 10,000 after 9 h on stream albeit some decrease of conversion indicating catalyst instability was observed after 2 h. The cross-metathesis of **5** with dimethyl maleate also performed well although a selectivity issue was evidenced since the self-metathesis of **5** became predominant with regards to the cross-metathesis reaction after a few hours. In both cases, the ruthenium content in the final product determined by ICP-OES analysis remained very low, typically below 15 ppm.

Another type of SILP was prepared by immobilization of **C25** into [bmim][PF₆] supported onto a Starmem 228 nanofiltration membrane in order to prepare a catalytic membrane reactor [89]. After impregnation of the membrane with the

ionic liquid, this membrane was mounted in a filtration cell before a suspension of **C25** in toluene was introduced and a trans-membrane pressure of 3 bar applied. The immobilized catalyst was tested in the RCM of **14**. Assuming full catalyst immobilization, the RCM performed with modest performances since the conversion dropped quickly upon a second reuse of the initial 2.5 mol% load. However, full conversion could be obtained provided extension of the reaction duration from 1 to 2.5 h at 35°C.

3 Conclusion

Over the last decade many efforts have been devoted to the transfer of homogeneous olefin metathesis reactions from conventional organic media to RTILs. Owing to their poor solubility in RTILs neutral catalysts have quickly shown some limitations. This problem was however easily solved by employing ionic tags of various types. The tagged complexes have shown very good activities in various types of RCM reactions but it is presently difficult to conclude that reactions carried out in RTILs performed better than in conventional organic solvents. In some cases the ionically tagged catalysts could be recycled or reused several times. However with the recent developments on the boomerang mechanism it is very likely that what is seen as recycling is rather due to the formation of a catalyst reservoir in the RTILs. Most of the recycling tests were done at room or low temperature on RCM reaction of unhindered dienes with unusually high catalyst loadings. As a general trend, the higher the initial loading was the higher the number of cycles. When more demanding substrates and reaction conditions were necessary, the recycling properties of the catalysts dropped. Surprisingly, one example showed good reusability when a low initial catalyst loading was employed and this result was obtained with a Grubbs type catalyst (supposedly not recyclable) rather than with a Hoveyda type catalyst (supposedly recyclable). This last result clearly raises the question of the operating mode of all these catalysts in ionic liquid media having in mind that these features are not yet clearly established in classical organic solvent in the case of Hoveyda type catalysts [90, 91]. If the nature of the reusability cannot be truly established, several results have shown the interest of using ionic tags for the minimization of catalyst leaching and consequently the amount of residual metal in the reaction products. This point raises a second question yet in strong relationship with the operating mode of the catalyst. Indeed, whatever the catalytic mechanism, the ligand bearing the ionic tag is decoordinated from the metal centre in the initiation step thus releasing a neutral complex in the media. Without return of the tagged ligand this neutral compound or species arising from its decomposition should be extracted by organic solvent unless highly soluble in RTILs. Answers to these questions will be required in the near future in order to continue developing olefin metathesis processes in RTILs.

References

1. Fürstner A (2000) *Angew Chem Int Ed* 39:3012–3043
2. Hoveyda AH, Zhugralin AR (2007) *Nature* 450:243–251
3. Deshmukh PH, Blechert S (2007) *Dalton Trans* 2479–2491
4. Schrock RR, Hoveyda AH (2003) *Angew Chem Int Ed* 42:4592–4633
5. Vougioukalakis GC, Grubbs RH (2010) *Chem Rev* 110:1746–1787
6. Samojłowicz C, Bieniek M, Grela K (2009) *Chem Rev* 109:3708–3742
7. Diesendruck CE, Tzur E, Lemcoff NG (2009) *Eur J Inorg Chem* 4185–4203
8. Fischmeister C, Dixneuf PH (2007) pp 3–27. New ruthenium catalysts for alkene metathesis. In: *Metathesis chemistry: from nanostructure design to synthesis of advanced materials*. İmamođlu Y, Dragutan V (eds) Springer, Dordrecht, The Netherlands
9. Hérissou JL, Chauvin Y (1971) *Makromol Chem* 141:161–176
10. Chauvin Y (2006) *Angew Chem Int Ed* 45:3740–3747
11. Schrock RR (2006) *Angew Chem Int Ed* 45:3748–3759
12. Grubbs RH (2006) *Angew Chem Int Ed* 45:3760–3765
13. Donohe TJ, Fishlock LP, Procopiou PA (2008) *Chem Eur J* 14:5716–5726
14. Nicolaou KC, Bulger PG, Sarlah D (2005) *Angew Chem Int Ed* 44:4490–4527
15. van Otterlo WAL, de Koning CB (2009) *Chem Rev* 109:3743–3782
16. Gradillas A, Perez-Castells J (2006) *Angew Chem Int Ed* 45:6086–6101
17. Kress S, Blechert S (2012) *Chem Soc Rev* 41:4389–4408
18. Leitgeb A, Wappel J, Slugovc C (2010) *Polymer* 51:2927–2946
19. Buchmeiser MR (2000) *Chem Rev* 101:1565–1604
20. Schwendeman JE, Church AC, Wagener KB (2002) *Adv Synth Catal* 344:597–613
21. Mutlu H, Montero de Espinosa L, Meier MAR (2011) *Chem Soc Rev* 40:1404–1445
22. Meier MAR (2009) *Macromol Chem Phys* 210:1073–1079
23. Rybak A, Meier MAR (2008) *Green Chem* 10:1099–1104
24. Rybak A, Meier MAR (2007) *Green Chem* 9:1356–1361
25. Miao X, Malacea R, Fischmeister C, Bruneau C, Dixneuf PH (2011) *Green Chem* 13:2911–2919
26. Miao X, Fischmeister C, Bruneau C, Dixneuf PH, Dubois J-L, Couturier J-L (2012) *ChemSusChem* 5:1410–1414
27. Elevance Renewable Science will develop a biorefinery based on metathesis technology in Malaysia. www.elevance.com
28. Vougioukalakis GC (2012) *Chem Eur J* 18:8868–8880
29. Buchmeiser MR (2004) *New J Chem* 28:549–557
30. Buchmeiser MR (2009) *Chem Rev* 109:303–321
31. Keraani A, Renouard T, Fischmeister C, Bruneau C, Rabiller-Baudry M (2008) *ChemSusChem* 1:927–933
32. Schoeps D, Bühr C, Dijkstra M, Ebert K, Plenio H (2009) *Chem Eur J* 15:2960–2965
33. van der Gryp P, Barnard A, Cronje J-P, de Vlieger D, Marx S, Vosloo HCM (2010) *J Membr Sci* 353:70–77
34. Kajetanowicz A, Czaban J, Rajesh Krishnan G, Malińska M, Wozniak K, Siddique H, Peeva LG, Livingston AG, Grela K (2013) *ChemSusChem*. 6:182–192
35. Fürstner A, Ackerman L, Beck K, Hori H, Koch D, Langeman K, Liebl M, Six C, Leitner W (2001) *J Am Chem Soc* 123:9000–9006
36. Yao Q, Zhang Y (2004) *J Am Chem Soc* 126:74–75
37. Kingsbury JS, Hoveyda AH (2005) *J Am Chem Soc* 127:4510–4517
38. Vorfalt T, Wannowius KJ, Thiel V, Plenio H (2010) *Chem Eur J* 16:12312–12315
39. Fischmeister C (2007) p 483–501. Catalytic alkene metathesis in ionic liquids. In: *Metathesis chemistry: from nanostructure design to synthesis of advanced materials*. İmamođlu Y, Dragutan V (eds) Springer, Dordrecht, The Netherlands
40. Śledź P, Mauduit M, Grela K (2008) *Chem Soc Rev* 37:2433–2442

41. Chauvin Y, Olivier-Bourbigou H (1995) *Chemtech* 25:26–30
42. Buijsman RC, van Vuuren E, Sterrenburg JG (2001) *Org Lett* 3:3785–3787
43. Mayo KG, Nearhoof EH, Kiddle JJ (2002) *Org Lett* 4:1567–1570
44. Garbacia S, Desai B, Lavastre O, Kappe CO (2003) *J Org Chem* 68:9136–9139
45. Ding X, Lv X, Hui B, Chen Z, Xiao M, Guo B, Tang W (2006) *Tetrahedron Lett* 47:2921–2924
46. Bradley D, Williams G, Ajam M, Ranwell A (2006) *Organometallics* 25:3088–3090
47. *Mol JC* (2002) *Green Chem* 4:5–13
48. Warwel S, Tillack J, Demes C, Kunz M (2001) *Macromol Chem Phys* 202:1114–1121
49. Thurier C, Fischmeister C, Bruneau C, Olivier-Bourbigou H, Dixneuf PH (2008) *ChemSusChem* 1:118–122
50. Thomas PA, Marvey BM (2009) *Int J Mol Sci* 10:5020–5030
51. Thomas PA, Marvey BB, Ebenso EE (2011) *Int J Mol Sci* 12:3989–3997
52. Mutlu H, Meier MAR (2010) *Eur J Lipid Sci* 112:10–30
53. Vasnev AV, Greish AA, Kustov LM (2004) *Russ Chem Bull Int Ed* 53:2187–2191
54. Greish AA, Kustov LM, Vasnev AV (2011) *Mendeleev Commun* 21:329–330
55. Schrock RR, (2004) *J Mol Catal A Chem* 213:21–30
56. Gürtler C, Jautelat M Bayer AG EP 1035093A2 (2000) and US 6756500 B1 (2004)
57. Lee Miller A, Bowden NB (2007) *Chem Commun* 2051–2053
58. Fürstner A, Picquet M, Bruneau C, Dixneuf PH (1998) *Chem Commun* 1315–1316
59. Picquet M, Bruneau C, Dixneuf PH (1998) *Chem Commun* 2249–2250
60. Fürstner A, Liebl M, Lehmann CW, Piquet M, Kunz R, Bruneau C, Touchard D, Dixneuf P (2000) *Chem Eur J* 6:1847–1857
61. Sémeril D, Olivier-Bourbigou H, Bruneau C, Dixneuf PH (2002) *Chem Commun* 146–147
62. Csihony Sz, Fischmeister C, Bruneau C, Horváth IT, Dixneuf PH (2002) *New J Chem* 26:1667–1670
63. Gallagher MM, Rooney AD, Rooney JJ (2009) *J Mol Catal A Chem* 303:78–83
64. Audic N, Clavier H, Mauduit M, Guillemin JC (2003) *J Am Chem Soc* 125:9248–9249
65. Yao Q, Zhang Y (2003) *Angew Chem Int Ed* 42:3395–3398
66. Clavier H, Audic N, Mauduit M, Guillemin JC (2004) *Chem Commun* 2282–2283
67. Yao Q, Sheets M (2005) *J Organomet Chem* 690:3577–3584
68. Clavier H, Audic N, Guillemin JC, Mauduit M (2005) *J Organomet Chem* 690:3585–3599
69. Thurier C, Fischmeister C, Bruneau C, Olivier-Bourbigou H, Dixneuf PH (2007) *J Mol Catal A Chem* 268:127–133
70. Wakamatsu H, Blechert S (2002) *Angew Chem Int Ed* 41:2043–2405
71. Kinsbury JS, Harrity JPA, Bonitatebus PJ, Hoveyda AH (1999) *J Am Chem Soc* 121:791–799
72. Wakamatsu H, Saito Y, Masubuchi M, Fujita R (2008) *Synlett* 12:1805–1808
73. Grela K, Harutyunyan S, Michrowska A (2002) *Angew Chem Int Ed* 41:4038–4040
74. Rix D, Clavier H, Coutard Y, Gulajski L, Grela K, Mauduit M (2006) *J Organomet Chem* 691:5397–5405
75. Rix D, Caijo F, Laurent I, Gulajski L, Grela K, Mauduit M (2007) *Chem Commun* 3771–3773
76. Gulajski L, Mauduit M, Grela K (2009) *Pure Appl Chem* 81:2001–2012
77. Consorti CS, Aydos GLP, Ebeling G, Dupont J (2009) *Organometallics* 28:4527–4533
78. Chen S-W, Kim JH, Ryu KY, Lee W-W, Hong J, Lee S-g (2009) *Tetrahedron* 65:3397–3403
79. Ritter T, Hejl A, Wenzel AG, Funk TW, Grubbs RH (2006) *Organometallics* 25:5740–5745
80. Rybak A, Meier MAR (2007) *Green Chem* 9:1356–1361
81. Clavier H, Nolan SP, Mauduit M (2008) *Organometallics* 27:2287–2292
82. Liu G, Zhang J, Wu B, Wang J (2007) *Org Lett* 9:4263–4266
83. Consorti CS, Aydos GLP, Ebeling G, Dupont J (2008) *Org Lett* 10:237–240
84. Fogg DE, dos Santos EN (2004) *Coord Chem Rev* 248:2365–2379
85. Consorti CS, Aydos GLP, Dupont J (2010) *Chem Commun* 46:9058–9060
86. Hagiwara H, Okunaka N, Hoshi T, Suzuki T (2008) *Synlett* 1813–1816
87. Hagiwara H, Nakamura T, Okunaka N, Hoshi T, Suzuki T (2010) *Helv Chim Acta* 93:175–181

88. Duque R, Öchsner E, Clavier H, Caijo F, Nolan SP, Mauduit M, Cole-Hamilton DJ (2011) *Green Chem* 13:1187–1195
89. Keraani A, Rabiller-Baudry M, Fischmeister C, Bruneau C (2010) *Catal Today* 156:268–275
90. Thiel V, Hendann M, Wannowius K-J, Plenio H (2012) *J Am Chem Soc* 134:1104–1114
91. Nuñez-Zarur F, Solans-Monfort X, Rodríguez-Santiago L, Sodupe M (2012) *Organometallics* 31:4203–4215

Ionic Liquids in Transition Metal-Catalyzed Oligomerization/Polymerization

Anna M. Trzeciak

Abstract This short review presents selected examples of polymerization and oligomerization reactions catalyzed by transition metal complexes in ionic liquid media. Analysis of these data to some extent supports the popular opinion that ionic liquids are not inert solvents but rather should frequently be considered co-catalysts. In particular, the application of imidazolium salts makes possible the formation of carbene complexes and consequently changes catalytic activity in many cases.

Keywords Carbene complexes · Ionic liquids · Olefins oligomerization · Olefins polymerization · Phenylacetylene · Transition metal complexes

Contents

1	Introduction	309
1.1	Polymerization and Oligomerization of Olefins	309
2	Dimerization of Acrylates	316
2.1	Styrene and CO Copolymerization	317
2.2	Ring-Opening Metathesis Polymerization (ROMP)	317
2.3	Polymerization of Phenylacetylene	318
3	Conclusions	321
	References	322

Abbreviations

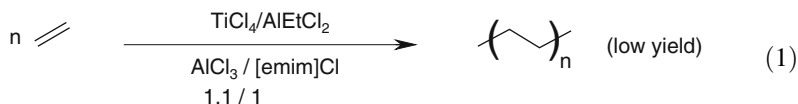
Ac	Acetyl
Acac	Acetylacetonate
Ar	Aryl
Bipy	2,2'-Bipyridyl
Bmim	1-Methyl-3-butylimidazolium cation
Bmim-y	1-Methyl-3-butylimidazol-2-ylidene
Bn	Benzyl
Bp	Bis-pyrazolylborate
Bu	Butyl
Bupy	1-Butyl-4-methylpyridinium cation
Cat	Catalyst
Cod	Cyclooctadiene
Cp	Cyclopentadienyl
Cy	Cyclohexyl
d	Day(s)
Dbmim	1,2-Dimethyl-3-butylimidazolium
DMF	Dimethylformamide
Emim	1-Ethyl-3-methylimidazolium
Et	Ethyl
h	Hour(s)
Hfacac	Hexafluoroacetylacetonate
i-Pr	Isopropyl
Me	Methyl
Mes	Mesityl, 2,4,6-trimethylphenyl (not methanesulfonyl)
Min	Minute(s)
Mokt	1-Methyl-3-octylimidazolium cation
Mol	Mole(s)
Nbd	Norbomadiene
Nu	Nucleophile
PE	Polyethylene
Ph	Phenyl
PPA	Polyphenylacetylene
Pr	Propyl
Py	Pyridine
Rt	Room temperature
s	Second(s)
<i>s</i> -Bu	<i>sec</i> -Butyl
<i>t</i> -Bu	<i>tert</i> -Butyl
Tf	Trifluoromethanesulfonyl (triflyl)
TFA	Trifluoroacetic acid
THF	Tetrahydrofuran
Tol	4-Methylphenyl
Tp	Tris-pyrazolylborate

1 Introduction

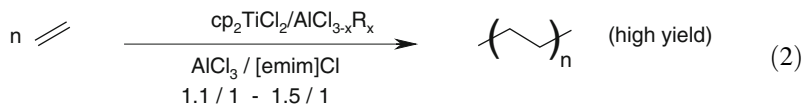
Ionic liquids have been used in various polymerization and oligomerization reactions of unsaturated compounds proceeding according to radical, cationic, or anionic pathways under metal-free conditions [1–7]. The activity of other types of systems used in polymerization stems from transition metal species acting as catalysts. Organic solvents are typically used in such reactions. Ionic-liquid non-volatile melts present an interesting alternative to organic solvents facilitating the recycling of the catalyst [8–13]. The commercialized Difasol process should be mentioned in this connection as an important example of an industrial technology using ionic liquids [8, 9]. Difasol, developed at ICP (Institut Francais du Petrole) by Y. Chauvin and H. Olivier-Bourbigou, is the nickel-catalyzed dimerization of short-chain alkenes into branched alkenes using chloroaluminate ionic liquids as solvents.

1.1 Polymerization and Oligomerization of Olefins

The first attempt at ethylene polymerization in an ionic liquid was reported by Wilkes et al. in 1990 [14]. In that experiment ethylene was bubbled at 1 atm into a melt composed of $\text{AlCl}_3 + [\text{emim}]\text{Cl}$ (1.1:1) (emim = 1-ethyl-3-methylimidazolium cation) and containing TiCl_4 and AlEtCl_2 , components of a Ziegler–Natta catalyst (1). The yield of polyethylene was relatively low; however, it was shown that polymerization can be performed in an ionic liquid. Moreover, spectroscopic studies evidenced structural transformations of the catalyst and the complete reduction of Ti(IV) to Ti(III) .

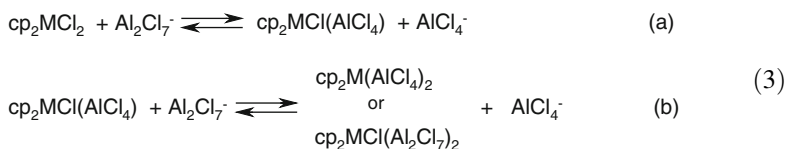


In subsequent studies, the same molten salt containing AlCl_3 and $[\text{emim}]\text{Cl}$ was employed with a catalyst composed of cp_2TiCl_2 and $\text{AlCl}_{3-x}\text{R}_x$ ($\text{R} = \text{Me}, \text{Et}$) (2) [15]. The Lewis acidity of this medium can be modulated by changing the $[\text{AlCl}_3]:[\text{emim}]\text{Cl}$ molar ratio. The dominant anions under basic conditions ($[\text{AlCl}_3]:[\text{emim}]\text{Cl} < 1$) were Cl^- and AlCl_4^- , while Al_2Cl_7^- and AlCl_4^- were present when acidic properties were stronger ($[\text{AlCl}_3]:[\text{emim}]\text{Cl} > 1$).



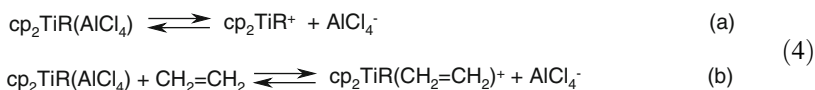
Importantly, it was found that catalysis did not occur in basic melts, where $\text{cp}_2\text{TiCl}_3^-$ was predominantly formed from the cp_2TiCl_2 precursor, whereas catalytic

activity was observed in acidic melts. Representative catalytic results were in the range from 0.02 to 0.15 (g PE) min⁻¹ (mmol Ti)⁻¹ min⁻¹. In contrast, cp₂ZrCl₂ and cp₂HfCl₂ did not exhibit any catalytic activity under the same conditions. In order to explain the observed differences, spectroscopic studies (¹H NMR) were undertaken. Two complexation processes can be considered when the cp₂MCl₂ complex is dissolved in an acidic ionic liquid containing AlCl₃ and [emim]Cl (3):



In all cases, AlCl₄⁻ coordinated in a monodentate fashion forming M–Cl–Al bridging structures [15].

It was found that the value of the equilibrium constant K₁ for reaction 1 (3) was much higher for Ti (>10⁵) than for Zr (22 ± 4) or Hf (4.1 ± 0.8), which means that the M–Cl bonding in Zr and Hf complexes is much stronger than Ti–Cl. This was assumed to be the main reason for the observed high catalytic ability of Ti with respect to Zr and Hf. Two active Ti species were proposed, both formed from AlCl₄⁻-containing intermediates (4):



In the presence of a high excess of AlCl₄⁻, as was the case in an acidic ionic liquid, displacement of coordinated AlCl₄⁻ by ethylene was proposed as the step responsible for the formation of a catalytically active form, cp₂TiR(CH₂=CH₂)⁺.

In 1995, Chauvin described the dimerization of propene performed in a two-phase system containing ionic liquids that played the role of a regioselective solvent enabling the maximization of the yield of 2-methylpentene and 2,3-dimethylbutene [16]. After hydrogenation, these branched alkenes can be used to increase the octane number of gasoline.

NiCl₂L₂ (L=PⁱPr₃, PBu₃, PCy₃, PBn₃, py) complexes, air stable and easy to handle, were used as catalyst precursors. The reaction medium contained [bmim]Cl, AlCl₃ and AlCl₂Et as alkylating agents. In the basic ionic liquid, where the molar fraction of AlCl₃ was <0.5 and an excess of free Cl⁻ was present, catalytic activity was not observed because the nickel precursor formed a blue paramagnetic tetrahedral anionic species of the type NiCl₄²⁻. In contrast, in an acidic medium a catalytically active nickel hydrido complex of the type [HNi(PR₃)]⁺A⁻ was formed enabling an efficient catalytic process.

The composition of the melt influenced the kind of aluminum anions present in the reaction medium (Table 1):

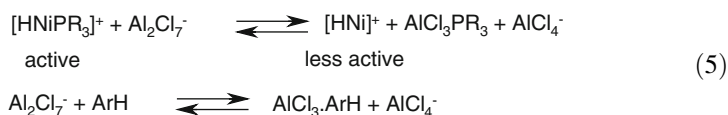
The best results were obtained in the third ionic liquid (Table 1). For example, 84% of 2,3-dimethylbutenes was obtained in reaction catalyzed by NiCl₂(PCy₃)₂.

Table 1 Aluminum anions present in ionic liquids

IL	Composition	Aluminum anions
[bmim]Cl/AlEtCl ₂	1:1.2	AlEtCl ₂ ⁻ , Al ₂ Et ₂ Cl ₅ ⁻
[bmim]Cl/AlCl ₃ /AlEtCl ₂	1:0.82:0.26	AlCl ₄ ⁻ , AlEtCl ₃ ⁻ , Al ₂ Et ₂ Cl ₅ ⁻
[bmim]Cl/AlCl ₃ /AlEtCl ₂	1:1.2:0.1	AlCl ₄ ⁻ , Al ₂ Cl ₇ ⁻ , Al ₂ EtCl ₆ ⁻ , Al ₂ Et ₂ Cl ₅ ⁻

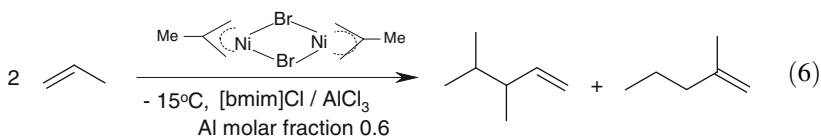
The same catalyst produced 76% of 2,3-dimethylbutenes in [bmim]Cl/AlCl₃/AlEtCl₂.

Analysis of the composition of dimerization products obtained with nickel catalysts containing different phosphines made it possible to realize the effect of phosphine, discussed in terms of competition between the bonding of phosphine to the active nickel species (soft) and to AlCl₃ (hard). Thus, [HNiPR₃]⁺ loses phosphine forming a less active hydride [HNi]⁺ (5). This hypothesis was proved by ³¹P NMR, where the formation of a phosphine–AlCl₃ complex was evidenced. To prevent the formation of such species, another soft base was added to the catalytic system, an aromatic hydrocarbon, ArH. Consequently, an Al₂Cl₇⁻ anion formed an AlCl₃·ArH adduct instead of AlCl₃·PR₃ (5):



The hydrocarbons that formed adducts with AlCl₃, such as tetramethylbenzene or pentamethylbenzene, facilitated the formation of 2,3-dimethylbutane with high yield. The system recommended for practical applications contained [NiCl₂(PR₃)₂] – [NiCl₂(pyridine)₂] dissolved in an AlCl₃/[bmim]Cl ionic liquid with small additions of AlEtCl₂ and aromatic hydrocarbons (1,2,3,5-tetramethylbenzene or toluene) [16].

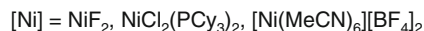
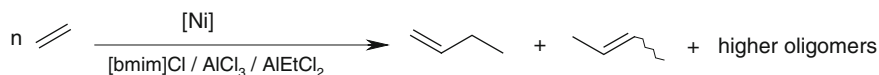
An acidic molten salt containing AlCl₃ and [bmim]Cl (molar fraction of Al = 0.6) used without any nickel complex transformed propene to oligomers, typical for cationic reactions [17]. This can be explained by the presence of some free protons. In contrast, in the same acidic conditions, η³-methylallylnickel bromide produced 67% of 2-methylpentenes (6). In the basic melt (molar fraction of Al = 0.45), the nickel complex was not active.



Cationic side reactions causing a decrease in reaction selectivity were suppressed by the application of AlEtCl₂, acting as a proton scavenger instead of AlCl₃. Under these conditions, other nickel precursors, such as Ni(acac)₂ or NiCl₂(^tPr₃P)₂, were also quite active. For example, 2,3-dimethylbutenes were

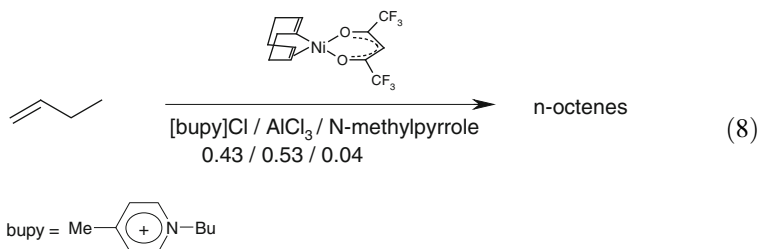
obtained with a yield of 76% in an $\text{AlCl}_3/[\text{bmim}]\text{Cl}$ medium (molar fraction of $\text{Al} = 0.7$) with a $\text{NiCl}_2(\text{P}^i\text{Pr}_3)_2$ catalyst. Interestingly, the steric effect of phosphine resulted in the formation of 2,3-dimethylbutane as the main product. The lack of catalytic activity in acidic melts is explained by the formation of NiCl_4^- and NiCl_3L^- (molar fraction of $\text{Al} = 0.45$) anionic species.

Three nickel complexes, NiF_2 , $\text{NiCl}_2(\text{PCy}_3)_2$, and $[\text{Ni}(\text{MeCN})_6][\text{BF}_4]$, were used as catalysts for ethylene dimerization in $\text{AlCl}_3-[\text{bmim}]\text{Cl}$ [18]. The reactions were performed in the presence of AlEtCl_2 (7). Interestingly, the addition of toluene to the reaction mixture was essential for the modulation of ethylene dimerization activity and selectivity. Other hydrocarbons promote the formation of higher oligomers instead of dimers. The best results, a high yield of 1-butene (83%), were obtained with a dicationic catalyst. The same catalyst was used in the heptane-catalyzed formation of 2-butenes with the yield 66%. The most active catalyst, $\text{NiCl}_2(\text{PCy}_3)_2$, gave lower selectivity to the butenes.



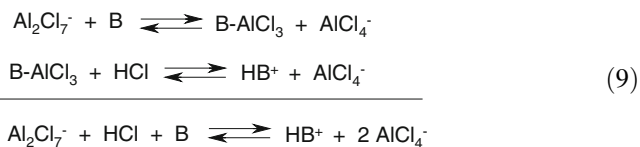
(7)

The phosphine-free nickel complex $[\text{Ni}(\text{H-COD})(\text{hfacac})]$ ($\text{H-COD}=\eta\text{-4-cycloocten-1-yl}$) without an aluminum co-catalyst was used for the dimerization of 1-butene to linear octenes in slightly acidic pyridinium chloroaluminate [19]. The chloroaluminate ionic liquid was buffered with small amounts of weak organic bases such as pyrrole and *N*-methylpyrrole (8). The addition of *N*-methylpyrrole resulted in the suppression of all cationic side reactions and only dimerization products were formed. Moreover, the reaction proceeded much faster in the ionic liquid than in toluene, indicating a facilitated activation of the catalyst. Excellent selectivity to the dimeric product, 98%, was obtained using $[\text{bupy}]\text{Cl}/\text{AlCl}_3/\text{N}$ -methylpyrrole (0.43/0.53/0.04) or $[\text{bupy}]\text{Cl}/\text{AlCl}_3/\text{chinoline}$ (0.43/0.53/0.04). Interestingly, the application of LiCl as a buffering agent in $[\text{bupy}]\text{Cl}/\text{AlCl}_3$ (0.45/0.55) resulted in 75% selectivity to dimers [19].



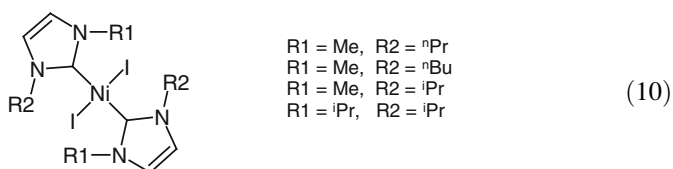
The efficiency of the buffering function can be correlated with selectivity to dimers and the suppression of oligomer formation. It was found that the extent of

cationic side reactions correlated well with the content of Al_2Cl_7^- , and the action of the added base B (*N*-methylpyrrole, pyridine, chinoline) can be illustrated by the following set of equilibria (9):



Thus, the base traps any free acidic species present in the melt and as a result cationic side reactions are reduced.

A similar concept, based on the application of a buffered chloroaluminate–imidazolium ionic liquid, was used for the dimerization of 1-butene with Ni(II) dicarbene complexes (10) [20]. The first catalytic attempts were performed in toluene; however, after the addition of an AlEt_2Cl cocatalyst, Ni(0) was formed and dimerization was not observed. Similarly, no products were found when AlCl_3 or MAO were used as cocatalysts. In contrast, in an ionic liquid being a mixture of $[\text{bmim}]\text{Cl}$, AlCl_3 , and *N*-methylpyrrole (at a molar ratio of 0.45:0.55:0.1) at room temperature, TOF values as high as 3,820–7,020 h^{-1} were achieved. Under the same conditions, $\text{NiCl}_2(\text{PCy}_3)_2$ was less active, giving TOF of 2,950 h^{-1} . Isomer proportions after hydrogenation were similar for $\text{NiCl}_2(\text{PCy}_3)_2$ and for carbene complexes, 3,4-dimethylhexane being the dominating product.



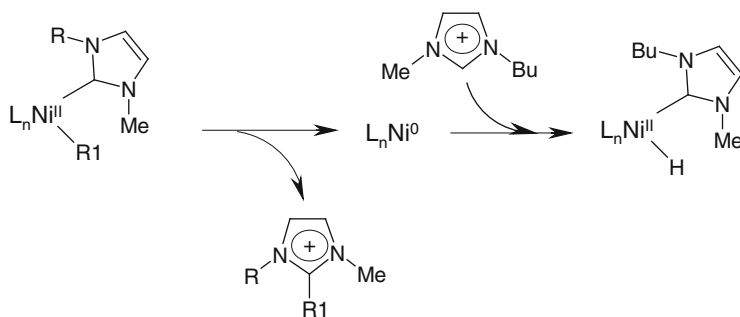
R1 = Me, R2 = ⁿPr
 R1 = Me, R2 = ⁿBu
 R1 = Me, R2 = ⁱPr
 R1 = ⁱPr, R2 = ⁱPr

One carbene complex was also tested in propene dimerization [20]. However, 2-methylpentane was formed as the main product instead of the desirable, highly-branched 2,3-dimethylbutane, which was preferentially formed with $\text{NiCl}_2(\text{PCy}_3)_2$.

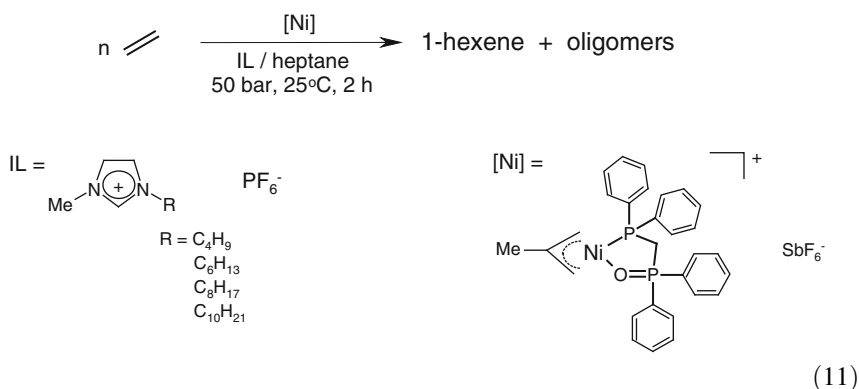
The selectivity of carbene complexes can change during the reaction due to replacement of carbene ligands in ionic liquid medium (Scheme 1).

A cationic nickel complex was used for the first time in the selective biphasic oligomerization of ethylene to 1-olefins (11) [21]. It was shown that ionic liquids with a PF_6^- anion played an important role and very promising results, with high selectivity to *n*-hexene and high activity (TOF 12,712 h^{-1}), were observed in $[\text{bmim}]\text{PF}_6$ [21]. The activity decreased when alkyl chain length increased.

The catalyst dissolved in an ionic liquid was recycled twice with almost the same selectivity but with lower activity.



Scheme 1 Formation of modified Ni(II) carbene complex after reductive elimination of imidazolium cation

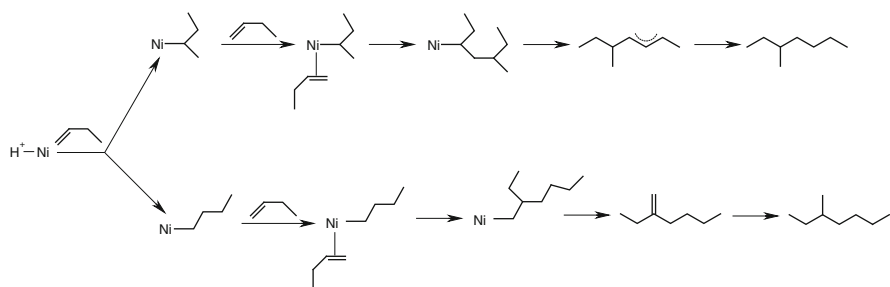


On the basis of solvent basicity studies, it was proposed that the very high catalytic activity of the complex in [bmim]PF₆ can be explained by a unique combination of high polarity and low coordination power displayed by this ionic liquid. In conclusion, ionic liquids with PF₆⁻ anions were recommended as an appropriate reaction medium that makes it possible to achieve a good compromise between solvating and coordination properties [21].

Butene oligomerization was performed in a two-phase system containing a 1-butyl-3-methylimidazolium chloro-ethyl-aluminate ionic liquid, containing 57 mol% of Al, prepared by mixing AlCl₃, AlEtCl₂ and [bmim]Cl [22]. The good solubility of nickel complexes in polar non-ionic liquids and the poor solubility of olefins in these media enables efficient separation of the reaction products from the catalyst by simple decantation.

A nickel cationic complex [Ni(MeCN)₆][BF₄]₂, was used in the presence of PPh₃, PBu₃, PCy₃, and PCy₃.CS₂ to produce dimers from 2-butene with a selectivity of 92–98%. The highest rate constant, ca. 9 mol Ni⁻¹ s⁻¹, was noted when PCy₃.CS₂ was applied.

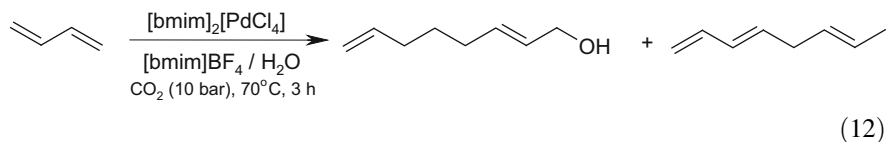
In the absence of AlCl₃, lower TOF values were obtained, similarly as observed for propene dimerization [22]. This was interpreted as a result of a strong influence of the anion associated with the cationic active species. The structure of C₈ products



Scheme 2 Possible pathways to 3-methylheptene

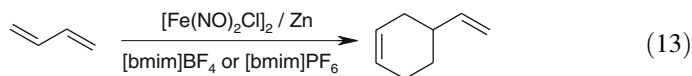
was practically unaffected by the kind of phosphine used. The distribution of C₈ products was similar to that obtained with the homogeneous system (Dimersol), with 3-methylheptene dominating over dimethylpentenes (Scheme 2).

An interesting example of palladium-catalyzed hydrodimerization of 1,3-butadiene to octa-2,7-dien-1-ol in [bmim]BF₄ and [bmim]PF₆ has been reported by Dupont et al. (12) [23]. Palladium compounds of the formula [η³-C₄H₇PdCl]₂, [η³-C₄H₇Pd(COD)]BF₄, and Pd(OAc)₂ were used as catalyst precursors; however, during the reaction they decomposed with the formation of metallic palladium. Nevertheless, octa-2,7-dien-1-ol was formed as the main product in the absence as well as in the presence of CO₂ pressure (5–10 atm). In the latter case, an increase in TOF values to 150–200 h⁻¹ was noted. A higher stability of the catalyst was achieved for the anionic complex [bmim]₂[PdCl₄], which was reused four times with almost the same activity.



It is worth noting that [bmim]₂[PdCl₄] reacted with water in [bmim]BF₄ forming the imidazole complex Pd(im)₂Cl₂, whose catalytic activity in hydrodimerization was similar to that of its anionic precursor [23].

The cyclodimerization of 1,3-butadiene and isoprene catalyzed by an iron–nitrosyl complex was studied in [bmim]BF₄ and [bmim]PF₆ in a two-phase system (13) [24].

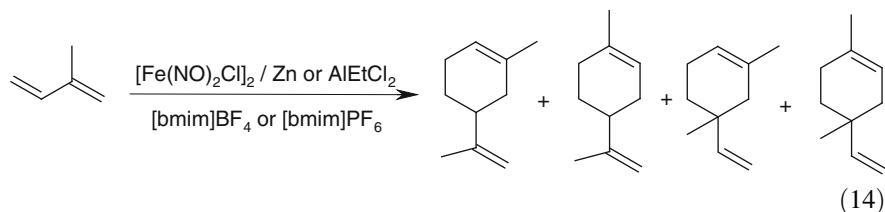


The iron precursor [Fe(NO)₂Cl]₂, was reduced in situ by metallic Zn, AlEtCl₂, or BuLi, and Zn appeared the most efficient in terms of high conversion of 1,3-butadiene and high selectivity to 4-vinyl-1-cyclohexene. The maximum TOF value, 1,404 h⁻¹, was obtained at 50°C. In further investigations, the effect of

different phosphines on the reaction course was studied; a decrease in catalytic activity was noted in all cases.

The same catalytic system was successfully applied in the cyclodimerization of isoprene to methyl-4-(1-methylethenyl)cyclohexenes and dimethyl-4-vinylcyclohexenes (14).

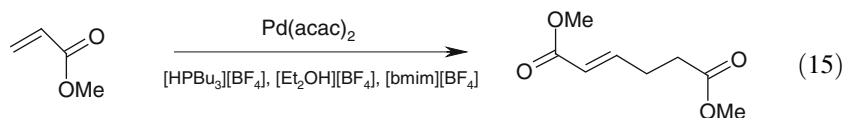
Selectivity to 4-vinyl-cyclohexene derivatives was the highest in both ionic liquids and increased in the presence of phosphine. Consequently, 1,4-dimethyl-4-vinylcyclohexene was obtained with 65–70% selectivity when phosphine was present, whereas without phosphine selectivity to this product was 46–65%.



2 Dimerization of Acrylates

The first continuous, biphasic dimerization of methylacrylate to Δ^2 -dihydrodimethylmuconate catalyzed by $\text{Pd}(\text{acac})_2$ was performed using $[\text{bmim}]\text{BF}_4$ as the catalyst solvent (15) [25]. An acceleration of the dimerization process was demonstrated by comparing the results obtained with the addition of PBu_3 and $\text{PBu}_3/[\text{bmim}]\text{BF}_4$. The TON values obtained after 24 h were 1,024 and 2,986, respectively. When the bidentate ligand $\text{PBu}_2(\text{CH}_2)_2\text{NMe}_2$ was used instead of PBu_3 , a further increase in TON values was noted. It was also observed that toluene played an important role in the reaction system facilitating a biphasic mode of the process and making it possible to overcome the inhibiting influence of the reaction products.

It was noted that imidazolium and pyridinium salts had similar rate-enhancing effects. Thus, the formation of a carbene palladium complex was rather unlikely. Moreover, acidic conditions do not facilitate carbene formation.



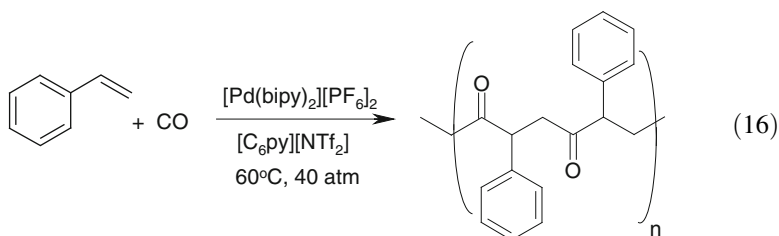
In continuous flow reaction an overall TON of more than 4,000 was realized after 50 h indicating the high stability of the catalytic system [25].

Methyl methacrylate was polymerized by a living radical process mediated by a copper complex formed in situ from CuBr and *N*-propyl-2-pyridylmethanimine in $[\text{bmim}]\text{PF}_6$ [26]. When the ratio of the ligand to $\text{Cu}(\text{I})$ increased, the rate of polymerization also increased. As the $\text{Cu}(\text{I})$ catalyst is soluble in $[\text{bmim}]\text{PF}_6$ but not in toluene, poly(methyl methacrylate) can be easily extracted to the organic phase. The possibility of recycling the catalyst dissolved in an ionic liquid after such extraction was not tested.

2.1 Styrene and CO Copolymerization

An improvement in the yield of polyketone formed by the copolymerization of styrene with CO was observed when ionic liquids were used as solvents instead of methanol or trifluoroethanol in reaction catalyzed by $[\text{Pd}(\text{bipy})_2][\text{PF}_6]_2$ (16) [27]. The yield of the product depended on the kind of anion present in the ionic liquid and decreased in order: $\text{NTf}_2 > \text{PF}_6 > \text{BF}_4$ for pyridinium and imidazolium salts. The structure of the cation, in particular the length of the alkyl chain, also influenced the reaction yield. In the series of $[\text{C}_n\text{py}][\text{NTf}_2]$ salts, the yield of polyketone increased with the increase in the number of carbon atoms from $n = 4$ to $n = 10$. It was suggested that different reaction mechanisms operated in methanol and in ionic liquids; however, further mechanistic considerations were not presented.

Copolymerization performed in the absence of any oxidant gave a rather low yield of the product; therefore, 1,4-benzoquinone was preferably used. Under optimized conditions, productivity as high as 24 kg of polymer $(\text{g Pd})^{-1}$ was achieved at 80°C within 8 h. Good recyclability of the catalyst was demonstrated in four subsequent runs with similar productivity, molecular weight, and polydispersity of polyketone.

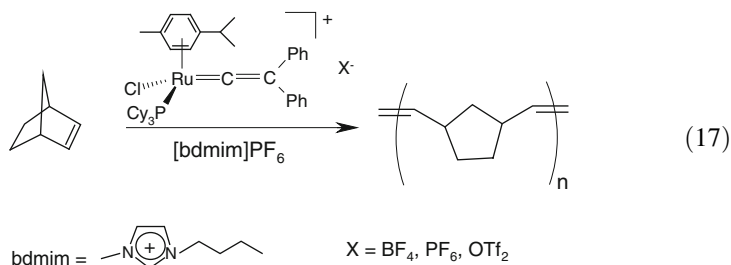


The same process was studied using $(\text{bipy})\text{Pd}(\text{OAc})_2$ as a catalyst in a $[\text{C}_6\text{py}][\text{NTf}_2]$ medium [28]. A pyridinium ionic liquid was used to avoid the formation of Pd-carbene complexes, which can be expected in imidazolium salts. In the typical procedure some amount of methanol was present and the highest productivity of the system at 70°C and 40 bar CO was 2.7 kg of the polymer $(\text{g Pd})^{-1}$. The catalyst was recycled twice; however, its activity was significantly lower. It was stressed that the replacement of typically used methanol with an ionic liquid inhibited chain transfer and catalyst decomposition indicating a higher stability of the catalyst in the ionic liquid.

2.2 Ring-Opening Metathesis Polymerization (ROMP)

The ROMP of norbornene, catalyzed by an allenylidene ruthenium complex, was carried out in a biphasic medium containing an ionic liquid and toluene [29].

As far as the ionic liquid is concerned, the PF_6^- anion was selected because of its hydrophobic properties making it possible to dissolve ruthenium salt. In order to avoid the formation of a carbene ruthenium complex, an imidazolium cation substituted at the C2 carbon was used ($[\text{bdmim}]\text{PF}_6$) (17):



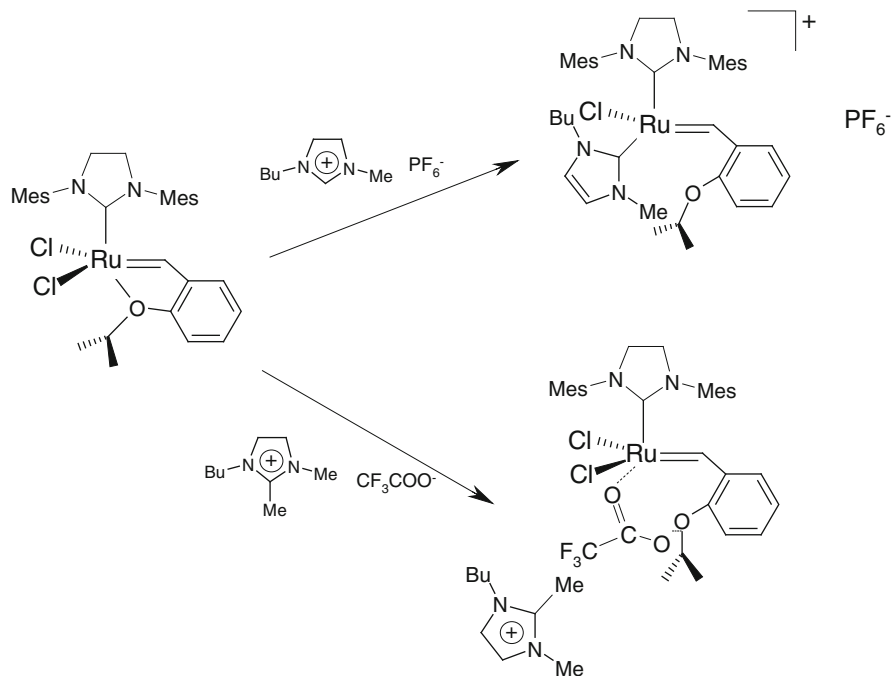
Using the mixture of the ionic liquid and toluene, it was possible to recycle the catalyst five times with a high yield of the polymer. The second catalyst tested, an allenylidene Grubbs complex rapidly lost its catalytic activity and no polymer was formed in the second recycle. Better results were obtained with a more bulky complex; however, a decrease in the yield of the polymerization product was also observed in this case in the third recycle. The highest efficiency of the allenylidene catalyst can be explained by its ionic structure, in contrast to the allenylidene catalyst.

The same reaction of functionalized norbornenes was studied using ruthenium catalysts bearing *N*-heterocyclic carbene ligands [30].

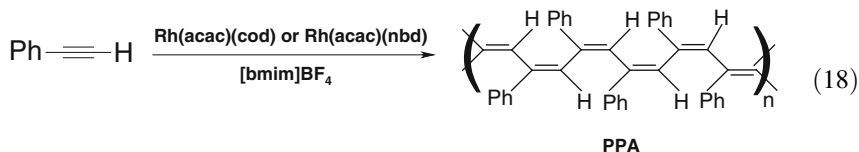
It was observed that the yield of the polymer depended on what catalysts, ionic liquids, and substrates were used. In particular, ionic liquids containing chloride, or nitrate anions are not suitable for obtaining polymers, whereas weakly coordinating anions, BF_4^- or PF_6^- , enable high-yield synthesis of the product. Spectroscopic investigations allowed to characterize the specific interactions between ruthenium catalyst and ionic liquids (Scheme 3).

2.3 Polymerization of Phenylacetylene

The rhodium-catalyzed polymerization of phenylacetylene to polyphenylacetylene (PPA) was performed in the ionic liquids $[\text{bmim}]\text{BF}_4$ and $[[\text{bupy}]\text{BF}_4$ by Mastronilli et al. in 2002 (18) [31]. β -Acetylacetonato complexes of Rh(I), $[\text{Rh}(\text{acac})(\text{nbd})]$, and $[\text{Rh}(\text{acac})(\text{cod})]$ with diene ligands, highly active in organic solvents, were selected as catalysts. It was found that a basic co-catalyst, namely NEt_3 , was necessary to get PPA.



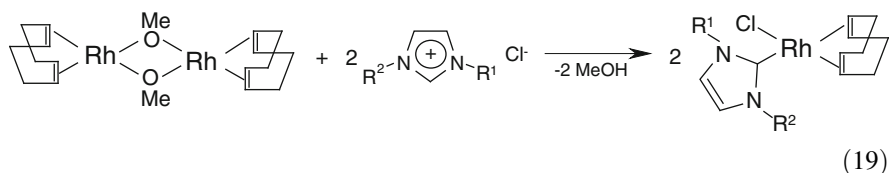
Scheme 3 Proposed interactions of Ru catalyst with ionic liquids



While the presence of NEt₃ played a very important role in the catalytic process, the influence of the ionic liquid structure was less visible and both of the ionic liquids used made it possible to obtain similar yields of PPA. The molecular weight of PPA varied from 55,000 to 196,000 Da, and the *cis* configuration in the polymer chain dominated. If the effect of the rhodium precursor structure is considered, the norbornadiene complex exhibited higher activity, making it possible to obtain a 95–100% yield of PPA within 5 min. Additionally, catalytic experiments performed with [(nbd)RhCl]₂ and [(cod)RhCl]₂ dimers confirmed the higher catalytic ability of acetylacetonato complexes. Moreover, an Rh(acac)(nbd) catalyst was recovered in the ionic liquid and showed almost unchanged activity in the second run [31]. In contrast to the [(cod)RhCl]₂ chlorido-free rhodium dimer, [(cod)Rh(OMe)]₂ catalyzed polymerization of phenylacetylene in ionic liquids without any co-catalyst [32]. The highest yield (92%) of PPA was obtained in [bupy]BF₄, whereas only 57% of PPA was formed in [bmim]I. The addition of NEt₃ caused an increase in polymerization yield in almost all ionic liquids with the exception of

[mokt]Cl, where yield decreased from 75% in reaction without NEt_3 to 51% in its presence. At the same time, molecular weight increased from 72,400 to 94,400 Da. In general, in almost all the ionic liquids studied, the presence of an NEt_3 co-catalyst caused an increase in M_w while the reverse effect was observed after cod addition.

The fact that a different polymerization course was observed in [mokt]Cl than in other ionic liquids inspired spectroscopic studies oriented towards the identification of possible new rhodium species formed in the reaction mixture [33]. In fact, UV-vis and $^1\text{H NMR}$ data made it possible to propose the formation of a new carbene complex in reaction of $[(\text{cod})\text{Rh}(\text{OMe})_2]$ with [mokt]Cl (19). Although this product was not isolated, its analogs of the formula $[\text{Rh}(\text{bmim-}y)\text{X}(\text{cod})]$ were obtained and fully characterized, including X-ray analysis [33]. It was also confirmed that the dimer $[(\text{cod})\text{Rh}(\text{OMe})_2]$ reacted only with imidazolium salts bearing halide anions. The formation of a carbene rhodium complex using imidazolium salt with the BF_4^- anion was also possible in the presence of a $[\text{Bu}_4\text{N}]\text{Cl}$ additive.



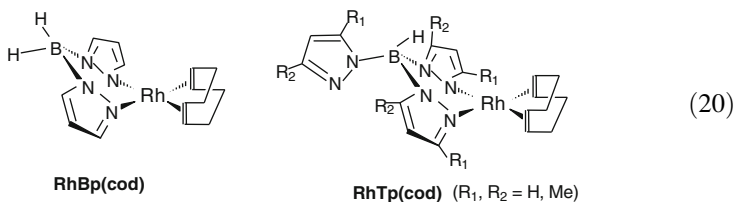
Rh(I) carbene complexes were tested as catalysts of phenylacetylene polymerization. However, the catalytic results were in most cases worse than with the application of $[(\text{cod})\text{Rh}(\text{OMe})_2]$. Only in [mokt]Cl were the results similar, indicating an important role of carbene complexes in the polymerization course [33].

Transition metal complexes bearing *N*-heterocyclic carbene ligand have found many applications in catalysis [34, 35], including olefin polymerizations [36].

A very positive effect of ionic liquids was noted when rhodium complexes with bis- and tris-pyrazolylborate ligands were used for phenylacetylene polymerization (20) [37]. Thus, in reaction with $[\text{RhBp}(\text{cod})]$ as a catalyst in ionic liquids, 28–58% of PPA was formed. The molecular weight of PPA increased remarkably in comparison with reactions performed in CH_2Cl_2 and polydispersity decreased.

Even more spectacular improvement in the polymerization process was observed in reaction catalyzed by $\text{RhTp}(\text{cod})$, which was almost inactive in CH_2Cl_2 . The highest yield of PPA was obtained in reaction performed in [bmim]Cl (43% after 1 h and 64% after 24 h). Interestingly, a clear effect of the anion present in the ionic liquid was found: higher yields of polymerization were obtained in ionic liquids containing Cl^- anions than in an analogous BF_4^- containing salt.

Attempts to reuse the catalyst $\text{RhTp}(\text{cod})$ in [bmim]Cl resulted in a 75% yield of PPA, which was even higher than obtained in the first run (51%).



Another tris-pyrazolylborate Rh(I) complex, $\text{RhTp}^{\text{Me}_2}(\text{cod})$, used in ionic liquids appeared more active than its non-substituted analog, $\text{RhTp}(\text{cod})$. In all cases, the yield of PPA obtained within 2 h was in the range 50–69%, whereas $\text{RhTp}(\text{cod})$ produced 17–56% of PPA. The molecular weight of the PPA was similar, ranging from 57,500 to 80,400 Da for $\text{RhTp}(\text{cod})$ and from 61,600 to 54,800 Da for $\text{RhTp}^{\text{Me}_2}(\text{cod})$. Interestingly, the activity of $\text{RhTp}(\text{cod})$ increased not only in the presence of imidazolium or pyridinium salts but also after the addition of tetralkylammonium salts. In experiments performed in CH_2Cl_2 at a fourfold excess of salt versus rhodium, the yield of PPA was 13–81% and the best result was noted for $[\text{Bu}_4\text{N}]\text{Cl}$. This is a remarkable increase in yield, as only 2% of PPA was formed in CH_2Cl_2 .

Tetralkylammonium salts also positively modified the catalytic activity of $\text{RhBp}(\text{cod})$ making it possible to obtain up to 100% of PPA. Interestingly, the presence of $[\text{Et}_4\text{N}]\text{Br}$ and $[\text{Bu}_4\text{N}]\text{Br}$ resulted in the formation of the polymer with the lowest M_w , ca. 6,900 Da, and a relatively high polydispersity index, 3.9.

3 Conclusions

The first applications of ionic liquids in polymerization and oligomerization of olefins were based on organoaluminum ionic liquids. Composition of these salts influenced remarkably on the reaction course and positive results were obtained only in acidic ionic liquids containing molar fraction of Al > 0.5. One problem associated with the use of chloroaluminum ionic liquids was their moisture sensitivity. Thus, any trace of water should be excluded from the reactants and equipment involved in the process. Moreover, the presence of high concentration of chloride anion, typical for acidic ionic liquid, facilitated formation of MCl_4^{2-} or MCl_3L^- species which were catalytically not active.

Imidazolium and pyridinium salts, air- and water-stable alkylaluminum-free ionic liquids, can be considered as the second generation that found applications in catalytic transformations of olefins. When imidazolium ionic liquids are used as solvents formation of carbene metal complexes is very plausible, in particular for salts bearing halide anions. Formation of carbene complexes frequently changes the original activity of the catalytic system. To prevent formation of less active carbene complexes imidazolium salts substituted at C2 carbon can be used. However, there are also examples of carbene complexes that exhibit high catalytic activity in polymerization of olefin and acetylenes.

References

1. Erdmenger T, Guerrero-Sanchez C, Vitz J, Hoogenboom R, Schubert US (2010) *Chem Soc Rev* 39:3317
2. Kubisa P (2005) *J Polym Sci Part A: Polym Chem* 43:4675
3. Kubisa P (2004) *Prog Polym Sci* 29:3
4. Kubisa P (2009) *Prog Polym Sci* 34:1333
5. Dou J, Liu Z, Mahmood K, Zhao Y (2012) *Polym Int* 61:1470
6. Vijayaraghavan R, Macfarlane DR (2012) *Sci China Chem* 55:1671
7. Illescas J, Ortiz-Palacios J, Esquivel-Guzman J, Ramirez-Fuentes YS, Rivera E, Morales-Saavedra OG, Rodriguez-Rosales A, Alzari V, Nuvoli D, Scognamiglio S, Mariani A (2012) *J Polym Sci Part A: Polym Chem* 50:1906
8. Freemantle M (2010) *An introduction to ionic liquids*. RSC Publishing, Cambridge
9. Wasserscheid P, Welton T (eds) (2003) *Ionic liquids in synthesis*. Wiley, Weinheim
10. Olivier-Bourbigou H, Magna L, Morvan D (2010) *Appl Catal A: General* 373:1
11. Dupont J, de Souza RF, Suarez PAZ (2002) *Chem Rev* 102:3667
12. Sheldon R (2001) *Chem Commun* 2399
13. Plechkova NV, Seddon KR (2008) *Chem Soc Rev* 37:123
14. Carlin RT, Osteryoung RA, Wilkes JS, Rovang J (1990) *Inorg Chem* 29:3003
15. Carlin RT, Wilkes JS (1990) *J Mol Catal* 63:125
16. Chauvin Y, Einloft S, Olivier H (1995) *Ind Eng Chem Res* 34:1149
17. Chauvin Y, Gilbert B, Guibard I (1990) *J Chem Soc Chem Commun* 1715
18. Einloft S, Dietrich FK, de Souza RF, Dupont J (1996) *Polyhedron* 15:3257
19. Ellis B, Keim W, Wasserscheid P (1999) *Chem Commun* 337
20. McGuinness DS, Mueller W, Wasserscheid P, Cavell KJ, Skelton BW, White AH, Englert U (2002) *Organometallics* 21:175
21. Wasserscheid P, Gordon CM, Hilgers C, Muldoon MJ, Dunkin IR (2001) *Chem Commun* 1186
22. Chauvin Y, Olivier H, Wyrvalski CN, Simon LC, de Souza RF (1997) *J Catal* 165:275
23. Dullius JEL, Suarez PAZ, Einloft S, de Souza RF, Dupont J, Fischer J, de Cian A (1998) *Organometallics* 17:815
24. Ligabue RA, Dupont J, de Souza RF (2001) *J Mol Catal A Chem* 169:11
25. Zimmermann J, Wasserscheid P, Tkatchenko I, Stutzmann S (2002) *Chem Commun* 760
26. Carmichael AJ, Haddleton DM, Bon SAF, Seddon KR (2000) *Chem Commun* 1237
27. Hardacre C, Holbrey JD, Katdare SP, Seddon KR (2002) *Green Chem* 4:143
28. Klingshirn MA, Broker GA, Holbrey JD, Shaughnessy KH, Rogers RD (2002) *Chem Commun* 1394
29. Csihony S, Fischmeister C, Bruneau C, Horvath IT, Dixneuf PH (2002) *New J Chem* 26:1667
30. Vygodskii YS, Shaplov AS, Lozinskaya EI, Filippov OA, Shubina ES, Bandari R, Buchmeister MR (2006) *Macromolecules* 39:7821
31. Mastrorilli P, Nobile CF, Gallo V, Suranna GP, Farinola G (2002) *J Mol Catal A: Chem* 184:73
32. Gil W, Trzeciak AM, Ziółkowski JJ (2006) *Appl Organometal Chem* 20:766
33. Gil W, Lis T, Trzeciak AM, Ziółkowski JJ (2006) *Inorg Chim Acta* 359:2835
34. Budagumpi S, Haque RA, Salman AW (2012) *Coord Chem Rev* 256:1787
35. Glorius F (ed) (2007) *N-heterocyclic carbenes in transition metal catalysis*. Springer, Berlin
36. Nolan SP (ed) (2006) *N-heterocyclic carbenes in synthesis*. Wiley, New York
37. Trzeciak AM, Ziółkowski JJ (2004) *Appl Organometal Chem* 18:124

Ionic Liquids in Transition Metal-Catalyzed Enantioselective Reactions

Yong Li, Yan-Mei He, and Qing-Hua Fan

Abstract Transition metal-catalyzed asymmetric reactions provide a powerful access to the optically active molecules that serve as precursors to pharmaceutically significant compounds. However, separation and recycling of these often expensive chiral catalysts are rather difficult and thus limit their applications in industry. As one of the most promising solutions to these problems, immobilization of a chiral homogeneous catalyst can, in principle, facilitate its separation and recycling, and thus is of considerable interest to both academia and industry. Although many methods have been developed for the immobilization of chiral catalysts via attachment of the catalyst onto a solid support via covalent attachment or noncovalent interactions, obvious decrease in catalytic activity and/or stereoselectivity is often observed due to mass transfer and accessibility of the active sites. Alternatively, chiral catalysts have also been immobilized by the use of aqueous, fluoruous, supercritical CO₂ (scCO₂) and ionic liquid phase systems. In this chapter, we present the recent significant achievements of the transition metal-catalyzed asymmetric reactions in ionic liquids (ILs). Their unique properties render ILs ideal “mobile supports” for the immobilization of chiral transition metal catalysts without laborious catalyst modification, and consequently facilitating catalyst separation and recycling through a biphasic operation. Moreover, chiral transition metal catalysts in ILs often show improved catalytic activities and/or stereoselectivities.

Y. Li

Beijing National Laboratory for Molecular Sciences, CAS Key Laboratory of Molecular Recognition and Function, Institute of Chemistry, Chinese Academy of Sciences (CAS), Beijing 100190, People's Republic of China

Department of Chemistry, Henan Institute of Education, Zhengzhou 450046, People's Republic of China

Y.-M. He and Q.-H. Fan (✉)

Beijing National Laboratory for Molecular Sciences, CAS Key Laboratory of Molecular Recognition and Function, Institute of Chemistry, Chinese Academy of Sciences (CAS), Beijing 100190, People's Republic of China
e-mail: fanqh@iccas.ac.cn

Representative examples suggested that asymmetric catalysis in ILs would combine the advantages of both traditional homogeneous and heterogeneous catalysis. The positive “IL effects” together with different strategies and concepts (e.g., catalyst with ionic tag and ionic liquid-supported phase catalysis) of IL use in catalytic applications will also be discussed.

Keywords Asymmetric catalysis · Catalyst immobilization · Catalyst recycling · Ionic liquid · Transition metal catalyst

Contents

1	Introduction	324
2	Asymmetric Reductions in ILs with Transition Metal Catalysts	325
2.1	Asymmetric Hydrogenation	325
2.2	Asymmetric Transfer Hydrogenation	333
3	Asymmetric Oxidations in ILs with Transition Metal Catalysts	333
3.1	Asymmetric Epoxidation of Olefins	333
3.2	Asymmetric Dihydroxylation of Olefins	334
4	Asymmetric C–C and C–Heteroatom Bond Formation in ILs with Transition Metal Catalysts	336
4.1	Asymmetric Diels–Alder Reaction	336
4.2	Asymmetric Cyclopropanation	338
4.3	Asymmetric Allylic Substitution	339
4.4	Asymmetric Ring-Opening Reactions of Epoxides	340
4.5	Other Asymmetric Reactions	341
5	Conclusion and Perspectives	342
	References	343

1 Introduction

Asymmetric catalysis provides a powerful access to the optically active molecules that serve as precursors to pharmaceutically significant compounds [1, 2]. Over the past four decades, a plethora of chiral catalysts have been reported, and many of them are known to be highly effective in the asymmetric formation of C–H, C–C, C–O, C–N and other bonds. However, their practical applications in industrial processes are still very limited due to their high costs, particularly in the cases with catalyst loading in the range of 1–10 mol%, and difficulties in removing trace amounts of the often toxic transition metals from the products. To overcome these problems, homogeneous chiral catalysts have been immobilized by anchoring the ligand and/or the catalyst onto a solid support via covalent attachment or noncovalent interactions [3, 4]. Despite the advantage of easy separation, however, most of these traditional immobilized chiral catalysts often result in lowered catalytic activity and stereoselectivity due to mass transfer and accessibility of the active sites. Thus, the search for more efficient immobilization methods has received considerable attention in the past decades.

As an important alternative approach, the use of aqueous, fluoruous, supercritical CO₂ (scCO₂) and ionic liquid phase systems has shown their potential for immobilization of chiral catalysts [3, 4]. Nevertheless, when water or fluorinated solvents are used as reaction media, modification of the catalyst is often necessary to ensure its solubility. For the scCO₂ system, the critical conditions may limit its application. In this context, ionic liquids (ILs) as green and alternative solvents have been highlighted as one of the most promising candidates for the facile recovery and reuse of catalysts [5, 6].

ILs consist entirely of organic cations and organic or inorganic anions, and are regarded as green alternatives to volatile organic solvents due to their negligible vapor pressure and nonflammable nature. Their physicochemical properties, such as polarity and solvent miscibility, can be fine-tuned by altering the combination of cations and anions. These unique properties render them ideal mobile supports for anchoring the chiral transition metal catalysts without laborious catalyst modification, and consequently facilitating catalyst separation and recycling through a biphasic operation. Moreover, chiral transition metal catalysts in ILs often show improved catalytic activities and/or stereoselectivities, and in some cases, they can catalyze the reactions that are not possible to conduct in common organic solvents. This positive effect might be attributed to their unique ionic nature as well as the stabilization of catalytically active intermediates in ILs [7]. Thus, asymmetric catalysis in ILs would combine the advantages of traditional homogeneous and heterogeneous catalysis.

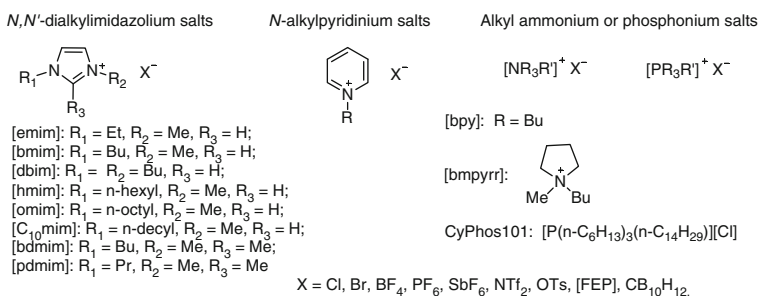
Since the pioneering work of Chauvin in 1995, who first reported the use of ILs as reaction media for asymmetric hydrogenation and demonstrated the potential of ILs in immobilization and recycling of the expensive chiral catalysts [8], many applications of ILs have been described in asymmetric biocatalysis, organocatalysis and transition metal catalysis, which have already been reviewed in the recent literatures [9–11]. In this chapter, we present the recent significant achievements of the transition metal-catalyzed asymmetric reactions in achiral IL and chiral IL (CIL), with emphasis on those showing obvious “IL effects” as well as those with excellent recyclability. Some different strategies and concepts (e.g., catalyst with ionic tag and ionic liquid-supported phase catalysis) of IL use in catalytic applications are also highlighted. However, the IL-modified chiral ligands for asymmetric catalysis without use of ILs are not included in this chapter. The representative ILs used in transition metal-catalyzed enantioselective reactions are listed in Fig. 1.

2 Asymmetric Reductions in ILs with Transition Metal Catalysts

2.1 Asymmetric Hydrogenation

Transition metal-catalyzed asymmetric hydrogenation of carbon–carbon and carbon–heteroatom double bonds is one of the most effective, economical and

a Conventional ILs used for asymmetric catalysis



b Chiral ILs used for asymmetric catalysis

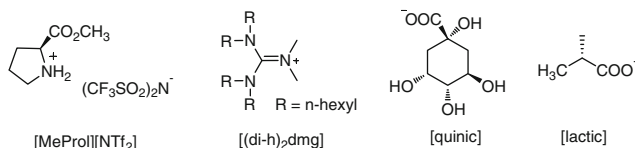
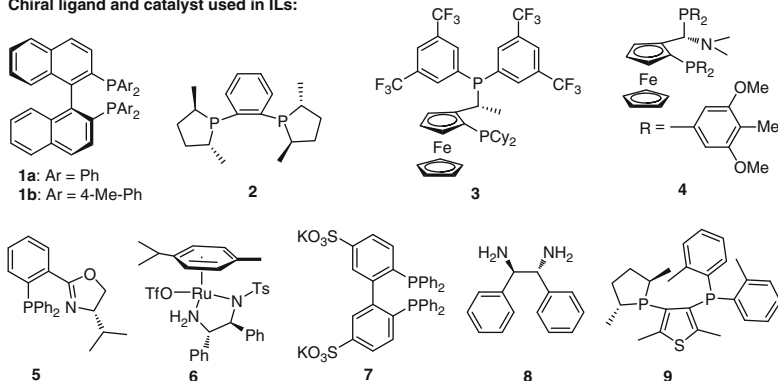
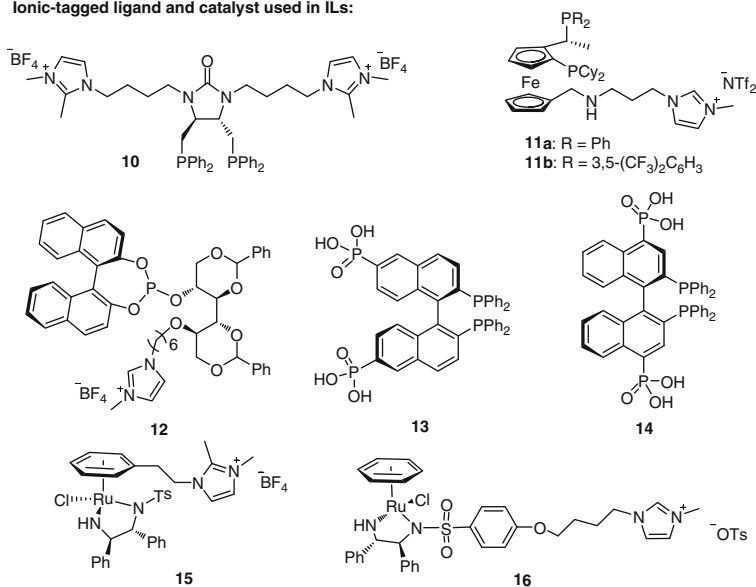


Fig. 1 Representative ILs used in transition metal-catalyzed asymmetric reactions

environmentally friendly methods for the preparation of optically active compounds [1, 2]. Excellent enantioselectivity and activity have been achieved using Rh, Ru, Ir and Pd complexes. However, these catalysts are usually expensive and air sensitive. It is difficult to recycle homogeneous phosphine-containing catalysts due to their low stability toward oxidation. Immobilization of these catalysts in ILs offers a practical way to tackle these challenges. Since the first report on asymmetric hydrogenation in ILs by Chauvin in 1995 [8], a large number of asymmetric hydrogenation in ILs with complexes of chiral phosphine- and nitrogen-containing ligands (as shown in Fig. 2) have been reported. In most cases, co-solvents are commonly needed to improve catalytic activity and/or enantioselectivity because of the poor hydrogen solubility in ILs and the important role of organic solvents on the catalytic performance. Although successful results have been achieved with direct immobilization of the unmodified chiral catalysts, incorporation of ionic moieties into catalyst structure would reduce the catalyst leaching, particularly in the case of noncharged catalysts. Another significant contribution is the application of CILs for this transformation, which acted as both the reaction media and the only chiral source.

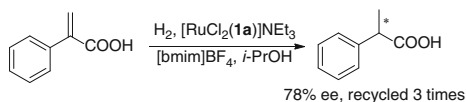
In 1997, Dupont et al. reported the asymmetric hydrogenation of 2-arylacrylic acids catalyzed by $[\text{RuCl}_2(\mathbf{1a})_2]\text{NET}_3$ complex in a mixture of [bmim]BF₄ and alcohol [12]. When methanol was used as co-solvent, the homogeneous hydrogenation gave the products with 86% ee. In contrast, when 2-propanol was employed, the biphasic system with catalyst immobilized in IL phase was formed, in which 78% ee was achieved. The results demonstrated that the hydrogenation in IL phase performed well and gave the products with better enantioselectivity in comparison with the homogeneous reaction in *t*-PrOH. The catalyst in ILs could be reused three times with no significant decline in activity and enantioselectivity

a Chiral ligand and catalyst used in ILs:**b** Ionic-tagged ligand and catalyst used in ILs:**Fig. 2** Representative chiral ligands and catalysts for asymmetric reduction

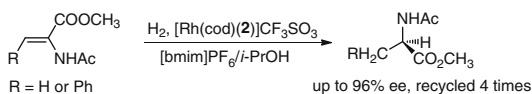
(Scheme 1). Subsequent studies found that the solubility of H₂ in [bmim]BF₄ is almost four times higher than that in [bmim]PF₆; and H₂ concentration in the ILs rather than hydrogen pressure had a remarkable effect on the reactivity and enantioselectivity of the reaction [13].

Similarly, the hydrogenation of α -dehydroamino acid esters catalyzed by [Rh(cod)(2)]CF₃SO₃ in a biphasic system of [bmim]PF₆/*i*-PrOH proceeded smoothly to give the product with 96% ee [14]. In contrast to the hydrogenation in alcohol, all manipulations could be performed in air without significant loss of enantioselectivity. This result suggests that the IL could stabilize the highly air-sensitive catalysts.

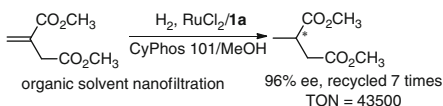
Scheme 1 Ru-catalyzed hydrogenation of α -arylacrylic acids in ILs



Scheme 2 Rh-catalyzed hydrogenation of α -dehydroamino acid esters in ILs



Scheme 3 Ru-catalyzed hydrogenation of dimethyl itaconate in ILs

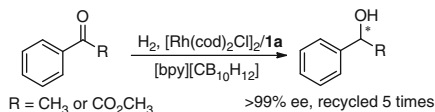
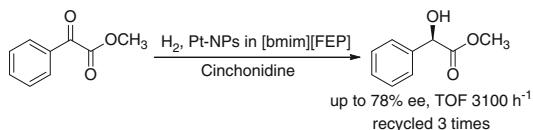
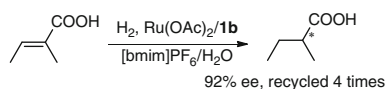


Thus, the catalyst could be easily recovered and reused at least four times with no loss of enantioselectivity but in gradually decreased yields (Scheme 2).

The same reaction could also be conducted by Rh/diphosphine (**3** or **4**) complexes in wet ILs [15]. Superior results comparable to those in organic solvents or biphasic ILs/organic co-solvent media were achieved, which were not due to the lower H₂ solubility, but more likely due to the differences in catalyst solvation in different solvent systems. The rhodium catalyst could be recycled at least seven times with full conversions and more than 99% ee. Moreover, even at a high S/C ratio of 10,000, the hydrogenation of methyl α -acetamidoacrylate in wet [omim]BF₄ afforded a full conversion and 95% ee in 3 h.

In 2006, Livingston et al. described the enhanced enantioselectivity and catalytic stability in the Ru-catalyzed asymmetric hydrogenation of dimethyl itaconate in homogeneous ILs/methanol mixture [16]. Complete conversion and 96% ee at an S/C ratio of 6,000 in CyPhos101/methanol (75% ee in methanol) were obtained. Notably, the product was separated from the reaction mixture via solvent nanofiltration; and the catalyst in ILs could be recycled at least seven times with a total TON of 43,500 (Scheme 3).

Encouraged by the excellent achievements in asymmetric hydrogenation of olefins, simple and functional ketones were also subjected to hydrogenation in ILs. In 2003, Zhu et al. reported the asymmetric hydrogenation of acetophenone and ethyl benzoylformate in ILs with a rhodacarborane-BINAP catalyst [17]. In neat ILs such as [omim]BF₄, [bmim]PF₆ and a new carborane-based IL [bpy][CB₁₀H₁₂] at 50°C, full conversions and excellent enantioselectivities (99.1% ee for acetophenone and 99.5% ee for ethyl benzoylformate in [bpy][CB₁₀H₁₂]) were observed, which are better than those obtained in THF (91.3% ee and 85.7% ee, respectively). In addition, the catalyst could be recycled five times with similar activity and enantioselectivity (Scheme 4).

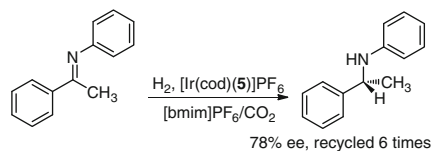
Scheme 4 Rh-catalyzed hydrogenation of ketones in ILs**Scheme 5** Pt/NPs-catalyzed hydrogenation of methyl benzoylformate in ILs**Scheme 6** Ru-catalyzed α,β -unsaturated acids in ILs

Transition metal nanoparticles have been effectively prepared in ILs, in which the IL can act as a support and stabilizer against agglomeration [18]. This new class of catalysts has received increasing attention over the past several years [19]. However, their use in asymmetric catalysis is less explored. In 2011, Baiker et al. first reported the IL-supported Pt nanoparticles as catalysts for asymmetric hydrogenation [20]. With cinchonidine as a costabilizer as well as the chiral source, Pt nanoparticles with a mean size of 2–3 nm could hydrogenate methyl benzoylformate in [bmim] tris(pentafluoroethyl)trifluorophosphate ([FEP]) to give the product with 78% ee and 3,100 h⁻¹ TOF. The catalyst could be recycled three times with the slight decline in conversion and retained enantioselectivity (Scheme 5).

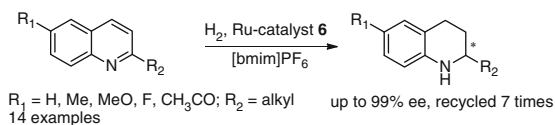
The use of scCO₂ proves to be an interesting alternative to common organic solvents due to its nontoxic nature as well as its recoverability and ease of separation [21]. In addition, scCO₂ can dissolve quite well in ILs while ILs cannot dissolve in scCO₂, which provides a means of IL recycling without product contamination. With Ru(*R*)-tolBINAP as catalyst, Jessop et al. reported the asymmetric hydrogenation of tiglic acid in ILs, where the reduced product could be readily isolated by using scCO₂ extraction [22]. Notably, the catalyst could be recycled four times with retained activity and even enhanced enantioselectivity. Moreover, in wet [bmim][PF₆], higher enantioselectivity (92% ee) was observed as compared with the biphasic IL/*i*-PrOH system, which was probably due to the higher H₂ concentration in IL/H₂O under the same pressure (Scheme 6).

Based on the similar concept of IL/scCO₂ combination, Leitner et al. reported multiphase catalytic asymmetric hydrogenation of imines in IL/CO₂ mixture with a cationic Ir-phosphinooxazoline catalyst [23]. Improved reaction rate in the presence of scCO₂ was observed, which might result from a strongly increased H₂ solubility and/or reduced viscosity of ILs. Moreover, the IL led to enhanced stability of the catalyst. An additional benefit is that the product was readily separated by scCO₂ extraction; and the catalyst in IL phase could be recycled at least six times with almost the same conversion and enantioselectivity (Scheme 7).

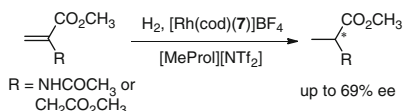
Scheme 7 Ir-catalyzed hydrogenation of imines in ILs and *sC*CO₂



Scheme 8 Ru-catalyzed hydrogenation of quinolines in ILs



Scheme 9 Rh-catalyzed hydrogenation in CILs

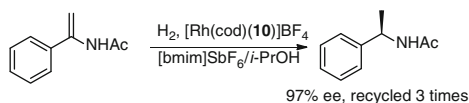


Despite great progress made in the asymmetric hydrogenation of olefins and ketones in ILs, no example of hydrogenation of heteroaromatic compounds [24] in ILs was reported till 2008. Fan et al. first used phosphine-free cationic Ru-TsDPEN catalysts for the asymmetric hydrogenation of quinolines [25]. A variety of 2-alkyl quinolines were hydrogenated smoothly in neat [bmim]PF₆ to furnish 1,2,3,4-tetrahydroquinolines in high yields (87–97%) with excellent enantioselectivities (96–99% ee), which were better than those obtained in methanol (Scheme 8). More interestingly, the hydrogenation in ILs was selective for C=N (quinoline) over C=O bond, which were both reduced in methanol. In addition, the catalyst stability was remarkably enhanced in ILs. Even after 30 days, almost the same activity and enantioselectivity were observed. The drastic enhancement of the catalyst stability in ILs was probably attributed to the solvation effect of [bmim]PF₆ on the cationic Ru catalyst and/or the very low solubility of oxygen in ILs. The catalyst in ILs could be easily recovered by solvent extraction, and recycled at least seven times without obvious decrease in reactivity and enantioselectivity.

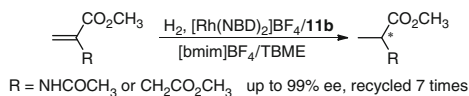
In addition to achiral ILs, CILs have recently attracted increasing interest because of their potential chiral discrimination capabilities [26]. In 2007, Leitner and Klankermayer et al. reported the asymmetric hydrogenation of methyl 2-acetamidoacrylate and dimethyl itaconate catalyzed by Rh-catalyst containing tropos biphenylphosphane ligand in readily available amino acid-based CILs [27]. With the protic (*S*)-proline-derived CILs as chiral media, complete conversion and up to 69% ee were achieved (Scheme 9). After extraction of the product with *sC*CO₂, the catalyst could be successfully recycled, though the decrease in activity and enantioselectivity was observed. Later, they found that the key role of the CIL was to effectively block the catalytic cycle for one of the two enantiomers of the catalyst [28].

Although direct immobilization of the unmodified chiral transition metal catalysts in ILs has proven to be very successful, an obvious decrease in activity was often noted after several cycles. The main cause of this decrease might be

Scheme 10 Rh-catalyzed hydrogenation with IL-tagged bisphosphine ligand



Scheme 11 Rh-catalyzed hydrogenation with IL-tagged Josiphos ligands



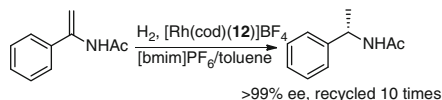
catalyst leaching during product extractions with organic solvents from the reaction mixture. Generally, the attachment of an ionic tag into catalyst structure would be a straightforward way to minimize catalyst leaching [29]. In 2003, Lee et al. reported the introduction of two imidazolium units into chiral bisphosphine ligand for the Rh-catalyzed hydrogenation of enamide [30]. With this modified ligand/Rh complex as catalyst, an enamide was smoothly hydrogenated in [bmim]SbF₆⁻/i-PrOH biphasic system in full conversion with 97% ee. Notably, improved catalyst stability in ILs was also observed. Moreover, the catalyst could be recycled three times without any loss of catalytic efficiency (Scheme 10).

Similarly, two imidazolium-tagged Josiphos ligands **11** were also prepared and tested in the Rh-catalyzed asymmetric hydrogenation of methyl acetamidoacrylate and dimethyl itaconate in the biphasic co-solvent/ILs system [31]. The introduction of imidazolium moieties afforded catalyst with sufficient affinity to [bmim]BF₄. The IL-tagged catalysts showed excellent enantioselectivity comparable to those obtained with the unmodified parent ligands. Moreover, in ^tBuOMe/[bmim]BF₄ system, the catalyst could be easily recovered and recycled seven times with only 15% decrease in TOFs and retained enantioselectivity (Scheme 11).

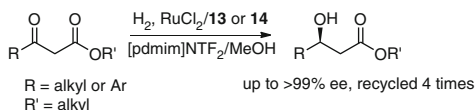
In 2011, series of ionic monophosphite ligand **12** bearing the carbohydrate group were reported by Xia et al. for Rh-catalyzed asymmetric hydrogenation of functionalized olefins [32]. For the asymmetric hydrogenation of enamides in the biphasic [bmim]PF₆/toluene system, full conversion and >99% ee were obtained. Moreover, the catalyst could be recycled at least ten times without obvious loss of catalytic efficiency (Scheme 12).

In addition to the commonly used imidazolium groups, other ionic tags such as phosphonic or sulfonic acid and ammonium salt were also documented. In 2003, Lin et al. developed the phosphonic acid-functionalized BINAP ligands **13** and **14** for the Ru-catalyzed asymmetric hydrogenation of β-ketoesters in ILs [33]. Several β-alkyl ketoesters were successfully hydrogenated in complete conversion with excellent enantioselectivity in homogeneous MeOH/ILs ([bmim]BF₄, [bmim]PF₆ or [pdmim]NTf₂) system, which are comparable to or better than those obtained in MeOH. Moreover, the modified catalysts could be recycled by simple solvent extraction and reused for four times without any deterioration of activity and enantioselectivity (Scheme 13). Later, the 4,4'-phosphonic acid-derived BINAP ligand was also applied to the highly asymmetric hydrogenation of β-aryl ketoesters in MeOH/ILs with excellent catalytic performance [34].

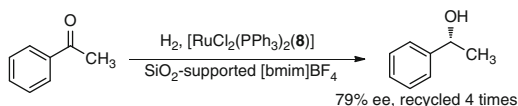
Scheme 12 Rh-catalyzed hydrogenation with IL-tagged monophosphite ligands



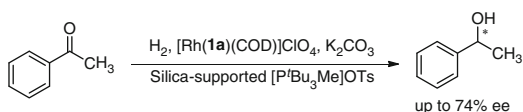
Scheme 13 Ru-catalyzed hydrogenation with phosphonic acid-tagged ligands



Scheme 14 Ru-catalyzed hydrogenation of acetophenone in SILP



Scheme 15 Rh-catalyzed hydrogenation of acetophenone in SILP

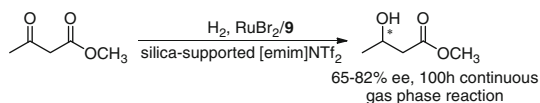


To reduce the amount of ILs utilized, which are also expensive, and further facilitate catalyst separation from reaction mixture, a “heterogenized” type of homogeneous ionic liquid catalyst system, described as supported ionic liquid phase (SILP) catalyst, has recently been introduced [35]. This new concept of supported ionic liquid catalysis combines the advantages of ILs with those of heterogeneous support materials. In 2008, Liu et al. reported the successful immobilization of chiral $[\text{RuCl}_2(\text{PPh}_3)_2(\text{S,S-DPEN})]$ complex into the channels of IL-modified mesoporous materials such as MCM-48, MCM-41, SBA-15 or amorphous SiO_2 [36]. In the hydrogenation of acetophenone, comparable catalytic activity and enantioselectivity to those of homogeneous counterpart were achieved. These heterogeneous catalysts were stable and could be recycled at least four times without noticeable decrease in reactivity and enantioselectivity (Scheme 14).

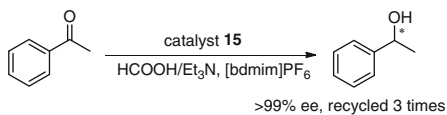
Similarly, Müller et al. reported the immobilization of rhodium catalysts containing chiral diphosphine ligands in silica-supported thin films of phosphonium-based ILs [37]. The heterogenized catalysts showed good enantioselectivity in the asymmetric hydrogenation of acetophenone, while no enantioselectivity was observed in MeOH (Scheme 15). This effect was probably due to the enhanced substrate–catalyst (S–C) interactions by the formation of solvent cage of IL around the complexes.

In 2011, Wasserscheid et al. extended the SILP catalyst concept to continuous gas phase asymmetric hydrogenation for the first time [38]. With a Ru complex containing chiral diphosphine as the catalyst, hydrogenation of methyl acetoacetate in $[\text{emim}]\text{NTf}_2$ on silica afforded the product with 65–82% ee, which was obtained from more than 100 h time-on-stream continuous operation (Scheme 16).

Scheme 16 Ru-catalyzed continuous gas phase hydrogenation in SILP



Scheme 17 Ru-catalyzed transfer hydrogenation of ketones in ILs



2.2 Asymmetric Transfer Hydrogenation

Asymmetric transfer hydrogenation provides a powerful alternative to asymmetric hydrogenation because of its versatility and practical simplicity [1, 2]. However, so far, few examples of transfer hydrogenation have been reported in ILs.

In 2004, Dyson et al. developed a versatile ruthenium precursor for IL biphasic asymmetric transfer hydrogenation [39]. With an imidazolium-tagged Noyori–Ikariya Ru-TsDPEN catalyst (**15** in Fig. 2), transfer hydrogenation of acetophenone by the HCOOH/Et₃N azeotrope in [bdmim]PF₆ proceeded smoothly to give the product in quantitative conversion and excellent enantioselectivity (>99% ee). The catalyst could be recycled three times with the same enantioselectivity but at the expense of decreased activity (Scheme 17).

Similarly, Ohta et al. reported another imidazolium-tagged Ru/diamine catalyst (**16** in Fig. 2), in which an “IL-philic” ionic tag was attached to the diamine ligand [40]. This catalyst was also applied in the same reaction in [bmim]PF₆ to afford 98% conversion and 93% ee; and the recovered catalyst showed slight decrease in conversion and enantioselectivity.

3 Asymmetric Oxidations in ILs with Transition Metal Catalysts

3.1 Asymmetric Epoxidation of Olefins

Asymmetric epoxidation of unfunctionalized olefins with Mn-salen catalysts is a useful method for the synthesis of chiral epoxides, which are important building blocks in the preparation of many pharmaceuticals and fine chemicals [1, 2]. The representative salen ligands used in asymmetric epoxidation in ILs are listed in Fig. 3.

In 2000, Song et al. reported the asymmetric epoxidation of olefins with chiral Jacobson’s Mn(III)-salen **17** catalyst in [bmim]PF₆/CH₂Cl₂ [41]. The epoxidation of several alkenes afforded the product with up to 96% ee. Notably, the Mn catalyst performed more effectively in the presence of IL, giving an enhanced activity

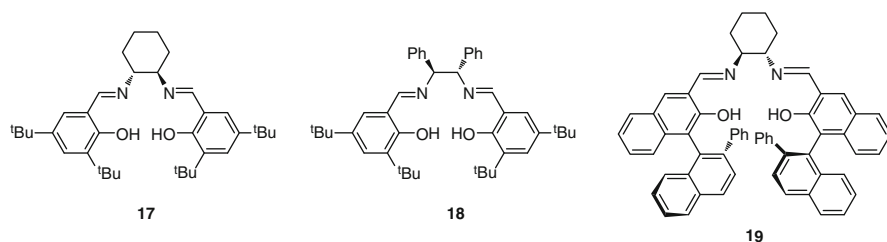
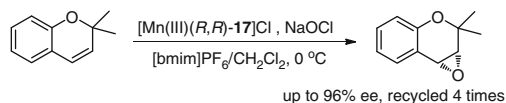
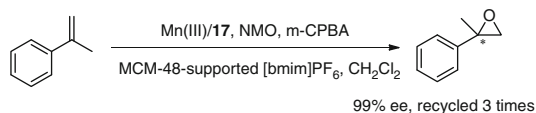


Fig. 3 Representative chiral ligands for asymmetric epoxidation of olefins



Scheme 18 Mn-catalyzed epoxidation of olefins in ILs



Scheme 19 Mn-catalyzed epoxidation of olefins in SILP

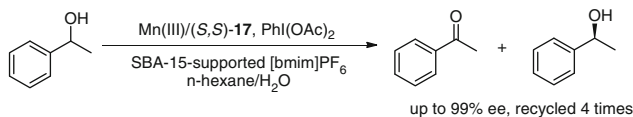
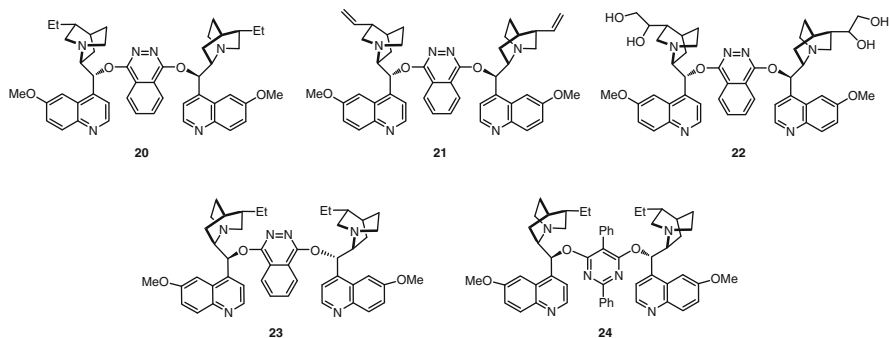
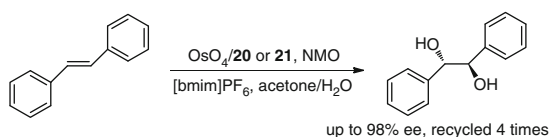
comparable to that obtained in pure CH_2Cl_2 . In addition, this catalyst in ILs could be recycled four times, but both the enantioselectivity and the activity decreased slightly upon successive use (Scheme 18). Similar results by using a Katsuki-type catalyst Mn(III)-**19** were subsequently obtained by Smith et al. [42].

To improve separation and recyclability of the catalyst, Liu et al. recently applied solid-supported ILs for the immobilization of chiral Mn-salen catalysts [43]. The IL phase of $[\text{bmim}]\text{PF}_6$ containing chiral Mn(III)-salen (**17** or **18**) complexes was immobilized onto the IL-modified mesoporous silica MCM-48. The heterogenized catalysts exhibited good to excellent activities and enantioselectivities in the asymmetric epoxidation of several unfunctionalized olefins. Notably, these SILP catalysts were stable and could be recycled three times without the loss of activity and enantioselectivity (Scheme 19).

With the similar strategy, Halligudi et al. also reported the immobilization of chiral Mn(III)-**17** complex onto the IL-modified mesoporous silica SBA-15 [44, 45]. The SILP catalysts displayed moderate to excellent activities and enantioselectivities in the oxidative kinetic resolution of several secondary alcohols. Moreover, the catalyst could be recycled four times without obvious loss of activity and enantioselectivity (Scheme 20).

3.2 Asymmetric Dihydroxylation of Olefins

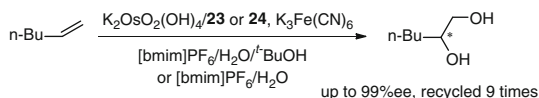
The Os-catalyzed asymmetric dihydroxylation of olefins is one of the most general methods for the synthesis of chiral vicinal diols, which are important building

**Scheme 20** Mn-catalyzed oxidative kinetic resolution of alcohols in SILP**Fig. 4** Representative chiral ligands for asymmetric dihydroxylation of olefins**Scheme 21** Os-catalyzed dihydroxylation of olefins in ILs by Song et al

blocks in the preparation of biologically active compounds [1, 2]. Due to the high cost of both osmium and the alkaloid-derived ligands and the toxicity of the metal, catalytic systems that can allow the facile and efficient separation of the catalyst from the reaction mixture are highly desirable. In addition to the organic polymer or inorganic material-supported alkaloids, systems using ILs have proven to be promising approach to recycle both the ligand and the metal. Some representative alkaloid ligands used in ILs are listed in Fig. 4.

In 2002, Song et al. reported the Os-catalyzed asymmetric dihydroxylation of olefins using NMO as co-oxidant in ILs/acetone–H₂O mixture [46]. With bis(cinchona) alkaloid **20** or **21** as the ligand, excellent yields and enantioselectivities were obtained in the asymmetric dihydroxylation of *trans*-stilbene and methyl-*trans*-cinnamate (Scheme 21). Notably, the Os catalyst bearing a new bis(cinchona) alkaloid **22**, generated in situ from ligand **21**, showed superior recyclability to the Os/**20** catalytic system. The recovered IL phase containing osmium and **22** could be recycled several times, even in the recycle experiments using 0.1 mol% OsO₄; and the total TON was up to 2,370. In addition, the IL suppressed over-oxidation of the resulting diols, a commonly observed side reaction in organic solvents. Later, a similar effect of the chiral ligand structure on recyclability was also observed by Sheldon et al. in the same transformation [47].

Scheme 22 Os-catalyzed dihydroxylation of olefins in ILs by Afonso et al



Almost at the same time, Afonso et al. described the Os-catalyzed asymmetric dihydroxylation of unfunctionalized olefins using $K_3Fe(CN)_6$ as co-oxidant in ILs/co-solvent media [48, 49]. With $K_2OsO_2(OH)_4$ -**23** or **24** as the catalyst, the reaction in the biphasic $[bmim]PF_6/H_2O$ or the monophasic $[bmim]PF_6/H_2O-t-BuOH$ mixture afforded good to excellent yields and enantioselectivities, which are comparable to or better than those achieved in the homogenous $H_2O-t-BuOH$ mixture. This catalytic system could be reused at least nine times without significant loss of activity and enantioselectivity (Scheme 22).

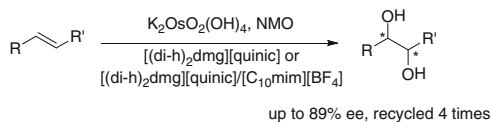
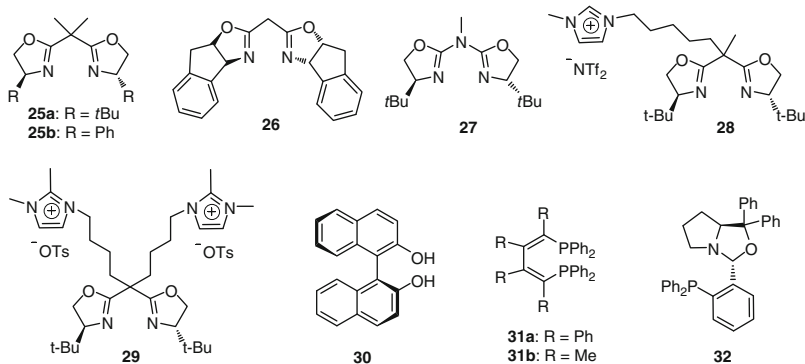
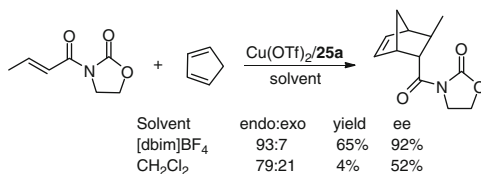
Subsequently, Afonso et al. developed a cleaner Os-catalyzed asymmetric dihydroxylation of olefins by the combination of ILs as solvent with the use of $scCO_2$ in the separation process [50]. Dihydroxylation of 1-hexene and styrene using the aforementioned catalytic systems proceeded smoothly in neat ILs, such as $[bmim]NTf_2$, $[omim]BF_4$, $[dmbim]PF_6$, $[dmbim]BF_4$ and $[dmbim]NTf_2$, affording the chiral diols in high yields (87–98%) and enantioselectivities (90–97% ee) without the need of a slow addition of olefin. In a model dihydroxylation of 1-hexene in $[bmim]NTf_2$, the chiral diol product was readily isolated via $scCO_2$ extraction without osmium contamination; and the catalyst could be reused eight times without obvious loss of activity and enantioselectivity. In contrast, the organic extraction method led to 1–2% catalyst leaching and resulted in osmium contamination of the product.

Most recently, the same group further reported the Os-catalyzed asymmetric dihydroxylation by using CILs as both the chiral source and reaction media [51, 52]. With chiral guanidinium ILs and $K_2OsO_2(OH)_4$ catalyst, dihydroxylation of several olefins containing aliphatic and aromatic units proceeded smoothly to afford very good yields (up to 95%) and enantioselectivities (up to 89%), which are comparable to or better than those obtained from the conventional system based on Sharpless chiral ligand. More interestingly, the system of $[(di-h)_2dmg][quinic]$ combined with conventional achiral IL such as $[omim]PF_6$ and $[C_{10}mim]PF_6$ also provided good performance (Scheme 23). In addition, the chiral diol product could be isolated by organic solvent or $scCO_2$ extraction; and in the latter case, the catalyst was successfully recycled at least four cycles without significant decrease in yield and enantioselectivity.

4 Asymmetric C–C and C–Heteroatom Bond Formation in ILs with Transition Metal Catalysts

4.1 Asymmetric Diels–Alder Reaction

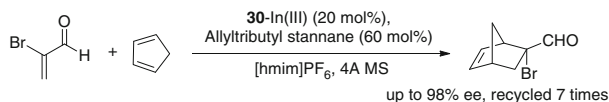
The Diels–Alder reaction is one of the most efficient bond-forming reactions widely used in synthetic organic chemistry. The homogeneous Lewis acid-catalyzed

**Scheme 23** Os-catalyzed dihydroxylation of olefins in CILs**Fig. 5** Representative chiral ligands for asymmetric D—A reaction**Scheme 24** Cu-catalyzed D—A reaction in ILs

asymmetric Diels–Alder reaction has been extensively studied over the past decades [1, 2]. Efforts were also made in the heterogeneous asymmetric Diels–Alder reaction to facilitate the catalyst recycling. Some representative chiral ligands used in ILs are listed in Fig. 5.

In 2003, Oh et al. reported the first asymmetric Diels–Alder reaction in ILs [53]. With [dbim]BF₄ as reaction media, remarkable enhancement of catalytic activity and stereoselectivity was observed. The reaction between *N*-crotonyloxazolidione and cyclopentadiene catalyzed by chiral Cu/25a complex gave good yield and excellent diastereoselectivity and enantioselectivity, whereas the same reaction in CH₂Cl₂ exhibited much poor yield and selectivity (Scheme 24). More recently, Kim et al. studied the same kind of Diels–Alder reactions with chiral bis(oxazoline) 26/Cu catalyst in ILs [54]. It was found that the catalytic performance was highly dependent on the property of ILs. Similar enhanced reactivity and stereoselectivity were observed. In addition, the catalyst could be recycled up to 17 times with slight deterioration of yield and selectivity.

To minimize catalyst leaching, Doherty et al. recently developed recyclable copper catalysts bearing imidazolium-tagged bis(oxazoline) ligands 28 for Diels–Alder reactions in ILs [55]. In comparison with CH₂Cl₂, the reaction in



Scheme 25 In-catalyzed D—A reaction in ILs

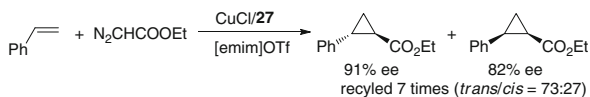
[emim][NTf₂] provided much faster rates and significantly enhanced enantioselectivities. Remarkably, the catalyst loading could be decreased to 0.5 mol% in the IL to give complete conversion within 2 min with retained enantioselectivity (95% ee). In addition, this catalyst could be readily recycled at least ten times without any loss of activity and enantioselectivity; and much lower metal leaching was observed as compared with those of the original ligand without an IL-tag.

Similarly, C₂-symmetry imidazolium-tagged bis(oxazoline) ligands were also successfully utilized for the same reactions in [bmim]NTf₂, furnishing the products with 98% conversion and 97% ee. The catalyst Cu/**29** could be recycled at least 20 times without an obvious loss of activity and enantioselectivity [56].

In addition to bis(oxazoline) ligands, other chiral ligands, including BINOL (**30**) [57], diphosphines (**31**) [58] and phosphinooxazolidine (**32**) [59], have also been used for Diels–Alder reactions. For example, Loh et al. recently described the In(III)/**30**-catalyzed Diels–Alder reaction in [hmim]PF₆ [57]. The cycloaddition of both cyclic and acyclic dienes to 2-methacrolein and 2-bromoacrolein resulted in high yields and enantioselectivities (up to 98% ee). The catalyst could be recycled at least seven times with similar yields and enantioselectivities (Scheme 25).

4.2 Asymmetric Cyclopropanation

Cyclopropane subunits have been found in many important natural and synthetic compounds, and the chiral bis(oxazoline)-Cu complexes are the most extensively used catalysts for asymmetric cyclopropanation reactions [1, 2]. Recently, Mayoral et al. extensively investigated the Cu-catalyzed asymmetric cyclopropanation reactions between alkenes and ethyl diazoacetate in ILs. In 2001, they reported the first asymmetric cyclopropanation in ILs and demonstrated the possibility to recycle the catalyst [60]. The reaction with catalyst CuCl₂/**25a** in [emim]NTf₂ gave the best results in terms of diastereoselectivity and/or enantioselectivity. Their further studies revealed that the ionic Cu/**25a** or **25b** catalysts in ILs were more robust than those supported on anionic solids [61]. This behavior was likely due to the higher stability of the catalyst in IL media than those attached onto the solid supports. Moreover, the nature of both the anion and the cation, the presence of water and the IL/catalyst molar ratio could strongly influence both catalytic performance and catalyst recycling. The catalyst CuCl/**25a** in [emim]OTf or [bmim]OTf could be recycled five times with retained reactivity but decreased enantioselectivity, which was due to the ligand decoordination. To overcome this problem, a more stable Cu catalyst containing azabis(oxazoline) (**27** in Fig. 5) was further

Scheme 26 Cu-catalyzed cyclopropanation in ILs

utilized in the asymmetric cyclopropanation in [emim]OTf [62]. The catalyst could be recycled at least seven times without any loss of activity and selectivity (Scheme 26).

In 2007, the same group developed SILP as two-dimensional nanoreactors for the Cu-catalyzed asymmetric cyclopropanation in [bmim]PF₆ [63]. With layered clay with negative charges as the support, the SILP catalyst Cu(I)/**25b** displayed greatly different catalytic behaviors comparable to bulk IL media due to the confinement effects of the nanoreactors. For example, the cyclopropanation of styrene changed from a preference of the (1*S*,2*S*)-*trans* isomer in bulk solution to the (1*R*,2*S*)-*cis* isomer in the SILP.

Davies et al. also reported the Cu-catalyzed cyclopropanation between styrene and ethyl diazoacetate [64]. They found that the cyclopropanation catalyzed by Cu(OTf)₂/**25a** could be carried out in different ILs with good yield and enantioselectivity; and the purity of ILs had a marked effect on the catalytic performance. The catalyst could be recycled at least four times without any drop of yield and enantioselectivity.

4.3 Asymmetric Allylic Substitution

Palladium-catalyzed asymmetric allylic substitution reaction represents a useful process for enantioselective formation of carbon–carbon and carbon–heteroatom bonds [1, 2]. Some representative chiral ligands used in ILs are listed in Fig. 6.

In 2000, Toma et al. first reported the asymmetric allylic substitution reaction of racemic (*E*)-1,3-diphenyl-3-acetoxyprop-1-ene with dimethyl malonate catalyzed by Pd complexes containing diphosphine ligands **33** or **34** in [bmim][PF₆]. A significant enhancement in enantioselectivity was observed in ILs as compared with those in THF [65] (Scheme 27). The catalyst could be recycled but with reduced yield and enantioselectivity. In a subsequent study, the influence of chiral ligands, bases and other reaction conditions was further investigated and up to 92% ee was achieved [66].

In 2011, Teuma et al. reported the Pd-catalyzed asymmetric allylic substitution reactions with chiral carbohydrate-based diphosphite ligands in neat ILs [67]. With [bmpyrr]NTf₂ as reaction media, the catalyst Pd/**35** was found to be highly active and induced excellent enantioselectivity in the allylic alkylation and amination. In the case of allylic amination, the catalyst could be reused at least nine times with retained enantioselectivity and activity (Scheme 28).

In addition to the chiral bidentate phosphorus ligands, other chiral ligands, including monodentate phosphoramidite (**36**) [68], tridentate NPN ligand (**37**)

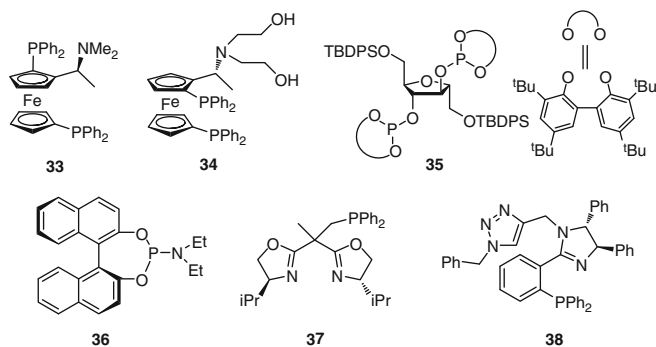
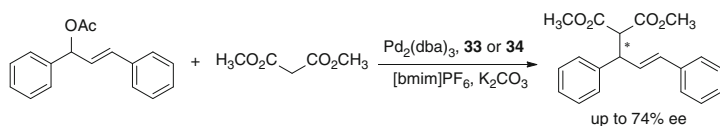
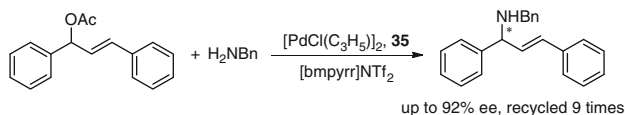


Fig. 6 Representative chiral ligands for asymmetric allylic substitution



Scheme 27 Pd-catalyzed allylic alkylation in ILs



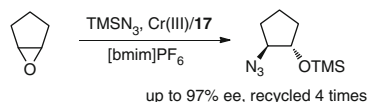
Scheme 28 Pd-catalyzed allylic amination in CILs

[69] and phosphine–imidazoline ligand (**38**) [70], have also been used for asymmetric allylic substitution reactions. For example, Claver et al. developed a Pd/**38** catalytic system for the allylic substitution in ILs under microwave conditions [70]. High conversion and excellent enantioselectivity (up to 96% ee) were achieved in [bdmim]BF₄. The catalyst could be recycled three times but with gradually decreased activity and enantioselectivity.

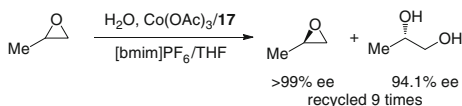
4.4 Asymmetric Ring-Opening Reactions of Epoxides

Epoxides are valuable intermediates for the stereocontrolled synthesis of complex organic compounds, and the asymmetric ring opening of such chiral epoxides extends their utilities [1, 2]. In 2000, Song et al. reported the asymmetric ring-opening of epoxides with TMSN₃ catalyzed by Cr(III) complex containing salen ligand (**17**, Fig. 3) in ILs for the first time [71]. They found the nature of the anion of ILs strongly affected the reactivity and enantioselectivity of catalyst. With

Scheme 29 Cr-catalyzed ring-opening of epoxides with TMSN₃ in ILs



Scheme 30 Co-catalyzed HKR of epoxides in ILs



hydrophobic [bmim]PF₆ as the reaction media, the reaction proceeded smoothly to provide up to 97% ee. The catalyst could be recycled four times without any loss of activity and enantioselectivity (Scheme 29).

Subsequently, hydrolytic kinetic resolution of racemic epoxides was also reported by the same group [72]. The reaction catalyzed by Co(III)/17 in [bmim]PF₆/THF mixture afforded the chiral epoxides and diols with up to 99% ee and up to 94% ee, respectively. Notably, IL proved to stabilize the Co(III) complex against reduction, which usually occurred in organic solvent. In addition, the catalyst could be recycled up to nine times with the loss of catalytic activity and enantioselectivity (Scheme 30).

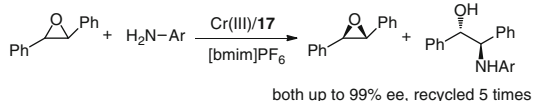
In 2010, Kureshy et al. described aminolytic kinetic resolution (AKR) of *trans*-epoxides catalyzed by chiral Cr(III)/17 complex in ILs [73]. They demonstrated that the AKR of *trans*-epoxides with different anilines as nucleophile proceeded well in [bmim]PF₆, affording anti-β-aminoalcohols in excellent yields with high enantioselectivity. More importantly, the reaction was five times faster in the presence of ILs than in conventional organic solvents. In addition, the recycling test allowed the catalyst to be reused five times with unchanged yield and ee value (Scheme 31).

4.5 Other Asymmetric Reactions

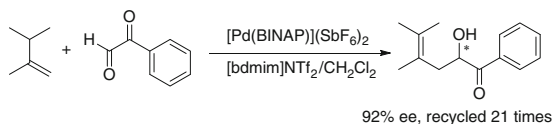
In addition to the asymmetric C–C bond formation reactions described above, some attempts were recently made to use ILs in other types of asymmetric reactions, such as carbonyl-ene reaction [74, 75], carbonyl alkylation [76–78], Mukaiyama aldol reaction [79], Michel addition [80], Henry reaction [81], Mannich reaction [82], hydrovinylation [83], Heck reaction [84] and so on. However, in most cases, the catalytic performance and/or the catalyst recycling were still less satisfactory as compared with those achieved in the asymmetric hydrogenation and oxidation reactions. Here, we only highlighted the recent results achieved in asymmetric carbonyl-ene reaction in ILs.

In 2007, Luo et al. reported the asymmetric carbonyl-ene reaction between arylglyoxals and alkenes with a chiral Pd(II)-BINAP catalyst in ILs [74]. Moderate yields and high enantioselectivities were achieved in [bdmim]NTf₂/CH₂Cl₂

Scheme 31 Cr-catalyzed
AKR of *trans*-epoxides in ILs



Scheme 32 Pd-catalyzed
carbonyl-ene reaction in ILs



mixture, which are comparable to those obtained in organic solvent. Remarkably, this chiral Lewis Pd catalyst was very stable in ILs, and could be recycled 21 times with retained enantioselectivity and activity (Scheme 32).

Most recently, Kim et al. also investigated the same reaction with Cu(II) catalyst containing bis(oxazoline) (**25**, Fig. 5) in ILs [75]. Reaction between α -methyl styrene and ethyl glyoxylate in neat [bmim]PF₆ exhibited remarkably enhanced reactivity and enantioselectivity, which greatly exceed those of the corresponding reactions in dichloromethane. Moreover, the catalyst could be recycled eight times with no significant decrease in catalytic efficiency.

5 Conclusion and Perspectives

As being described in this chapter, room temperature ILs as an effective alternative to common volatile organic solvents have been extensively employed as reaction media for various transition metal-catalyzed asymmetric reactions in recent years. The use of ILs allows chiral organometallic catalysts to be recycled more easily, which often requires no ligand modification. More importantly, large increases in reactivity and/or stereoselectivity in many cases have been achieved as compared with conventional solvents. In addition, the combination of IL as reaction media with new concepts and/or techniques, such as scCO₂ extraction, nanofiltration and SILP catalysis, has made asymmetric catalytic reactions in ILs greener and more economical. CILs as both the reaction medium and source of chirality provide a promising tool for transition metal-catalyzed asymmetric reactions without the use of common chiral ligands.

Despite of significant progress made in this field, some challenges still retain. First, a great amount of organic solvents are often required to realize satisfactory catalytic performance and/or to isolate the product. Replacement of organic solvents with greener media such as scCO₂ is highly desirable in the future. Second, high cost of IL may limit practical applications of catalysis in ILs. The SILP catalysis together with scCO₂ extraction appears to be successful examples. Expectedly, there is a large potential to realize practical asymmetric transformations in both liquid phase and gas phase by using the combination of

ILs with solid catalysts. Third, although some interesting and even unprecedented “IL effects” have been observed in different catalytic systems, the nature of these effects and detailed mechanistic understanding of reaction pathways in ILs remain to be extensively investigated in the future. On the basis of the mechanistic understanding, to develop more effective asymmetric reactions with higher TOF and TON values in ILs than those achieved in conventional organic solvents is also highly desirable.

In conclusion, the examples described in this chapter have demonstrated that ILs represent a unique class of reaction media for transition metal-catalyzed asymmetric reactions. In addition, asymmetric catalysis in ILs can combine the advantages of conventional homogeneous and heterogeneous catalysis, and will continue to attract increasing research interest from both academia and industry.

Acknowledgments We are grateful to the financial support from the National Natural Science Foundation of China (No. 21232008 and 21202038) and National Basic Research Program of China (973 program, Nos. 2010CB833300 and 2011CB8086000).

References

1. Noyori R (1994) *Asymmetric catalysis in organic synthesis*. Wiley, New York
2. Ojima I (ed) (2000) *Catalytic asymmetric synthesis*, 2nd edn. Wiley, New York
3. Ding K, Uozumi Y (eds) (2008) *Handbook of asymmetric heterogeneous catalysis*. Wiley, Weinheim
4. Fan QH, Li YM, Chan ASC (2002) Recoverable catalysts for asymmetric organic synthesis. *Chem Rev* 102:3385
5. Dupont J, de Souza FR, Suarez PAZ (2002) Ionic liquid (molten salt) phase organometallic catalysis. *Chem Rev* 102:3667
6. Hallett JP, Welton T (2011) Room-temperature ionic liquids: solvents for synthesis and catalysis 2. *Chem Rev* 111:3508
7. Lee JW, Shin JY, Chun YS, Jang HB, Song CE, Lee S (2010) Toward understanding the origin of positive effects of ionic liquids on catalysis: formation of more reactive catalysts and stabilization of reactive intermediates and transition states in ionic liquids. *Acc Chem Soc* 43:985
8. Chauvin Y, Mussmann L, Olivier H (1995) A novel class of versatile solvents for two-phase catalysis: hydrogenation, isomerization, and hydroformylation of alkenes catalyzed by Rhodium complexes in liquid 1,3-dialkylimidazolium salts. *Angew Chem Int Ed* 34:2698
9. Song CE (2004) Enantioselective chemo- and bio-catalysis in ionic liquids. *Chem Commun* 1033
10. Durand J, Teuma E, Gómez M (2007) Ionic liquids as a medium for enantioselective catalysis. *C R Chimie* 10:152
11. Lijin X, Xiao J (2009) Asymmetric catalysis in ionic liquids. In: Benaglia M (ed) *Recyclable and recoverable catalysts*. Wiley, Chichester
12. Monteiro AL, Zinn FK, de Souza RF, Dupont J (1997) Asymmetric hydrogenation of 2-arylacrylic acids catalyzed by immobilized Ru-BINAP complex in 1-*N*-butyl-3-methylimidazolium tetrafluoroborate molten salt. *Tetrahedron Asymmetry* 8:177
13. Berger A, de Souza RF, Delgado MR, Dupont J (2001) Ionic liquid-phase asymmetric catalytic hydrogenation: hydrogen concentration effects on enantioselectivity. *Tetrahedron Asymmetry* 12:1825

14. Guernik S, Wolfson A, Herskowitz M, Greenspoon N, Geresh S (2001) A novel system consisting of Rh-DuPHOS and ionic liquid for asymmetric hydrogenation. *Chem Commun* 2314
15. Pugin B, Studer M, Kuesters E, Sedelmeier G, Feng X (2004) Mixture of ionic liquids and water as a medium for efficient enantioselective hydrogenation and catalyst recycling. *Adv Synth Catal* 346:1481
16. Wong HT, See-Toh YH, Ferreira FC, Crook R, Livingston AG (2006) Organic solvent nanofiltration in asymmetric hydrogenation: enhancement of enantioselectivity and catalyst stability by ionic liquids. *Chem Commun* 2063
17. Zhu YH, Carpenter K, Bun CC, Bahnmueller S, Chan PK, Srid VS, Kee LW, Hawthorne MF (2003) (R)-Binap-mediated asymmetric hydrogenation with a rhodacarborane catalyst in ionic-liquid media. *Angew Chem Int Ed* 42:3792
18. Dupont J, Fonseca GS, Umpierre AP, Fichtner PFP, Teixeira SR (2002) Transition-metal nanoparticles in imidazolium ionic liquids: recyclable catalysts for biphasic hydrogenation reactions. *J Am Chem Soc* 124:4228
19. Migowski P, Dupont J (2007) Catalytic applications of metal nanoparticles in imidazolium ionic liquids. *Chem Eur J* 13:32
20. Beier MJ, Andanson JM, Mallat T, Krumeich F, Baiker A (2012) Ionic liquid-supported Pt nanoparticles as catalysts for enantioselective hydrogenation. *ACS Catal* 2:337
21. Jutz F, Andanson JM, Baiker A (2011) Ionic liquids and dense carbon dioxide: a beneficial biphasic system for catalysis. *Chem Rev* 111:322
22. Brown RA, Pollet P, McKoon E, Eckert CA, Liotta CL, Jessop PG (2001) Asymmetric hydrogenation and catalyst recycling using ionic liquid and supercritical carbon dioxide. *J Am Chem Soc* 123:1254
23. Solinas M, Pfaltz A, Cozzi PG, Leitner W (2004) Enantioselective hydrogenation of imines in ionic liquid/carbon dioxide media. *J Am Chem Soc* 126:16142
24. Wang DS, Chen QA, Lu SM, Zhou YG (2012) Asymmetric hydrogenation of heteroarenes and arenes. *Chem Rev* 112:2557
25. Zhou HF, Li ZW, Wang ZJ, Wang TL, Xu LJ, He YM, Fan QH, Pan J, Gu LQ, Chan ASC (2008) Hydrogenation of quinolines using a recyclable phosphine-free chiral cationic ruthenium catalyst: enhancement of catalyst stability and selectivity in ionic liquid. *Angew Chem Int Ed* 47:8464
26. Payagala T, Armstrong DW (2012) Chiral ionic liquids: a compendium of syntheses and applications. *Chirality* 24:17
27. Schmitkamp M, Chen DJ, Leitner W, Klankermayer J, Francio G (2007) Enantioselective catalysis with tropos ligands in chiral ionic liquids. *Chem Commun* 4012
28. Chen DJ, Schmitkamp M, Francio G, Klankermayer J, Leitner W (2008) Enantioselective hydrogenation with racemic and enantiopure binap in the presence of a chiral ionic liquid. *Angew Chem Int Ed* 47:7339
29. Šebesta R, Kmentova I, Toma S (2008) Catalysts with ionic tag and their use in ionic liquids. *Green Chem* 10:484
30. Lee S, Zhang YJ, Piao JY, Yoon H, Song CE, Choi JH, Hong J (2003) Catalytic asymmetric hydrogenation in a room temperature ionic liquid using chiral Rh-complex of ionic liquid grafted 1,4-bisphosphine ligand. *Chem Commun* 2624
31. Feng XD, Pugin B, Kusters E, Sedelmeier G, Blaser HU (2007) Josiphos ligands with an imidazolium tag and their application for the enantioselective hydrogenation in ionic liquids. *Adv Synth Catal* 349:1803
32. Zhao YW, Huang HM, Shao JP, Xia CG (2011) Readily available and recoverable chiral ionic phosphite ligands for the highly enantioselective hydrogenation of functionalized olefins. *Tetrahedron Asymmetry* 22:769
33. Ngo HL, Hu AG, Lin WB (2003) Highly enantioselective catalytic asymmetric hydrogenation of β -keto esters in room temperature ionic liquids. *Chem Commun* 1912

34. Hu AG, Ngo HL, Lin WB (2004) Remarkable 4,4'-substituent effects on Binap: highly enantioselective Ru catalysts for asymmetric hydrogenation of β -aryl ketoesters and their immobilization in room-temperature ionic liquids. *Angew Chem Int Ed* 43:2501
35. Mehnert CP (2005) Supported ionic liquid catalysis. *Chem Eur J* 11:50
36. Lou LL, Peng XJ, Yu K, Liu SX (2008) Asymmetric hydrogenation of acetophenone catalyzed by chiral Ru complex in mesoporous material supported ionic liquid. *Catal Commun* 9:1891
37. Fow KL, Jaenicke S, Muller TE, Sievers C (2008) Enhanced enantioselectivity of chiral hydrogenation catalysts after immobilization in thin films of ionic liquid. *J Mol Catal A Chem* 279:239
38. Öhsnera E, Schneidera MJ, Meyera C, Haumannb M, Wasserscheid P (2011) Challenging the scope of continuous, gas-phase reactions with supported ionic liquid phase (SILP) catalysts-Asymmetric hydrogenation of methyl acetoacetate. *Appl Catal A Gen* 399:35
39. Geldbach T, Dyson PJ (2004) A versatile ruthenium precursor for biphasic catalysis and its application in ionic liquid biphasic transfer hydrogenation: conventional vs task-specific catalysis. *J Am Chem Soc* 126:8114
40. Kawasaki I, Tsunoda K, Tsuji T, Yamaguchi T, Shibuta H, Uchida N, Yamashita M, Ohta S (2005) A recyclable catalyst for asymmetric transfer hydrogenation with a formic acid-triethylamine mixture in ionic liquid. *Chem Commun* 2134
41. Song CE, Roh EJ (2000) Practical method to recycle a chiral (salen)Mn epoxidation catalyst by using an ionic liquid. *Chem Commun* 837
42. Smith K, Liu SF, Ei-Hiti GA (2004) Use of ionic liquids as solvents for epoxidation reactions catalyzed by a chiral Katsuki-type salen complex: enhanced reactivity and recovery of catalyst. *Catal Lett* 98:95
43. Lou LL, Yu K, Ding F, Zhou W, Peng XJ, Liu SX (2006) An effective approach for the immobilization of chiral Mn(III) salen complexes through a supported ionic liquid phase. *Tetrahedron Lett* 47:6513
44. Sahoo S, Kumar P, Lefebvre F, Halligudi SB (2008) A chiral Mn(III) salen complex immobilized onto ionic liquid modified mesoporous silica for oxidative kinetic resolution of secondary alcohols. *Tetrahedron Lett* 49:4865
45. Sahoo S, Kumar P, Lefebvre F, Halligudi SB (2009) Oxidative kinetic resolution of secondary alcohols using chiral Mn-salen complex immobilized onto ionic liquid modified silica. *Appl Catal A Gen* 354:17
46. Song CE, Jung D, Roh EJ, Lee S, Chi DY (2002) Osmium tetroxide-(QN)₂PHAL in an ionic liquid: a highly efficient and recyclable catalyst system for asymmetric dihydroxylation of olefins. *Chem Commun* 3038
47. Liu QB, Zhang ZH, van Rantwijk F, Sheldon RA (2004) Osmium-catalyzed asymmetric dihydroxylation of olefins in ionic liquids: the effect of the chiral ligand structure on recyclability. *J Mol Catal A Chem* 224:213
48. Branco L, Afonso CAM (2002) Catalytic asymmetric dihydroxylation of olefins using a recoverable and reusable OsO₄²⁻ in ionic liquid [bmin][PF₆]. *Chem Comm* 3036
49. Branco L, Afonso CAM (2004) Ionic liquids as a convenient new medium for the catalytic asymmetric dihydroxylation of olefins using a recoverable and reusable osmium/ligand. *J Org Chem* 69:4381
50. Branco L, Serbanovic A, da Ponte MN, Afonso CAM (2005) Clean osmium-catalyzed asymmetric dihydroxylation of olefins in ionic liquids and supercritical CO₂ product recovery. *Chem Commun* 107
51. Branco L, Gois PMP, Lourenco NMT, Kurteva VB, Afonso CAM (2006) Simple transformation of crystalline chiral natural anions to liquid medium and their use to induce chirality. *Chem Commun* 2371
52. Branco L, Serbanovic A, da Ponte MN, Afonso CAM (2011) Chiral guanidinium ionic liquids for asymmetric dihydroxylation of olefins with recycling of the catalytic system by supercritical CO₂. *ACS Catal* 1:1408

53. Meracz I, Oh T (2003) Asymmetric Diels–Alder reactions in ionic liquids. *Tetrahedron Lett* 44:6465
54. Yeom CE, Kim HW, Shin YJ, Kim BM (2007) Chiral bis(oxazoline)-copper complex catalyzed Diels–Alder reaction in ionic liquids: remarkable reactivity and selectivity enhancement, and efficient recycling of the catalyst. *Tetrahedron Lett* 48:9035
55. Doherty S, Goodrich P, Hardacre C, Knight JG, Nguyen MT, Parvulescu VI, Paun C (2007) Recyclable copper catalysts based on imidazolium-tagged bis(oxazolines): a marked enhancement in rate and enantioselectivity for Diels–Alder reactions in ionic liquid. *Adv Synth Catal* 349:951
56. Zhou ZM, Li ZH, Hao XY, Dong X, Li X, Dai L, Liu YQ, Zhang J, Huang HF, Li X, Wang JL (2011) Recyclable copper catalysts based on imidazolium-tagged C₂-symmetric bis(oxazoline) and their application in D–A reactions in ionic liquids. *Green Chem* 13:2963
57. Fu F, Teo YC, Loh TP (2006) Catalytic enantioselective Diels–Alder reaction in ionic liquid via a recyclable chiral In(III) complex. *Org Lett* 8:5999
58. Doherty S, Goodrich P, Hardacre C, Luo HK, Rooney DW, Seddon KR, Styring P (2004) Remarkable enantioselectivity enhancements for Diels–Alder reactions in ionic liquids catalysed by platinum diphosphine complexes. *Green Chem* 6:63
59. Takahashi K, Nakano H, Fujita R (2007) Reuse of chiral cationic Pd-phosphinooxazolidine catalysts in ionic liquids: highly efficient catalytic asymmetric Diels–Alder reactions. *Chem Commun* 263
60. Fraile JM, Garcia JI, Herrerias CI, Mayoral JA, Carrie D, Vaultier M (2001) Enantioselective cyclopropanation reactions in ionic liquids. *Tetrahedron Asymmetry* 12:1891
61. Fraile JM, Garcia JI, Herrerias CI, Mayoral JA, Gmough S, Vaultier M (2004) Comparison of the immobilization of chiral bis(oxazoline)-copper complexes onto anionic solids and in ionic liquids. *Green Chem* 6:93
62. Fraile JM, Garcia JI, Herrerias CI, Mayoral JA, Reiser O, Vaultier M (2004) The importance of complex stability for asymmetric copper-catalyzed cyclopropanations in [emim][OTf] ionic liquid: the bis(oxazoline)-azabis(oxazoline) case. *Tetrahedron Lett* 45:6765
63. Castillo MR, Fousse L, Fraile JM, Garcia JI, Mayoral JA (2007) Supported ionic-liquid Films (SILF) as two-dimensional nanoreactors for enantioselective reactions: surface-mediated selectivity modulation (SMSM). *Chem Eur J* 13:287
64. Davies DL, Kandola SK, Patel RK (2004) Asymmetric cyclopropanation in ionic liquids: effect of anion and impurities. *Tetrahedron Asymmetry* 15:77
65. Toma Š, Gotov B, Kmentová I, Solcániová E (2000) Enantioselective allylic substitution catalyzed by Pd⁰-ferrocenylphosphine complexes in [bmim][PF₆] ionic liquid. *Green Chem* 2:149
66. Kmentová I, Gotov B, Solcániová E, Toma Š (2002) Study of ligand and base effects on enantioselective allylation catalyzed by Pd⁰ phosphine complexes in [bmim][PF₆] ionic liquid. *Green Chem* 4:103
67. Favier I, Gastillo AB, Godard C, Castillon S, Claver C, Gomez M, Teuma E (2011) Efficient recycling of a chiral palladium catalytic system for asymmetric allylic substitutions in ionic liquid. *Chem Commun* 47:7869
68. Lyubimov SE, Davankov VA, Gavrilov KN (2006) The use of an ionic liquid in asymmetric catalytic allylic amination. *Tetrahedron Lett* 47:2721
69. Castillo MR, Castillon S, Claver C, Fraile JM, Gual A, Martin M, Mayoral JA, Sola E (2011) Tridentate chiral NPN ligands based on bis(oxazolines) and their use in Pd-catalyzed enantioselective allylic substitution in molecular and ionic liquids. *Tetrahedron* 67:5402
70. de la Fuente V, Fleury-Bregeot N, Castillon S, Claver C (2012) Recycling of allylic alkylation Pd catalysts containing phosphine–imidaoline ligands in ionic liquids. *Green Chem* 14:2715
71. Song CE, Oh CR, Roh EJ, Choo DJ (2000) Cr(salen) catalysed asymmetric ring opening reactions of epoxides in room temperature ionic liquids. *Chem Commun* 1743

72. Oh CR, Choo DJ, Shim WH, Lee DH, Roh EJ, Lee S, Song CE (2003) Chiral Co(III)(salen)-catalysed hydrolytic kinetic resolution of racemic epoxides in ionic liquids. *Chem Commun* 1100
73. Kureshy RI, Kumar M, Agrawal S, Khan NH, Abdi SHR, Bajaj HC (2010) Aminolytic kinetic resolution of trans epoxides for the simultaneous production of chiral *trans* β -amino alcohols in the presence of chiral Cr(III) salen complex using an ionic liquid as a green reaction media. *Tetrahedron Asymmetry* 21:451
74. Luo HK, Khim LB, Schumann H, Lim C, Jie TX, Yang HY (2007) Enantioselective carbonyl-ene reactions of arylglyoxals with a chiral palladium(II)-BINAP catalyst. *Adv Synth Catal* 349:1781
75. Kim M, Jeong HS, Yeom CE, Kim BM (2012) Enhanced reactivity and enantioselectivity in catalytic glyoxylate-ene reactions using chiral bis(oxazoline)-copper complex in an ionic liquid. *Tetrahedron Asymmetry* 23:1019
76. Ji SJ, Qian R, Chen JP, Liu Y, Loh TP (2004) InCl₃-promoted allylation of aldehydes in ionic liquid: scope and enantioselectivity studies. *Synlett* 3:534
77. Teo YC, Goh EL, Loh TP (2005) Catalytic enantioselective allylation of aldehydes via a chiral indium(III) complex in ionic liquids. *Tetrahedron Lett* 46:4573
78. Lu J, Ji SJ, Loh TP (2005) Enantioselective allylation of aldehydes catalyzed by chiral indium(III) complexes immobilized in ionic liquids. *Chem Commun* 2345
79. Doherty S, Goodrich P, Hardacre C, Parvulescu V, Paun C (2008) Efficient heterogeneous asymmetric catalysis of the Mukaiyama aldol reaction by silica- and ionic liquid-supported Lewis acid copper(II) complexes of bis(oxazolines). *Adv Syn Catal* 350:295
80. Hamashima Y, Takano H, Hotta D, Sodeoka M (2003) Immobilization and reuse of Pd complexes in ionic liquids: efficient catalytic asymmetric fluorination and Michael reactions with β -ketoesters. *Org Lett* 5:3225
81. Khan NH, Prasetyanto EA, Kim YK, Ansari MB, Park SE (2010) Chiral Cu(II) complexes as recyclable catalysts for asymmetric nitroaldol (Henry) reaction in ionic liquids as greener reaction media. *Catal Lett* 140:189
82. Chen SL, Ji SJ, Loh TP (2003) Asymmetric Mannich-type reactions catalyzed by indium(III) complexes in ionic liquids. *Tetrahedron Lett* 44:2405
83. Bosmann A, Francia G, Janssen E, Solinas M, Leitner W, Wasserscheid P (2001) Activation, tuning and immobilization of homogenous catalysts in an ionic liquid/compressed CO₂ continuous-flow system. *Angew Chem Int Ed* 40:2697
84. Poszak R, Trzeciak AM, Pernak J, Borucka N (2011) Effect of chiral ionic liquids on palladium-catalyzed Heck arylation of 2,3-dihydrofuran. *Appl Catal A: General* 409–410:148

Index

A

Accelerator electron beam, 37
Acetophenone, asymmetric hydrogenation, 328
Acrylates, dimerization, 316
Alcohols, 6, 99, 129, 149, 163, 335
 allylic, hydroformylation, 129
 epoxidation, 226
 oxidation, 6, 174
Alkenes, 2, 88, 95, 121, 145, 241, 258, 309, 341
 carbonylation, 146
 CO₂ hydroformylation, 134
 cyclopropanation, 31, 338
 epoxidation, 198–204, 211, 225, 333
 hydroformylations, 95, 99, 114, 118, 122, 129
 hydrogenation, 2, 5, 132, 310
 isomerization, 102
 oxidations, 6
 solubility, 104
Alkenyl halides, carbonylations, 152
Alkoxy carbonylation, 145, 147, 152
Alkylammonium decatungstate, 172
Alkylation, 79, 87, 90, 339
Alkyl carbonylation, 10
1-Alkyl-3-methylimidazolium bis
 (trifluoromethylsulfonyl)amide, 42
1-Alkyl-3-methylimidazolium cations, 103
Alkylpyridinium-based, 246
Alkynes, 44, 146, 151, 269
Alloys, 55
Allylic alcohols, Heck coupling, 243, 259
Allylic substitution, asymmetric, 339
Aminocarbonylation, 145, 151, 156

2-Arylacrylic acids, asymmetric
 hydrogenation, 326
2-Aryl-2,3-dihydrofurans, 257
Aryl halides, 7, 145, 247, 258, 261, 263, 267, 272
 carbonylations, 152, 155
Aryl iodides, 154, 157, 159, 242, 250, 255, 257, 267, 270
2-Arylpropanoic acids, 146
Au-NP-decorated multiwalled carbon
 nanotubes (Au-MWCNT), 32

B

Benzothiophene (BT), 164
7-Benzyloxy-2H-chromene, oxyarylation, 256
Biodesulfurization, 164
Biphenyl carbinol, oxidation, 177
Bis(cinchona) alkaloids, 335
Bis(3-sodium sulfonatophenyl)
 phenylphosphine (TPPDS), 112
Bis-(4-tert-butylphenyl)(3-sodium
 sulfonatophenyl)phosphine, 113
Bromobenzene, hydroxycarbonylations, 155
1,3-Butadiene, cyclodimerization, 315
 hydrodimerization, 315
 hydrogenation, 4
1-Butene, 127, 312
 dimerization, 289, 313
2-Butene, 87, 89, 128, 312, 314
Butoxycarbonylation, 153
1-Butyl-3-methylimidazolium chloro-ethyl-
 aluminate ionic liquid, 314

C

Carbene complexes, 307
 Carbon dioxide (CO₂), 95
 *sc*CO₂, 95, 118, 325
 Carbon monoxide, 145
 Carbonyl alkylation, 341
 Carbonylation, 9
 Carbonyl-ene reaction, 341
 Carene, 208
 Catalysis, 1, 17, 55
 asymmetric, 323
 heterogeneous, 1, 185, 222, 249
 homogeneous, 1, 99, 145, 176, 185, 324
 metal-free, 256
 Catalysts, immobilization, 287, 323
 ionic, 294
 ionically tagged, 295
 metal-free, 185, 215, 256
 recycling, 323
 C–C bond forming reactions, 237
 C–C coupling, 7
 Cellulose, 30
 Cetyltrimethylammonium bromide
 (CTAB), 70
 Chalcones, epoxidation, 201, 215
 Chloroaluminate, 88
 6-Chloro-dimethylchromene,
 epoxidation, 204
 Chloroindanate, 88
 Chlorometallate ILS, 82
 Chloroperoxidase (CPO), 221
 Chromones, epoxidation, 205, 215, 217
 Cinchonidine, 329
 Cinnamic esters, 243
 Colloids, 55
 Coordination structure, 83
 Couplings, 7
 Cross-coupling reactions, 237
 CS₂, catalyst poisoning, 3
 α-Cyclodextrins, 110
 Cyclohexanol, oxidation, 176
 Cyclohexene, hydroformylation, 134
 hydrogenation, 32, 46
 Cyclohexyl acrylate, 255
 Cyclooctadiene (COD), 39, 57, 153
 Cyclooctane, 68
 Cyclooctatriene (COT), 39, 57
 Cyclooctene, epoxidation, 186, 192, 197
 oxidation, 195
 Cyclooctene oxide, 207

Cyclopropanation, asymmetric, 338

D

1-Decene, 206
 Dehalogenation, 9
 α-Dehydroamino acid esters, hydrogenation,
 327
 Derjaguin–Landau–Verwey–Overbeek
 (DLVO) theory, 21
 Dialkylimidazolium ILS, 246
 Diallyltosylamine, RCM, 298
 Dibenzo[a,e]cyclooctatetraene (DCT), 3
 Dibenzothiophene (DBT), 164
 Diels–Alder, asymmetric, 336
 Diethyl diallylmalonate (DEDAM), 290
 Dihaloarenes, carbonylation, 158
 1,2-Dihydronaphthalene, epoxidation, 221
 Dihydroxylation, asymmetric, 334
 Dihydroxytetrahydronaphthalene, 221
 Dimerization, 10
 Dimethylbutenes, 310
 Dimethyl itaconate, 100
 Ru-catalyzed hydrogenation, 328
 Dimethyl 1,18-octadec-9-enedioate, 301
 Dioxomolybdenum(VI), 187
 Diphenyl-3-acetoxyprop-1-ene, 339
 Diphenylmethane, 88
 Dodecene, hydroformylation, 108

E

Earth-abundant metals, 55
 Electrodeposition, 21
 Electron beam, 37
 Electroreduction, 21, 34
 Enantioselectivity, 323
 Energy, 55
 Epoxidation, 185, 189, 191, 205
 asymmetric, 333
 metal-free, 215
 Epoxides, asymmetric ring-opening, 340
 Ethenolysis, 291
 Ethyl benzoylformate, asymmetric
 hydrogenation, 328
 Ethylene, 128
 1-Ethyl-3-methylimidazolium ethyl sulfate, 29
 Extraction and oxidative desulfurization
 (EODS), 165
 Extractive desulfurization (EDS), 164

F

- Fatty acid methyl esters (FAMEs), metathesis transformations, 291
- Fischer–Tropsch reaction, 9
- Friedel–Crafts reactions, 88

G

- Gamma-irradiation, 37
- Gas-liquid interfacial discharge plasma (GLIDP), 36
- Gas–phase synthesis, 35
- Geraniol, 208
- Glow-discharge electrolysis (GDE), 36
- Gold, 55
- Gold nanoparticles, 30
- Green chemistry, 163
- Grubbs catalyst, 290, 300
- Guggulsterone, epoxidation, 211

H

- Halometallates, coordination, 83
- Heck coupling, chiral ionic liquids, 256
- Heck reaction, 237, 241
- Henry reaction, 341
- Heterogeneous catalysis, 1, 185, 222, 249
- 1-Hexene, 102, 113, 116, 119, 122, 133, 149, 293, 313, 336
 - dihydroxylation, 336
- Homogeneous catalysis, 1, 99, 145, 176, 185, 324
- Hoveyda catalysts, 288, 293, 298
- Hydroarylation, 11
- Hydrodesulfurization (HDS), 164
- Hydroesterification, 9
- Hydroformylation, 9, 95
 - Pt-based, 131
 - Ru-based, 132
- Hydrogenation, 4
 - asymmetric, 325
- Hydrosilylation, 10
- Hydrovinylation, 341
- Hydroxycarbonylation, 150, 155
- 1-(2'-Hydroxyethyl)-3-methylimidazolium cation, 6
- 4-Hydroxy styrene, epoxidation, 220

I

- Ibuprofen, 146
- Imidazolium, 246

- Inclusion complexes, 106
- Iodobenzene, hydroxycarbonylations, 155
- 3-Iodo-2-cyclohexen-1-one, 175
- Ionic liquid glow-discharge electrolysis (IL-GDE), 36
- Ionic liquids, 1, 17, 19, 79, 163, 185, 237, 287, 323
 - room temperature (RT-ILs), 19
- Iridium nanoparticles, 2, 28
- Iron, 211
- Iron oxide, 55
- Iron(III) porphyrin, 212
- Ir-phosphinooxazoline, 329
- Isoflavones, epoxidation, 215
- Isomerization, 10

J

- Jacobsen-type Mn-salen, 199, 206, 226, 333
- Jeffery conditions, 243

K

- Ketoprofen, 146

L

- Lactones, macrocyclic, 301
- Ligands, 55
- Limonene, 208
- Lipases, 218

M

- Magnetron sputtering, 36
- Manganese, 199, 226
- Mannich reaction, 341
- Menthol, 256
- Mercury, catalyst poisoning, 3, 4
- Metal carbonyls, 38
- Metal
 - catalysts, 1
 - nanocrystals, 55
 - nanoparticles, 2, 17, 20
 - oxides, 55
 - salts, solvation, 81
 - speciation, 79
- Methyl 2-acetamidoacrylate, asymmetric hydrogenation, 330
- hydrogenation, 328
- Methyl acrylate, 100
- Methyl benzoylformate, Pt/NPs-catalyzed hydrogenation, 329

1-Methyl-3-butyylimidazolium decatungstate,
177

Methyl 9-decenoate, 291

3-Methyleneisindolin-1-ones, 158

3-Methylheptene, 315

Methyl linoleate, epoxidation, 191

Methyl methacrylate, 316

Methyl oleate, 301

Methyl oleate oxide, 213

Methylpentanoate, 132

Methyl-3-pentenoate, 100

Methyl ricinoleate, self-metathesis, 293

Methyltrioxorhenium (MTO), 179

Michael addition, 256, 341

Mn-porphyrin, 199

Molybdenum, 187, 222, 287

Monoterpenes, MTO-catalyzed epoxidation,
208

Mukaiyama aldol reaction, 341

N

N-Alkyl-3,4-dihydroquinolinium salts, 218

Nanoclusters, 55

Nanocrystals, 55

Nanoparticles, 2, 17, 55

oxo processes, 131

Nanostructures, 55

Naproxen, 146

N-Butylimidazole (BIm), 29

N-Crotonyloxazolidione, 337

Negishi coupling, 237, 240, 275

Nerol, 208

N-Heterocyclic carbenes (NHCs), 4, 63,
117, 292

Noble metals, 55

Norbornadiene, 319

Norbornenes, 100, 104, 192, 199, 294, 318

polymerization, 295

ROMP, 294, 317

Novozym 435, 220

Nucleophiles, 145

O

9-Octadecene, 301

Octa-2,7-dien-1-ol, 315

1-Octene, epoxidation, 204

hydroformylation, 109, 130

self-metathesis, 291

Olefins, asymmetric dihydroxylation, 334

asymmetric epoxidation, 333

epoxidation, 185, 189, 193, 196, 206, 219

metathesis, 9, 287

oligomerization, 307, 309

polymerization, 307, 309

Oleic acid, epoxidation, 213

Organometallics, 55

Organomolybdenum, 188

Ostwald ripening, 18

Oxidation, 6

asymmetric, 333

metal-catalyzed, 163

Oxidiperoxomolybdenum, 194

Oxo process, 99

P

Palladium, 237

nanoparticles, 28, 237

Pauson–Khand reaction, 9

Peroctanoic acid, 219

Perrhenate, 210

Phenylacetylene, 307

polymerization, 318

Phenylborylation, 11

1-Phenylethanol, 179

Phenyl(3-sodium sulfonatophenyl)(4-tert-
butylphenyl)phosphine, 113

Phosphine-imidazolylidene palladium, 262

Phosphinooxazolidine, 338

Physical vapor deposition, 37

α -Pinene, 192

epoxidation, 209

Plasma deposition, 36

Plasma electrochemical deposition (PECD), 36

Platinum, 55

nanoparticles, 28, 36

Polyether guanidinium methanesulfonates, 109

Polyoxometals (POMs), 171, 196

Polyoxotungstate, 196

Propene, 123, 125, 130

dimerization, 310, 314

Pulsed electrodeposition (PED), 34

Pyridinium-based ILs, 246

Pyridinium chloroaluminate, 312

Q

Quinolines, Ru-catalyzed hydrogenation, 330

R

Reduction, asymmetric, 325

chemical, 21, 28

electrochemical, 34

photochemical, 33

sonochemical (ultrasound), 34

Rhenium, 206, 228

Rhodium, 104, 114, 131, 318, 332

nanoparticles, 3, 32, 45
Ring-opening metathesis polymerization (ROMP), 317
Room temperature ionic liquids (RTILs), 19, 287
Ruthenium, 55, 214, 287, 290
 allenylidene, cationic, 294

S

*sc*CO₂, 95, 118, 325
Schrock catalysts, 295
SILPs. *See* Supported ionic liquid phases (SILPs)
Silver, 55
Sodium triphenylphosphine-3-monosulfonate (TPPMS), 100, 112, 117, 120, 123
Sonogashira coupling, 269
Stabilization, 17
Stilbenoids, 248
Stille cross-coupling, 267
Styrene, 100, 104, 147, 192, 200, 248, 317
 alkoxycarbonylation, 147
 carbonylation, 150
 CO copolymerization, 317
 cyclopropanation, 339
 dihydroxylation, 336
 epoxidation, 203, 207, 226
 hydroformylation, 104, 132
 hydrogenation, 64
 self-metathesis, 290
Sulfides, 163
 oxidation, 164
Sulfoxidation, 6
Supported ionic liquid phases (SILPs), 95, 121, 254
Surface chemistry, 55
Suzuki coupling, 4–9, 240, 248
Suzuki–Miyaura reaction, 237, 261

T

Tetraalkylammonium ionic liquids, 243
Tetrabutylammonium decatungstate, 173

Tetradecene, 102, 104, 291
Tetramethylguanidinium lactate, 32
Tetra-*n*-decyltriethylphosphonium chloride (THPC), 263
Thermally reduced graphite oxide (TRGO), graphene, 45
Thiocarbonylation, 159
Thiocyanatodioxomolybdenum complexes, 189
TPPMS. *See* Sodium triphenylphosphine-3-monosulfonate (TPPMS)
Transition metals, 55, 79, 185, 307, 323
Trimethyl-1,4-benzoquinone (TMBQ), 180
Trimethylphenol (TMP), 181
Tris(imidazolium)-tetrakis(diperoxotungsto)phosphate, 179
Tri(3-sodium sulfonatophenyl)phosphine (TPPTS), 112
Tungsten, 225

U

Ullmann homo-coupling, 272
Ultra low sulfur diesel (ULSD), 164

V

Vanadium, 186
 peroxides, 186
Vinyl acetate, 100
Vinylarenes, 129
4-Vinyl-1-cyclohexene, 214, 315
2-Vinylnaphthalene, 100, 129
 hydroformylation, 108
Vitamin K, 215

X

Xantphos, guanidinium-modified, 115

Z

Zerovalent metal precursors, 38